

# **The potential utilisation of contaminated biomass following phytoremediation**

**Douglas George Bray**

Submitted in accordance with the requirements of the degree of Doctor of Philosophy  
as part of the Integrated PhD with MSc in Bioenergy

ESPRC Centre for Doctoral Training

Bioenergy, Fertiliser and Clean Water from Aquatic Macrophytes (BEFWAM)

**Faculty of Engineering and Physical Sciences**

School of Chemical and Process Engineering

The University of Leeds

June 2023



The candidate confirms that the work submitted is his own, except where work which has formed part of jointly authored publications has been included. The contribution of the candidate and the other authors to this work has been explicitly indicated below. The candidate confirms that appropriate credit has been given within the thesis where reference has been made to the work of others.

1. **Bray DG**, Nahar G, Grasham O, Dalvi V, Rajput S, Dupont V, Camargo-Valero MA, Ross AB. (2022). The Cultivation of Water Hyacinth in India as a Feedstock for Anaerobic Digestion: Development of a Predictive Model for Scaling Integrated Systems. *Energies*. 15(24): 9599. **10.3390/en15249599**
2. Apurba Koley, **Douglas G. Bray**, Sandipan Banerjee, Sudeshna Sarhar, Richih Ghosh Thahur, Amit Kumar Hazra, et al. (2022). Water Hyacinth (*Eichhornia crassipes*) A Sustainable Strategy for Heavy Metals Removal from Contaminated Waterbodies. In: *Bioremediation of Toxic Metal(loid)s*. CRC Press;

Publication 1 contributed towards Chapter 7; the candidate designed and conducted the experimental cultivation work, contributed to the data analysis of the cultivation and techno-economic work and contributed to the draft and review process of the publication.

- Dr Gaurav Nahar designed and performed the methodology and experimental work for the anaerobic digestion. Dr Nahar also reviewed and provided feedback to the publication.
- Dr Oliver Grasham designed the methodology for the techno-economic assessment and contributed towards the draft and review process of the publication.
- Dr Vishwanath Dalvi, Dr Shailendrasingh Rajput, Dr Valerie Dupont, Dr Miller A. Camargo-Valero and Dr Andrew B. Ross reviewed and provided feedback to the publication.

The candidate contributed towards publication 2 through literature analysis, draft preparation and review and feedback.

This copy has been supplied on the understanding that it is copyright material and that no quotation from the thesis may be published without proper acknowledgement.

The right of Douglas George Bray to be identified as Author of this work has been asserted by him in accordance with the Copyright, Designs and Patents Act 1988.

The dataset associated with this thesis is openly available from the University of Leeds Data Repository at <https://doi.org/10.5518/1367>.

# Acknowledgements

Firstly, I would like to thank my supervisor Dr Andrew Ross for his incredible support and guidance throughout my PhD. I have had some incredible experiences because of his desire to see my work succeed and I could not have achieved this without you. I would also like to thank my supervisor Dr Miller Alonso Camargo-Valero for his time and effort in designing the best project I could have asked for.

I would also like to thank Dr Jessica Adams for hosting me at the Institute of Biological, Environmental and Rural Sciences, Aberystwyth University and providing me with material that I could not have received from elsewhere. The time I was able to spend at Aberystwyth was an amazing experience and your support was greatly appreciated.

I would also like give a special mention to Dr Gaurav Nahar and his team at Defiant Renewables Ltd., without your help and support I could not have made it through my PhD; in addition to the dedication, you showed towards our work during an incredibly difficult time, I cannot thank you enough. Finally, thank you for hosting me on so many occasions, my time India is something I will never forget and was the best thing about my PhD.

I would like to thank everyone who worked so tirelessly to collect and prepare all the samples that I have analysed throughout my work, in particular Dr Shailendrasingh Rajput Dr Opio Innocent Miria and Apurba Koley. I would also like to thank the technical and administrative staff at the University of Leeds, especially Dr. Adrian Cunliffe, Karine Alves Thorne, Simon Lloyd, Emily Bryan-Kinns and James McKay. I would like to acknowledge the Engineering and Physical Sciences Research Council (EPSRC) for providing the funding to support this research degree, as well as the BEFWAM project (Bioenergy, fertiliser and clean water from invasive aquatic macrophytes) for supporting my work.

Thank you to all friends and colleagues that have helped me along the way, your support has kept me going through every barrier that appeared. I would like to specifically mention Dr Aaron Brown, Dr Scott Wiseman and Dr James Hammerton, your friendship during the quiet days meant more than I can possibly say. Next to Dr Nicholas Davison for helping me make the most of our time in India. I'd also like to extend my gratitude to, Innes Deans, Poppy Cooney, Jessica Quintana-Najera, Jaime Borbolla-Gaxiola, Flora Brocza, Oliver Grasham, Adan Yusuf and the Energy group. Outside of the university I would like to thank all of the Newton-Le-Willows cricket club for keeping me going every Saturday; Nathan Haris for forcing me to enjoy myself; and all of my friends in Bristol for giving me time away in the final months.

I would like to thank my family, Lucy Baker, Kevin Bray and Josh Bray (and all the rest), for helping get to where I am today and continually being there for me at every step of the journey.

Finally, I want to thank Anna Rogers, for never letting me give up, pushing me to always be the best I can and supporting with everything you have.

# Abstract

Bioenergy and bioproducts are widely regarded as one of the key contributors to reducing global greenhouse gas emissions. Utilisation of wastes or pests could provide an alternative feedstock to avoid land use complications and reduce costs. An example of a potential feedstock is the invasive aquatic macrophyte water hyacinth (WH), however, due to its heavy metal content, moisture content and cost of removal, it has yet to be valorised or used on a large scale. The aim of this thesis was to demonstrate the potential utilisation of WH in a biorefinery concept, to produce bioproducts, with a focus on protein and bioenergy.

This work focussed on the comparison of biomass composition across various locations, pollution sources and degrees, and timescales. The results demonstrated that water hyacinth has a high variability across locations with particular impact from the residence time of the waterbody: a lower residence time appeared to increase plant contamination despite reduced pollutant concentration within the water. The phenological study demonstrated that if a growth period can be identified, then clear trends can be observed, in particular where growth methods by WH are identified. However, all sites demonstrated increased heavy metal content at the same time as reduced protein content, suggesting that either protein recovery or heavy metal removal should be prioritised when harvesting plants.

When cultivated under controlled conditions, it was evidenced that WH growth rate had a strong linear relationship with water nitrogen concentration but that other factors such as plant density and temperature did have an impact. The source of nutrients did have a significant impact on growth, but all nutrient sources fit within a 95% confidence of the linear relationship. However, the relationship identified here resulted in a lower growth than literature, suggesting that optimisation was still possible.

The potential for protein extraction from water hyacinth was examined, utilising an alkali acid extraction. This demonstrated that a safe protein precipitate could be produced from water hyacinth leaves, but the yields were lower than other feedstocks. The fibrous residue, from the alkali extraction, demonstrated an improved biogas yield as compared with the raw biomass. The data was utilised in various scenarios, it was demonstrated that a WH biorefinery was not economically viable on a large scale due to the high running costs, but on a small scale could provide enough biogas to replace 1- 6 cylinders of liquid petroleum gas, 14.2 kg cylinder for a single family. Whilst optimisation could improve the viability of the large-scale systems, the value of digestate would be the most significant change, whilst non-direct benefits from harvesting should be investigated further.

# Table of contents

Acknowledgements.....	II
Abstract .....	III
Table of contents .....	IV
List of figures .....	IX
List of plates.....	XXIII
List of tables.....	XXIV
List of equations.....	XXIX
Abbreviations & nomenclature .....	XXX
Chapter 1. Introduction .....	1
1.1. Energy and food security .....	1
1.2. Pollution of freshwater ecosystems .....	2
1.3. Water hyacinth infestation .....	4
1.4. Aims, objectives and structure .....	5
1.4.1. Aims and objectives .....	5
1.4.2. Structure .....	6
Chapter 2. Literature review.....	7
2.1. Introduction into water hyacinth biomass .....	7
2.1.1. Global distribution of water hyacinth.....	8
2.1.2. Morphology of water hyacinth .....	13
2.1.3. Phenology of water hyacinth .....	18
2.2. Impact of environmental parameters on the growth of water hyacinth.....	21
2.2.1. Temperature .....	21
2.2.2. Light intensity .....	22
2.2.3. Waterbody .....	22
2.2.4. Nutrient availability .....	23
2.2.5. Biomass density .....	26
2.2.6. Toxic substances .....	28
2.3. Utilisation of water hyacinth biomass .....	28
2.3.1. Harvesting water hyacinth .....	28

2.3.2. Influence of composition on utilisation technique .....	31
2.3.3. Phytoremediation.....	32
2.3.4. Energy generation.....	45
2.3.5. Fertiliser production .....	49
2.3.6. Protein source.....	50
2.4. Introduction to water lettuce .....	54
2.5. Summary of methodologies for protein extraction.....	57
2.5.1. Protein release.....	57
2.5.2. Protein recovery.....	62
2.5.3. Methods for further investigation .....	66
2.6. Research gaps .....	66
Chapter 3. Materials, equipment and experimental methods .....	68
3.1. Material collection, preparation and storage .....	68
3.1.1. Biomass feedstocks .....	68
3.1.2. Water .....	78
3.1.3. Inoculum .....	78
3.2. Cultivation protocol.....	78
3.2.1. Material collection, preparation and storage.....	79
3.2.2. Small crate cultivation .....	79
3.2.3. Large tank cultivation .....	80
3.3. Material characterisation .....	82
3.3.1. Proximate analysis.....	82
3.3.2. Ultimate analysis.....	83
3.3.3. Volatile solids.....	84
3.3.4. Elemental analysis .....	84
3.3.5. Biochemical analysis.....	84
3.4. Water characterisation .....	86
3.5. Utilisation potential indicators .....	86
3.5.1. Protein extraction.....	86
3.5.2. Biomethane potential .....	87

3.5.3. Higher heating value .....	89
Chapter 4. Natural variations of water hyacinth .....	91
4.1. Introduction.....	91
4.1.1. COVID-19 impact statement .....	91
4.2. Geographical and water quality study of water hyacinth .....	92
4.2.1. Water analysis .....	93
4.2.2. Whole plant samples.....	97
4.2.3. Water hyacinth tissue variations.....	102
4.3. Phenological variations.....	111
4.3.1. Murchison Bay, Lake Victoria.....	112
4.3.2. Pune, Maharashtra.....	124
4.3.3. Goyal Para, West Bengal.....	141
4.4. Summary of composition .....	151
4.5. Conclusions.....	153
Chapter 5. Cultivation of water hyacinth.....	157
5.1. Introduction.....	157
5.1.1. COVID-19 impact statement .....	158
5.2. Impact of nitrogen on growth rate .....	158
5.3. Impact of nutrient source on growth rate.....	161
5.4. Large-scale cultivation .....	166
5.5. Impact of nitrogen and nutrient source on utilisation potential indicators.....	169
5.6. Phenological study .....	172
5.6.1. Impact of the rain shelter.....	172
5.6.2. Variations in growth rate.....	173
5.6.3. Logistic Growth Model.....	177
5.6.4. Impact on Utilisation Potential Indicators.....	185
5.7. Conclusions.....	187
Chapter 6. Alkali acid extraction.....	189
6.1. Introduction.....	189
6.1.1. COVID-19 Impact Statement.....	190



6.2. Alkali acid extraction from wild and cultivated water hyacinth .....	190
6.2.1. Raw biomass characterisation .....	190
6.2.2. Protein extract.....	192
6.2.3. Fate of trace elements .....	201
6.2.4. Alkali acid extraction solid residue analysis.....	206
6.3. Comparison of alkali acid extraction conditions on water lettuce .....	209
6.3.1. Effect of extraction time on alkali acid extraction.....	211
6.3.2. Effect of temperature on alkali acid extraction.....	214
6.3.3. Influence of alkali concentration on alkali acid extraction .....	221
6.3.4. Fate of trace nutrients and heavy metals in water lettuce.....	227
6.3.5. Residue analysis in water lettuce.....	228
6.3.6. Optimisation of extraction.....	230
6.4. Conclusions.....	234
Chapter 7. Development of an Aquatic biomass biorefinery.....	237
7.1. Introduction .....	237
7.2. Scenario description.....	238
7.2.1. Wild harvested scenarios .....	238
7.2.2. Cultivated scenarios.....	240
7.3. Cost assumptions.....	243
7.3.1. Capital cost .....	243
7.3.2. Annual operating costs .....	245
7.3.3. Product value.....	247
7.4. Wild water hyacinth scenarios .....	247
7.4.1. Wild water hyacinth as a resource .....	247
7.4.2. Scenario wild anaerobic digestion (W-AD) .....	253
7.4.3. Scenario wild alkali acid extraction (W-AAE).....	258
7.4.4. Secondary benefits of the wild scenarios .....	266
7.5. Cultivated water hyacinth scenarios .....	266
7.5.1. Cultivated biomass as a resource .....	266
7.5.2. Scenario cultivated anaerobic digestion (C-AD) .....	270

7.5.3. Scenario cultivated cow manure (C-CM) .....	271
7.5.4. Scenario cultivated co-digestion (C-CoD).....	271
7.5.5. Costings of the cultivated water hyacinth scenarios .....	272
7.6. Conclusions.....	274
Chapter 8. Conclusions and Future Work .....	277
8.1. Conclusions.....	277
8.2. Future work .....	282
8.2.1. Bioaccumulation and the role of water hyacinth in urban water bodies.....	282
8.2.2. Increasing the economic sustainability of a water hyacinth biorefinery .....	283
References .....	286
Appendix A. Global distribution of water hyacinth.....	317
Appendix B. Analysis of individual sites .....	318
B.1. Phenological analysis of water quality indicators .....	318
B.2. Biomass composition of water hyacinth samples for geographical and pollution analysis .....	321
Appendix C. Nutrient composition in growth trials .....	322

# List of figures

Figure 2.1-1: Cultivation of water hyacinth in a botanical garden [35].....	9
Figure 2.1-2: Distribution of water hyacinth showing the tropic zone (adapted from [35]). .....	10
Figure 2.1-3: Elemental analysis of water hyacinth by time and plant tissue in the River Nile. Adapted from [62]. a) macronutrient; b) trace element. ....	20
Figure 2.1-4: Heavy metal concentration in water hyacinth by season and plant tissue in Srepok River. Adapted from [14]. ....	20
Figure 2.2-1: Maximum growth rate of water hyacinth against water nitrogen concentration from literature [33,90–97]; ○ - low growth rate results. a) linear fit including low growth rate values; b) LitFit. ....	25
Figure 2.3-1: Water heavy metal concentration against percentage removal by water hyacinth, from studies in Table 2.3-2.....	34
Figure 2.5-1: Mock solubility curve of protein in lignocellulosic biomass. Representative of lignocellulosic biomass described in literature [268,270]. ....	64
Figure 3.1-1: Sample collection locations in India. ....	69
Figure 3.1-2: Sample collection locations in Uganda: 1) clean water; 2) Nakivubo Channel; 3) Ugandan Brewery Ltd. ....	69
Figure 3.1-3: Goyal Para pond sampling point in Santinkean, West Bengal (credit S. Balachandran). ....	75
Figure 3.1-4: Clean water site sampling point in Murchison Bay, Lake Victoria (credit O.I. Miria). ....	75
Figure 3.1-5: Nakivubo channel site sampling point in Murchison Bay, Lake Victoria (credit O.I. Miria). ....	76
Figure 3.1-6: Ugandan Brewery Ltd. site sampling point in Murchison Bay, Lake Victoria (credit O.I. Miria). ....	76
Figure 3.2-1: Addition of metal frame and net for the small crate growth trial (credit G. Nahar).....	80
Figure 3.2-2: Rain shelter over large tanks (Credit G. Nahar). ....	82
Figure 3.3-1: Temperature profile of the thermo-gravimetric analyser for proximate analysis.....	83
Figure 4.2-1: Water analysis of the Murchison Bay sites. Error bars represent the standard error of the mean due to the phenological variations at each site. a) heavy metals, 5 samples in duplicate; b) nitrogen compounds	

(NH<sub>4</sub>, NO<sub>3</sub> and TKN) and phosphate (PO<sub>4</sub>), 7 samples in duplicate; c) chemical oxygen demand (COD) and total suspended solids (TSS), 7 samples in duplicate..... 93

Figure 4.2-2: Map of the Indrayani and Mula rivers, demonstrating the flow of the river and the major sources of pollution. ● = sewage pollution locations; ● = industrial pollution locations; MIDC= Maharashtra Industrial Development Corporation; ⊗ = biomass and water collection locations. a) Indrayani River, Pimpri Chinchwad; b) Mula River, Pune..... 95

Figure 4.2-3: Water analysis of Pune and Pimpri Chinchwad sites. Error bars represent the standard error of the mean due to the phenological variations at each site. a) heavy metals, 3 samples in duplicate; b) nitrogen (TN and TKN), 2 samples in duplicate..... 96

Figure 4.2-4: Water analysis of West Bengal site. Error bars represent the standard error of the mean due to the phenological variations at each site, 6 samples in duplicate..... 96

Figure 4.2-5: Proximate (a) and ultimate (b) composition of whole water hyacinth and water lettuce samples for geographical and pollution analysis. Each sample was run in duplicate. .... 97

Figure 4.2-6: Inorganic composition of whole water hyacinth and water lettuce samples for geographical and pollution analysis. a) heavy metals; b) nutrients. Each sample was run in duplicate. .... 100

Figure 4.2-7: Proximate composition of water hyacinth tissue samples for geographical and pollution analysis. a) leaf; b) root; c) petiole. Each sample was run in duplicate; each of location was an average of all phenological samples: Maharashtra had 4 samples, West Bengal had 3 samples, Murchison Bay (Uganda) had 8 samples. .... 103

Figure 4.2-8: Ultimate composition of water hyacinth tissue samples for geographical and pollution analysis. a) leaf; b) root; c) petiole. Each sample was run in duplicate; each of location was an average of all phenological samples: Maharashtra had 4 samples, West Bengal had 3 samples, Murchison Bay (Uganda) had 8 samples. .... 104

Figure 4.2-9: Utilisation potential indicators of water hyacinth tissues for geographical and pollution analysis. Error bars represent the represent the variation due to the phenological variations at each site. a) maximum theoretical biomethane potential; b) C:N ratio; c) theoretical higher heating value; d) protein content. Each sample was run in duplicate; each of location was an average of all phenological samples: Maharashtra had 4 samples,

West Bengal had 3 samples, Murchison Bay (Uganda) had 8 samples. .....	105
Figure 4.2-10: Modified Gompertz model, depicting the experimental biomethane potential of water hyacinth tissues for geographical and pollution analysis. Error bars represent the represent the analysis variation. a) Indrayani Moshi, May 2021; b) Mula Baner, May 2021; c) Murchison Bay (Uganda) Clean Water, September 2019; Brown (Unpublished). $H_m$ = maximum biomethane yield; $R_m$ = peak biomethane production rate; $\lambda$ = lag phase. Each sample was run in duplicate.....	107
Figure 4.2-11: Averaged inorganic composition (heavy metals) of water hyacinth samples for geographical and pollution analysis. a) leaf; b) root; c) petiole. Each sample was run in duplicate; each of location was an average of all phenological samples: Maharashtra had 4 samples, West Bengal had 3 samples, Murchison Bay (Uganda) had 8 samples.....	109
Figure 4.2-12: Averaged inorganic composition (nutrients) of water hyacinth samples for geographical and pollution analysis. a) leaf; b) root; c) petiole. Each sample was run in duplicate; each of location was an average of all phenological samples: Maharashtra had 4 samples, West Bengal had 3 samples, Murchison Bay (Uganda) had 8 samples. ....	111
Figure 4.3-1: Average phenological variations of environmental conditions for Murchison Bay, Lake Victoria, Uganda. Error bars represent the variations over the selected period, of 1984-2021. a) average temperature at 2m; b) average solar irradiance (all sky surface shortwave downward irradiance); c) precipitation. Raw data was taken from NASA Prediction Of Worldwide Energy Resources [73].....	113
Figure 4.3-2: Phenological variations of water quality indicators for Murchison Bay, Lake Victoria, Uganda. Each sample was analysed in duplicate and averaged between the three sites (clean water, Navikubo Channel, Ugandan Brewery Ltd.). a) heavy metals; b) nitrogen and phosphorous; c) other. ....	114
Figure 4.3-3: Phenological changes of the average ash content in biomass from Murchison Bay, Lake Victoria, Uganda. Each sample was analysed in duplicate and averaged between the three sites; the error bars represent the standard deviations of these variations. *= extreme values. ....	115
Figure 4.3-4: Phenological changes of the heavy metal translocation factor in biomass from Murchison Bay, Lake Victoria, Uganda. Each sample was analysed in duplicate and averaged between the three sites; the error bars	

represent the standard deviations of these variations. a) non-essential; b) essential..... 116

Figure 4.3-5: Phenological changes of non-essential heavy metal content in biomass from Murchison Bay, Lake Victoria, Uganda. Each sample was analysed in duplicate and averaged between the three sites; the error bars represent the standard deviations of these variations. \*= extreme values. a) aluminium; b) cadmium; c) chromium; d) lead; e) titanium..... 118

Figure 4.3-6: Phenological changes of essential heavy metal content in biomass from Murchison Bay, Lake Victoria, Uganda. Each sample was analysed in duplicate and averaged between the three sites; the error bars represent the standard deviations of these variations. \*= extreme values. a) copper; b) iron; c) nickel; d) zinc..... 119

Figure 4.3-7: Phenological changes of the nutrient translocation factor in biomass from Murchison Bay, Lake Victoria, Uganda. Each sample was analysed in duplicate and averaged between the three sites. a) macro-nutrients; b) micro-nutrients. .... 120

Figure 4.3-8: Phenological changes of macro-nutrient content in biomass from Murchison Bay, Lake Victoria, Uganda. Each sample was analysed in duplicate and averaged between the three sites; the error bars represent the standard deviations of these variations. \*= extreme values. a) nitrogen; b) potassium; c) calcium; d) magnesium..... 121

Figure 4.3-9: Phenological changes of micro-nutrient content in biomass from Murchison Bay, Lake Victoria, Uganda. Each sample was analysed in duplicate and averaged between the three sites; the error bars represent the standard deviations of these variations. \*= extreme values. a) cobalt; b) molybdenum; c) sodium. .... 122

Figure 4.3-10: Phenological changes of utilisation potential indicators in biomass from Murchison Bay, Lake Victoria, Uganda. Each sample was analysed in duplicate and averaged between the three sites; the error bars represent the standard deviations of these variations. a) maximum theoretical biomethane potential and theoretical biomethane potential; b) C:N ratio; c) protein content; d) theoretical higher heating value. .... 123

Figure 4.3-11: Average phenological variations of environmental conditions for Pune, Maharashtra, India. Error bars represent the variations over the selected period, of 1984-2021. a) average temperature at 2m; b) average solar irradiance (all sky surface shortwave downward irradiance); c)

precipitation. Raw data was taken from NASA Prediction Of Worldwide Energy Resources [73].....	125
Figure 4.3-12: Phenological variations of water quality indicators for Pune, Maharashtra, India. Each sample was analysed in duplicate and averaged between the four sites (Indrayani Moshi, Indrayani Alandi, Mula Baner, Mula Sangvi). a) elemental; b) nitrogen. ....	126
Figure 4.3-13: Phenological changes in dry weight proportions of tissues in water hyacinth biomass from river sites in Pune, Maharashtra. a) Indrayani Moshi; b) Indrayani Alandi; c) Mula Baner; d) Mula Sangvi. ....	127
Figure 4.3-14: Water hyacinth coverage on 11/03/2021 from Maharashtra, India: a) Indrayani Moshi; b) Mula Baner; c) Indrayani Alandi; d) Mula Sangvi (credit G. Nahar). ....	127
Figure 4.3-15: Phenological changes of ash content in biomass from river sites in Pune, Maharashtra. Each sample was analysed in duplicate; the error bars represent the standard deviation of the replications. a) Indrayani Moshi; b) Indrayani Alandi; c) Mula Baner; d) Mula Sangvi. ....	128
Figure 4.3-16: Phenological changes of the heavy metal translocation factor in biomass from river sites in Pune, Maharashtra. Each sample was analysed in duplicate. a) Indrayani Moshi; b) Indrayani Alandi; c) Mula Baner; d) Mula Sangvi. i] non-essential; ii] essential.....	129
Figure 4.3-17: Phenological changes of non-essential heavy metal content in biomass from Maharashtra, India. Each sample was analysed in duplicate; the error bars represent the standard deviation of the replications. Error bars represent the variations. a) aluminium; b) cadmium; c) chromium; d) lead; e) titanium. ....	131
Figure 4.3-18: Phenological changes of essential heavy metal content in biomass from Maharashtra, India. Each sample was analysed in duplicate; the error bars represent the standard deviation of the replications. a) copper; b) iron; c) nickel; d) zinc. ....	132
Figure 4.3-19: Alandi, Indrayani River, Pimpri Chichwad, India on 20/01/2021 (credit G. Nahar).....	132
Figure 4.3-20: Water Hyacinth biomass from Alandi, Indrayani River on 20/01/2021 (credit G. Nahar). ....	133
Figure 4.3-21: Phenological changes of the nutrient translocation factor in biomass from river sites in Pune, Maharashtra. Each sample was analysed in	

duplicate. a) Indrayani Moshi; b) Indrayani Alandi; c) Mula Baner; d) Mula Sangvi. i] macro-nutrient; ii] micro-nutrient. ....	134
Figure 4.3-22: Phenological changes of the maximum average tissue macro-nutrient content in biomass from Pune, Maharashtra. Each sample was analysed in duplicate; the error bars represent the standard deviation of the replications. a) nitrogen (leaf); b) potassium (petiole); c) calcium (leaf); d) magnesium (root). ....	136
Figure 4.3-23: Phenological changes of the maximum average tissue micro-nutrient content in biomass from Pune, Maharashtra. Each sample was analysed in duplicate; the error bars represent the standard deviation of the replications. a) cobalt (Root); b) molybdenum (Root); c) sodium (Petiole). ....	137
Figure 4.3-24: Water hyacinth coverage on 01/02/2021 at Sangvi, Mula River, Pune, India (credit G. Nahar). ....	137
Figure 4.3-25: Phenological changes of the maximum theoretical biomethane potential and theoretical biomethane potential in biomass from river sites in Pune, Maharashtra. Each sample was analysed in duplicate; the error bars represent the standard deviation of the replications. a) Indrayani Moshi; b) Indrayani Alandi; c) Mula Baner; d) Mula Sangvi. ....	138
Figure 4.3-26: Phenological changes of the carbon to nitrogen ratio in biomass from river sites in Pune, Maharashtra. Each sample was analysed in duplicate; the error bars represent the standard deviation of the replications. a) Indrayani Moshi; b) Indrayani Alandi; c) Mula Baner; d) Mula Sangvi. .	139
Figure 4.3-27: Phenological changes of the protein concentration in biomass from river sites in Pune, Maharashtra. Each sample was analysed in duplicate; the error bars represent the standard deviation of the replications. a) Indrayani Moshi; b) Indrayani Alandi; c) Mula Baner; d) Mula Sangvi. .	140
Figure 4.3-28: Phenological changes of the higher heating value in biomass from river sites in Pune, Maharashtra. Each sample was analysed in duplicate; the error bars represent the standard deviation of the replications. a) Indrayani Moshi; b) Indrayani Alandi; c) Mula Baner; d) Mula Sangvi. .	141
Figure 4.3-29: Average phenological variations of environmental conditions for Goyal Para, West Bengal, India. Error bars represent the variations over the selected period, of 1984-2021. a) average temperature at 2m; b) average solar irradiance (all sky surface shortwave downward irradiance); c) precipitation. Raw data was taken from NASA Prediction Of Worldwide Energy Resources [73]. ....	142



Figure 4.3-30: Phenological variations of water quality indicators of Goyal Para, West Bengal, India. Each sample was analysed in duplicate. a) nitrogen (TKN), total suspended solids (TSS) and dissolved oxygen (DO); b) total dissolved solids (TDS). .....	143
Figure 4.3-31: Phenological changes in tissue weight proportion in water hyacinth biomass from Goyal Para, West Bengal, India. a) wet weight proportion; b) dry weight proportion; c) moisture content. ....	143
Figure 4.3-32: Phenological changes of ash content in biomass from Goyal Para, West Bengal. Each sample was analysed in duplicate; the error bars represent the standard deviation of the replications. ....	144
Figure 4.3-33: Phenological changes of the heavy metal and nutrient translocation factors in biomass from Goyal Para, West Bengal, India. Each sample was analysed in duplicate. a) i] non-essential heavy metals; a) ii] essential heavy metals; b) i] macro-nutrients; b) ii] micro-nutrients. ....	146
Figure 4.3-34: Phenological changes of non-essential heavy metal content in biomass from Goyal Para, West Bengal, India. Each sample was analysed in duplicate; the error bars represent the standard deviation of the replications. a) aluminium; b) cadmium; c) chromium; d) lead; e) titanium. ....	147
Figure 4.3-35: Phenological changes of essential heavy metal content in biomass from Goyal Para, West Bengal, India. Each sample was analysed in duplicate; the error bars represent the standard deviation of the replications. a) copper; b) iron; c) nickel; d) zinc. ....	148
Figure 4.3-36: Phenological changes of the macro-nutrient content in biomass from Goyal Para, West Bengal, India. Each sample was analysed in duplicate; the error bars represent the standard deviation of the replications. a) nitrogen; b) potassium; c) calcium; d) magnesium. ....	149
Figure 4.3-37: Phenological changes of the micro-nutrient content in biomass from Goyal Para, West Bengal, India. Each sample was analysed in duplicate; the error bars represent the standard deviation of the replications. a) cobalt; b) molybdenum; c) sodium. ....	150
Figure 4.3-38: Phenological changes of utilisation potential indicators in biomass from Goyal Para, West Bengal, India. Each sample was analysed in duplicate; the error bars represent the standard deviation of the replications. a) maximum theoretical biomethane potential; b) C:N ratio; c) protein content; d) theoretical higher heating value.....	151

Figure 5.2-1: Absolute growth rate, of trial 1, 2 and 5, against starting water nitrogen concentration, with cow manure as the sole nutrient source. The error bars represent the standard deviation of the replications.....	160
Figure 5.2-2: Linear regression for absolute growth rate against starting water nitrogen concentration for small crate trials. The error bars represent the standard deviation of the replications.....	161
Figure 5.3-1: Average nitrogen solubilisation in small- and large-scale trials, from various nutrient sources. The error bars represent the standard deviation of the replications.....	163
Figure 5.3-2: Absolute growth rate of nutrient source, trial three, against starting water nitrogen concentration, overlaid with LitFit and TrialFit. The error bars represent the standard deviation of the replications. ....	164
Figure 5.3-3: Absolute growth rate against starting water nitrogen concentration for the nutrient source small crate trials, overlaid with LitFit and TrialFit. The error bars represent the standard deviation of the replications. ....	165
Figure 5.4-1: Absolute growth rate against starting water nitrogen concentration for the $N_0$ trials, overlaid with large tanks trials, LitFit and TrialFit. The error bars represent the standard deviation of the replications. ■= control; ●= 6.35 kg tank; ▲ = 12.7 kg tank; all black symbols= small crate trials. ....	167
Figure 5.4-2: Absolute growth rate against starting water nitrogen concentration for the FCM and CM large tank trial, overlaid with LitFit and TrialFit. The error bars represent the standard deviation of the replications.....	168
Figure 5.4-3: Absolute growth rate against starting water nitrogen concentration for the digestate and CM large tank trial, overlaid with LitFit and TrialFit. The error bars represent the standard deviation of the replications. ....	168
Figure 5.5-1: Change in leaf tissue nitrogen and protein content with respect to time for the variable cow manure trial. The error bars represent the standard deviation of the replications. a) nitrogen; b) protein. ....	170
Figure 5.5-2: Leaf and whole plant nitrogen concentration and starting water nitrogen concentration for digestate and filtered cow manure large tank trials. The error bars represent the standard deviation of the replications. a) filtered cow manure trial; b) digestate trial.....	171
Figure 5.5-3: Biomethane potential and starting water nitrogen concentration for digestate and filtered cow manure large tank trials. The error bars represent the standard deviation of the replications. a) filtered cow manure trial; b) digestate trial. ....	172

Figure 5.6-1: Solar irradiance inside and outside of the rain shelter from 15/06-09/07/2021. a) 1000; b) 1200; c) 1500; d) 1800. ....	173
Figure 5.6-2: Environmental conditions data for phenological study trials- a) solar irradiance; b) air temperature at 2m. Raw data was taken from NASA Prediction Of Worldwide Energy Resources [73]......	175
Figure 5.6-3: Weight changes over time for control tanks in the large tank phenological trials. The error bars represent the standard deviation of the replications. ....	176
Figure 5.6-4: Weight changes over time for fertilised tanks in the large tank phenological trials. The error bars represent the standard deviation of the replications.....	177
Figure 5.6-5: Changes in experimental and calculated density ( $P$ ) and residual sum of squares (RSS) for an example of logistic growth model fit for large scale winter trial control tank 1. ....	178
Figure 5.6-6: Residual sum of squares (RSS) for intrinsic growth rate of the phenological study large tank trial with a carrying capacity of 640 and 2,569 g DW/ m <sup>2</sup> . The error bars represent the standard deviation of the replications. a) control; b) fertilised.....	180
Figure 5.6-7: Change in total residual sum of squares (RSS) for logistic growth model by varying carrying capacity ( $k$ )......	180
Figure 5.6-8: Change in total residual sum of squares (RSS) for logistic growth model for the control and fertilised tanks by varying carrying capacity ( $k$ )......	181
Figure 5.6-9: Change in total residual sum of squares (RSS) for logistic growth model for the low and high nitrogen dosed tanks by varying carrying capacity ( $k$ ). ....	181
Figure 5.6-10: Change in intrinsic growth rate ( $r$ ) for logistic growth model for the control and fertilised tanks by varying carrying capacity ( $k$ ). a) control tanks; b) fertilised tanks. ....	182
Figure 5.6-11: Change in fresh weight intrinsic growth rate ( $r$ ) and starting water nitrogen concentration ( $N_0$ ) for phenological study in large tank trial. The error bars represent the standard deviation of the replications. ....	183
Figure 5.6-12: Change in fresh weight intrinsic growth rate ( $r$ ), normalised for starting water concentration ( $N_0$ ) in the phenological study large tank trial. x-error represents variation across the whole study; y-error represents replicate variation. a) temperature; b) solar irradiance.....	184

Figure 5.6-13: Changes in final protein content for the whole plant and leaf, and starting water nitrogen concentration ( $N_0$ ) in the phenological study large tank trial. The error bars represent the standard deviation of the replications. a) control tanks; b) fertilised tanks.....	185
Figure 5.6-14: Changes in theoretical biomethane potential ( $BMP_{th}$ ) and starting water nitrogen concentration ( $N_0$ ) in the phenological study large tank trial. The error bars represent the standard deviation of the replications. a) control tanks; b) fertilised tanks.....	186
Figure 5.6-15: Modified Gompertz model, depicting the experimental biomethane potential of whole water hyacinth plants from seasonal large-scale cultivation analysis. Error bars represent the represent the analysis variation. $H_m$ = maximum biomethane yield; $R_m$ = peak biomethane production rate; $\lambda$ = lag phase. Each sample was run in duplicate.....	186
Figure 6.2-1: Comparison of plant parts of water hyacinth from Lake Victoria from January 2020, a) biochemical composition; b) protein content. Error bars demonstrate the replicate variation.....	191
Figure 6.2-2: Comparison of plant parts of water hyacinth from Maharashtra rivers from June 2019, a) biochemical composition; b) protein content. Error bars demonstrate the replicate variation.....	191
Figure 6.2-3: Comparison of water hyacinth whole biomass; from Murchison Bay (Dec 2018), West Bengal (June 2019), Mula Baner (June 2019) and water lettuce from Indrayani Moshi (June 2019). Error bars demonstrate the replicate variation. ....	192
Figure 6.2-4: Comparison of alkali acid extraction from water hyacinth plant tissues, from Indrayani Moshi Jun-19- a) precipitate weight; b) protein recovery; c) protein content and increase compared with raw biomass; d) ash content. Error bars demonstrate the replicate variation. ....	195
Figure 6.2-5: Comparison between whole plant and leaf precipitates at 40°C/1.0M/150 minutes, a) difference in precipitate weight; b) protein content; c) protein recovery. Error bars demonstrate the replicate variation. ....	196
Figure 6.2-6: Comparison of alkali acid extraction from a variety of locations at 40°C/1.0M/150 minutes, a) precipitate weight; b) protein content; c) protein recovery. Error bars demonstrate the replicate variation.....	198
Figure 6.2-7: Example of a linear fit of a biochemical component plotted against a alkali acid extraction result- lignin and precipitate weight. Error bars demonstrate the replicate variation.....	199

Figure 6.2-8: Comparison of alkali acid extraction from wet and dry samples from an IBERS heavy metal spiked small-crate trial at 40°C/1.0M/150 minutes, a) precipitate weight; b) protein content; c) protein recovery. Error bars demonstrate the replicate variation. ....	201
Figure 6.2-9: Trace elemental composition of raw water hyacinth tissues and protein extract from Indrayani Moshi Jun-19, utilising alkali acid extraction at 40°C/1.0M/150 minutes- a) low concentration elements; b) high concentration elements. ....	203
Figure 6.2-10: Elemental composition of raw biomass, residue from alkali extraction and protein precipitate from acid precipitation for whole water lettuce plant, cultivated water hyacinth whole plant and leaf sample- a) low concentration elements; b) high concentration elements. ....	204
Figure 6.2-11: Trace elemental comparison of raw biomass and residue from alkali acid extraction on cultivated Pune Jun-21 whole plant and leaf samples at 40°C/1.0M/150 minutes. ....	208
Figure 6.2-12: Experimental bio-methane potential of raw biomass and residue from alkali acid extraction on cultivated water hyacinth Pune Jun-21 whole plant and leaf samples at 40°C/1.0M/150 minutes. Error bars demonstrate the replicate variation. ....	208
Figure 6.3-1: Composition of water lettuce reference material for alkali acid extraction and comparative water hyacinth samples- a) heavy metals; b) nutrients. ....	210
Figure 6.3-2: The effect of extraction time on the precipitate weight from water lettuce utilising alkali acid extraction (☆ - maximum value for condition with data label). Error bars demonstrate the replicate variation. ....	212
Figure 6.3-3: The effect of extraction time on the protein concentration from water lettuce utilising alkali acid extraction (☆ - maximum value for condition with data label). Error bars demonstrate the replicate variation. ....	213
Figure 6.3-4: The effect of extraction time on the protein recovery from water lettuce utilising alkali acid extraction (☆ - maximum value for condition with data label). Error bars demonstrate the replicate variation. ....	214
Figure 6.3-5: The effect of extraction time on the ash content from water lettuce utilising alkali acid extraction (☆ - minimum value for condition with data label). Error bars demonstrate the replicate variation. ....	214

Figure 6.3-6: The effect of temperature on the precipitate weight from water lettuce utilising alkali acid extraction. Error bars demonstrate the replicate variation. a) 0.1M NaOH; b) 1.0M NaOH.....	216
Figure 6.3-7: Percentage relative difference (calculated via Equation 6-4) between precipitate of each condition, with respect to extraction time, for alkali acid extraction. Error bars demonstrate the replicate variation. a) 0.1 M NaOH; b) 1.0 M NaOH. ....	217
Figure 6.3-8: The effect of temperature on the protein content of protein precipitate from water lettuce utilising alkali acid extraction. Error bars demonstrate the replicate variation. a) 0.1M NaOH; b) 1.0M NaOH.....	218
Figure 6.3-9: The effect of temperature on the protein recovery from water lettuce utilising alkali acid extraction. Error bars demonstrate the replicate variation. a) 0.1M NaOH; b) 1.0M NaOH.....	219
Figure 6.3-10: The effect of temperature on the ash content from water lettuce utilising alkali acid extraction. Error bars demonstrate the replicate variation. a) 0.1M NaOH; b) 1.0M NaOH. ....	220
Figure 6.3-11: The effect of temperature on the total ash weight from water lettuce utilising alkali acid extraction. Error bars demonstrate the replicate variation. a) 0.1M NaOH; b) 1.0M NaOH.....	221
Figure 6.3-12: The effect of alkali concentration on the precipitate weight from water lettuce utilising alkali acid extraction. Error bars demonstrate the replicate variation. a) 40°C; b) 65°C c) 90°C.....	222
Figure 6.3-13: Percentage relative difference (calculated via Equation 6-4) between precipitate of 0.1 and 1.0 M of NaOH, with respect to extraction time. a= 0.1 M NaOH; b= 1.0 M NaOH. Error bars demonstrate the replicate variation. ....	223
Figure 6.3-14: The effect of alkali concentration on the protein concentration of the protein precipitate from water lettuce utilising alkali acid extraction. Error bars demonstrate the replicate variation. a) 40°C; b) 65°C c) 90°C. ....	224
Figure 6.3-15: The effect of alkali concentration on the protein recovery from water lettuce utilising alkali acid extraction. Error bars demonstrate the replicate variation. a) 40°C; b) 65°C c) 90°C.....	225
Figure 6.3-16: The effect of alkali concentration on the percentage ash content of protein precipitate from water lettuce utilising alkali acid extraction. Error bars demonstrate the replicate variation. a) 40°C; b) 65°C c) 90°C. ....	226

Figure 6.3-17: Elemental composition of precipitate from water lettuce utilising alkali acid extraction at a variety of conditions- temperature (°C) / alkali concentration (M) time (minutes). a) low concentration elements; b) high concentration elements.....	228
Figure 6.3-18: Trace elemental comparison of raw biomass and residue from alkali acid extraction on cultivated water lettuce at 40°C/1.0M/150 minutes. low concentration elements; b) high concentration elements.....	230
Figure 6.3-19: Experimental bio-methane potential of raw biomass and residue from alkali acid extraction on water lettuce at 40°C/1.0M/150 minutes. Error bars demonstrate the replicate variation. ....	230
Figure 6.3-20: The effect of washing on elemental composition of precipitate from water lettuce utilising alkali acid extraction - a) low concentration elements; b) high concentration elements. ....	232
Figure 6.3-21: The impact of changing the precipitation pH. Error bars demonstrate the replicate variation. a) precipitate weight; b) protein content; c) protein recovery.....	233
Figure 6.3-22: The impact of changing the precipitation pH. Error bars demonstrate the replicate variation. a) precipitate weight; b) protein content; c) protein recovery.....	234
Figure 7.2-1: Process flow of water hyacinth biorefinery, utilising wild harvested, dried and shredded biomass to produce biogas via anaerobic digestion. Green= raw plant biomass; blue= end product.....	238
Figure 7.2-2: Process flow of water hyacinth biorefinery, utilising wild harvested, dried and shredded biomass to produce protein extract and biogas via alkali acid extraction and anaerobic digestion. Green= raw biomass; grey= interim product; blue= end product; orange= potential waste; broken line= potential flow.....	240
Figure 7.2-3: Process flow of water hyacinth biorefinery, utilising wild harvested, dried and shredded biomass to produce biogas via anaerobic digestion. Green= raw biomass; grey= interim product; blue= end product; dark blue= external product. a) scenario cultivated anaerobic digestion; b) scenario cultivated cow manure; c) scenario cultivated co-digestion...	241
Figure 7.2-4: Process flow of water hyacinth biorefinery, utilising wild harvested, dried and shredded biomass to produce biogas via anaerobic digestion. Green= raw biomass; blue= end product; brown= external nutrient source; dark blue= external product; broken line= potential flow. a)	

scenario cultivated domestic wastewater anaerobic digestion; b) scenario cultivated domestic wastewater ruminant feed; c) scenario cultivated domestic wastewater co-digestion.....	242
Figure 7.4-1: Phenological assumptions for biomass availability in Murchison Bay, Lake Victoria.....	248
Figure 7.4-2: Estimated biomass density in a Pune river.....	250
Figure 7.4-3: Time required for different numbers of harvesters to clear Indrayani River of water hyacinth, from Moshi to Alandi.....	253
Figure 7.4-4: Distribution of annual costs for scenario wild anaerobic digestion. ....	258
Figure 7.4-5: Distribution of annual costs for scenario wild alkali acid scenario. a) wet feedstock; b) dry feedstock. ....	265
Figure 7.5-1: Quantity of digestate produced and required by a farm pond cultivating water hyacinth for anaerobic digestion. ....	269
Figure 7.5-2: Payback period for each liquid petroleum gas replacement scenario, where digestate is utilised by the user. Error bars demonstrate the impact on economic performance based on variations in feedstock methane yield. ....	274
Figure B.1-1: Phenological variations of heavy metal water concentration of Murchison Bay, Lake Victoria, Uganda. a) clean water; b) Nakivubo channel; c) Ugandan Brewery Ltd. ....	318
Figure B.1-2: Phenological variations of nitrogen and phosphorus concentration of Murchison Bay, Lake Victoria, Uganda. a) clean water; b) Nakivubo channel; c) Ugandan Brewery Ltd. ....	319
Figure B.1-3: Phenological variations of chemical oxygen demand and total suspended solids concentration of Murchison Bay, Lake Victoria, Uganda. a) clean water; b) Nakivubo channel; c) Ugandan Brewery Ltd.....	320
Figure B.1-4: Phenological variations of water quality indicators of Pune, Maharashtra, India. a) Indrayani Moshi; b) Indrayani Alandi; c) Mula Baner; d) Mula Sangvi).....	320
Figure B.2-1: Minimum and maximum inorganic composition (heavy metals) of water hyacinth samples for geographical and pollution analysis. a) leaf; b) root; c) petiole. ....	321



# List of plates

The Plate label has been utilised to denote photographs taken by the author.

Plate 1.3-1: Water hyacinth flower from Pune, India (May 2019).....	4
Plate 2.1-1: Water hyacinth flower from Pune, India (May 2019).....	8
Plate 2.1-2: Cross section of a water hyacinth float from Pawana River, Pune, India (April 2019). .....	14
Plate 2.1-3: Water hyacinth, with daughter plant, from Pawana River, Pune, India (April 2019). .....	15
Plate 2.4-1: Mature water lettuce plants from Pawana River, India, May 2019. a) Leaf rosette; b) Feathery hanging roots .....	55
Plate 3.1-1: Shredded whole water hyacinth plants.....	70
Plate 3.1-2: Water hyacinth whole with indication of tissues. ....	70
Plate 3.1-3: Shredded water hyacinth tissues: a) leaf; b) petiole (including float); c) root. .....	70
Plate 3.1-4: Water lettuce whole plant with indication of the tissues.....	71
Plate 3.1-5: Indrayani River sampling points, Pimpri-Chinchwad. a) Moshi (May 2019); b) Alandi (March 2022).....	72
Plate 3.1-6: Water hyacinth from Indrayani River, Pimpri Chinchwad (May 2019).....	72
Plate 3.1-7: Mula River sampling points, Pune. a) Baner (May 2019); b) Sangvi (March 2021). .....	73
Plate 3.1-8: Water hyacinth from Mula Mudtha River, Pune (May 2019). .....	74
Plate 3.1-9: Cultivation of water hyacinth at the Institute of biological, environmental and rural sciences glasshouses (June 2021). .....	77
Plate 3.2-1: Small crate growth trial set up in March 2020. ....	80
Plate 3.2-2: Large tank with net and pulley system (February 2020). .....	81
Plate 3.2-3: Weighing water hyacinth mat in large tank with net and pulley system (February 2020). .....	81
Plate 5.3-1: Evidence of the increased viscosity and surface tension from high dose cow manure trials. a) 4 kg b) 8 kg c) 12 kg.....	166
Plate 6.3-1: Product formed in the thermo-gravimetric analysis crucible at 900°C.....	227

# List of tables

Table 2.1-1: Changes biochemical composition of water hyacinth by location (% of dry weight). .....	12
Table 2.1-2: Biochemical analysis of water hyacinth tissues (% dry weight). .....	16
Table 2.1-3: Changes in trace element concentration water hyacinth roots by location (ppm, dry weight). .....	17
Table 2.1-4: Nutrient variation in water hyacinth tissues. ....	18
Table 2.2-1: Water hyacinth biomass density. ....	27
Table 2.3-1: Average heavy metal concentrations for water hyacinth below and above water tissues, from studies in Table 2.3-2. ....	34
Table 2.3-2: Heavy metal removal by water hyacinth. ....	36
Table 2.3-3: Average higher heating value of various biomass, adapted from [174]. ....	46
Table 2.3-4: Amino acid profile of water hyacinth protein and pea protein, displayed as concentration in the protein extract (%). ....	54
Table 2.4-1: Composition variations for water lettuce. ....	56
Table 2.5-1: Cornell net carbohydrate and protein system [263–265]. ....	63
Table 3.1-1: Water hyacinth sample collection locations. ....	69
Table 3.5-1: Equations for theoretical higher heating value estimation. ....	90
Table 3.5-2: Sample types for bomb calorimetry. ....	90
Table 3.5-3: Higher heating value results from bomb calorimetry and various theoretical higher heating value equations. ....	90
Table 4.2-1: Utilisation potential indicators of whole water hyacinth and water lettuce samples for geographical and pollution analysis. ....	99
Table 4.2-2: Water hyacinth collection sites included in the geographical and pollution study. ....	102
Table 4.2-3: Biomethane potential and biodegradability index of water hyacinth biomass for geographical and pollution study. ....	106
Table 4.4-1: Range of composition and utilisation potential indicator values for water hyacinth biomass from Murchison Bay, Maharashtra and West Bengal. ....	152
Table 5.2-1: Nitrogen solubilisation in cow manure growth trials. ....	159
Table 5.3-1: Nutrient source growth trials. ....	162
Table 5.3-2: Nitrogen solubilisation in nutrient source growth trials. ....	163

Table 5.3-3: Comparison of growth yields for different cultivated biomasses. ....	166
Table 5.6-1: Impact of rain shelter on absolute growth rate in large tank trials. ....	172
Table 5.6-2: Environmental conditions and starting water nitrogen concentration for phenological study trials. ....	175
Table 5.6-3: Intrinsic growth rate of the phenological study large tank trial with a carrying capacity of 640 kg DW/ m <sup>2</sup> . ....	179
Table 5.6-4: Intrinsic growth rate of the phenological study large tank trial with a carrying capacity of 2,569 kg DW/ m <sup>2</sup> . ....	179
Table 5.6-5: Intrinsic growth rate of the phenological study large tank trial with a carrying capacity of 1000 g DW/ m <sup>2</sup> . ....	183
Table 6.2-1: Samples for alkali acid extraction. ....	193
Table 6.2-2: Statistical analysis of the relationship between biochemical components and alkali acid extraction outputs for whole plants (Indrayani Mosh Jun-19 <i>Pistia stratiotes</i> ; West Bengal Jan-20; and Murchison Bay Dec-18). ....	199
Table 6.2-3: Statistical analysis of the relationship between biochemical components and alkali acid extraction outputs for water hyacinth parts and whole plants (Indrayani Moshi Jun-19 <i>Pistia stratiotes</i> ; West Bengal Jan-20; Murchison Bay Dec-18; leaf, root and petiole Indrayani Moshi Jun-19). ....	200
Table 6.2-4: Recommended daily allowance of various trace elements and protein compared with protein precipitate, from cultivated Pune leaf Jun-21; a commercial vegan multivitamin; and a commercial pea protein. ....	205
Table 6.2-5: Trace nutrient and protein composition of water hyacinth precipitate, from cultivated Pune leaf Jun-21, in comparison with Indian soybean meal. ....	206
Table 6.2-6: Comparison of the composition of raw biomass and residue from alkali acid extraction on cultivated Pune Jun-21 whole plant and leaf samples at 40°C/1.0M/150 minutes. ....	207
Table 6.3-1: Composition of water lettuce reference material for alkali acid extraction and comparative water hyacinth samples. ....	210
Table 6.3-2: Percentage change in precipitate weight with respect to extraction time. ....	212
Table 6.3-3: Percentage change in protein content of precipitate with respect to extraction time. ....	213

Table 6.3-4: Composition of raw biomass and residue from alkali acid extraction on water lettuce at 40°C/1.0m/150 minutes.....	229
Table 6.3-5: Analysis of protein precipitate after washing in comparison to reference and raw biomass. ....	231
Table 7.3-1: Quotes for heavy duty excavator for use in Pune, India.....	243
Table 7.3-2: Quotes for heavy duty excavator for use in Kampala, Uganda. ....	243
Table 7.3-3: Anaerobic digester unit and associated equipment costs. ....	244
Table 7.3-4: Deenbandhu fixed dome digesters costs.....	244
Table 7.3-5: Bioreactor unit and associated equipment costs. ....	245
Table 7.3-6: Maintenance cost of biorefinery equipment in Kampala and Pune. ....	245
Table 7.3-7: Electricity cost in Uganda [382]. ....	246
Table 7.3-8: Labour costs for skilled and unskilled workers in India and Uganda. ....	246
Table 7.3-9: Cost of chemicals for biorefinery in India and Uganda.....	247
Table 7.4-1: Biomass composition range from Murchison Bay, Lake Victoria.....	249
Table 7.4-2: Cu, Ni, Pb, Ti and Zn concentration range from Murchison Bay, Lake Victoria.....	249
Table 7.4-3: Biomass composition range from Pune Rivers, May 2021.....	251
Table 7.4-4: Cu, Ni, Pb, Ti and Zn concentration range from Pune Rivers, May 2021. ....	251
Table 7.4-5: Harvestable biomass from Murchison Bay, Lake Victoria. ....	251
Table 7.4-6: Biomethane potential of wild harvested water hyacinth biomass parts in Murchison Bay, Lake Victoria. ....	254
Table 7.4-7: Digestate quantity and nutrient content from anaerobic digestion of water hyacinth from biomass in Murchison Bay, Lake Victoria. ....	255
Table 7.4-8: Mass, biomethane production and digestate quantity and nutrient content from anaerobic digestion of water hyacinth leaf and petiole from Murchison Bay, Lake Victoria. ....	255
Table 7.4-9: Biomethane potential of wild harvested water hyacinth biomass and plant parts in Pune, India. ....	256
Table 7.4-10: Mass and digestate quantity and nutrient content from anaerobic digestion of water hyacinth from biomass in Pune, India. ....	256
Table 7.4-11: Mass, biomethane production and digestate quantity and nutrient content from anaerobic digestion of water hyacinth leaf and petiole from Pune, India.....	257

Table 7.4-12: Capital costs, annual costs, income and payback time of the scenario wild anaerobic digestion based in Kampala and Pune. ....	258
Table 7.4-13: Protein production of wild harvested water hyacinth whole plant and leaf in Murchison Bay, Lake Victoria. ....	259
Table 7.4-14: Mass and nutrient flow for protein precipitation from water hyacinth whole plant from Murchison Bay, Lake Victoria. ....	259
Table 7.4-15: Mass and nutrient flow for protein precipitation from water hyacinth leaf from Murchison Bay, Lake Victoria. ....	260
Table 7.4-16: Biomethane potential of four scenarios containing water hyacinth biomass parts from Murchison Bay, Lake Victoria. ....	261
Table 7.4-17: Mass and nutrient content of digestate and raw biomass from four scenarios, in Murchison Bay, Lake Victoria. ....	261
Table 7.4-18: Protein production of wild harvested water hyacinth whole plant and leaf in Pune, India. ....	262
Table 7.4-19: Mass and nutrient flow for protein precipitation from water hyacinth whole plant from Pune, India. ....	262
Table 7.4-20: Mass and nutrient flow for protein precipitation from water hyacinth leaf from Pune, India. ....	263
Table 7.4-21: Biomethane potential of four scenarios containing water hyacinth biomass parts from Pune, India. ....	263
Table 7.4-22: Mass and nutrient content of raw biomass compared with digestate from four scenarios, in Pune, India. ....	264
Table 7.4-23: Reduction in nutrient content of digestate, as compared with cow manure [138]. ....	264
Table 7.4-24: Capital costs, annual costs, income and payback time of the scenario wild alkali acid extraction based in Kampala and Pune. ....	265
Table 7.5-1: Intrinsic growth rate and final harvest yield. ....	267
Table 7.5-2: Biomass composition range for large tank cultivated biomass. ....	268
Table 7.5-3: Cu, Ni, Pb, Ti and Zn concentration range for large tank cultivated biomass. ....	268
Table 7.5-4: Biomethane potential of wild harvested water hyacinth biomass cultivated in Pune, India. ....	270
Table 7.5-5: Digestate quantity and nutrient content from anaerobic digestion of water hyacinth from biomass cultivated in India. ....	270

Table 7.5-6: Surplus water hyacinth and cow manure after cultivation and diet supplementation, based on the cultivation area and requirements of the cattle. ....	271
Table 7.5-7: Area and digestate required for water hyacinth cultivation to fulfil requirements of co-digestion with cow manure.....	272
Table 7.5-8: Scenarios considered for liquid petroleum gas consumption and methane requirement to meet demand. ....	273
Table 7.5-9: Daily inventory of water hyacinth, cow manure and water for digester operation.....	273
Table 7.5-10: Subsidised installation costs, material costs and value of liquid petroleum gas offset. ....	273
Table A-1: List of Countries for the Global Distribution of Water Hyacinth.....	317
Table C-1: Composition of cow manure, from small crate nutrient Trial 1 via ICP-OES, vs. Hoagland’s solution. ....	322

# List of equations

Equation 2-1: Translocation factor. ....	20
Equation 2-2: Bioconcentration factor. ....	21
Equation 3-1: Hydrogen correction for moisture content. ....	83
Equation 3-2: Calculation of oxygen-content, by difference, on an as received basis..	84
Equation 3-3: Calculation of cellulose. ....	85
Equation 3-4: Calculation of hemicellulose.....	85
Equation 3-5: Calculation of lignin.....	85
Equation 3-6: Boyle's equation for theoretical biomethane potential [301]. ....	87
Equation 3-7: Calculation of experimental biomethane potential. ....	88
Equation 3-8: Modified Gompertz model.....	88
Equation 3-9: Calculation of anaerobic biodegradability index. ....	89
Equation 3-10: Modified Buswell and Neave equation for theoretical conversion of organics to methane and carbon dioxide.....	89
Equation 5-1: Specific growth rate as a factor of temperature [80]. ....	174
Equation 5-2: Changes in weight by time as a function of specific growth rate [80]...	174
Equation 5-3: Logistic growth model [81]. ....	177
Equation 5-4: Ratio between intrinsic growth rate of control and fertilised large tanks. .....	183
Equation 5-5: Intrinsic growth rate normalised for starting water nitrogen concentration. .....	184
Equation 5-6: Ratio between intrinsic growth rate of control and fertilised large tanks, utilising higher starting water nitrogen concentration for the monsoon trial.....	184
Equation 6-1: Protein weight in precipitate. ....	213
Equation 6-2: Protein recovery percentage. ....	214
Equation 6-3: Relative difference between precipitate weights, under conditions a and b, at time t. ....	216
Equation 6-4: Percentage relative difference between precipitate weight at time t. ...	216
Equation 6-5: Ash weight at time t. ....	219
Equation 7-1: Final growth rate calculated utisiling normalised growth rate for nitrogen content.....	267

# Abbreviations & nomenclature

<b>AAE</b>	Alkali acid extraction
<b>AAS</b>	Atomic absorption spectroscopy
<b>AD</b>	Anaerobic digestion
<b>ADF</b>	Acid detergent fibre
<b>ADL</b>	Acid detergent lignin
<b>AGR</b>	Absolute growth rate
<b>AMD</b>	Acid mine drainage
<b>AMPTS</b>	Automatic methane potential test system
<b>AN</b>	Ammoniacal nitrogen
<b>aNDF</b>	Amylase treated-neutral detergent fibre
<b>ANOVA</b>	Analysis of variance
<b>APHA</b>	Animal and Plant Health Agency
<b>Ash%<sub>t</sub></b>	Percentage ash content at time t
<b>Ash<sub>t</sub></b>	Ash weight at time t
<b>BCF</b>	Bioconcentration factor
<b>BDL</b>	Below detectable limits
<b>BI</b>	Biodegradability index
<b>BM</b>	Buffalo manure
<b>BMP</b>	Biomethane potential
<b>BMP<sub>ex</sub></b>	Experimental biomethane potential
<b>BMP<sub>th</sub></b>	Actual theoretical biomethane potential
<b>BOD</b>	Biological oxygen demand
<b>C-AD</b>	Scenario cultivated anaerobic digestion
<b>C-CM</b>	Scenario cultivated cow manure
<b>C-CoD</b>	Scenario cultivated co-digestion
<b>C-DoAD</b>	Scenario cultivated domestic wastewater anaerobic digestion
<b>C-DoCo</b>	Scenario cultivated domestic wastewater co-digestion
<b>C-DoRF</b>	Scenario cultivated domestic wastewater ruminant feed
<b>CFW</b>	Cooked food waste
<b>CH<sub>4</sub></b>	Methane
<b>CM</b>	Cow manure
<b>CN</b>	End harvest tissue nitrogen content
<b>CN</b>	Plant nitrogen concentration
<b>CNCPS</b>	Cornell net carbohydrate and protein system
<b>CO<sub>2</sub></b>	Carbon dioxide
<b>COD</b>	Chemical oxygen demand
<b>CREEC</b>	Centre for research in energy and energy conservation
<b>C<sub>t</sub></b>	Tissue nitrogen content with respect to time
<b>CuSO<sub>4</sub>.5H<sub>2</sub>O</b>	Copper sulphate



<b>CW</b>	Clean water
<b>DB</b>	Dry basis
<b>DM</b>	Dry matter
<b>DO</b>	Dissolved oxygen
<b>DR</b>	Defiant Renewables Ltd.
<b>DSC</b>	Differential scanning calorimetry
<b>DuW</b>	Duckweed
<b>DW</b>	Dry weight
<b>EC</b>	Electrical conductivity
<b>ETP</b>	Extractable true protein
<b>EUR</b>	Euro
<b>FC</b>	Fixed carbon
<b>FCM</b>	Filtered cow manure
<b>FeSO<sub>4</sub>.7H<sub>2</sub>O</b>	Iron sulphate
<b>FW</b>	Fresh weight
<b>GHG</b>	Greenhouse gas
<b>GP</b>	Goyal Para
<b>GPS</b>	Global positioning system
<b>H<sub>2</sub>O</b>	Water
<b>H<sub>2</sub>SO<sub>4</sub></b>	Sulphuric acid
<b>HCl</b>	Hydrochloric acid
<b>HHV</b>	Higher heating value
<b>HHV<sub>ex</sub></b>	Experimental higher heating value
<b>HHV<sub>th</sub></b>	Theoretical higher heating value
<b>HM</b>	Heavy metal
<b>H<sub>m</sub></b>	Peak experimental biomethane potential
<b>HTC</b>	Hydrothermal carbonisation
<b>HTL</b>	Hydrothermal liquefaction
<b>IBERS</b>	Institute of biological, environmental and rural sciences
<b>ICP-MS</b>	Inductively coupled mass spectrometry
<b>ICP-OES</b>	Inductively coupled optical emission spectroscopy
<b>INR</b>	Indian rupee
<b><i>k</i></b>	Carrying capacity
<b>KOH</b>	Potassium hydroxide
<b>LAI</b>	Leaf area index
<b>LD<sub>50</sub></b>	Median lethal dose
<b>LPG</b>	Liquid petroleum gas
<b>MAE</b>	Microwave-assisted extraction
<b>Maximum BMP<sub>th</sub></b>	Maximum theoretical biomethane potential
<b>MIDC</b>	Maharashtra Industrial Development Corporation
<b>MPCB</b>	Maharashtra Pollution Control Board
<b>MPL</b>	Maximum permissible limits

<b><math>N_0</math></b>	Starting water nitrogen concentration
<b>NaCl</b>	Sodium chloride
<b>NaHCO<sub>3</sub></b>	Sodium biocarbonate
<b>NaOH</b>	Sodium hydroxide
<b>NC</b>	Nakivubo Channel
<b>ND</b>	No data
<b>NH<sub>3</sub></b>	Ammonia
<b>NH<sub>4</sub><sup>+</sup></b>	Ammonium
<b>NO<sub>2</sub><sup>-</sup></b>	Nitrite
<b>NO<sub>3</sub></b>	Nitrate
<b><math>N_t</math></b>	Change in water nitrogen concentration over time
<b><math>N_{th}</math></b>	Starting theoretical water nitrogen concentration
<b>OM</b>	Organic matter
<b><math>P</math></b>	Density
<b>Pb(NO<sub>3</sub>)<sub>2</sub></b>	Lead nitrate
<b><math>P_N</math></b>	Leaf nitrogen concentration
<b>PO<sub>4</sub></b>	Phosphate
<b>PR</b>	Pearson's r value
<b><math>r</math></b>	Intrinsic growth rate
<b><math>r_d</math></b>	Ratio of intrinsic growth rate between control and fertilised large tanks
<b>RDA</b>	Recommended daily intake
<b><math>R_m</math></b>	Peak biomethane production rate
<b><math>r_N</math></b>	Intrinsic growth rate normalised for starting water nitrogen concentration
<b>RPD<sub>t</sub></b>	Percentage relative difference between precipitate weight at time t
<b>RSS</b>	Residual sum of squares
<b><math>r_x</math></b>	Final intrinsic growth rate normalised for starting water nitrogen concentration
<b>SD</b>	Standard deviation
<b>SDG</b>	Sustainable development goals
<b><math>S_g</math></b>	Specific growth rate
<b>SO<sub>2</sub></b>	Sulphur dioxide
<b>T</b>	Temperature
<b>t</b>	Time
<b>TC</b>	Antibiotic tetracyclines
<b>TDS</b>	Total dissolved solids
<b>TF</b>	Translocation factor
<b>TGA</b>	Thermo-gravimetric analyser
<b>TKN</b>	Total Kjeldhal nitrogen
<b>TN</b>	Total nitrogen

<b>UAE</b>	Ultrasound-assisted extraction
<b>UBL</b>	Ugandan Brewery Ltd.
<b>UGX</b>	Uganda dollar
<b>UPI</b>	Utilisation potential indicator
<b>USD</b>	United States dollar
<b>UV-Vis</b>	Ultraviolet-visible
<b>VBU</b>	Visva-Bharati University
<b>VM</b>	Volatile matter
<b>VS</b>	Volatile solids
<b>W-AAE</b>	Scenario wild alkali acid extraction
<b>W-AD</b>	Scenario wild anaerobic digestion
<b>WH</b>	Water hyacinth
<b>WL</b>	Water lettuce
<b>WQI</b>	Water quality indicator
<b><math>W_{t_a}</math></b>	Precipitate weight at time t under conditions a
<b><math>W_{t_b}</math></b>	Precipitate weight at time t under conditions b
<b>WWTP</b>	Wastewater treatment plant
<b><math>Zn(NO_3)_2 \cdot 6H_2O</math></b>	Zinc nitrate
<b><math>\Delta W_t</math></b>	Relative change between precipitate weight, under conditions a and b, at time t
<b><math>\lambda</math></b>	Lag phase

## Chapter 1.

# Introduction

Human evolution has been impacted by major events throughout our development; the control of fire through to the invention of the internet, our lives have been shaped by many different events. Arguably one of the most significant events, in the span of the modern human, has been the industrial revolution which has defined our lives and led to a significant impact on the planet. This industrial revolution allowed humans to thrive, in ways that had previously not been possible, resulting in a dramatic increase in population and consumption. This has culminated in the declaration of a climate emergency [1]: the continual rise of human population and anthropogenic pollution, in particular greenhouse gas (GHG) emissions, has resulted in significant damage to the natural world. The sustainable development goals (SDG) define the issues that face humanity and are therefore the focus of modern-day research and innovation [2]. The most recent SDG report details the impacts of the COVID-19 pandemic, the conflict in Ukraine and the ever-present threat of climate change, as the most pressing threats to humanity. Chief amongst these threats are energy and food security that, for the first time, the Ukraine conflict has thrown into the spotlight for the developed as well as the developing nations.

### 1.1. Energy and food security

Population rises and threats from climate change have resulted in a disparity between developing and developed nations. Whilst the conflict in Ukraine and the COVID-19 pandemic have threatened the energy and food security of developed nations, these issues have been prevalent in developing nations for decades, and have only been worsened by global challenges; in 2021, 150 million more people were faced with hunger than in 2019, with 2.3 billion people in a state of food insecurity [2]. This is a direct result of the COVID-19 pandemic, resulting in 47% of the global population under the stress of inflated food prices [2]. However, this has been further exacerbated: in early 2022, the global food market was 30% higher than the previous year, reaching an all-time high as a result of inflated energy and fertiliser prices, amongst other factors [2].

The disparity, between developed and developing countries, is evident when comparing energy security. Whilst the conflict in Ukraine has led to a mass reluctance of utilising Russian gas, 100% of people living in Europe, Northern America, Australia

and New Zealand have access to electricity [2]. Whereas, in sub-Saharan Africa it is just 48.1% [2]. Secondly, ~2.4 billion people rely on biomass/polluting cooking systems, predominantly within Brazil, China, India, Indonesia and Pakistan [2]. Energy from biomass, or bioenergy, will not disappear overnight: millennia of tradition and exploitation cannot be eradicated and despite efforts to reduce biomass reliance, through the implementation of liquid petroleum gas (LPG) initiatives [3], bioenergy continues to be a key source of fuel for a large number of communities. Bioenergy offers significant advantages over alternative renewable energy sources, wind, solar, etc., due to the potential for continuous use, off- or micro-grid use and storage potential. Another significant potential is for the generation of secondary products in small scale biorefineries [4], in particular the generation of clean water.

## **1.2. Pollution of freshwater ecosystems**

Pollution of our aquatic environments has increased dramatically since the industrial revolution and removal/treatment is not able to keep pace with waste production. As of 2020, just 74, 54 and 71% of the global population had access to safely managed drinking water, safely managed sanitation and basic hygiene, respectively [2]. The disparity shown in energy security is reflected in drinking water availability, with half of the people that have access to safe drinking water living in developing countries, whilst all countries, who are at critical levels of fresh water stress, are located in northern Africa and western/south Asia [2]. Aquatic environments have been particularly impacted by the effect of nutrient loading [5] and industrial wastewaters [6], yet 80% of global wastewater goes untreated [5]. The ratio, between treated and untreated wastewaters, is much greater in developing countries, as compared with developed [5]. Nutrient loading is the increased presence of nutrients within an ecosystem, primarily the introduction of nitrogen and phosphorous and can result in eutrophication. Eutrophication is a natural process that occurs in all water systems, where nutrient levels are increased, therefore primary production increases, increasing food availability at high trophic levels [7]. However, if the nutrient content is excessive, then the increased primary production can result in disturbances to the balance of organisms (decrease in biodiversity, higher chance of invasion, mass death) and quality of the water (hypoxic zones, cyanobacteria blooms) [8,9]. Since the turn of the century, eutrophication has become one of the biggest global challenges due to the increase in nutrient use in agriculture [8–11]. The pollution of vital water resources is not only a hugely damaging issue for animal or plant life but has detrimental effects for humans using the systems for drinking, fishing, recreation and other economic purposes.

Industrial wastewater occurs in any mass production cluster, whether this is manufacturing, agriculture, urban environments, or others. Industrial activity is the greatest source of heavy metals (HMs), a term used to describe any “metal and metalloid element with a relatively high density” [12], of  $\geq 5 \text{ g/cm}^3$ , encompassing ~53 elements [13]. HMs like Cu, Zn, Fe, Mn, Cr and Co, often play a vital role in biochemical functions of plants as essential nutrients, provided they do not exceed certain concentrations [13,14], beyond this, essential HMs become extremely toxic, predominantly through enzyme disruption [15]. The non-essential HMs, like Cd, As, Pb and Hg, are toxic in much smaller concentrations and cause stress in plants at low concentrations [13]. HMs are non-degradable and extremely persistent in the environment, therefore, the increasing levels of HMs in the environment, due to anthropogenic activities, are a serious cause for concern. The routes of HMs into aquatic systems are numerous and complex, predominantly due to anthropogenic activities, however, the background levels of HMs is often produced by geological weathering in areas of metal-bearing formations [15].

Traditional methods of pollution control are expensive and rarely 100% effective, resulting in contaminated water released to the environment or significant production of waste [16–19], therefore, alternative methods, in particular nature based methods, is a research area that has been gaining traction for several decades. One example is phytoremediation, where natural plant mechanisms are utilised to remove pollutants from an environment [20,21]. Phytoremediation can be achieved through phytoextraction/ accumulation, rhizofiltration, phytostabilization, and phytotransformation/ degradation and phytovolatilization. Phytoremediation can be applied to the removal of organic compounds, radionuclides and metals in freshwater systems [20,21]. Certain plants are able to hyperaccumulate pollutants, this is defined as more than 0.1% by dry weight of plant tissue, however, this is  $>1\%$  for more common pollutants like macro- and micro-nutrients [22]. The main criteria, for selecting a hyperaccumulating plant for phytoremediation, are: accumulating capacity; tolerance capacity; removal efficiency; bioconcentration factor (BCF) index and translocation factor (TF) index [20]. Hyperaccumulator plants can retain  $>100$  times greater concentrations of metals, in above ground tissue, than non-hyperaccumulators and have a BCF of  $>1$  [20]. However, utilisation of the contaminated biomass can be challenging based on the elevated levels of nutrients or toxic pollutants; therefore, plant selection is vital.

The potential introduction of biorefineries that could clean water, whilst producing energy, food and fertiliser, are an innovative option that could act as a transition whilst the global community attempts to change the way that modern day humans live.

### 1.3. Water hyacinth infestation

Water Hyacinth (WH), *Eichhornia crassipes* (Mart.) Solms, is one example of a hyper accumulator that has the potential to be utilised in a biorefinery.

WH is an invasive free floating aquatic macrophyte, native to the Amazonian Basin, Brazil [23,24]. Once admired for its beautiful and decorative flowers, see Plate 1.3-1, WH has been branded as the most problematic weed in the globe, resulting in the colloquial name the “beautiful devil” [25]. WH was introduced to the tropics through horticultural trade, spreading across a large span throughout the 19<sup>th</sup> and 20<sup>th</sup> centuries [26]. Despite a widespread ban in some USA states and the entirety of the EU [27], seeds are still available for purchase on the internet. The persistence of WH has led to a wealth of published literature, encompassing a wide variety of disciplines, including animal nutrition, high value product feedstock, water purification and energy.



**Plate 1.3-1:** Water hyacinth flower from Pune, India (May 2019).

WH is extremely fast growing, capable of growing at 0.26 tonnes of dry biomass per hectare per day, however, this has a large range depending on environmental conditions [28]. WH can thrive in a variety of conditions, demonstrating a tolerance of 6-40°C and up to 15% salinity [23,29]. This high range of tolerance and rapid growth rate allows WH to outcompete other plant species; additionally, WH forms thick dense mats, reducing light penetration and dissolved oxygen (DO), causing concentrated anaerobic zones, reducing biodiversity [28,30].

WH is capable of accumulating high levels of both nutrients and HMs, yet contains the majority of these in its roots, indicating a low TF [24,31]. The high growth rate, accumulation potential, low TF and easy harvesting due to its floating nature, makes WH a highly desirable plant for selection in a biorefinery. Secondly, WH is an invasive species, in many countries it is considered a nuisance that must be removed and

significant amounts of money and resources are spent on its eradication [25,32]. The use of WH in a biorefinery would valorise the biomass, making its removal/harvest a viable economical decision as well improving the local ecosystem services. This study aims to understand the viability of WH as a resource and demonstrate a feasible method of utilisation.

## **1.4. Aims, objectives and structure**

### **1.4.1. Aims and objectives**

The overall aim of this study is to demonstrate the potential utilisation of WH in a biorefinery concept, to produce food and energy. This will contribute to SDG 2 (zero hunger); SDG 6 (clean water and sanitation); and SDG 7 (affordable and clean energy) [2].

To achieve this aim, several objectives were completed:

*Objective 1: Water hyacinth in the wild.*

- WH was characterised in terms of proximate, ultimate and inorganic composition.
- Water lettuce (WL) was characterised as a comparison to WH
- Potential utilisation indicators were used to determine the applicability of each feedstock for further conversion.
- Variations between the feedstocks were analysed based on morphological, geographical, water quality and phenological variation.

*Objective 2: Water hyacinth in controlled conditions.*

- WH was cultivated to determine the resource availability in a controlled environment.
- Nitrogen loading and source were varied to understand their impact on growth rate and final density.
- The logistic growth model was employed to understand the impacts of temperature and solar irradiance on growth rate and final density.

*Objective 3: Water hyacinth in a biorefinery.*

- Alkali acid extraction was performed on variety of WH feedstocks to determine the variation that occurred across conditions.
- WL was utilised as a comparison to WH.
- The sample with the optimal extraction yield was selected for further extractions to understand the variation caused by extraction conditions.



- The potential for anaerobic digestion of residue from alkali acid extractions was assessed.
- Information from objectives 1 and 2 was utilised to determine the potential mass and nutrient flows within a biorefinery under different scenarios.

#### 1.4.2. Structure

The thesis is comprised of 8 chapters, organised as follows:

**Chapter 1** introduction to the research topic and outline and aims and objectives of the investigation.

**Chapter 2** provides an overview of the published research underpinning this study, investigating WH biomass, cultivation conditions, utilisation methods and the summarisation of different protein extraction methods from biomass in general.

**Chapter 3** describes the various experimental protocols and methodologies used throughout this study. This includes biomass collection, cultivation and characterisation; water characterisation; and utilisation potential indicators.

**Chapter 4** determines the differences in biomass composition and utilisation potential due to geographical, water quality and phenological variations.

**Chapter 5** investigates the potential for cultivation of WH, based on variations in nutrient loading, nutrient source, and environmental conditions.

**Chapter 6** describes the impact of sample selection and extraction conditions on the potential for protein extraction from WH and WL. This is followed by the variation in biogas yield from the extraction residue.

**Chapter 7** details a biorefinery under different scenarios, pulling on the information from the previous chapters.

**Chapter 8** describes the conclusions of the is work and defines the future work

## Chapter 2.

# Literature review

A key aspect of this work is to produce a comprehensive review of the literature and identify key knowledge gaps in the cultivation and utilisation of contaminated WH biomass. Initially, WH biology, distribution and composition are introduced, followed by the impact of various environmental parameters that impact the growth of WH. Finally, the various utilisation methods are described, with a focus on protein extraction.

### 2.1. Introduction into water hyacinth biomass

WH, *Eichhornia crassipes* (Mart.) Solms, is an invasive free floating aquatic macrophyte, native to the Amazonian Basin, Brazil [23,24]. Once admired for its beautiful and decorative flowers, Plate 2.1-1, WH has been branded as the most problematic weed in the globe and was named the 'beautiful devil' [25]. WH arrived in the tropics through horticultural trade and spread throughout the 19<sup>th</sup> and 20<sup>th</sup> centuries [26]. The persistence of WH has led to a wealth of published literature, encompassing a wide variety of disciplines leading to WH being used in animal feed, agriculture, water purification and energy.

WH is extremely fast growing, capable of growing at ~72 grams dry weight (DW) per m<sup>2</sup> per day [33], though this number varies with conditions and location [28]; in comparison, microalgae raceway ponds can produce a maximum productivity of 40 g DW/m<sup>2</sup>/day [34]. The high growth rates and range of tolerance allows WH to outcompete other plant species; additionally, WH forms dense mats that reduces light penetration and dissolved oxygen (DO), due to decomposition of biological material and reduced gas mixing, causing concentrated anaerobic zones, reducing biodiversity [28,30].



**Plate 2.1-1:** Water hyacinth flower from Pune, India (May 2019).

#### 2.1.1. Global distribution of water hyacinth

WH originated in Brazil, where samples were collected and taken to Europe to be grown in various botanical gardens, see Figure 2.1-1, such as Royal Botanical Gardens Kew, Gottingen and Monaco.

The first recorded introduction of WH was Louisiana in 1884 [23], however, there is some evidence that the plant had already been introduced into Japan at this time [25]. Records do not give a complete answer surrounding the introduction of WH to the rest of the world, however, it is generally believed that plants were brought on ships by early European explorers and grown in botanical gardens, evidenced by the seemingly simultaneous introduction of WH into several continents [25]. WH then showed its true nature: escaping into natural water bodies, WH was able to spread rapidly and begin to cause global devastation [25]. Whilst WH primarily came from Europe, the European climate is too temperate for WH to dominate freshwater systems and therefore only Portugal was significantly affected [25]. Africa had documented infestations in early to mid-1900s, in Egypt, South Africa and Congo before extending along major rivers (White Nile, the Nile Delta) and was escalated by high floods [25], it is now a major issue in many water bodies [25,32].



**Figure 2.1-1:** Cultivation of water hyacinth in a botanical garden [35].

Today, WH grows freely across 6 continents and almost 100 countries, portrayed in Figure 2.1-2; the full list is described in Appendix A. Figure 2.1-2 demonstrates the global domination of WH, however, there are significant gaps in the literature where WH has been documented, this most likely due to lack of published data. This is particularly a problem in countries in Central Africa, including South Sudan, Central African Republic and Chad.

Chad is a prime risk for WH infestation due to many international tributaries, an internationally shared lake and favourable fertile basin [36]. However, it has been suggested that WH is not present in Chad [37], despite several false alarms from Lake Chad [36]. The ecology of Lake Chad is dominated by other macrophytes, water lettuce (WL), submergent reeds and reeds (mostly *Cyperus papyrus*) [36], which reduce the nutrient levels of the lake and may contribute to the absence of WH.

Libya has a high risk for infestation due to optimal climate and location, countries with access to the Mediterranean are at high risk of infestation [38], however, there is no definitive evidence for any infestation. The majority of the Libyan population have access to clean and sanitary water [39], this suggests that the ground water, which accounts for 95% of the water reserves, may contain low concentrations of pollution, both industrial and nutrient rich, therefore reducing the probability that WH can dominate the water systems.

Somalia is situated to the east of Ethiopia and Kenya; these countries have large areas that are dominated by WH but despite this, WH has yet to be reported in Somalia [38,40]. This is likely be due to the topography around the borders of Somalia: the area between Somalia and Kenya is largely arid therefore they is little water or plant transfer between the countries [41].

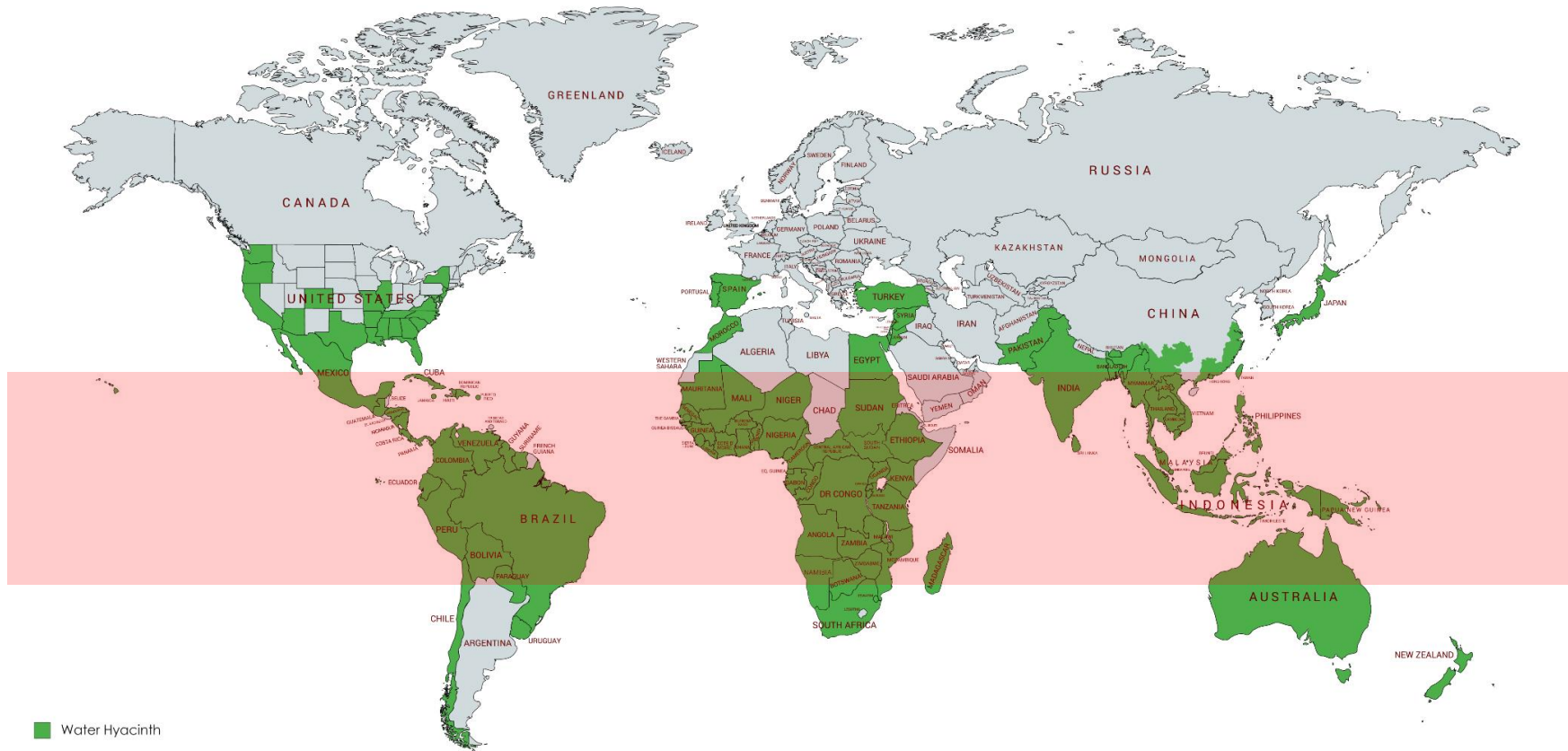


Figure 2.1-2: Distribution of water hyacinth showing the tropic zone (adapted from [35]).

#### 2.1.1.1. Composition variation

WH has colonised many water bodies across a large proportion of the globe; the changes in location demonstrate variations in the composition of the biomass, see Table 2.1-1. The ratio between cellulose and hemicellulose varies, from 0.4 to 1.4, suggesting that environmental conditions have an impact on these structural fibres. WH has a low lignin content: with the exception of Poddar *et al.* [42], the lignin content was less than 10% dry matter (DM). In comparison to other floating aquatic plants, WH has a higher cellulose and lignin content than *Pistia stratiotes* (water lettuce) and *Limnobium laevigatum* [43], however, there is variation within the literature, WL in particular can contain higher levels of lignin [44,45]. The protein content of WH shows a large range, similar to that shown by WL, which ranges from 11.1-18.4% [44–46]. The ash content of WH is considered high for a plant that would be utilised for bioenergy [47,48], however, when compared with WL, WH demonstrates a lower ash content. Sudiarto *et al.* demonstrated that WH had a lower ash content in different conditions, ranging from 16.8-17.9% DM, in comparison with 19.8-22.2% DM for WL [43]; other studies have shown an ash content of >20% for WL [45,46].

**Table 2.1-1:** Changes biochemical composition of water hyacinth by location (% of dry weight).

Reference	[42] <sup>1</sup>	[49]	[50]	[51]	[48]	[52]	[53]	[54]	Overall
Waterbody	Unknown	Unknown	Ponds	River	Sewage Lagoons	Canal	Canal and Ditch	Tank	N/A
Pollution Source	Unknown	Unknown	Unknown	Unknown	Sewage	Unknown	Unknown	Unknown	N/A
Location	Unknown	India	India	China	USA	Egypt	Egypt	India	N/A
Moisture Content	-	-	-	-	95.0	93.8	90.5	90.6	90.5- 95.0
Organic Matter	83.6	-	-	-	-	-	74.3	83.7	74.3- 83.7
Fat	-	-	-	-	1.6-2.2	-	-	-	1.6- 2.2
Protein	16.3	11.9	-	-	9.7-23.4	17.0	20.0	-	9.7- 23.4
Esther Extract	1.6	-	-	-	-	-	3.5	-	1.6- 3.5
Fibre	16.3	-	-	-	18.6-19.5	-	18.9	-	16.3- 19.5
Nitrogen Free Extract	49.4	-	-	-	-	-	31.9	-	31.9- 49.4
Ash	16.4	20.2	-	-	11.1-20.4	-	25.7	-	11.1- 25.7
Neutral Detergent Fibre	56.1	-	-	-	-	-	62.3	-	56.1- 62.3
Acid Detergent Fibre	37.7	-	-	-	-	-	29.0	-	29.0- 37.7
Cellulose	25.6	17.8	24.7	25.6	-	31.0	19.7	18.0	17.8- 31.0
Hemicellulose	18.4	43.4	32.2	31.8	-	22.0	33.4	34.0	18.4- 43.4
Lignin	9.9	7.8	3.2	3.6	-	7.0	9.3	26.4	3.2- 26.4

<sup>1</sup>Referenced from Valk (2015) [55]

## 2.1.2. Morphology of water hyacinth

### 2.1.2.1. Seedling

Mature WH plants develop 500 ovules with approximately 50 seeds per capsule, which can rise to 500. The seeds are extremely small, 0.5mm-4mm x 1.0mm, and sink to the bottom of the water, or can become trapped on the mat, where they lie dormant until optimal conditions arise, which can exceed 20 years [23,26]. WH seeds require warm and shallow water to germinate, producing 5 small leaves before the sixth and further leaves allow the seedling to break from the rootstock and reach the surface [56].

Numerous fibrous roots form at the base of the stem of the juvenile, before forming feathery hairs surrounding the main fibrous roots [26,56]. Leaves form at the apical bud at the centre of the rosette; these tend to elongate as crowding occurs [56].

### 2.1.2.2. Shoot

The shoot exhibits sympodial branching, producing stolons with short internodes, each bearing a leaf and roots [25,56]. The axillary buds are predominantly stolon buds but do not all develop into stolons [25]. The stolon tends to be purple/violet in colour and can reach 50 cm in length before breaking off to allow the daughter plant to breakaway easily [25,26]. This occurs less regularly in plants that are in overcrowded areas, like the centre of the mat, compared to plants at the edge of the mat [25,26].

### 2.1.2.3. Root

The root morphology is dependent on the depth and flow of the river [25,26,56]. WH produces main fibrous roots surrounded by feathery hairs that give it a high surface area and can allow it to thrive on very short but ample roots [25]. The roots can be up to 3m long and make up half of the biomass of the plants, but when in nutrient rich waters, the roots can be one fifth the size of the petioles, compared with nutrient poor zones where the roots can be over 3 times the length of the petioles [25,26]. It has been shown that the ratio of roots: leaves and/or petioles, demonstrates a linear negative correlation, corroborating the hypothesis that as root size increases, due to poor nutrient conditions, the leaf and petiole size decreases [57]

The roots of WH are predominantly white when grown in darkness, however, if exposed to light they develop a pink/purple hue [25,26]; it has been reported that this is a defensive adaptation to make the roots less visible to aquatic organisms, though there is little evidence of this [25].

The feathery roots of WH allow the roots to stay suspended in the water, however it is possible for WH to root into the ground [26]; this tends to produce the midget form of



water hyacinth: WH has been reported in four different forms; midget, small, medium and large/giant [23,58].

#### 2.1.2.4. Leaf and petiole

Leaves develop from the apical meristem until this is consumed during the flowering process [25,56]. The axillary bud is enclosed in a tubular leaf structure (prophyll), as the bud develops, a small primary leaf emerges before normal foliage appears; consisting of petiole and waxy leaves [25]. The leaves form a spirally arranged phyllotaxy with elongated petioles of up to 1m in length with an average of 6-8 leaves per plant (discounting attached daughter plants) [25,56].

The petioles vary depending on the morphological growth form [23]: each flower variant produces different sized floats in the centre of the petiole, the floats contain intercellular spaces filled with air to aid with flotation [23,25,26,56], see Plate 2.1-2. These floats are the main variation between the different variants of WH: the larger variants produce floats that are thinner and longer, whereas the smaller variants have floats that are extremely fat, see Plate 2.1-3. The petioles, specifically the float, is one reason that WH is an unsuitable source of food for many animals: the petioles can absorb significant amounts of water during digestion forcing animals to “drink more and feel repleted” despite the low nutritional value of the petioles [52].

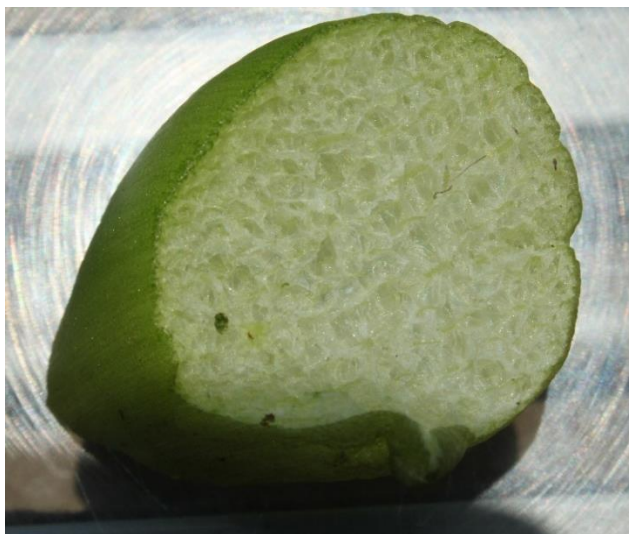


**Plate 2.1-2:** Cross section of a water hyacinth float from Pawana River, Pune, India (April 2019).

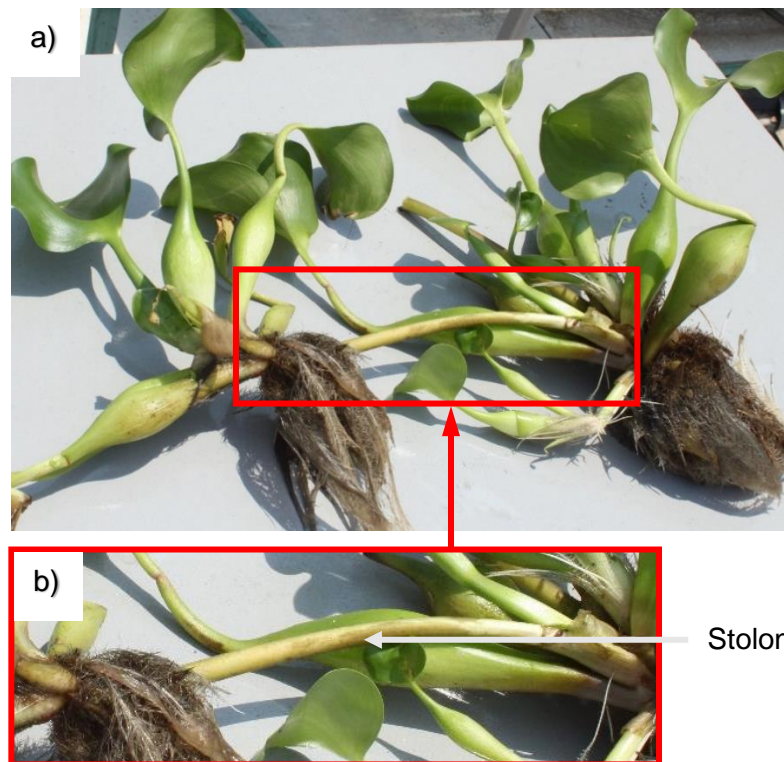


**Plate 2.1-3:** Water hyacinth, with daughter plant, from Pawana River, Pune, India (April 2019).

#### 2.1.2.5. Flower

The lilac flowers develop on a terminal inflorescence that has between 4 and 25 flowers, depending on the size and variation of the plant [25,26]. The flowers contain six stamens though pollinators are largely unknown: Barrett states that a major factor limiting sexual reproduction are low and inefficient pollination [59]. The flowers are beautifully coloured but short lived; during summer the average cycle is completed with two days [23,25]. Penfound and Earle describe the anthokinetic cycle in detail, suggesting that the bud starts to open at ~1700 and is beginning to wilt by the same time the next day [23]. The stem begins to bend before the flower head dips into the water where the fruit develops. The curvature occurs due to elongation of the epidermal and hypodermal cells [25].

WH belongs to the Pontederiaceae family, this is one of very few families to exhibit the floral variation known as tristily, characterised by three differing forms: long styles and two anther levels below the stigma (long-style); one set of anthers above and one below the stigmas (mid-style); and anthers at two level above the stigmas (short-style) [60]. These variations are all compatible and show little variation in seed production. The pollinators for WH have been poorly studied, vary from location to location and are considered to be the limiting factor in the sexual reproduction of WH [59,60].

### 2.1.2.6. Morphological composition variation

The parts of the plants that comprise the majority of the plant are the leaf, root and petiole, therefore, these are the most widely studied. However, there is little consensus on how biochemical composition varies between the tissues, see Table 2.1-2. The protein content of the above water parts, leaf and petiole, are often higher than the below water below water tissue, root. This is also true for WL [61], however, the protein content is lower than WH. The opposite is true for ash content, due to the high heavy metals (HM) concentrations in the root, see Table 2.1-3, WH roots tend to have a greater concentration of ash than above water tissues, however, petioles can store excess nutrients which can form high concentrations, see Table 2.1-4. As previously stated, whole WL plants contain higher ash concentrations than WH, this is replicated in the tissue analysis: Wasagu *et al.* reported values of 35.2 and 44.5% for the ash content of the leaf and root, respectively [61]. This shows that WL has a higher ash content than all but one example in Table 2.1-2, and that the root contains greater ash than the leaf. The HM concentration in WH roots demonstrates that various elements are concentrated more than others: Cr, Cu, Fe, Mn and Zn are all concentrated more than the other elements listed in Table 2.1-3. Further investigation into the phytoremediation properties of WH will be described later in this study. Table 2.1-4 demonstrates that nutrient concentrations vary amongst the tissues, however, there is not enough evidence to demonstrate a trend from this data. K appears to be concentrated in high amounts with all tissues, followed by Na, then Mg and Ca.

**Table 2.1-2:** Biochemical analysis of water hyacinth tissues (% dry weight).

Ref.	Plant Part	Cellulose	Hemi-cellulose	Lignin	Protein	Total Carbohydrate	Lipid	Ash
[62]	Leaf	-	-	-	15.9	31.5	-	14.4
	Petiole	-	-	-	15.9	31.2	-	12.4
	Root	-	-	-	15.2	28.4	-	12.5
[63]	Leaf	8.7	8.4	11.5	-	-	-	19.9
		12.8	24.0	14.3	-	-	-	12.4
	Petiole	8.4	3.0	4.5	-	-	-	26.8
		14.2	25.8	5.9	-	-	-	14.4
	Root	16.0	7.7	13.4	-	-	-	26.0
		15.9	27.5	8.8	-	-	-	14.6
[64]	Leaf	29.9	31.8	5.5	22.0	-	1.9	13.1
	Petiole	29.3	28.4	18.4	7.7	--	1.0	21.2
	Root	18.1	16.2	15.7	3.3	-	0.7	50.1

**Table 2.1-3:** Changes in trace element concentration water hyacinth roots by location (ppm, dry weight).

	[65]	[66]	[67]	[68]	[69]	[70]	Overall
Water Body	Wetland	Tank (collected from River)	Tank (unknown collection)	Reservoir	Pond	Irrigation Canal	N/A
Pollution Source	Industrial	Industrial	Mixture	Mixture	Industrial	Unknown	N/A
Location	Brazil	Ivory Coast	Iran	México	Pakistan	Egypt	N/A
As	-	-	-	9.3	-	-	9.3
Ba	-	-	-	86.6	-	-	86.6
Co	-	-	-	18.6	-	-	18.6
Cd	0.2-0.4	0.7	19.9	0.4	3.5-5.8	0.1-0.3	0.1-19.9
Co	-	-	-	18.6	-	14.5-21.7	14.5-21.7
Cr	3.3-4.6	655.3	-	63.6	-	36.8-86.8	3.3-655.3
Cu	0.5-0.9	225.2	-	74.6	666.7-1313.0	16.5-41.5	0.5-1313.0
Fe	-	-	-	-	-	9987.9-22612.0	9987.9-22612.0
Mn	-	-	-	-	-	2623.9-7198.2	2623.9-7198.2
Mo	-	-	-	9.6	-	-	9.6
Ni	0.4-0.7	104.5	0.1	69.6	-	20.3-50.3	0.1-104.5
Pb	0.4-5.2	1792.7	-	37.6	1049.0-1738.0	0.1-4.5	0.1-1792.7
Ti	-	-	-	900.0	-	-	900
V	-	-	0.2	80.6	-	-	0.2-80.6
Zn	3.1-5.5	-	-	249.0	-	42.8-136.2	3.1-249.0

**Table 2.1-4:** Nutrient variation in water hyacinth tissues.

Reference	Plant Part	Concentration (ppm), dry weight				
		K	Na	Ca	Mn	Mg
[62]	Leaf	12,128	11,430	8541	4980	7,243
	Petiole	12,618	11,566	7436	5392	6,453
	Root	12,292	11,611	7176	4662	6,336
[48]	Leaf	36,000	18,300	7,560	69	8,490
		36,000	18,300	2890	69	8,490
	Petiole	27,300	12,100	8,760	88	1,540
		33,000	6,570	4110	176	2,570
	Root	30,300	10,200	6,860	41	1,810
		28,000	25,600	5420	356	2,830

### 2.1.3. Phenology of water hyacinth

WH is persistent throughout the tropics and has extended its reach outside, displayed in Figure 2.1-2, despite the reduction in growth WH exhibits at low temperatures. WH grows rapidly during elevated temperature periods, whilst during winter its growth is minimal due to death of leaves [23]. Center and Spencer have given a detailed analysis of WH growth cycle in a climate with near freezing temperatures; however, this may not be representative of plants in more tropical conditions [56].

WH produces seeds in the spring, where the ovary produces a small capsule containing approximately 500 seeds [23,26], that sink to the bottom of the water body. However, the plants predominantly reproduce via clonal propagation [26,56,71]; daughter cells are produced at the end of fragile stolons, see Plate 2.1-3b, that are easily broken to allow the dispersal of ramets into the water body [26]. The cold temperatures during winter cause losses of WH which can have significant population reductions, before clonal growth intensifies in spring due to small pockets of plants that survive [24,25,56,72]. This data is predominantly for countries that experience high temperature based seasonal variation (e.g., USA); for countries whose seasons are less severe, reduction in growth is more likely. Countries that experience powerful monsoon seasons, similar reductions may occur due to strong water flow from high rains, potentially requiring seed repopulation, however, there is little evidence of this in literature.

The density of WH mats rapidly increase during the spring before decreasing during early summer but remaining constant for the rest of the season [23,24,56]. This is in contrast to leaf length which peaks in summer before declining over the winter months [23,56]. Flowering begins in mid-late spring and is at maximum bloom during early summer [23], although flowering is not uniform across the mats and often occurs in small portions of a population [25]. Flowering is affected by a variety of factors; the

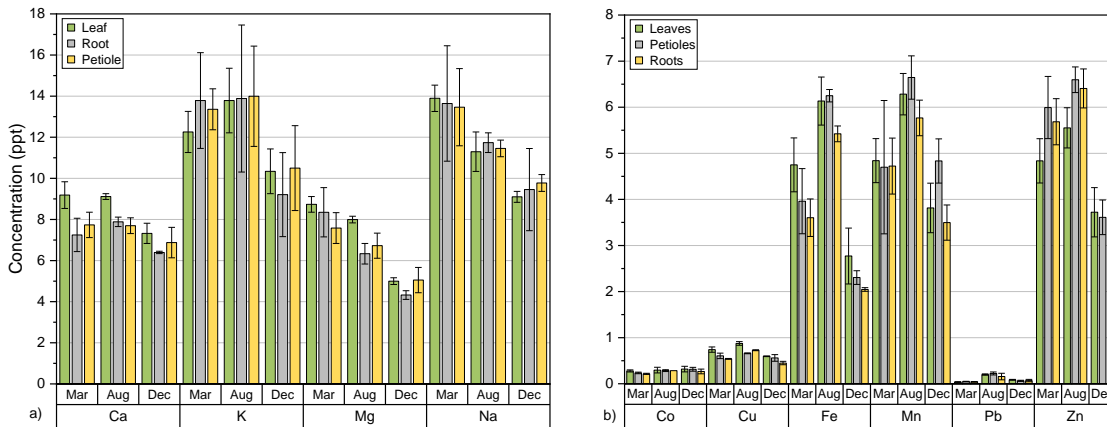
dominant of which is plant density and is usually more profuse in areas of lower densities (number of plants per unit of area) [25]. The fruit of WH usually occurs in the water to increase the dispersal of seeds and to ensure that a minimal amount of the seeds are trapped on the mat [25]. Center and Spencer determined three distinct periods of growth; the first phase starts after the shoots are killed during winter and results in a redistribution of the biomass before the plant begins the second phase in spring and starts to rapidly increase clonal propagation [56]. The third phase is the increase in total plant and leaf size as smaller plants are lost and the larger plants dominate and start to flower. This cycle is very different depending on the climate; Gopal suggests evidence of plants flowering in January in southern India [25], as opposed to September in southern USA [23].

The anthokinetic cycle of WH consists of two main phases, the flowering phase and bending phase. During the summer months of the USA, the cycle can be complete within 48 hours, though the buds can be visible for up to 10 days before flowering [23]. The flowers open in morning, taking ~1 hour to fully open; after one day the inflorescence begins to bend downwards from just below the inflorescence [23]. The ovaries develop over a 20 day period and do not need to be in the water to develop though the fruit production does generally occur in the water, and can develop more quickly in the water [23,25].

As the fruit reaches maturity, it is detached from the inflorescence before releasing the seeds which sink to the bottom and lie until suitable conditions for germination arise [23,25,26]. The seeds root into the ground before growing float leaves to allow the plant to leave the sediment and float on the surface [23,25].

#### *2.1.3.1. Phenological composition variation*

Abdel Shafy *et al.* studied both seasonal and organ variations in WH from the River Nile for a selected number of trace elements [62], see Figure 2.1-3. The data presented shows that Mg and Na peak during the March but Ca and K both peak slightly in the August whereas all macronutrients drop in the December. Similarly, all HMs peak in the August and reach minimum during December. August is the penultimate month of the dry season, where temperatures are at the peak and there is little rain [73], therefore, increased nutrient and HM retention could be due to concentrated elements within the low water levels, therefore increasing uptake. For variation in the tissues, Abdel Shafy *et al.* found little significant variation, though stated that other authors had found that these elements accumulated in the root more than the leaf and petiole [62].



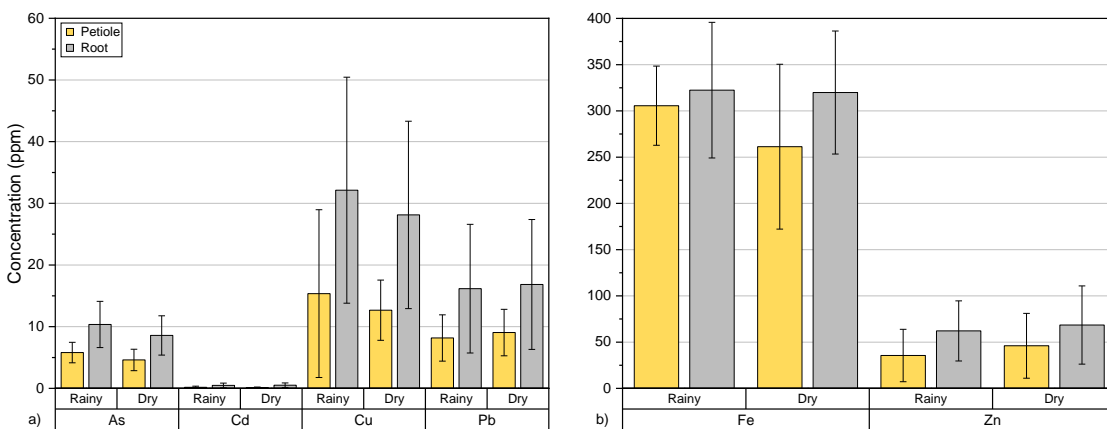
**Figure 2.1-3:** Elemental analysis of water hyacinth by time and plant tissue in the River Nile. Adapted from [62]. a) macronutrient; b) trace element.

Figure 2.1-4 shows the HM concentration variations between the rainy and dry season in Vietnam [14]. This clearly demonstrates that the HMs accumulate in the roots, this would result in a low TF; the TF is the ratio between the concentration of an element in tissues below the water and the concentration in tissues above the water, for WH this is calculated via Equation 2-1 [70].

**Equation 2-1:** Translocation factor.

$$TF = \frac{\text{Leaf Concentration} + \text{Petiole Concentration}}{\text{Root Concentration}}$$

WH has been stated to have a low TF for most HMs [66,74], however, without data from the leaf, it is not possible to determine a TF from Figure 2.1-4. Chernykh *et al.* concluded that the environmental conditions had a significant impact on HM concentration/ accumulation [14]. The variation between Figure 2.1-3 and Figure 2.1-4 demonstrates that geographic/environmental conditions impact the accumulation of HMs: accumulation of Cu, Fe and Zn was greater from the River Nile [62], whereas Pb was greater from the Srepok River [14].



**Figure 2.1-4:** Heavy metal concentration in water hyacinth by season and plant tissue in Srepok River. Adapted from [14].

Neither study investigated the elemental concentration of the water, therefore a BCF could not be calculated. The BCF is the ratio between the concentration of an element or chemical within whole biomass or tissue to the concentration within the water or soil, this is calculated via Equation 2-2 [70]. Without a value for the BCF, it is impossible to determine the efficiency of contaminant removal and removal could be considered negligible over time.

**Equation 2-2:** Bioconcentration factor.

$$BCF = \frac{\text{Biomass Concentration}}{\text{Water Concentration}}$$

Chernykh states that the areas sampled were influenced by wastewater entering the areas, however, there were no results stating the level of contamination (e.g. HM concentration) and therefore the accumulation of HM may be negligible over a long period of time [14].

## **2.2. Impact of environmental parameters on the growth of water hyacinth**

WH has a high growth rate across a variety of conditions: extensive studies have shown that WH can double its weight in under two weeks with optimal conditions [23,25,56,75]. However, growth rate can vary significantly, depending on temperature, light, water type and quality, nutrient availability and biomass density. The effect of these parameters on the survivability and growth rate of WH are discussed below.

### **2.2.1. Temperature**

WH can be found in a variety of freshwater water bodies, from flowing rivers to temporary ponds and marshes [23,25,32,76,77], as well rooting in banks and becoming stranded during times of low rainfall, but at a reduced success [23,29]. Figure 2.1-2 shows that WH is abundant in the tropic zone due to a preferred water temperature of 22-33°C, where biomass can double in weight over two weeks at optimal temperatures [23,25,56]. Water temperatures of over 33°C can cause inhibition of some vital functions and plants can survive for ~1 month in temperatures of over 34°C [23,56,71,78,79]; Gopal suggests that growth ceases entirely at a water temperature >40°C [25]. WH can survive below freezing, at a minimum of -6.5°C, but only for short periods, with a UK winter enough for total eradication of a population [23,24,29].

Imaoka and Teranishi demonstrated that when growth rate was normalised for impact of N and plant density, it increased exponentially, with the equation  $0.063(1.087^{T-20})$  where T is temperature [80]. As ambient air temperature was increased from 14-29°C, the growth rate increased [80]. In contrast, Wilson *et al.* described a linear relationship up to an optimum, where, above this temperature, the rate decreased linearly [81].



### 2.2.2. Light intensity

WH grows best under intensive light, this is important for flowering and formation of key tissues, including leaves, roots and floats [25]. Penfound and Earle found that in America, the floats of mature plants only form in early spring when maximum solar radiation reaches juveniles, however, plants that grow in the absence of full radiation, if they were shaded by trees or growing on the bank, of below an average light intensity of 1400 lux, will not grow floats [23]. The elongated petioles of mature plants ensure maximum solar radiation reaches the leaves and if shaded, to below an average light intensity of 1400 lux, plants will die, although starch storage in the roots can take 12 days to deplete [23]. This is important in lab-based experiments to ensure that average light intensity is ~5000 lux to simulate required solar radiation [23].

### 2.2.3. Waterbody

WH can grow in a large variety of water bodies, including; lakes, streams, ponds, waterways, ditches and backwater areas in temperate and tropical zones [25,71]. However, WH seedlings require warm shallow water to allow germination and rooting into the sediment before they become buoyant enough to float [26,56]. WH mats are able to stabilize pH levels and temperature in still water; this prevents stratification and the mixing of gases into and within the water column [71]. The stabilization of physical factors by WH mats, produces a water body with higher carbon dioxide (CO<sub>2</sub>) tension, lower DO, a more uniform temperature and higher acidity [23]. WH can survive in a wide range of pH levels, 4-10, but is most successful in neutral water [71]; acidic waters have caused problems for WH for initial infestations and has reduced its impact in Guinea [82].

The depth of the waterbody can result in significant morphological changes in WH; plants that are rooted in shallow water tend to have a smaller root structure than floating plants, larger roots tend to provide greater growth and adaptability to drought conditions [25]. In countries that experience monsoons, the plants are often washed away from the high flood areas, this can lead to rapid spread of WH if the conditions are favourable.

WH has a high rate of evapotranspiration, due to the increased size of its stomatal apertures, compared with other plants [23,25], this can be up to 3 times higher than local flora and reduces the water table [71], though this figure is highly variable depending on the location and the period of the year [25]. This increase has been linked with increased nitrogen supply: the increased nitrogen supply leads to a high leaf area index (LAI), which could account for this increase in evapotranspiration. This has caused problems in America, WH plants reduced the water table and affected the

irrigation of crops [23]. In Hindi, WH is named “samudra sokh”, or the one which can absorb the ocean, in association with its ability to rapidly increase the loss of water compared with open water [25].

There is some evidence to suggest that WH is affected by the flow rate of the river; Penfound and Earle stated that the variety of clone is dependent on the waterbody [23]. Midget clones are mainly found on land and small clones on the fringes of larger mats where the water is more stagnant. Medium plants tend to be found in water that is slow moving whereas the giant and large clones are in fast moving and well aerated water [23]. However, Penfound and Earle did not comment on the suspected cause of these differences. Center *et al.* characterised clones by the size of lamina (blade like organ of the leaf or petal that is primarily responsible for photosynthesis) and the size of the petioles; however, did not comment on the cause or differences (other than appearance and abundance) of the clones [58].

WH has been shown to tolerate low levels of salinity, surviving in estuaries and some brackish waters, even tolerating short periods of time in seawater [23,82]. However, WH cannot tolerate a salinity of 0.525-0.6%, [23,83]; at a salt concentration of 2%, the plants wilt and die rapidly [23]. It has been suggested that the damage caused by a salinity above 0.9% would be irreversible due to the salt-retention properties and specific ionic ratios of minerals in particular wastewaters [83]. However, this was significantly higher than the lethal level described by Gopal, and Muramoto and Oki, 0.23% [23] and 0.6-0.8% [84], respectively. WH has a high level of tolerance for variable conditions like nutrient availability, water level and velocity, pH and temperature, but increased salinity will damage the plant irreparably. However, there is a suggestion that it has the ability to adapt to salinity: Toy demonstrated that some plants did not show distress until 0.7%, and could develop a new ‘ecotype’ in certain locations [85]. It is clear that WH is impacted by high salinity, however it has been shown to have greater resilience than both WL and pennywort [86].

#### 2.2.4. Nutrient availability

Nutrient availability is important in two respects, nutrient uptake and impact on growth rate; the former will be discussed later in this study. Optimum levels of macronutrients results in an increased growth rate; greater plant height, in particular petiole growth; shorter roots (inversely to plant height); and a darker green colour in the leaves [25]. In contrast, reduced nutrients will result in reduced growth rates; shorter plants, longer and wider spread roots; and the development of a deep purple colour of the roots [25].

The concentration of N and P have been stated as the key nutrients to consider when investigating nutrient impact on growth rate [80,81,87]. P concentration appears to

have a lower impact on growth rate: Reddy *et al.* demonstrated that maximum growth rate was reached at a water concentration of 1.06 mg P/L [87]. This is supported by the findings of Imaoka and Teranishi, who stated that growth was independent of P concentration, within the biomass, from 2.0-10.1 mg P/g [80]. However, P concentration has been shown to impact the uptake rates of N and K [87,88]. It can be assumed that if P is above the limiting concentration, suggested to be 1.06 mg P/L [87], then it will have limited impact on the growth rate of WH.

In contrast, increases in N concentration generally result in increases of growth and nutrient uptake rate. Wilson *et al.* suggested that the relationship between growth rate and water N concentration would begin to demonstrate a plateau beyond 10 mg N/L [81], however, this study did not include data beyond 10 mg N/L and produced an  $r^2$  of 0.29 and 0.47, suggesting a weak fit. An examination of literature revealed that there were few studies that investigate the impact of water N-concentration ( $N_t$ ) on the absolute growth rate (AGR). These results from these studies were plotted, with  $N_t$  against maximum growth rate; this demonstrated a weak linear relationship, following the equation  $AGR = (0.64N_t) + 27.6$ , see Figure 2.2-1a, with a slope that was significantly different from 0. Reddy *et al.* reported a maximum AGR of 39.7 g DW/m<sup>2</sup>/day for 50.5 mg N/L and 32.2 g DW/m<sup>2</sup>/day for 25.5 mg N/L, these results represent reduced growth rate in comparison to the linear fit. Therefore, it is possible that these were anomalous results, or high  $N_t$  resulted in reduced growth. Removing these points produced stronger linear relationship with an equation of  $AGR = (1.6N_t) + 22.3$ , the p-value from the t-test was <0.05 and therefore, the relationship was significant; this fit is described as the LitFit from this point. This suggests that beyond 30 mg N/L, the relationship may not be linear. This is similar to the conclusions drawn by Wilson *et al.*, however, this study had a positive correlation beyond 10 mg N/L. In contrast, Fox *et al.* suggested that plant weight was increased up 80 mg N/L [89], however, this study gave no growth rate or initial plant weights so could not be included in this study.

This study was based on few reports and could not be extended beyond 30 mg N/L. Therefore, this was identified as key literature gap; in an integrated system a predicted nutrient requirement would aid end users in minimising excess nutrient addition and predicting biomass production.

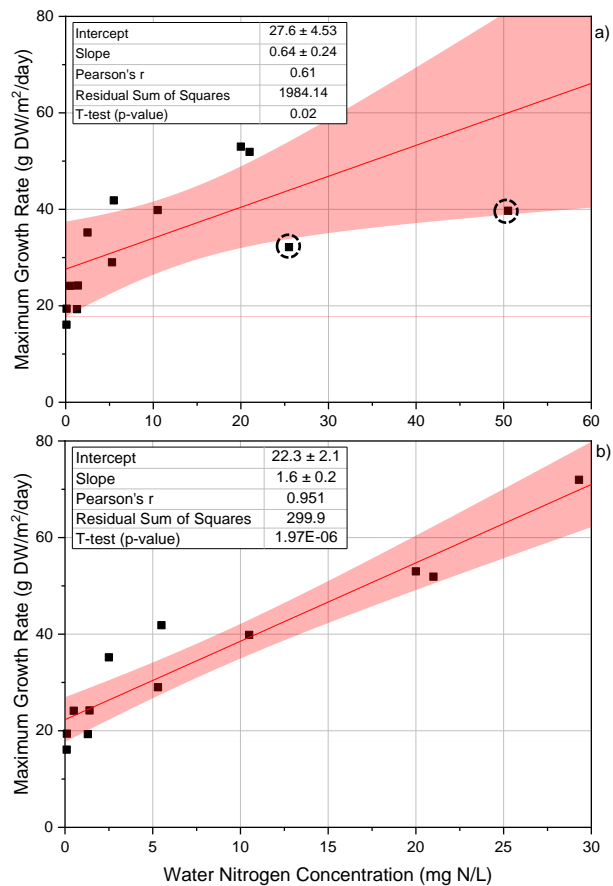


**Figure 2.2-1:** Maximum growth rate of water hyacinth against water nitrogen concentration from literature [33,90–97]; ○ - low growth rate results. a) linear fit including low growth rate values; b) LitFit.

Imaoka and Terranishi examined the relationship between plant N concentration ( $C_N$ ), and growth rate; it was demonstrated that above 20 mg N/L, growth rate was independent of plant nitrogen concentration, whereas below 20 mg N/L, growth rate increased according to the equation  $AGR = 0.063 (C_N - 4.29)$  [80]. Wilson *et al.* concurred with this statement, assuming a linear relationship between leaf N concentration ( $P_N$ ), and growth rate [81]. The young expanding leaves, located in the centre of the rosette, have a high  $P_N$  [81]. This decreases as the leaves mature, then after maturity the  $P_N$  stabilises; therefore, the third leaf, the first mature leaf, is the first leaf that can be taken to given an accurate representation of  $P_N$  [81].

The form of N is an important consideration, however, there is little unanimity in the literature. Gopal suggested that the source of nitrogen, between ammonia and nitrate, does not affect growth, however, a mixture does increase growth rate [25]. Delgado *et al.* and Fernando both found that ammonia was preferred over nitrate [98,99]; Delgado *et al.* used WH to treat pig slurry and removed 88% of ammonium during summer, but only 60% of nitrate [98]. Reddy and Tucker demonstrated that nitrate increased growth rate over ammonia [94]; nitrate and ammonia were absorbed more as a mixture, followed by nitrate alone then ammonia alone. The uptake rate is also affected by

season, specifically temperature and plant maturity [25]. The reduction in temperature reduces growth rate which is followed by nutrient uptake, suggesting a relationship between growth rate and uptake [25,94].

WH has a high nutrient uptake rate that follows a linear relationship with nutrient availability [25], this relationship eventually plateaus as storage of nutrients begins to increase [100,101]. Nutrient storage is relatively high in WH: Ho and Wong described a nutrient concentration of 5.42%, 1.97% and 4.57% DM for N, P and K, respectively [101]. However, this varies, as luxury nutrients can be stored in floats or laminas [100,101], demonstrating a positive correlation between concentration of nutrients in the water and the plant [87,99].

### 2.2.5. Biomass density

Table 2.2-1 displays a range of maximum densities, carrying capacity, from a variety of studies. Biomass density impacts the growth rate for all plants, through restriction of nutrients, sunlight, water, and other limiting factors. Reddy and D'Angelo demonstrated that regular harvests, can result in an increased average growth rate; increased DO; increased nutrient uptake; and reduced detritus accumulation [102], indicating that uncontrolled density increases, negatively impacts cultivation. This impact has been suggested to begin at 101 g DW/m<sup>2</sup>, however, when normalised to remove the impact of temperature, this was increased to 125 g DW/m<sup>2</sup> [80]. Temperature appears to impact the maximum density, with most studies reporting peak density in warmer months [56,91,103,104]. The availability of nutrients also appears to impact the maximum density: Reddy *at al.* demonstrated that increased water N loading increased the maximum plant density, across the range of 0.5 to 50.5 mg N/L [97].

The individual size of each plant varies as density changes: the height of each plant increases as the density increases [56,104], suggesting that vertical growth is prioritised over horizontal growth (asexual reproduction). This is achieved by the loss of daughter plants (ramets) due to restricted water and nutrient access [56]. Center and Spencer concluded that increase in size, vertical growth, and increase in number, horizontal growth, are alternative growth strategies [56]; a newly formed population will begin by prioritising horizontal growth to dominate the space, once space is restricted and there are limiting factors to growth, like space, light, nutrient and water availability, the plants will prioritise vertical growth. This was corroborated by Eid and Shaltout, who showed that individual plant weight and leaf area size have a negative correlation with number of individual plants [104], demonstrating that as the number of plants increases, the size of the plants is reduced. Conversely, as the number of plants decreases, the leaf size and plant weight increase [56,104].

**Table 2.2-1:** Water hyacinth biomass density.

Reference	Details	Plant Biomass Density*	
		(kg FW/m <sup>2</sup> )	(kg DW/m <sup>2</sup> )
[23]	Field Study in Los Angeles, Seasonal Peak	46.3	2.71
[56]	Field Study in Florida	25.0	2.50
	Drainage Canal, Lake Wauburg, Florida	32.6	3.26
	Drainage Canal, Paynes Prairie, Florida	25.5	2.55
	Farm Pond, Florida	23.1	2.31
	Lake Alice, University of Florida	22.6	2.26
[57]	Biven's Arm, Florida	20.8	2.08
	Sewage Plant, Florida	18.6	1.86
	SR-23-B Pond, Florida	10.5	1.05
	SR-23-A Pond, Florida	7.0	0.70
	River Styx, Florida	6.7	0.67
	Chairel Lagoon, Mexico	50.5	2.84
	Cruz Pintada Dam, Mexico	76.0	4.27
	Sanalona Dam, Mexico	57.0	3.20
[75]	Solís Dam, Mexico	63.0	3.54
	Requena Dam, Mexico	51.0	2.87
	Endhó Dam, Mexico	51.0	2.87
	Valle de Bravo Dam, Mexico	67.0	3.76
	Field Study in Florida	40.4	2.4
[78]	Field Study in Florida	42.2	2.5
[91]	Small Ponds, Auburn University, Alabama	21.3	2.13
[92]	1000L Concrete Tanks, Florida	10.0	1.00
[96]	Pond Series, Louisiana	29.7	2.97
[97]	1000L Concrete Tanks, Florida	16.0	1.60
[102]	1000L Concrete Tanks, Florida	67.0	6.70
[103]	Lake Ramgarh, Gorakhpur, India	12.5	0.72
[105]	Small Enclosures, Belo Horizonte, Brazil	20.3	2.03
	Giant Water Hyacinth	25.0	2.50
	Dwarf Water Hyacinth	6.4	0.64
	Dymond (1974), cited by (Mitsch, 1974)	14.0	1.40
	Penfound (1956), cited by (Mitsch, 1974)	31.6	3.16
	Westlake (1963), cited by (Mitsch, 1974)	15.0	1.50
[106]	Wahlquist (1972), as cited by (Mitsch, 1974): No Fertiliser	17.4	1.74
	Wahlquist (1972), as cited by (Mitsch, 1974): P addition	55.0	5.50
	Wahlquist (1972), as cited by (Mitsch, 1974): P+N addition	59.0	5.90

\*If not stated, 90% was used as moisture content to calculate fresh weight (FW) and dry weight (DW)

## 2.2.6. Toxic substances

As previously discussed, pH and salt concentration have a significant effect on WH growth and survival. Another toxic substance to WH are herbicides, which have been used to control populations of WH in Florida, USA since the 1970's [107].

WH has been shown to grow in polluted waters [13,14,24,25,108–113], including artificially spiked water, heavy metal rich industrial effluent, sewage wastewater and polluted rivers. This has shown that WH is capable of surviving significant concentrations of HMs: Majumdar *et al.* spiked cultivated WH with As, Pb and Cd up to 100x the concentration of the natural water bodies (10, 2 and 0.5 mg/L respectively) [13]. This led to significant uptake by WH, of which the majority remained in the roots; however, some metal poisoning was evident due to the high concentration. In polluted wastewater, as opposed to spiked laboratory grown plants, HMs can accumulate within WH organs without displaying signs of metal poisoning [14]; Gopal showed that there is significant variation in metal concentration within WH, Fe varying from 232-15,500 ppm across the literature cited [25]. However, some HMs appear to have a greater toxicity to WH than others: Palihakkara *et al.* showed that a Cu concentration of 4 mg/L is toxic to WH whereas Cd at the same concentration was not [112]; however, this Cu concentration is unlikely to be reached under normal conditions. The phytoremediation capacity of WH will be discussed later in this study.

## 2.3. Utilisation of water hyacinth biomass

The utilisation of WH has been comprehensively reviewed, particularly in recent times [55,114–118]. These areas are varied and numerous, and include:

- Conversion to energy
- Food (animal and human)
- Fertiliser/compost
- Construction
- Pulp, paper and rope
- Homeopathic medicine
- Growth substrate
- Effluent treatment

This suggests a plant that has multiple applications; however, the composition of the biomass is vital in the success of each method.

### 2.3.1. Harvesting water hyacinth

Two aspects were considered here: the regularity of harvest and the methods of harvests. The impact of harvesting regularity has been investigated multiple times; Reddy and D'angelo found that increasing the number of harvests increased the biomass production and the nutrient removal, varied between 1, 3 or 21 harvests in a 13 month experiment [102]. Secondly, it reduced the detritus formed in the base of the cultivation tank, therefore, reducing biomass loss and the cleaning requirements in

long-term cultivation [102]. This harvesting interval was ~19 days, under half that of Fernando, who demonstrated that a harvesting interval of 40 days increased the yield to 566 from 348 g DW/m<sup>2</sup>, for a 30 day harvesting interval [99], suggesting that Reddy and D'Angelo may have over harvested the biomass. Sun and Zhu produced a decision model to examine the maximum sustainable yield when a population is harvested weekly; the study found that 14,059 m<sup>2</sup> could be harvested, out of a maximum 154,649 m<sup>2</sup> (9.1%) [119].

The harvesting interval may vary as growth rate does: Ho and Wong suggested that harvesting intervals should be reduced in summer to increase the nutrient removal potential of the plant [101]. This is due to the increased nutrient removal potential of plants that are regularly harvested, in comparison to populations that are not harvested [120]. Lorber investigated three harvesting simulation strategies; varying the harvesting intensity to fit uniform harvesting, medium intensity across the year; gas demand, high intensity during winter and low intensity in the summer; and growth rate, high harvesting intensity in the summer and low in the winter [121]. The target yield, of 55 t/ha/yr, was only achieved by the uniform and growth rate strategies, however, the target average density was only achieved by the growth rate strategy as the uniform strategy reached minimum densities over the winter due to over harvesting [121].

Harvesting of WH has two predominant methods: manual and mechanical removal. Manual removal requires a large amount of labour hours and therefore can incur high costs [122,123], however, it is suitable for small scale harvesting [124]. Gunnarsson and Petersen estimated that one person can harvest 200 kg FW/hour, provided the plants are close to the shoreline [125], whilst Ramaprabhu and Ramchandran suggested that it would take one person 360-900 hours to clear one hectare (ha), assuming a mat density of 20-30 kg/m<sup>2</sup> [126], a density that was lower than the average found in Table 2.2-1. This clearance was similar to that of WL and *Salvinia*, however, the biomass density was higher for WH [126]. If a density of 20-30 kg/m<sup>2</sup> was applied to 200 kg FW/hour, the clearance rate would be 1000-1500 hours/ha, for one person, or 6.7-10 m<sup>2</sup> per hour. In comparison, Dar found that a specialist WH harvester could clear 40 m<sup>2</sup> per hour, utilising 7 L of diesel [127]; further analysis must be conducted to determine the cost effectiveness of the mechanical harvester, in comparison to manual harvesting, however mechanical harvesters can collect biomass from deep and fast flowing water that humans would not be able to access [124], as well as operating at a higher speed for greater lengths of time.

The mechanical harvester described by Dar, utilised two conveyers and cutters on a floating structure [127]. The cutters are important to the harvesting of WH due to the density of the mats, which can be linked across multiple plants through the stolon [25],



and therefore should be broken up before being added to the conveyor [127]. Chopping is also important for transporting WH: WH has a low bulk density of  $\sim 96 \text{ kg/m}^3$ , compared with  $700\text{-}1100 \text{ kg/m}^3$  for coal [128], making transportation costly, nevertheless, when utilising a 'chopper *cum* crusher', Mathur and Singh were able to reduce the average specific volume from  $8.25$  to  $5.28 \text{ m}^3/\text{t}$  [129]. However, it has been reported that cutters become easily clogged by plants or debris which slows the removal [33]. Other issue faced by Dar were regular overheating of the engine, full capacity performance, contamination of the motor with water and manoeuvrability in shallow water [127].

There are many types of aquatic weed harvesters, including mechanical cutters, rotovation, rototilling, hydro-raking, rollers and sweeper [130]; these can include fully functional aquatic machines, small boat attachments, or portable boat mounted devices [130]. Wolverton and McDonald examined three different harvesters: a conveyor and cutter; a conveyor and a clamshell bucket with dragline [33]. The conveyors were limited by the success of the boats guiding biomass onto the conveyor which reduced the percentage of time the conveyor was loaded with WH, however, a better system design would increase the effectiveness, for example, the inclusion of funnels to direct the biomass onto the conveyor [33]. The clamshell was named as the most versatile, as it could be easily converted from standard equipment and the waterbody had little impact on its functionality: boats could be employed to move the biomass to the shore for easy removal. The conveyor and cutter had the lowest removal rate,  $2.3 \text{ t/hr}$  on average, compared with  $9.3 \text{ t/hr}$  for the conveyor and the clamshell bucket [33]; this was largely due to the clogging of the cutter with debris. However, all systems performed better than the harvester described by Dar: assuming a biomass density of  $42.9 \text{ kg FW/m}^2$ , calculated as the average density from Table 2.2-1, the harvester would achieve a biomass recovery of  $1.7 \text{ t/hr}$  [127]. Musil and Breen described a study, by Van Dyke [131], that was able to recover  $0.61 \text{ t/hr}$ , assuming an 8 hour working day, the lowest performing study described [132]. In contrast, Su *et al.* discussed a WH harvester from Shanghai that was able to recover  $70\text{-}80 \text{ t/hr}$  [124], however, this was stated without any reference to the company or machine so this cannot be verified. Due to the disparity between this value and the recovery yields described, this value seems improbable.

The cost of harvesters vary depending on the complexity and location, similar harvesters to that described by Dar cost from USD  $\$69,980$  to  $199,980$  plus transportation costs [133], therefore, investment must be considered carefully. Greenfield estimated that mechanical harvesting may range from USD  $\$500\text{-}800$  per acre plus the initial start-up cost [130]. In contrast, a later study by Greenfield estimate the costs as

little as USD \$477 to 2,146/ha during the spring, a cost comparable to that of chemical herbicide application [134]. Harvesters are available worldwide, with many companies operating in the USA and China [124,130,133], suggesting that purchasing a harvester would be possible from anywhere in the world.

One harvester design in literature is particularly intriguing, Valk, through discussions with designer of dredging equipment, designed a boat that was able to harvest WH and split the biomass into leaves and roots, the biomass was then shredded to reduce bulk density for transport [55]. This design would remove the time required to split the roots manually and therefore remove significant concentrations of HMs from the utilisation methodology; the roots could then be disposed of safely or utilised in a different method. The estimated costs of the harvester and shredder were €650,000 and €250,000, respectively; with an energy requirement of 400 and 500 kW, respectively [55]. The maintenance and operational costs of the machinery was assumed to be €32,490 and €12,500, for the harvester and shredder, respectively [55]. Whilst the theoretical potential of this harvester is encouraging, it was not be possible to identify any practical application of the design.

### 2.3.2. Influence of composition on utilisation technique

The chemical composition of WH has been described on many occasions throughout the several decades of study. Some examples are displayed in Table 2.1-1; this demonstrates that WH varies by location/ environmental conditions, however, it also demonstrates phenological and morphological variations, see sections 2.1.2.6 and 2.1.3.1, respectively.

There are clear variations between the studies, for whole biomass, however, there are consistent trends: lignin is consistently below 10% dry weight, with the exception of one study, whereas holocellulose accounts for ~50% dry weight; water content is >90%; protein content is approximately >10%; and ash content is >10%. Lignin content and lignin-carbohydrate interactions are key limiters in the anaerobic digestion (AD) of biomass because lignin is largely insoluble and resistant to degradation by anaerobic bacteria, present in AD [135]. WH has a relatively high lignin content, lower than typical grasses but higher than WL and seaweed [43,136,137], suggesting that it is not an optimal feedstock for AD. However, WH does contain higher cellulose than WL and similar amounts to grass. WH also contains higher concentrations of NPK, in comparison to traditional feedstocks, like cow manure (CM), used in rural AD [138]. This would likely improve the quality of digestate, as a fertiliser, in comparison to CM digestate.

The high-water content of WH would reduce the applicability of thermal conversion methods, like combustion and pyrolysis. Secondly, WH has a higher ash content than most biomass utilised for thermal energy conversion [47]. Therefore, it is unlikely that WH would be considered for thermal conversion; however, it is possible that WH residue, from an alternative process like protein extraction, or WH roots could be disposed of utilising incineration. The high HM concentrations within the roots could be an obstacle for this method. The high HM content of WH could be a challenge for a variety of methods, in particular biological routes: the impact of toxic metals could reduce efficiency of biological conversion methods. Combustion would also be affected, where high HM or ash content can result in issues with slagging or fouling [139] and toxic emissions [140].

Whilst a protein content of >10% is lower than other biomass utilised for protein extraction, soybean typically contains 40% protein [141], the variation in tissue protein content demonstrates that this biomass could be utilised as a feedstock for a variety of different methods. For example, high protein content within the leaves, low lignin content within the petioles and high trace metal concentrations in the roots could be utilised to for protein, AD and phytomining or high value element extraction, respectively.

### 2.3.3. Phytoremediation

Phytoremediation is the process of removing contaminants from soil or water. Various plants have been considered in literature, including WH, WL, *Azolla pinnata* and *Lemna minor* (Duckweed- DuW) [110,117,142,143], depending on their affinity for different contaminants. The key pollutants discussed here are HMs and nutrients.

#### 2.3.3.1. Heavy metals

The phytoremediation of HMs from wastewater and polluted aquatic systems produces biomass containing high concentrations of toxic HMs, therefore, disposal or utilisation of this biomass is highly problematic.

WH can tolerate high concentrations of HMs due to a low TF for a variety of metals. This includes Cd, Cr, Cu, Pb and Zn; when compared with *Echinochloa polystachya*, WH was able to accumulate higher concentrations, of these elements, in its roots, whilst containing lower concentrations in the above water tissues [65]. Similarly, WH has been shown to have a higher BCF, for Cd, Cr and Pb, than WL [66]. In this study, both WH and WL had a BCF of >1000, for Cu, Cr, Pb and Zn, indicating that the biomass contained 1000 times the concentration in the water, therefore, these plants would be considered hyperaccumulators [66]. The WH roots in this study had an increased BCF, compared with the whole plants, and reached 950 for Cd, indicating

that the roots alone contain a high enough concentration to be considered a hyperaccumulator for Cd, Cu, Cr, Pb and Zn. In contrast, Shirinpur-Valadi *et al.* found that WH shoots had a higher BCF than the roots, for Cd, Ni and V [67]; this is a highly unlikely result based on the low TF shown by previous studies. Shirinpur-Valadi *et al.* also reported that DuW accumulated greater concentrations of Cd, Co, Ni, Pb, V and Zn than WH [67]. This is in contrast to other comparisons of WH and DuW: Alvarado *et al.* demonstrated that WH was able to accumulate 600 mg As/ha/day, in comparison to 140 mg As/ha/day for DuW, however, this was largely due to increased biomass production of WH [17]. Rai demonstrated that WH was able to accumulate greater quantities of Cu, Cr, Fe and Zn, than DuW, regardless of the concentration [143]. However, the increased concentrations of HM resulted in physiological/biochemical: reduction of chlorophyll, protein and sugar [143]; this is important as these components are vital for survival and utilisation. Gameda *et al.* compared the uptake of Cr by WH and DuW; WH was able to accumulate greater total Cr and Cr (III), however, DuW was able to remove greater quantities of Cr (VI) [144]. This is an important distinction, it is vital to understand the nature of the pollutant, whilst WH was able to accumulate greater concentrations of Cr (III), if this was not the predominant form of Cr in the water, it would not be an appropriate choice for phytoremediation.

As previously stated, WH has a low translocation factor for a range of metals and it has been demonstrated that WH roots can accumulate ten times more than the above water tissues [145]. However, translocation of toxic elements can occur: Victor *et al.* stated a translocation factor 3.35 for Cd [66], and Fawzy *et al.* showed highest concentration of Pb in the leaves [146]. However, for both studies, there were other metals that accumulated in greater amount in the roots. This translocation of metals is not a problem in low quantities, however, there is evidence that the presence of metals in the leaves reduces transpiration, even at low concentrations [147]. At higher concentrations, significant toxicity is exhibited [112], however, if the concentration in the water is still low then metals can be accumulated in significant quantities.

WH has been suggested for biomonitoring due to the positive correlation between Cd concentration in the water and the roots [148]. However, it could be suggested that this is site dependent, corroborated by the findings of Majumdar *et al.*, who demonstrated that the accumulation of As, Cd and Pb were not dose dependent [13].

The removal of HMs by WH appears to be highly element and site specific: Table 2.3-2 displays a range of study locations, environmental conditions, HMs, concentrations and results. However, most studies agree that WH has a low TF and high BCF for the majority of elements studied. Figure 2.3-1 depicts the water HM concentration against the percentage removal, of various elements, from the studies shown in Table 2.3-2.

This demonstrates that there is significant variation between the studies and elements, with only Cd removing >60% for all conditions studied.

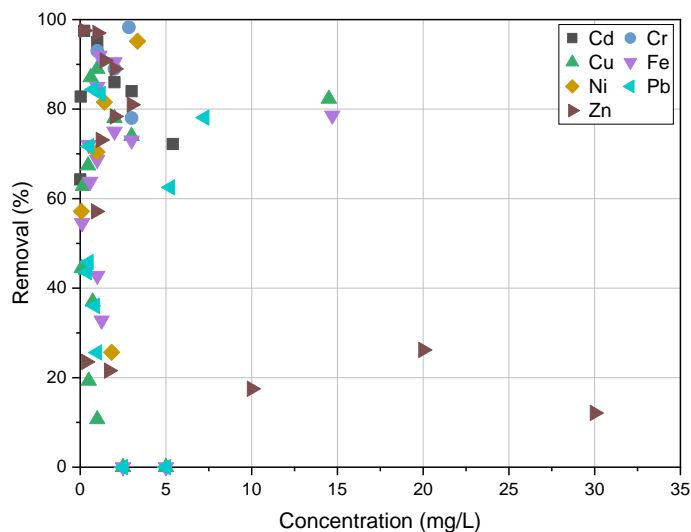


**Figure 2.3-1:** Water heavy metal concentration against percentage removal by water hyacinth, from studies in Table 2.3-2.

The translocation of metals, by WH, has been shown to be relatively low, this is corroborated by the studies of Table 2.3-2; these studies have been summarised and averaged in Table 2.3-1. This demonstrates that only Cd had a translocation factor >1, however, the large range resulted in an error margin that suggests that this may be insignificant. Out of the eight studies, that included Cd, listed in Table 2.3-2, five demonstrated a TF of >1, whilst two of the other three were <0.01. This implies that Cd translocation is highly variable, depending on the conditions.

**Table 2.3-1:** Average heavy metal concentrations for water hyacinth below and above water tissues, from studies in Table 2.3-2.

Element	Concentration of tissue (ppm)		Translocation Factor
	Below Water	Above Water	
Cd	1.3 ± 1.7	0.9 ± 1.3	2.4 ± 2.9
Co	5013.9 ± N/A	1164.3 ± N/A	0.2 ± N/A
Cr	45.4 ± 35.9	10.3 ± 6.4	0.4 ± 0.3
Cu	44.5 ± 34.2	19.6 ± 12.8	0.6 ± 0.3
Fe	7916.9 ± 8949.7	1351.5 ± 1788.1	0.1 ± 0.0
Mn	9.6 ± N/A	4.6 ± N/A	0.5 ± N/A
Ni	31.3 ± 30.8	15.6 ± 16.5	0.4 ± 0.3
Pb	166.9 ± 455.2	23.2 ± 42.7	0.7 ± 0.8
Ti	900.0 ± N/A	166.7 ± N/A	0.2 ± N/A
Zn	105.3 ± 127.8	74.2 ± 78.6	0.8 ± 0.2

The translocation of metals is related to the method of retention by the biomass; Vesik *et al.* investigated the localisation of HMs within the root tissue of WH [149]. This study determined that Al, Fe, Mn and Ti were localised on the surface of the roots, whereas Cu, Pb and Zn were in greater concentrations within the inner sections of the roots. All metals showed spikes in specific locations of the root, with the exception of Pb, which appeared to be consistent across a large range of the root, suggesting that it was at a low level distribution [149]. There was some increase in K and Mg within the centre of the root, this is likely due transportation of these elements to the stele for translocation up the plant [149]. The retention of Al, Mn, Ti and Fe on the epidermis external walls, suggests that there will be lower retention of these metals in comparison to metals contained within the biomass or cells [149]. It is believed that the toxicity of reduced forms, of Fe and Mn, is avoided through oxidation [149]. The external retention is likely to reduce the translocation of elements to the upper tissues.

Translocation of HMs can lead to significant impacts on the survival of a plant; firstly, HMs can induce deficiencies in essential elements, this can be through dilution of essential elements or substitution of the HM into metalloproteins [150]. Substitution of HMs can impact photosynthesis, with targets sites including photosynthetic pigments and enzymes, and photosystems [150]. One important damage mechanism is the substitution of the chlorophyll central atom, Mg, by HMs (Cd, Cu, Hg, Ni, Pb, and Zn) to produce a HM-chlorophyll molecule [151]. This primarily occurs at low light levels and often produce a complex that is more stable to irradiance than Mg-chlorophyll [151]. It has been shown that stress by Cu, impairs photosynthetic pathways quicker than impairments to cell division [152]; the blue-green Cu-chlorophyll complex is highly stable and appears vital even when dead [151].

**Table 2.3-2:** Heavy metal removal by water hyacinth.

Area of Study	Metals/ Metalloids	Conditions (mg/L unless stated)	Accumulation (mg/kg unless stated)	Removal (%)	General Results	Reference
IISER, Kolkata, India	As, Pb, Cd	Spiked Solution: 1, 5, 10 As 0.5, 1, 2 Pb 0.1, 0.3, 0.5 Cd	Root (Highest): As 1mg/L- 58.8; Pb 1mg/L- 34.3; Cd 0.3mg/L- 2.5 Petiole (Highest): As 1mg/L- 16.74; Pb 1mg/L- 18.7; Cd 0.3mg/L- 1.9 Leaf (Highest): As 1mg/L- 12.2; Pb 1mg/L- 11.6; Cd 0.3mg/L- 1.4	N/A	Used as substrate for vermicomposting. Control soil contained As 134.69 mg/kg compared to 23.9 for vermicompost. Trial on fruit bearing plants showed little contamination and improved growth.	[13]
Sleman, Yogyakarta, Indonesia	Fe, Cu, Cd, Pb	Leachate from Integrated Waste Disposal Management Plant	N/A	Using Electro- Assisted Phytoremediation 77.8, 22.0, 31.6 and 30.0% was removed after 11 days (Fe, Cu, Cd, and Pb)	Decrease in TDS, EC but increase in DO.	[109]
Bukit Besi, Terengganu, Malaysia	Fe	Polluted lake: Fe 2	N/A	Fe 90.5%	After 28 days the WH was healthier than WL. WH was more effective at reducing P, COD and EC than WL and <i>S. molesta</i> .	[110]
Bolgoda Lake, Panadura, Sri Lanka	Cd, Cu	Stock Solution Cd 0.005, 0.01, 0.02 Cu 1.02, 2.46, 4.78	N/A	100% Cd Removal: 0.005- 2 days 0.01- 2 days 0.02- 3 days 100% Cu Removal: 1.02- 2 days	No plant survived more than 14 days. Rapid decrease of Cd in first 24 hours (sorption)	[112]

					2.46- N/A (>6 days) 4.78- N/A (>6 days)		
Loktak Lake, Manipur, India	Cu, Cd, Cr, Zn, Fe	Spiked Solution: 1, 2, 3	N/A		1, 2 and 3 mg/L (15 days): Fe 85, 75, 73 Cu 89, 78, 74 Cd 95, 86, 84 Cr 93, 89, 78 Zn 97, 89, 81	Maximum removal on 12th day. WH was more efficient than <i>L. minor</i> and <i>A.</i> <i>pinnata</i> . Reduction in chlorophyll, protein and sugar with increased HMs.	[143]
Caximba Landfill, Parana, Brazil	Cu, Cr, Zn, Ni, Pb, Cd	Landfill leachate treatment lagoon Natural wetlands with several species (WH dominant)	Root: Cu 0.5-0.9; Cr 3.3-4.6; Zn 3.1-5.5; Ni 0.4-0.7; Pb 0.4-5.2; Cd 0.2-0.4 Above Water: Cu 0.3- 1.9; Cr 2.0-3.5; Zn 2.5-5.5	N/A		Reduction of 75% BOD, 63% COD, 84% ammoniacal N, 89% TN, 70% P. Higher Cd, Cr, Pb in roots than <i>E.</i> <i>polystachya</i> . Lower metals in above water.	[65]
Unknown River, Ivory Coast	Zn, Cd, Pb, Cu, Cr	Industrial Park Wastewater	Root: Zn 1792.7 Cd 0.7* Pb 104.5 Cr 655.3 Cu 225.2		Zn 97.6 Cd 64.3 Pb 87.5* Cu 71.2* Cr 8.3*	Cd had a TF of 3.35 (rest were <0.5). Roots had a BCF of 957-8428 for all metals.	[66]
Rasht, Gilan, Iran	Pb, Zn, Cr, Cd	Various Rivers and Lagoons: Cd 0.027- 0.052 Cr 0.01-0.65 Zn 2,7-26.5	Roots Mean: Cd 19.93; V 0.19; Ni 0.09 Above Water Mean: Cd 173.9; Co 4.91; V 2.17; Cr 21.78; Zn 241.6; Ni 2.6; Pb 115.7	N/A		Compared with DuW, <i>Cyperus alterifolius</i> , <i>Canna x generalis</i> DuW fronds had highest uptake of Cd, Co, V, Cr, Zn, Ni and Pb.	[67]



		Pb 0.15-16.51 Control solution (all 10)			The control water had the highest uptake rate.	
Loktak Lake, Manipur, India	Fe, Cu, Cd, Cr, Zn, Ni, As	Effluent Discharge point	N/A	Fe 83 Cr 66 Cu 63 Cd 6 Zn 79 Ni 67 As >60*	WH was more efficient than WL and S. polyrhiza. No visible adverse effects. TF was <1 for all but >0.5 for Fe, Cr, Cu, Cd, Zn and Ni	[74]
Hattar, Pakistan	Cd, Pb, Hg, Ni	Effluent: Cd 0.24 Pb 1.20 Hg 4.97 Ni 3.34	N/A	Cd 97.50 Pb 83.40 Hg 99.94 Ni 95.18	Performed better than sludge at reducing EC, turbidity, COD, ammonia, phosphate, Ni, Pb.	[153]
Yeltsovka River, Novosibirsk, Russia	Cd	Control and 130 µg/L	Leaf: Control- 0.3 130 µg/L - 31	N/A	Sorption of Cd onto roots and localised to cortex and rhizodermis of roots before translocation	[154]
Hayatabad, Khyber Pakhtunkhwa, Pakistan	Al, As, Cd, Cr, Cu, Fe, Mn, Pb, Zn	Effluent: Al 22.17 As 5.03 Cd 0.03 Cr 2.84 Cu 0.16 Fe 14.70 Mn 20.37 Pb 5.25 Zn 2.01	Whole: Al 16.16 As 1.31 Cd 0.02 Cr 1.78 Cu 0.13 Fe 9.00 Mn 9.69 Pb 3.28 Zn 1.58	Al 72.91 As 26.07 Cd 82.80 Cr 98.28 Cu 62.82 Fe 78.57 Mn 61.14 Pb 62.51 Zn 78.35	WH had a higher efficiency than WL. Al, Cr, Fe, Mn, Zn, Pb accumulated at higher concentrations in the above water tissues.	[155]

Eutrophied Lake (Not Stated)	Zn, Cr	Stock Solution Zn(NO <sub>3</sub> ) <sub>2</sub> ·6H <sub>2</sub> O K <sub>2</sub> Cr <sub>2</sub> O <sub>7</sub> ·5H <sub>2</sub> O	N/A	Zn 0 Nutrients- 97 0.5 Nutrients- 91 1 Nutrients- 86 Cr 0 Nutrients- 90 0.5 Nutrients- 87 1 Nutrients- 82	Maximum removal at neutral pH, low salinity, low metal concentrations, lack of nutrients	[156]
Dhanbad, Jharkhand, India	Mn, Cu, Pb, Cd	Mine Waste: Mn 0.06-0.22 Cu 0.002-0.009 Pb 0.010-0.014 Cd 0.001-0.005	Leaf: Mn 62.9-67.9 Cu 3.86-13.54 Pb 3.4-5.06 Cd 0.037-0.13	N/A	More metals in sediment than water. Root concentrates metals but leaves are 75% of above water dry matter so can reach high total.	[157]
Freshwater Ponds, Lahore, Punjab, Pakistan	Zn, Pb, Fe, Cu, Ni	Leachate Addition (%): 0, 25, 50, 75, 100	N/A	Highest Removal (75% Leachate): Zn 90.09 Pb 84.44 Fe 87.10 Cu 92.96 Ni 81.56	Significant reduction of pH, TDS, BOD and COD for 50% and 75% leachate. Removal was poor for 100%. TF <1.	[158]
Aquaculture Store, Bogor, West Java, Indonesia	Zn	Artificial AMD: 10, 20, 30 AMD: 7790, pH 3	10: 1581.16 20: 3165.31 30: 3967.92 7790: 1190.02	10: 0-19.4 20: 7.1-27.8 30: 8.3-18.2 7790: 0-21.6	Artificial AMD showed a pH increase and no adverse effects. AMD showed toxicity symptoms in the 2-week period. pH rapid increase over 1st 3 days then slow increase.	[159]

Nile Delta, Egypt	Cd, Co, Cr, Cu, Fe, Mn, Ni, Pb, Zn	River Water: Co 0.01-0.08 Cr 0.22-2.99 Cu 0.03-0.05 Fe 1.08-4.20 Mn 0.12-0.54 Ni 0.22-2.93 Pb 0.01-0.05 Zn 0.09-0.43 Cd (ug/L) 0.67-1.50	Co 0.3-21.4 Cr 1.7-82.2 Cu 3.2-30.4 Fe 353.9-20752.2 Mn 182-7195.9 Ni 1.5-49.2 Pb 0.4-2.9 Zn 7.6-133.6 Cd 0.07-0.20	N/A	BCF >1 for all; TF <1 for all but Pb; Higher levels in Roots. Concentrations in tissues showed correlations with water concentration suggesting biomonitoring potential.	[160]
Valsequillo Reservoir, Puebla, México	Co, Zn, As, Ni, Cu, Pb, Ti, Cr, Ba, Mo, V, Hg, Cd	Valsequillo Reservoir (ug/L): Co 1.2 Zn 6.9 As 3.4 Ni 4.8 Cu 1.7 Pb 0.9 Ti 3.2 Cr 2.0 Ba 78.9 Mo 1.4 V 4.7 Cd 0.6 Hg 0.6	Submerged Mean: Co 18.6; Zn 249.0; As 9.3; Ni 69.6; Cu 74.6; Pb 37.6; Ti 900.0; Cr 63.6; Ba 86.6; Mo 9.6; V 80.6; Cd 0.4; Hg BDL Above Water Mean: Co 2.6; Zn 159; As BDL; Ni 23.3; Cu 18.0; Pb 15.0; Ti 166.7; Cr 14.3; Ba 175.6; Mo 4.6; V 15.3; Cd BDL; Hg BDL	N/A	Higher sediment metal concentration than water. All TFs <1 except Ba (3.49). Mirroring of roots and sediment HMs, prediction that root deposition contributes to pollution.	[68]
Ayetoro waterways of Ilaje Local Government Area (LGA), Ondo State, Nigeria	Pb, Cu, Fe	Stock Solution 1000 mg/L of each metal 1, 2, 5 and 10 mL of stock solution	Root Mean (mg/g): Pb 10.78 Cu 5.88 Fe 183.18 Petiole Mean (mg/g): Pb 3.46 Cu 3.65 Fe 10.48	1mL- Pb 45.81; Cu 19.29; Fe 72.03 2mL- Pb 25.62; Cu 10.69; Fe 42.77 5 and 10 mL- No significant reduction	No visible effects from 1 or 2 but 5 and 10 had high Cu so no removal (21 and 30 mg/L), suggested due to reduction in transpiration. Fe showed low	[161]

			Leaf Mean (mg/g): Pb 0.56 Cu 0.74 Fe 7.58		retention in deionised water.	
Hayatabad Industrial Estate, Peshawar, Pakistan	Cd, Cu, Pb	Industrial Park Wastewater: Cd 5.4 Cu 14.5 Pb 7.25	Root: Cd 3.5-5.8 Cu 663.7-1313 Pb 1049-1738 Above Water: Cd 1.4-3.3 Cu 97.2-101.5 Pb 118.3-155.4	Cd 72.2 Cu 82.3 Pb 78.1	BCF: Cd 62; Cu 3666; Pb 10383. Highest root accumulation of Cu and Pb, WL highest Cd. Translocation: Cattail<WL<WH<DuW	[69]
Lian River, Guangdong, China	Ag, Cd, Co, Cr, Cu, Mn, Ni, Pb, Sb, Sn, Tl, Zn	13 sites- Sediment (mg/kg): Ag 0.29-84.3 Cd 0.76-17.6 Co 8.3-24.7 Cr 66.4-211 Cu 60.1-4901 Mn 363-868 Ni 55.4-1115 Pb 80.3-2225 Sb 35.6-459 Sn 26.2-388 Tl 1.13-1.47 Zn 318-2060	Leaf: Ag 0.007-0.579 Cd 0.044-0.521 Co 0.12-1.81 Cr 14.6-86.2 Cu 15.0-43.5 Mn 221-958 Ni 2.87-32.3 Pb 1.26-5.57 Sb 0.30-15.4 Sn 0.68-18.3 Tl 0.005-0.040 Zn 36.9-197	N/A	All sites measured had Cu above the tolerable limits for Sheep and 1 for cattle. Relationship between root and sediment concentration ( $R^2 > 0.75$ ) for Ag, Cd, Ni	[162]

Sawangan, Depok, West Java, Indonesia	Pb, Cd, Cu	Water from Situ Agathis Lake, Depok, West Java, Indonesia	<p>Root:</p> <p>Small- Pb 1.34; Cd 0.047; Cu 53.5</p> <p>Medium- Pb 2.17; Cd 0.89; Cu 83.8</p> <p>Large- Pb 0.009; Cd 0.805; Cu 84.4</p> <p>Petiole:</p> <p>Small- Pb 0.15; Cd 0.05; Cu 16.7</p> <p>Medium- Pb 0.01; Cd 0.03; Cu 15.7</p> <p>Large- Pb BDL; Cd 0.018; Cu 11.2</p> <p>Leaf:</p> <p>Small- Pb 0.06; Cd 0.05; Cu 7.69</p> <p>Medium- Pb 0.08; Cd 0.02; Cu 15.1</p> <p>Large- Pb BDL; Cd 0.0007; Cu 17.6</p>	N/A	<p>Decreasing metal accumulation with size. Roots accumulate more HMs TDS reduced from 261 to 204ppm. TSS reduced from 0.0449 to 0.0151 ppm.</p>	[163]
Clementi Station, Singapore (plants purchased from shop)	Pb, Cu, Cd, As	Stock solution: 2 or 8 of individual metals 2 combined	<p>Root Mean: 393-3192</p> <p>Leaf Mean: 6-10</p>	<p>Pb 2- 100 (1 day); 8- 100 (1 day) Cu 2- 100 (2 day); 8- 100 (2 day) Cd 2- 99; 8- 89.5 As 2- 100 (2 day); 8- 99.5 Combined- All 100. Pb 1 day; Cu 2 day; Cd 4 day; As 4 day Max 7 days</p>	<p>Hyperaccumulator for Pb and moderate for the rest. Ligands (O-H; C-O; C- C; C-H) aid in accumulation of HMs in tissues.</p>	[164]

Nile Delta, Egypt	Cd, Co, Cr, Cu, Fe, Mn, Ni, Pb, Zn	River Water (ug/L): Cd 0.2-2.0 Co 10.0-83.0 Cr 218.0- 2993.0 Cu 6.9-73.9 Fe 383.0- 6870.4 Mn 64.3- 629.3 Ni 223.5- 2934.0 Pb 8.5-170.0 Zn 70.0-788.4	Root: Cd 0.1-0.3; Co 15-22; Cr 37-87; Cu 17-42; Fe 9988-22612; Mn 2624- 7198; Ni 20-50; Pb 0.1-4.5; Zn 43-136 Petioles: Cd 0.1-0.2; Co 0.4-1.6; Cr 1.4-6.3; Cu 2.7- 16.8; Fe 351-1473; Mn 209-604; Ni 1.5-6.4; Pb 0.1-1.5; Zn 7.1-39.5 Leaf: Cd 0.1-0.3; Co 0.1- 1.7; Cr 5.0; Cu 14.4; Fe 396-2197; Mn 180-391; Ni 2.8-7.9; Pb 0.1-2.0; Zn 15.9-29.7	N/A	BCF >1 for all HMs. TF <1 for all HMs. T-values were not significant indicating a good fit of the equations to forecast HM uptake in the Nile Delta. R <sup>2</sup> for BCF vs Water Concentration was >0.9 for Co, Cr, Cu, Fe, Ni.	[70]
Marriott Lake, Alexandria Governorate, Egypt	Fe, Cu, Ni, Pb	Lake Water (ug/L): Fe 19.3 Cu 4.6 Ni 5.3 Pb 2.3	Root: Fe 5847.45 Cu 28.20 Ni 50.99 Pb 32.38 Above Water: Fe 653.03 Cu 13.58 Ni 40.20 Pb 18.68	N/A	70% WH coverage, 25 cm depth and retention time of 3-5 days was the optimum design.	[165]

\*Estimated from Paper (graphical representation/calculation); BOD= Biological oxygen demand; COD= Chemical oxygen demand; EC= Electrical conductivity; TN= Total nitrogen; TDS= Total dissolved solids; DO= Dissolved oxygen; AMD= Acid mine drainage.

### 2.3.3.2. Nutrients

WH has a high nutrient uptake rate which helps it to outcompete other aquatic plants; its high growth rate and uptake rate has led to WH being utilised as a method of reducing nutrients in natural ecosystems or nutrient based industrial waste waters.

In Lake Caohai, WH was used in an attempt to stop eutrophication by removing P [166]; after the deliberate introduction of WH, downstream of the cultivation sites had reduced P by over half, as well as an increase in DO, despite the coverage of WH mats. Iamchaturapatr *et al.* compared the uptake of N and P by 21 different wetland plants, both emergent and floating, and demonstrated the WH had a poor nutrient uptake on an area basis, likely due to the high coverage of floating plants in comparison to emergent plants [167]. However, on a weight basis WH performed better than 16 and 19 plants for N and P, respectively; water caltrop and Manchurian wild rice out performed WH in the recovery of both N and P [167]. This is in contrast to a study comparing WH to WL, *Limnobiium laevigatum* and *Lemna sp.*, where WH recovered the lowest percentage of TN, however, it had the highest growth rate and greatest resilience to the swine wastewater effluent [43]. WH showed a maximum growth rate of 5.2 g DW/m<sup>2</sup>/day, demonstrating a large decrease in the predicted growth rate shown in Figure 2.2-1. Another impact of the effluent was the reduction in lignin content of the plants [43]; this suggests that WH utilised in wastewater phytoremediation may be easy to break down and produce greater yields during certain energy conversion techniques. Swine effluents have been studied multiple times and recovery has been shown to be high: 88% and 100% of ammoniacal nitrogen (AN) and COD were removed, respectively [98]. This clearly shows that WH can remove high levels of nutrients from nutrient rich waste waters. The next step is to retain the nutrients and remove the biomass; in a study remediating sewage treatment effluent, WH tissues contained 5.42, 1.97 and 4.57% for N, P and K, respectively [101].

The concentration of nutrients in the water is likely to have an impact on the removal of nutrients, for example, a reduced N:P ratio has been shown to reduce the adsorption of phosphorous [25,94]. This can occur due to increased denitrification of waters, a process that is exemplified by the presence of WH [168]. Fox *et al.* demonstrated that the percentage of N removal decreased as water N increased [89]. This relationship was from 40 to 300 mg N/L, in contrast, Imaoka and Teranishi examined the relationship of N recovery and water N concentration, from 0-50 mg N/L. This showed that recovery increased as N concentration increased, up to ~10 mg N/L, where the relationship plateaued [80]. The same relationship was true for water P concentration and P recovery, however, the plateau occurred above ~1 mg P/L [80]. Imaoka and Teranishi also showed that at a plant density >100 g/m<sup>2</sup>, the recovery of N and P was

reduced; secondly, the uptake of both nutrients were increased as temperature was increased [80]. Polomski *et al.* also showed that the plant N and P concentration followed a linear relationship with the total supply of these nutrients [169].

The presence of certain contaminants in a wastewater can result in reduced nutrient uptake: Caldelas *et al.* demonstrated that the presence of Hg reduced the accumulation of P, K, S, Ca and Mg in submerged tissues [170]. This was also true for the presence of Cu and antibiotic tetracyclines, where the reduction in removal was greater in the roots than the above water tissues; overall, the growth rate and uptake rate, of N, were reduced by increased Cu and TCs [171]. Similar impacts were observed in paper mill effluent: WH was unable to grow in 100 or 75% paper mill effluent, which resulted in poor removal [108]; however, at 50% the maximum removal was achieved and was able to reduce EC, TDS, BOD, COD, N, P and K by at least 70% within 60 days [108]. This removal is similar to that found in domestic waste water, by Rezania *et al.*, where COD, N and P were reduced by 80, 75 and 75%, respectively, in just one week [172].

#### 2.3.4. Energy generation

WH has been outlined as a source of biomass for the conversion to energy as far back as the 1930's [25]. The main areas of interest are the production of biogas, ethanol, hydrogen and bio-oil. WH grows quickly, has high cellulose and low lignin and is easily hydrolysed, making it a priority plant for the production of bio-fuels [173].

##### 2.3.4.1. Thermal conversion

###### 2.3.4.1.1. Combustion

Combustion of sun-dried WH could provide a simple and cheap option and provide fertiliser from the ash. However, the high moisture and ash content, as well as low calorific value makes this less suitable. Table 2.3-3 displays the higher heating value (HHV) of various biomass groups, demonstrating an average HHV, of all the biomass was 18.87 MJ/kg. In comparison, Lara-Serrano *et al.* determined the HHV of dry WH to be 14.4 MJ/kg, therefore suggesting that even once dried, WH is not an appropriate material for direct combustion [63].



**Table 2.3-3:** Average higher heating value of various biomass, adapted from [174].

Biomass	Number of Samples	Average HHV (MJ/kg)
Energy Grass, <i>Miscanthus</i>	25	19.14
Energy Grass, other	17	18.04
Wood Material	18	19.58
Wood Waste	9	18.47
Cereals	16	18.61
Millet	6	18.17
Sunflower	6	20.26
Hemp	6	18.04
Waste	13	15.97
Other Plant Material	28	19.79
Other Non-Plant Material	10	20.32
All	154	18.87

\*This study, analysed via bomb calorimetry

There is little information on the effect of heavy metals in direct incineration of WH; however, combustion of coal high in arsenic leads to increased arsenic content in children [140], suggesting that hyperaccumulating plants like WH are not suitable for direct incineration. Further study of this is important as the use of residues for combustion may provide some energy recovery at the end of a different conversion process.

#### **2.3.4.1.2. Pyrolysis**

Pyrolysis is the thermochemical decomposition of organic materials in an inert atmosphere [175]. Pyrolysis and incineration work best when samples are dried; this suggests that these techniques are not suitable for WH, due to the high moisture and ash content, see Table 2.1-1. In experimental conditions, Biswas *et al.* demonstrated that pyrolysis of WH had a maximum yield of 24.6, 40.2 and 48.0% for bio-oil, gas and biochar, respectively, at temperatures varying from 300-450°C [175]. WH produced a higher yield of gas and char at its maximum conversion, compared with *Azolla* and *Sargassum tenerrimum* [175]. The analysis of the bio-oil showed a high concentration of functional groups, phenolic, ketones and nitrogen-containing groups, showing a high promise of a fuel [175].

#### **2.3.4.1.3. Briquetting**

Briquetting produces a uniform fuel and increases certain characteristics to produce a better fuel. The main characteristics that are altered are a reduction in moisture content and increased energy density [176]. In general, briquettes have certain advantages over wood [176]:

- Greater heat intensity
- Cleanliness
- Convenience in use
- Smaller storage required

When compared with charcoal and wood, WH briquettes (14.55-17.17 MJ/kg) have a similar calorific value to firewood (14.40-17.40 MJ/kg) but lower than that of charcoal (15-27 MJ/kg) [177–179]. However, the gas analysis of WH briquettes showed a reduction in the amount of S, N and chlorides suggesting it could be used in fuel applications [177]. The calorific value varies depending on the use of a binder, or binder; however, Davies and Davies suggested that without binder, WH would not meet minimum requirements for use as a fuel [180]. The binder also affects the moisture, ash, fixed carbon (FC) and volatile matter (VM): molasses increased moisture, VM and FC, whilst reducing ash, as content is increased [179]; as compared with empty fruit bunch fibres and cassava starch which decreased moisture, ash and FC, with an increase in VM as content is increased [178].

When examining WH briquettes as a cooking fuel, it was determined that both firewood and charcoal had a greater specific fuel consumption. However, the use of WH briquettes boiled water faster than charcoal, though slower than traditional firewood [181]. The boiling of water was sped up through the addition of firewood pieces, which resulted in cooking times quicker than kerosene [182]. Whilst WH briquettes are not ideal for energy or cooking fuels, the use of WH briquettes to reduce dependence on firewood or charcoal and reduce the impact of uncontrolled WH populations, means that WH still has potential to be used as a fuel, and has been suggested as an option for local communities in developing countries [183].

The studies discussed here all have a common gap: the inorganic content of WH can reach high concentrations, as discussed in 2.3.3.1, however, no study has discussed the potential implications of HM content in briquettes, this is an area that should be investigated.

#### **2.3.4.1.4. Hydrothermal processing**

The use of hydrothermal techniques has potential for biomass with a high moisture content, due to the removal of the need for drying. However, the use of WH in hydrothermal liquefaction (HTL) and hydrothermal carbonisation (HTC) have been sparsely reported.

Elliot *et al.* compared five feedstocks for HTL, demonstrating that WH had a similar oil production as wood in aqueous slurries with a higher H:C ratio and lower oxygen content [184]. Despite this, oils from WH had a high nitrogen content which could be a

problem if used as a fuel. Another study produced 16% oil weight percentage, which was increased to 23% with the addition of a catalyst [185], this was 3% lower than the yield achieved by the previous study.

Brown *et al.* produced hydrochars, via HTC, at 150, 200 and 250°C; this demonstrated that whilst it was possible to increase the energy yield of WH, with the maximum increase at 150°C, the chars could not be used for in large scale combustion due to issues with slagging and fouling [139]. The authors suggested that the chars were used in energy storage, batteries and super capacitors, soil amendments, low-cost phytoremediation sorbents and carbon sequestration [139].

#### 2.3.4.2. Anaerobic digestion

Biogas, a mixture composed primarily of methane (CH<sub>4</sub>) and CO<sub>2</sub>, is produced by the AD of biodegradable materials, including lignocellulosic biomass and biological wastes, like sewage or agricultural residues. The physio-chemical analysis of WH suggests that it has high potential for the production of biogas through AD: WH has a high moisture and soft organic matter content, as well as high levels of cellulose/hemicellulose with low lignin and a C:N ratio that falls within the “ideal range”, which varies from 12 to 32 [186–189]. WH has been compared with other feedstocks, including *Salvinia*, channel grass and water chestnut, and demonstrates a higher maximum cumulative production of biogas, as well as a higher methane content/electrical generation potential [186,187,189].

The use of WH in phytoremediation and subsequent utilisation for biogas production through AD, has demonstrated that WH can be utilised in cohesion to treat industrial effluent (paper and pulp, distillery, brass and electroplating effluent) and produce biogas [186,187]. However, whilst the studies showed that the use of WH for phytoremediation resulted in a increase in C:N ratio in the effluent, and thus a greater production of biogas than the control, the plants were only able to grow on a maximum of 40% effluent (diluted with deionized water) before growth was inhibited, whilst 20% resulted in the highest production of biogas. This was due to inhibitory effects of toxic metals on methanogenesis [187] and therefore reduces the applicability of WH to treat this waste and subsequently be used for the production of biogas.

However, the treatment of WH with HTC, followed by AD has been shown to have promise due to the high energy output from hydrochar combustion [139]. The combustion of hydrochar and biogas formed from AD of the process waters produced more than three times the energy than utilisation of the untreated WH, however, issues with slagging and fouling were noted and the presence HMs were not considered [139].

### 2.3.5. Fertiliser production

WH is an attractive feedstock for nutrient recovery, especially composting, due to its high mineral content [63]. Composting aids in stabilising organic matter with the aid of microbes under aerobic conditions [190]. The optimal C:N ratio for composting is variable, according to literature, and is given as ~15-40, which puts WH at the lower end of the range, suggesting that some additional feedstock is required [125,186]. WH has high moisture and key nutrients (N, P and K) so other than minor addition of some feedstock to increase C:N ratio, little is needed for good composting of WH. However, the accumulation of HMs in WH requires methods to reduce the concentration or bioavailability of these metals.

One method of reducing the bioavailability of HMs is the addition of waste lime to compost [191,192]. Singh *et al.* showed that the addition of waste lime to compost resulted in a significant reduction in bioavailability and all metals were reduced to low or zero risk categories within the compost through the combination of rotary drum composting and lime additions [191]. However, Singh and Kalamdhad demonstrated that the addition of CM and sawdust, to vary the C:N ratio, resulted in a reduced effectiveness of lime and that the addition of lime had no effect on Mn [192]. The results from both studies showed that, in compost, bioavailability is more important than total concentration, in regard to toxicity.

Another method of restricting the movement of HMs is vermicomposting; vermicomposting utilises interactions between microorganisms and earthworms to breakdown complex organic matter into smaller less complex fractions [13]. The earthworms are able to actively uptake non-essential toxic metals through their digestive systems [193]. It has been shown that Cu and Cd accumulated significantly with some accumulation of Zn and Pb though high levels of metals were still found in the coprolites (dung) of the worms [193]; however, the metals have a greatly reduced bioavailability [13]. Despite this reduced bioavailability, after growth trials utilising the compost, as a fertiliser, lettuce plants still had levels of HMs, Ni and Zn, above the critical toxic level, although Jordão *et al.* stated there were no visible signs of toxic stress [194]. In contrast, when fruit bearing plants (chickpea, chilli, coriander and tomato) were grown utilising vermicompost, the fruits contained significant amounts less HMs than the control, reaching negligible levels of HMs [13]. However, this study contained WH artificially spiked with As, Cd and Pb but did not include the Ni and Zn; this is a significant omission as Zn has been suggested to accumulate less in earthworms in vermicomposting [193,194].

### 2.3.6. Protein source

Plants are vital portion of animal feed, however, as a result of climate change, farming in tropical regions is becoming increasingly unstable [195], therefore, alternative sources of protein are rapidly developing [196]. Several studies have reported that WH has a high proportion of crude protein, Table 2.1-1, and in some cases even producing more protein per ha than soybeans [197]. However, this varies on the environmental conditions [198], as well as throughout the plant and across the season [62,199], peaking in juvenile leaves and during the spring/early growing season. However, WH contains high levels of cellulose, which is likely to reduce protein extraction from biomass [200], and HMs, making it a less favourable feedstock for protein extraction.

#### 2.3.6.1. Animal feed substitution

WH has been used in many feeding trials, predominantly focussing on ruminants; however, most studies focus on partitioned plants due to high inorganic content of the roots, see Table 2.1-3, and the intercellular spaces in the petioles that can soak up water, requiring animals to drink greater amounts water to feel repleted, reducing their intake of feed [52]. Despite this, there are reports of WH trials that utilise more than just the leaves in feeding trials. de Vasconcelos *et al.* utilised whole sun-dried WH plants, or WH hay, to replace 0-80% Tifton-85 hay (on a DW basis) in the diets of sheep [198]. The trial demonstrated that dry matter (DM) intake was reduced, likely due to the inclusion of petioles, yet the blood plasma levels of urea, glucose, aspartate aminotransferase and gamma-glutamyl transferase were not impacted [198]. The authors suggested that WH hay could be economically advantages in the diets of sheep, despite a protein content of 15.9% [198]. This value would fit within the average protein content of WH shown in Table 2.1-1 and therefore could be increased if harvested at a different time or location, potentially increasing the value of the WH hay. In a similar experiment, Abdelhamid and Gabr fed WH hay, without roots, to sheep, however, they found that 50% was the optimal replacement due to the increased chance of tetany [53], possibly due to reduced levels of Ca, K or Mg. The authors also found that DM intake, digestibility, and nutritive values reduced as WH proportion increased, however, WH hay performed better than rice straw [53]. Neither report considered the long-term impacts of HM concentration on the animals, whereas Mekuriaw *et al.* utilised WH leaves in diet replacement sheep, determining that the HM concentration was below safe limits [201]. However, the authors found that WH leaves reduced the daily weight gain as proportion of diet was increased, with the DM intake, digestibility and protein intake also reducing [201]. Whilst the authors stated that HMs were below safe limits, no analysis of the milk or meat was conducted, therefore, the conclusion about safety cannot be confirmed. When introducing WH as 50% of the diet

in bull cattle, it was demonstrated that the dry matter intake was not affected, whilst the protein intake and daily weight gain were increased [202]. In a similar fashion, when introducing up to 45% WH in the diet of Red Sindhi cattle, protein intake and digestibility were increased. However, bloating also increased whilst rice straw intake reduced [203], likely due to the petioles soaking up water [52]. Therefore, a maximum of 30% was suggested. The inclusion of WH as 30% of the diet in dairy cattle required 784 g FW/day [204].

WH has also been utilised in the diets of goats [205,206] and Awassi lambs [207]. When utilised as goat feed, WH demonstrated a reduction in weight gain, as compared with the control diet, however, both studies concluded the reduction was low enough for WH to be considered an acceptable low costs alternative [205,206]. In contrast, diet replacement in Assawi lambs [207] and bull cattle [202] resulted in significant increases in protein intake, as well as total and daily weight gain.

There are several examples of feeding trials to animals other than ruminants, Fouzi and Deepani used leaf powder to evaluate the impact of replace soy bean and fish meal in the diets of Tilapia [208]. This demonstrated that there was no significant difference between the feed conversion ratio and growth rate between the diets, therefore, WH could be utilised to replace 20% of high cost feeds, soybean meal was 120 Rs/kg and fish meal was 290 Rs/kg [208]. Secondly, Moses *et al.* fed WH, with the roots removed, to rabbits, replacing up 15% of wheat bran; however, above 5% the growth rates were negatively impacted, despite the increase in protein content within the feed [209]. In contrast, Lu *et al.* demonstrated that ducks feed with 50 g of fresh WH per day, with the roots removed, had an increased daily feed intake, egg-laying ratio and egg weight, by 5.9, 9.8 and 2.4%, respectively [4].

The majority of the reports discussed so far do not consider the potential long-term impacts of HMs within WH biomass. Wu *et al.* examined the use of WH leaves in the diets of mice [210]; the authors determined the concentration of Ag, Al, Ba, Cd, Hg, Pb, Pd, Pt, Sb, Sn were all within the maximum limits for food additives of animal feed and established that the median lethal dose (LD<sub>50</sub>) was more than 16g per kg of body weight [210], a value greater than ascorbic acid [211].

#### 2.3.6.2. Protein extraction from water hyacinth

Removing the roots can be costly and time consuming, as described in section 2.3.1, therefore, other methods of utilising WH for animal, or human, consumption have been considered. Protein extraction, or concentration, utilises a variety of different methods to increase the concentration of protein and reduce contaminants. Examples of protein extraction from WH are described here, whilst further methods are discussed in section 2.4.

Bolenz *et al.* examined five different methods of protein extraction from WH plants (without the roots): mechanical chopping, chemical, thermal and chemical, enzymatic and lactic acid fermentation [52]. The addition of sodium hydroxide (NaOH), to achieve pH 8.5, achieved the highest extraction yields, reaching a pellet protein concentration of 58%, however, the protein recovery was only 18.5%, with over half the protein left within the press cake [52]. This press cake had high fibre content and therefore could be used as a feed for ruminants, it is likely the digestibility was increased by the process, however, the use of NaOH may result in high levels of Na salts. Hontiveros and Serrano also studied the use of NaOH to extract protein [212]; NaOH was added to WH leaves, to attain pH 9, before the liquid was filtered and hydrochloric acid (HCl) was added, pH 2, to flocculate the protein [212]. Further flocculation was achieved by heating the liquid to 60-80°C. The resultant protein precipitate had a 248% greater protein concentration than the original biomass [212]. However, this was still just 23% protein, due to the low initial raw biomass protein concentration, 9%, therefore, it is possible that a greater concentration could be achieved with a better starting product. The precipitate was then fed to Tilapia, where the digestibility was high at 76%; the concentration Cr, Cu and Pb were below maximum permissible limits (MPL); and the amino acid index was 0.88 [212]. This suggests that alkali acid extraction (AAE) would be suitable to produce a WH protein extract that would make an appropriate feed for Tilapia, however, the HM concentration of the meat was not analysed, therefore, bioaccumulation could not be estimated.

Another technique for improving the protein content, from WH leaves, is blanching in acetic acid followed by soaking in ethanol to remove fat [197,213]. Adeyemi and Osubor blanched WH leaves in 5% acetic acid, resulting in a protein concentrate that contained 50% protein and 33% carbohydrates, all 17 amino acids analysed were present, whilst 13 HMs were analysed and found to be <0.15 mg/kg, therefore, were within safe limits for human consumption [213]. However, all amino acids were either the same or lower than that found by the AAE from Hontiveros and Serrano [212], see Table 2.3-4; secondly, the HM concentration of the raw biomass was not stated, therefore, it is not possible to determine if the technique was responsible for low HM concentration [213].

Wu and Sun, followed a similar principle, however, the leaves were blanched in 0.5% acetic acid [197]; the protein concentrate contained 18.7 mg/kg of alkaloids (<10% of the MPL); <0.4 mg/kg of 10 HMs (less than the MPL for all); and the LD<sub>50</sub> was greater than 20.5 g/kg of body weight in a feeding trial with mice [197]. The replicate of low HM concentrations suggests that this technique can successfully reduce HM concentration and increase the protein content from WH leaves.

The value of WH protein extract would be hard to define due to the nature of new products on the market and the potential markets that the protein could be employed. Firstly, the soybean meal market would be targeted as a potential replacement for ruminant feed. In 2022, the price of soybean meal varied between USD \$450-550 per metric tonne [214], however, in India, the price was significantly higher, ~ USD \$750 per metric tonne, due to high process costs [215]. This could allow WH protein to exploit the Indian market as a low cost alternative, as well easing the supply issues faced [215]. The second market would be fish feed: Fouzi and Deepani stated that replacing 20% of Tilapia feed, with dried WH leaves, could reduce the cost by 30% [208]. However, extracting the protein would increase the costs of feed, likely removing this saving. Without further information on protein extract feeding trials, it would be possible to estimate the value of WH in fish feed. The final market would be human consumption, this market would contain the most unknowns due to the high HM concentration and lack of evidence behind digestibility and nutritional value for humans. However, many new protein products have entered the market, the largest being soy protein [141]. Another more recent protein product is pea protein; the amino acid profile of a commercially available pea protein is displayed in Table 2.3-4. This demonstrates that pea protein has a similar amino acid profile as the product produced by Hontiveros and Serrano [212], based on the 9 amino acids reported on the pea protein. However, the pea protein contains 83% protein compared with just 23% from WH [212,216]. Petersen *et al.* estimated that pea protein isolates cost USD \$6.50–8.10 per kg [196]; based on the amino acid profile, it could be assumed that WH would fit into the lower end of this range, however, the lower protein concentration suggests that this would not be this case. An assumption could be made that the proportion of protein within the isolates could be used a conversion factor, valuing the WH protein precipitate at ~ USD \$1.80-2.45 per kg. There is currently no WH protein extract product available, therefore any value assigned would require assumptions.



**Table 2.3-4:** Amino acid profile of water hyacinth protein and pea protein, displayed as concentration in the protein extract (%).

Reference	[212]	[213]	[216]	[217]
Method	Alkali Acid Extraction	Acetic Acid Concentration	Alkali Acid Extraction	Raw
Feedstock	Water Hyacinth Leaf	Water Hyacinth Leaf	Pea	Soy
Alanine	6.5	3.2	-	2.8
Arginine	6.6	3.8	-	4.8
Aspartic acid	10.2	5.0	-	-
Cysteine	0.4	0.7	-	0.2
Glutamic acid	7.3	6.0	-	12.4
Glycine	6.5	3.0	-	2.7
Histidine	2.2	1.1	2.5	1.5
Isoleucine	5.5	2.3	4.8	1.9
Leucine	9.6	5.0	8.5	5.0
Lysine	5.1	3.7	7.5	3.4
Methionine	1.3	1.3	1.9	0.3
Phenylalanine	6.0	3.7	5.5	3.2
Proline	5.6	2.7	-	3.3
Serine	10.2	2.5	-	3.4
Threonine	5.3	2.6	3.7	2.3
Tryptophan	1.4	-	1.0	-
Tyrosine	2.9	2.2	-	2.2
Valine	7.5	2.8	5.0	2.2

## 2.4. Introduction to water lettuce

WL has been utilised as a comparative biomass to WH in multiple studies, comparing treatment of various wastewaters and subsequent growth rates [93,218,219], responses to HMs [66,110,158,220] and comparison of biochemical compositions [64]. WL grows well in similar conditions to WH, has a similar morphology and is an invasive species that likely originated in a similar area as WH [221], and has therefore been selected as suitable biomass for comparison.

WL is also a free-floating aquatic macrophyte capable of rapid vegetative propagation [222]. It has widespread distribution in the tropics, but unlike WH has spread to more temperate climates as well [222]. According to the EPPO Global Database, WL has a greater global distribution than WH with a presence in 125 countries and a greater presence in American, Australian and Chinese states, as well as Europe [35].

WL from Pawana River, India, shown in Plate 2.4-1. WL produces long feathery hanging roots and spongy and hairy leaves, which are most prominent in juvenile stage [223,224]. The leaves are often swollen with air containing tissues to allow the plant to float, as they do not contain floats like WH [223,224]. Whilst WL is capable of sexual

reproduction, its primary form of spread is their rapid vegetative reproduction via the production of stolons [223,225], similar to that of WH. This allows the plants to form dense mats across the waterbody, causing damage to the environment and biodiversity, impeding human activities and creating a health hazard through insects and snails [225]. Whilst up to 175.1 plants per m<sup>2</sup> have been observed in Egypt, the high moisture content of WL, stated as 93.8% at peak dry matter (DM), results in a peak DM weight of 3.8 g per plant [225]. In comparison to WH, the leaf of WL is the primary fraction: Galal *et al.* found that in general WL tissues proportions were 7.6, 10.7 and 78.5% for roots, stem-bases and leaves respectively [225].

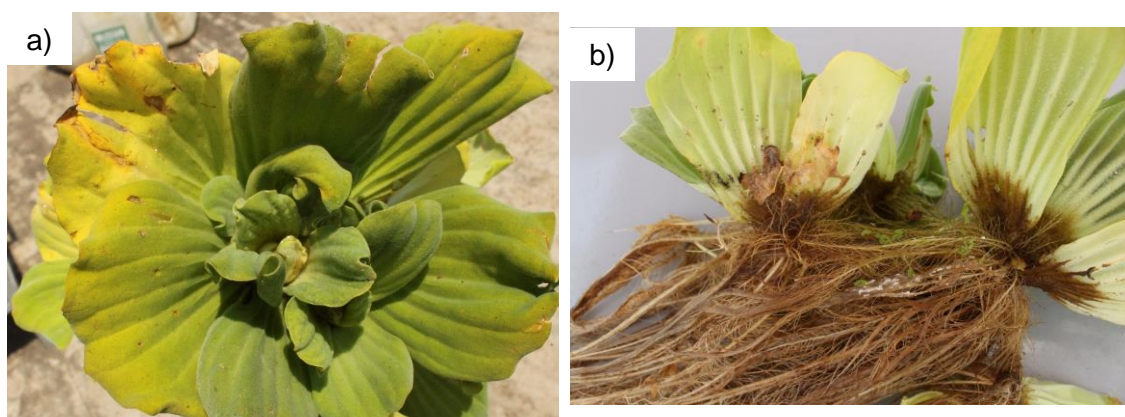


**Plate 2.4-1:** Mature water lettuce plants from Pawana River, India, May 2019. a) Leaf rosette; b) Feathery hanging roots

Whilst WL appears to grow rapidly, 58.81 g/m<sup>2</sup> day in one study [226], it does not appear to be able to achieve the plant density of WH: Gala *et al.* demonstrated a peak density of 665 g DW/m<sup>2</sup> [226], compared with Table 2.2-1 which showed a minimum WH plant density of 670 g DW/m<sup>2</sup>. This is likely due to the size of WH which can grow vertically due to the presence of large petioles.

The biochemical composition of WL has been previously compared with WH, suggesting that WL has a lower cellulose content, higher ash and lignin content, and similar protein content. A range of compositions are displayed in Table 2.4-1.

**Table 2.4-1:** Composition variations for water lettuce

Reference	[43]		[44]	[45]	[46]	[61]		[64]		Whole plant Range
						Leaf	Root	Leaf	Root	
Waterbody	Tank	Tank	Ponds	Pond	Tank	Unknown		Unknown		N/A
Pollution Source	Swine wastewater	Hoaglands' solution	Industrial wastewater	Aquaculture	N/A	Unknown		Unknown		N/A
Location	Korea	Korea	Turkey	China	India	Nigeria		India		N/A
Moisture Content	95.1	94.7	-	-	-	-	-	90.0	90.0	94.7 - 95.1
Volatile Solids	-	-	80.3	57.9	-	-	-	-	-	57.9 - 80.3
Organic Matter	77.8	80.1	-	-	-	-	-	-	-	77.8 - 80.1
Protein	-	-	-	18.4	16.0	7.0	3.2	19.8	1.4	16.0 - 18.4
Lipid	-	-	-	3.9	5.1	2.2	1.8	0.7	0.4	3.9 - 5.1
Fibre	-	-	-	-	11.1	17.5	20.5	-	-	11.1
Nitrogen Free Extract	-	-	-	27.6	45.7	-	-	-	-	27.6 - 45.7
Ash	22.2	19.9	-	25.1	22.2	35.2	44.5	11.1	30.1	19.9 - 25.1
Cellulose	-	-	34.4	16.1	-	-	-	27.6	16.1	16.1 - 34.4
Hemicellulose	-	-	26.3	-	-	-	-	29.7	14.2	26.3 - 35.2
Lignin	-	-	11.6	-	-	-	-	3.5	13.6	11.6

## 2.5. Summary of methodologies for protein extraction

There are two key aspects of protein extraction: release of protein; and recovery of protein. The first step can occur through breaking cells and/or solubilising the protein; the main methods are physical treatment, like grinding or pressing [141,227,228], or through chemical treatments like acid hydrolysis or alkali solubilisation [141,228–233]. There are two approaches for this step, concentration or extraction; in the process of protein concentration, non-protein compounds are removed, as opposed to releasing or extracting the protein. The primary advantage of concentration is that it does not require a recovery step, however, it is likely to require multiple steps to remove all non-protein compounds [197,213]. In protein extraction, the primary method for recovery is isoelectric precipitation, either by heat or acid [228–231,234].

One of the most well-known examples is the production of soybase, a product that forms the base of soymilk and tofu, among other goods [141]. This process begins with mechanical disruption before solubilisation of the protein followed by filtration to remove non-soluble matter [141].

The sections below discuss the various methods of releasing and removing protein in greater detail.

### 2.5.1. Protein release

#### 2.5.1.1. *Physical and physical/chemical treatments*

Physical treatment of biomass can occur via multiple methods, however, industrial processing of biomass often occurs at harvest with minor physical treatment by cutting, shredding, or other processing methods [235]. However, this level of processing would be unlikely to disrupt the cells enough to allow for full release of protein. Further reduction of particle size causes a greater proportion of cell disruption and increases the surface area available for interaction with solvents [141]. There are different methods for reducing particle size or mechanically disrupting cells, some are detailed below.

The production of soybase has been improved by utilising different particle size reduction methods; the traditional methods utilised a mill to grind the soybean and reduce its particle size [141]. Protein recovery from soy flour was increased from 40 to 52% by reducing particle size from 223.4 to 89.5  $\mu\text{m}$  using a centrifugal mill [236]. This increase in protein recovery was also found when soy flour and okara (waste from the whole soybean extraction process [141]) were ground to  $<75 \mu\text{m}$ : protein recovery reached 97 and 93% for the soy flour and okara [237]. However, increasing the particle size improves fermentation of silages in a rumen simulation system [238], suggesting

that any waste from the protein recovery may not be suitable as an animal feed, reducing the market value.

The use of a screw press can transform biomass or residues into a different fractions, most notably a fibre rich press cake and protein rich green juice [239]. This process can occur at large scale [235] and as batch or continuous [240]. Santamaría-Fernández *et al.* proposed a process utilising a screw press to obtain a plant juice which was subjected to acidic fermentation to precipitate the protein [241]. The press cake and residual juice were then used to produce biogas with a yield of 219-539 mL CH<sub>4</sub>/g VS [241]. A similar approach was used in a demonstration scale-study to evaluate the scalability of processing grass clover mixtures [235]. The demonstration plant had an input of 10 tonnes per hour and successfully operated for four days, processing 444 tonnes of biomass and producing 1 tonne of dried protein concentrate, 7 tonnes of protein paste, and 223 tonnes of press cake; however, the total recovery of protein was low as 72.4% of the crude protein was in the press cake [235]. This is similar to results found by Larsen *et al.* who utilised a twin-screw press on tall fescue and reed canary grass [227]. The biomass was processed at room temperature in a press equipped with a 1mm screen; 200g of wet biomass was added to 200g of demineralized water and pressed. The juice was then subjected to heat coagulation and centrifugation to remove the protein. The pulp fraction (or press cake) accounted for 71-78% of the total crude protein [227], again demonstrating that recovery of protein is low, suggesting a low percentage of protein release from mechanical disruption. There are many reactions that can reduce the solubility of protein and therefore reduce the yield, one such example occurs in biomass that contain phenols. During pressing, phenols are released from the biomass and bind to proteins, reducing the extractability and digestibility of the protein [242]. These compounds are then oxidised, though the activity of enzymes, to more reactive quinones which can polymerise into brown pigments and may react with the proteins causing aggregation of proteins and reducing solubility [242]. Through the addition of antioxidants, mainly sulphur containing agents, this redox reaction can be inhibited and therefore increase the solubility of protein, resulting in higher protein yields [242].

The two methods presented so far are simple and have a relatively low energy consumption; the methods presented below are examples of more novel extraction techniques. These will not be considered for method selection in this project due their complexity and immaturity in practise.

Ultrasound-assisted extraction (UAE) is a non-thermal extraction technique that implodes cavities on the surface of the feedstock, resulting in micro-jetting which generates surface peeling, erosion and particle breakdown [243]. UAE has been applied to various types of biomass to produce high value products for food,

nutraceutical, cosmetic, pharmaceutical and bioenergy applications [243]; its application to protein extraction is limited to laboratory- and some pilot-scale. When applied during alkali extraction of protein from rice dreg flour, the yield was increased from 43.2 to 88.44%, even when the alkali concentration was just 0.1M NaOH and temperature was 50°C [244]. The increased protein recovery was also demonstrated with cyanobacteria, where 2 minutes of sonication resulted in a protein recovery increase from 60 to 96% and reduced the process duration from ~2 hours to 7 minutes [245]. When utilised with cauliflower residue, the optimised time period of sonication was 15 minutes [246], suggesting a large variation in optimum times for different biomass. Whilst UAE improves protein recovery, it has been shown that there is a disparity between laboratory- and pilot-scale results: when using UAE to enhance protein extraction from soybeans, the improvements reduced from 11-12% at lab-scale to just 4.2% in a pilot-scale test [141]. UAE is considered a rapid and cost-effective extraction method for food production [243], however, examples of protein extraction from lignocellulosic material are limited.

Microwave-assisted extraction (MAE) transmits microwaves through the biomass, the microwaves are absorbed and converted to thermal energy which heats the moisture in cells causing pressure increases cells which improves porosity in the biomass, allowing for better penetration by solvents [240,247]. The use of MAE in extracting natural bioactive compounds has been well documented [247], but is more novel for protein extraction as MAE can result in protein hydrolysis [240]. To avoid hydrolysis of proteins, Ye and Li repeated 30 second heating followed by cooling to room temperature [248]. In contrast, for the production of soy milk, MAE reached the extraction point, 90°C, in 20-50 minutes, depending on the power level, compared with 40 minutes for conventional methods [249]. The resultant milk had 44% more protein, which was 39.6% more soluble, suggesting no production of hydrolysed insoluble protein fractions, than conventional methods [249]. MAE has been shown to increase protein extraction, however, high-energy inputs can lead to the protein hydrolyse and solvent evaporation [250].

#### *2.5.1.2. Chemical treatments*

The use of chemicals in protein extraction predominantly involves the application of solvents as a method of releasing the protein. The two types of solvents commonly used are organic and alkaline [240].

Organic solvents, such as ethanol, isopropanol and chloroform, have been used to solubilise proteins from a variety of agricultural residues [240], primarily the alcohol soluble storage proteins, such as prolamins, which can be extracted free of lipids using chloroform solubilisation and acetone precipitation [251]. Organic solvents have also

been utilised to extract vegetable oils from biomass with high oil content [240,251,252]; for example, a yield of up to 80% oil was obtained from rice bran; for protein, the yield was 8.9-20.4% depending on the water content of the solvent and temperature of extraction [253]. The protein yield increased with water content of the solvent; a similar result was found with soybean, however, the yield was only 11% when using the same solvents and conditions [252]. These low yields could be explained by the nature of the proteins in biomass, mainly albumins and globulins, and the potential coagulation caused by incorrect mixtures of the solvent: in some cases alcohols can be used to precipitate proteins and others will cause conformational changes in their structure if the percentage of alcohol is too high [240,254].

Alkali treatments simultaneously cause cell disruption and solubilise the protein [255], thus allowing subsequent recovery of the protein by precipitation or membrane filtration. There are several key aspects to alkali solubilisation: time, temperature and amount of solvent; these three variables, along with feedstock selection, largely determine the protein extraction yield [255]. A review of alkali solubilisation looked at the relationship between temperature, time and protein yield [255]; whilst there was no optimum time or temperature, most likely due to the variation in feedstocks, there was a positive trend showing greater extraction with longer time periods and higher temperatures. Extraction from *Azolla* showed that at room temperature significantly less biomass was solubilised, including a reduction in solubilised N, when compared with 45°C [230]. The results in the protein precipitate were less conclusive but also suggested that less nitrogen was present at room temperature; when the temperature reached 95°C, the amount of solubilised N and biomass was the highest, however there was less protein recovered, suggesting that this temperature hydrolysed the protein and therefore it was not recoverable [230]. Whilst, time and temperature are key aspects in alkali solubilisation, it is the absolute amount of alkali that has the defining role [256]; the absolute amount of alkali is directly related to pH, solid-to-liquid ratio and agent concentration [240]. The effect of alkali on protein extraction occurs through two mechanisms: alteration of the cell wall and protein properties [255]. Whilst acid will degrade the cell wall more effectively than alkali, most proteins are least soluble near their isoelectric point, which is often pH 4-5, and therefore precipitate at a lower pH and fully solubilise at a higher pH [240,255]. The alkali disrupts the cell wall by reducing surface tension, partially removing lignin, and complete removal of uranic or acetyl ester groups of hemicellulose [257]. The importance of alkali amount is due to the influence of the biomass on the alkali: components of the biomass, like lignin, can react with the alkali and buffer the system, therefore reducing the amount of alkali that is available [255]. Alkaline extraction of protein has been studied for many decades but despite its low cost, the yield was always low; the understanding of these three

principles has led to an increase in protein yields. In a study that utilised green tea residue for protein extraction, the variation of temperature, time and alkali amount, led to an increase of protein solubilisation from ~20% to 95% [256]. The optimum conditions were pH 12.5, 95°C and 32 mL NaOH/g biomass (recovery increased disproportionately with greater liquid addition) [256].

Alkali extraction is the most likely chemical method for use on lignocellulosic biomass due to the effect of alkali on cell walls and higher yields. However, it is possible to combine the two processes and recover high amounts of protein: using a feedstock of corn distiller's grain, a 90% protein yield was obtained with a mixed solvent of 45% ethanol and 55% 1M NaOH [258].

The chemical treatments described here are primarily focussed on removing the protein from the biomass and producing a protein extract. Another option is removing the other organic material and leaving a protein concentrate. The methodology consists of high temperature acid treatment followed by soaking the biomass in ethanol to remove the fat [197,213], resulting in a product that has a significant proportion of protein, ~56%, and contains all the essential amino acids [213]. However, the 'blanching' of biomass could be considered dangerous, particularly on a small scale.

#### 2.5.1.3. *Biological treatments*

Biological treatments are mainly utilised when physical and/or chemical treatments are producing a low yield. The main problem with protein extraction is the low solubility of proteins, therefore, a variety of enzymes, including carbohydrases and peptides, can be utilised to aid in the solubilising of protein [240].

Cellulose and oil hamper the extraction of protein from biomass [255], therefore, by using carbohydrase enzymes, it is possible to promote the hydrolysis of the lignocellulosic material, resulting in a release of protein associated with cell wall and increase the penetration by the solvent [240]. The multi-enzyme mixture, Viscozyme®, has been used on a variety of biomass, including cereals and seaweed [259–261], to improve the protein extraction. Viscozyme® contains a wide variety of carbohydrases, including arabinose, cellulase,  $\beta$ -glucanase, hemicellulase, and xylanase [259]. The addition of Viscozyme®, to defatted rice bran meal, was shown to increase the protein isolate mass yield from 10.2%, for standard AAE, to 22.4% and recovered over double the protein present in the feedstock (82.6%) [261]. The isolate yield and recovery efficiency was marginally higher than microwave treatment followed by homogenisation, which achieved an isolate yield of 22.3% and efficiency of 82.5% [261]. When compared with similar treatments of seaweed, the efficiency was significantly reduced: Viscozyme® treatment achieved a maximum of 48.5% protein recovery from *Eucheuma denticulatum*, significantly lower than Alcalase® (59.4%)



[259]. The efficiency of Viscozyme® was similar with *Palmaria palmata* as a feedstock and showed no variation from the control, AAE; whereas Alcalase®, had a recovery of >80% [260].

Proteases can also be utilised to increase extraction yield, the enzyme reduces the size of proteins which allows for easier extraction, resulting in lower alkalinity requirements [255]. The use of protease, on soybean, demonstrated an increase from 80 to 90% in protein yield [262].

When comparing the two types of enzymes, carbohydrase and protease, the feedstock plays a vital role in the success of the enzyme. Sari *at al.* carried out a multiple studies to demonstrate the impact of each enzyme; soybean performed poorly with carbohydrase, in comparison to the control, which was out performed by protease [255]. Whilst protease also performed best with *Moringa oleifera*, the carbohydrase performed better than the control; however, the extraction was lower than soybean for all except for the carbohydrase [255]. The extraction from rice bran performed in a similar manner, with the protease performing the best, followed by carbohydrase and the control, however, the extraction from rice bran was more successful than *Moringa oleifera* [255]. A combination of carbohydrase and protease was also conducted on the rice bran; however, this performed the worst of all the extractions on rice bran [255].

## 2.5.2. Protein recovery

The next step would be to recover the protein from the biomass, if the protein has undergone physical treatment it would most likely require a solvent to solubilise the protein for recovery, this could be acidic, neutral, alkaline or organic [240], though as previously described, it is most likely to be alkali. The solubilised protein must then be separated from the liquid; this can occur by isoelectric, temperature or organic precipitation, [240]. There are many other techniques, including ultrafiltration and membrane filtration [240], that will not be considered by this study due to the complexity/ high levels of technology required or are considered to be in their infancy. This decision was made as this study aims to find a procedure that can be used in developing countries, therefore, simple and low-cost procedures are favourable.

### 2.5.2.1. Isoelectric precipitation

The most commonly used method for protein precipitation is isoelectric precipitation, or acidic precipitation [240,255]. Most proteins are least soluble at their isoelectric point, which is often approximately pH 4 [240,255], therefore, by shifting the pH towards this point, most protein will become insoluble and can therefore be removed by centrifugation or filtration. The variation in precipitation has been demonstrated on fresh *Albizia lebbek*: the pH was set at 4, 7 and 9 to determine the yield of protein

[233]. The highest amount of precipitated protein was at pH 4 with 6.15 g and a protein content of 37.28%, compared with 4.88 and 4.17 g for pH 7 and 9, respectively, and a protein content of 32.73 and 34.52% [233].

The solubility of protein varies across the different types of protein due to their isoelectric points; this is described by the Cornell net carbohydrate and protein and system (CNCPS), see Table 2.5-1. The extractable true protein (ETP) is defined at neutral ETP or acid ETP, which includes B<sub>1</sub>+B<sub>2</sub> and B<sub>3</sub>, respectively; acid ETP accounts for ~75-85% in grasses [263]. This system states that fractions A and B are assumed digestible or extractable and are the focus of any attempt to concentrate protein.

**Table 2.5-1:** Cornell net carbohydrate and protein system [263–265].

Fraction	Type	Description	Extraction Method
A	Non-Protein Nitrogen	Nitrates, ammonia, amines and free amino acids	Trichloroacetic acid precipitate
B1	True Protein	Neutral Soluble	Borate phosphate buffer solution
B2	True Protein	Neutral Soluble	Neutral Detergent
B3	True Protein	Acid Soluble; Associated with Cells Walls	Acid Detergent
C	Unextractable	Acid Insoluble; Bound to Lignin	N/A

There is high variability of the proportions, of each fraction, across biomass; for example, amaranth meal proteins showed a minimum solubility of <20% at ~pH 4, yet had a solubility of ~35% at pH values <4 [266]. Whereas, soy protein isolate, which also had a minimum solubility at ~pH 4, was much less soluble at its minimum (<10%) and then increased substantially at a pH value <4 (>80%) [267]. It should be noted that the solubility of soy protein was more stable at acidic pH's (solubility of <20% at pH 4-5.5), whereas, amaranth had a solubility of >20% for all but pH 4, further emphasising the variation between different feedstocks [266,267]. Another example showed that dried alfalfa leaf protein had a minimum solubility of 2% at pH 4 [268]; the protein had a solubility of ~40% at the other values studied (2, 6, 8, and 10). The precipitation of protein from brewers' spent grain showed the highest values over the pH range 4-9, a much greater range than the previous examples. For pale brewers' spent grain, the highest precipitation was in the range of ~pH 6-12 [269]. However, it is generally accepted that the majority of biomass will have a lower solubility at pH 3-4; a mock protein solubility curve of protein solubility is displayed in Figure 2.5-1. This graph depicts the three stages of protein solubility: high and stable solubility in alkaline

conditions; reduced solubility until isoelectric point; and marginally increased solubility beyond isoelectric point (due to hydrolysis) [268,270].

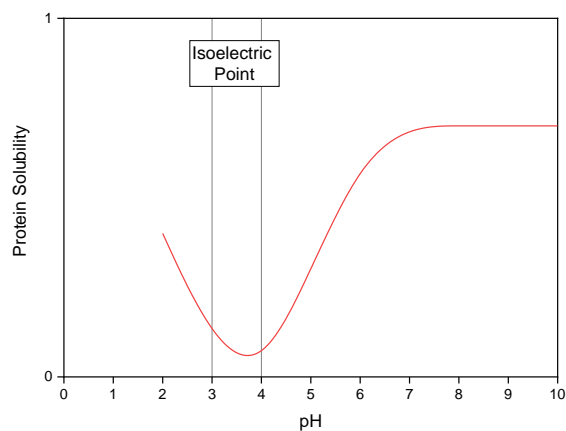


**Figure 2.5-1:** Mock solubility curve of protein in lignocellulosic biomass. Representative of lignocellulosic biomass described in literature [268,270].

There are two primary issues with acid precipitation: co-precipitation of lignin and formation of salts [229,240,271]. Lignin is partially soluble in alkali (pH 10), therefore can be fractionated with the protein in alkali solubilisation [271]. The shifting of the pH can result in lignin being precipitated out of solution (pH 2) with the protein. However, the required pH is significantly lower than the predicted isoelectric point and peptidase can be utilised to separate peptides from the lignin [240,271]. The salt formation is a greater problem, particularly when alkali (NaOH) is used for solubilisation as high volumes of sodium salts can be produced [229], coupled with the environmental concerns of using HCl [233], this reduces the effectiveness of AAEs. Alternative alkalis and acids can be used to reduce the impacts: the use of potassium hydroxide (KOH) has shown that it can produce yields identical to NaOH, as well as producing a K-rich salty wastewater that could be used as a fertiliser [229]. The utilisation of acetic and citric acid showed that whilst a higher quantity of acid was required to reach the desired pH, the environmental concerns over the use of HCl suggest that citric acid could be a preferable option [233].

It has been demonstrated that lactic acid fermentation can be utilised to produce protein product, precipitated due to the low pH of the fermentation, a press cake and lactic acid as a high value product [241]. This combination has been demonstrated at pilot scale and demonstrated that further large-scale biorefinery trials should be conducted, however, the lactic acid was not isolated during this trial, reducing the value of the final products [241]. However, this concept could be applied to WH to produce a biorefinery plant that was able to produce energy, food and clean water.

### 2.5.2.2. *Temperature precipitation*

Coagulating protein using temperature is another option that would not produce salts as a waste product. The coagulation often occurs with alongside hydrolysis of the proteins, which removes most of their functional but not their nutritional properties [255]. Utilising heat coagulation, protein yields from ryegrass were 45%, and for alfalfa were 53% [272]. The hydrolysis of proteins will occur at temperatures  $>140^{\circ}\text{C}$ , but can be as low as  $60^{\circ}\text{C}$  [240], indicating that the suggested maximum temperature,  $95^{\circ}\text{C}$ , should not result in mass hydrolysis of the protein. Temperature coagulation can be utilised in conjunction with acidic precipitation and has been demonstrated to increase precipitation yields as temperature increases [233]. The precipitated protein increased from 2.19 g and 21.71% protein content at  $50^{\circ}\text{C}$ , to 6.17 g and 37.64% protein content at  $100^{\circ}\text{C}$ . However, in this study, protein content was determined by N multiplied by the conversion factor (6.25), commonly used to determine protein content. This is not only a simplification and overestimation of protein quantity [273,274], it does not account for protein hydrolysis, therefore the quality of the protein is undetermined.

This method has been utilised at scale by the company 'BioRefine'; clover, grass and alfalfa were cut and pressed, the fibre was then used for biogas production and the juice heated to cause protein coagulation, before it was centrifuged to separate the protein [275]. The remaining liquid can be utilised as a fertiliser or in the production of biogas [275]. This is another biorefinery concept that could be applied to WH to fulfil the energy-water-food nexus.

### 2.5.2.3. *Acetone precipitation*

The precipitation of proteins with acetone is conventionally used in an analytical context [276]; according to Montealegre *et al.*, the most used procedure is precipitation with cold acetone at  $4^{\circ}\text{C}$  for 30 minutes, followed by filtration through a Whatman filter, elution with dioxane and tetrahydrofuran, and concentration by evaporating under nitrogen [276]. When compared with trichloroacetic acid, chloroform/methanol, ammonium sulphate and ultrafiltration for precipitation of proteins from human plasma, the results showed that acetone precipitation performed well, providing the levels of protein were high but was outperformed at dilute quantities by trichloroacetic acid [277]. This yield could be improved with the addition of low concentration sodium chloride (NaCl) (1-30 mM), increasing the precipitation efficiency from  $<15\%$  in 80% acetone, to 80-100% efficiency in a mixture acetone and NaCl [278]. However, precipitation with acetone requires large volumes of organic solvent, 3-4 times of the sample volume [277,278].

### 2.5.3. Methods for further investigation

The methods selected for further investigation aimed to be cheap, simple and demonstrate the extractability of protein from WH before more advanced methods were employed. The WH would first be treated physically by mechanical maceration to <1mm, then the protein would be solubilised by alkali treatment, and the protein then precipitated via acid. This was demonstrated by Bolenz *et al.* and outperformed a variety of other techniques when utilising WH as a feedstock [52]. However, the method could be improved to achieve a greater protein yield: firstly, NaOH was utilised to reach pH 8.5, a low pH in comparison to other alkali solubilisation methods [240]; secondly, ultrafiltration was used to separate the protein; finally, the temperature and solid to liquid ratio were not altered [52]. Additionally, the use of AAE has been shown to be the optimal methodology for other biomass, including seaweed [279]; Alamo switchgrass [228]; and defatted rice bran [240]. Another positive of AAE is the potential for improvements to the yield with complementary techniques, including, enzyme-, microwave- and ultrasound-assisted extractions.

## 2.6. Research gaps

The literature has demonstrated that there has been a significant amount of work surrounding WH and its potential to contribute to the transition to sustainable living, in particular the energy-water-food nexus. However, it is clear that the variations in composition could be a road block, as well as accurate estimations of biomass availability from cultivation. WH has been demonstrated to be an appropriate feedstock for animal and human feed, and a potential option for a biorefinery. Therefore, this study aims to address these gaps to develop the potential to introduce a WH biorefinery capable of producing energy, food and clean water.

Firstly, the composition and morphological variations of WH have been studied extensively, however, this has been within isolated projects that often do not consider the potential variations caused by water quality, environmental conditions or geographical location. Therefore, this study will attempt to rectify this by studying multiple populations across similar time periods. This information would be used to understand the optimal point of harvest, as well as the potential variation in yields from a biorefinery that utilised biomass from or was deployed in multiple locations.

Secondly, the studies of impact on environmental parameters on the growth of WH was outdated and incomplete, therefore, key parameters should be studied so that accurate estimations can be made for the potential feedstock availability from cultivation of WH. Therefore, the impact of the key environmental parameters (nutrient availability, solar irradiance and temperature) will be examined through a phenological study of WH growth characteristics in an artificial cultivation tank.

Protein extraction from WH has been investigated by several authors, however, the yields were poor in comparison to other lignocellulosic biomass. Secondly, the methods used to concentrate protein are unlikely to be considered for large-scale protein production due to high temperature and solvent requirements. Therefore, a simple and cheap method will be investigated to inform the potential for protein extraction from WH, with the option to improve extraction with complementary techniques.

Finally, biorefineries are an area of research that has exploded over the last decade, however, WH has little concrete evidence for an economically successful biorefinery, despite evidence that it can be used to produce energy or food and be cultivated in clean and polluted water. This study will attempt to link these two research areas by examining the potential utilisation of contaminated WH biomass following the phytoremediation of wastewater.

## Chapter 3.

# Materials, equipment and experimental methods

This chapter outlines the protocols, methodologies and equipment utilised whilst conducting the experimental work of this thesis. Initially, the sample collection, preservation, preparation and characterisation are discussed, followed by the tank-based cultivation protocol. Following this, the methodologies for the biomass utilisation methods are outlined.

### **3.1. Material collection, preparation and storage**

#### 3.1.1. Biomass feedstocks

A sample collection protocol was designed by the author and distributed to all collectors, to ensure replicability between the sites and comparisons between the data. This section has been adapted from this protocol.

##### *3.1.1.1. Biomass collection*

Samples were collected from three water bodies in India and three locations on Lake Victoria in Uganda; between May 2019 and August 2021. The locations are stated in Table 3.1-1, and depicted in Figure 3.1-1 and Figure 3.1-2. A further collection was undertaken at the institute of biological, environmental and rural sciences (IBERS), University of Aberystwyth. Further information on each location is give below.

**Table 3.1-1:** Water hyacinth sample collection locations.

Area	Waterbody	Location	Code	GPS <sup>1</sup>	
				Latitude	Longitude
West Bengal, India	Goyal Para	Santiniketan	GP	23°42'19"N	87°40'30"E
Pimpri-Chinchwad, India	Indrayani River	Moshi	Mosh	18°41'20"N	73°50'53"E
		Alandi	Ala	18°40'39"N	73°53'25"E
Pune, India	Mula River	Baner	Ban	18°33'50"N	73°47'23"E
		Sangvi	Sang	18°34'07"N	73°49'03"E
Murchison Bay, Kampala, Lake Victoria, Uganda	Murchison Bay, Lake Victoria	Clean water	CW	0°17'18" N	32°39'21"E
		Nakivubo Channel	NC	0°17'29" N	32°38'10"E
		UBL <sup>2</sup>	UBL	0°17'21" N	32°39'12"E
IBERS <sup>3</sup> , Aberystwyth, Wales	Glasshouses	Aberystwyth	IBERS <sup>3</sup>	52°25'09"N	4°03'58"W

<sup>1</sup>GPS Location is accurate to a minimum of 2500m; <sup>2</sup>Ugandan Brewery Ltd.; <sup>3</sup> Institute of biological, environmental and rural sciences.

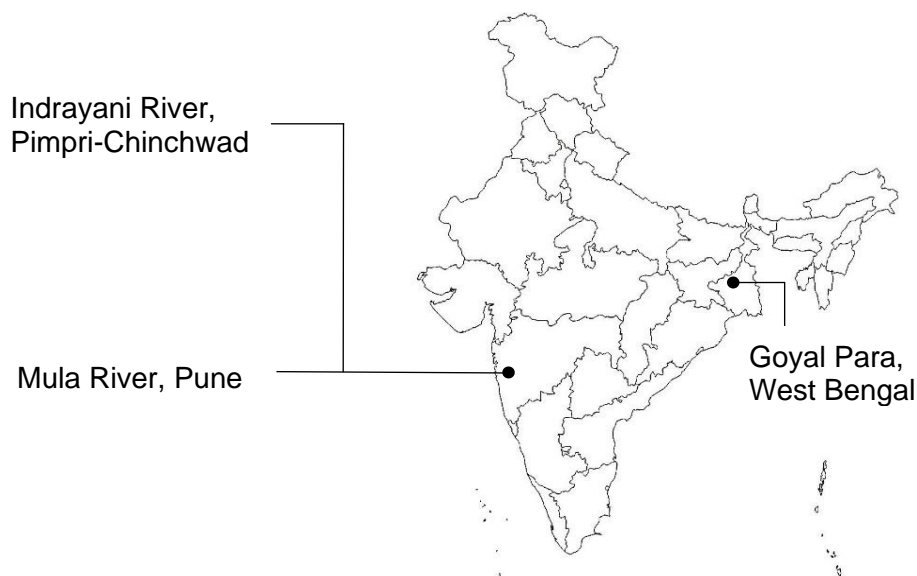


**Figure 3.1-1:** Sample collection locations in India.

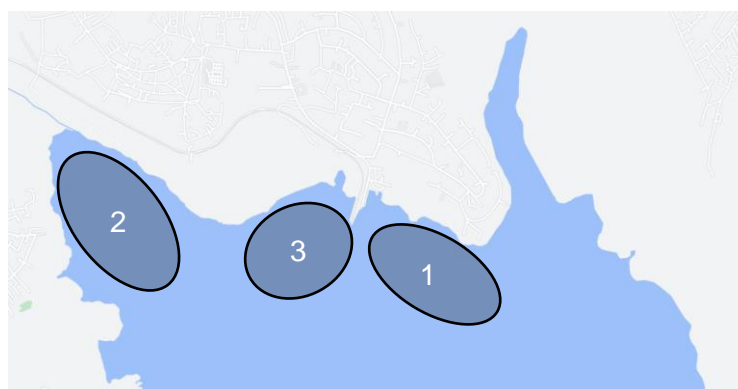


**Figure 3.1-2:** Sample collection locations in Uganda: 1) clean water; 2) Nakivubo Channel; 3) Ugandan Brewery Ltd.



At each location 10-30 plants were collected, depending on availability, and transported to the respective laboratory; multiple plants were collected to estimate the average of the population [280]. Half of the plants were shredded for analysis as whole plants, see Plate 3.1-1, and the other half used for tissue collection. For the tissues, the plant was split into three main parts: leaf, petiole (including float) and root; this is shown in Plate 3.1-2 and Plate 3.1-3. For WL the plants were only analysed as a whole plant; WL plants were only collected from Indrayani River.



**Plate 3.1-1:** Shredded whole water hyacinth plants.

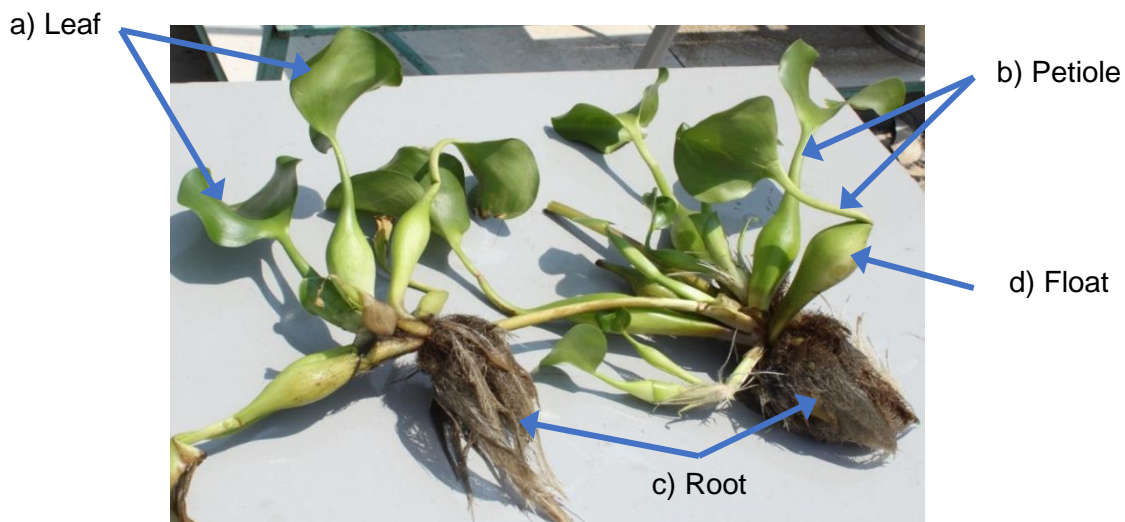


**Plate 3.1-2:** Water hyacinth whole with indication of tissues.



**Plate 3.1-3:** Shredded water hyacinth tissues: a) leaf; b) petiole (including float); c) root.

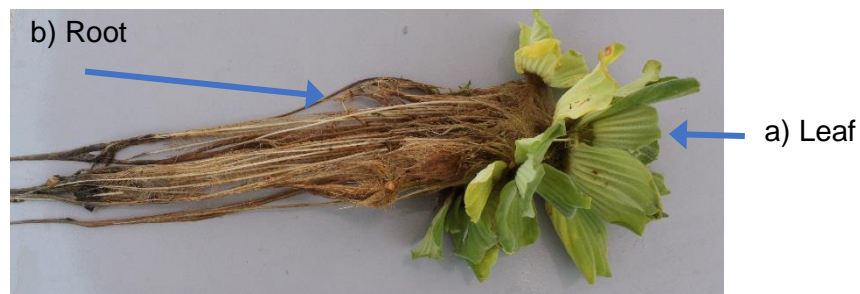


**Plate 3.1-4:** Water lettuce whole plant with indication of the tissues.

### 3.1.1.2. *Indrayani River*

Indrayani River originated at Kurvande in the Sahyadri ranges, where it then flowed through Kamshet, Talegaon, Dehu, Pimpri-Chinchwad and Alandi before it met the Bhima River at Tulapur [281]. The river was one of the major tributaries of the Bhima River and its flow was largely regulated by the hydroelectric dam, Valvan Dam [281]. The river was non-perennial and infested by WH for approximately half of the year before the monsoon rains remove much of the biomass. The stretch of river was predominantly utilised for irrigation. The river was polluted with raw sewage, up to 20 million litres per day and has been named as priority III (third highest priority level set for river pollution levels), by the Maharashtra Pollution Control Board (MPCB), from Moshi to Alandi due to high levels of BOD [281,282]. There was significant sewage pollution upstream from Moshi and Alandi, as well seasonal pollution due to large festival gatherings at Alandi, where the sanitation systems can not fit demand [283]. Whilst industrial waste release was not permitted in the river, there were 3 industrial estates, including two industrial parks and a floriculture site at Talegaon [283,284], with 44 major polluting industries that produced 23.07 million L/day of industrial effluent [281].

There were two MPCB sampling stations (sections of the river that are routinely sampled to determine river water quality) on the river stretch, one located in Moshi Gaon and one at Moshi Village, located between Moshi and Alandi, and a further station downstream from Alandi [285]. In 2017 and 2018, the water quality at all stations was not in compliance with the MPCB regulations, in particular due to high levels of BOD that reached 16 mg/L in May 2017, over five times the limit of 3 mg/L, however, this was an isolated event and the BOD was deemed to be between 3-10 mg/L and was classified as priority III [281].

The first sample collection point selected was located at Moshi Gaon, see Plate 3.1-5, underneath a major road out of Pimpri-Chinchwad. This area was partially harvested by the local authority in April 2019, the biomass was left to rot on the banks of the river

and was therefore of no value. The second sample point was located under a small vehicle bridge in Alandi; both points are within the priority III stretch of river.

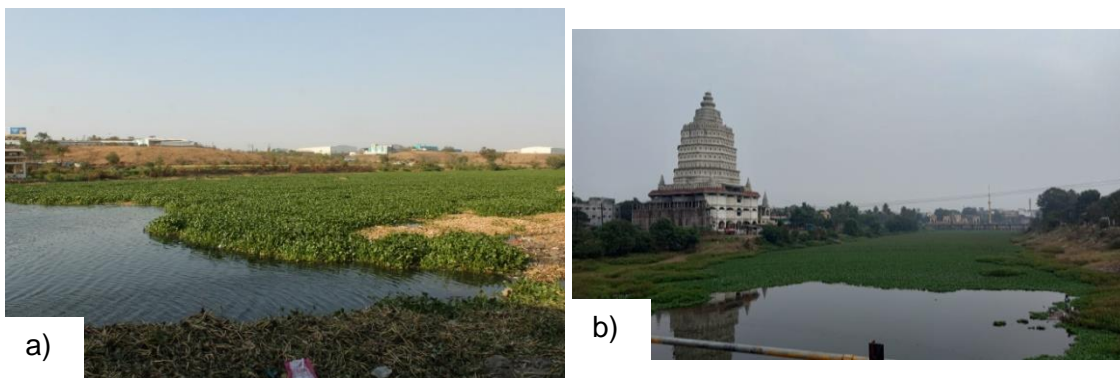


**Plate 3.1-5:** Indrayani River sampling points, Pimpri-Chinchwad. a) Moshi (May 2019); b) Alandi (March 2022).

The WH plants were large clones with petioles of over 50cm and narrow floats, most likely due to the high flow rate and sewage pollution, however, the roots were almost as long as the petioles, shown in Plate 3.1-6, which was larger than expected. Collection and preparation of the biomass was carried out by the author in May 2019 and February-March 2020; from May 2019-January 2020 and May 2020 onwards, the collection was undertaken by Dr Gaurav Nahar of Defiant Renewables Ltd. (DR). Whole WL plants were also collected at this site, in addition to individual parts.



**Plate 3.1-6:** Water hyacinth from Indrayani River, Pimpri Chinchwad (May 2019).

### 3.1.1.3. Mula River

The source of the Mula River was Mulshi Lake in the Western Ghats of Maharashtra; the Mulshi dam was the key component in the flow of the river for the majority of the year, however, the river was non-perennial [286]. Downstream, the river entered Pune where it was highly polluted, largely through sewage and household waste [286]; the high level of pollution resulted in the MPCB classifying the water quality as Class IV.

The river has been named the 'lifeline' of Pune due to its use as drinking, bathing, and industrial and irrigation waters [286]. The Mula and Mutha rivers cover the majority of Pune and are therefore key recipients in the disposal of solid, domestic, medical and industrial waste streams, as well as agricultural run-off [286]. There were 18 industries within the vicinity of the Mula River, including the Hinjewadi industrial site [283], however, the MPCB stated that no industrial pollution was permitted [282,286].

As of 2019, 744 million litres of sewage was generated per day in Pune, of which 477 million L/day was effectively treated, therefore, 267 million L/day of raw sewage was left un-treated [282,286]. It is unclear how much was directly pumped into the Mula River; however, the river stretch has been deemed a priority level I for the MPCB and it is therefore likely that a significant portion was pumped into the river.

There were two MPCB sampling stations in operation; at Aundh Gaon (between Baner and Sangvi) and at Bopodi (downstream of Sangvi where the Mula meets the Pawana River) [285]. In 2017 and 2018, the water quality was not in compliance with the MPCB regulations, in particular due to high levels of BOD that reached 22 mg/L in May 2017, over seven times the limit of 3 mg/L [286].

The first wild WH sample collection point, see Plate 3.1-7, was downstream of the Baner Water Treatment Plant, near a main road joining the Pune with Pimpri-Chinchwad. This point is within the stretch of river that was deemed priority I and was likely to be in non-compliance with the MPCB regulations. The second sample point was within the district of Sangvi and was also in the priority I stretch of the river.

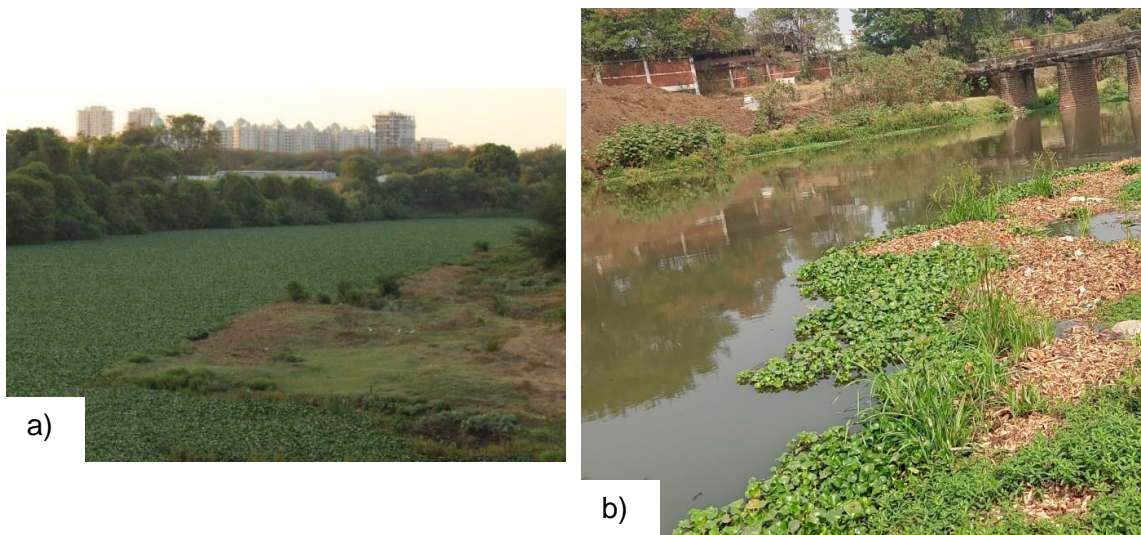


**Plate 3.1-7:** Mula River sampling points, Pune. a) Baner (May 2019); b) Sangvi (March 2021).

The river was left unharvested and produced a dense mat with large/giant clones, similar to that of Indrayani River. Whilst the plants were similar, the roots were significantly shorter than Indrayani, Plate 3.1-8, suggesting a higher nutrient content

than Indrayani, this was likely due to the high input of raw sewage. The river here was difficult to ascertain the flow rate due to the density of the mat, however, the areas of bare river suggest a flow rate higher than the Indrayani River. Collection and preparation of the biomass was carried out by the author in May 2019 and February-March 2020; from May 2019-January 2020 and May 2020 onwards, the collection was undertaken by Dr Gaurav Nahar of DR.



**Plate 3.1-8:** Water hyacinth from Mula Mudtha River, Pune (May 2019).

#### *3.1.1.4. Santiniketan*

Santiniketan is a small village in West Bengal. It is located 3 km north of Visva-Bharati University (VBU) and contains a small assortment of ponds, GP, which contained a large number of WH, Figure 3.1-3. The ponds were stagnant, except during monsoon, and the only source of contamination was the sewage from the village. This contamination was minimal when compared with urban sewage pollution. The plants were of small size, most likely due to the stagnant nature of the water not allowing for regular nutrient turnover. Collection and preparation of the biomass and water was undertaken by Apurba Koley, a masters' student at VBU.



**Figure 3.1-3:** Goyal Para pond sampling point in Santinkean, West Bengal (credit S. Balachandran).

#### 3.1.1.5. *Lake Victoria*

Lake Victoria is one of the great African lakes; the lake is shared by Kenya, Uganda and Tanzania. Water hyacinth exists as floating mats across the lake, most likely due to the high level of nutrient pollution from the various settlements and large catchment area. There were three sampling points selected within Murchison Bay, Kampala; with the aim to find two different WH mats that were affected by a point pollution source and one that demonstrated the effect of the background pollution, Figure 3.1-2. Collection and preparation of the biomass was undertaken by Dr Opio Innocent Miria, a PhD student at Makerere University.

Site 1 had no specific point source and has been determined a clean area (CW); the water is clear compared to the other sites. This site gives an indicator for the background pollution of the lake/ bay.



**Figure 3.1-4:** Clean water site sampling point in Murchison Bay, Lake Victoria (credit O.I. Miria).

Site 2 was at the opening of a sewage pipe, NC; the water was visibly darker due to high turbidity, there was a putrid odour and visible bubbles, Figure 3.1-5.



**Figure 3.1-5:** Nakivubo channel site sampling point in Murchison Bay, Lake Victoria (credit O.I. Miria).

Site 3 was near the opening of a waste stream from Ugandan Breweries Ltd. (UBL); the water was a dark green colour and had high turbidity, Figure 3.1-6.



**Figure 3.1-6:** Ugandan Brewery Ltd. site sampling point in Murchison Bay, Lake Victoria (credit O.I. Miria).

#### *3.1.1.6. Institute of biological, environmental and rural sciences (IBERS)*

Live WH plants were collected from Kew gardens, approximately 25, under a permit issued by the Animal and Plant Health Agency (APHA) within article 35(1) (a) and (b) of the Invasive Alien Species (Enforcement and Permitting) Order 2019, and transported to a secure facility at the University of Aberystwyth. The plants were allowed to proliferate utilising Chempack EC fertiliser 20-20-20 NPK with micronutrients, at a

semi-controlled temperature of 20-25°C, variation was due to external temperature variation.

Eight tanks were also spiked with a HM solution to produce contaminated material for protein extraction. A stock solution of 1000 ppm was prepared, utilising analytical grade HM salts, and used to spike the tanks to 4 ppm of each HM. The salts utilised were copper sulphate ( $\text{CuSO}_4 \cdot 5\text{H}_2\text{O}$ ), iron sulphate ( $\text{FeSO}_4 \cdot 7\text{H}_2\text{O}$ ), zinc nitrate ( $\text{Zn}(\text{NO}_3)_2 \cdot 6\text{H}_2\text{O}$ ) and lead nitrate ( $\text{Pb}(\text{NO}_3)_2$ ).

The cultivation work was carried out by Andrew Taravella (IBERS glasshouse staff member) under direction of the author. The HM spiked cultivation work was conducted by the author.



**Plate 3.1-9:** Cultivation of water hyacinth at the Institute of biological, environmental and rural sciences glasshouses (June 2021).

#### *3.1.1.7. Preservation and storage*

The collected biomass was preserved through various drying methods depending on the capabilities of the location. Samples from Uganda were air dried and oven dried to a moisture content of approximately 7%, by the Centre for Research in Energy and Energy Conservation (CREEC, Makerere University Kampala, Uganda). Samples from India and IBERS were oven dried according to BS EN ISO 18134-1:2015 [287]. The dried biomass was placed in Ziploc bags and transported to the University of Leeds for analysis.

Half of the samples collected at IBERS were collected and place into a NutriBullet blender, the plants were then frozen (-20°C) to allow direct use of wet and dry WH during protein extraction; described in 3.5.1.



### 3.1.1.8. Particle size reduction

To comply with internal phyto-sanitation laws, all samples from India were ground to 1mm using a Bajaj Grinder. These samples were passed through a 1mm screen to ensure homogeneity. All other dried samples were ground cutting mill (Retsch, Germany, SM300) and passed through a 1mm screen to obtain the correct particle size fraction.

The particle size was reduced further, to  $<100\mu\text{m}$ , for proximate, ultimate and inorganic analysis. This reduction in particle size was achieved using a cryomill (Retsch, Germany).

### 3.1.2. Water

At each location, described in 3.1.1.1, approximately one litre of water was collected and poured into a 50 ml centrifuge tube. This was repeated twice more to produce three random samples from the location. This was designed based on the information within BS EN ISO 5667-14:2016 [288].

### 3.1.3. Inoculum

Inoculum was utilised in biomethane potential (BMP) experiments, described in 3.3.5. The inoculum was collected from the outlet of an anaerobic digester at Esholt wastewater treatment plant (WWTP) in West Yorkshire, UK. The anaerobic digester processes wastewater biosolids from an urban population of ~750,000 and was operated under mesophilic temperatures ( $37^{\circ}\text{C}$ ) [289]. The inoculum was collected during steady-state operation of the anaerobic digester. Inoculum was passed through a 1mm sieve to remove large particulates and stored at  $4^{\circ}\text{C}$ . Prior to setting up an experimental BMP ( $\text{BMP}_{\text{ex}}$ ) test, the inoculum was incubated at  $37^{\circ}\text{C}$  for approximately 48-hr to reduce residual methane emissions. The inoculum was stored for less than one month before utilisation.

## 3.2. Cultivation protocol

During this work, a cultivation protocol was determined to ensure the replicability and validity of these experiments; the protocol is described below. Trials and cultivation work were carried out on the roof of DR building;  $18^{\circ}38'03.5''\text{N}$   $73^{\circ}47'16.3''\text{E}$  (Kant Helix, Bhoir Colony, Chinchwad, Pune-411033, India). Sample collection and cultivation trials occurred from May 2019- May 2021. The trials were conducted by the author during fieldwork from February 2020 to March 2020; post-March 2020, the trials were conducted with support from Dr Gaurav Nahar, under the direction of the author. The stock feedstock cultivation was conducted by Dr Gaurav Nahar, under the direction of the author.

Cultivation work was also conducted at the IBERS facility, Aberystwyth University, utilising the small crate protocol.

### 3.2.1. Material collection, preparation and storage

WH was collected from Indrayani River, see 3.1.1.1., and moved to the DR building. The biomass was placed in large tanks (approximately 1.5 m<sup>2</sup>) that was fed with CM once every 14-21 days to ensure the plants were healthy. Whilst the plants were stored in the tanks, there was an obvious change in the growth of the WH, with the proportion of roots growing larger; indicating nutrient deficit when compared with Indrayani River [25,26]. The daughter plants grew to significantly smaller sizes (demonstrating a medium clonal variety rather than the giant that was collected); whilst there was no analysis to conclude that this was due to a nutrient deficit, this was the likely scenario when compared with Indrayani River. The leaves became significantly darker, which was in stark contrast to the previous two changes in morphology as this indicates a nutrient rich plant [25]. The conclusion was that the plants obtained high levels of nutrients in the biomass, but the lack of flowing water suggests that the replenishment of nutrients were diminished, therefore, nutrient deficient characteristics were displayed. The biomass cultivated in these tanks was used as the starter material for the growth trials conducted at DR. Before adding to the tanks, the daughter plants were removed and the plants cleaned to reduce nutrients contaminating the crates.

### 3.2.2. Small crate cultivation

Trials were conducted in small opaque crates, see Plate 3.2-1, of the dimensions 65 x 45 x 31.5 cm, that were filled with 55 L of tap water from the DR water tank. For each trial, three samples of water were analysed and used as the reference value for the trial. Plants were collected from the biomass stock tanks; the plants selected were all  $\sim 150 \pm 50$  g FW; three plants were placed in each crate. The weighing procedure was changed from May 2020 due to the necessity for lone working in India. Before May 2020, the plant roots were gently squeezed until there was a gap of 5 seconds between water drops. After May 2020, removable metal frames were constructed with net in the centre, see, Figure 3.2-1. The frames were held above the crate until there was a gap of 5 seconds between water drops.



**Plate 3.2-1:** Small crate growth trial set up in March 2020.



**Figure 3.2-1:** Addition of metal frame and net for the small crate growth trial (credit G. Nahar).

Once the plants were weighed, they were added to the crates and left to acclimatise for four days. After acclimatisation, the water level was raised back to 55 L; the nutrient sources were then added to the crates and the water agitated to increase solubilisation and then collected for analysis, utilising the same collection method as described in 3.1.2. Each condition was conducted in triplicate, unless stated otherwise. The water level was raised back to 55 L once every 7 days.

### 3.2.3. Large tank cultivation

Large metal tanks were constructed, of the dimensions 1.22 x 1.22 x 0.31 m, and filled with 350 L of tap water from the DR water tank. The tanks were fitted with a metal frame with a net in the centre, as displayed in Plate 3.2-2, this was similar to that shown on the small crates in Figure 3.2-1. The frame was attached to a pulley system to measure the mass of the WH 'mat'.



**Plate 3.2-2:** Large tank with net and pulley system (February 2020).

For each tank,  $35 \pm 5$  plants were collected from the biomass stock tank. The plants chosen were of varying sizes to mimic a new WH mat in the early stages of the growth season. The mats produced weighed  $5.0 \pm 1.0$  kg. The mat was weighed by raising the frame, then hanging the rope supports onto a weight balance, accurate to 50 g, see Plate 3.2-3. The frame was held in the air for one minute to allow the water to drain and then weighed repeatedly until two consecutive weights read equally (a minimum of three repeats).



**Plate 3.2-3:** Weighing water hyacinth mat in large tank with net and pulley system (February 2020).

Once the mat was weighed, the plants were left to acclimatise for 4 days. After acclimatisation, the nutrient source was added. To ensure solubilisation, the nutrient source was added to a drum of tap water and mixed thoroughly before addition to the

tanks. The water level was then raised back to the 350 L mark and the water agitated to facilitate solubilisation. The water level was raised back 350 L once every 7 days. For the seasonal analysis trials, nutrients were added to the tank every 14 days (unless specified in the trial variations).

### 3.2.3.1. Rain shelter construction

The first tank trial, conducted March-April 2020, was halted early; when repeated in July 2020, the impact of an early monsoon caused this trial to be abandoned. The impact of monsoon can lead to raised water levels which causes water overflow, this reduces the nutrient content and removes plants from the tanks. To combat the issues with large rainfall, a shelter was constructed out of semi-transparent plastic sheets mounted on a metal frame, see Figure 3.2-2. The rain shelter will impact the solar radiation reaching the tank, but would be necessary for mass cultivation of WH in India.



**Figure 3.2-2:** Rain shelter over large tanks (Credit G. Nahar).

## 3.3. Material characterisation

### 3.3.1. Proximate analysis

The proximate analysis of a sample determined its four basic constituents: moisture, ash, VM and FC. Proximate analysis was conducted in duplicate via a thermogravimetric analyser (TGA/ Differential scanning calorimetry (DSC) 1, Mettler Toledo). Approximately 10 mg of sample, <100µm particle size, was placed into a pre-weighed ceramic crucible. The TGA was programmed to follow the temperature profile described in Figure 3.3-1. The sample was placed in an atmosphere of N and heated at 25°C/min up to 105°C, where it was held for 10 minutes, the weight change was used to determine moisture. The sample was then further heated to 900°C in the same conditions and the same rate. When 900°C was achieved the temperature was held for

a further 10 minutes; the weight change was used to determine VM. The N atmosphere was then replaced with air and the temperature held at 900°C for 15 minutes to allow the oxidation of carbon, therefore, the weight change determined the FC. The final residue weight was used to determine the ash content of the sample.

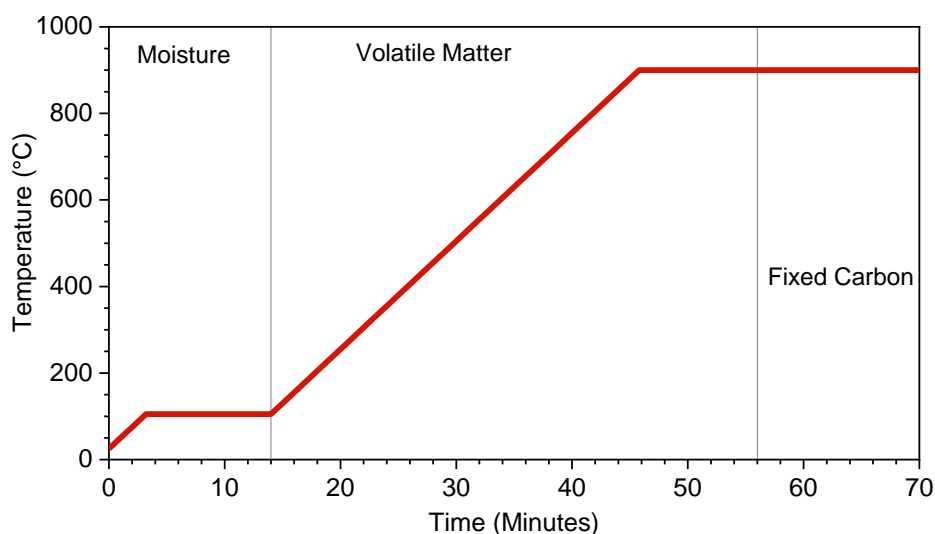


**Figure 3.3-1:** Temperature profile of the thermo-gravimetric analyser for proximate analysis.

### 3.3.2. Ultimate analysis

Ultimate analysis was used to determine the carbon, hydrogen, nitrogen, sulphur and oxygen content of the sample. Ultimate analysis was conducted in duplicate using an EA112 Flash Analyser. The instrument was calibrated with certified reference materials, like oatmeal and 2,5-Bis(5-tert-butyl-2-benzo-oxazol-2-yl) thiophene (Elemental Microanalysis, Devon, UK). A sample of 2.5- 3.5 mg was weighed into a tin capsule which was then crimped and pressed to remove atmospheric air. For samples with a high sulphur content (<5%), ~3 mg of vanadium pentoxide was added to improve combustion.

Samples were placed in an autosampler and injected into the instrument which was purged with helium (He) and combusted at 900°C in a known quantity of oxygen. The gaseous products, CO<sub>2</sub>, water (H<sub>2</sub>O), nitrogen (N<sub>2</sub>) and sulphur dioxide (SO<sub>2</sub>), were passed through a gas chromatography column, where each is separated. The gases were then detected via a thermal conductivity detector to determine the relative fractions of the elemental constituents. The H fraction was corrected for moisture according to Equation 3-1. The O-content was determined by difference through Equation 3-2.

**Equation 3-1:** Hydrogen correction for moisture content.

$$\text{Corrected } H (\%) = H (\%) - (\text{Moisture}(\%) \times \left(\frac{2}{18}\right))$$

**Equation 3-2:** Calculation of oxygen-content, by difference, on an as received basis.

$$O(\%) = 100 - \text{Moisture}(\%) + \text{Ash}(\%) + C(\%) + H(\%) + N(\%) + S(\%)$$

### 3.3.3. Volatile solids

The volatile solids (VS) content of raw and treated biomass were determined in duplicate according to APHA 2540E [290]. Approximately 1 g of sample was dried at 105°C (Mettler Drying Oven) with subsequent ashing at 550°C (Nabertherm B180 furnace). The same methodology was conducted to calculate the VS content of the inoculum, however, ~25mL was added.

### 3.3.4. Elemental analysis

Quantification of the elemental composition of biomass can be achieved by a variety of different methods, including atomic absorption spectroscopy (AAS), inductively coupled mass spectrometry (ICP-MS), inductively coupled optical emission spectroscopy (ICP-OES) and ultraviolet-visible (UV-Vis) spectrometry. These methods require digestion of the sample within acid. A variety of reagents and procedures are applicable for this digestion, however, for this analysis, 10ml of 69% nitric acid was added to 0.2g of sample in a flat-bottomed conical flask and placed on a hot plate, at temperature level 7 until dry. The flasks were then left to cool for ~2 minutes, filled with a further 10ml of 69% nitric acid and swirled, fitted with a reflux funnel and placed on the hot plate for a further 15 minutes at temperature level 5. The samples were left overnight to cool then made up to 50ml with de-ionised water. The sample was then utilised for elemental analysis via ICP-MS and ASS.

The leaf samples collected from the cultivation tanks were analysed by DR laboratory technicians, for total Kjeldhal N (TKN) using the modified Kjeldhal methodology [291], as suggested by Baethgen and Alley [292].

### 3.3.5. Biochemical analysis

#### 3.3.5.1. Structural fibres

The structural fibres (cellulose, hemicellulose and lignin) were quantified utilising the Gerhardt Fibretherm fibre analyser. The samples were required to be <1mm and >100µm. Approximately 1g of sample was placed in a fibre bag, which was placed within a pre-weighed quartz crucible and held open with a glass spacer. The collection was then placed within the Fibretherm carousel and run under standard conditions with neutral detergent solution and heat-stable alpha amylase (amylase was added after 1 hour of run time), prepared according to BS EN ISO 16472:2006 [293]. The sample was then oven dried overnight (Mettler Drying Oven). After 12 hours of drying, the

samples were cooled and weighed, the weight equated to the amylase treated-neutral detergent fibre (aNDF) and ash content.

The samples were then replaced into the Fibretherm carousel and run under standard conditions with acid detergent solution, prepared according to BS EN ISO 13906:2008 [294]. The samples were then oven dried overnight (Mettler Drying Oven). After 12 hours of drying, the samples were cooled and weighed, the weight equated to the acid detergent fibre (ADF) and ash content.

The samples were then placed in a Gerhardt stainless-steel carousel and placed in a beaker of 72% sulphuric acid and rotated slowly for 1 minute every 5 minutes for 30 minutes, before it was allowed to rest for 1 hour and 30 minutes. The carousel was then raised and allowed to drain before being plunged into glass beakers filled with water. This was repeated until the water remained clear after plunging to reduce the contamination from sulphuric acid. The samples were placed in the Fibretherm carousel and run on a water only wash cycle to remove sulphuric acid contamination from the samples. The samples were then oven dried overnight (Mettler Drying Oven). After 12 hours of drying, the samples were cooled and weighed, the weight equated to the acid detergent lignin (ADL) and ash content.

The samples were then placed in a Gerhardt incinerator module and ashed for 2 hours at 550°C (Nabertherm B180 furnace). Once cooled, the samples were weighed, the weight equated to the ash content of the sample. However, this was not a true ash content due to the removal of some inorganics in the Fibretherm process.

Once the ash content has been subtracted, the aNDF, ADF and ADL can then be utilised to calculate the structural fibre content: aNDF is primarily cellulose, hemicellulose and lignin; ADF is primarily made up of cellulose and lignin; and ADL is the lignin content of a sample. The calculations for each structural fibre are displayed in Equation 3-3, Equation 3-4 and Equation 3-5.

**Equation 3-3:** Calculation of cellulose.

$$\text{Cellulose (\%)} = \frac{\text{ADF}(g) - \text{ADL}(g)}{\text{Sample weight (g)}} \times 100$$

**Equation 3-4:** Calculation of hemicellulose.

$$\text{Hemicellulose (\%)} = \frac{\text{aNDF}(g) - \text{ADF}(g)}{\text{Sample weight (g)}} \times 100$$

**Equation 3-5:** Calculation of lignin.

$$\text{Lignin (\%)} = \frac{\text{ADL}(g)}{\text{Sample weight (g)}} \times 100$$



### 3.3.5.2. Protein

Protein content was calculated theoretically through the use of a conversion factor from the N-concentration of each sample. Traditionally, a value of 6.25 has been used to convert N to protein, however, Magomya *et al.* demonstrated that 6.25 is an overestimation of protein in plant samples [273]. Magomya *et al.* determined that the N: protein factors ranged from 3.24 to 5.29, and averaged at 4.64. For the purposes of this study, all protein calculation utilised a conversion factor of 4.64.

## 3.4. Water characterisation

Each location had different capabilities for the analysis of water, therefore, each site was analysed for different water quality indicators.

In Santiniketan, the water was analysed for TKN according to EPA Method 351.1 [295]. Total dissolved solids (TDS) and total suspended solids (TSS) were analysed via a gravimetric analysis according to method 2540C and 2540D, respectively, in the standard methods for the examination of water and wastewater [290]. Dissolved oxygen (DO) was calculated via the Winkler titration method [296].

In Uganda the water was analysed for ammonium ( $\text{NH}_4^+$ ), via Hach Method 8155 [297]; nitrate ( $\text{NO}_3$ ), according to APHA 4500-NO3E [290]; TKN, according to APHA 4500-N C [290]; COD, according to APHA 5220 D [290]; and Cd, Cr, Cu and Ni, according to APHA 3111 B [290]. TSS was calculated using the same method as in Santiniketan.

In Maharashtra, the water collected from rivers was analysed by a third party. The water was analysed for TN and TKN according to APHA: 1992 [298], and for elemental concentrations by ICP-OES according to the ASTM D1976-18 standard [299]. The water collected from the cultivation tanks was analysed by DR laboratory technicians, for TKN using the modified Kjeldhal methodology [291], as suggested by Baethgen and Alley [292].

## 3.5. Utilisation potential indicators

### 3.5.1. Protein extraction

Protein extraction was conducted via alkali acid extraction. Dried samples were milled to ~1 mm particle size, as previously described; one gram was added to 40 mL, unless otherwise stated, of 0.1 or 1.0M NaOH in a 250 mL Duran bottle. The solution was then agitated by hand to mix the solids with the NaOH and placed in a water bath at 40-90°C and 60 RPM, for up to 6 hours. The solution was then filtered through a Whatman 4 filter paper. The solid residue was dried according to BS EN ISO 18134-1:2015 [287]. If required, the solution was stored at 5°C overnight. Sulphuric acid ( $\text{H}_2\text{SO}_4$ ), of varying concentrations, was then added to the solution to reduce the pH to 3.5. The pH of the

solutions was analysed after each addition to ensure the pH did not overshoot. The solution was then centrifuged for 10 minutes at 3500g, this produced a solid protein isolate and a liquid containing NaOH and H<sub>2</sub>SO<sub>4</sub>. The protein isolate was placed in an ALPHA 1-2 LD plus freeze drier (CHRIST, Osterode am Harz, Germany) for 48 hours. For the comparison on wet and dry biomass, the moisture content of the biomass was calculated and utilised to add 1 g of biomass on a dry basis.

### 3.5.2. Biomethane potential

#### 3.5.2.1. Maximum theoretical biomethane potential ( $BMP_{th}$ )

The maximum theoretical biomethane potential (maximum  $BMP_{th}$ ) was determined using Boyle's equation, see Equation 3-6, where  $c$ ,  $h$ ,  $o$  and  $n$  represent the molar fraction of C, H, O and N, respectively. The equation uses units of mL CH<sub>4</sub>/g VS and assumes 1 mole of gas has a volume of 22,400 mL under normalised conditions. The Boyle equation was developed as an update to the Buswell equation [300] to include nitrogen containing fractions of biomass, such as protein. The Boyle equation assumes complete conversion of a substrate, with no concession for biodegradability of the substrate [137], therefore, the Boyle's  $BMP_{th}$  was assumed to be the maximum theoretical biomethane potential. To calculate the "actual" theoretical biomethane potential ( $BMP_{th}$ ), the maximum  $BMP_{th}$  must be converted utilising the biodegradability index (BI), described in section 3.5.2.4.

**Equation 3-6:** Boyle's equation for theoretical biomethane potential [301].

$$BMP_{th}(\text{mL CH}_4/\text{g VS}) = \frac{22400 \left( \frac{c}{2} + \frac{h}{8} - \frac{o}{4} - \frac{3n}{8} \right)}{12c + h + 16o + 14n}$$

#### 3.5.2.2. Experimental biomethane potential ( $BMP_{ex}$ )

The  $BMP_{ex}$  was determined utilising the automatic methane potential test system (AMPTS) II. The system was maintained at 37°C for 30 days. A 2:1 inoculum-to-substrate ration was utilised, on a VS basis, by diluting samples, with distilled water, to 10 g VS/L, and the inoculum to 20 g VS/L. A 200 mL aliquot of sample and inoculum was added to each reactor, resulting in a 400 mL working volume with a 100 mL headspace. Blank reactors, containing 200 mL inoculum and 200 mL distilled water, were run in parallel to account for biomethane emissions from the inoculum. The generated biomethane was normalised, to be expressed on a VS basis, using Equation 3-7, where  $V_{CH_4\text{Sample}}$  is the volume (mL) of the biomethane originating from the sample;  $V_{CH_4\text{Blank}}$  is the volume of biomethane stemming from the blank (mL);  $CVS$  is the concentration of VS added (10 g VS/L); and  $V_{\text{Sample}}$  is the volume of sample added to the reactor (0.2L).

**Equation 3-7:** Calculation of experimental biomethane potential.

$$BMP_{ex\ Solids} = \frac{(VCH_4Sample - VCH_4Blank)}{CVS \times VSample}$$

The headspace was flushed with N to ensure anaerobic conditions. The pH was unadjusted. All measured gas volumes were automatically normalised to standard conditions (1 atm, 0°C and zero moisture content). Each sample was conducted in duplicate.

The AMPTS system calculates biomethan generation via water displace: the biogas travelled down Tygon® tubing where CO<sub>2</sub>, and other acidic gases, were removed by 3M NaOH. The CH<sub>4</sub> then travelled along more tubing where it displaced water, the volume of displaced water was equal to the CH<sub>4</sub> production in the AMPTS system.

The modified Gompertz model was used to fit the BMP<sub>ex</sub> data to describe the process kinetics [302]. The model is described in Equation 3-8, where  $H_m$  is the maximum biomethane yield (mL CH<sub>4</sub>/g VS),  $R_m$  is the peak biomethane production rate (mL CH<sub>4</sub>/g VS/d),  $\lambda$  is the lag phase (d),  $t$  is the time (d) and  $e=2.71828$  [137]. The parameters were estimated via the least squares method and the accuracy of the modified Gompertz model was calculated through the squared correlation coefficient ( $R^2$ ) between the experimental and the modelled data [137].

**Equation 3-8:** Modified Gompertz model.

$$H = H_m \exp \left[ -\exp \left( \frac{R_m e}{H_m} (\lambda - t) + 1 \right) \right]$$

### 3.5.2.3. Large scale biomethane potential

Large scale biomethane potential was conducted in a 200L semi-batch reactor by Dr G. Nahar, as described by Bray *et al.* [138], to replicate a rudimentary-type reactor, often used in rural Indian locations, such as Deenbandhu fixed-dome digesters [303]. The reactor was loaded at a 20:80 ratio of WH:CM on a wet basis, representing a 15:1 inoculum-to-substrate ratio on a VS basis. Further material was added to maintain the ISR ratio.

The head space was flushed with nitrogen, and the gas generation was measured using a pressurised gauge. The generated gas was passed through a water trap to remove the condensable material, such as water vapour and fine dung particles, and stored in an sport utility vehicle tyre tube. The stored biogas was measured on alternate days using a biogas pump provided by SP ecofuel, Gujarat, India. The biogas flow was measured using a flow meter provided by PS Instruments, Mumbai, India.

The gas composition was analysed using a gas chromatograph (GC, Agilent 7890 B Gas Chromatograph, Germany). The gas analysis was performed using argon as a

carrier gas, and detection was achieved by means of a thermal conductivity detector. The average yield of methane that evolved in the test reactor was used to predict the expected yields in a typical fixed-dome digester for the techno-economic analysis.

#### 3.5.2.4. Biodegradability

The biodegradability, or the biodegradability index (BI), of a sample is defined as the methane conversion efficiency of a sample and is calculated utilising the  $BMP_{ex}$  and the maximum  $BMP_{th}$  [304], see Equation 3-9:

**Equation 3-9:** Calculation of anaerobic biodegradability index.

$$BI (\%) = \frac{BMP_{ex}}{Max\ BMP_{th}} \times 100$$

#### 3.5.2.5. Theoretical mass balance

A modified Buswell and Neale equation [305], shown in Equation 3-10, was utilised to calculate the theoretical conversion of the biomass to  $CH_4$  and  $CO_2$ , where  $n$ ,  $a$  and  $b$  equates to  $C_nH_aO_b$ .

**Equation 3-10:** Modified Buswell and Neave equation for theoretical conversion of organics to methane and carbon dioxide.

$$\%CH_4 = \frac{\left(\frac{n}{2} + \frac{a}{8} - \frac{b}{4}\right)}{\left(\frac{n}{2} + \frac{a}{8} - \frac{b}{4}\right) + \left(\frac{n}{2} - \frac{a}{8} + \frac{b}{4}\right)}$$

To calculate the mass and N flow, the BI was utilised.

### 3.5.3. Higher heating value

#### 3.5.3.1. Theoretical higher heating value

The theoretical HHV ( $HHV_{th}$ ) can be calculated using a multitude of equations [47], predominantly calculated by utilising ultimate and/ or proximate analysis. To assess this, eight equations were selected, see Table 3.5-1. To determine the optimal equation for calculating  $HHV_{th}$ , eight samples, see Table 3.5-2, were selected for analysis via bomb calorimetry, as described in 3.5.3.2, and the residual sum of squares (RSS) calculated; the results are displayed in Table 3.5-3. Equations 7 and 8 utilised ash content to determine HHV, however, in comparison to traditional biomass feedstocks for combustion, WH has a high ash content [47,48]. Therefore, the HHV from equations 7 and 8 were discounted due to over or underestimated HHV.

Equation 5 produced the lowest RSS, however, the equation calculated HHV using just C; the calculation of HHV is the enthalpy of complete combustion, where all carbon and hydrogen, and other products, are completely oxidised [174]. Therefore, this equation may poorly estimate HHV when applied to a greater range of samples. To account for

this, equation 3 was selected: this equation utilised C, H and O and had the second lowest RSS.

**Table 3.5-1:** Equations for theoretical higher heating value estimation.

Equation No.	Reference	Equation
1	[137]	$HHV = (0.3383C) + (1.422 \times (H - (O/8)))$
2	[306]	$HHV = 0.196FC + 14.119$
3	[307]	$HHV = -1.3675 + 0.3137C + 0.7009H + 0.0318O$
4	[174]	$HHV = 3.55C^2 - 232C - 2230H + 51.2C \times H + 131N + 20600$
5	[308]	$HHV = 0.3699C + 1.3178$
6	[308]	$HHV = 0.3856 \times (C + H) - 1.6938$
7	[47]	$HHV = 19.914 + 0.2324Ash$
8	[47]	$HHV = 4.9422 + -2.5170Ash + 0.2678C + 0.0653 \times (Ash \times C)$

**Table 3.5-2:** Sample types for bomb calorimetry.

Sample No.	Location	Plant Part	Date
1	Indrayani Moshi	Whole	May-21
2	Indrayani Moshi	Root	Feb-21
3	Indrayani Moshi	Leaf	Jan-21
4	Ugandan Brewery Ltd.	Petiole	Aug-20
5	Mudtha Baner	Root	May-21
6	Mudtha Baner	Petiole	Feb-21
7	Ugandan Brewery Ltd.	Root	Jun-20
8	Nakivubo Channel	Root	Sep-20

**Table 3.5-3:** Higher heating value results from bomb calorimetry and various theoretical higher heating value equations.

Sample No.	Bomb Colorimeter	Equation Number					
		1	2	3	4	5	6
1	15.5	11.4	16.5	13.8	15.2	14.2	13.4
2	13.7	9.3	16.1	12.5	14.8	13.0	12.0
3	17.0	13.3	16.7	15.2	16.1	15.4	14.9
4	13.5	9.1	17.1	13.7	15.0	13.9	13.0
5	8.8	7.5	15.0	7.5	15.0	9.3	7.5
6	13.3	8.0	16.7	12.4	15.1	13.0	11.8
7	11.8	9.2	16.4	11.4	14.6	12.3	11.1
8	10.7	8.5	15.9	10.5	14.3	11.3	10.1
RSS	-	110.2	117.5	9.7	66.3	5.9	16.6

### 3.5.3.2. Experimental higher heating value

The experimental HHV ( $HHV_{ex}$ ) was calculated for a select number of samples to inform the equation selection for all the samples. This was performed on a Parr (USA) 6200 bomb calorimeter, according to BS ISO 1928:2009. This work was carried out by Karine Alves Thorne (University of Leeds laboratory technician).

## Chapter 4.

# Natural variations of water hyacinth

### 4.1. Introduction

WH has significant potential as a resource, as demonstrated in Chapter 2; it can grow rapidly and reach a high density, resulting in a large amount of biomass that has the characteristics to be used across many disciplines. However, it was also shown that biomass can vary by location, and even across a population. Therefore, it is vital to understand if these variations will change the potential utilisation of WH and if the biomass can be trusted to fall within certain limits regardless of the locality, water quality and time of harvest.

The key objective of this chapter was to assess WH as a resource; this was achieved via the following sub-objectives:

- WH was characterised in terms of proximate, ultimate and inorganic composition;
- WL was characterised as a comparison to WH;
- Potential utilisation indicators were used to determine the applicability of each feedstock for further conversion;
- Variations between feedstocks were analysed based on morphological, geographical, water quality and phenological variation.

Initially, the biomass and water were characterised and analysed based on the average composition within the sites selected, see Chapter 3 for a list of the sites. This allowed a comparison across the sites to understand the potential impacts of varied environmental conditions, based around geographical location, and water body type/quality. The whole biomass and parts of the plant were analysed. The characterisation was utilised to determine a variety of utilisation potential indicators (UPI), including biomethane potential (BMP), higher heating value (HHV) and protein quantity. Next, the characterisation was utilised to demonstrate the phenological variations in biomass that occurred at each site. The UPIs were also calculated for the phenological variation.

#### 4.1.1. COVID-19 impact statement

The impact of COVID-19 was significant on the fieldwork that could be conducted in this chapter, as well as the laboratory experiments. Collection of biomass and water

could not be undertaken by the author for much of the study due to international and local lockdowns. In Maharashtra, collection was conducted by the author in June 2019 and March 2020. These collections were utilised to generate a sampling protocol for the project, see Chapter 3. In Maharashtra, sample collection was undertaken by Dr Gaurav Nahar of Defiant Renewables Ltd., however due to COVID-19, sample collection was abandoned for January, April and May 2021. All water samples from Maharashtra were sent to third-party laboratories for analysis. Due to the closure of these, certain samples were disposed of after long term storage. In Goyal Para, West Bengal, sample collection was undertaken by Apurba Koley of VBU. However, due to issues of travelling to the site, biomass collection could only be undertaken at three points of time. All water analysis was conducted by Apurba Koley on site. In Uganda (Murchison Bay, Lake Victoria), sample collection was undertaken by Dr Opio Innocent Miria of CREEC. Due to limited sample, all biomass was split into tissues to understand the variation in plant part composition. Water collection was due to start in early 2020, however, this was delayed due to COVID-19; all water was analysed on site by Dr Opio Innocent Miria. All biomass was transferred to the University of Leeds for analysis. Due to the closure of laboratories at the University of Leeds, biochemical analysis of the biomass was removed from this study. However, a small-scale study was conducted on a subset of the samples and is discussed in Chapter 6.

#### **4.2. Geographical and water quality study of water hyacinth**

Six sites were selected for this study: one from Murchison Bay, Lake Victoria, Uganda (eventually split in three sites for individual parts) and five from India (four from Pune, Maharashtra and one from Santiniketan, West Bengal), a full list is described in Chapter 3. There are multiple differences between the sites that impacted the composition; these include but are not limited to: type/size of water body; flow rate of the water; pollution source and quantity; climatic conditions; seasonal variation in biomass and climatic conditions; WH clonal variety; dominance of WH; and WH coverage. The four samples from Maharashtra (Indrayani and Mula) were collected from rivers with consistent flows and high raw sewage pollutions. The West Bengal site contained small ponds polluted with local village sewage, therefore it is likely to be cleaner than Maharashtra and have a higher residence time. Lake Victoria is one of the great African lakes and has high nutrient pollution; the lake has a high residence time, with many WH mats floating around the lake. Collection was undertaken in Murchison Bay, Lake Victoria, a site adjacent to Kamapala and was polluted from a variety of industries.

#### 4.2.1. Water analysis

The three sites from Murchison Bay, Lake Victoria, CW, NC and UBL, were analysed for a variety of water quality indicators (WQIs). Figure 4.2-1 displays the HM and nutrient concentration of the Murchison Bay sites. Each site was analysed 5-7 times, depending on the type of analysis, over a two-year period; these were averaged to demonstrate the geographical and pollution source variations. All analysed parameters demonstrated the greatest variation at NC, this suggests that the introduction of sewage had a greater impact than industrial pollution. NC had the highest levels of Cu, NH<sub>4</sub>, NO<sub>3</sub>, TKN, COD, TSS and phosphate (PO<sub>4</sub>); these are all likely to be associated with sewage pollution [309,310]. The CW site can be assumed as background level of pollution, suggesting that Ni pollution occurs throughout the bay and is not associated with the point sources selected in this study. There was little variation between CW and UBL, suggesting that the brewery effluent had little impact on the selected WQIs.

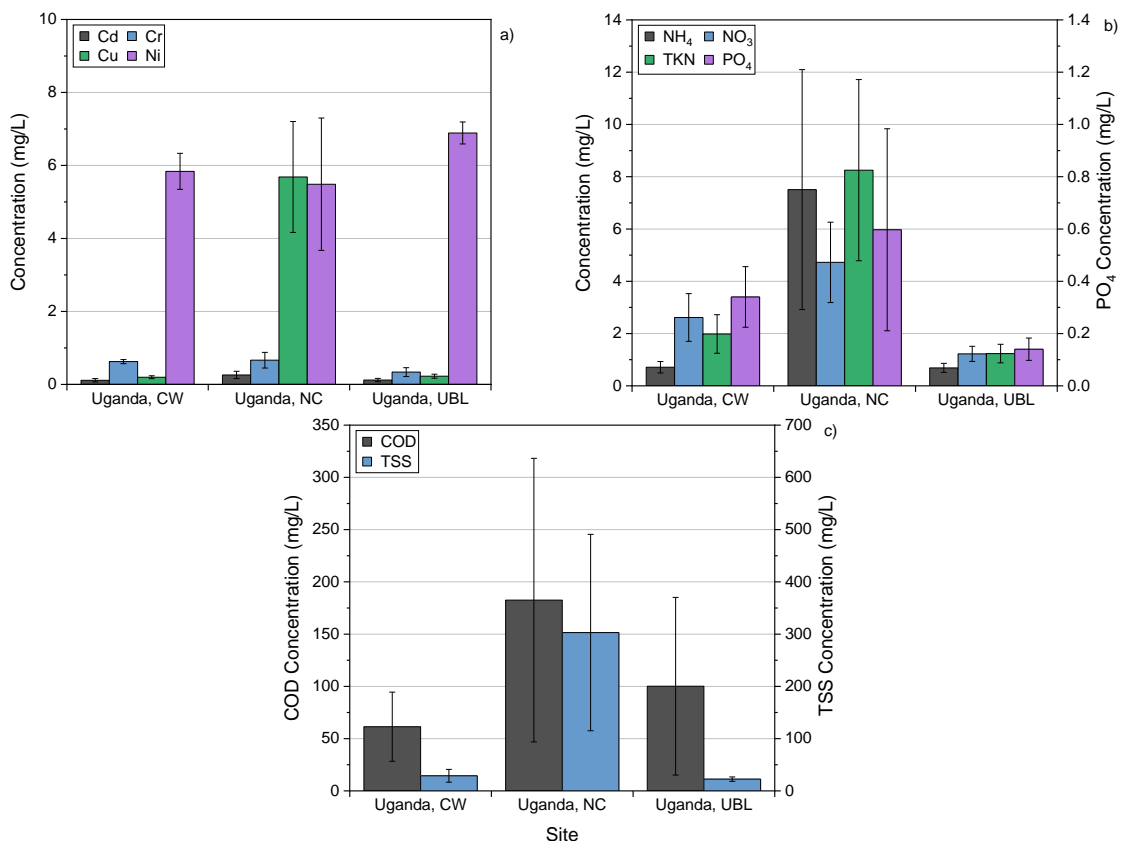


**Figure 4.2-1:** Water analysis of the Murchison Bay sites. Error bars represent the standard error of the mean due to the phenological variations at each site. a) heavy metals, 5 samples in duplicate; b) nitrogen compounds (NH<sub>4</sub>, NO<sub>3</sub> and TKN) and phosphate (PO<sub>4</sub>), 7 samples in duplicate; c) chemical oxygen demand (COD) and total suspended solids (TSS), 7 samples in duplicate.

The sites in Maharashtra were on two rivers, two sites on the Indrayani River and two on the Mula River, as described in section 3.1.1.1. The rivers both received untreated sewage, 20 million L/day [281] and 267 million L/day [286] to the Indrayani and Mula



River, respectively. Figure 4.2-2 demonstrates the flow of the rivers and the major points of pollution on the way to the sample points. On the Mula River: the Baner WWTP had the capacity to treat 30 million L/day; Sangvi could treat 15 million L/day; Bopodi treated 18 million L/day; Mundhwa treated 45 million L/day; and Tanajiwadi could treat 17 million L/day [283,286]. It is unknown how much raw sewage entered the river at these sites. To the west of the city is located the Hinjewadi Maharashtra Industrial Development Corporation (MIDC) site, the plots are mainly software companies, with 2-3 thousand employees in total, and produced 2.5 million L/day of effluent, of which 1.7 million L cannot be treated on site [283,284].

In Lonavla (not on the figure), on the Indrayani River, of the 12.3 million L/day of sewage generated, only 3.7 million L/day were treated; Talegaon had no WWTP and generated 7 million litres of untreated sewage [283]; Dehu treated 8.2 of the 8.5 million L/day of sewage; at Alandi there was no WWTP and therefore released 2.4 million L/day of raw sewage into the Indrayani River [283]. Secondly, unquantified mass pollution events occur annually along the Indrayani River, including the bi-annual yatras, Sanskrit for journey or procession, where hundreds of thousands of 'yatras' gather in Alandi [283]. On the Northern side of the river from Talegaon is a MIDC site, on this site were various engineering corporations like Larsen and Toubro Ltd., producing 1.6 million L/day of industrial effluent [283,284]. North east from Dehu is the Chakan MIDC site, it houses over 750 large and small industries, including a high number of automotive companies (like the Volkswagen Group and Jaguar Land Rover) and food processors, producing 4.8 million L/day of industrial effluent [283,284]. To the southwest of Dehu is the Talawade MIDC site, the site produces 1.6 million L/day of effluent and with most plots containing software centres [283,284].

The water was analysed for inorganics, Ag, Al, Au, B, Ba, Ca, Cd, Cr, Cu, Fe, K, Mg, Mn, Mo, Na, Ni, P, Pb, Si, Sn, Ti and Zn, and nitrogen, TN and TKN; the results are displayed in Figure 4.2-3 show the inorganics that had one or more values above 0 mg/L.

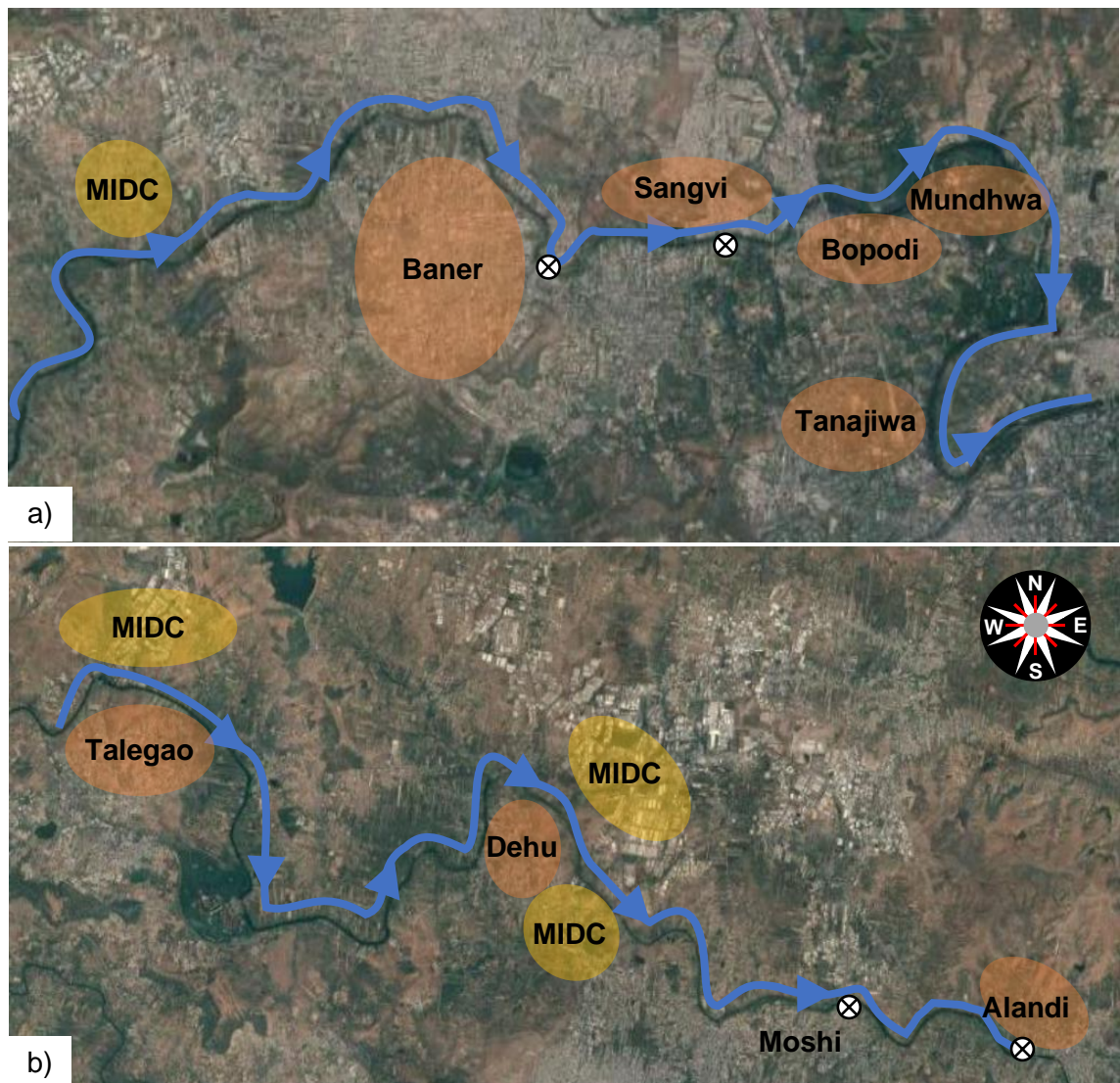


**Figure 4.2-2:** Map of the Indrayani and Mula rivers, demonstrating the flow of the river and the major sources of pollution. ● = sewage pollution locations; ● = industrial pollution locations; MIDC= Maharashtra Industrial Development Corporation; ⊗ = biomass and water collection locations. a) Indrayani River, Pimpri Chinchwad; b) Mula River, Pune.

Due to the high phenological variability, there is little that can be discerned from the differences in HMs and N across the locations. The highest inorganic concentration was Ca, Mg and Na, these are not traditionally associated with raw sewage pollution [309,310]. The analysis of Cr, Ni, Pb and Zn were below detectable limits (BDL) suggesting that the WH mats were successful at removing the HM pollution from the water. Similarly, Cu and Fe were only above the detectable limits at one collection point.

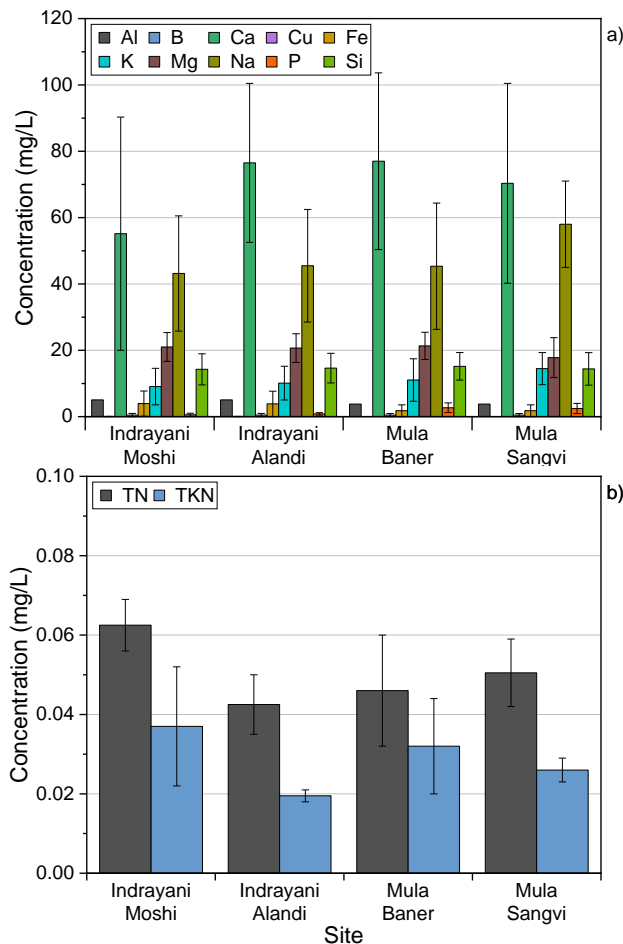


**Figure 4.2-3:** Water analysis of Pune and Pimpri Chinchwad sites. Error bars represent the standard error of the mean due to the phenological variations at each site. a) heavy metals, 3 samples in duplicate; b) nitrogen (TN and TKN), 2 samples in duplicate.

TKN, TSS, DO and TDS were analysed at the West Bengal site; these were analysed six times over an 18-month period, see Figure 4.2-4. The TSS of West Bengal was 9.7% of CW, Murchison Bay, suggesting it to be water body with the lowest pollution, therefore, these results are the baseline for a “clean waterbody” in comparison to urban waterbodies.

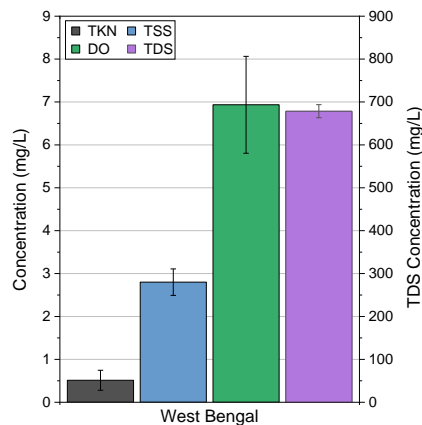


**Figure 4.2-4:** Water analysis of West Bengal site. Error bars represent the standard error of the mean due to the phenological variations at each site, 6 samples in duplicate.

The TKN analysis was conducted at all sites; the results demonstrated that the Maharashtra rivers had the lowest concentration of TKN, this was likely due to the higher flow rate of water, constant refreshing of the water will dilute the pollution, however, over time plants would have been exposed to a greater total nutrient quantity. Murchison Bay had a greater TKN than West Bengal, confirming that West Bengal was likely to receive the lowest pollution concentration. This was also true for TSS, which hit a maximum of 4.2 mg/L in West Bengal, compared with 1350.7 mg/L for Murchison Bay.

The HM analysis showed that Maharashtra had significantly lower metal concentration than Murchison Bay: Maharashtra rivers were BDL at all sampling points for Cd, Cr and Ni, and BDL for Cu for all except for one. This one result was 1.45 and 1.40 mg/L in Indrayani and Mula River, respectively; in comparison to an average result of 0.2, 5.7 and 0.2 mg/L at CW, NC and UBL (Murchison Bay), respectively. These results follow a similar relationship to TKN, where the concentration was lower, but due to a high flow rate, it is likely that the plants were exposed to a greater total HM content.

#### 4.2.2. Whole plant samples

A whole sample was selected from each location, with the addition of a sample of *Pistia stratiotes* (Water Lettuce- WL) from Indrayani Moshi and analysed for proximate, ultimate, and inorganic composition, displayed in Figure 4.2-5 and Figure 4.2-6. Table 4.2-1 displays UPIs of the biomass and the date of collection. The whole sample from Murchison Bay was collected in Murchison Bay but prior to multi-site allocation and was situated outside of the zones, however, it is likely to be similar to CW which was closest to the background levels of the lake.

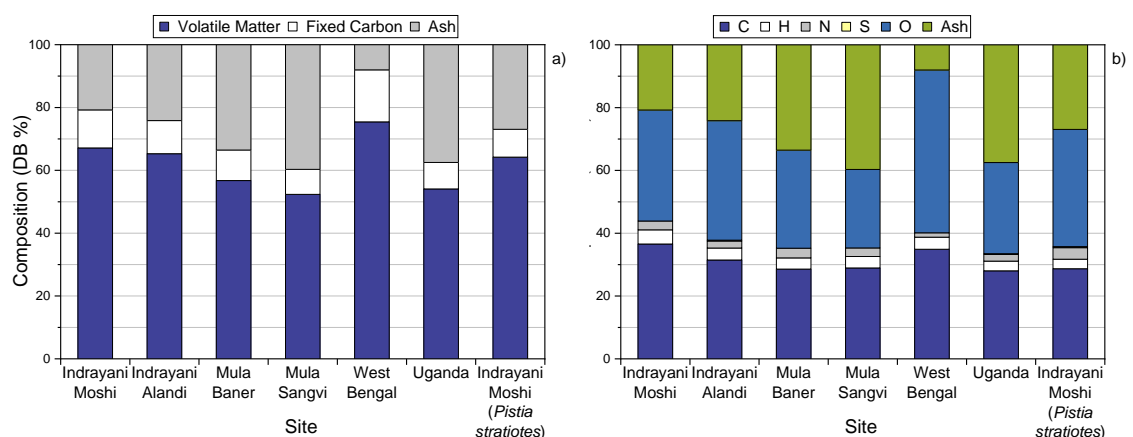


**Figure 4.2-5:** Proximate (a) and ultimate (b) composition of whole water hyacinth and water lettuce samples for geographical and pollution analysis. Each sample was run in duplicate.

The proximate analysis was conducted by thermogravimetric analysis to understand the variations, in the proportion of VM, FC and ash, of the different sites. The results

are presented on a dry basis (DB): no moisture fraction is presented. VM represents the greatest fraction across all sites, ranging from 52.4 (Mula Sangvi) to 75.4% (West Bengal). WL was within the range of WH samples with a VM of 64.2%. The FC fraction ranged from 8.0 (Mula Sangvi) to 16.6% (West Bengal); Table 2.1-1 demonstrated that literature suggests that the organic matter (OM) fraction, VM plus FC, ranged from 74.3- 83.7%, in comparison to the range of 60.3 (Mula Sangvi) to 92.0% (West Bengal). The organic matter contributes to towards the energy potential of a feedstock, the ash and moisture are considered inert in terms of energy potential, therefore, these results suggest that WH has a large range of energy potential. In comparison to the feedstocks studied by Brown, WH had a greater range of OM, with the majority of samples containing a lower fraction of OM [137]. This was corroborated by the statement in section 2.1.1.1: the ash content of WH is considered high for a plant that would be utilised for bioenergy. This results in a high inert fraction; in tandem with a high-water content, raw WH biomass would not be an ideal energy feedstock. This study demonstrated an ash content range of 8.0 (West Bengal) to 39.7% (Mula Sangvi), again, this shows a greater range than literature. There appears to be no trend based on the geographical or pollution variations, however, West Bengal had a lower ash content, possibly due to reduced pollution in the ponds. The average value was 27.3%, for WH only, this suggests that this study has a greater ash content than was reported in literature. It was previously stated that WH has a lower ash content than WL, however, this study reports an ash content of 27.0% for WL.

The CHNSO content of each location has been displayed in Figure 4.2-6; the O content was calculated by difference. The average abundance of elements follows  $O > C > H > N > S$ , however, Brown suggests that when O content of WH was directly measured, the result was significantly lower than by difference [137]. This would make C the most abundant element, ranging from 28.0 (Murchison Bay) to 36.6% (Indrayani Moshi), as would be expected in lignocellulosic biomass [137]. The H, N and S content represents a smaller fraction than C and O. WL contained a greater N content, 3.7%, than WH, 1.4 to 3.1%. The S content was BDL for four out of the seven samples, and WL (0.33%) contained the highest proportion of S out of all the samples. There appears to be no trend based on the geographical or pollution variations.

The UPIs, displayed in Table 4.2-1, focussed on utilisation by AD, protein extraction and direct combustion. The maximum  $BMP_{th}$  is a measure of the maximum theoretical yield of biomethane, on a dry basis, from a feedstock [301]. The maximum  $BMP_{th}$  of lignocellulosic biomass tends to range from 426- 599 mL  $CH_4/g$  VS [311], this would suggest that WH has a low potential for AD in comparison to other lignocellulosic biomass. However, a more realistic  $BMP_{th}$  can be calculated utilising the BI, this is the

ratio between maximum  $BMP_{th}$  and  $BMP_{ex}$  to demonstrate the methane conversion efficiency of a feedstock [137,304]. Brown reported that WH had a BI of 12-61% [137], compared with Allen *et al.* who found that a range of 33-90% for a variety of other lignocellulosic biomass [311]. This would suggest that raw WH is poorly converted through AD and corroborates the fact that it could make a poor feedstock for AD. A further example of this is the C:N ratio: an optimal C:N ratio, for the AD of WH, is ~32.1 [312], over twice the ratio found in this study.

The protein content of WH, at all sites, was lower than WL and lower than major animal products in human diets, for example, chicken (23.1%), beef (21.4%), salmon (18.7%), cod (16.6%) and canned tuna (26.5%) [313,314]. The protein content of WL was higher than raw tofu (15.8%) [313,314], however, raw soybean has a protein content of over twice that of WL and WH [141].

The  $HHV_{th}$  was <15 MJ/kg for all samples, this would be considered low for a biomass fuel [306,308,315]: Friedl *et al.* examined 154 different biomasses and found an average  $HHV_{th}$  of 18.9 MJ/kg [174]. This suggests that WH would not be a suitable choice for solid fuel combustion. Secondly, the high ash content of the root may suggest that WH would not be suitable for direct incineration [140]. The inorganic content of WH is displayed in Figure 4.2-6.

**Table 4.2-1:** Utilisation potential indicators of whole water hyacinth and water lettuce samples for geographical and pollution analysis.

Site	Date	Max $BMP_{th}^*$ (mL $CH_4$ /g VS)	C:N ratio*	$HHV_{th}$ (MJ/kg)*	Protein (%)*†
Indrayani Moshi	May-21	412.6±3.7	12.9±0.2	14.4±0.1	13.1±0.1
Indrayani Alandi	May-21	336.0±21.8	14.1±0.2	12.4±0.3	10.3±0.2
Mula Baner	May-21	358.9±6.7	9.2±0.2	11.1±0.1	14.3±0.1
Mula Sangvi	May-21	445.4±0.2	10.6±0.0	11.1±0.0	12.7±0.1
West Bengal	Jan-20	264.3±11.2	24.7±0.9	13.9±0.2	6.6±0.3
Murchison Bay‡	Dec-18	374.7±30.6	13.1±0.1	10.5±0.4	10.0±0.1
Indrayani Moshi ( <i>Pistia stratiotes</i> )	Jun-19	274.7±0.3	7.8±0.1	10.9±0.0	17.1±0.3

\*Calculated on a dry basis; †Calculated via conversion factor, on N content, of 4.64 [273]; ‡Lake Victoria

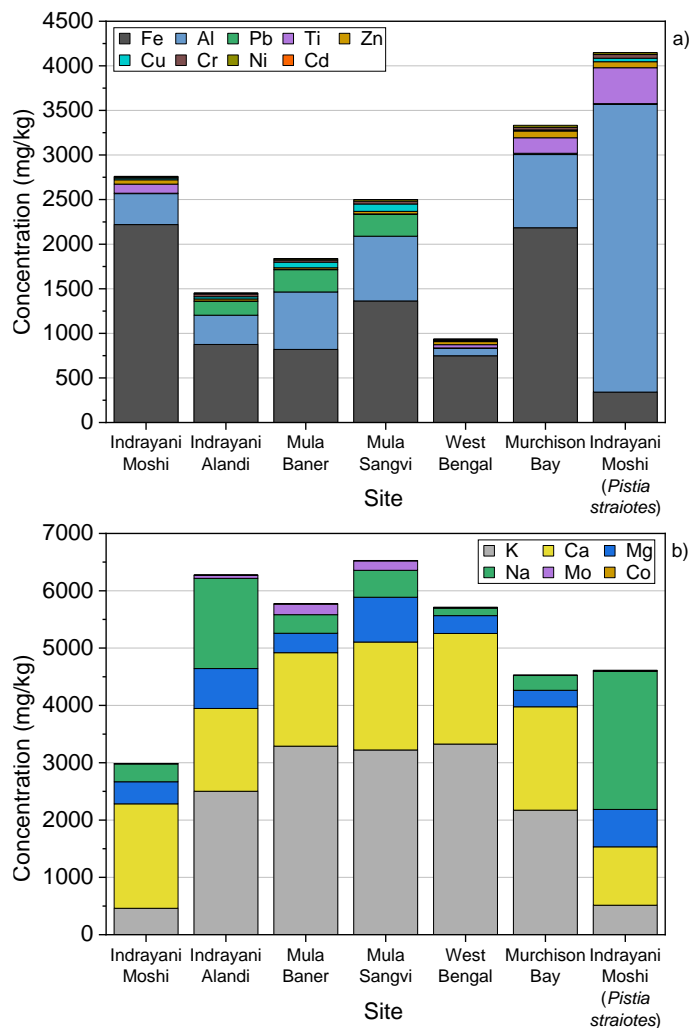


**Figure 4.2-6:** Inorganic composition of whole water hyacinth and water lettuce samples for geographical and pollution analysis. a) heavy metals; b) nutrients. Each sample was run in duplicate.

The WH samples contained high levels of HMs, in particular Fe and Al, see Figure 4.2-6. The Fe content ranged from 748 (West Bengal) to 2220 mg/kg (Indrayani Moshi), greater than the range for Al: 86 (West Bengal) to 821 mg/kg (Murchison Bay). Murchison Bay had a greater total HM content than any site in India, this was possibly due to the zero-tolerance policy for industrial pollution within Maharashtra rivers [281]. However, there are large concentrations of untreated sewage released into both rivers; this is likely to contain elevated levels of Al, Cr, Cu, Fe, Ni, Pb and Zn [309,310].

The order of the average concentration, for each HM, is displayed in the legend of Figure 4.2-6; this demonstrates that Fe, Al and Ti are three of the four highest concentration HMs; this is likely due to the method of uptake: Fe, Al and Ti are elements that are adsorbed to the root surface [149], as opposed to actively taken up.

The presence of Ti at Indrayani Moshi does imply that another source of pollution occurs. The discharge of Ti to the environment is likely to originate from chemical and pharmaceutical; glass, ceramic, textile and tanning; metallurgy; and pigment, dye and

paint industries [6,12,16,316]. Whilst industrial pollution is prohibited, there are 44 major industries that utilise water from the river, generating 23.07 million L/day of industrial effluent, within the Indrayani Moshi area [281]. The presence of Ti, and the formation of toxic foams [317], implies that a zero tolerance of industrial pollution may not have been adhered to; an alternative is the presence of scrap traders/ yards along the river before the Moshi site [318]. The Ti could have been introduced by illegal dumping or runoff during heavy rains; this possibility would clarify the reduction in Ti at Alandi, where there are no scrap traders, and the levels of Ti would have been reduced by the uptake from WH.

The second site on each river (Alandi and Sangvi), show different trends: Indrayani samples demonstrate lower total HM content on the second site, whereas Mula demonstrates an increase at the second site. It is suggested that was due to the difference in pollution: Mula receives regular pollution along the river and therefore the WH consistently reduces the HM content within the river, suggesting that significant pollution occurs between the two sites, likely from Baner side Water Treatment Plant; in contrast, Indrayani receives greater quantities of pollution before the city, therefore, WH reduces the pollution as it travels down the river and therefore samples in Alandi are subjected to lower concentrations. Further analysis of the water quality and sites downstream would be required to confirm this hypothesis.

WL demonstrated the highest total HM content, with a high concentration of Al but low concentration of Fe, in comparison with WH. It has been shown that WL has a greater bioaccumulation of Cd, Cu and Zn than WH [66]; in this study, WL had the third and second highest concentration of Cu and Zn, respectively. WL also contained high concentrations of Ti, corroborating the assumption that industrial pollution does occur in the Indrayani River.

The nutrient concentration demonstrates less variation than HMs, with the exception of Indrayani Moshi, the total nutrient content range was 4531 (Murchison Bay) to 6529 mg/kg (Mula Sangvi). The highest concentration was from K and Ca, the low K concentration at Indrayani Moshi was responsible for the low total concentration of nutrients in these samples. Indrayani Alandi is a site for the bi-annual assembly of yatras and is therefore a site for high sewage pollution events, suggesting that the higher nutrient content, in comparison to Moshi, could be due to this event. There appears to be little conclusive trend for geographical or pollution variation in nutrient content. WL contains similar total nutrient concentration; however, this is due to high concentrations of Na, with a lower K and Ca content.



### 4.2.3. Water hyacinth tissue variations

The same collection sites, as used for the whole plant analysis, were used for the WH tissue analysis. However, for Murchison Bay, three sites were selected for tissue analysis. Multiple collections were undertaken at each site and averaged to understand total variation in the sample, described in Table 4.2-2. The samples were analysed for ultimate, proximate and inorganic composition analysis.

**Table 4.2-2:** Water hyacinth collection sites included in the geographical and pollution study.

Site	Water Body	Main Pollution Source	Dates Included Start	End	Collections
Moshi, Pimpri Chichwad	Indrayani River	Treated Sewage	Jan-21	May-21	4
Alandi, Pimpri Chinchwad	Indrayani River	Treated Sewage	Jan-21	May-21	4
Baner, Pune	Mula River	Raw Sewage	Jan-21	May-21	4
Sangvi, Pune	Mula River	Raw Sewage	Jan-21	May-21	4
Santiniketan, West Bengal	Goyal Para Ponds	Minimal	Dec-19	Jul-20	3
Uganda, CW	Murchison Bay*	No point source	Oct-19	Sep-20	8
Uganda, NC	Murchison Bay*	Treated Sewage	Oct-19	Sep-20	8
Uganda, UBL	Murchison Bay*	Industrial (Brewery)	Oct-19	Sep-20	8

\*Lake Victoria

The proximate analysis, displayed in Figure 4.2-7, demonstrated that the leaf and petiole have the least variation across the locations. The standard deviation (SD) of the leaf was 2.0, 1.7 and 3.4%, for the VM, FC and ash, respectively and the petiole was 2.2, 1.5 and 3.3%. In contrast, the root had larger variations in the ash and VM content across the locations; the SD was 10.4, 3.7 and 13.8%, for the VM, FC and ash, respectively. The ash content of the root was replicated in the trend across the other tissues: the sites with the highest ash content in the root, also have the highest ash content in the leaf and petiole.

The river sites, Indrayani and Mula, contained the highest ash content, suggesting that the flow rate had a greater impact on ash content than pollutant concentration. Between the two rivers Mula had greater ash content, likely due to the higher sewage pollution which could result in a greater inorganic uptake. NC had a pollutant concentration of up 10x that of the other sites in Murchison Bay, yet only displayed a

marginal increase in ash content. In contrast, West Bengal had the lowest pollution and demonstrated the lowest ash content.

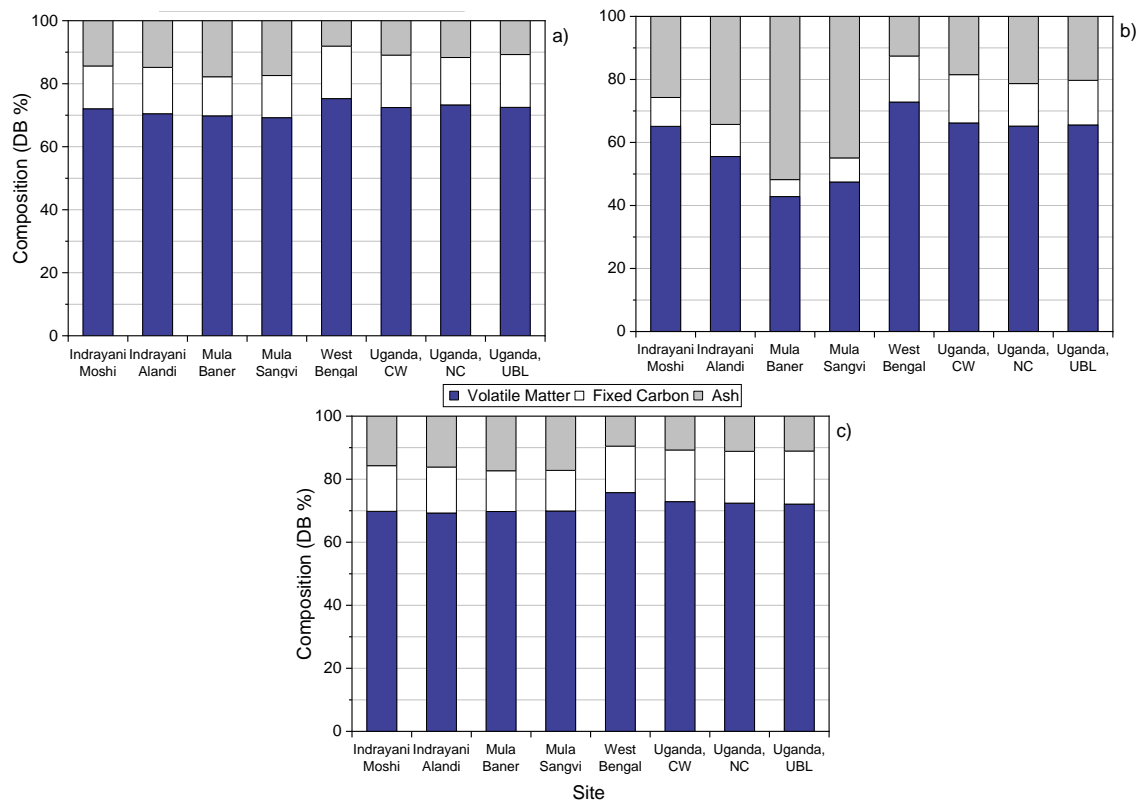


**Figure 4.2-7:** Proximate composition of water hyacinth tissue samples for geographical and pollution analysis. a) leaf; b) root; c) petiole. Each sample was run in duplicate; each of location was an average of all phenological samples: Maharashtra had 4 samples, West Bengal had 3 samples, Murchison Bay (Uganda) had 8 samples.

The ultimate composition, see Figure 4.2-8, demonstrated a similar trend to the whole sample analysis: samples with lower ash content had higher C content, the exception was West Bengal. The river samples contained the greatest N concentrations, in the leaf and petiole, suggesting that N uptake was greater due to increased flowrate. This corroborates the suggestion that flow has a greater impact than pollutant concentration, as all river sites had an average water TKN of at least 10x lower than the other sites. The S content was low in the leaf and petiole; in the root it was in greatest concentrations in the river samples, with the exception of Mula Baner, which was BDL.

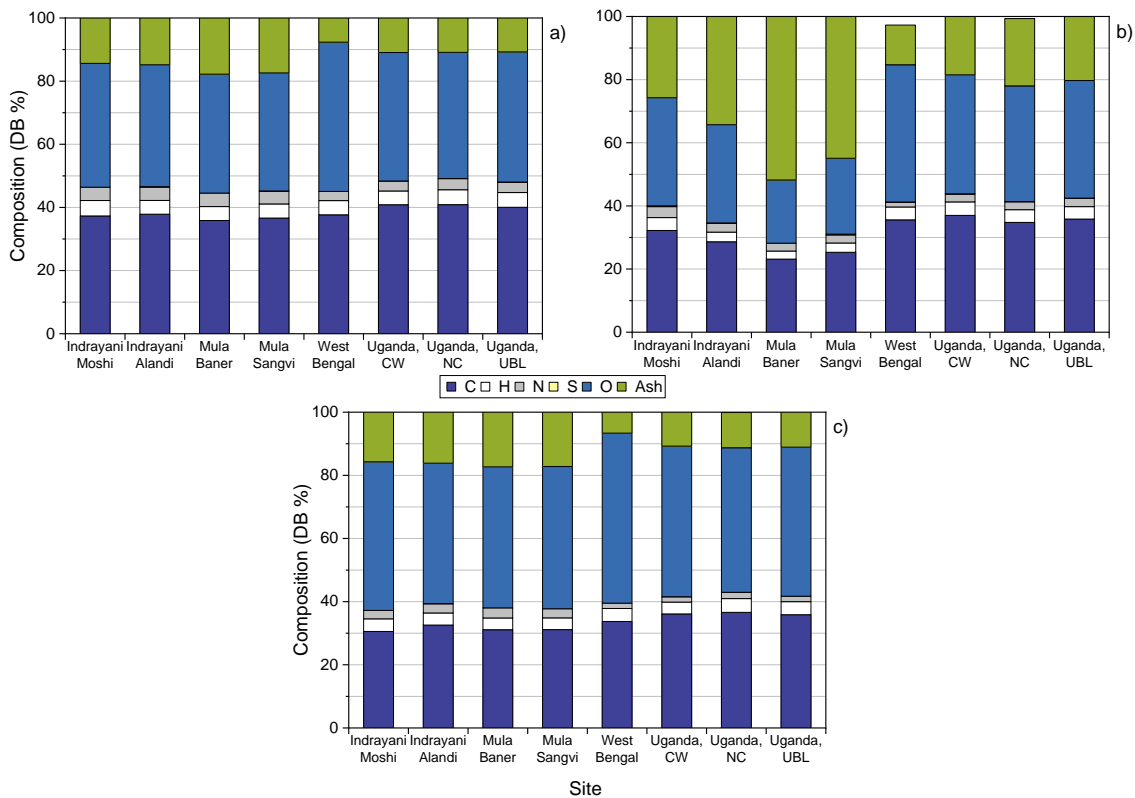


**Figure 4.2-8:** Ultimate composition of water hyacinth tissue samples for geographical and pollution analysis. a) leaf; b) root; c) petiole. Each sample was run in duplicate; each of location was an average of all phenological samples: Maharashtra had 4 samples, West Bengal had 3 samples, Murchison Bay (Uganda) had 8 samples.

The UPIs of each plant part, displayed in Figure 4.2-9, demonstrated that the composition variation, between tissues, resulted in large variations in the UPIs of each tissue. The leaf and root demonstrated a similar maximum  $BMP_{th}$  across all sites, with the petiole displaying a lower value, this was due to the high O and low C concentration within the petiole. All sites had similar maximum  $BMP_{th}$ , with the exception of West Bengal, which had a lower value, this was also due to the high O concentration of the West Bengal sample. Whilst most samples had similar maximum  $BMP_{th}$ , the experimental  $BMP_{th}$  is likely to be different: the C:N ratio of the rivers samples was considerably lower than the other samples, likely resulting in a lower  $BMP_{ex}$  unless co-digestion is introduced to increase this ratio [312]. The same was true for the leaf and root, which had a lower C:N for many samples, however, there was significant variation.

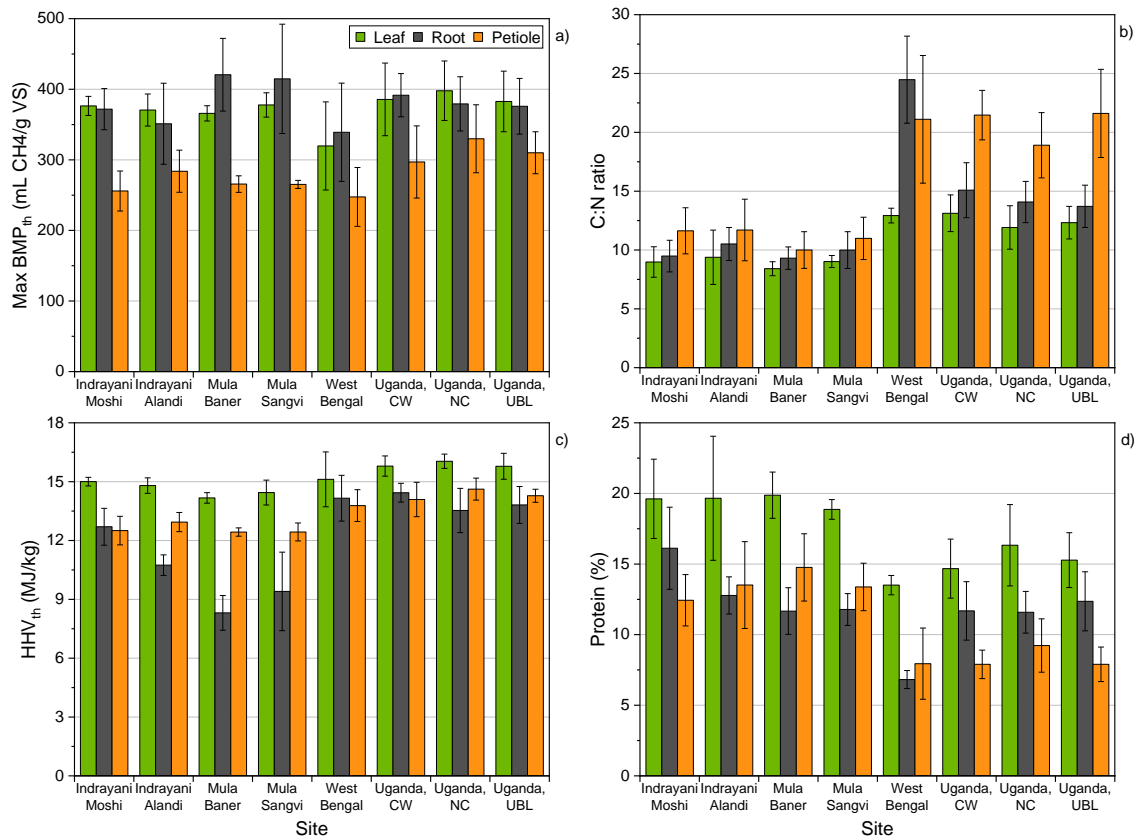


**Figure 4.2-9:** Utilisation potential indicators of water hyacinth tissues for geographical and pollution analysis. Error bars represent the represent the variation due to the phenological variations at each site. a) maximum theoretical biomethane potential; b) C:N ratio; c) theoretical higher heating value; d) protein content. Each sample was run in duplicate; each of location was an average of all phenological samples: Maharashtra had 4 samples, West Bengal had 3 samples, Murchison Bay (Uganda) had 8 samples.

The BMP of WH tissues was investigated further by analysing a subset for the  $BMP_{ex}$ , allowing the calculation of the BI from the different parts. One collection date for two sites were used, Indrayani Moshi and Mula Baner from May 2021, and one site from Murchison Bay, CW, was added for comparison, conducted by Brown (unpublished); the results are displayed in Table 4.2-3 and Figure 4.2-10. Peak biomethane production rate ( $R_m$ ), peak  $BMP_{ex}$  ( $H_m$ ) and lag phase ( $\lambda$ ) are displayed on the figure. The results in Table 4.2-3 demonstrate that there was significant variation between the locations, in both the theoretical and the experimental methane yields, and therefore the BI. With the exception of the root, Indrayani Moshi had the highest maximum  $BMP_{th}$ , yet had a lower  $BMP_{ex}$  than Mula Baner for all parts. This resulted in a lower BI for all parts. The petiole had the highest BI, this could be due to the increased C:N of the petiole sample, however, it has also been suggested that the petiole contains a lower lignin concentration, as compared with the other plant tissues [63], which would increase the BI of the petiole [137,319]. The root BI was half that of the leaf, despite suggestions of similar lignin and higher cellulose content [63]. This was likely due to

increased ash content and potential toxicity of the HMs to bacteria; however, this has been poorly studied.

Figure 4.2-10 shows that Mula Baner also had a higher  $R_m$ . The  $R_m$  of the root varied significantly between the sites: at Mula Baner, the root was only lower than the leaf, whereas at Indrayani Moshi and CW (Murchison Bay), the root was the lowest sample and showed a small  $\lambda$  at Indrayani Moshi. Indrayani Moshi had higher VM and C content, likely the reason behind the higher  $BMP_{th}$ , yet had a lower BI, further analysis should be conducted of WH tissues to understand their digestion behaviour.

The methane production of the leaf and petiole was greater than what was described for the whole plant by Brown *et al.*, who demonstrated a yield of 103 mL  $CH_4/g$  VS for the whole plant [139]. At the CW site (Murchison Bay), the roots accounted for ~32% of the biomass, the leaves ~24% and the petioles ~44%, on a dry basis. Using these values, an approximate whole plant  $BMP_{th}$  can be calculated, resulting in a value of ~123 mL  $CH_4/g$  VS. This is similar to the whole plant calculations made by Brown *et al.* [139] but higher than demonstrated by Quintana-Najera *et al.* for another sample from Murchinson Bay [304].

**Table 4.2-3:** Biomethane potential and biodegradability index of water hyacinth biomass for geographical and pollution study.

Site	Plant Part	Max $BMP_{th}$ (mL $CH_4/g$ COD)	$BMP_{ex}$ (mL $CH_4/g$ COD)	Biodegradability Index (%)
Indrayani Moshi	Whole	412.6 ± 3.7	104.0 ± 13.7	25.2 ± 3.1
	Leaf	387.5 ± 14.8	129.6 ± 7.2	33.4 ± 0.6
	Root	391.0 ± 3.2	67.7 ± 10.9	17.3 ± 2.9
	Petiole	273.5 ± 45.1	166.7 ± 7.7	62.0 ± 13.1
Mula Baner	Whole	358.9 ± 6.7	148.4 ± 9.0	41.4 ± 3.3
	Leaf	366.1 ± 1.2	176.7 ± 7.7	48.3 ± 2.3
	Root	454.0 ± 22.0	82.3 ± 11.2	18.1 ± 1.6
	Petiole	255.8 ± 6.3	180.5 ± 1.5	70.6 ± 2.3
Murchison Bay Clean Water*	Leaf	249.7 ± 5.2	150.8 ± 10.4	60.5 ± 5.4
	Root	313.9 ± 85.7	56.8 ± 0.1	18.8 ± 5.2
	Petiole	176.7 ± 10.5	158.2 ± 5.2	89.8 ± 8.3

\*Brown (Unpublished)

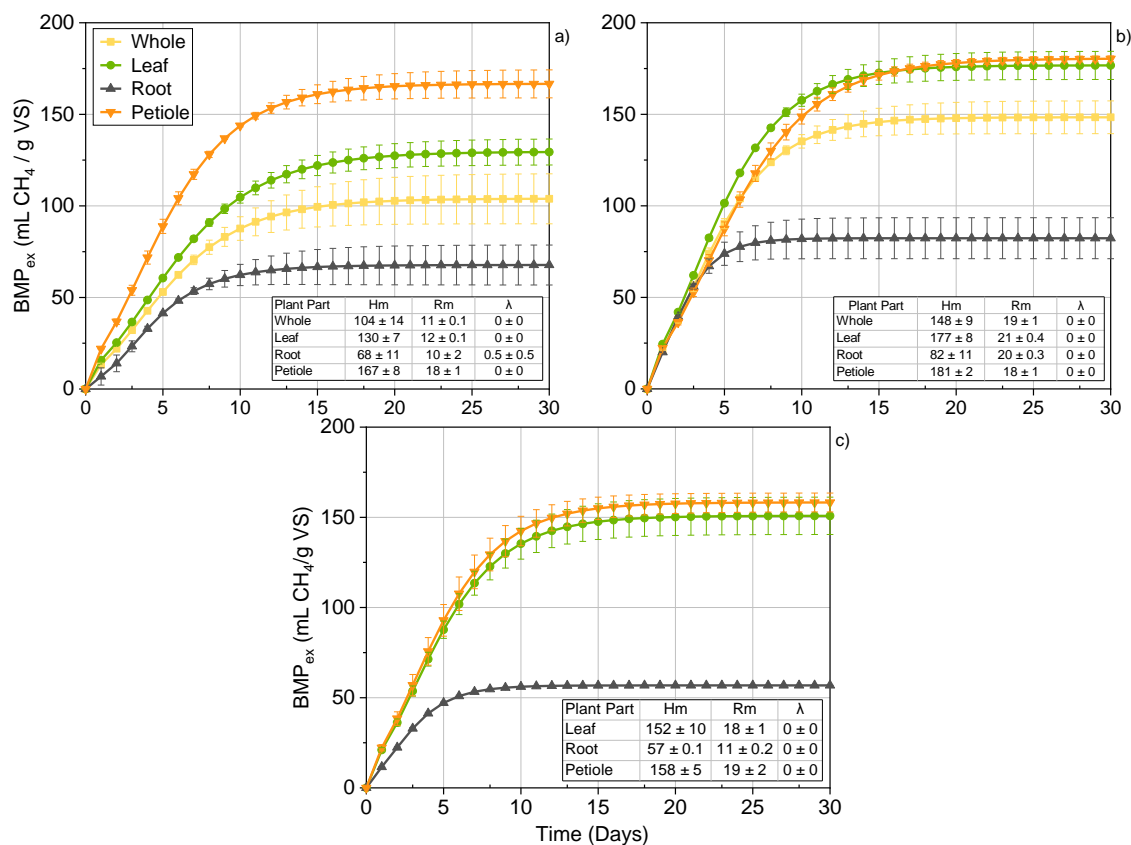


**Figure 4.2-10:** Modified Gompertz model, depicting the experimental biomethane potential of water hyacinth tissues for geographical and pollution analysis. Error bars represent the represent the analysis variation. a) Indrayani Moshi, May 2021; b) Mula Baner, May 2021; c) Murchison Bay (Uganda) Clean Water, September 2019; Brown (Unpublished). H<sub>m</sub>= maximum biomethane yield; R<sub>m</sub>= peak biomethane production rate; λ= lag phase. Each sample was run in duplicate.

The lower C:N ratio, in Figure 4.2-9b, was largely due to the high concentration of N, in particular within the WH leaf. This resulted in elevated protein concentrations: the maximum protein content was 24.5, 18.7 and 18.3% in the leaf, root and petiole, respectively. Therefore, WH leaves could be higher than major animal products, though lower than canned tuna (26.5%) [313,314]. Whilst the river locations had the lowest water TKN value, the plant protein content was highest, corroborating the theory that water flow had a greater impact on uptake than pollutant concentration. However, this is based on a small range of nutrient conditions and further analysis should be conducted to confirm this. West Bengal had the lowest pollution levels, of the high residence time samples, and consequently had the lowest protein content.

The leaf was the only tissue to have a HHV<sub>th</sub> >15 MJ/kg, however, this would still be considered a low energy density for a biomass fuel [306,308,315]. The river samples had the lowest HHV<sub>th</sub>.

The inorganic analysis of WH tissues is displayed in Figure 4.2-11 and Figure 4.2-12; the tissue analysis demonstrates that the root contains greater concentrations of HMs,

than the leaf or petiole. The low residence time samples, Indrayani and Mula River samples, had greater concentrations of HMs within all tissues, further demonstrating the theory that flow rate had a greater impact on pollutant uptake than pollutant concentration. The Mula River sites had the highest average total HM concentration, with elevated concentrations of Al, Cu, Cr, Fe Ni and Pb; these elements are often high in untreated raw sewage [309,310]. The Indrayani Moshi sample had elevated Ti and Zn levels, in comparison to other samples. As previously stated, this was likely to have come from industrial effluent, generated in the Moshi region, despite MCPB assurances that “no industrial pollution is permitted” [281]. However, the presence of Ti in West Bengal cannot be explained here. NC had marginally greater average total HM concentration than the other higher residence time sites, West Bengal and Murchison Bay, likely due to the sewage pollution that occurs in the area. The other high residence time samples showed little variation. However, if Al and Fe are removed, West Bengal had the highest total HM concentration, due to higher concentrations of Cu, Ti and Zn; further investigation must be conducted to understand how these HMs were introduced to the village ponds.

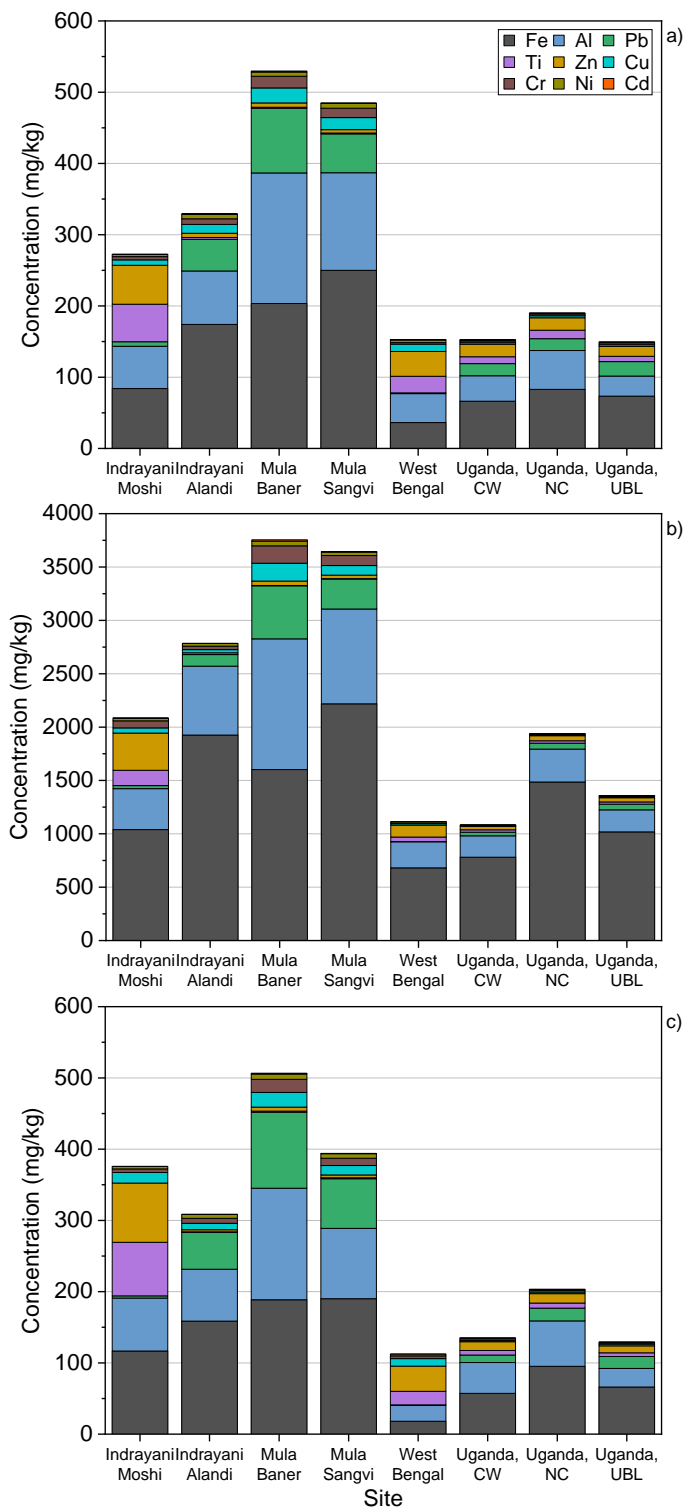


**Figure 4.2-11:** Averaged inorganic composition (heavy metals) of water hyacinth samples for geographical and pollution analysis. a) leaf; b) root; c) petiole. Each sample was run in duplicate; each of location was an average of all phenological samples: Maharashtra had 4 samples, West Bengal had 3 samples, Murchison Bay (Uganda) had 8 samples.

The maximum and minimum total HM content, at a single collection point, are displayed in Appendix B.2; this demonstrates that there was considerable phenological variations, for example, Mula Baner had a maximum total HM concentration of 5677



mg/kg, in March 2021, and a minimum of 2638 mg/kg, in February 2021. This analysis also demonstrates that UBL had spikes in the analysis period: in June 2020, the concentration of Al, Cd, Co, Cr, Cu, Mg, Mo and Pb all showed substantial spikes. This occurred at regular intervals throughout the year, suggesting that the brewery effluent was responsible for intermittent pollution, whereas the background pollution of the lake was responsible for the average HM concentration. Brewery effluent is likely to contain Cd, Cu, Cr, Ni, Pb and Zn [320–323], therefore another point source may be responsible for some of the pollution spike. This will be discussed in more detail in section 4.3.

The analysis of nutrient content, see Figure 4.2-12, demonstrates that the petiole contained the highest average total nutrient concentration; this is due to the ability of WH to store luxury nutrients in the floats of the petiole [100,101]. West Bengal contained the highest total concentration in the root and petiole, due to high concentrations of K and Ca, in contrast to previous assumptions on the impact of flow rate on uptake and the low pollution in the village ponds. NC contained the highest total concentration of nutrients, in comparison to the other Lake Vicotria samples, likely due to the presence of sewage pollution. In contrast to previous observations, the river samples contained lower or equal total nutrient concentration in all tissues, with the exception of the leaf at Mula Sangvi. It is possible that was due to different growth focuses: WH has two primary growth mechanisms [56], horizontal and vertical growth, which are determined by the conditions of the population. Horizontal growth focusses on dominating a water body through asexual reproduction, whereas vertical growth seeks to generate greater biomass size, see section 2.2.5. The river samples were collected during a period of variable growth strategy, possibly reducing the uptake at certain points of the cycle, resulting in a lower average value. The difference in these growth strategies will be discussed further in section 4.3.

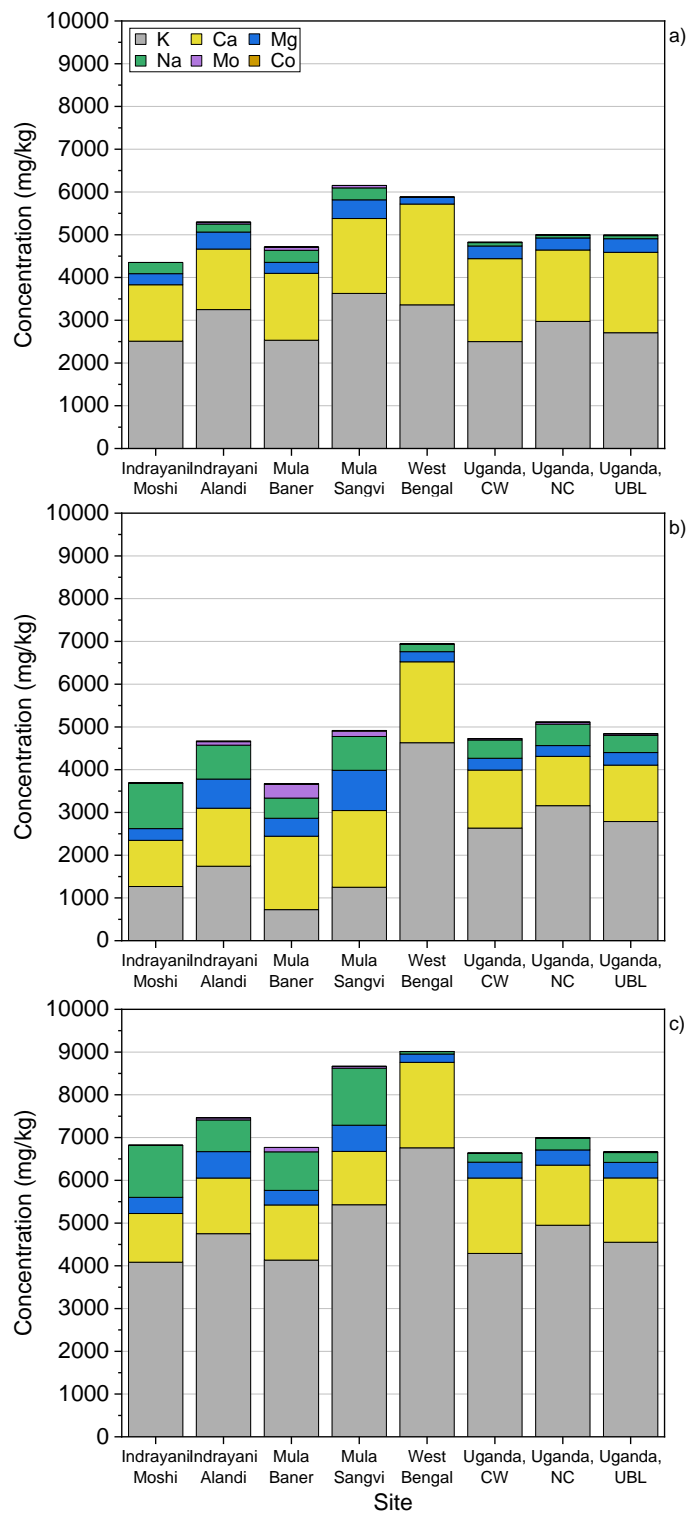


**Figure 4.2-12:** Averaged inorganic composition (nutrients) of water hyacinth samples for geographical and pollution analysis. a) leaf; b) root; c) petiole. Each sample was run in duplicate; each of location was an average of all phenological samples: Maharashtra had 4 samples, West Bengal had 3 samples, Murchison Bay (Uganda) had 8 samples.

### 4.3. Phenological variations

Composition variation, across the growth season, would result in different yields when the biomass was processed, therefore, understanding these variations is important.

The impact of monsoon on WH populations, at the Maharashtra locations, meant that biomass was lost, therefore, biomass was only available from December/ January to May/ June. Murchison Bay and West Bengal were sampled over the entire year, see Table 4.2-2. WQIs and environmental conditions were examined at each site. The environmental conditions were taken from NASA's Prediction of Worldwide Energy Resources [73]. The conditions examined were:

- Average air temperature at 2m above the ground- °C
- Average solar irradiance (all sky surface shortwave downward irradiance)- kWh/m<sup>2</sup>/day
- Precipitation- mm

#### 4.3.1. Murchison Bay, Lake Victoria

Murchinson Bay demonstrated mild seasonal variation, with the year split into four periods of higher or lower precipitation. The periods of higher precipitation were March-May and September- November; whereas the periods of lower precipitation periods lasted from December- February and June- August, see Figure 4.3-1c. Temperature was at its minimum in June/ July and then increased until the peak in February, Figure 4.3-1a. Solar irradiance followed a similar trend as temperature, Figure 4.3-1b. All three conditions peaked during the first four months of the year, then reached a trough in June/ July before they increased. The sites in Murchison Bay were within 4 km<sup>2</sup>, therefore the variations in environmental conditions were considered negligible.

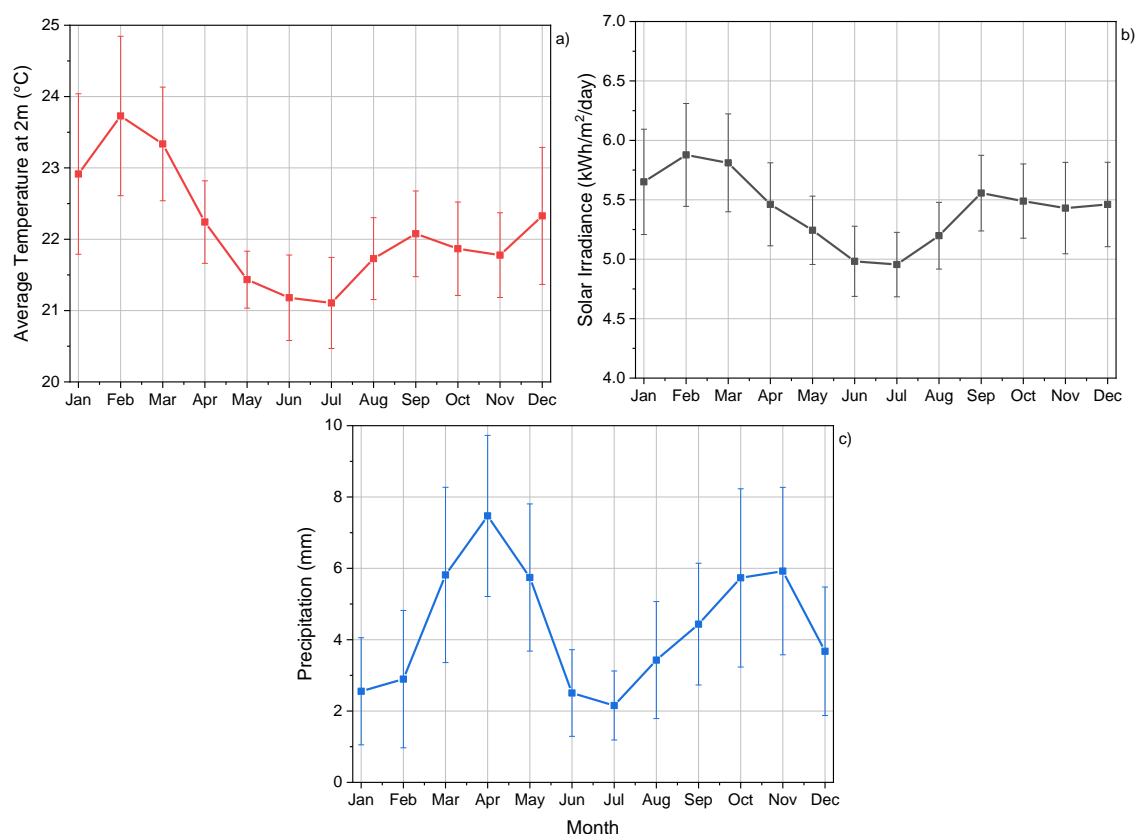


**Figure 4.3-1:** Average phenological variations of environmental conditions for Murchison Bay, Lake Victoria, Uganda. Error bars represent the variations over the selected period, of 1984-2021. a) average temperature at 2m; b) average solar irradiance (all sky surface shortwave downward irradiance); c) precipitation. Raw data was taken from NASA Prediction Of Worldwide Energy Resources [73].

The averaged WQIs, discussed in section 4.2.1, are displayed against time in Figure 4.3-2; the individual sites are presented in Appendix B.1. The metals peaked during the second rainy season of 2021, excluding Cu and Ni at CW (Murchison Bay), possibly due to the increased surface runoff during increased rainfall. This was similar to results demonstrated by Kumar *et al.*, who found a greater HM concentration after monsoon rains in India [324]. The first analysis of NC water showed the lowest content of all samples, then increased until September 2021. This suggests that pollution occurred at this site to increase the inorganic content, between September 2020 and September 2021, increasing by 0.6, 1.4, 9.2, and 12.4  $\mu\text{g/L}$  for Cd, Cr, Cu and Ni, respectively; the HM content then decreased. These results suggest that there was little variation temporally, with distinct increases that are likely to have been a point source pollution event, however, these occurred in the rainy season and therefore could be due surface runoff. This resembles the results of Outa *et al.*, who found that minimal variation in HM and nutrient concentration occurred, within the water and sediment, with respect to time [325].

There appears to be no relationship between N containing compounds and environmental conditions, however,  $\text{NO}_3$  and TKN both showed a slight increase in the first rainy season; in contrast,  $\text{PO}_4$ , COD and TSS increased in the second rainy season. This disparity between the indicators is unusual, however it still suggests that nutrient increase occurred due to surface runoff. However, investigation of the individual sites demonstrated that the individual sites had similar baseline levels: each site had separate spikes. This suggests that individual pollution would be the cause, as suggested by the HM results.

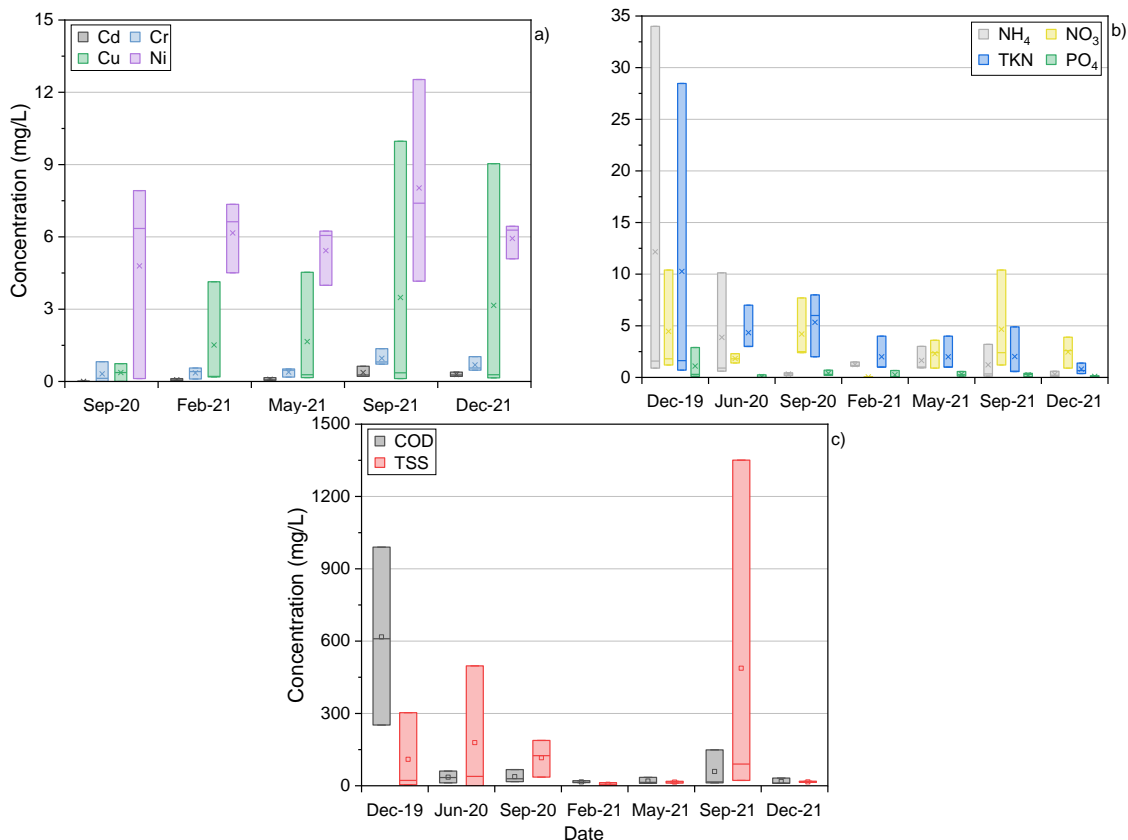


**Figure 4.3-2:** Phenological variations of water quality indicators for Murchison Bay, Lake Victoria, Uganda. Each sample was analysed in duplicate and averaged between the three sites (clean water, Navikubo Channel, Ugandan Brewery Ltd.). a) heavy metals; b) nitrogen and phosphorous; c) other.

The total inorganic content of the biomass is contained within the ash, therefore, the variations in ash content can be viewed as an indicator of HM and nutrient content. Figure 4.3-3 shows the average for Murchison Bay, the individual sites are available as a raw dataset [326]. The ash content has clear variations across the year, displaying peaks and troughs at distinct points, however, all results were within the typical range of ash content in WH tissues [63,64,327]. There are three clear troughs, with a maximum range of almost 10%; this range appears to be higher than expected. It is possible that this was due to sampling errors and further phenological sampling would be required to confirm this, however, one sample, in each of the two respective years,

were collected just 15 days apart (1<sup>st</sup> October 2019 and 15<sup>th</sup> September 2020), these results showed a variation of 0.5, 1.2 and 0.3% for the leaf, root and petiole, respectively. This suggests that the phenological variations presented here may be replicable.

The root contained the highest ash content, as would be expected in WH [65,66,145,148]. Conventional bioenergy feedstocks have an ash content of <8%, such as willow (4.1%), miscanthus (4.9%) and oak wood (7.4%) [328]. Assuming that the plant proportions were 24, 32 and 44%, for the leaf, root and petiole respectively, as previously described, then whole plant would have a minimum and maximum ash content of 7.6 and 17.1%, respectively. This suggests that WH from Murchison Bay may not be an appropriate biomass for bioenergy.

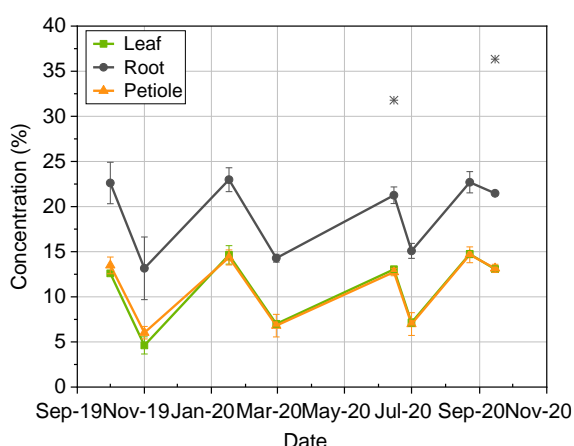


**Figure 4.3-3:** Phenological changes of the average ash content in biomass from Murchison Bay, Lake Victoria, Uganda. Each sample was analysed in duplicate and averaged between the three sites; the error bars represent the standard deviations of these variations. \*= extreme values.

The translocation factor (TF) is an important indicator when examining a hyperaccumulating plant. A high TF indicates that the plant is able to translocate the element from the root, up the plant, with ease. This would allow the plant to utilise the nutrient easily or, in the case of toxic elements, be quickly overwhelmed and killed by the pollutant. As previously described, WH has a low TF for many HMs [66,74], this has been reiterated in this study, see Figure 4.3-4; the individual sites are available as a raw dataset and graphical representation [326]. The key spikes in TF occurred in the dry seasons of Murchison Bay, Lake Victoria (January- February and June- August). However, there was no clear relationship with temperature, and subsequently growth rate.

A TF of <1 suggests that the plant is able to accumulate the element within the root without translocating it to other parts of the plant, therefore it cannot be used within the leaf or petiole either positively or negatively. Whilst all HMs were below <1 for much of

the year, only Al and Fe did not breach a TF of >1. This suggests that the localisation of the elements within the tissue, as analysed by Vesk *et al.* [149], plays a vital role in the translocation of the elements. Vesk *et al.* determined that Al, Fe and Ti were located on the surface of the roots, where as Cu, Pb and Zn were in greater concentrations within the inner sections of the roots [149]. The low translocation of Al and Fe suggests that these were poorly taken up by the plant, corroborating the theory that they are retained on the epidermis external walls. In contrast, Ti demonstrated spikes >1; it has been previously been reported that Ti had a low TF in WH but the bioconcentration factor (BCF) was the highest of all analysed metals [68]. Therefore, it is possible that a high level of Ti in the water of Murchison Bay could lead to an increased translocation. However, this cannot be confirmed; further analysis into the localisation of metals in the root and the mechanisms of uptake would increase the understanding of this area.

Previous studies suggest that Cr, Pb, Cu, Fe, Ni and Zn have a TF of <1, regardless of conditions. TF calculated from Table 2.3-2 demonstrated that these metals have a TF value of <1 in most scenarios, however, similarly to Figure 4.3-4, there are cases where the plant is unable to contain the metals in the below water tissue. Cd displayed a TF of >1 in 5 out of 8 studies and appears to be independent of conditions. Majumdar *et al.* demonstrated that at a concentration of 0.1 and 0.5 mg of Cd/L, the TF was <1, whereas at 0.3 mg/L, the TF is >1 [13], this appears to confirm that the TF was independent of water concentration.

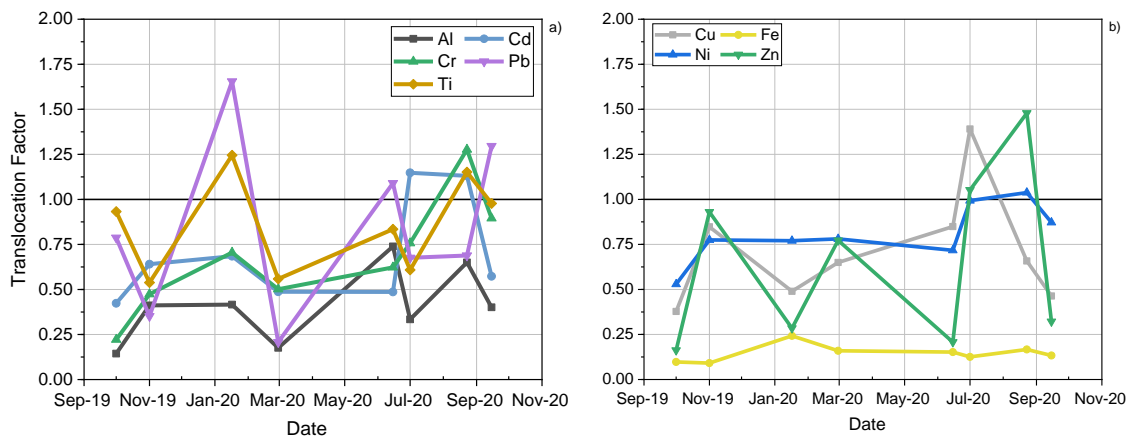


**Figure 4.3-4:** Phenological changes of the heavy metal translocation factor in biomass from Murchison Bay, Lake Victoria, Uganda. Each sample was analysed in duplicate and averaged between the three sites; the error bars represent the standard deviations of these variations. a) non-essential; b) essential.

The total concentration of HMs is presented in Figure 4.3-5 and Figure 4.3-6; as with ash content, there are distinct peaks and troughs throughout the year. The samples collected in October 2019 and September 2020 demonstrate similar values, except for Al, suggesting that annual replicability may occur. With the exception of Fe, all HMs

displayed their peak between June and September, once extreme/ anomalous values have been discounted. This is a period of low precipitation and low temperature; therefore, low growth and no surface runoff suggests that a pollution event could have occurred from Kampala during this period. On the other hand, the uptake of metals is not instantaneous, particularly in a large lake due to high dispersal, therefore, it is possible that the concentration in the water was increased during the rainy season which resulted in greater increase in the plant in subsequent months. Further analysis of the phenological changes in BCF and water quality would be required to identify this. Fe did not follow the same trend, likely due to the method of uptake: Fe was predominantly adsorbed to the surface of roots and is marginally translocated to the upper tissues [161], therefore the lower retention could mean that Fe was largely independent of conditions. The peaks in TF occurred over the same period, indicating that as root concentration increases, so does translocation.

The HMs show a trend of three peaks during the study: January/ February; June/ July; and September-November, as shown in Figure 4.3-5 and Figure 4.3-6. The first two peaks occurred during a period of low precipitation, in contrast to peak 3 which was during high precipitation. Peaks 1 and 3 were at higher temperatures, whereas peak 2 was at low temperature. This data suggests that high growth, assuming temperature dependent growth, or precipitation periods, demonstrate an increase in HM uptake and concentration in WH. Abdel Shafy *et al.* demonstrated that Cu, Fe, Pb and Zn peaked during the latter stages of the Egyptian dry season [62], where the temperature is at the highest point [73]. The point of peak biomass density in Egypt is the end of July [329], suggesting that HM concentration peaked at the end of the growth cycle. Assuming that temperature and biomass density have a positive relationship [80,81], then peak 1 would follow a similar trend. Peak 3 occurred during a small temperature spike, therefore increased growth could be the primary factor in HM uptake increase. In contrast, peak 2 was likely due to increased precipitation increasing the surface runoff as suggested by the increase in HM water concentration during the second rainy season, see Figure 4.3-2. This was also found in Vietnam where As, Cu, Pb and Fe all peaked during the rainy season [14], which occurs as temperatures begin to drop [73]. The maximum value for each HM was in the following order: Fe > Al > Pb > Zn > Ti > Cu > Cr > Ni > Cd; there appears to be no trend for the essential and non-essential metals. Outa *et al.* examined the uptake of trace metals by *Vossia cuspidata* in Murchison Bay, determining a replicable order as this study [325], with the exception of Pb, suggesting that the uptake from these two plants is linked to background concentrations of HMs.



The HM concentration in the WH tissues, from Murchison Bay, was typically lower than the results displayed in Table 2.3-2. In particular, the Cd, Fe, Ni and Ti concentrations in above water tissues. However, the biomass did contain greater than expected concentrations of Pb in the above water tissue. The biomass would not be considered as an acceptable food additive due to the concentrations of Pb and Cd, particularly in the roots [330,331].

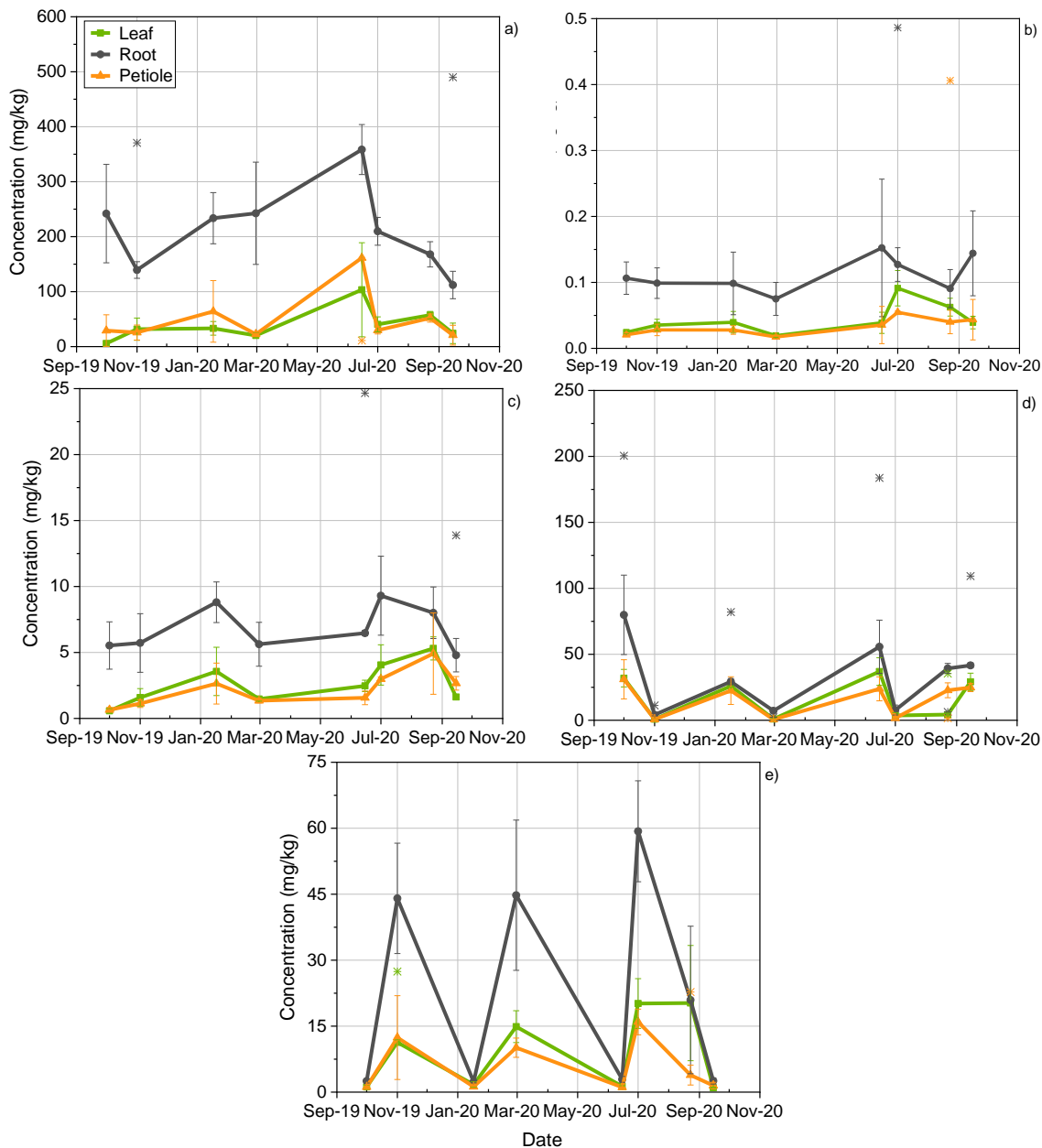


**Figure 4.3-5:** Phenological changes of non-essential heavy metal content in biomass from Murchison Bay, Lake Victoria, Uganda. Each sample was analysed in duplicate and averaged between the three sites; the error bars represent the standard deviations of these variations. \* = extreme values. a) aluminium; b) cadmium; c) chromium; d) lead; e) titanium.

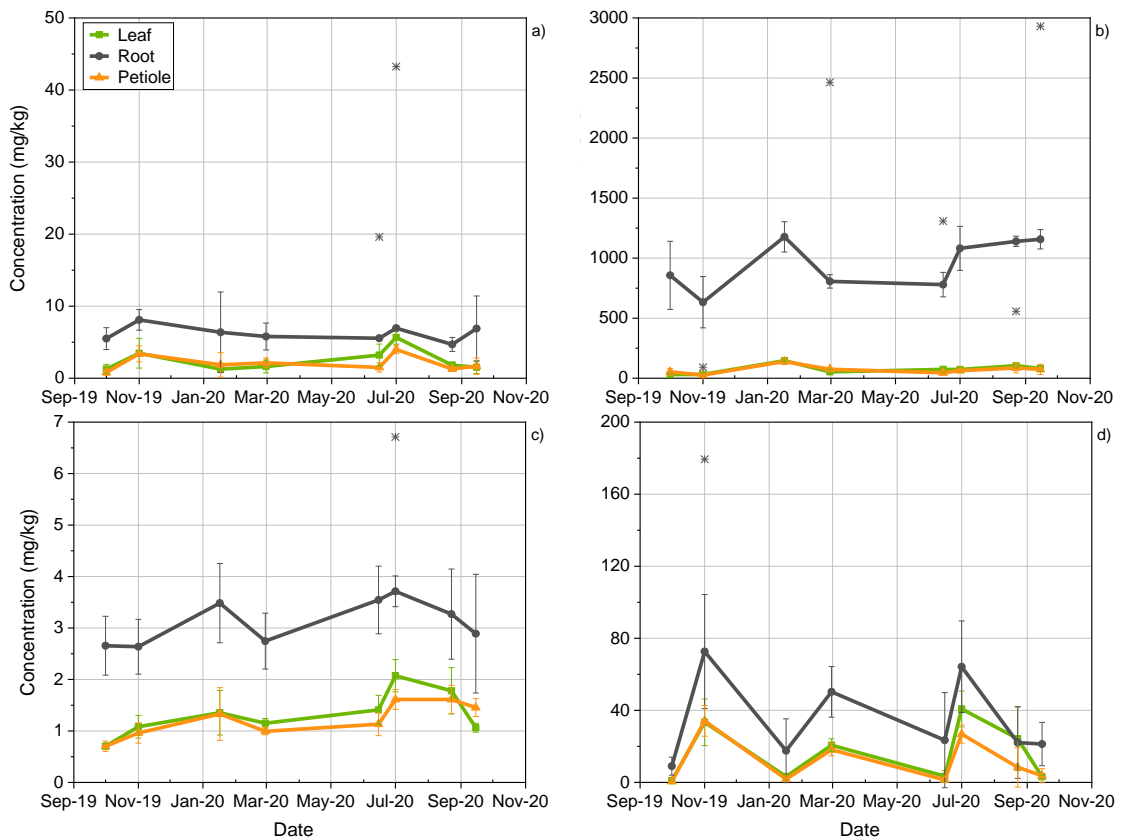


**Figure 4.3-6:** Phenological changes of essential heavy metal content in biomass from Murchison Bay, Lake Victoria, Uganda. Each sample was analysed in duplicate and averaged between the three sites; the error bars represent the standard deviations of these variations. \* = extreme values. a) copper; b) iron; c) nickel; d) zinc.

Nutrients are taken up through the roots and transported up the plant via translocation; this process is vital to a plant's survival; therefore, it is likely that the TF of nutrients would be higher than that seen in HMs. The macro-nutrients demonstrated a TF of  $>1.9$  for all elements, see Figure 4.3-7. Ca peaked in July- September, the same peak that was present in the HMs. The micro-nutrient TF was similar to the HMs: demonstrating a TF of  $<1$  for most of the year, with peaks occurring at specific points, however, only Mo had the same sharp peak in July-September. Macro-nutrients appear to have been easily translocated by WH, whereas micro-nutrients are contained to the roots where they have a reduced toxicity to the plant.

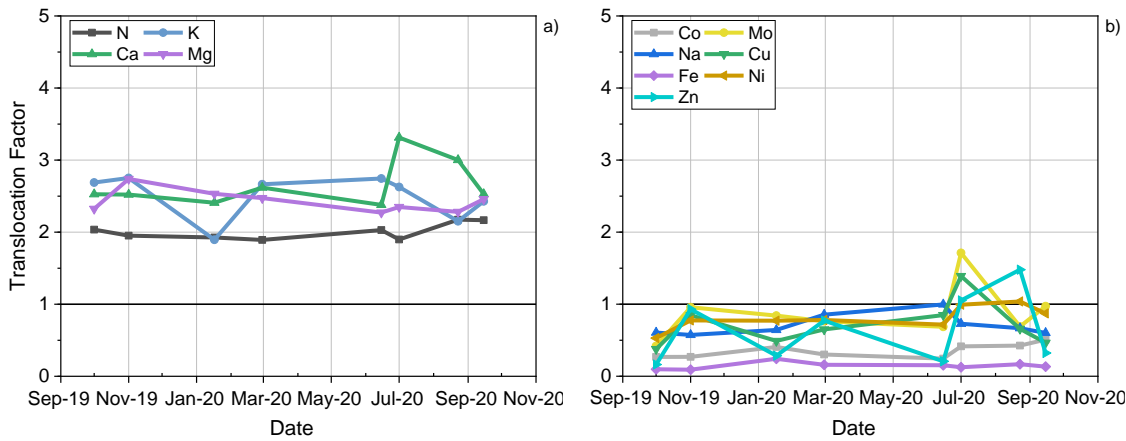


**Figure 4.3-7:** Phenological changes of the nutrient translocation factor in biomass from Murchison Bay, Lake Victoria, Uganda. Each sample was analysed in duplicate and averaged between the three sites. a) macro-nutrients; b) micro-nutrients.

The concentration of macro-nutrients, displayed in Figure 4.3-8, demonstrates that macro-nutrients are primarily concentrated within the leaf or petiole. It has previously been suggested that WH can store luxury nutrients within the petiole [100,101], this has been corroborated by the presence of Ca, K and Mg in equal or greater concentrations than the leaves or roots. Whilst there are high concentrations of macro-nutrients within the roots, these are similar concentrations to HMs like Al, Fe and Zn, with the exception of N. This suggests that WH can actively transport high concentrations of macro-nutrients without the same occurring with toxic elements. The nutrients showed similar trends to the HMs: each nutrient demonstrates clear peaks, with the key peaks occurring January/ February; June/ July; and September-November. However, within these peak periods, certain nutrients also demonstrate a trough, suggesting an error in collection, or these periods had high uptake of inorganics. The dramatic rise in certain nutrients suggest that uptake of this level would not be representative of a population and suggests error in collection. This can occur if the sampling was not representative of the population or was contaminated.

The peaks occurred in periods of high growth and/ or high precipitation, in contrast to the results by Abdel Shafy *et al.*, who determined little variation occurred between the end of the wet season and the dry season [62]. Whereas, at the start of the wet season had the lowest concentration for all nutrients, except Co. This suggests that the high precipitation during the wet season and high temperatures in the dry season increased nutrient content in the biomass.

The extreme values displayed in Figure 4.3-8 and Figure 4.3-9 were all associated with one site, NC, with the exception of two points for Co. This is likely due to the increased sewage pollution that is likely to contain high concentrations of nutrients and therefore cause spikes in nutrient concentration.

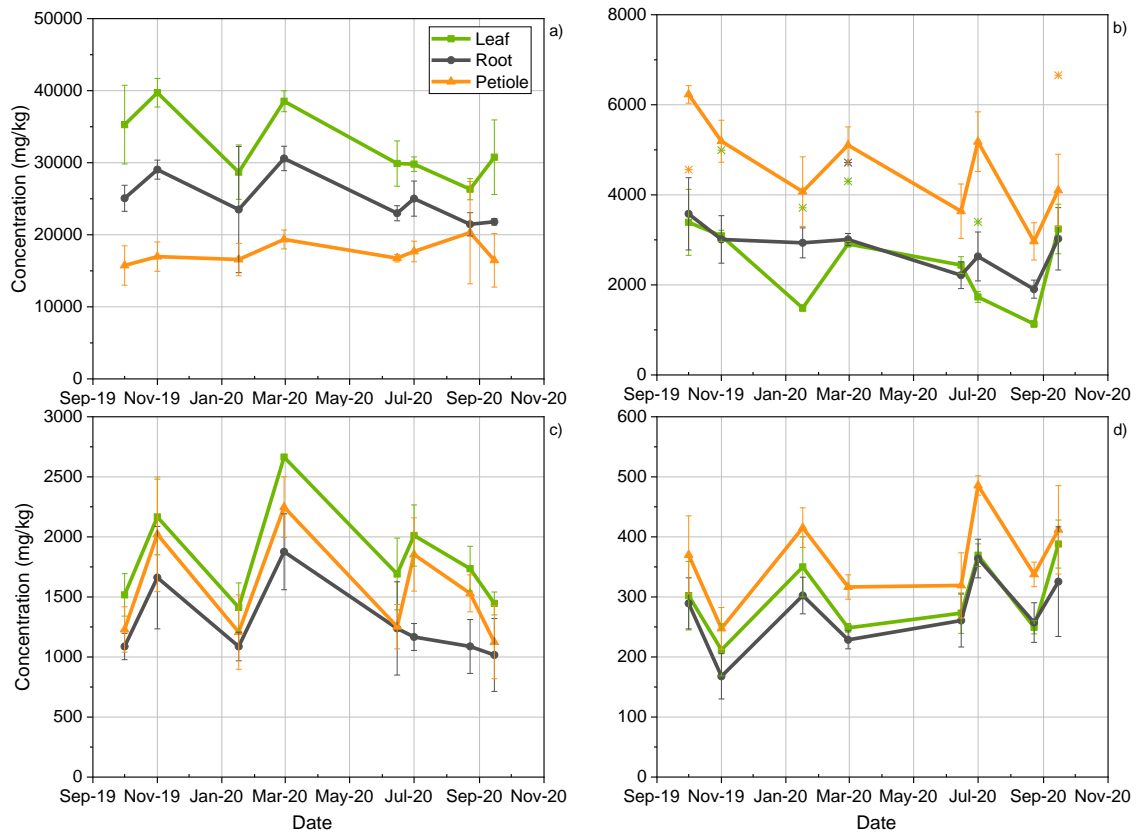


**Figure 4.3-8:** Phenological changes of macro-nutrient content in biomass from Murchison Bay, Lake Victoria, Uganda. Each sample was analysed in duplicate and averaged between the three sites; the error bars represent the standard deviations of these variations. \* = extreme values. a) nitrogen; b) potassium; c) calcium; d) magnesium.

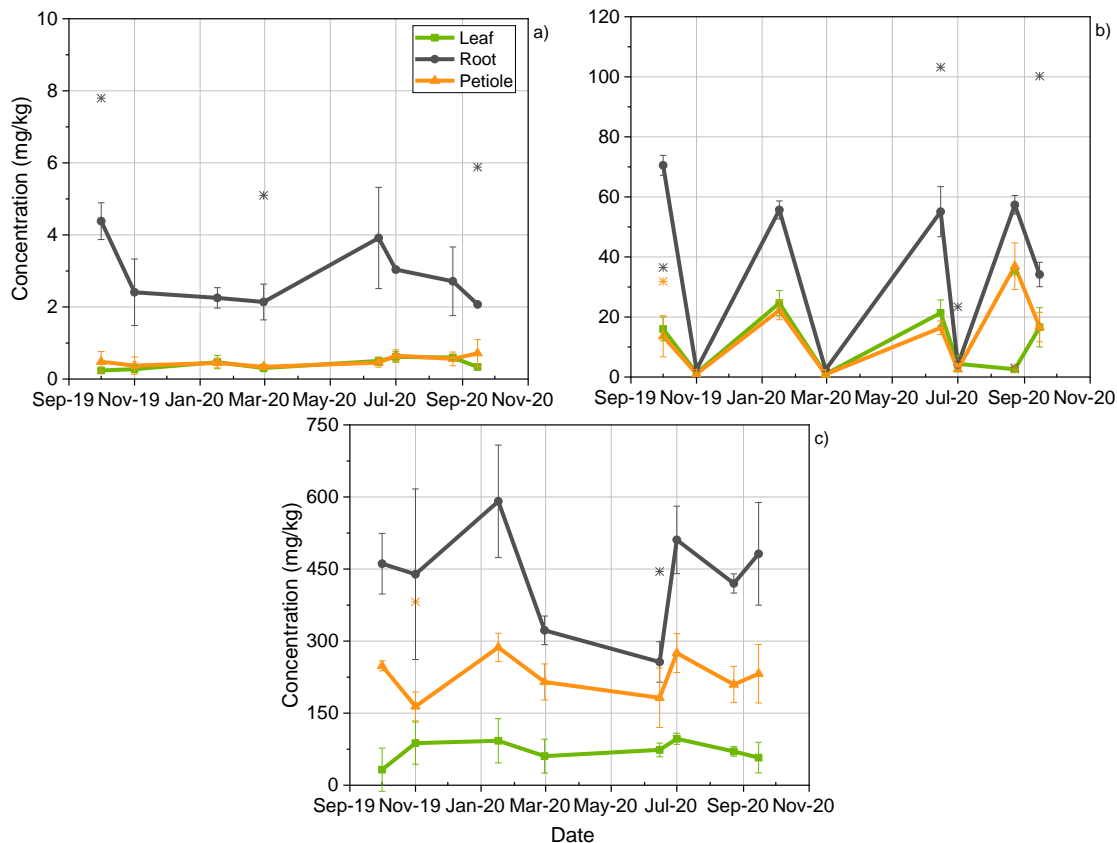


**Figure 4.3-9:** Phenological changes of micro-nutrient content in biomass from Murchison Bay, Lake Victoria, Uganda. Each sample was analysed in duplicate and averaged between the three sites; the error bars represent the standard deviations of these variations. \* = extreme values. a) cobalt; b) molybdenum; c) sodium.

The maximum  $BMP_{th}$  and  $BMP_{th}$  are displayed in Figure 4.3-10a; the  $BMP_{th}$  was calculated by multiplying the maximum  $BMP_{th}$  by the BI, as described in Equation 3-9, to estimate the  $BMP_{ex}$ , shown in Table 4.2-3. Both demonstrate that the peaks and troughs are opposite to that shown by protein, Figure 4.3-10c. The C:N ratio is an important aspect of methane generation in AD [312]; the optimal C:N is 32.09, however, the ratio for each part of the plant was significantly lower than this, with no sample greater than 27.5. Therefore, it is unlikely that the Murchison Bay WH could be used as a sole feedstock for AD. The differences in the phenological changes of the  $BMP_{th}$  and C:N ratio for the petiole should be examined further through  $BMP_{ex}$ .

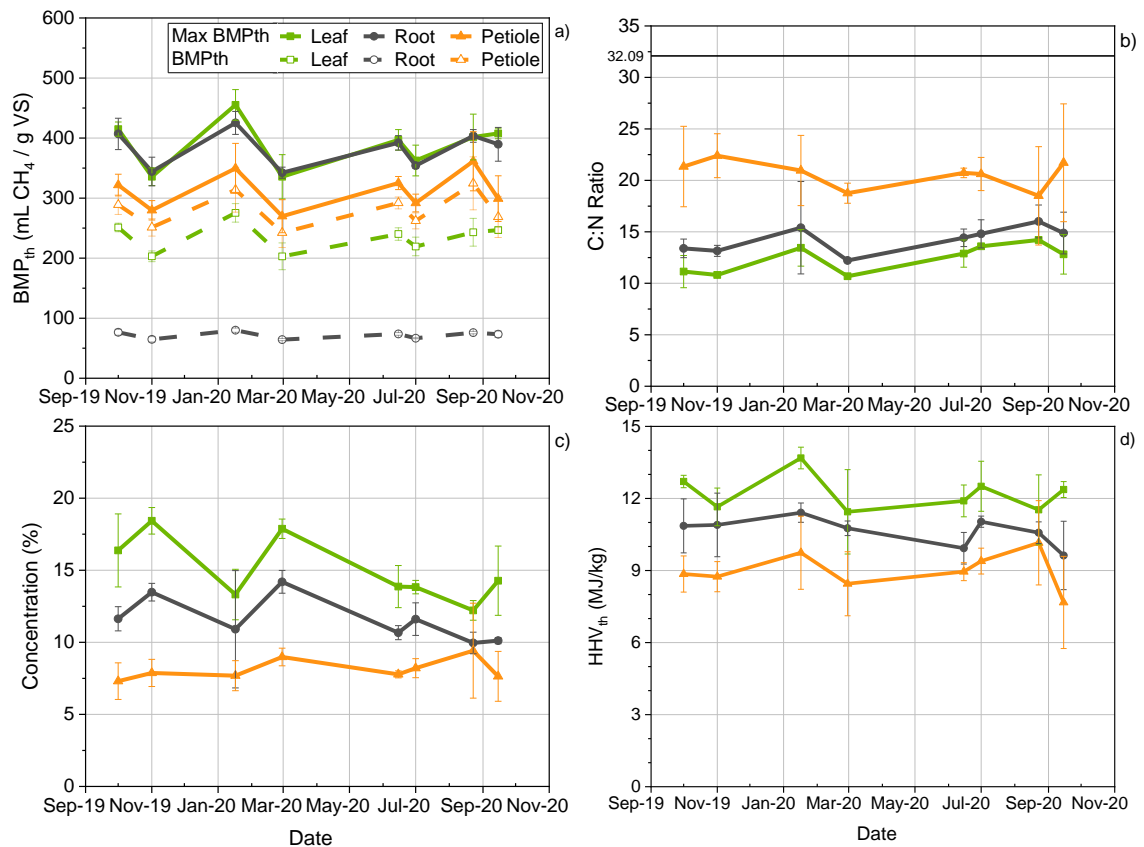


**Figure 4.3-10:** Phenological changes of utilisation potential indicators in biomass from Murchison Bay, Lake Victoria, Uganda. Each sample was analysed in duplicate and averaged between the three sites; the error bars represent the standard deviations of these variations. a) maximum theoretical biomethane potential and theoretical biomethane potential; b) C:N ratio; c) protein content; d) theoretical higher heating value.

Figure 4.3-10c shows that the protein content peaks in November and February. These are periods of low HM translocation and therefore would reduce the potential toxicity of the biomass making them optimal points of harvest. The peak protein content of the leaves was similar to that described by Sivasankari and Ravindran, whose results suggested 22.0, 3.3 and 7.7% protein content for the leaf, root and petiole, respectively [64]. Figure 4.3-10c demonstrated that all root samples had greater protein content than the petioles and the values suggested by Sivasankari and Ravindran [64].

The protein content of leaves was similar to that expected in chicken (23.1%), beef (21.4%), salmon (18.7%), cod (16.6%) and raw tofu (15.8%) [313,314]. However, it was lower than raw soybean (36.5%) and canned tuna (26.5%) [313,314]. WH leaves are a suitable protein source throughout the year; however, whilst the leaves have been deemed as not acutely toxic when utilised in animal feed [210], it has been observed that only a portion of ruminant diet can be replaced by WH [207]. The WH whole samples from Murchison Bay had a protein content of 10%; throughout the study, the leaves contained a greater protein content. Secondly, the leaves contained lower levels of HMs, than the whole plant, therefore, plant separation should be considered.

Alternatively, the extraction of protein from WH has been shown to reduce the HM content within the protein product [197]. To be considered as a protein supplement, a substance should contain >20% protein [212]; one example of WH protein extraction resulted in an increased protein content by >200%, and would be considered as an acceptable protein supplement if Murchison Bay WH was utilised to the same effect. The HHV<sub>th</sub> was below 15 MJ/kg for all samples, see Figure 4.3-10d, which is considered low for a biomass fuel [306,308,315]. Table 2.3-2 displays a variety of different biomasses, of which no value was <15 MJ/kg; the average HHV<sub>th</sub> was 6.6, 8.2 and 10.0 MJ/kg greater than the average WH leaf, root and petiole HHV<sub>th</sub>, respectively. This suggests that WH is not a suitable choice for solid fuel combustion. There was little phenological variation, however, small peaks occurred in January and July, and a small trough in March. Other peaks and troughs were part specific and therefore possibly anomalous. This was particularly evident for the petioles, which showed the greatest variation.

A limitation of this study is the equation utilised to predict the HHV<sub>th</sub>: the database utilised, to produce the equation used in this study, contained a multitude of different biomasses, with an experimental HHV range of 14.0-22.5 MJ/kg and an ash content of 0-25%, with only 7 samples >20% [307]. This HHV<sub>ex</sub> is higher than any result in this study, whilst the ash content was lower than the average for the Murchison Bay samples. This suggests that the equation may not be appropriate for these samples.

#### 4.3.2. Pune, Maharashtra

The river samples were all collected within the Maharashtra region, either in the city of Pimpri Chinchwad or Pune. Maharashtra had greater seasonal variability than Kampala; for the purposes of this analysis, the year was split into spring (January-March), summer (April- mid-June, variable due to monsoon), monsoon (mid-June- mid-September) and winter (mid-October-December). Spring was characterised by low rainfall and rapid increases in temperature and solar irradiance, see Figure 4.3-11. Summer also had low rainfall with the peak temperature and solar irradiance. Monsoon had high rainfall and reduced temperature and solar irradiance, compared with summer. However, the start and end are variable, this was greater in recent times due to climate change [332,333]. Winter was characterised by a slight increase in solar irradiance and reduction in rainfall as the monsoon cloud cover and rains receded; the temperature also reduced during winter. The sites in Maharashtra were within 70 km<sup>2</sup> of each other, whilst this was a larger than distance Murchison Bay, the impact of environmental conditions was also considered negligible. Samples could not be collected after June due to the monsoon rains: the plants were washed downstream

due to the strength of the water flow. Therefore, plants were collected from January (when a mat was first observed in all rivers) until monsoon began.

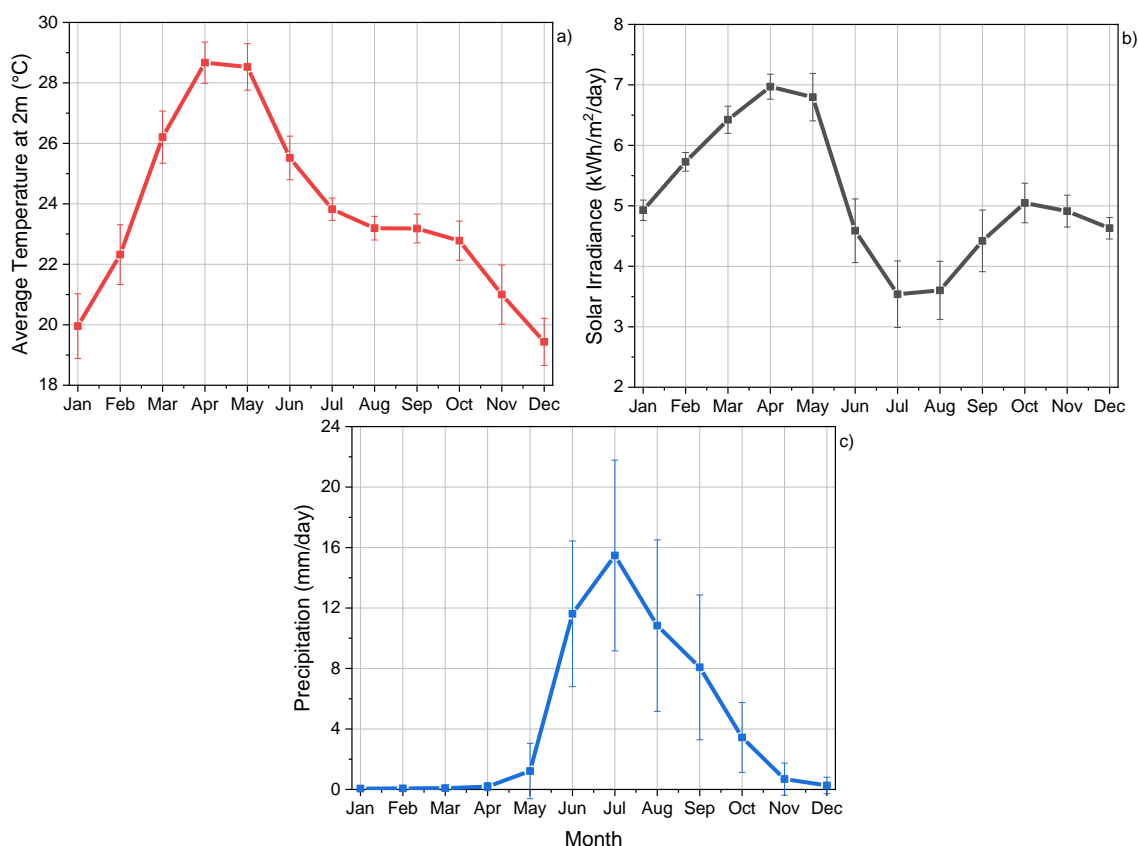


**Figure 4.3-11:** Average phenological variations of environmental conditions for Pune, Maharashtra, India. Error bars represent the variations over the selected period, of 1984-2021. a) average temperature at 2m; b) average solar irradiance (all sky surface shortwave downward irradiance); c) precipitation. Raw data was taken from NASA Prediction Of Worldwide Energy Resources [73].

The WQIs for Maharashtra are displayed in Figure 4.3-12, the individual sites are displayed in Appendix B.1; the HM concentration varied between 2019 and 2020, this is likely due to inconsistent pollution events and high flow rate. There appears to be no clear trend in HMs or N, between January and June 2020, this contrasts with the annual variation, suggesting that the HM and nutrient pollution was consistent before the monsoon rains, it is possible that these rains altered the background level of pollution. However, there is not enough data in this study to conclusively determine a trend. Another possibility is the impact of flow on water quality: the water was replenished with regularity therefore it had the potential to vary day to day depending on the pollution input.



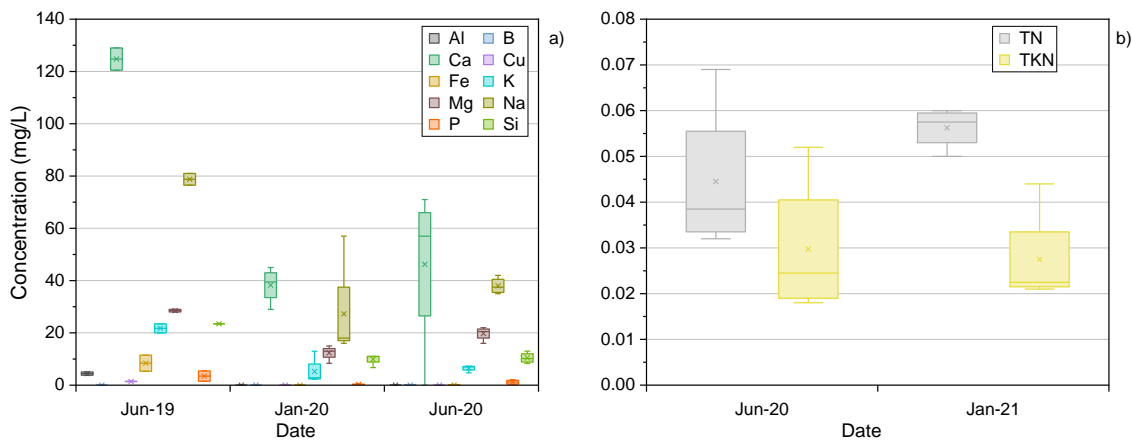


**Figure 4.3-12:** Phenological variations of water quality indicators for Pune, Maharashtra, India. Each sample was analysed in duplicate and averaged between the four sites (Indrayani Moshi, Indrayani Alandi, Mula Baner, Mula Sangvi). a) elemental; b) nitrogen.

The Maharashtra samples were all weighed to determine dry weight ratios of the tissues. It was assumed that roots would have a greater percentage of the biomass at the beginning of the season, before reducing when the plant began to grow vertically, once space was restricted [56]; this would be mirrored in petiole proportion which would increase when vertical growth began. The results are displayed in Figure 4.3-13, this demonstrates that each site has varied tissues proportions, in particular at Mutha Baner where the roots had the largest proportions of all tissues. However, at all sites the petiole increased from the start of the season to the end, except for Alandi, where the petiole sample was spoilt so no proportion could be calculated. The Indrayani River had increased petiole proportion in March, suggesting that a vertical growth shift occurred between February and March collection. This was evidenced by the coverage demonstrated by Figure 4.3-14: except for Sangvi, all sites had 100% coverage in March, therefore vertical growth would be prioritised. The leaf proportion reduced or did not change over season, as the plants increase vertically, the leaves increase in size, therefore it can be assumed that either there were less leaves, or they had an increased moisture content by the end of the of the season. Results from West Bengal samples demonstrated that the tissues moisture content varied from 88.5- 93.6, 83.3- 94.9 and 91.1- 95.7% for the leaf, root and petiole respectively.

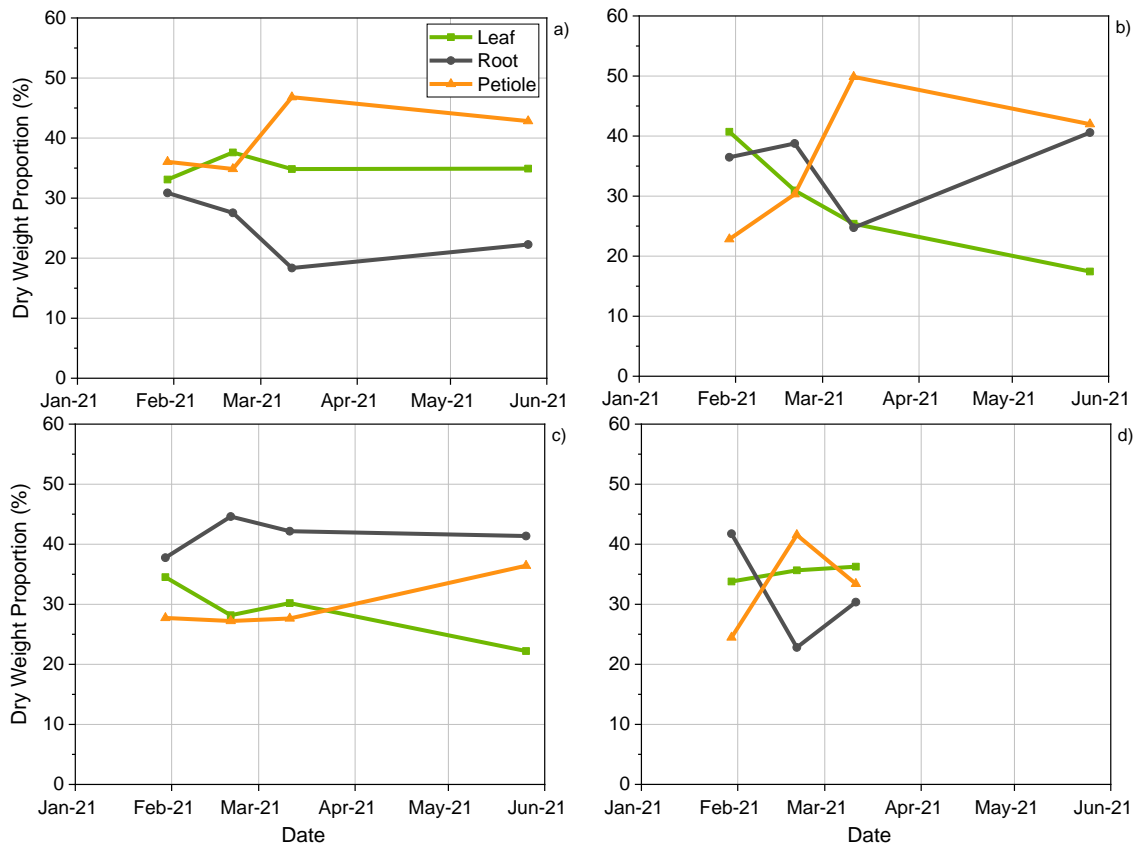


**Figure 4.3-13:** Phenological changes in dry weight proportions of tissues in water hyacinth biomass from river sites in Pune, Maharashtra. a) Indrayani Moshi; b) Indrayani Alandi; c) Mula Baner; d) Mula Sangvi.

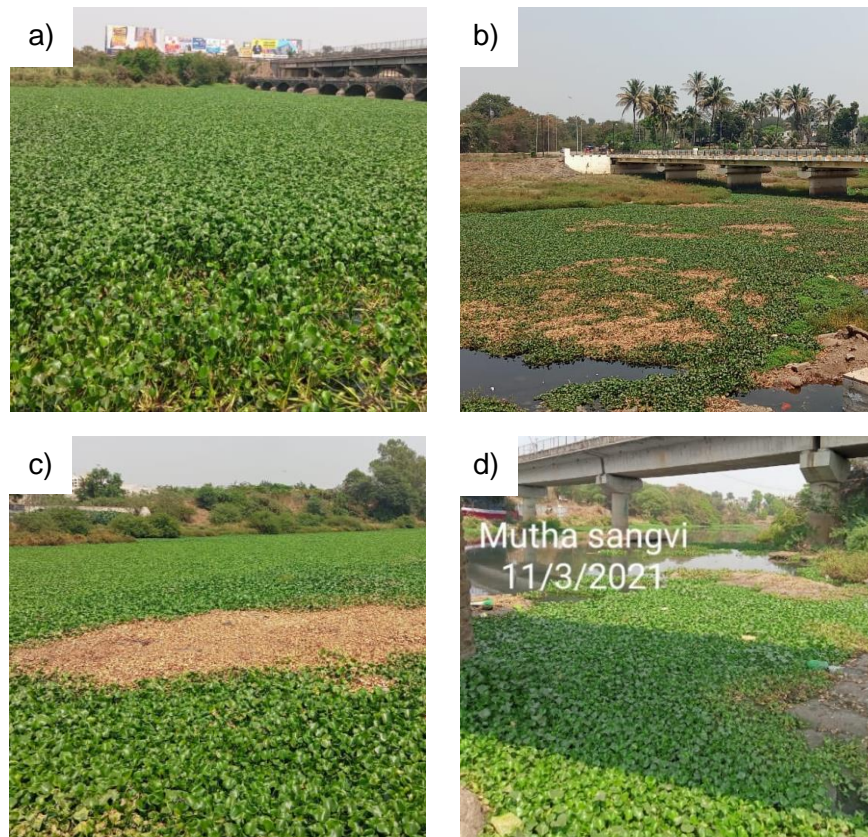


**Figure 4.3-14:** Water hyacinth coverage on 11/03/2021 from Maharashtra, India: a) Indrayani Moshi; b) Mula Baner; c) Indrayani Alandi; d) Mula Sangvi (credit G. Nahar).

As with the ash content in Murchison Bay, Figure 4.3-15 shows that WH roots contain a higher ash content than the above water tissues. All sites peaked at the end of the growing season (June), similar to what show in Murchison Bay where ash peaked during periods of high growth. All sites in Maharashtra produced an ash content higher than Murchison Bay, with the Mula river sites reaching double the concentration.

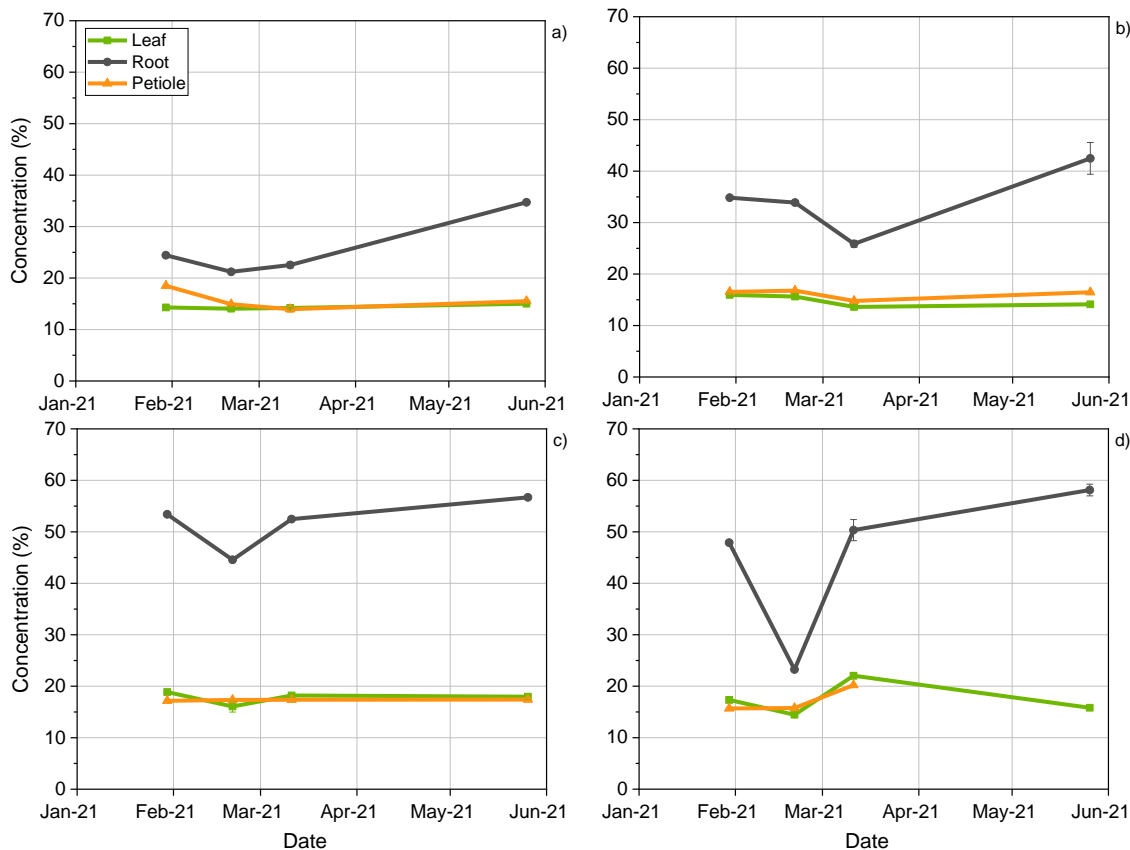


**Figure 4.3-15:** Phenological changes of ash content in biomass from river sites in Pune, Maharashtra. Each sample was analysed in duplicate; the error bars represent the standard deviation of the replications. a) Indrayani Moshi; b) Indrayani Alandi; c) Mula Baner; d) Mula Sangvi.

The TF for essential and non-essential HMs suggests that the majority of metals are contained to the roots, with the exception of localised spikes, see Figure 4.3-16. One metal that was exempt from this trend was Ti; as discussed previously, Ti is unlikely to have been introduced to the rivers via raw sewage, the predominant source of pollution in these rivers. It is possible that Ti could have been introduced via industrial pollution, despite the regulations from the MCPB; however, as shown in Figure 4.3-12, the presence of Ti in the water was not detected at any of the sites. The localised spikes of high TF were also replicated in the results for Murchison Bay; secondly, it has been demonstrated that Ti can be accumulated at high levels [68]. There appears to be no difference between the essential and non-essential HMs; nor was there a phenological trend for the majority of HMs, however, particular HMs exhibited a reduced TF with time.

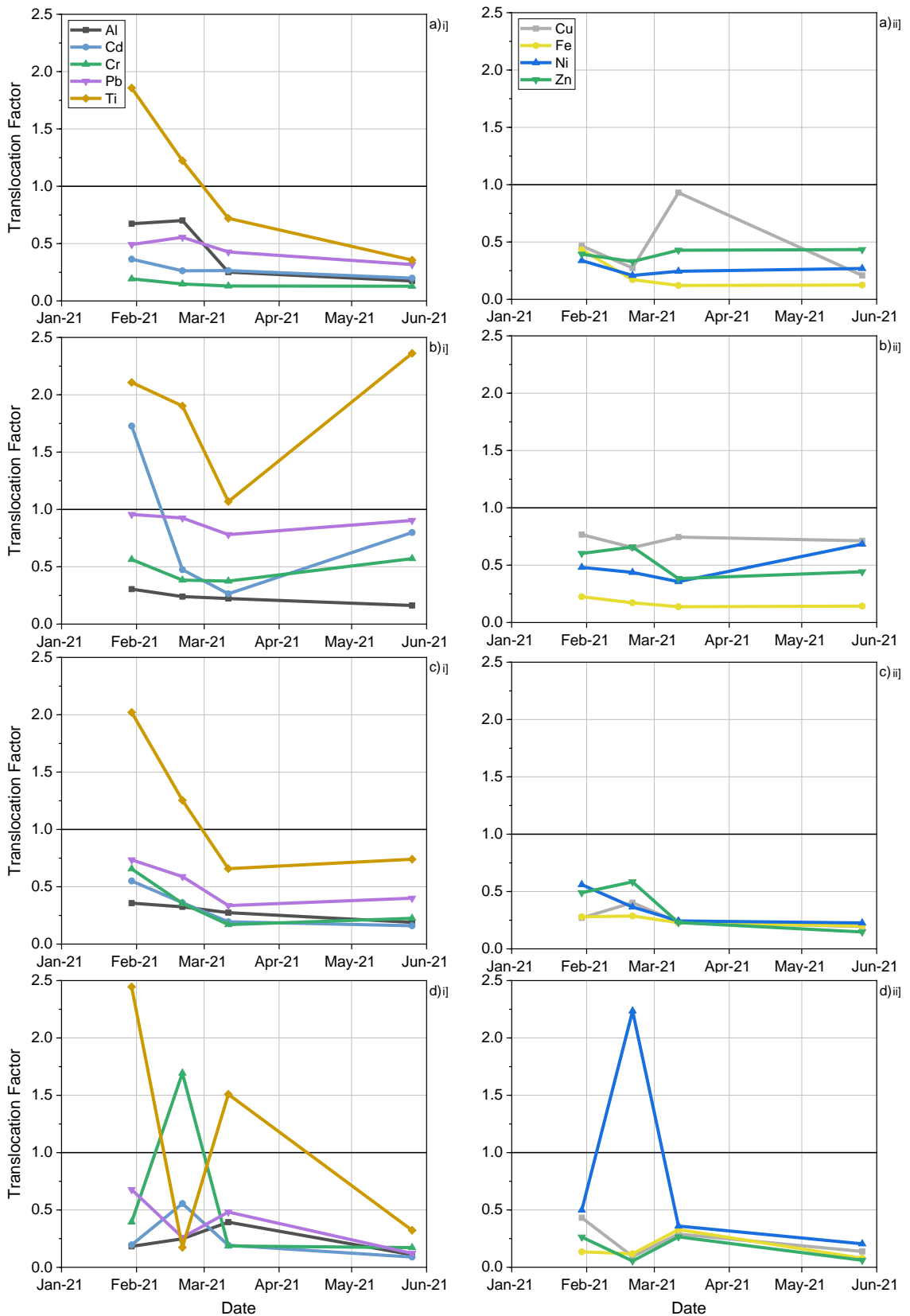


**Figure 4.3-16:** Phenological changes of the heavy metal translocation factor in biomass from river sites in Pune, Maharashtra. Each sample was analysed in duplicate. a) Indrayani Moshi; b) Indrayani Alandi; c) Mula Baner; d) Mula Sangvi. i] non-essential; ii] essential.

The HM concentration in WH was predominantly concentrated in the roots, therefore, for illustrative purposes, only the roots are displayed here, see Figure 4.3-17 and Figure 4.3-18; the individual tissues are available as a raw dataset and graphical representation [326]. Each site showed distinct variation; however, there were general trends observed. Firstly, as stated, the HM concentration in the roots was higher than the other tissues, often exceeding twice the concentration of the leaf and petiole combined. The second general trend was that the HM content generally increased as the growing season progressed, with most HMs ending with a greater concentration at the end of the period of collection as compared with the start. It is possible that this was due to the variation in growth priorities over the season.

Whilst the majority of HMs appear to increase over the season, many of the HMs exhibit a reduction from in February, suggesting that the biomass was on a downwards trend from a peak earlier in the year. The first biomass collection occurred on the 20/01/2021, however, initial biomass appeared in late December, therefore, collection occurred after approximately one month of growth, where it was likely the concentration changed. This one month period had high growth rate, where the biomass prioritised horizontal growth [56], this resulted in a rapid spread across the river, see Figure 4.3-19, however, the plants remained small with bulbous petioles, dense roots and small leaves, see Figure 4.3-20. The plant was aiming to dominate the river as quickly as possible, despite the sub-optimal growth conditions. This high rate of growth is likely to increase the HM concentration within the biomass. However, as there is no data to confirm this, another theory could be possible: horizontal growth results in reduced concentrations of HMs within the biomass due to the distribution of pollutants to ramets via the stolon. There was no literature found discussing these theories, however, the reduction of HM concentration from January to February suggests that horizontal growth may result in a dilution of HM concentration within the population. Further analysis should be conducted to understand this.

Once the horizontal growth has rendered WH the dominant species in a water body, the plant will attempt to focus growth vertically, increasing weight and strength of the plant, therefore, increasing the likelihood of survival. This change in focus, coupled with the increased growth rate as temperature increased, may be the cause of the increased HM content over the growth season.

The Mula Baner site demonstrated a different trend to the other sites, whilst all sites had spikes of individual HMs throughout the collection period, Mula Baner had a specific increase of all HMs in March. All HMs exhibited this increase, although the degree of the increase varied with the HM. This increase also occurred at Mula Sangvi, however, not all HMs increased, and the degree of increase tended to be reduced in

comparison. This increase could be attributed to a point source of pollution downstream from Baner, therefore, the WH mat would have removed some of the pollutants and therefore reduced the pollutant uptake in the plants at the second site.

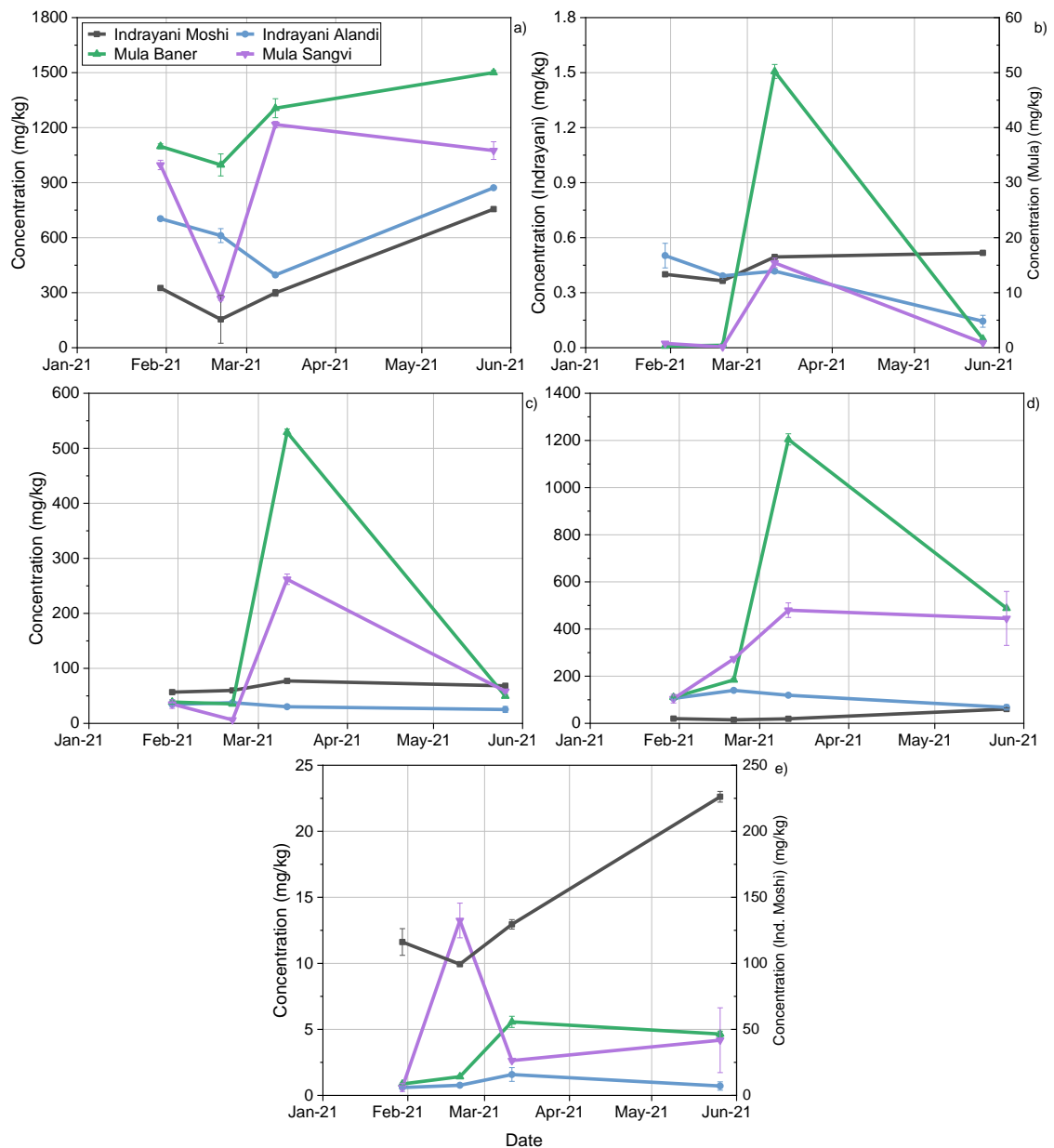


**Figure 4.3-17:** Phenological changes of non-essential heavy metal content in biomass from Maharashtra, India. Each sample was analysed in duplicate; the error bars represent the standard deviation of the replications. Error bars represent the variations. a) aluminium; b) cadmium; c) chromium; d) lead; e) titanium.

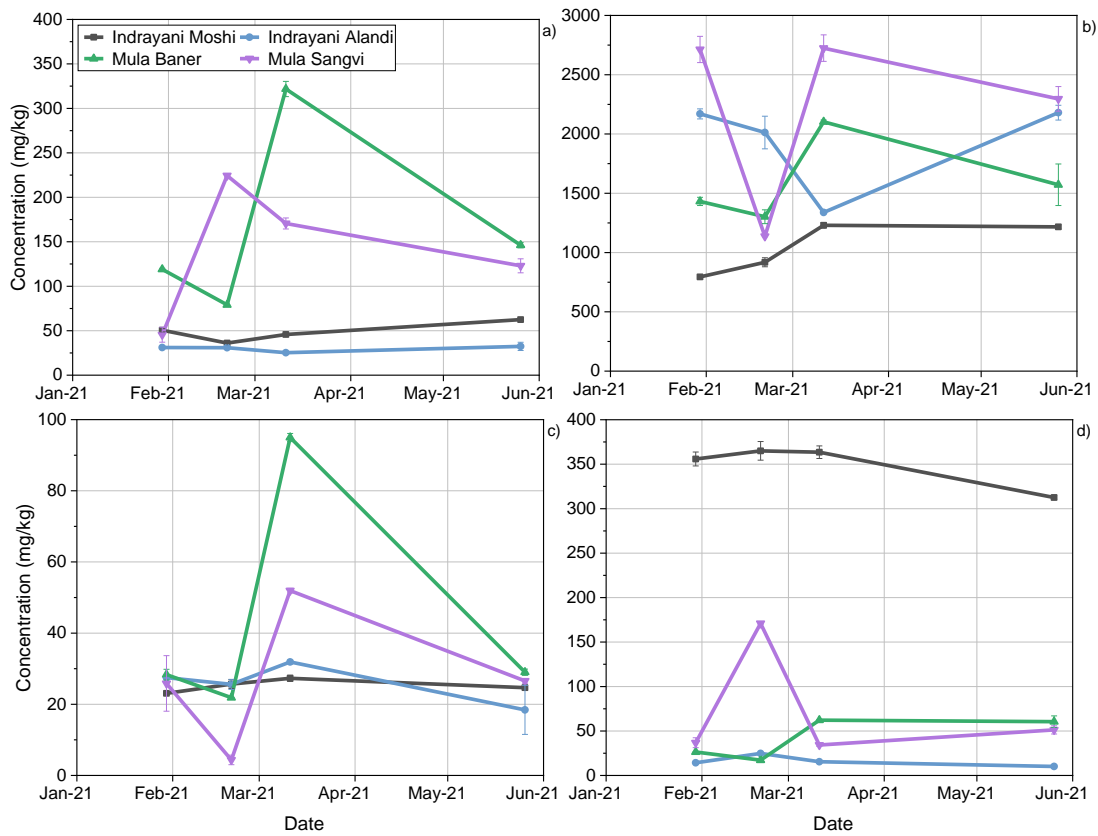


**Figure 4.3-18:** Phenological changes of essential heavy metal content in biomass from Maharashtra, India. Each sample was analysed in duplicate; the error bars represent the standard deviation of the replications. a) copper; b) iron; c) nickel; d) zinc.



**Figure 4.3-19:** Alandi, Indrayani River, Pimpri Chichwad, India on 20/01/2021 (credit G. Nahar).



**Figure 4.3-20:** Water Hyacinth biomass from Alandi, Indrayani River on 20/01/2021 (credit G. Nahar).

The TF of the macro-nutrients demonstrated similar results to Murchison Bay: all macro-nutrients were  $>1$ , peaking at  $\sim 15$ , see Figure 4.3-21. All micro-nutrients had a TF  $<1$ , except for Na which was  $>1$  at all times, except for Mula Sangvi in June. The majority of sites had micro-nutrients with a TF of  $<1$ , emulating the trends found in HMs. The exception was Mula Sangvi, where all micro-nutrients had a TF of  $>1$  in February; there were no increases in HMs that would suggest uptake increased in at this point. However, all sites demonstrated a decrease in Na TF at this point.



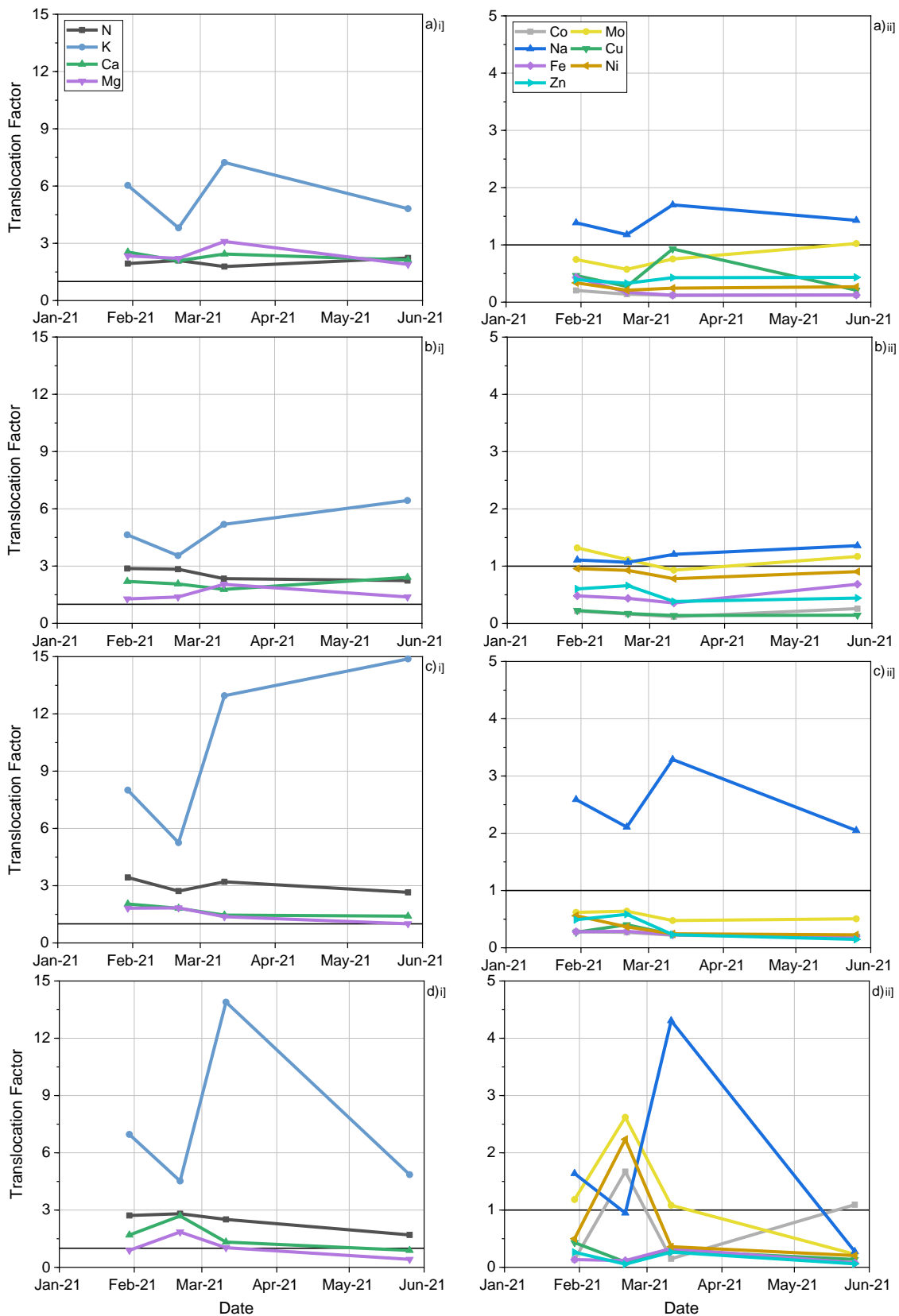


**Figure 4.3-21:** Phenological changes of the nutrient translocation factor in biomass from river sites in Pune, Maharashtra. Each sample was analysed in duplicate. a) Indrayani Moshi; b) Indrayani Alandi; c) Mula Baner; d) Mula Sangvi. i) macro-nutrient; ii) micro-nutrient.

As suggested by the TF, the macro-nutrients were in greater concentrations within the leaf and petiole as compared with the HMs. For illustrative purposes, the tissue containing the maximum average concentration, for each element, are displayed here, see Figure 4.3-22 and Figure 4.3-23. The individual tissues are available as a raw dataset and graphical representation [326]; unless stated, all tissues follow similar trends as displayed in Figure 4.3-22 and Figure 4.3-23. The tissue with the highest concentration varied depending on the nutrient and site:

- Nitrogen- Leaf (all data points)
- Potassium- Petiole (all data points)
- Calcium- Leaf (highest early in the season but higher in the root at the end of the season)
- Magnesium- Petiole (root was similar throughout the season)
- Cobalt- Root (all data points, one apparent anomalous result)
- Molybdenum- Root (all data points, one apparent anomalous result)
- Sodium- Petiole (root was similar throughout the season)

The N concentration was highest in the leaf, likely due to the high protein and chlorophyll content within WH leaves [64,220]. The trends changed between the rivers: the sites on the Indrayani River peaked in January before reducing over the growing season. This could be attributed to the high N/ protein content of juvenile leaves [81]: early in the season, the plants favour rapid horizontal growth, therefore, the number of juvenile plants/ leaves would be greater early in the season, increasing the N content of the total population. However, the Mula River did not follow this trend; this could be due to the difference in WH dominance between the rivers. In the Indrayani River, the plants demonstrated almost 100% coverage by the first collection, shown in Figure 4.3-19, therefore, the plants would soon promote vertical growth. This vertical growth would reduce the number of ramets being produced and therefore increased the average age of the population, corresponding to a reduction in the N content of the leaf. The root and petiole were unaffected by this, however, they appear to increase in N content in February/ March. This is possibly due to the increased growth rate of WH resulting in a greater uptake rate, therefore concentrations would increase within the biomass, as ramet production was reduced, and therefore N concentration would increase within the non-leaf tissues, where luxury nutrients are often stored [100,101].

In contrast to Indrayani River, the Mula River was not dominated by WH in February 2020, see Figure 4.3-24. This resulted in a reduced N concentration, which eventually peaked in March. Whilst the river was not completely covered in WH by March, see Figure 4.3-14, it is likely that the river was 100% covered soon after the collection, therefore, the N content would have reduced from that point.

Juvenile leaves also contain higher concentrations of K, whereas Ca is found to increase with maturity [334]. Therefore, K follows a similar trend to N, however, the petiole has a greater peak compared with the leaf, suggesting that the storage of luxury nutrients occurred once the plants had reached 100% coverage and focussed on vertical growth. Ca increased throughout the season, confirming that population age increased as the season continued. However, the Mula River demonstrated elevated Ca concentration in January, there is no known theory as to why this occurred, however, it is possible that increased pollution increased the Ca concentration of the water.

Co and Mo demonstrate similar trends to that shown by the HMs: increased concentration over the growing season with a spike in March. In contrast with this, Na decreased over the season, however, the February/ March peak still occurred. The March peak only occurred in the Mula River, as with the HMs, suggesting that this was due to a specific point source pollution event.

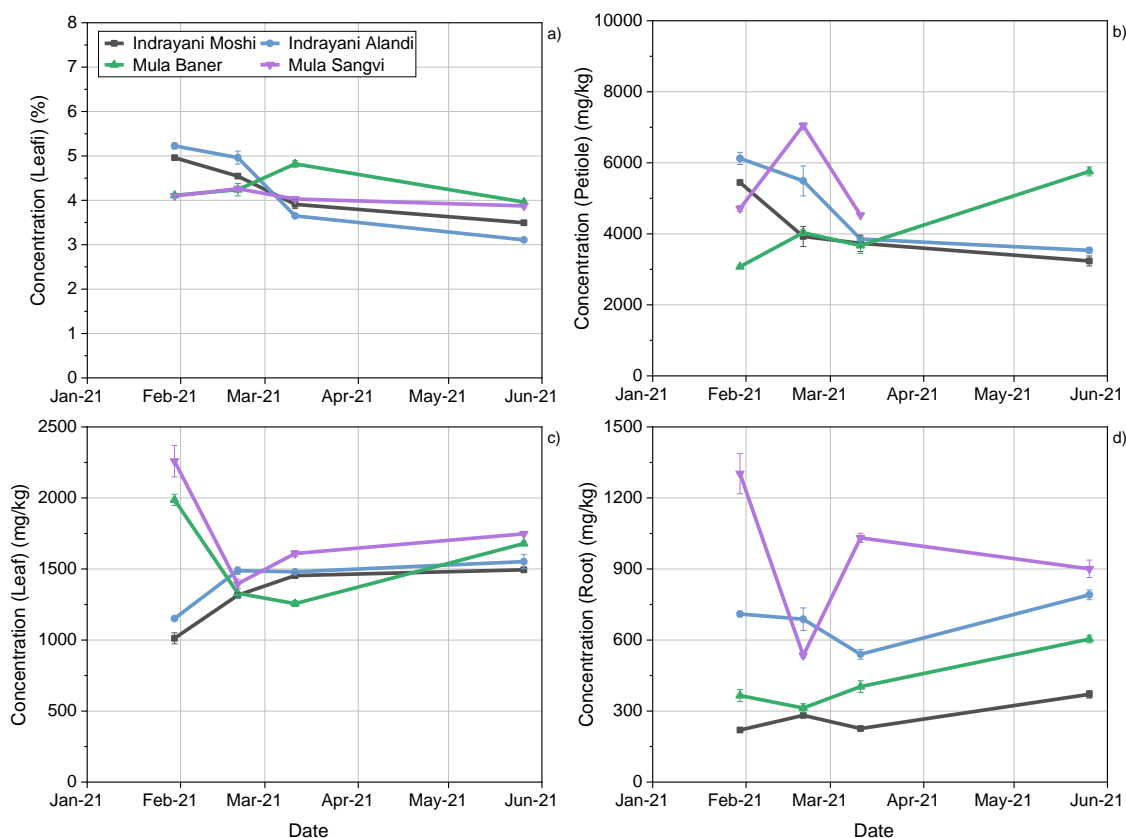


**Figure 4.3-22:** Phenological changes of the maximum average tissue macro-nutrient content in biomass from Pune, Maharashtra. Each sample was analysed in duplicate; the error bars represent the standard deviation of the replications. a) nitrogen (leaf); b) potassium (petiole); c) calcium (leaf); d) magnesium (root).

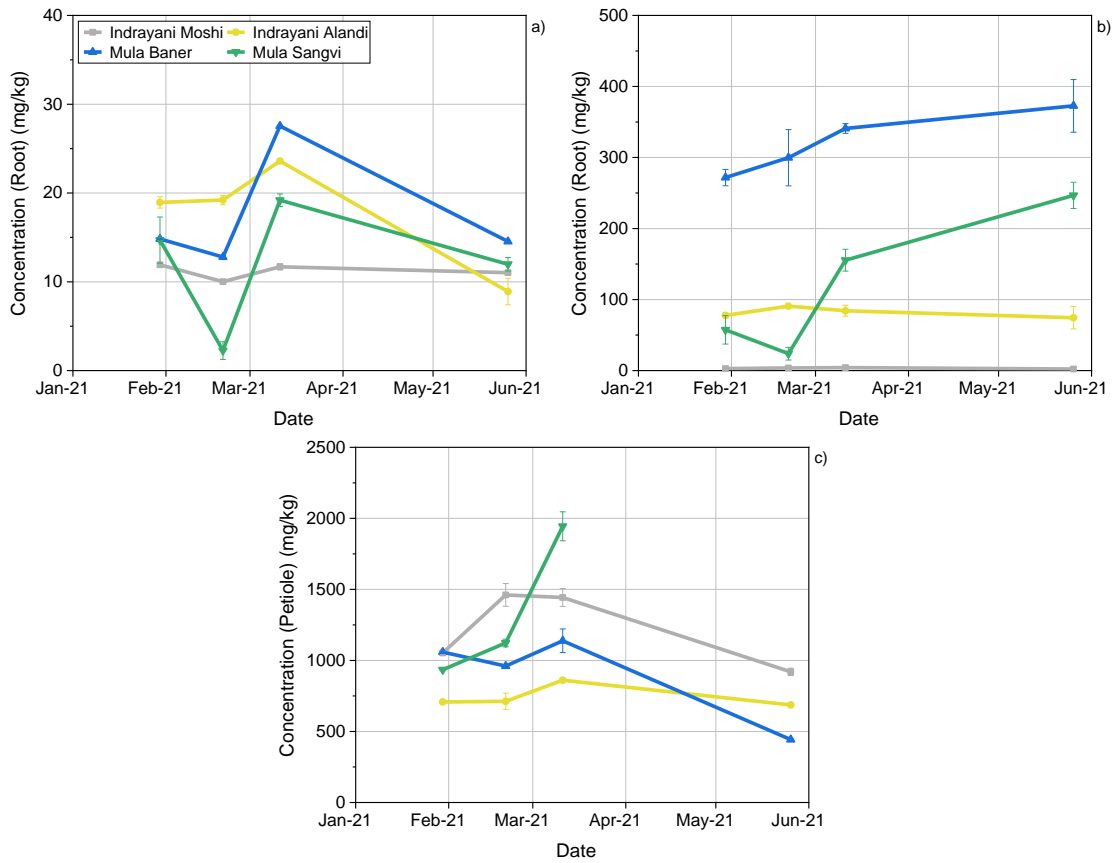


**Figure 4.3-23:** Phenological changes of the maximum average tissue micro-nutrient content in biomass from Pune, Maharashtra. Each sample was analysed in duplicate; the error bars represent the standard deviation of the replications. a) cobalt (Root); b) molybdenum (Root); c) sodium (Petiole).



**Figure 4.3-24:** Water hyacinth coverage on 01/02/2021 at Sangvi, Mula River, Pune, India (credit G. Nahar).

The maximum  $BMP_{th}$  and  $BMP_{th}$ , for all four sites, are displayed in Figure 4.3-25; with the exception of Alandi, all sites increased in March. Alandi, Baner and Sangvi all increased over the growing season, whilst Moshi showed no significant difference from

the initial collection point. As with Murchison, all sites demonstrate the opposite trend to protein, see Figure 4.3-27, which decreased over the season as overall maturity of the mat increases. This is reflected in the C:N ratio, Figure 4.3-26, which increased over the season as protein levels dropped. At all sites, the  $BMP_{th}$  of the root appeared to peak at the end of the season; in a biorefinery these could be used for AD, suggesting that late in the season would be the optimal time to harvest, however, this would reduce protein content.

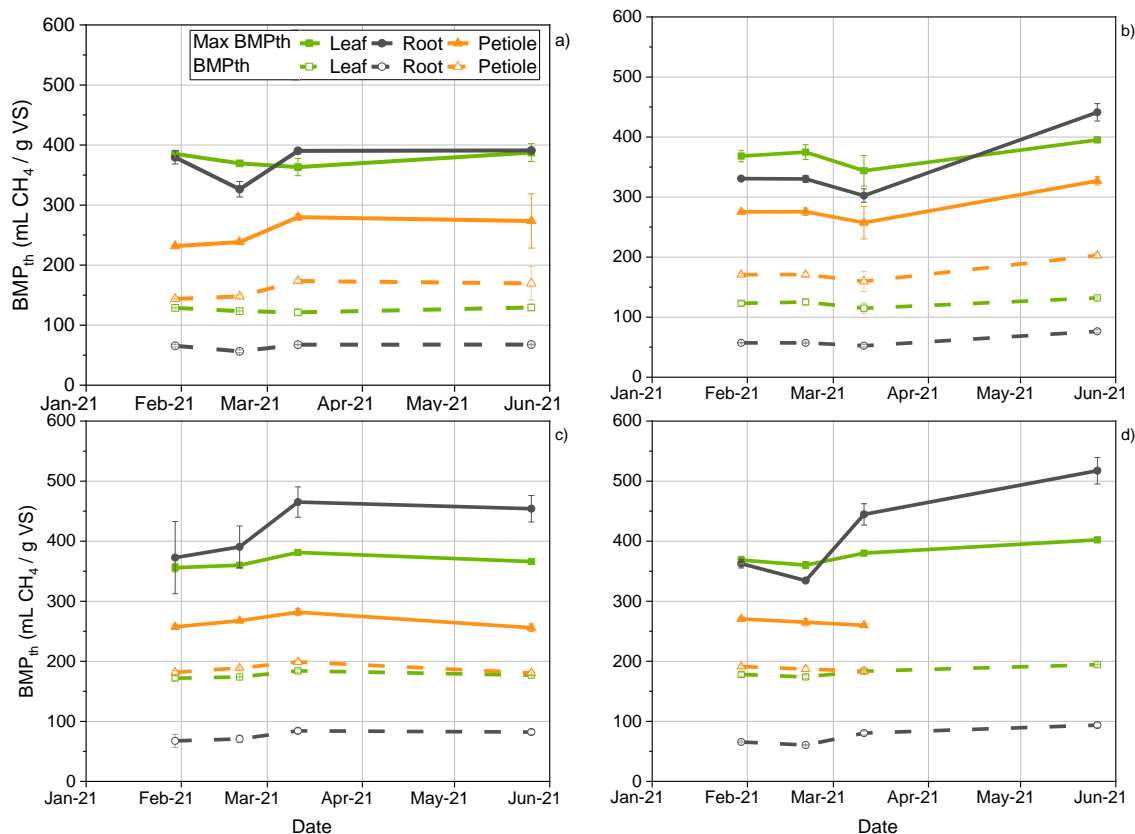


**Figure 4.3-25:** Phenological changes of the maximum theoretical biomethane potential and theoretical biomethane potential in biomass from river sites in Pune, Maharashtra. Each sample was analysed in duplicate; the error bars represent the standard deviation of the replications. a) Indrayani Moshi; b) Indrayani Alandi; c) Mula Baner; d) Mula Sangvi.

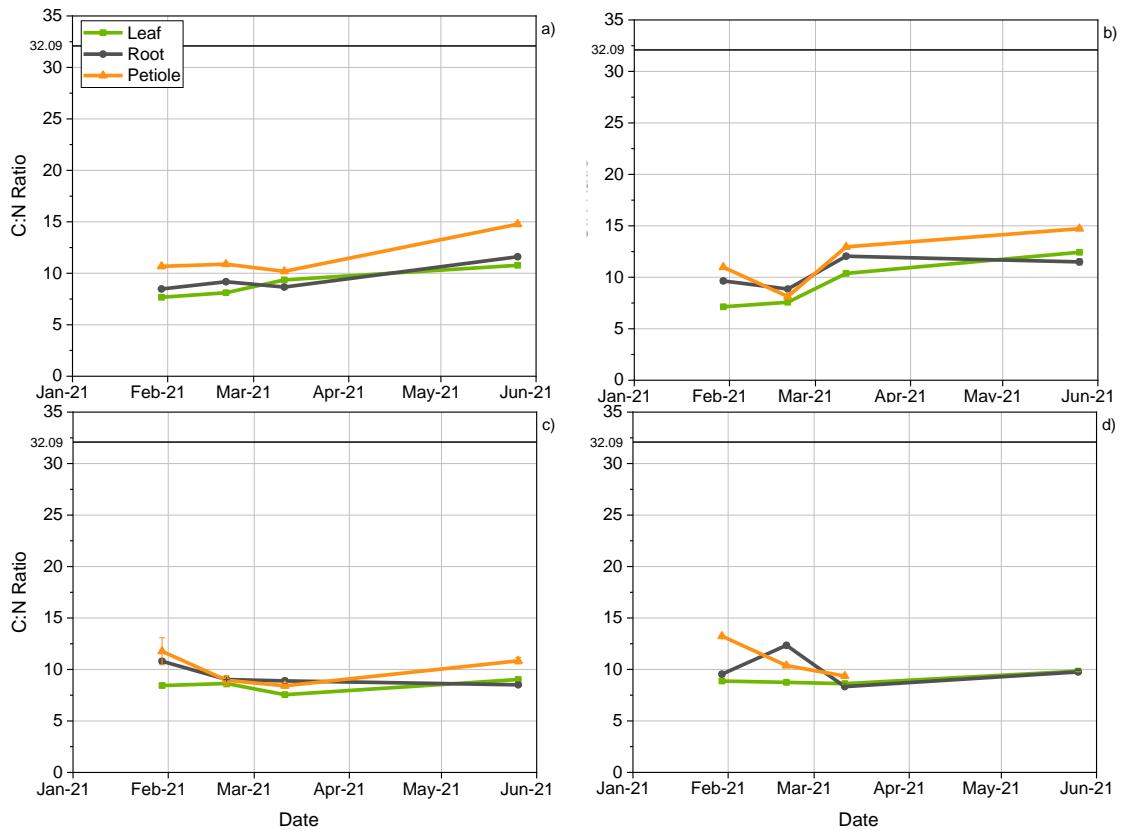


**Figure 4.3-26:** Phenological changes of the carbon to nitrogen ratio in biomass from river sites in Pune, Maharashtra. Each sample was analysed in duplicate; the error bars represent the standard deviation of the replications. a) Indrayani Moshi; b) Indrayani Alandi; c) Mula Baner; d) Mula Sangvi.

The peak protein levels vary from site to site, see Figure 4.3-27; whilst the peak protein occurred in March for Baner, this was a point of HM increase within above water tissues, suggesting that this would not be an optimal point of harvest. Whilst the protein reduced in June, this may be the optimal point of harvest to increase profitability and impact of the harvest. Pre-March, the biomass was small and does not cover 100% of the river, see Figure 4.3-14, therefore, the protein content was high but the total protein within the mat would have been low. Secondly, the TF of certain HMs peaked early in the season, suggesting that the leaves may have high HM content. In comparison, only Alandi demonstrated a TF above 1 in June; the root HM content peaked for a variety of HMs and sites, and the biomass was at maximum coverage and size. This suggests that above water biomass HM content was at a similar level to the rest of the year, yet the root had the highest level, therefore increasing the HM removal from the water. The total protein content of the mat would have been at its highest in March or June, suggesting that June was the optimal point of harvest, for these sites for the times sampled. It should be noted that further analysis may demonstrate that annual variation was significant and the missed collections between March and June could be significant, however, for the purposes of this study, it was assumed that June was the

optimal harvest point from the Maharashtra rivers to maximise protein recovery potential, HM removal and biogas potential.

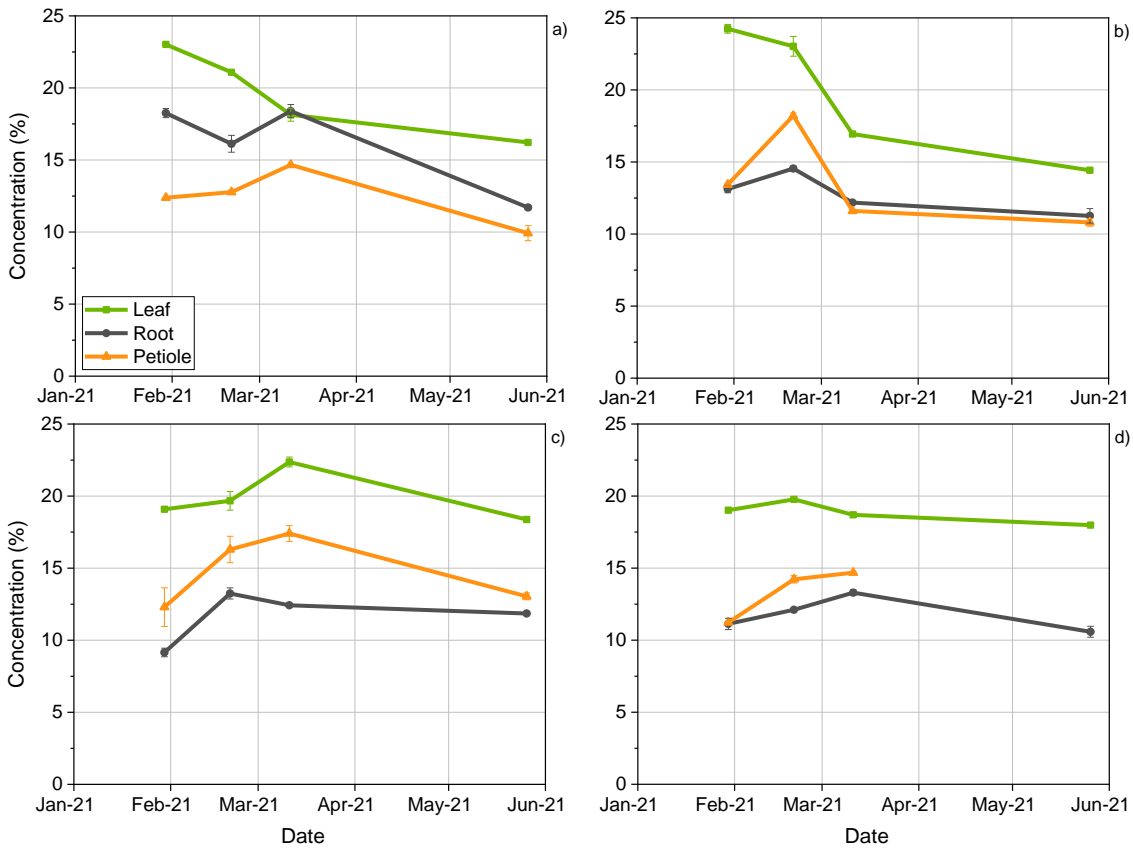


**Figure 4.3-27:** Phenological changes of the protein concentration in biomass from river sites in Pune, Maharashtra. Each sample was analysed in duplicate; the error bars represent the standard deviation of the replications. a) Indrayani Moshi; b) Indrayani Alandi; c) Mula Baner; d) Mula Sangvi.

As shown in Murchison Bay, no value for  $HHV_{th}$  was above 14 MJ/kg, suggesting it is not appropriate to directly combust the biomass. There appears to be no trend across the sites, see Figure 4.3-28, with each site demonstrating different peaks and troughs, however, most had higher or equal  $HHV_{th}$  at the end of the season compared with the start.

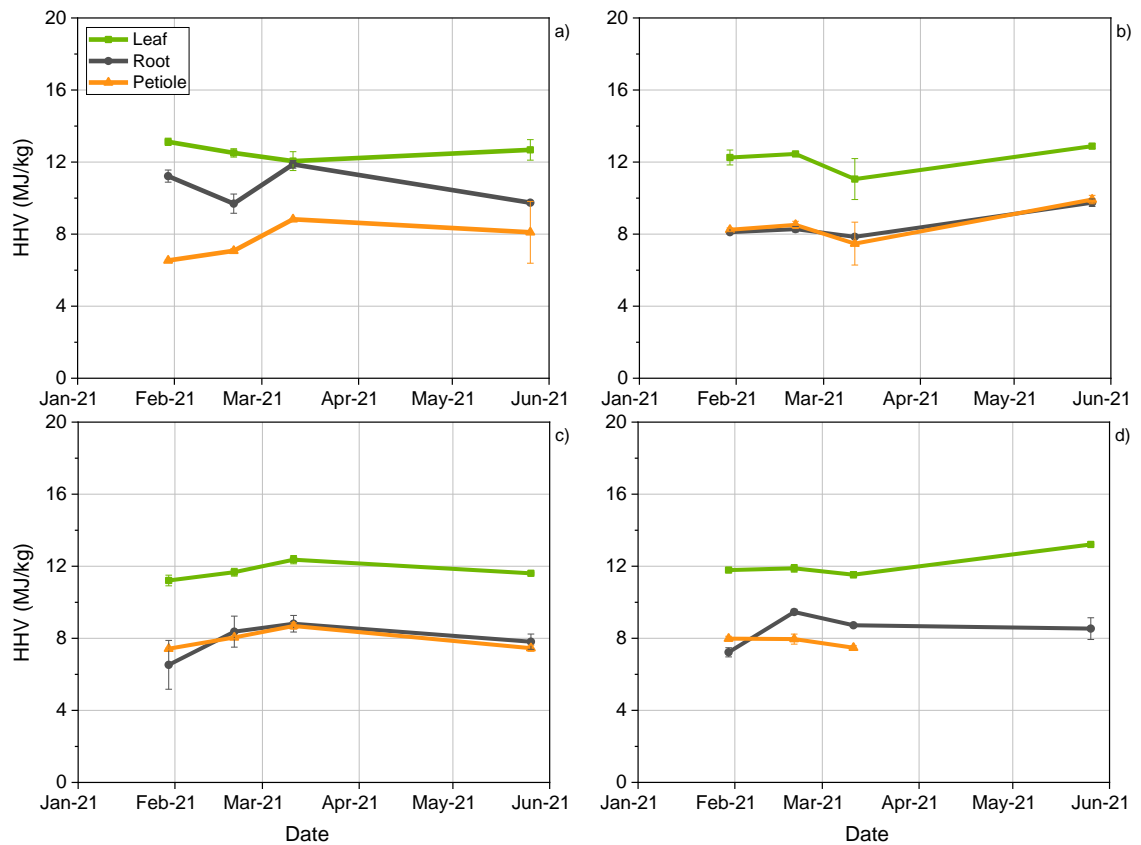


**Figure 4.3-28:** Phenological changes of the higher heating value in biomass from river sites in Pune, Maharashtra. Each sample was analysed in duplicate; the error bars represent the standard deviation of the replications. a) Indrayani Moshi; b) Indrayani Alandi; c) Mula Baner; d) Mula Sangvi.

#### 4.3.3. Goyal Para, West Bengal

The environmental conditions at Goyal Para, West Bengal, were similar to those in Maharashtra, see Figure 4.3-29, with a reduced impact of monsoon. The temperature and solar irradiance increased rapidly from January- April/ May. The monsoon rains then caused a reduction in temperature and solar irradiance until October. The rain then receded, which increased solar irradiance marginally before the temperature and solar irradiance reduced in winter. The lighter monsoon rains meant that plants were not washed away during monsoon, therefore a sample could be collected in winter, however, the conditions during monsoon were deemed unsafe for collection.



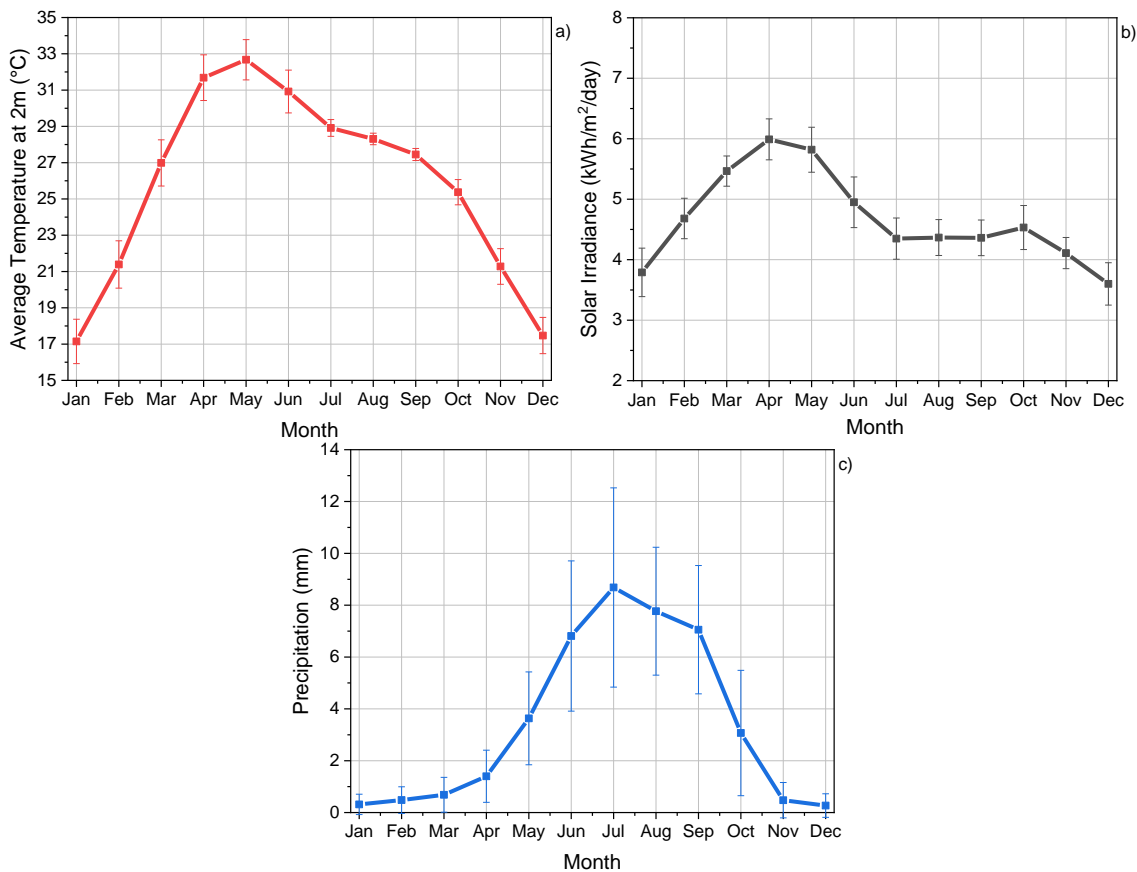


**Figure 4.3-29:** Average phenological variations of environmental conditions for Goyal Para, West Bengal, India. Error bars represent the variations over the selected period, of 1984-2021. a) average temperature at 2m; b) average solar irradiance (all sky surface shortwave downward irradiance); c) precipitation. Raw data was taken from NASA Prediction Of Worldwide Energy Resources [73].

The WQIs for West Bengal are displayed in Figure 4.3-30; TSS and TDS all showed an increase at the start of winter, suggesting that surface run off from monsoon rains caused an increase in pollution levels. DO reduced at the start of winter then increased, corroborating this theory. In comparison with Murchison Bay, the TSS levels in West Bengal were lower, demonstrating that it was likely to contain lower levels of pollution. TKN also increased in winter 2020/21 but not 2019/20. As with the water analysis in Murchison Bay and Maharashtra, further analysis would be required to determine a reliable phenological trend.

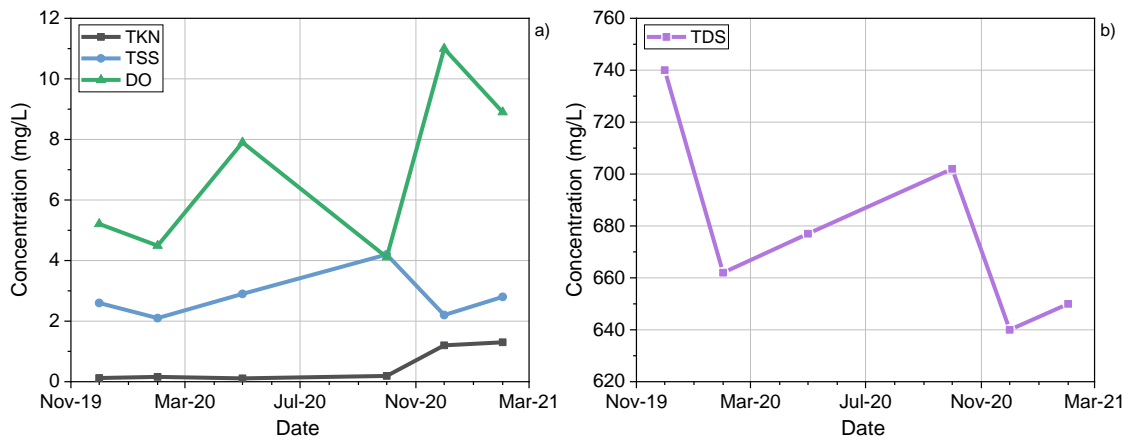


**Figure 4.3-30:** Phenological variations of water quality indicators of Goyal Para, West Bengal, India. Each sample was analysed in duplicate. a) nitrogen (TKN), total suspended solids (TSS) and dissolved oxygen (DO); b) total dissolved solids (TDS).

The tissue proportions demonstrates that the petiole had the greatest proportion whilst wet and dry, at all sample points, whilst the leaf had the lowest, except for the dry weight in December. Due to the variety for WH present at West Bengal, forming small clones, this was expected as the leaves tend to be small yet numerous whilst the petioles tend to be short and bulbous, and the roots tend to be large to extract nutrients from the water. There was little variation in wet weight across the collections, suggesting that moisture content was the biggest variation.

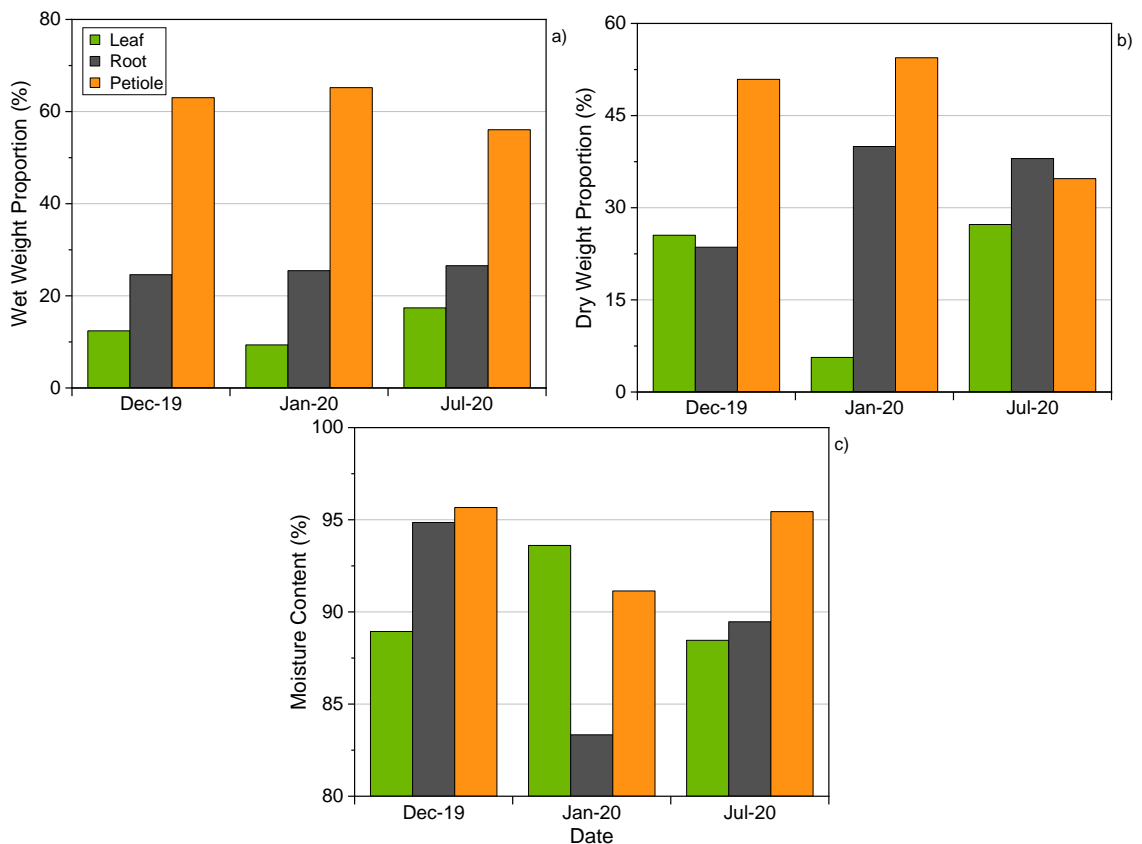


**Figure 4.3-31:** Phenological changes in tissue weight proportion in water hyacinth biomass from Goyal Para, West Bengal, India. a) wet weight proportion; b) dry weight proportion; c) moisture content.

As expected, the root contained a greater concentration of ash than the leaf or petiole, see Figure 4.3-32. The spike in January suggests that the WH had begun its growth period, despite the sub-optimal conditions. It is possible that this was due to a pollution event, however, there have been no large pollution events associated with the ponds in question, therefore, this is unlikely.

The reduction in ash in July was likely due to the impact of monsoon: the reduced growth rate in May/ June would reduce uptake and therefore, reduce ash content. The petioles demonstrated a spike of ash in July, this was possibly due to the increased storage of luxury nutrients in petioles [100,101], at the end of the growing season. The gap of collections between January and July result in unknown composition of the growth period in West Bengal, therefore the phenological changes across the season are speculation. However, it was evident that West Bengal WH had a reduction in ash content between the start and end of the growth period, with the exception of the petiole.

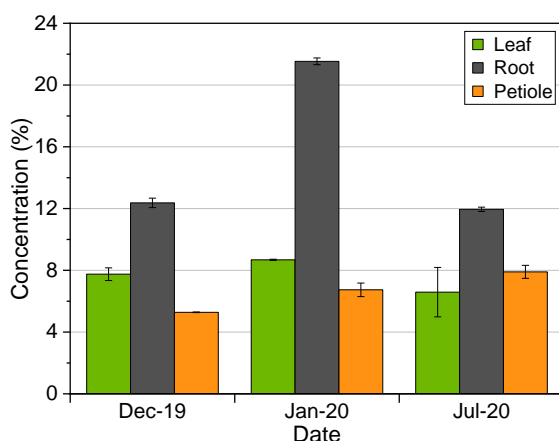


**Figure 4.3-32:** Phenological changes of ash content in biomass from Goyal Para, West Bengal. Each sample was analysed in duplicate; the error bars represent the standard deviation of the replications.

The ash content suggested that the overall TF would be lowest in January, whilst December and July would be similar. The TF was >1 for five out of nine HMs in January and was the lowest of all the collection points, see Figure 4.3-33. However, whilst December had the highest TF for four non-essential HMs and two essential HMs, July had a similar TF to January for all HMs. The results suggests that certain elements were translocated in peak growth conditions whilst others were translocated during dormant periods of the year. The high TF of HMs was in contrast with other sites: whilst Ti was demonstrated to have a TF of >1 in Maharashtra and periodically >1 in Murchison Bay, no site had a TF of over 2.5 for any HM, in particular, Cr only had a TF of >1 in two results at West Bengal. The TF for Cd in December was >6, whilst this is

much higher than any other site, other studies have shown that the TF for Cd can be over 8, see Table 2.3-2.

This contrasts with the nutrients which had a lower TF than all other sites: Murchison Bay had a TF for macro-nutrients of >2, whilst Maharashtra had a more similar TF. One suggestion for the cause of this is the variety of WH clone in the ponds of West Bengal: the plants were in stagnant water with low nutrient replenishment; therefore, the plants were only able to grow to a small size, producing large petioles with dense roots. Further analysis of the varieties should be conducted to understand the variations in uptake rate, however, as previously suggested, plants prioritising vertical growth may have a higher uptake rate. This uptake rate could lead to greater translocation, however, if the plant is unable to grow vertically this would reduce uptake.

The average macro-nutrient TF was highest for January and lowest for December, indicating that the suspected increase in growth increased translocation of nutrients to the upper tissues of the plants. Whilst the leaf and petiole ash content were higher in January than December, this was not the case in July, despite a similar TF. However, there was a significantly higher TF for Na in July, this element is often in high concentrations within WH, as discussed previously, and therefore could contribute to a higher ash content in the petioles in July.

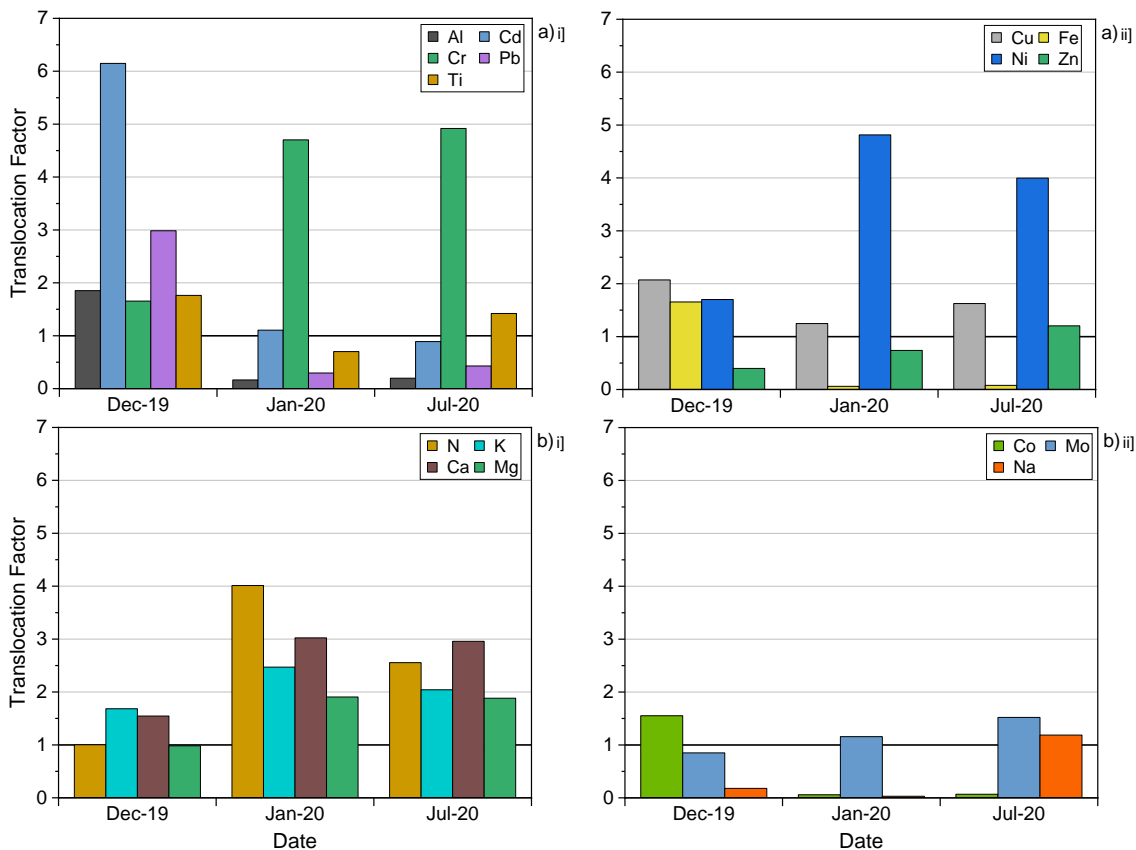


**Figure 4.3-33:** Phenological changes of the heavy metal and nutrient translocation factors in biomass from Goyal Para, West Bengal, India. Each sample was analysed in duplicate. a) i] non-essential heavy metals; a) ii] essential heavy metals; b) i] macro-nutrients; b) ii] micro-nutrients.

The reduced HM TF in January suggests that root inorganic concentrations would be increased and upper tissue concentrations reduced; Figure 4.3-34 and Figure 4.3-35 demonstrate that the HM root concentrations were increased in January. However, the same was true for leaf and petiole, indicating a greater translocation occurred with the greater concentrations. The increased concentration was likely due to the suspected increased growth rate in January. The decrease in concentrations from January to July cannot be accounted for due to the large gap in collection: this period would contain the highest growth rate changes and therefore would result in the greatest variation in uptake rate and concentrations. Secondly, the impact of monsoon cannot be confirmed: the water contamination suggests that the monsoon increased the nutrient content of the water, likely due to surface runoff, however, there was no data on HM concentration.

The low Fe root concentration and high leaf Cd concentration in January appear to be anomalous. This would explain the high TF results in Figure 4.3-33.

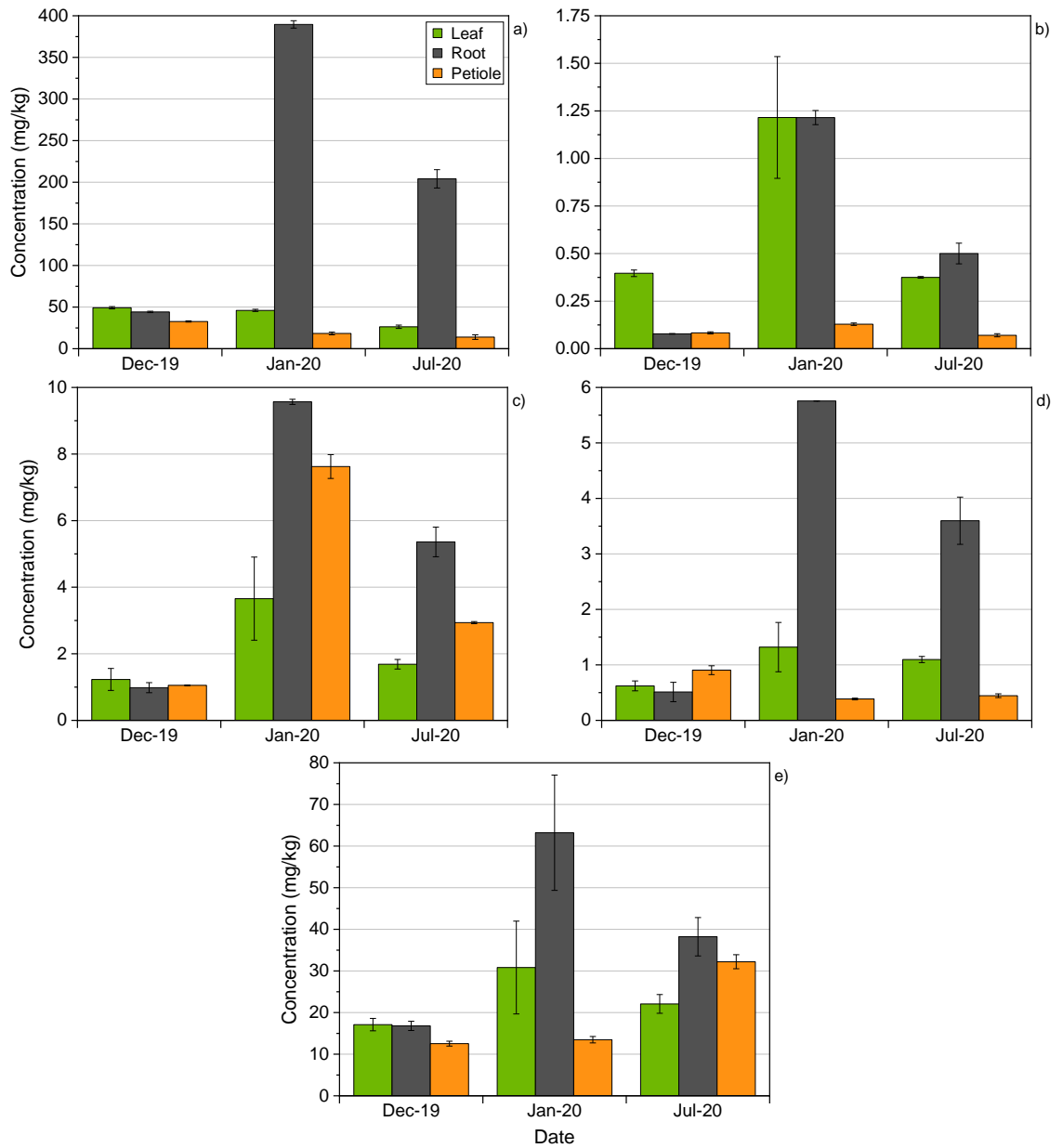


**Figure 4.3-34:** Phenological changes of non-essential heavy metal content in biomass from Goyal Para, West Bengal, India. Each sample was analysed in duplicate; the error bars represent the standard deviation of the replications. a) aluminium; b) cadmium; c) chromium; d) lead; e) titanium.

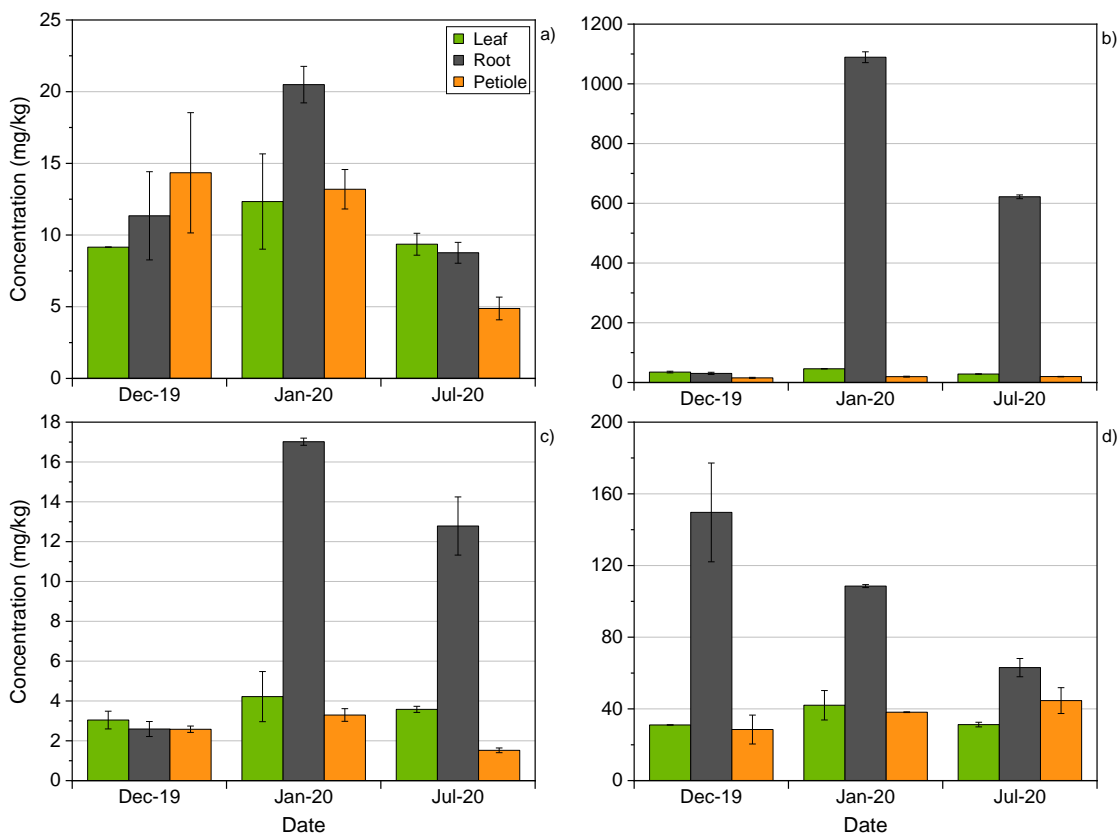


**Figure 4.3-35:** Phenological changes of essential heavy metal content in biomass from Goyal Para, West Bengal, India. Each sample was analysed in duplicate; the error bars represent the standard deviation of the replications. a) copper; b) iron; c) nickel; d) zinc.

The root nutrient concentrations were highest in December, with the exception of Co which followed the same trend as Fe, then fell in January and were similar in July, see Figure 4.3-36. The drop between December and January could be attributed to the change in growth focus that could have occurred in January: the January sample was collected on 29/01/2020, therefore, the temperature would have increased and likely resulted in an increased growth rate. This increased growth rate is likely to have allowed the plant to expand horizontally and therefore increase the number of plants, this would spread the nutrients among a larger population and therefore, dilute the nutrient concentration within the plant. There were no other trends that can be identified due to the lack of collection points.

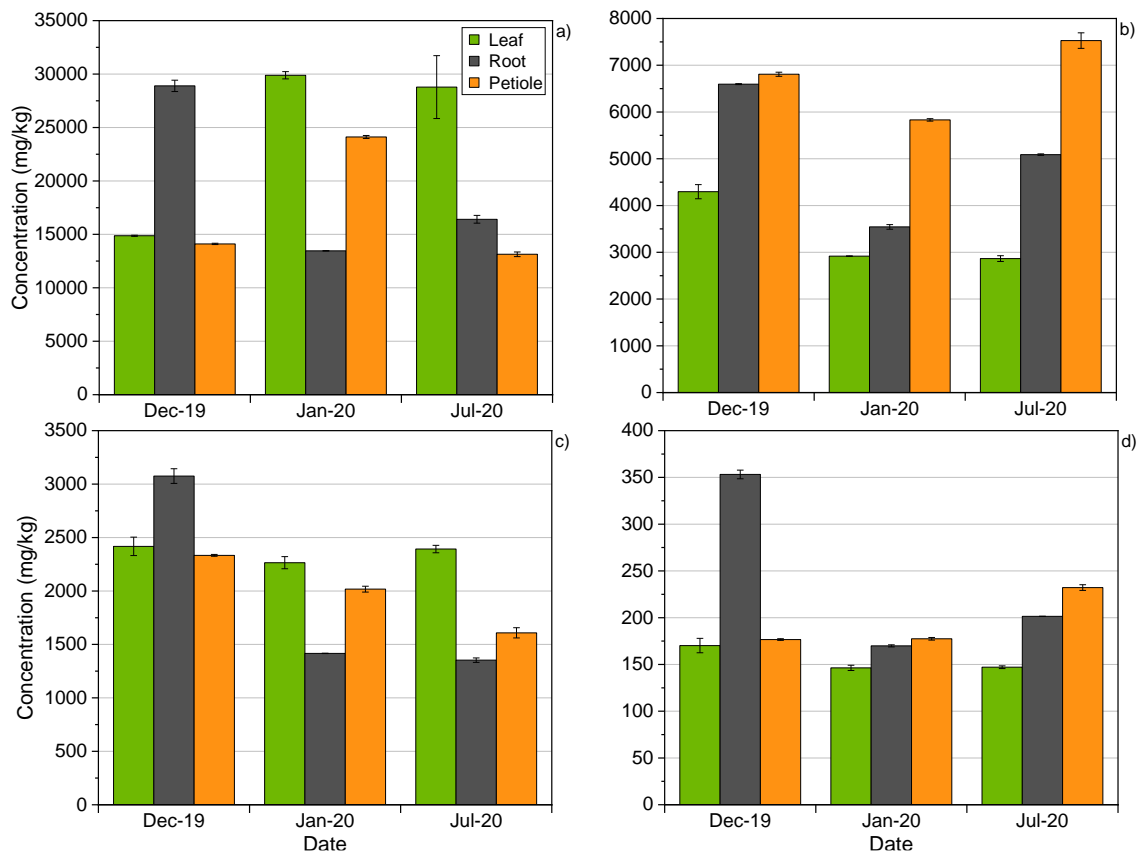


**Figure 4.3-36:** Phenological changes of the macro-nutrient content in biomass from Goyal Para, West Bengal, India. Each sample was analysed in duplicate; the error bars represent the standard deviation of the replications. a) nitrogen; b) potassium; c) calcium; d) magnesium.



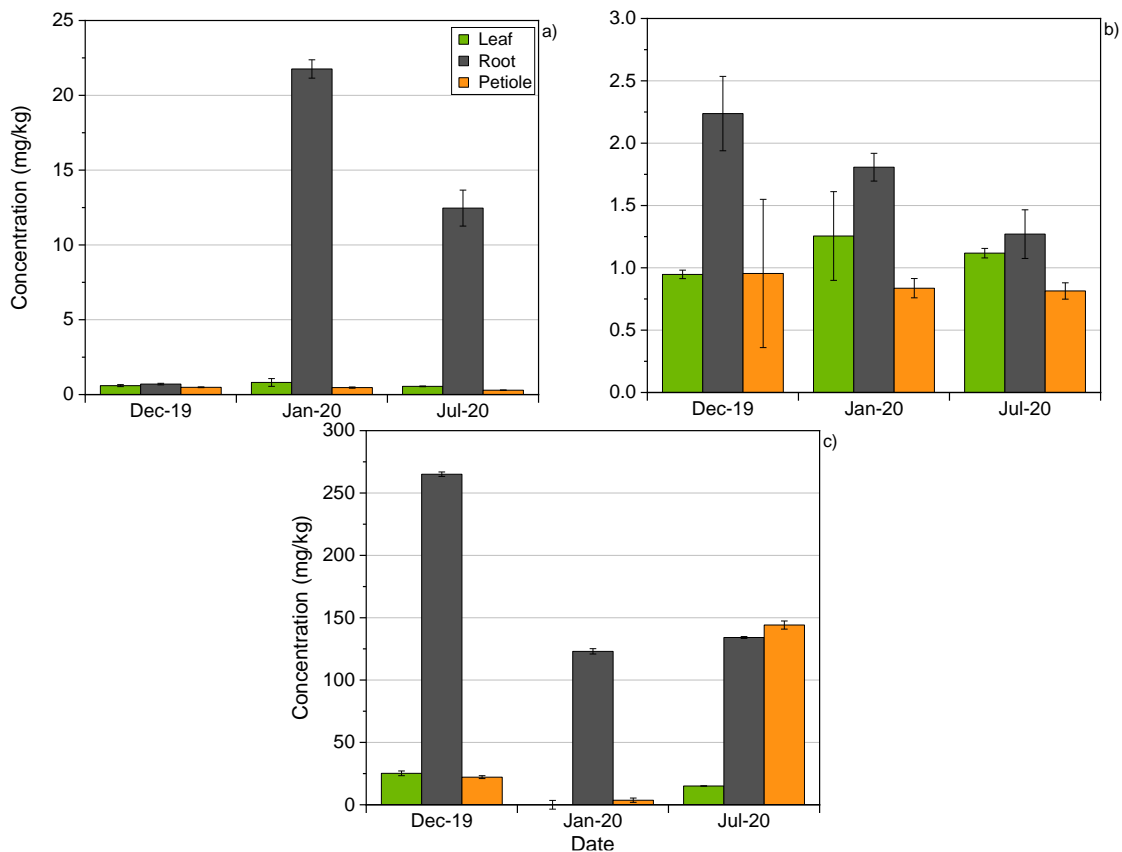


**Figure 4.3-37:** Phenological changes of the micro-nutrient content in biomass from Goyal Para, West Bengal, India. Each sample was analysed in duplicate; the error bars represent the standard deviation of the replications. a) cobalt; b) molybdenum; c) sodium.

Unlike the phenological variations shown in Murchison Bay and Maharashtra, the max  $BMP_{th}$  in West Bengal does not appear to be inverse to the protein content or follow the same trend as the C:N ratio, see Figure 4.3-38, this was likely due to the high oxygen concentration in the West Bengal samples. Secondly, the maximum  $BMP_{th}$  was lower than Murchison Bay and Maharashtra, on average, with results for the leaves and roots dropping below 300 and only error breaking 400 mL  $CH_4/g$  VS. The petiole demonstrated different trends to that seen in Murchison Bay: in July, the petiole had higher max  $BMP_{th}$  and  $HHV_{th}$  than the root, something that did not occur at any point in Murchison Bay. Similarly, the petiole had higher protein content and lower C:N ratio than the root in January. These results demonstrate that different locations result in significantly different trends and utilisation potentials.

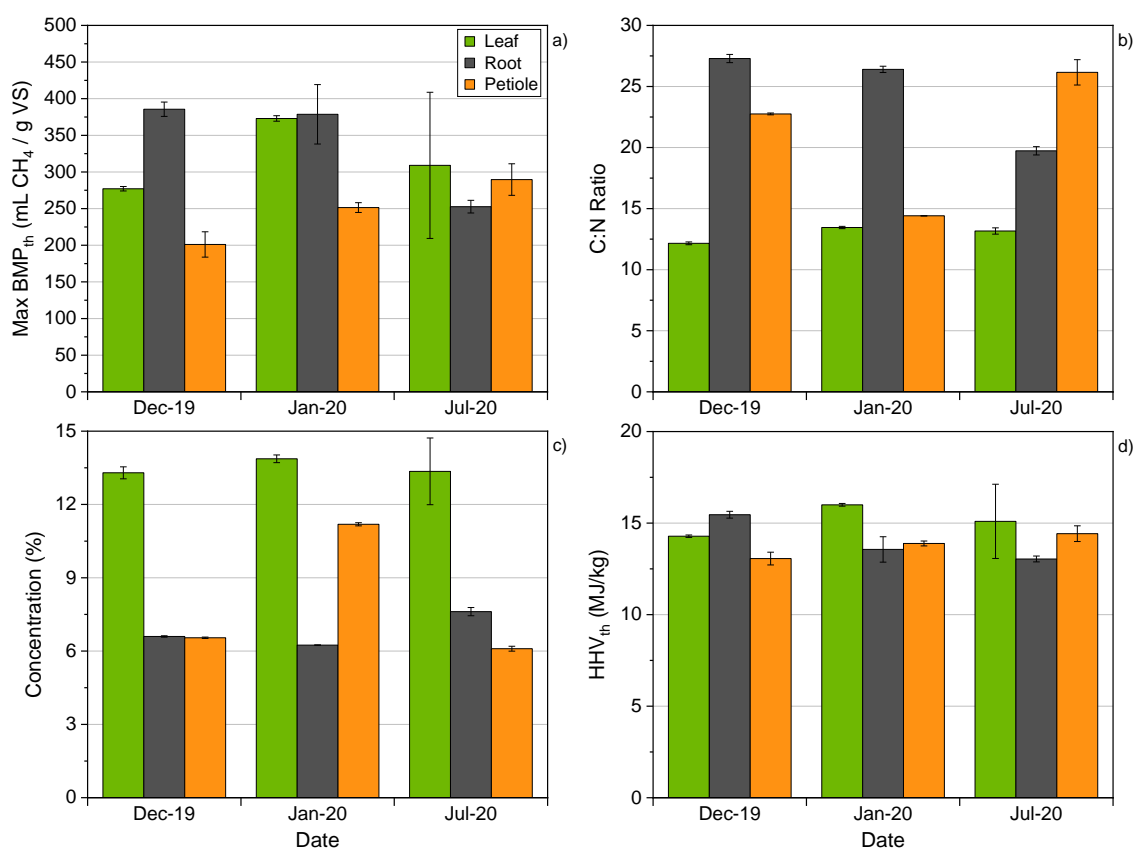


**Figure 4.3-38:** Phenological changes of utilisation potential indicators in biomass from Goyal Para, West Bengal, India. Each sample was analysed in duplicate; the error bars represent the standard deviation of the replications. a) maximum theoretical biomethane potential; b) C:N ratio; c) protein content; d) theoretical higher heating value.

The C:N ratio was below 27.5 for all results, and therefore would be unlikely to be utilised as a sole feedstock in AD. The protein content of the leaves was lower than the previous sites, suggesting it would be less appropriate for protein extraction or animal feed. Secondly, the protein spikes, January and July, coincided with increases of HMs within all parts, reducing its applicability. As with all other samples, the HHV<sub>th</sub> was below 16 MJ/kg, suggesting that WH would not be an appropriate combustion fuel.

#### 4.4. Summary of composition

Table 4.4-1 displays the range of composition and UPIs for parts of the plant at Murchison Bay, Maharashtra and West Bengal. This gives the possible composition and utilisation potential indicators for WH at these sites.

**Table 4.4-1:** Range of composition and utilisation potential indicator values for water hyacinth biomass from Murchison Bay, Maharashtra and West Bengal.

Parameter	Murchison Bay			West Bengal			Maharashtra			
	Leaf	Root	Petiole	Leaf	Root	Petiole	Whole	Leaf	Root	Petiole
C (% DW)	37-44	28-39	34-40	35-40	32-39	32-35	29-37	36-39	22-29	30-34
H (% DW)	3.1-5.8	2.9-5.2	1.6-5.2	4.3-4.8	3.7-4.8	3.6-4.8	3.6-4.5	4.4-4.9	2.4-3.6	3.7-4.0
N (% DW)	2.6-4.3	1.9-3.5	1.3-3.0	2.9-3.0	1.3-1.6	1.3-2.4	2.2-3.1	3.1-4.0	2.3-2.6	2.1-2.8
S (% DW)	0.0-0.2	0.0-0.4	0.0-0.1	0.0-0.0	0.0-0.4	0.0-0.0	0.0-0.3	0.0-0.3	0.0-0.5	0.0-0.1
O (% DW)*	35-47	29-44	37-53	43-50	38-50	52-58	25-38	37-39	14-30	43-47
VM (% DW)	69-90	55-73	69-78	75-76	69-76	72-79	52-67	67-72	36-69	66-71
FC (% DW)	6-19	9-18	14-20	15-18	15-16	12-16	8-12	11-16	3-12	11-15
Ash (% DW)	4-15	11-36	5-16	7-9	12-22	5-8	21-40	14-16	21-45	14-17
Total HMs (mg/kg)	322-632	917-3925	349-762	273-336	613-1898	286-354	2210-3454	423-1623	1969-6449	640-1346
BMP <sub>th</sub> (mL CH <sub>4</sub> / g VS) <sup>1</sup>	189-288	61-84	217-375	87-117	17-25	78-112	112-148	150-164	69-92	170-217
C:N	9-15	10-19	13-28	12-13	20-27	14-26	9-14	7-12	8-12	8-15
Protein (% DW) <sup>2</sup>	12-20	9-16	6-14	13-14	6-8	6-11	10-14	14-24	9-18	10-18
HHV (MJ/kg)	10-16	10-13	7-11	14-16	13-16	13-14	11-14	14-15	8-14	12-14

<sup>1</sup>Calculated using maximum theoretical methane potential multiplied by biodegradability index; <sup>2</sup>Calculated via conversion factor, on N content, of 4.64 [273]

## 4.5. Conclusions

This chapter aimed to assess WH as a resource by characterising the biomass for proximate, ultimate and inorganic composition; utilising this to investigate UPIs and determine the applicability of WH for AD, combustion and protein extraction; and understand the variation that occurs due to differences in location, water quality and phenological variation. WL was also characterized as a comparison to WH.

To understand the morphological the geographical and water quality variations, biomass and water were collected from three locations in Murchison Bay and five in India. These sites were split into three categories: sewage pollution; industrial pollution; and no point source pollution. The water analysis demonstrated that in Murchison Bay, the site with sewage pollution (NC) had the highest levels of Cu, NH<sub>4</sub>, NO<sub>3</sub>, TKN, PO<sub>4</sub>, COD and TSS, all of which are often present within treated sewage wastewater. The no point source pollution site in India (West Bengal) was chosen to demonstrate the baseline for a clean urban waterbody, whereas the no point source pollution site in Murchison Bay estimated the background pollution in Murchison Bay. In comparison with the no point source pollution site in Murchison Bay (CW), the TSS and TKN at West Bengal was 9.7 and 25.8% lower, respectively, confirming that it was the site with lowest pollution. The sites in Maharashtra (Indrayani and Mula rivers) had the lowest N and HM concentration, however, these were the only sites located on a river, therefore the flow rate and replenishment of nutrients was greater. It is likely that whilst these sites had the lowest concentrations, the high level of raw sewage pollution and replenishment, would expose the plants to a greater total value of pollutants. Despite this, the whole plant river samples had a lower ash content and total HM content than the sample from Murchison Bay; however, these samples did contain greater total nutrient content, likely due to the raw sewage pollution into the rivers. All sites had a high ash content, averaging at 27.3% across the samples, and a HHV<sub>th</sub> of less than 15 MJ/kg; this ash content was higher than conventional bioenergy crops, like oak wood (7.4%) [328], whilst the HHV<sub>th</sub> was less than conventional bioenergy crops [174]. This suggests that WH would be a poor choice for combustion. As a feedstock for AD, the samples had a maximum BMP<sub>th</sub> of 264-445 mL CH<sub>4</sub>/g VS and have been shown to have a poor BI [139]. This would make WH a poor choice of feedstock for AD compared with traditional feedstocks that have higher BI and a maximum BMP<sub>th</sub> of 426-599 mL CH<sub>4</sub>/g VS. In contrast, WH had a protein content range that was higher than raw tofu [313,314] suggesting that it could be a useful protein source. The location and water quality variation did not demonstrate clear trends, however, the river samples tended to have higher maximum BMP<sub>th</sub> and protein content, whereas West Bengal had the lowest maximum BMP<sub>th</sub> and protein, but the highest C:N ratio and HHV<sub>th</sub>.

The individual plant parts were also analysed: root, petiole and leaf; this demonstrated that the root had the highest ash content but also had the greatest variation. The petiole had the highest nutrient content, which was unexpectedly the highest in West Bengal. The rivers sites had the highest ash content, whilst West Bengal had the lowest, corroborating that the flow rate increased the exposure of inorganics to the plants and that West Bengal had the lowest pollution levels. The rivers also had the highest concentrations of N and S within the individual tissues. A subset of the samples were used to analyse the  $BMP_{ex}$  of the whole and parts of the plant. This demonstrated that the petiole had the highest methane production and BI, potentially due to the low lignin content. The root had the lowest methane production, likely due to the high concentration of HMs within the tissue. When comparing the two river samples (Indrayani Moshi and Mula Baner), Baner had a higher BI for all parts and the whole sample. This was unexpected due to the higher max  $BMP_{th}$ , C:N ratio and C content for Indrayani Moshi whole and part samples. However, Indrayani Moshi whole had a greater HM concentration, including a greater Zn content, in the whole and parts, which is known to reduce the methane production in AD [335].

The phenological analysis looked at Murchison Bay biomass across one full year and Indian biomass from December/ January through to May/ June. In Murchison Bay there were no conclusive relationships drawn from the water quality analysis, however, it appeared that pollution may have increased during the wet season, potentially from surface runoff. In the biomass, the HMs demonstrated a TF of  $<1$ , however, there were spikes above 1 for all HMs except for Al and Fe. These elements have been shown to be localised on the surface of the epidermis of the roots [149] and therefore are taken up less within the tissue and less translocation occurs. Total concentration in the tissues peaked at all sites in July-September, suggesting that the biomass had a greater uptake of HMs within the wet season, as this was the first collection after the wet season. Certain metals peaked later than others suggesting that uptake may have been slower for these metals either due to a lower affinity or lower concentration within the water. This increase was not due to point source of either sewage pollution (NC) or the brewery wastewater (UBL), as the peak also occurred at CW. Other peaks occurred that were not present at all sites, predominantly within periods of higher temperature or precipitation, suggesting that increased growth rate or surface runoff was responsible. These peaks were most extreme at NC, suggesting that the sewage pollution had the greatest pollution impact. The troughs in HM concentration occurred at the same sampling point as the peaks in protein content, whilst the peaks in HM concentration were identical to the peaks in maximum  $BMP_{th}$ . This outlines that if protein recovery is the target, then HM removal would be low, but the plant would be

less toxic. In comparison, increased methane production would also result in increased HM removal from the lake.

In Maharashtra, there was little variation between the WQIs across the year; due to the high flow rate it would be difficult to estimate the variation of water quality without a greater regularity of monitoring, however, both rivers are categorised as highly polluted by the MPCB. The HM content, of the biomass, predominantly peaked at the end of the growth season, whereas nutrients varied depending on the element. The HMs had a reduction early in the growth season, attributed to the effect of dilution as the plants spread horizontally across the waterbody. The increase at the end of the season was attributed to increased growth rate, due to temperature increase and the switch of focus to vertical growth. The nutrient concentration changed after the plants reached 100% coverage and stopped spreading horizontally, this resulted in an increase in vertical growth and maturity of the population, which resulted in decreased N and K and increased Ca. The UPIs demonstrated that  $BMP_{th}$  generally increased over the growth season, similar to HM concentration, and had an inverse relationship to protein content. This suggests that early season harvest would be optimal for protein recovery, whilst late season harvest would be optimal for methane production and HM removal. However, biomass density and coverage were highest at the end of the season, suggesting that total protein, HM content and methane potential would be higher at the end of the season.

West Bengal had reduced impact of the monsoon; therefore, the biomass was available across the whole year; however, the impact of COVID-19 and collection conditions, resulted in reduced biomass collections. The TSS and TDS increased during monsoon, potentially due to the increase of soil particulates from surface runoff. All WQIs were at elevated levels during spring. Despite the reduced pollution in West Bengal, all tissues had a greater TF for HMs, than the other sites, in particular for Cr and Cd; however, the TF was lower for the nutrients. There appeared to be no phenological trend for the TF of either HMs or nutrients, however, this was likely due to the lack of sampling points. The HM concentration data demonstrated that all tissues had an increased HM content in January, suggesting that as root HM concentration increased, translocation increased. The nutrient concentration was highest in December, this was attributed to the increased horizontal growth that would have occurred from January. The concentration in July would likely be lower than in April or May due to the impact of monsoon. The maximum  $BMP_{th}$  had no obvious trend across the parts; in contrast to the other sites, it did follow an opposing trend to the protein content, however, this again could be due to the lack of sample points. Another contrasting trend was the protein and HM concentration, which both peaked at the

same collection points, in particular within the leaves. This was not found at any of the other sites and could make West Bengal biomass poor choice of feedstock for protein extraction. This demonstrates that a greater number of sites must be studied to understand if this was an anomalous result, or if this is consistent amongst some WH populations.

In comparison with WL, WH had a similar average ash content, nutrient content, HHV<sub>th</sub> and max BMP<sub>th</sub> across all samples, whereas N, protein content and HM content were lower in WH. Both plants would not be ideal feedstocks for combustion or anaerobic digestion, however, have high enough protein to be considered as feedstocks for protein extraction or direct feeding. Despite this, WH and WL are both considered invasive weeds and therefore represent an important resource for bioenergy and bioproducts. WH could be considered the better choice of feedstock based on growth rate and plant density, whereas WL had better characteristics for use in AD and protein extraction.

## Chapter 5.

# Cultivation of water hyacinth

### 5.1. Introduction

Chapter 4 described the variations in composition that can occur in wild WH, detailing the proximate, ultimate and inorganic composition, as well as the different UPIs. In Murchison Bay, biomass was available throughout the year, but was spread across the Murchison Bay, potentially resulting in costly and time-consuming harvesting. In Goyal Para, the biomass was also available across the year, but the biomass did not grow to large size. In Pune, the biomass was only available for half of the year, due to the impact of monsoon on plant populations, but grew to a large size. To ensure a sufficient supply of biomass, cultivation of biomass in tanks could be an option. This would allow a further supply of biomass to supplement the WH that was harvested, with a secondary advantage of reducing HM contamination within the biomass. For large-scale cultivation to be a plausible addition to a biorefinery, it must be possible to estimate the quantity of biomass that could be produced across a range of nutrient and environmental conditions and ensure this biomass is of sufficient quality.

The key objective of this chapter was to investigate the potential for cultivation of WH, and was achieved via the following tasks:

- WH was cultivated to determine the resource availability in a controlled environment.
- Nitrogen loading and source were varied to understand their impact on growth rate and final density.
- The logistic growth model was employed to understand the impacts of temperature and solar irradiance on growth rate and final density.

Initially, the relationship between starting water N-concentration ( $N_0$ ) and absolute growth rate (AGR) was examined, to further the work discussed in 2.2.4. Next, this relationship was studied utilising different nutrient sources, including filtered cow manure, water soluble fertiliser and digestate from AD. These experiments were preliminary trials to inform large-scale trials that further examined the relationship between the  $N_0$  and AGR in a real-world scenario. Secondly, the successful nutrients from the small crate trials, like filtered cow manure, were also used in the large-scale trials. The impacts of nutrient choice on feedstock quality were evaluated through



estimation of the  $BMP_{th}$  and protein content, providing an approximation of expected yields from biomass harvests. Finally, a phenological study of large-scale cultivation was conducted, demonstrating the potential variations across the year. The logistic growth model was employed to predict the intrinsic growth rate and carrying capacity of a WH cultivation tank. The variations in  $BMP_{th}$  and protein content were identified.

#### 5.1.1. COVID-19 impact statement

The impact of COVID-19 was most significant on the work carried out at Defiant Renewables Ltd., India. Firstly, the analysis of water samples during cultivation was restricted to N only. This was due to lack of staff on-site and closure of third-party laboratories. As demonstrated in Chapter 2, this would not diminish the importance of this study: N has been shown to be the predominant growth limiting nutrient for WH. For trial 3, nutrient source in May 2020, see section 5.3, N analysis was not possible due to a local lockdown in Maharashtra.

Secondly, the work carried out by the author was limited due to the reduced time that could be spent in India. Initial small crate and large-scale trials, February-March 2020, were conducted by the author. All further trials were designed by the author. The experiments that were fully conducted by Defiant Renewable staff were: small crate trials 2 and 3; and large-scale nutrient source and phenological trials. Leaf harvests during the seasonal spring trial, see Figure 5.5-1, were reduced due to a local lockdown, therefore, harvesting occurred as often as possible.

The final impact was on the seasonal trials; firstly, the trial conducted in March 2020 had to be cut short; therefore, it was treated as a preliminary trial to inform all future trials. No data has been presented. Secondly, the summer trial was delayed due to a local lockdown in Maharashtra. This resulted in the trial being impacted by the Monsoon.

## 5.2. Impact of nitrogen on growth rate

It has been demonstrated that the water N-concentration is one the primary limiting factors in the growth of WH, see section 2.2.4. Therefore, it is important to understand how N-concentration affects the growth rate of WH. Section 2.2.4 demonstrated that a linear relationship can be seen between water N-concentration and AGR, up to ~30 mg N/L. However, it is unknown whether this relationship can be replicated in a single study, or extended beyond 30 mg N/L.

To examine this relationship, a single nutrient source was selected as a control, cow manure (CM), and compared with a control (no nutrients added), in three small crate trials. In all trials, varying quantities of CM was mixed into 55L of water, see Table 5.2-1. The solubility of N within CM was calculated by determining the starting

theoretical water N-concentration ( $N_{th}$ ) if 100% of the N was solubilised. The  $N_{th}$  was greater than the analysed  $N_o$  due to the poor solubility of CM. The solubilisation was extremely variable, however, there was a general increase in percentage solubilisation as CM quantity was increased. This was unexpected as the quantity increases it would be closer to the saturation limit; however, a saturation limit was not found. CM was collected from a single cow shed throughout the trials; however, due to the multiple collections required, it is possible that, due to the variable nature of CM, the fibre content and the ratio of N containing compounds (e.g.,  $NH_3$ ,  $NH_4^+$ ,  $NO_2^-$  and  $NO_3^-$ ) within the manure varied and thus the solubilisation varied.

All CM samples were analysed for N-concentration, however, only CM from trial 1 was analysed by ICP-OES to determine the NPK ratio. The NPK ratio was 0.22:0.02:0.06, on a dry weight basis, see Appendix C. Assuming that P and K solubilised at the same percentage as N, above 200g of CM, neither P and K would be limiting factors and increased P would be unlikely to impact growth rate [87,88].

**Table 5.2-1:** Nitrogen solubilisation in cow manure growth trials.

Trial No.	Quantity of CM (kg)	$N_{th}$ (mg N/L)	$N_o$ (mg N/L)	Solubilisation
1	0.00	0.0	8.2	0%
	0.05	2.0	9.6	75%
	0.25	9.9	9.8	16%
	0.50	19.8	10.4	11%
	1.00	39.6	12.5	11%
	2.00	79.3	23.6	19%
2	0.00	0.0	2.9	0%
	4.00	149.8	103.5	67%
	8.00	299.6	169.8	56%
	12.00	449.5	255.3	56%
5	0.00	0.0	1.2	0%
	0.25	6.8	4.6	50%
	0.50	13.6	3.7	18%
	0.75	20.5	5.2	20%
	1.00	27.3	7.7	24%
	1.50	40.9	11.1	24%
	2.00	54.5	14.8	25%
	2.50	68.2	19.1	26%
	3.00	81.8	36.7	43%
	3.50	95.5	29.9	30%
4.00	109.1	44.4	40%	

The changes in weight ( $W_t$ ) and nitrogen ( $N_t$ ) are available as a raw dataset [326]. The AGR of Trials 1-3 was plotted against the  $N_o$ , shown in Figure 5.2-1. It is possible to

observe a general positive relationship between the AGR and the  $N_0$  up to  $\sim 15$  mg N/L; from here there were not enough data points to give a conclusive relationship and the level of error increased in the range of 25-50 mg N/L. However, there appears to be a negative correlation as the  $N_0$  increases beyond 25 mg N/L, particularly beyond 50 mg N/L, as shown by trial 2. From this data it is not possible to determine the optimum  $N_0$ . However, it can be assumed that the relationship either plateaus or becomes negative above 25 mg N/L. Therefore, the suggested fit would be a polynomial of order three. However it must be considered that other components in CM could be inhibitory at greater concentrations and further research should be conducted to examine other sources of N.

In contrast to this work, Wilson *et al.* suggested that the relationship was flat below 1 mg N/L, before a rapid increase between  $\sim 1$ -10 mg N/L, and finally a plateau above 10 mg N/L, demonstrating a polynomial fit of order three [81].

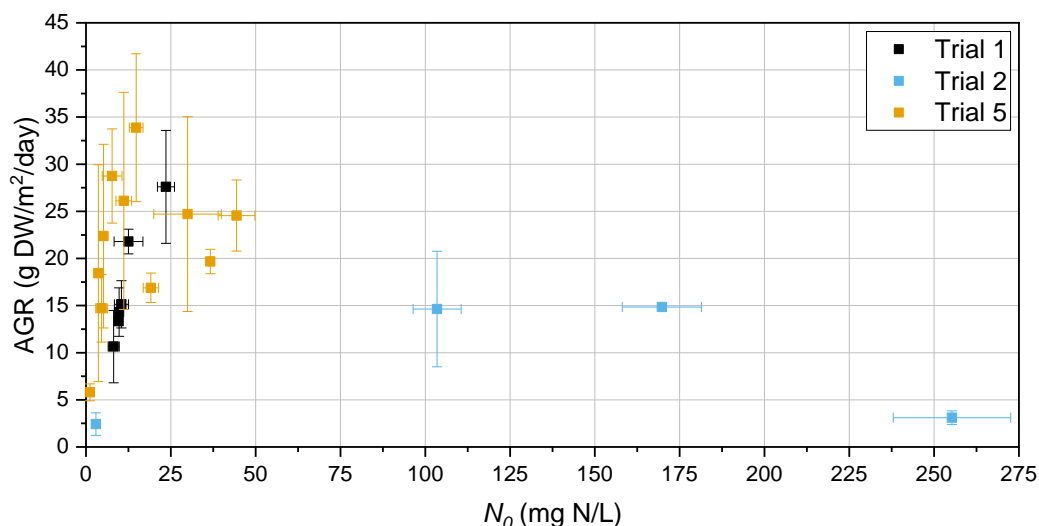


**Figure 5.2-1:** Absolute growth rate, of trial 1, 2 and 5, against starting water nitrogen concentration, with cow manure as the sole nutrient source. The error bars represent the standard deviation of the replications.

The literature review data, presented in section 2.2.4, demonstrated a strong positive linear correlation (LitFit), with a Pearson's  $r$  value (PR) of 0.95. The  $p$ -value was  $<0.05$ , therefore, the relationship was statistically significant, whilst the RSS was 299.95. However, the lack of data points suggests that this could be circumstantial. The trial data (TrialFit) demonstrated that when the  $N_0$  was below 30 mg N/L, there was a weaker correlation, PR of 0.73, yet a stronger fit, RSS of 31.34, see Figure 5.2-2. This demonstrates that there was a strong positive correlation that was statistically significant ( $p$ -value  $<0.05$ ). There was no consideration for the values above 30 mg N/L. The high level of error suggests that this data should be interpreted with caution,

however it is clear there was a positive correlation between  $N_0$  and AGR in the small-scale trials.

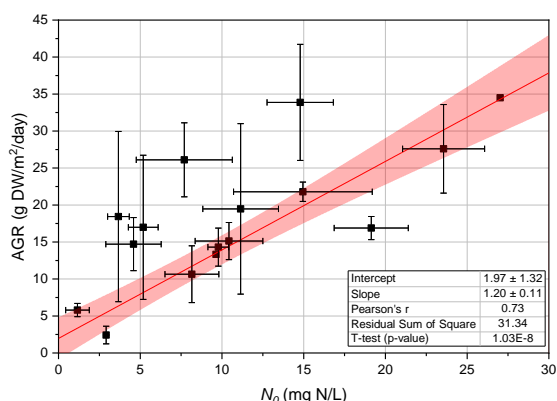


**Figure 5.2-2:** Linear regression for absolute growth rate against starting water nitrogen concentration for small crate trials. The error bars represent the standard deviation of the replications.

The linear regression equations were  $y = 1.75x + 18.43$  for the LitFit and  $y = 1.20x + 1.97$  for the TrialFit. This indicates that the values in literature had a greater AGR at low N values and the AGR increased at a faster rate as the N-concentration increased, as compared with the small crate trials. However, both sets of data suggests that a linear relationship between  $N_0$  and AGR was present below 30 mg N/L. The small crate trials were conducted utilising CM as a nutrient source; however, this relationship could be tested for a variety of different nutrient sources.

### 5.3. Impact of nutrient source on growth rate

Table 5.3-1 displays the nutrient sources utilised in the small crate trials, the N-concentration of the material and information on the collection. Buffalo manure (BM), CM, filtered CM (FCM) and cooked food waste (CFW) were selected because of their ease of access, low cost and relatively high nutrient concentration. Digestate was included to demonstrate the potential for a fully integrated system that would utilise WH, cultivated on digestate, as a feedstock for AD, which produced digestate as a waste product. NPK was used as a comparison against waste products; the cost of NPK suggests it would not be competitive, but it is important to demonstrate the differences between the two.

**Table 5.3-1:** Nutrient source growth trials.

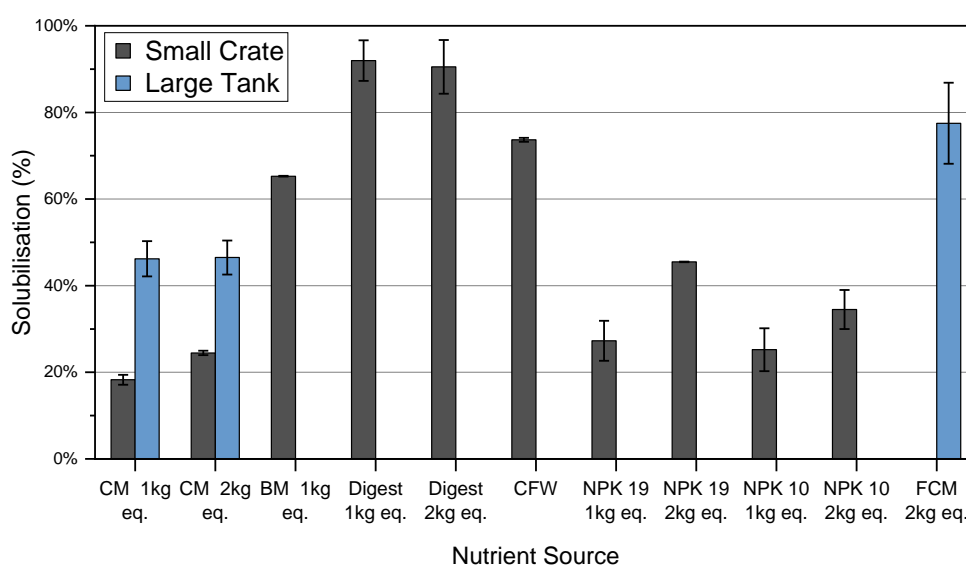
Nutrient Source	Abbreviation	N-Concentration (%)	Collection	Trial No.
Cow Manure	CM	0.23-0.42	Collected from a local cow shed before each trial.	All
Buffalo Manure	BM	0.30	Collected from a local cow shed before trial.	4
Digestate	Digest	0.03	Collected from a 1m <sup>3</sup> Anaerobic Digester fed with 10% KOH treated Water	4
Cooked Food Waste	CFW	1.11	Unknown cooked food waste collected from a local restaurant.	4
NPK (19:19:19)	NPK 19	19.00	Commercially available, water soluble NPK fertiliser. Solubility of 0.3 g/L.	4
NPK (10:26:26)	NPK 10	10.00	Commercially available, water soluble NPK fertiliser. Solubility of 1.0 g/L	4
Filtered Cow Manure	FCM	0.23	CM mixed with 15L of water, passed through a 2mm screen. 36.4% ( $\pm$ 3.85%) of	4

Figure 5.3-1 displays the N solubilisation for the different nutrient sources considered; the amount added, theoretical  $N_0$ , analysed  $N_0$  and solubilisation are shown in Table 5.3-2. Each nutrient source, except for CFW, was added to attain a  $N_{th}$  value of ~45 and ~90 mg N/L or the equivalent of 1 and 2 kg of CM per 55 L (1 kg eq. and 2 kg eq.), in the original trials. CM and NPK had the lowest N solubilisation; CM and NPK achieved higher solubilisation for 2 kg eq. than 1 kg eq., suggesting that the lower solubilisation was not due to saturation of the water. The NPK fertiliser for the 1 kg of CM eq. was added within the solubility limit. However, the 2 kg of CM eq. was greater than the solubility limit for NPK 10:26:26. There was evidence of poor solubilisation from NPK as the water became discoloured and reduced transparency. The solubilisation of N from CM was approximately twice as high in the large tanks compared with the small crates. The improved solubilisation of FCM compared with CM suggests that the fibrous material within the CM impacted the solubility of N. The different solubilisations resulted in variable  $N_0$ .

**Table 5.3-2:** Nitrogen solubilisation in nutrient source growth trials.

Nutrient Source	Amount Added	Theoretical Nitrogen (mg/L)	Analysed N (mg/L)	Solubilisation
Blank	-	-	3.3	-
Cow Manure*	1 kg	33.5	6.7	20.5%
	2 kg	66.9	14.5	22.2%
Buffalo Manure	0.83 kg	45.3	33.2	65.3%
Digestate	7.3 L	44.5	44.5	92.0%
	14.6 L	88.9	84.1	90.5%
Food Waste	0.125 kg	25.1	21.4	73.7%
NPK (19:19:19)	0.013 kg	44.9	15.9	27.3%
	0.026 kg	89.8	44.5	45.5%
NPK (10:26:26)	0.025 kg	45.5	15.1	25.2%
	0.050 kg	90.9	35.0	34.5%
Food Waste	0.125 kg	25.1	21.4	73.7%

\*Average of all nutrient source trials



**Figure 5.3-1:** Average nitrogen solubilisation in small- and large-scale trials, from various nutrient sources. The error bars represent the standard deviation of the replications.

The first nutrient source trial (overall trial three) investigated FCM and NPK 19; however, only theoretical  $N_0$  was available. The  $W_t$  is available as a raw dataset [326]. The  $N_0$  was estimated using the solubilisation values; this was then be plotted against the TrialFit, see Figure 5.3-2. This demonstrates that that FCM produced greater biomass than NPK 19, however, it is possible that higher solubilisation of FCM was responsible for this difference, as suggested by Figure 5.3-1. The AGR increase plateaued from FCM 45 and reduced from NPK 30, again suggesting that the solubilisation was higher than estimated. This initial trial demonstrated that FCM could

be used as a nutrient source, however, without  $N_0$  data, it is circumstantial. NPK 19 appeared to show poorer growth but must be investigated further.

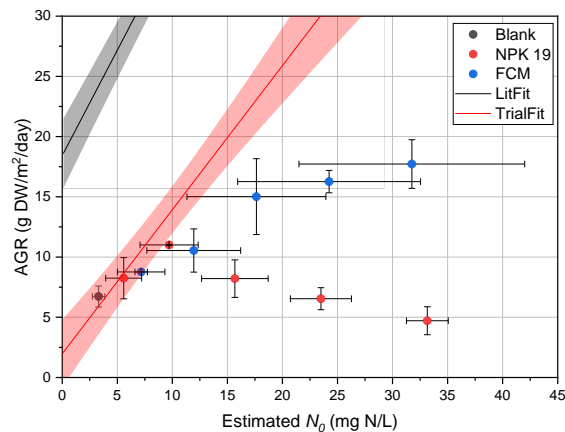


**Figure 5.3-2:** Absolute growth rate of nutrient source, trial three, against starting water nitrogen concentration, overlaid with LitFit and TrialFit. The error bars represent the standard deviation of the replications.

Nutrient source trial two investigated CFW, NPK 19, NPK 10, Digestate and BM. CFW was added at 125g per crate, the equivalent of 560 g of CM, due to limited quantity, whereas NPK19, NPK 10 and digestate were added to equal  $N_{th}$  to 1 and 2 kg CM eq.; BM was added at just 1 kg equivalence.  $W_t$  and  $N_t$  are available as a raw dataset [326].

Figure 5.3-3 shows AGR against  $N_0$ ; all  $N_0$  values below <40 mg N/L demonstrated a good fit with TrialFit, with the exception of CFW. The CFW had a lower AGR than the TrialFit, suggesting that CFW was not a suitable nutrient source. Secondly, the plants showed signs of distress due to drying out during the trial, further exemplifying that CFW would not be a suitable choice.

The digestate AGR did not fit the linear relationship, likely due to a higher solubilisation than CM which resulted in an  $N_0$  above 30 mg N/L. Whilst the AGR was significantly lower than the theoretical maximum, it was higher than what was achieved by Huurman *et al.* [336]. Huurman *et al.* utilised just 0.6 and 1.2L of digestate [336], which resulted in a maximum  $N_{th}$  of 31 and 62 mg/L. The AGR achieved, 8.38 and 9.04 g/m<sup>2</sup>/day [336], would be lower than predicted by the TrialFit, assuming a 90% solubilisation. For the lower  $N_0$ , the AGR would be expected to be almost three times greater. Therefore, to understand the effect of digestate on growth rate, further study should be conducted utilising a range of concentrations. Whilst digestate did not demonstrate improved AGR, likely due to the high  $N_0$ , it was considered further due to its application in an integrated system.

BM was within the expected bounds of the linear relationship, despite a  $N_0$  above 30 mg N/L, however, it showed high levels of variation. BM showed no significant advantages over CM and was therefore discounted for further investigation.

NPK 19 only had one result below 30 mg N/L, which fit within the expected bounds of the linear relationship. The higher N dose had significantly lower AGR, which reinforced the hypothesis that above 30 mg N/L, the impact of  $N_0$  on growth becomes negative. The use of NPK 19 had lower error margins than CM but otherwise demonstrated no advantages and due to the high cost was not investigated in large tanks.

NPK 10 also had just one value below 30 mg N/L; this value was closer to the LitFit than the TrialFit. This suggests that the waste product nutrient sources may limit growth due to low concentration or poor solubilisation of secondary nutrients. The higher N dose was over 30 mg N/L but was within the bounds of the TrialFit if it was extended past 30 mg N/L. Whilst NPK 10 showed a greater AGR than CM, it was not continued to the large tanks due to the high cost.

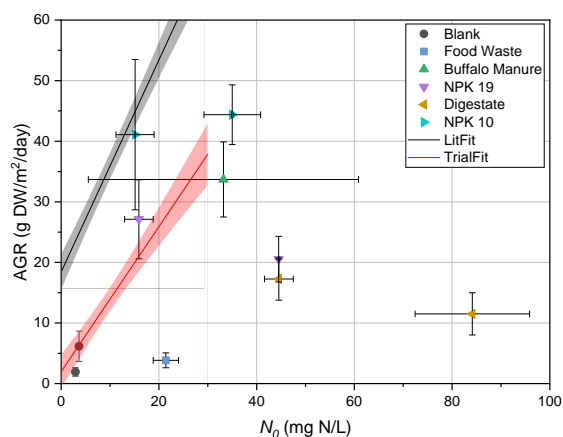


**Figure 5.3-3:** Absolute growth rate against starting water nitrogen concentration for the nutrient source small crate trials, overlaid with LitFit and TrialFit. The error bars represent the standard deviation of the replications.

The LitFit generated a maximum of 25.8 kg FW/m<sup>2</sup>/yr, compared with 13.8 for the TrialFit, at 30 mg N/L. This value was higher than various other crops cultivated in India, see Table 5.3-3. The lower maximum AGR for the TrialFit suggests that the small crates have a lower AGR than what is possible at a larger scale. Therefore, the impact of  $N_0$  on AGR was explored in large tanks. The nutrient sources explored further were CM, as a reference, FCM and digestate. FCM was selected to increase the solubilisation of CM and reduce the impact of viscosity and surface tension: during the original CM trials, crates that contained over 4 kg of CM had high viscosity and surface tension due to the fibrous material present in CM, see Plate 5.3-1. This provided an easy site for mosquito breeding, a serious issue when growing WH at scale or in the wild [337,338]. Digestate was selected to understand the possibility of an integrated system. The system would comprise of an AD system utilising WH as a primary feedstock, producing biogas and digestate. The digestate would be used to cultivate the WH and produce a cyclic system with the end result of biogas and other products.



**Table 5.3-3:** Comparison of growth yields for different cultivated biomasses.

Biomass	Yield (kg FW/m <sup>2</sup> /yr)	
Water Hyacinth	LitFit	25.8
	TrialFit	13.8
Lentils, dry <sup>1</sup>	0.09	
Soya beans <sup>1</sup>	0.10	
Maize (corn) <sup>1</sup>	0.32	
Wheat <sup>1</sup>	0.35	
Rice <sup>1</sup>	0.42	
Potatoes <sup>1</sup>	2.41	
Sugar cane <sup>1</sup>	7.86	

<sup>1</sup>FAOSTAT (2022), for cultivation in India [339]

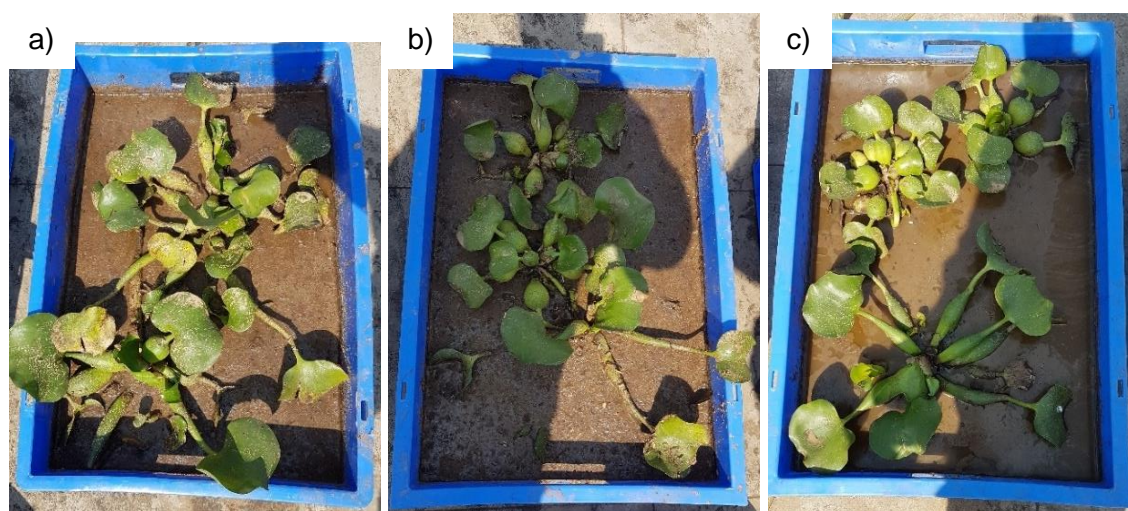


**Plate 5.3-1:** Evidence of the increased viscosity and surface tension from high dose cow manure trials. a) 4 kg b) 8 kg c) 12 kg.

#### 5.4. Large-scale cultivation

The reference nutrient source, CM, was utilised to vary  $N_0$  and investigate the impact on AGR in 350 L tanks. The trial was conducted in spring 2021; two tanks were fed with 12.7 kg of CM (the equivalent of 2 kg in the small crates) two tanks with 6.35 kg of CM, and two used as a tap water control. CM was added at day 1 and the trial was conducted for 14 days.  $W_t$  and  $N_t$  are available as a raw dataset [326]. Figure 5.3-1 shows that the solubilisation of N was much greater in the tanks compared with the small crates which resulted in a higher than predicted  $N_0$ . Figure 5.4-1 displays the AGR of the LitFit, TrialFit and the small crate  $N_0$  trials, Figure 5.2-2, overlaid with the results from the large tank. This demonstrates that the control and 6.35 kg CM fed tank had a higher AGR than predicted by the TrialFit but lower than the LitFit. However, both were within reasonable bounds of the trial data. The 12.7 kg CM fed tank was over the 30 mg N/L limit for the fit, however, if the fit was extended, it was within the 95%

confidence for the TrialFit, similar to what was seen with BM and NPK 10 in Figure 5.3-3, suggesting the trend could be extended. Despite the  $N_0$  of the 6.35 kg tanks being almost half the value of the 12.7 kg variation, the AGR shows only slight difference, 6.4% lower, suggesting that the growth had been affected by a higher  $N_0$ . This implies that the large tanks may not align with the TrialFit or the small crates.

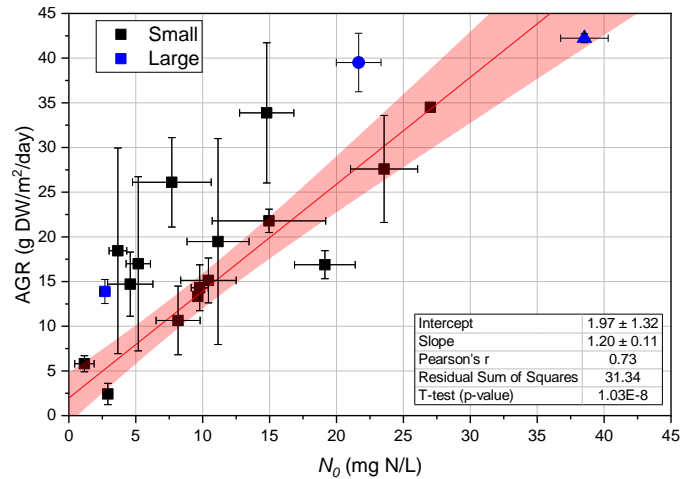


**Figure 5.4-1:** Absolute growth rate against starting water nitrogen concentration for the  $N_0$  trials, overlaid with large tanks trials, LitFit and TrialFit. The error bars represent the standard deviation of the replications. ■ = control; ● = 6.35 kg tank; ▲ = 12.7 kg tank; all black symbols = small crate trials.

Digestate and FCM were used as nutrient sources, in the large tanks, to demonstrate their potential for large scale growth. Digestate and FCM were cultivated during different seasons, so are not directly comparable; however, they are comparable with the CM control (12.7 kg).

FCM had a higher solubilisation than CM, therefore, the  $N_0$  was higher than CM. However, there was little variation in the AGR, see Figure 5.4-2. This suggests that either not all the N was bio-available, and therefore did not have a negative impact on AGR, or the reduction of fibrous material improved the growth rate. The reduction of fibrous material resulted in a lower viscosity and surface tension. Secondly, at the end of the trial, the fibrous material from the CM must be removed from the base of the tank, this would become problem over a year of cultivation; however, for the FCM this was not necessary, as the residue was reduced by filtering. This suggests that FCM would be a possible option for a nutrient source to cultivate WH at scale.

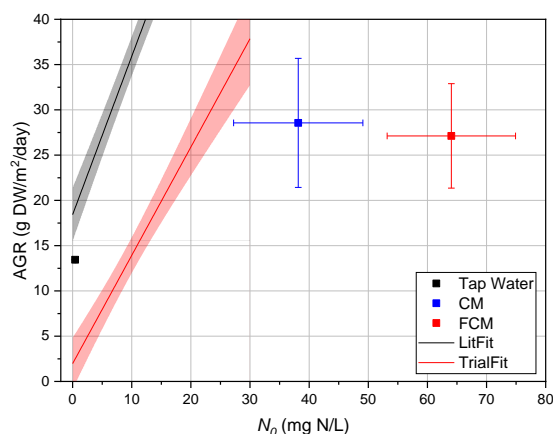


**Figure 5.4-2:** Absolute growth rate against starting water nitrogen concentration for the FCM and CM large tank trial, overlaid with LitFit and TrialFit. The error bars represent the standard deviation of the replications.

Digestate also had a higher solubilisation than CM, which resulted in a  $N_0$  over twice CM and FCM. The  $N_0$  was over four times higher 30 mg N/L, yet the AGR was equivalent to 22 mg N/L in the TrialFit. This suggests that the negative impact of an excessive  $N_0$  was not as great in the large tanks as compared with the small crates. The CM reference had a higher  $N_0$ , 61.5 mg N/L, than the maximum for the linear fits, 30 mg N/L; as with the digestate, the AGR was higher than the maximum predicted by the TrialFit. This does not lend weight to either argument about impact of excessive  $N_0$  or reduced fibre content as digestate would also have reduced fibrous material as compared with CM.

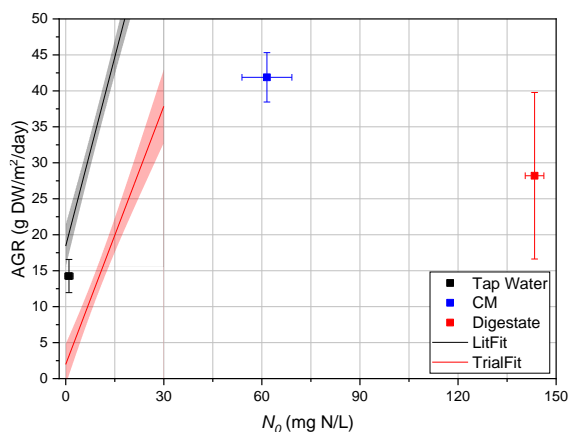


**Figure 5.4-3:** Absolute growth rate against starting water nitrogen concentration for the digestate and CM large tank trial, overlaid with LitFit and TrialFit. The error bars represent the standard deviation of the replications.

The relationship between AGR and  $N_0$  is important for mass cultivation; it is also important to understand the impacts on the utilisation of the biomass. The key UPIs considered were protein content, determined by tissue N-content, and theoretical BMP, determined via proximate and ultimate composition, as well as BI. These UPIs will inform the potential for an integrated biorefinery.

## 5.5. Impact of nitrogen and nutrient source on utilisation potential indicators

It has been shown that there was a positive correlation between tissue protein content and  $N_0$ , due to the positive correlation between nutrient concentration in the water and the uptake rate of nutrients by the plant [80,81], and between the  $N_0$  and the N-content of the leaves [87,99]. Therefore, it is important to understand if this will affect will impact the utilisation of the plant. Firstly, the tissue N-content ( $C_t$ ), where  $C$  was tissue N-content and  $t$  was time in days, and subsequently the protein concentration, was estimated across a single trial. Three leaves were harvested every 4 days, where possible, during the spring tank trial. Secondly, to understand the variation in protein across the cultivation season, biomass was harvested at the end of all large tank trials, and the end harvest tissue N-content ( $C_N$ ) was analysed.

$W_t$  and  $N_t$  for the leaf harvest trial are available as a raw dataset [326]. The trial lasted for 39 days, with CM added every ~14 days. The  $W_t$  demonstrated that the growth in tanks fed with CM were similar despite  $N_t$ , the 12.7 kg tanks reached approximately twice the value that was present in the 6.35 kg tanks. However, Figure 5.5-1a demonstrates that the higher CM dose resulted in a higher  $C_t$ . The results show that there was an increase in  $C_t$  with time, this suggests that as  $N_t$  increased, due to CM additions,  $C_t$  followed suit. These results support the theory of a positive correlation between water and plant tissue N-content [87,99].

The protein content was estimated, utilising the conversion factor of 4.64, and displayed in Figure 5.5-1b. Over the course of the trial, the protein content of the leaves was increased by 4.4, 6.9 and 8.3%, for the tap water control, 6.35 kg and 12.7 kg, respectively. This increase predominantly occurred from day 20; this suggests that a significant lag occurs between the addition of nutrients before the leaves increase in protein content. The protein content of the 12.7 kg tanks continued to increase up to the end of the trial, suggesting that it could increase further if left to grow. These considerations must be considered if cultivating WH for the production of protein. The maximum protein content (17.8%) was lower than for all of the river sites, but higher than the average for Goyal Para and all Uganda sites.

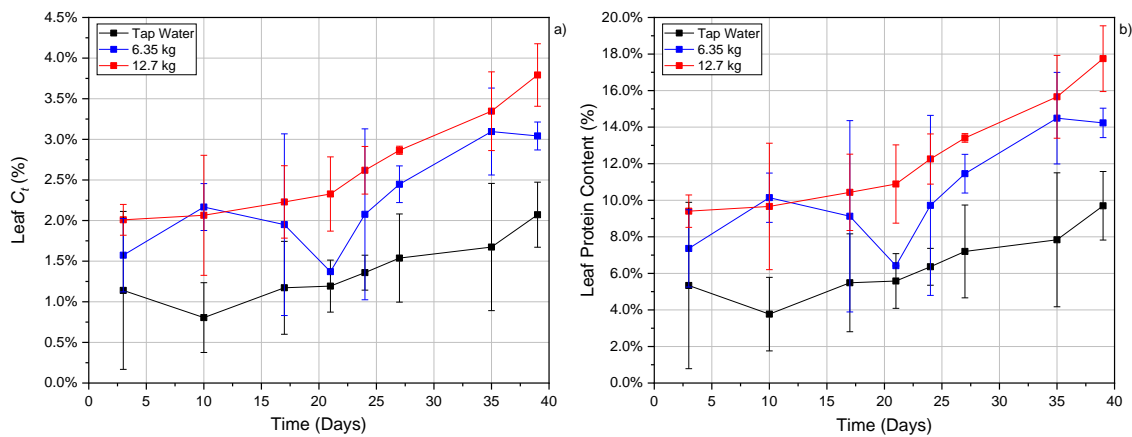


**Figure 5.5-1:** Change in leaf tissue nitrogen and protein content with respect to time for the variable cow manure trial. The error bars represent the standard deviation of the replications. a) nitrogen; b) protein.

Figure 5.5-2 depicts the differences in  $C_N$  for FCM, digestate, CM and control tanks. FCM produced a similar AGR to CM, however, the whole plant and leaf  $C_N$  was higher for FCM, Figure 5.5-2a. This is likely due to the higher  $N_t$  in the FCM tanks, similar to what was demonstrated in Figure 5.5-1. The protein content of the leaves and whole plant, from the FCM tanks, was approximately 15.8 and 14.6%, respectively. This was lower than what could be achieved: Wolverton and McDonald determined a leaf and whole plant protein 24.4 and 17.4%, in WH cultivated in sewage wastewaters [48]. This may have been due to environmental impacts or plant density.

The protein content from FCM was under half the estimated protein content of soybean, a commercially available protein extraction feedstock [141]. Soybean produces a protein extract of 65-70% crude protein; whereas for WH, it would be possible to produce a protein concentrate containing approximately 39 and 36% protein, via the method described by Hontiveros and Serrano Jr [212]. This was lower than soybean protein extract, but would be an acceptable protein supplement for animal feed [212]. However, this would be dependent on the HM content of the extract. This would be a significant advantage of cultivated biomass over the collection of wild biomass: the nutrients added to the cultivation tanks would be likely to have a lower concentration of toxic compounds than the natural environment.

Figure 5.5-2b shows the  $C_N$  for the CM and digestate trial. In previous analysis,  $N_0$  has been a significant factor in the final plant  $C_N$ ; however, this was not the case for the digestate tank: whilst the  $N_0$  was over twice that of CM, the final plant  $C_N$  was >1% lower for both the whole and leaf tissue. Further investigation would be required to determine the cause of the low  $C_N$ ; however, it can be suggested that this result makes digestate a poor choice of nutrient source when considering the production of feed additive or protein concentrate.

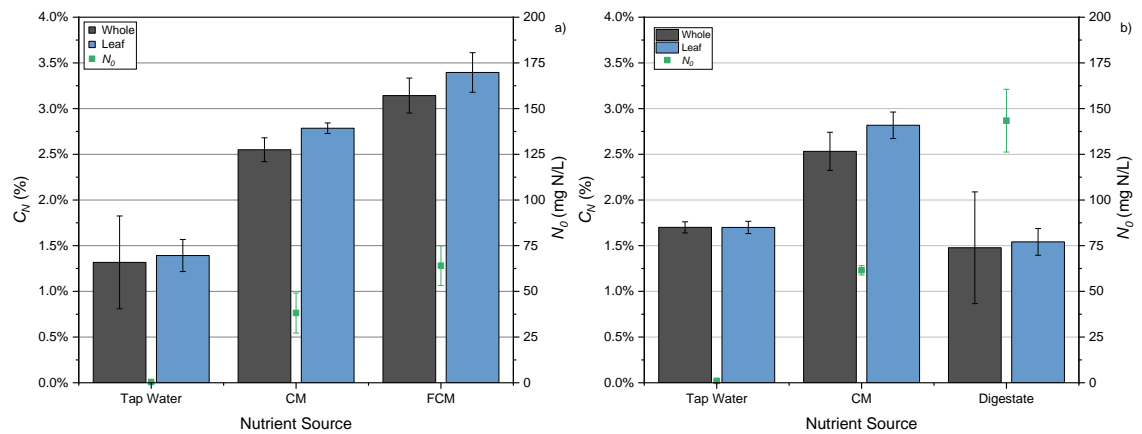


**Figure 5.5-2:** Leaf and whole plant nitrogen concentration and starting water nitrogen concentration for digestate and filtered cow manure large tank trials. The error bars represent the standard deviation of the replications. a) filtered cow manure trial; b) digestate trial.

The results of the max  $BMP_{th}$  and  $BMP_{th}$  are displayed in Figure 5.5-3. The  $BMP_{th}$  was calculated using a BI of 25.3 and 28.8% for the FCM and digestate, respectively; this was based off the  $BMP_{ex}$  for the CM plants described in section 5.6. The CM and FCM showed little variation, suggesting that the increased nutrient loading had little impact on the  $BMP_{th}$ . The digestate had a lower  $BMP_{th}$  than the control and CM tanks, predominantly due to a low H concentration. The results of  $BMP_{th}$  were similar to experimental results for untreated WH, as demonstrated by Brown *et al.*, who showed a biomethane yield of 103 mL  $CH_4/g$  VS [139]. However, it demonstrated that both the control tank and CM tank had variation between trials, this was investigated further in the phenological study.

The optimal C:N ratio of an anaerobic digester, utilising WH, is approximately 32.1 [312]. The end biomass results for all nutrient dosed tanks had a C:N ratio of below 15, suggesting that the  $BMP_{ex}$  may be less than the  $BMP_{th}$ , due to the high  $C_N$  of the biomass. The control tanks had an average C:N ratio of 25.1, therefore, when targeting biomass for anaerobic digestion, using low N dosed water, or removing leaves, or co-digestion, may increase biogas production.

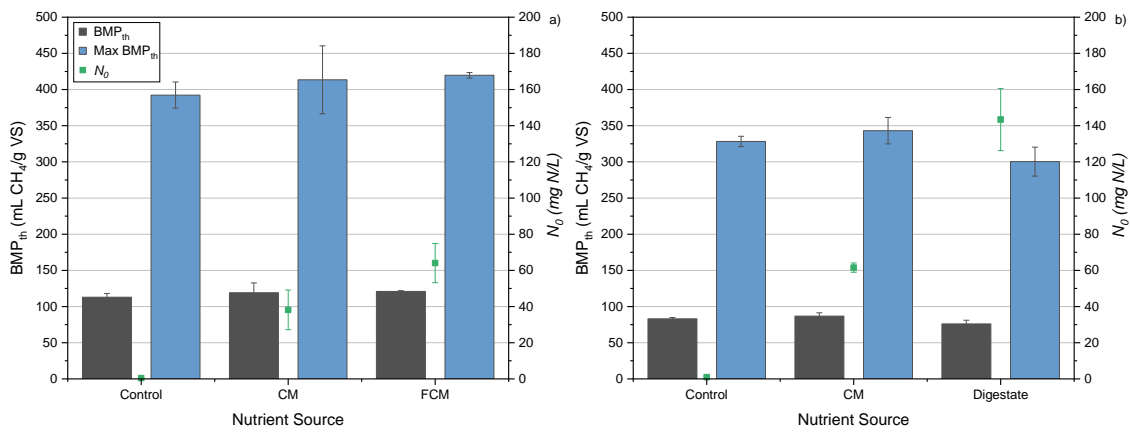


**Figure 5.5-3:** Biomethane potential and starting water nitrogen concentration for digestate and filtered cow manure large tank trials. The error bars represent the standard deviation of the replications. a) filtered cow manure trial; b) digestate trial.

The results shown here were discussed independently of phenological variations, like changes in temperature, cloud cover or solar irradiance. This is an important factor, as demonstrated in Chapter 4, and would have an impact on AGR and plant composition.

## 5.6. Phenological study

### 5.6.1. Impact of the rain shelter

As discussed in section 3.2.3.1, a rain shelter was constructed to protect the plants and trials from monsoon rain. The impact of the rain shelter was examined by comparing solar irradiance with and without the shelter, as well as comparing trials conducted in the spring of 2020 and 2021.

The trials are described in Table 5.6-1; this demonstrates that the tank with no rain shelter had a higher AGR. The  $N_0$  and average solar irradiance were marginally higher for the trial with no rain shelter, which may have increased the AGR. However, the temperature was higher during the rain shelter trial, this is likely to have had the largest impact on growth rate, suggesting that the rain shelter had an impact on growth rate.

**Table 5.6-1:** Impact of rain shelter on absolute growth rate in large tank trials.

Description	$N_0$ (mg/L)	AGR (g DW/m <sup>2</sup> /day)	Solar Irradiance (kWh/m <sup>2</sup> /day)	Temperature (°C)
No Rain shelter	3.17	14.3	6.3	22.2
Rain shelter	2.69	12.8	6.1	24.1

<sup>1</sup>NASA (2022) [73]

Solar irradiance data was collected at four different times of the day, between 15/06/2021-09/07/2021, to determine the difference between the irradiance inside and outside the rain shelter structure. The reduction in irradiance ranged from 11-75%, see

Figure 5.6-1; despite this variation, all data points from under the rain shelter were lower than outside of the rain shelter.

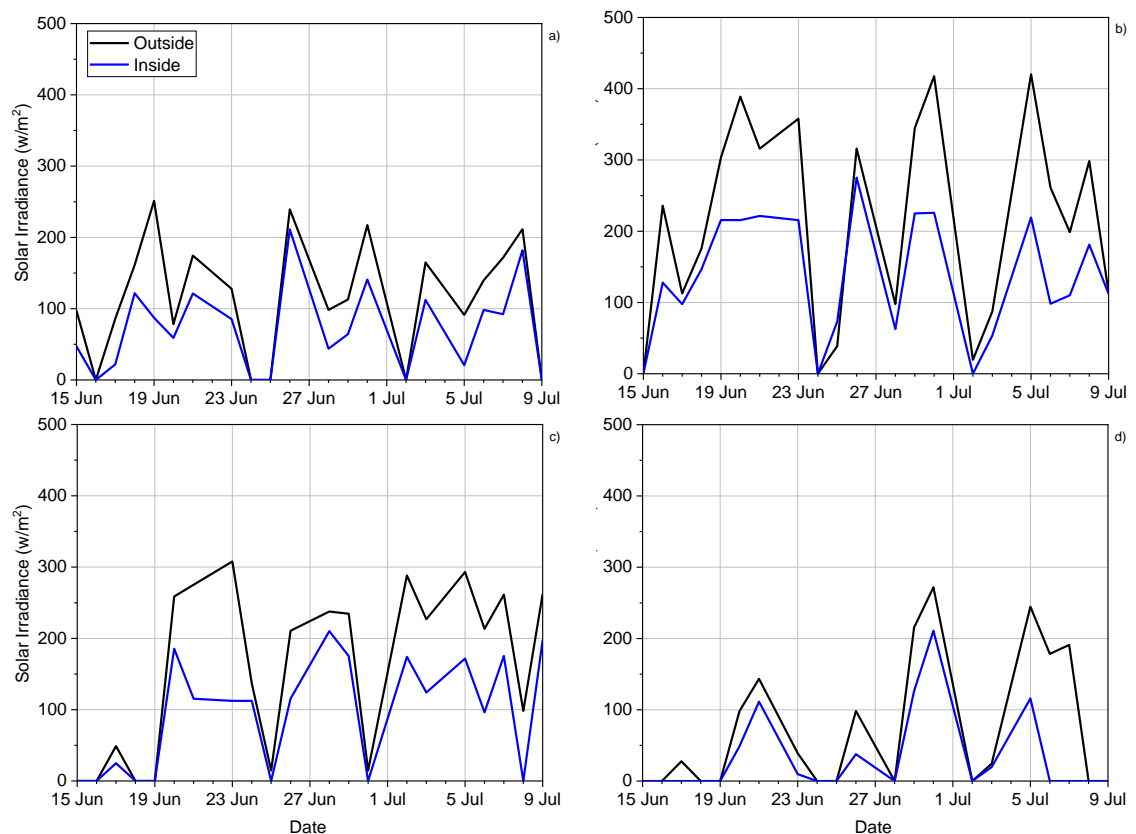


**Figure 5.6-1:** Solar irradiance inside and outside of the rain shelter from 15/06-09/07/2021. a) 1000; b) 1200; c) 1500; d) 1800.

It was not possible to quantify the impact of the rain shelter on AGR, due to the variations in nutrient and environmental conditions. However, it can be assumed that the rain shelter reduced the solar irradiance, as shown by the difference in measured solar irradiance; therefore, the AGR may have been affected. It is also possible that the temperature would be reduced, this could reduce evapotranspiration and potentially translocation of nutrients. These factors were not considered when calculating biomass availability as a cultivation tank would likely require protection during monsoon months and a permanent structure was the solution selected. Other options should be investigated further to reduce the impact on AGR.

### 5.6.2. Variations in growth rate

The phenological study consisted of four trials across the year, separated into each season: spring, summer, autumn (monsoon) and winter. Each trial consisted of four 350L tanks, two containing tap water (control) and two fed with 12.7 kg of cow manure (fertilised), the equivalent of 2 kg in small crates. Nutrients were added every two weeks, as predicted by the N removal and reduction in AGR shown in small crate trials



and preliminary tank trials, spring 2020, which occurred after 12-14 days. The trials were conducted for six weeks and therefore included three nutrient additions. All trials were covered by the rain shelter, the likely scenario for an integrated system.

The details for all the seasonal trials are described in Table 5.6-2 and Figure 5.6-2. The addition of CM resulted in variable  $N_0$ , see Table 5.6-2, and  $N_t$ , the raw dataset is available [326]. Both summer and winter had an  $N_0$  approximately twice the value of spring and monsoon. This suggests that these trials would have had a growth reduction due to high  $N_0$ , as seen in Figure 5.4-1. However, tank 2 for monsoon had a higher  $N_3$  than  $N_0$ , suggesting that the N had a delayed solubilisation; this could impact AGR.

The winter trial had high temperature variations, as well as the lowest average temperature, suggesting that the AGR was impeded. Imaoka and Teranishi determined specific growth rate via Equation 5-1 [80], where  $S_g$  was specific growth rate ( $\text{day}^{-1}$ ), and  $T$  was temperature. The  $k$  was then utilised to determine growth rate via Equation 5-2, where  $W_t$  was biomass weight at time  $t$  ( $\text{g}/\text{m}^2$ ).

**Equation 5-1:** Specific growth rate as a factor of temperature [80].

$$S_g = 0.063 (1.087)^{T-20}$$

**Equation 5-2:** Changes in weight by time as a function of specific growth rate [80].

$$\frac{dW_t}{dt} = S_g W_t$$

Assuming this would be applicable to the large tank trials conducted here, by applying this factor to the growth rate, utilising the average temperature, would suggest that the winter trial would have a reduced growth rate of 24, 36 and 33% when compared with monsoon, spring and summer, respectively. No trial had an average daily temperature of greater than 30°C, however, the hourly temperatures peaked at 39.1, 32.7, 29.8 and 29.7°C for spring, summer, monsoon and winter, respectively [80]. This suggests that the growth rate during summer, monsoon and winter was not impacted by high temperatures [78,80,81]. However, five days in the spring trial had temperatures over 37°C, with an average of over 4 hours at this temperature [80]; this suggests the growth rate would have been impacted over this time period. There was no applicable literature to determine the effect of the reduction in solar irradiance, however, due to the relationship between temperature and solar irradiance it was assumed that the effect may overlap.

The summer trial was affected by the onset of monsoon rains: after 14 days the average solar irradiance was 5.78 kWh/m<sup>2</sup>/day and the air temperature was 26.59 °C. However, this was reduced as the trial progressed to 4.24 kWh/m<sup>2</sup>/day and 24.17°C, for the final two weeks, due to the increased cloud cover and rain. The reduction in

temperature suggests a decrease in specific growth rate by 19%, for the first two weeks compared with the final two weeks [80]. The opposite occurred during the monsoon trial: the monsoon rains occurred early in 2020, which led to early receding of monsoon rains compared with preceding years. The solar irradiance and air temperature did not have a consistent rise but showed greater peaks and troughs due to the variable weather experienced during- and post-monsoon.

**Table 5.6-2:** Environmental conditions and starting water nitrogen concentration for phenological study trials.

Season	Dates	Solar Irradiance (kWh/m <sup>2</sup> /day)*	Temperature (°C)*	N <sub>0</sub> (mg N/L)	
				Control	Fertilised
Monsoon	24/08/2020-05/10/2020	4.03	23.85	0.43	38.16
Winter	07/12/2020-18/01/2021	4.20	20.63	2.29	60.40
Spring	19/02/2021-01/04/2021	6.21	26.06	2.69	38.53
Summer	21/05/2021-02/07/2021	4.64	25.42	0.99	61.54

\*Raw data was taken from NASA Prediction Of Worldwide Energy Resources [73].

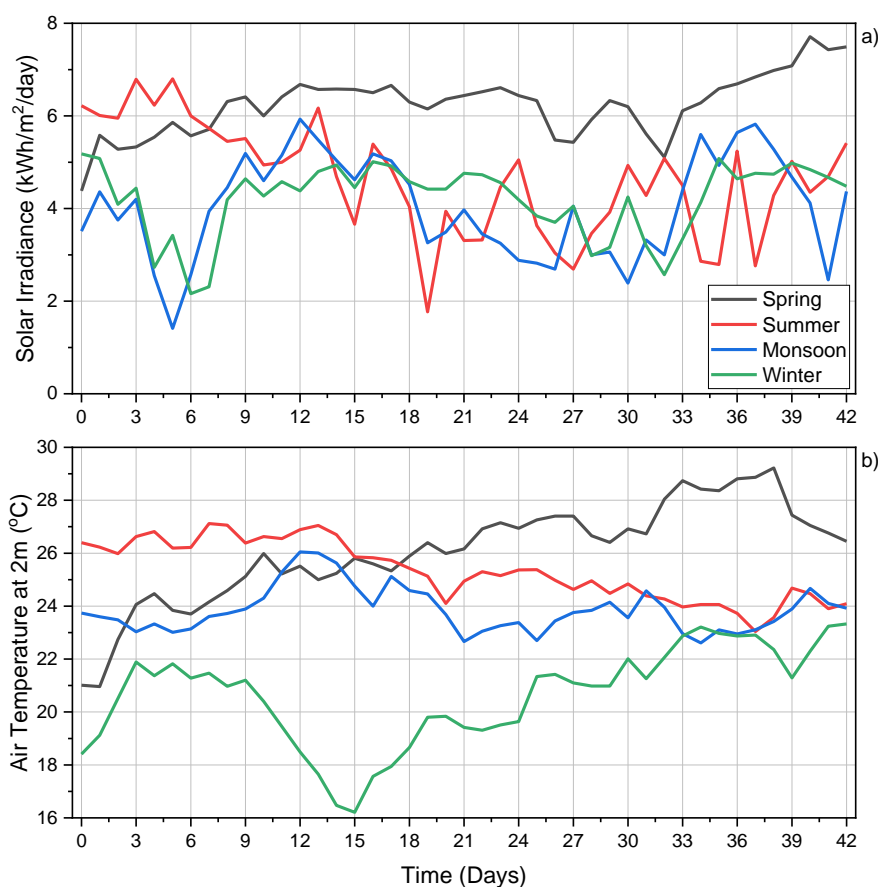


**Figure 5.6-2:** Environmental conditions data for phenological study trials- a) solar irradiance; b) air temperature at 2m. Raw data was taken from NASA Prediction Of Worldwide Energy Resources [73].

### 5.6.2.1. Control

The control tanks contained minimal nutrient addition and therefore were utilised as a basic method for normalisation of  $N_0$ . Figure 5.6-3 shows that there was minimal difference between final weight in three of the trials (summer, spring and monsoon). There was an error in weighing during the spring trial that resulted in the appearance of a large increase from day 20-21, this showed an apparent high growth rate during the second 14-day period and low growth during the final 14-day period. All trials showed similar growth during the first 14 days before the winter trial showed lower growth rate and diverged. The winter trial had a reduced final weight by 9, 13 and 17%, in respect to spring, summer and monsoon, respectively; based on the calculations determining impact of temperature on growth rate, from Equation 5-1 and Equation 5-2, this suggests that the average temperature was not the only factor affecting the weight variations.

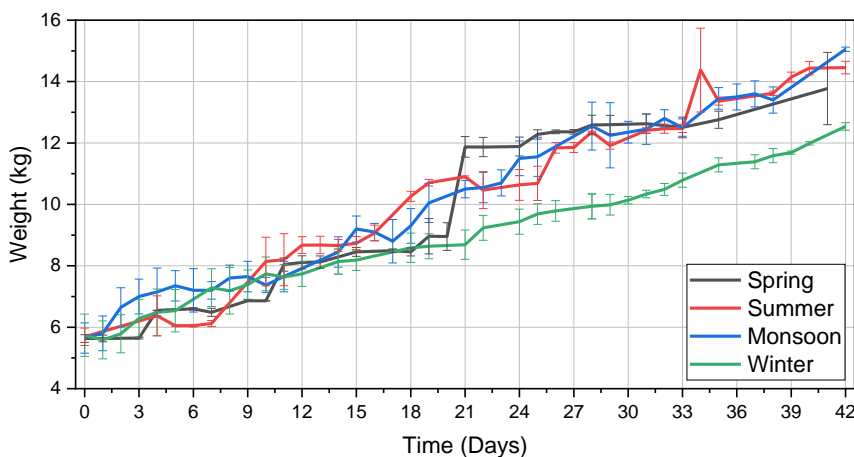


**Figure 5.6-3:** Weight changes over time for control tanks in the large tank phenological trials. The error bars represent the standard deviation of the replications.

### 5.6.2.2. Fertilised

The fertilised tanks had large variations in  $N_0$  due to the natural variations that occur with CM and the subsequent variation in solubilisation. Figure 5.6-4 shows  $W_t$  of the fertilised tanks for each season. The summer trial reached higher weight than the rest of the seasons. In contrast to the control tanks, there was minimal difference between monsoon, winter and spring trials. The increase in the growth of the winter and summer trials could be due to the higher  $N_0$ , compared to spring and monsoon, see Table 5.6-2. This suggests that an  $N_0$  of 60 mg N/L improved the growth rate, in contrast to the results stated in previous sections and that suggested by literature [80,81].

The monsoon trial also showed increased growth, compared with what was expected from the control tanks, suggesting that the delayed solubilisation meant that the value stated for  $N_0$  was not representative of the available N. Whilst the weighing error

present in the control tanks was not as obvious in the fertilised spring trial, the weight remained constant from day 16-28, this was due to the weighing error.

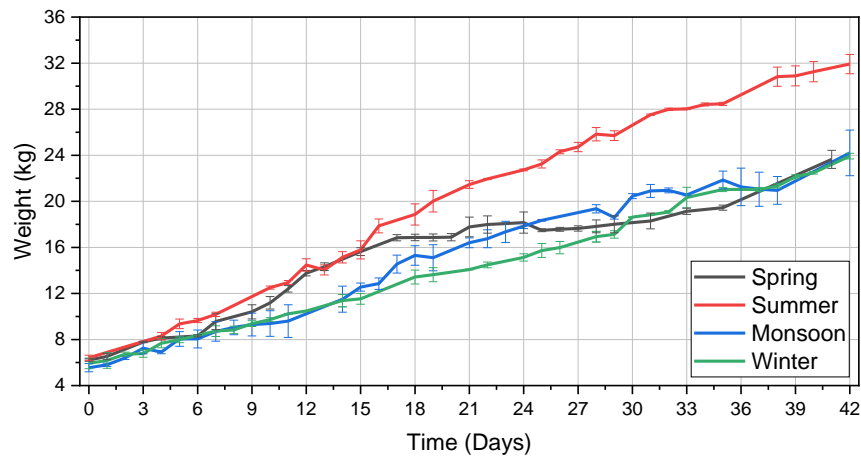


**Figure 5.6-4:** Weight changes over time for fertilised tanks in the large tank phenological trials. The error bars represent the standard deviation of the replications.

### 5.6.3. Logistic Growth Model

The analysis of WH populations via AGR produces a disparity due to the difference in weight; this disparity can produce similar growth rates despite different percentage increases. For example, Polomski *et al.* suggests that WH and WL produced similar increases in weight as total N supplied was increased [169]; however, WH had a percentage weight increase of ~71% compared with WL which increased by ~266%. Therefore, initial weight should be considered to compare growth rates of different populations. One method is the utilisation of the intrinsic growth rate: the intrinsic growth rate incorporates initial plant weight into the value, producing a unit of g/g/day [81].

To describe the different populations of WH, the logistic growth model, Equation 5-3, was used, where  $r$  was intrinsic growth rate (g/g/day),  $P$  was density (g DW/m<sup>2</sup>),  $k$  was carrying capacity (g/m<sup>2</sup>) and  $t$  was time (days). This differs from Imaoka and Teranishi, Equation 5-2, by introducing the carrying capacity as a limiting factor in growth rate [80]. The reduction of  $r$  in relation to  $k$  is important to the analysis of a populations growth and has been shown to be linear in WH [80,81].

**Equation 5-3:** Logistic growth model [81].

$$\frac{dP}{dt} = r \cdot P \cdot \left(1 - \frac{P}{k}\right)$$

Actual  $r$  and  $k$  values vary between studies: Wilson *et al.* demonstrated that literature values can vary from 0.005- 0.118 g/g/day (FW) and 640- 5310 g DW/m<sup>2</sup>, for  $r$  and  $k$  respectively. The value of  $k$  was maintained throughout the analysis of  $r$ .  $P$  was determined by converting wet biomass weight to dry, assuming a water content of 95%,

as determined by analysis from stock material. This value was different to that used by Wilson *et al.*, though it does fit within the range suggested by literature, 90.5-95.0% [42,48,52–54]. The fit of the model was maximised for each trial by solving for  $r$  to minimise the RSS, an example is depicted in Figure 5.6-5.

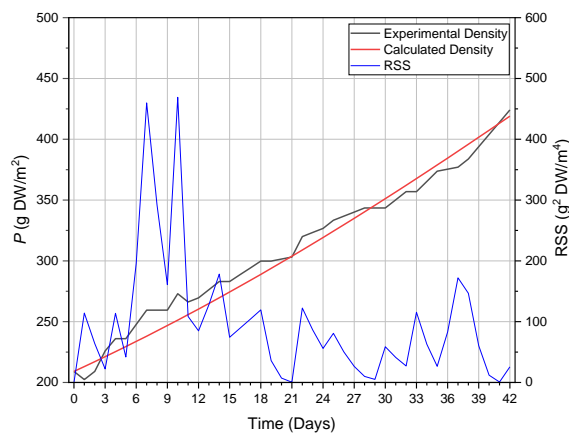


**Figure 5.6-5:** Changes in experimental and calculated density ( $P$ ) and residual sum of squares (RSS) for an example of logistic growth model fit for large scale winter trial control tank 1.

#### 5.6.3.1. Carrying capacity ( $k$ )

It is likely that  $k$  would be impacted by all environmental conditions, including  $N_0$ ,  $N_t$  and temperature, however, this model assumes a constant  $k$  value. The fit of the logistic growth model would be impacted by forcing  $k$  to remain constant. It is not possible to solve the equation with a varying  $k$ , as this will remove the comparability of the different  $r$  values. However, it possible to vary  $k$  multiple times whilst remaining constant across all the trials to understand the impact of  $k$  on  $r$ .

The value of  $k$  in literature varied from 640-5310 g DW/m<sup>2</sup> (average of 2570 g DW/m<sup>2</sup>), see section 2.2.5. One example of a parameter affecting  $k$ , was described by Mitsch, where giant WH reached 2500 g DW/m<sup>2</sup>, whereas, dwarf/small plants reached 640 g DW/m<sup>2</sup> [106]. The appearance of different clones has been shown to be dependent on waterbody, giant clones appear in fast moving and well aerated water compared to dwarf clones that are more common in the fringes of large mats [23]. This suggests that poor growth conditions can result in the growth of smaller clones. The plants utilised in large tanks were taken from Indrayani River as giant clones, however, storage in stock tanks resulted in changes to morphology, including longer roots and shorter petioles, which are characteristics of smaller clones [58]. Therefore, it is possible that a lower  $k$  value would be more appropriate for tank cultivation.

The results of the logistic growth model are described in Table 5.6-3, \*Fresh weight

Table 5.6-4 and Figure 5.6-6. The lower  $k$  value resulted in a greater  $r$  for the control tanks and a better fit than utilising the averaged literature value. However, the fertilised tanks had a poor fit for winter and summer, but a better fit for spring and monsoon. The size of the plants from the different trials was not measured and it is therefore impossible to determine the clonal variety present in the tanks. However, it is possible to conclude that the  $k$  value was impacted by the poor growing conditions of a cultivation tank. This was likely due to the lack of flowing water to replenish nutrients.

**Table 5.6-3:** Intrinsic growth rate of the phenological study large tank trial with a carrying capacity of 640 kg DW/ m<sup>2</sup>.

Season	Reference	$r$ (g/g/day)*		RSS (g <sup>2</sup> DW/m <sup>4</sup> )	
		Average	Standard Deviation	Average	Standard Deviation
Spring	Control	0.048	0.003	26,378	11,368
	Fertilised	0.137	0.003	129,030	22,081
Summer	Control	0.049	0.003	9,155	2,762
	Fertilised	0.183	0.008	1,962,468	148,957
Monsoon	Control	0.049	0.001	6,909	1,462
	Fertilised	0.127	0.012	202,704	143,470
Winter	Control	0.035	0.005	2,870	137
	Fertilised	0.103	0.001	173,404	7,451

\*Fresh weight

**Table 5.6-4:** Intrinsic growth rate of the phenological study large tank trial with a carrying capacity of 2,569 kg DW/ m<sup>2</sup>.

Season	Reference	$r$ (g/g/day)*		RSS (g <sup>2</sup> DW/m <sup>4</sup> )	
		Average	Standard Deviation	Average	Standard Deviation
Spring	Control	0.028	0.002	46,394	19,249
	Fertilised	0.043	0.001	344,507	17,537
Summer	Control	0.028	0.002	25,031	1,791
	Fertilised	0.057	0.002	343,190	42,110
Monsoon	Control	0.029	0.002	23,934	2,866
	Fertilised	0.047	0.001	255,954	170,664
Winter	Control	0.022	0.004	6,517	1,117
	Fertilised	0.043	0.002	51,542	4,475

\*Fresh weight

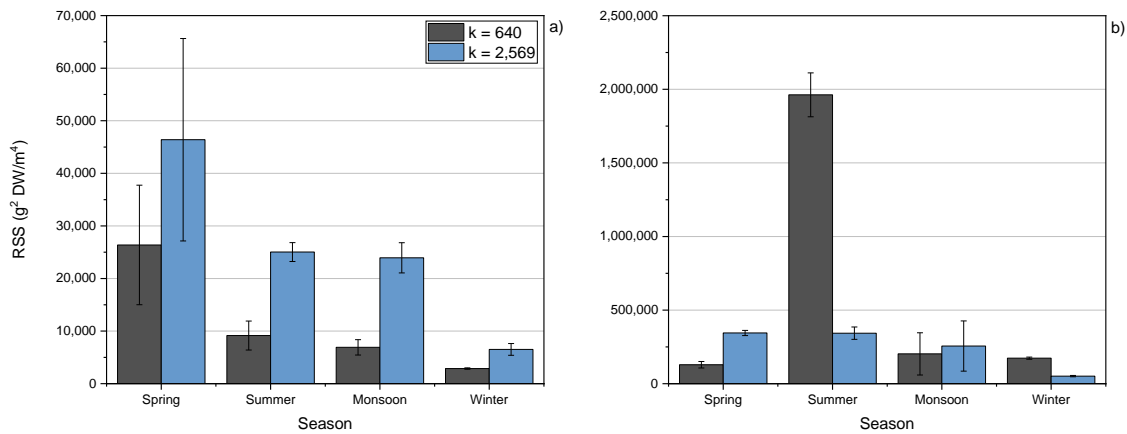


**Figure 5.6-6:** Residual sum of squares (RSS) for intrinsic growth rate of the phenological study large tank trial with a carrying capacity of 640 and 2,569 g DW/ m<sup>2</sup>. The error bars represent the standard deviation of the replications. a) control; b) fertilised.

The varying  $k$  value has shown that the literature averaged  $k$  was not the optimal fit for the large tank trials. Therefore, by altering the  $k$  it was possible to determine the optimum value for these trials; Figure 5.6-7 shows the logistic growth model results, solved to minimise total RSS, as a combination of all the trials (all seasons and all  $N$  doses combined). This suggests that the optimum value for  $k$  was approximately 1000 g DW/m<sup>2</sup>, to maximise the fit for all the trials. However, this does not mean each trial or tank had a maximised model fit.

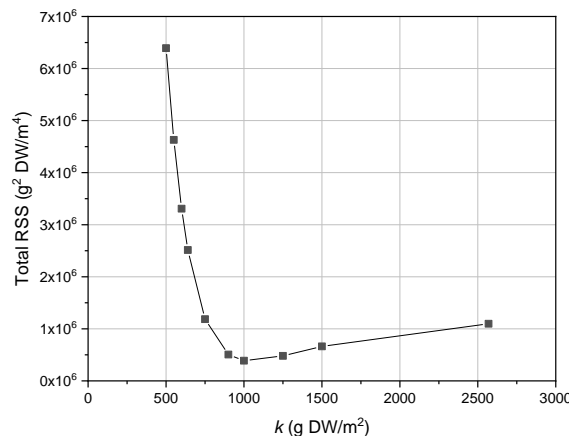


**Figure 5.6-7:** Change in total residual sum of squares (RSS) for logistic growth model by varying carrying capacity ( $k$ ).

As previously suggested,  $N_t$  and  $N_0$  may have impacted the value of  $k$ , therefore, the optimal  $k$  value would show differences between the control and fertilised tanks. Figure 5.6-8 shows the total RSS for the control and fertilised tanks; the combined value of control and fertilised equalled the total RSS shown in Figure 5.6-7. This demonstrates that whilst the total RSS was minimised at ~1000 g DW/m<sup>2</sup>, the control tanks have a minimised total RSS at ~600 g DW/m<sup>2</sup>. However, this has little impact on the overall total RSS as the control tanks have a lower total RSS by over one order of magnitude.

The  $k$  of the control tanks was similar to the value for small clones found by Mitsch [106], this suggests that the control tanks were dominated by the smaller clone variety, whilst the fertilised tanks had larger plants.

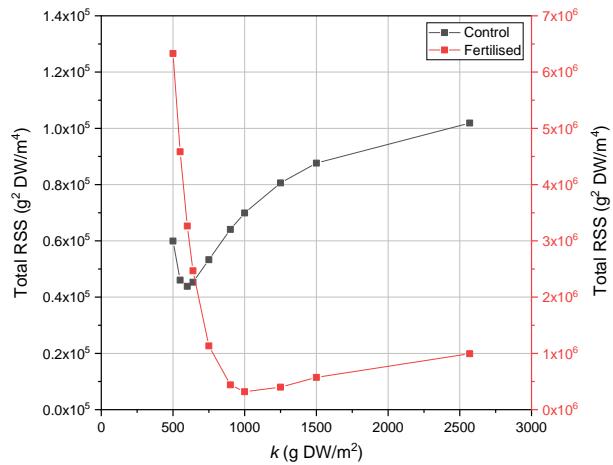


**Figure 5.6-8:** Change in total residual sum of squares (RSS) for logistic growth model for the control and fertilised tanks by varying carrying capacity ( $k$ ).

To further investigate the fit on the fertilised tanks, the tanks were split into low and high N doses, Figure 5.6-9. The low N doses were spring (38.5 mg N/L) and monsoon (38.2 mg N/L); the high N doses were winter (60.4 mg N/L) and summer (61.5 mg N/L). This shows that the high N doses had a minimum total RSS when  $k$  was  $\sim 1250$  g DW/m<sup>2</sup>, whereas the low N doses had a minimum total RSS at  $\sim 750$  g DW/m<sup>2</sup>. This corroborated the previous conclusion that better growing conditions increased the  $k$  value.

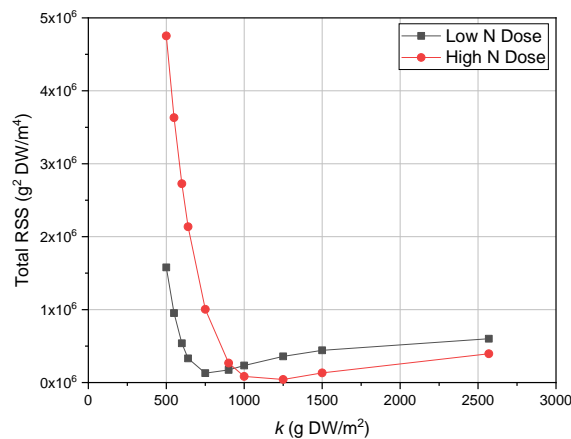


**Figure 5.6-9:** Change in total residual sum of squares (RSS) for logistic growth model for the low and high nitrogen dosed tanks by varying carrying capacity ( $k$ ).

The value of  $k$  impacted the fit of the model, which impacted the value of  $r$ , this is depicted in Figure 5.6-10. This illustrates that as  $k$  increased, the value for  $r$  decreased, as previously predicted [80,81]. All conditions were approaching a plateau at  $\sim 2600$  g DW/m<sup>2</sup>, the literature value for  $k$ , suggesting that carrying capacity had little impact on



the  $r$  in the phenological study: the trials were ended at a lower density than predicted by literature.

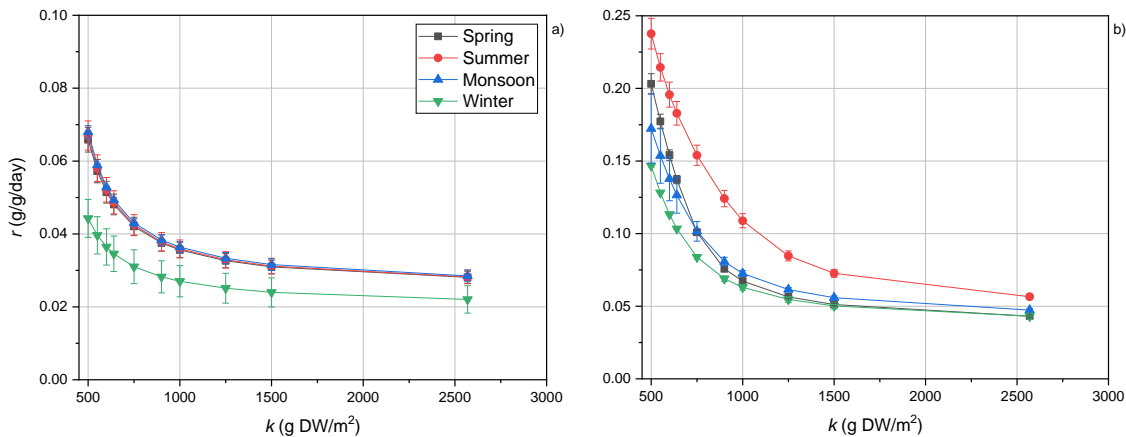


**Figure 5.6-10:** Change in intrinsic growth rate ( $r$ ) for logistic growth model for the control and fertilised tanks by varying carrying capacity ( $k$ ). a) control tanks; b) fertilised tanks.

The optimal  $k$  could be selected based on one of the following points:

1. The minimum overall total RSS
2. The point of intersection between the control and fertilised tanks total RSS
3. The point of intersection between the low and high dose

For the purposes of this study, the  $k$  value at the minimum overall total RSS was used, 1000 g DW/m<sup>2</sup>.

### 5.6.3.2. Intrinsic growth rate ( $r$ )

Once the  $k$  value was made constant, it was possible to solve the logistic growth model for  $r$  and compare the different trials; the results are described in Table 5.6-5 and Figure 5.6-11. The  $r$  value for control tanks, from spring, summer and monsoon, showed little variation, however, due to the weighing error in spring trial, the fit was poor in comparison. The winter trial had the lowest  $r$  value.

The fertilised tanks showed similar results for winter, spring and monsoon, whereas the summer trial had the greatest  $r$ . In comparison to the control tanks, the fits were poorer for the fertilised tanks, with the exception of winter. Based on the control results, it would be expected that summer and winter would have had lower  $r$  values, however, the increased  $N_0$  appears to have improved  $r$ . Monsoon also appears high, however, if  $N_3$  was utilised then the  $r$  value would appear to be correct.

**Table 5.6-5:** Intrinsic growth rate of the phenological study large tank trial with a carrying capacity of 1000 g DW/ m<sup>2</sup>.

Season	Reference	$r$ (g/g/day)*		RSS (g <sup>2</sup> /m <sup>4</sup> )	
		Average	Standard Deviation	Average	Standard Deviation
Spring	Control	0.036	0.002	35,490	16,842
	Fertilised	0.067	0.001	161,765	21,056
Summer	Control	0.036	0.002	15,826	719
	Fertilised	0.109	0.005	75,465	17,052
Monsoon	Control	0.036	0.001	14,165	2,284
	Fertilised	0.073	0.002	72,071	62,559
Winter	Control	0.027	0.004	4,427	415
	Fertilised	0.063	0.002	9,155	1,687

\*Fresh weight

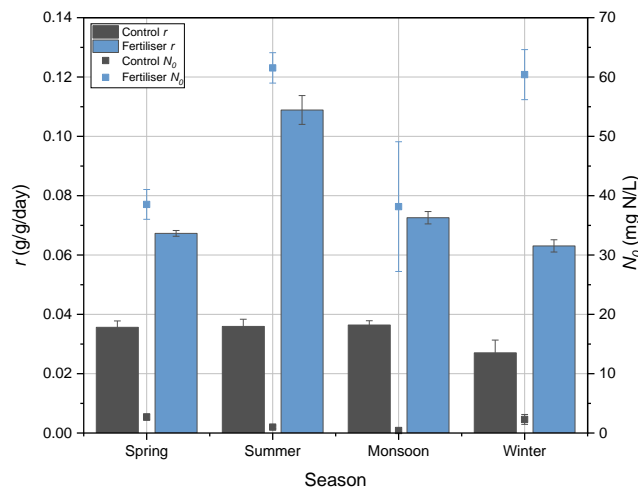


**Figure 5.6-11:** Change in fresh weight intrinsic growth rate ( $r$ ) and starting water nitrogen concentration ( $N_0$ ) for phenological study in large tank trial. The error bars represent the standard deviation of the replications.

### 5.6.3.3. Intrinsic growth rate normalised for starting water nitrogen concentration ( $r_N$ )

The ratio between the control and the fertilised tanks ( $r_d$ ) was greater in the tanks with the higher doses, confirming that the higher N doses increased  $r$ . Assuming that the effect of the different  $N_0$  in the control tanks was negligible, the ratio between the  $r$  of the control and fertilised tanks,  $r_d$ , can be utilised to normalise for the impact of  $N_0$  on the fertilised tanks.

By plotting  $N_0$  and  $r_d$ , the four trials produced a linear fit of  $N_0 = 21.4995.r_d - 0.0408$ ,  $PR = 0.85$ . By solving for  $r_d$  it was possible to calculate an  $r$  value that was normalised for  $N_0$  ( $r_N$ ) see Equation 5-4 and Equation 5-5.

**Equation 5-4:** Ratio between intrinsic growth rate of control and fertilised large tanks.

$$r_d = \frac{(N_0 + 0.0408)}{21.4995}$$

**Equation 5-5:** Intrinsic growth rate normalised for starting water nitrogen concentration.

$$r_N = r \cdot r_d$$

Utilising  $r_N$ , the impact of environmental factors was estimated, assuming a constant  $k$ , and is described in Figure 5.6-12. The temperature plot had a PR value of 0.85, demonstrating a strong fit, however, the p-value was  $>0.05$ , indicating that the relationship was not significant, as suggested by literature [80,81]. Solar irradiance had a PR of 0.35 and p-value  $>0.05$ .

The high error margin present in the monsoon trial was due to the difference between the  $N_0$  for the two fertilised tanks. In the monsoon trial,  $N_0$  had high variation, with an SD of 10.94. However, this variation reduced quickly:  $N_1$  had a SD of 4.13 and  $N_6$  had a SD of 0.64. This was due to N concentration in tank 2 increasing after  $N_0$ ; the difference became insignificant after  $\sim 6$  days of growth. This initial difference resulted in no increase of growth, suggesting that tank 2 either had a slower solubilisation or error in measurement. This could result in an under-estimation of the  $N_0$  and therefore explain why the monsoon  $r$  value was higher than expected. If the  $N_3$  for tank 1 was utilised, the relationship with temperature was significant, whilst solar irradiance was not. The  $N_3$  value was utilised from this point, with new values for  $r_d$  shown in Equation 5-6.

**Equation 5-6:** Ratio between intrinsic growth rate of control and fertilised large tanks, utilising higher starting water nitrogen concentration for the monsoon trial.

$$r_d = \frac{(N_0 - 7.9092)}{18.7940}$$

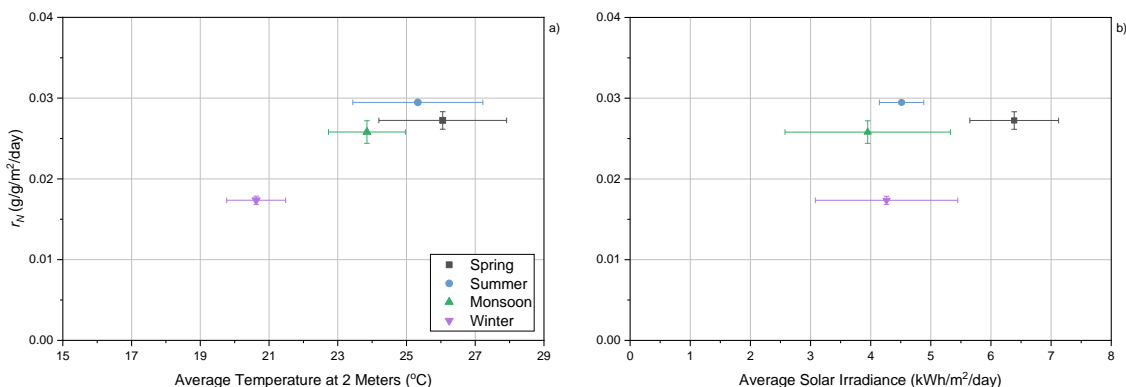
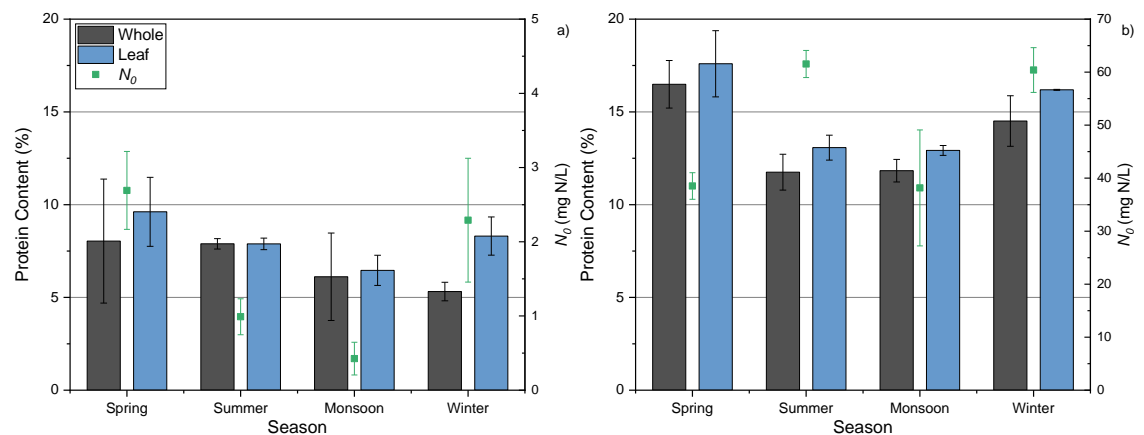


**Figure 5.6-12:** Change in fresh weight intrinsic growth rate ( $r$ ), normalised for starting water concentration ( $N_0$ ) in the phenological study large tank trial. x-error represents variation across the whole study; y-error represents replicate variation. a) temperature; b) solar irradiance.

#### 5.6.4. Impact on Utilisation Potential Indicators

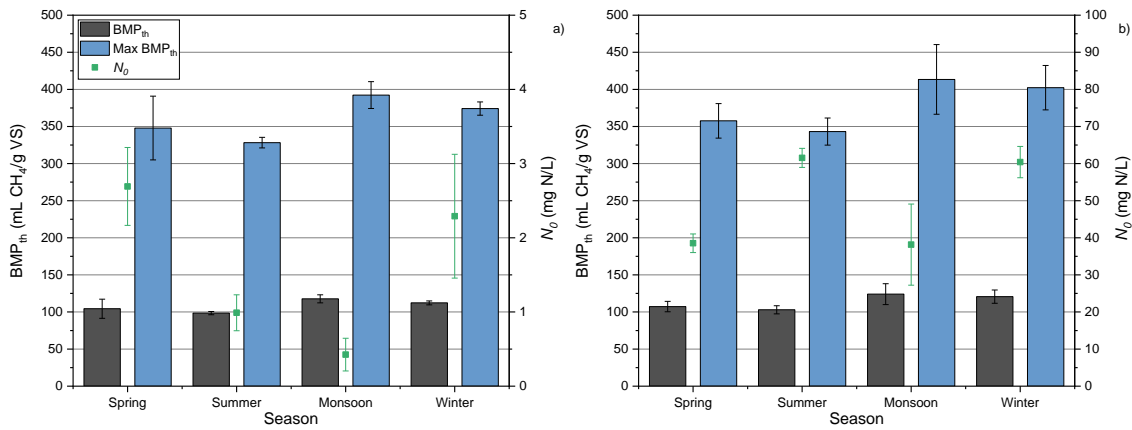
The analysis of wild WH, see Chapter 4, demonstrated variable leaf protein by location and season, with a range from 6.9- 27.2%. It is important to understand if the variation was as large in the cultivated samples.

Figure 5.6-13 shows the protein content of the whole plant and leaf for the phenological study. As with the wild samples, the leaf tended to have greater protein content than the whole plant. The control tanks demonstrated that protein increased from winter to spring, before a decrease through summer and the monsoon; this was similar to the results shown for Mula Baner and by Abdel Shafy *et al.*, who showed a reduction in plant protein from March through to December [62]. In the fertilised tanks there was a similar trend, however, the summer had a larger drop in protein content, resulting in a similar protein content to the monsoon trial. It is possible that this was due to reduction in growth rate that occurred at the latter stages of the summer trial in the fertilised tanks: the AGR of the fertilised summer tanks was 41.9, 48.0 and 26.4 g DW/m<sup>2</sup>/day for the first, second and third two weeks, respectively. This reduced growth rate would likely result in a reduction in juvenile leaf production and therefore reduced the protein content of the average leaf; without data from across the trial this was not possible to verify. The results demonstrated different trends to Indrayani River and the peak protein content was >2% lower than all Pune sites, except for Mula Sangvi.



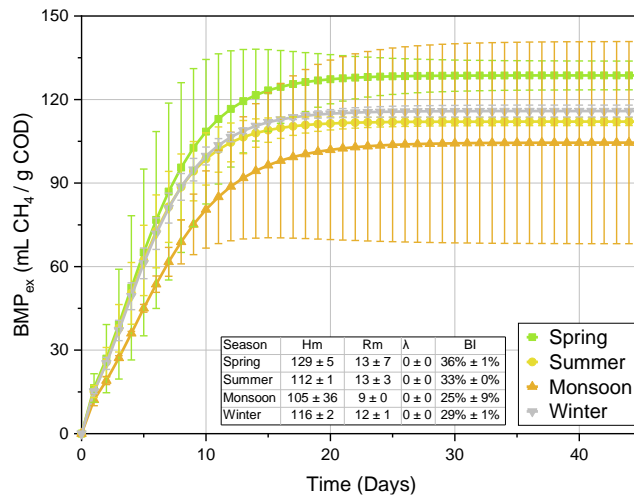
**Figure 5.6-13:** Changes in final protein content for the whole plant and leaf, and starting water nitrogen concentration ( $N_0$ ) in the phenological study large tank trial. The error bars represent the standard deviation of the replications. a) control tanks; b) fertilised tanks.

Figure 5.6-14 shows the  $BMP_{th}$  for the seasonal trials; the control tanks depicts that the highest average  $BMP_{th}$  was the monsoon trial, before it reduced throughout the rest of the year; however, due to the high error, there was little variation between the tanks. This was similar in the fertilised tanks. The  $BMP_{th}$  of the fertilised tanks appeared to be independent of the  $N_0$ .



**Figure 5.6-14:** Changes in theoretical biomethane potential ( $BMP_{th}$ ) and starting water nitrogen concentration ( $N_0$ ) in the phenological study large tank trial. The error bars represent the standard deviation of the replications. a) control tanks; b) fertilised tanks.

The  $BMP_{ex}$  for the whole plants, from the fertilised tanks, was analysed, see Figure 5.6-15. This demonstrates that whilst there was a difference in the methane production, the error margin resulted in no significant difference between the seasons. The most significant error was shown in the monsoon, particularly in the peak  $CH_4$  production ( $H_m$ ) despite a low standard deviation for the rate of change ( $R_m$ ). The BI demonstrated a similar story, with a high standard deviation from the monsoon trial, there was significant overlap between the samples, however, it appears that the spring trial had a greater BI than the other trials.



**Figure 5.6-15:** Modified Gompertz model, depicting the experimental biomethane potential of whole water hyacinth plants from seasonal large-scale cultivation analysis. Error bars represent the represent the analysis variation.  $H_m$ = maximum biomethane yield;  $R_m$ = peak biomethane production rate;  $\lambda$ = lag phase. Each sample was run in duplicate.

## 5.7. Conclusions

The aim of this chapter was to investigate the potential for large scale cultivation of WH for the use as a feedstock in a biorefinery. This included both small- and large-scale cultivation trials, as well as a phenological study.

The preliminary small crate trials, utilising a reference nutrient source of CM, appeared to demonstrate a polynomial relationship, of order three, between  $N_0$  and AGR. When the relationship was examined below 30 mg N/L, there was a strong linear fit, with a PR of 0.73 and RSS of 31.34. A fit that was weaker than the literature fit described in section 2.2.4. However, both the LitFit and TrialFit were statistically significant ( $p$ -value  $<0.05$ ).

Utilisation of other nutrient sources resulted in a distinct variation of  $N_0$  due to differences in solubilisation. CFW proved to be a poor choice of growth medium: the AGR of WH was poor and the leaves showed visual evidence of water loss. BM showed no improvement on CM and was discounted, however, it showed that it could be used in scenarios where BM was more accessible. Both NPK fertilisers (19:19:19 and 10:26:26) had similar or improved growth in comparison to CM, when  $N_0$  was  $<30$  mg N/L, however, both were not considered for further trials due to high costs. Digestate had high solubilisation that meant  $N_0$  was  $>30$  mg N/L, this was likely to have reduced the growth. However, the AGR was higher than achieved by Huurman *et al.* [336], and has potential for applications in an integrated system with an AD. FCM showed improved growth as dosage increased; viscosity and surface tension were reduced in comparison with CM. The latter points were the predominant reason it was selected for large-scale trials, due to the issues of attracting mosquitos and the fibrous remains that occurred with CM.

The relationship between  $N_0$  and AGR in the large tanks was similar to the small crates and when overlaid onto the TrialFit, it appeared to be within the bounds of the trial data. When cultivated with FCM, the  $N_0$  was higher than CM but still showed a similar AGR suggesting that the additional N did not have a negative impact on the AGR. Additionally, FCM had advantages over CM with reduced viscosity and surface tension, as well as a reduction in fibrous residue at the end of the trial. Digestate also had a higher  $N_0$  than CM but demonstrated an AGR similar to the TrialFit if  $N_0$  was  $\sim 22$  mg N/L. The high  $N_0$  of FCM and digestate tanks suggests that high  $N_0$  has a lower impact on AGR in the large tanks, compared with the small crates.

Leaves were harvested during a large tank trial and analysed for  $C_i$ ; this demonstrated that as  $N_i$  increased,  $C_i$  increased, as suggested by Wilson *et al.* [81]. At the end of each large tank trial, the biomass was harvested and analysed to determine the impact

on composition. FCM appeared to improve end trial harvest tissue N-content,  $C_N$ , when compared with CM. However, this was likely due to the higher  $N_0$ . Contrary to this, digestate reduced  $C_N$  compared with CM, despite a significantly higher  $N_0$ . The comparison of theoretical biomethane potential,  $BMP_{th}$ , showed that FCM had similar results to CM, whereas digestate reduced the  $BMP_{th}$ .

The phenological study showed that in the control tanks, winter had the lowest growth, whilst the other seasons were similar. In the fertilised tanks, the summer and winter trials had an increased  $N_0$ , which resulted in greater growth. Monsoon had a higher growth than expected, this was likely due to an error when determining  $N_0$ : in one tank, the  $N_t$  varied significantly over the first six days suggesting that some solubilisation was delayed. If the higher value was used, then the AGR was as predicted by the control tanks.

The logistic growth model was employed to determine an optimal carrying capacity ( $k$ ) for the large tanks. The optimal  $k$  appeared to vary depending on  $N_0$ : the optimal  $k$  value of the control tanks was lower than the fertilised tanks. The same relationship was true for the higher  $N_0$  fertilised tanks, summer and winter, compared with the lower  $N_0$  fertilised tanks, spring and monsoon. When solved for the intrinsic growth rate ( $r$ ), the logistic growth model showed similar results to AGR; however, it was possible to normalise  $r$  for  $N_0$  ( $r_N$ ). The result suggested that temperature had a significant impact on  $r$ , which was consistent with literature, whereas solar irradiance was insignificant.

The phenological variation in protein content showed that spring had the highest value before a drop to summer then a consistent increase throughout the year. The  $BMP_{th}$  peaked in monsoon before reducing throughout the year and appeared to be independent of nutrient increased loading. The plants were also analysed for experimental biomethane potential, however, due to high variation in the replicates, there was no significant difference between the seasons.

## Chapter 6.

# Alkali acid extraction

### 6.1. Introduction

Chapter 4 and Chapter 5 described various changes in the biomass composition and resource assessment for wild and cultivated biomass. This demonstrated that WH had a high protein content, often higher than various meat products and comparable with raw soybean. However, literature has yet to determine a suitable extraction methodology from WH. To ascertain if protein extraction would be a viable option, a simple methodology was employed, to determine the extractability of protein from WH. This was applied to the wild and cultivated samples to understand how the variations between the samples may affect protein extraction and the movement of HMs.

The aim of this chapter was to investigate the potential for protein extraction from WH and WL via alkali solubilisation and acidic precipitation. The key objectives were achieved via the following tasks:

- Alkali acid extraction was performed on variety of WH feedstocks to determine the variation that occurred across conditions.
- WL was utilised as a comparison to WH.
- The sample with the optimal extraction yield was selected for further extractions to understand the variation caused by extraction conditions.
- The potential for anaerobic digestion of residue from alkali acid extractions was assessed.

Initially, a selection of samples from Chapter 4 and Chapter 5 were selected to understand how the different feedstocks would affect yield and contamination levels within the protein extract. This included cultivated and wild WH, as well different plant parts and samples from different waterbodies. Secondly, a reference material was selected to undertake alkali acid extraction (AAE) under a variety of conditions. The parameters included were temperature, alkali strength and extraction time. Next, the best extraction condition was selected, and optimised to improve the yield/reduce contamination of the extract. This included variation in the pH of precipitation and washing the protein extract to remove sodium sulphate contamination.



### 6.1.1. COVID-19 Impact Statement

The impact of COVID-19 resulted in a reduction in the scale of the laboratory experiments conducted in Chapter 6. Initially, fermentation experiments, specifically lactic acid fermentation [235,340], were planned, but due to time limitations these were entirely removed. However, this is still viewed as a potential technique for protein extraction from WH and will be described in further work. Secondly, a greater range of extraction conditions were planned, including 0.5 and 1.5 M NaOH; 360-480 minutes; and an increased range of solid-to-liquid ratio conditions. Further optimisation experiments were planned, utilising a greater range of samples for removing sodium sulphates; a greater range of pH precipitation; and microwave- and sonication-assisted extractions [240,249].

The analysis of protein quality was not possible due to the loss of staff during the pandemic, this resulted in no amino acid analysis being conducted. Secondly, the biochemical analysis study was reduced due to delays in obtaining the equipment and method development.

## 6.2. Alkali acid extraction from wild and cultivated water hyacinth

### 6.2.1. Raw biomass characterisation

As discussed in Chapter 4 and Chapter 5, the protein content of WH differs considerably, depending on location, phenological variations and plant part; this study has shown variations from 4.2-27.7% protein. It has been shown that the biochemical composition varies depending on similar factors [55,64]. These are two parameters that will impact the efficiency of the AAE from the biomass [200].

There is little consensus in the literature on how the biochemical composition varies by plant part [63,64], therefore, a small study was conducted on the biochemical composition of a select number of samples, to understand the variations that occur between the different plant parts at different locations.

Figure 6.2-1a shows that cellulose is the predominant structural fibre in WH and appears to be in similar concentrations in the leaf and root, whereas the petiole contains between 5.9-9.34% more. Hemi-cellulose and lignin show similar trends: the leaf contains the highest hemi-cellulose and lignin, the root and petiole concentrations vary by location. Figure 6.2-1b shows that the protein content also peaks in the leaf, followed by the root and then the petiole, with the exception of UBL samples. The variations in structural fibre and protein composition, suggest that the petiole would be the most challenging tissue to extract protein, followed by the root, then leaf.

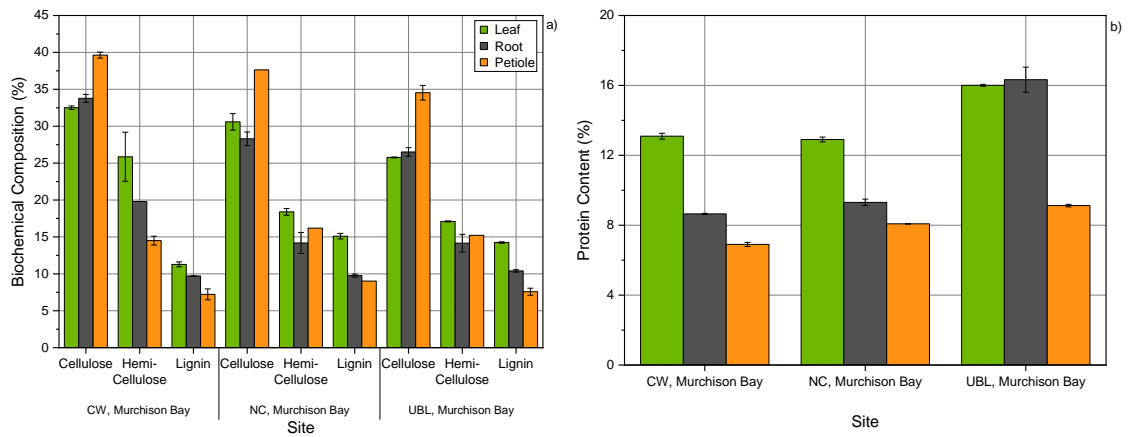


**Figure 6.2-1:** Comparison of plant parts of water hyacinth from Lake Victoria from January 2020, a) biochemical composition; b) protein content. Error bars demonstrate the replicate variation.

In comparison to the Lake Victoria biomass, the samples collected from Maharashtra, see Figure 6.2-2a, have a lower cellulose content within the petiole. The Maharashtra samples had the least cellulose in the leaf and greatest in the root. The hemicellulose was highest in the leaf and petiole, whilst the lignin was highest in the root. In both Uganda and Mula Baner, the petiole contained the lowest quantity of lignin. The protein varied between the sites, however, as shown in Chapter 4, this was expected. At Moshi, the petiole contained the least amount of protein, whereas at Baner, it was the root.

These results suggest that location has a significant impact on the biochemical composition of WH, validating the variable results previously found in literature.

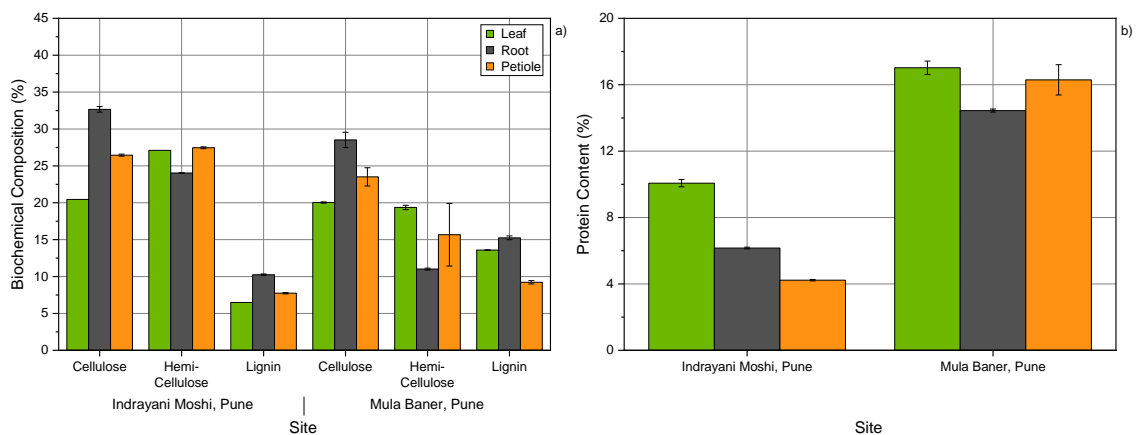


**Figure 6.2-2:** Comparison of plant parts of water hyacinth from Maharashtra rivers from June 2019, a) biochemical composition; b) protein content. Error bars demonstrate the replicate variation.

Figure 6.2-3 displays the variations that occurred in whole biomass from several locations and one sample of WL. This confirmed that location was significant for the biochemical composition for the WH samples. The cell wall components followed similar trends to the parts: cellulose was the highest concentration, then hemi-cellulose

and finally lignin. Hemi-cellulose showed the lowest variation, a range of 1.3%, followed by lignin and cellulose, 2.7 and 9.3%, respectively. The protein content was similar for West Bengal and Murchison Bay, whereas Mula Baner was greater. WL had approximately half the cellulose content of all the WH samples, a similar hemi-cellulose and a greater lignin content. The protein content was slightly lower than Mula Baner but greater than the rest. The low cellulose content suggests that AAE from WL would be more successful than WH, likely to release more protein at a quicker rate. However, the greater lignin content could result in more lignin fractionation and therefore, contamination of the precipitate [240,271].

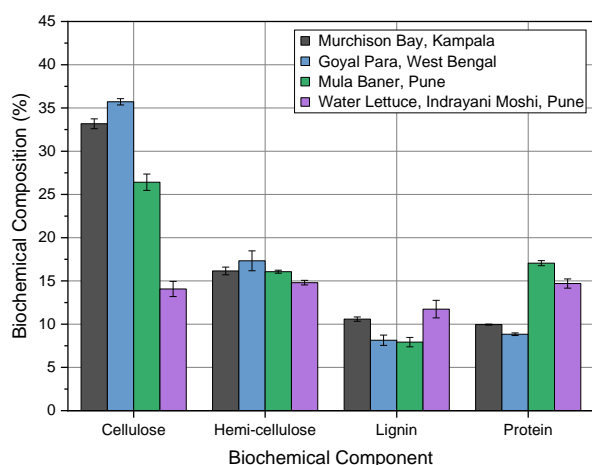


**Figure 6.2-3:** Comparison of water hyacinth whole biomass; from Murchison Bay (Dec 2018), West Bengal (June 2019), Mula Baner (June 2019) and water lettuce from Indrayani Moshi (June 2019). Error bars demonstrate the replicate variation.

### 6.2.2. Protein extract

A selection of samples from Chapter 4 and Chapter 5 were selected, see Table 6.2-1, and used in AAE at 40°C, 1.0 M NaOH and 150 minutes. The conditions were selected as WH contains high levels of cellulose [341], which reduces the extractability of protein [200], therefore, high temperatures and high molarity are recommended [255]. However, combining high temperature and high molarity can lead to changes in protein properties resulting in hydrolysis, racemisation and lysinoalanine formation [255]. Therefore, a high molarity with a moderate temperature was selected to increase hydrolysis without damaging the protein. Sari *et al.* found that most studies focussed on extraction times of <100 minutes [255], therefore, 150 minutes was selected to ensure all protein was solubilised.

Table 6.2-1 shows that the samples had a large range of protein content, ranging from 4.2-19.4%, and an ash content ranging from 3.9-39.7%. Samples included multiple collection times and locations: Maharashtra, cultivated and wild samples; West Bengal; Murchison Bay; and IBERS, cultivated under HM and nutrient conditions. The samples

also included different plant parts; however, the focus was on whole and leaf samples. These were selected as the optimal choices for AAE for the following reasons:

- Whole
  - Cheapest pre-processing (no separation required)
  - Lower HM content than root
  - Lower cellulose content than petiole
  - Easy homogenisation at the source
- Leaf
  - Lowest HM content
  - Lowest cellulose content (in Ugandan samples and one Indian sample)
  - Highest protein content for the majority of samples (see Chapter 4 and Chapter 5)

**Table 6.2-1:** Samples for alkali acid extraction.

Sample Location	Date	Plant Part	Protein Content (DB %)	Ash (DB %)
Water Lettuce, Indrayani Moshi, Pimpri Chinchwad, Maharashtra	Jun-19	Whole	17.1	26.9
Indrayani Moshi, Pimpri Chinchwad, Maharashtra	Jun-19	Leaf	10.1	8.6
		Root	6.2	9.8
	May-21	Petiole	4.2	7.3
		Whole	13.1	20.8
Indrayani Alandi, Pimpri Chinchwad, Maharashtra	May-21	Leaf	16.2	15.0
		Whole	10.3	24.2
Mula Baner, Pune, Maharashtra	May-21	Leaf	14.4	14.1
		Whole	14.4	33.6
Mula Sangvi, Pune, Maharashtra	May-21	Leaf	18.4	18.0
		Whole	12.7	39.7
Large-Tank Cultivated, Pune	Jun-21	Leaf	18.0	15.8
		Whole	11.8	17.6
Goyal Para, West Bengal	Jan-20	Leaf	13.1	7.7
		Whole	6.6	8.0
Murchison Bay, Lake Victoria	Dec-18	Leaf	14.4	6.6
CW, Murchison Bay, Lake Victoria	Nov-19	Whole	9.6	36.1
NC, Murchison Bay, Lake Victoria	Nov-19	Leaf	18.2	5.7
UBL, Murchison Bay, Lake Victoria	Nov-19	Leaf	19.5	3.9
Nutrient Small-Crate Cultivated, IBERS*	Jan-21	Leaf	17.7	4.2
		Whole	6.3	15.3
HM Small-Crate Cultivated, IBERS*	Jun-21	Leaf	16.3	15.4
		Whole	11.5	13.0
		Leaf	15.9	13.6

\*The Institute of Biological, Environmental and Rural Sciences, Aberystwyth, Wales

### 6.2.2.1. Comparison of alkali acid extraction from different parts of the plant

The comparison of the plant tissues, in section 6.2.1., suggested that the leaf would be the optimal tissue for AAE, followed by root, then the petiole. To examine this directly, plant tissues from Indrayani Moshi June 2019 were utilised for AAE, see Figure 6.2-4. Precipitate weight was calculated as a direct analysis; protein content of the precipitate was calculated by converting the N content, as described in Chapter 3; the protein recovery was calculated based on the protein content of the precipitate as a factor of the protein content in the original biomass. This sample had greater cellulose in the petiole, followed by the leaf, then root; the protein content followed the trend leaf > root > petiole.

The precipitate weight followed the protein content trend: leaf > root > petiole, implying that protein content had a greater impact on extraction than cellulose content. If the ash content was removed from the precipitate, the precipitate weight would be 60.4, 38.5 and 34.9 mg, for the leaf, root and petiole, respectively. This suggests that leaf was the most successful feedstock for AAE, whilst root and petiole had little difference, due to the overlap of error. The protein recovery yield showed little significant variation between the parts due to high error margins. However, the protein content of the precipitate demonstrated that the leaf precipitate was the highest, with little variation between the root and petiole. The protein increase revealed that the petiole had the most successful extraction, concentrating the protein in the precipitate and increasing its content by over 130%, compared with 70-75% for the leaf and root. This was unexpected due to the high cellulose content of the petiole; however, the petiole contained the highest concentration of lignin, therefore, it is possible that the alkali was able to fractionate the lignin and therefore release a greater proportion of the protein. Further analysis of the different parts would be required to fully understand this relationship.

These results suggest that the leaf produces the optimal protein extract, however, the petiole was the most successful protein concentration. It is unlikely that the root would be used for protein extraction due to the poor extraction and high ash content. Further analysis of the parts was conducted in section 6.2.3, to determine if the tissue precipitates differ in HM content.

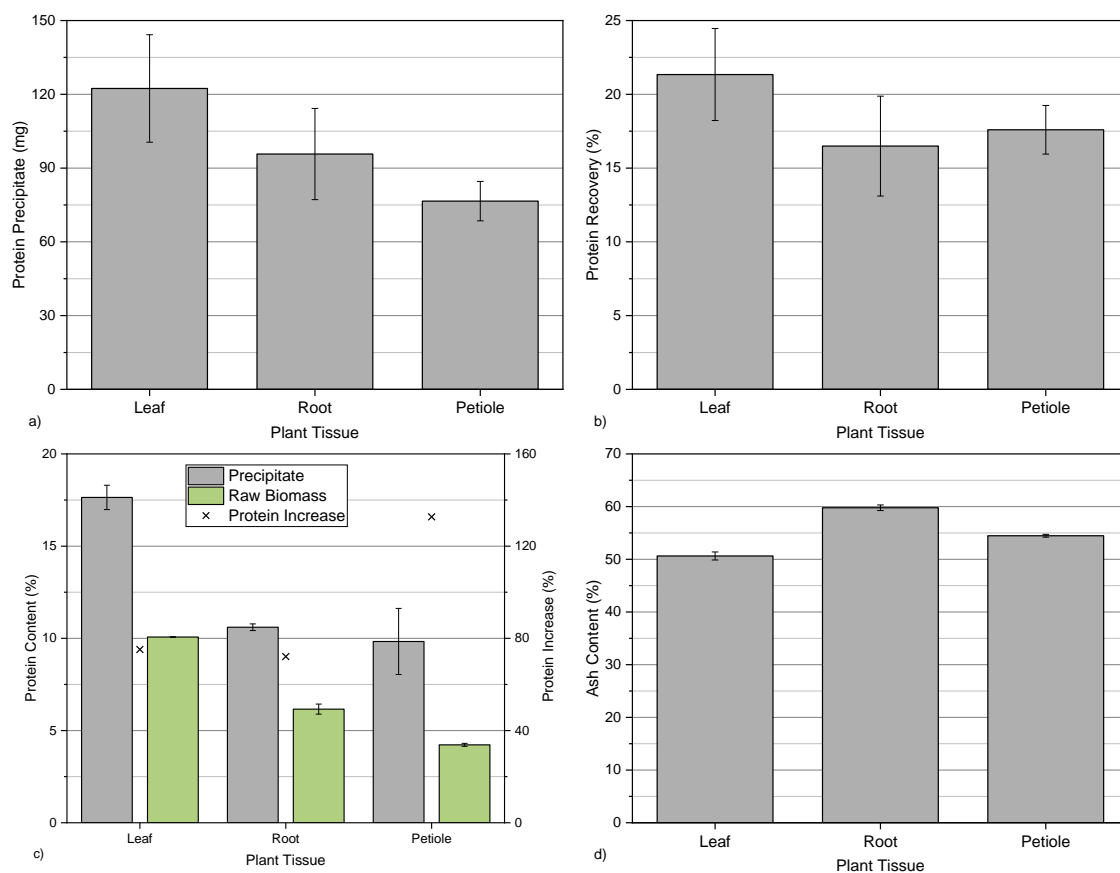


**Figure 6.2-4:** Comparison of alkali acid extraction from water hyacinth plant tissues, from Indrayani Moshi Jun-19- a) precipitate weight; b) protein recovery; c) protein content and increase compared with raw biomass; d) ash content. Error bars demonstrate the replicate variation.

The leaf was determined as the optimal tissue for AAE, however, it is important to understand how it performs against the whole biomass. Figure 6.2-5 shows the comparisons between the whole plant and leaf precipitates for a variety of samples. Figure 6.2-5a displays the difference between the whole and leaf precipitate weights; this demonstrates that with the exception of the cultivated Pune sample, all leaf precipitates had a greater precipitate weight. Secondly, Figure 6.2-5b shows that the protein content of all leaf precipitates were higher than the whole plant, resulting in a greater protein recovery, see Figure 6.2-5c, that was ~2x larger in the leaf than the whole, for one sample. However, the recovery was highly dependent on the sample: the Pune cultivated sample showed little difference in recovery, between the whole plant and the leaf.

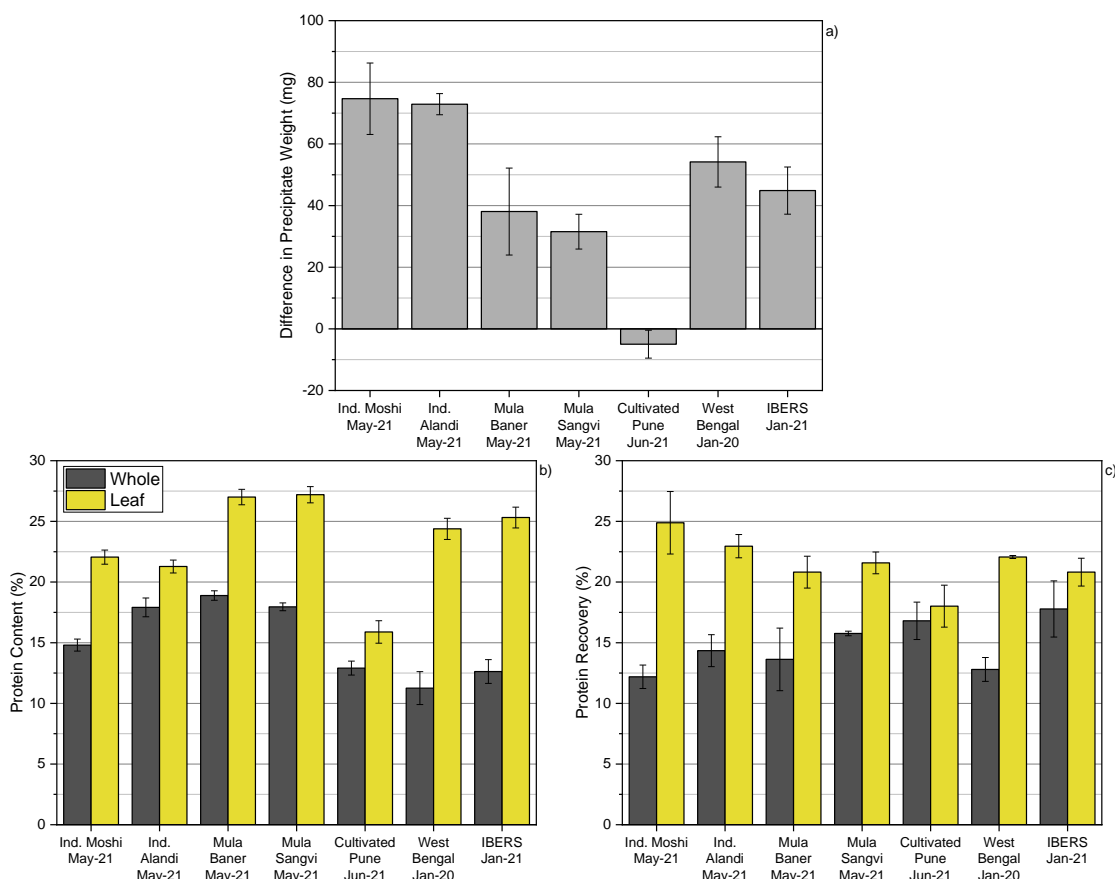


**Figure 6.2-5:** Comparison between whole plant and leaf precipitates at 40°C/1.0M/150 minutes, a) difference in precipitate weight; b) protein content; c) protein recovery. Error bars demonstrate the replicate variation.

Whilst the leaf samples improved protein recovery, the values are significantly lower than yields from similar biomass [342]. In a comparison of various biomass, Sari *et al.* showed that a low temperature alkali extraction liberated up to 80% of protein [200], the 25% recovery exhibited by WH leaves would be similar to microalgae meal, palm kernel meal and sugar beet pulp; with only raw microalgae and ryegrass producing a lower recovery [200]. This suggests that WH may be a poor choice of feedstock for AAE. However, the biomass investigated by Sari *et al.* were all high value biomass, whereas, WH was a highly invasive pest with a high growth rate, therefore, it may prove a better choice of feedstock.

#### 6.2.2.2. Comparison of alkali acid extraction from different locations

Chapter 4 demonstrated there was significant variation in composition of WH between the different locations. The range of AAE results, shown in 6.2.2.1, suggests a possible variation could occur from WH harvested at different locations, corroborated by the differences in biochemical composition shown in Figure 6.2-2.

Figure 6.2-6 demonstrates that there was variation between the locations, for both the whole and leaf samples. The whole sample demonstrated a standard deviation of 25.6

mg (excluding the WL) and the leaf sample was 20.1 mg. The protein recovery had a standard deviation of 2.0 and 3.5% for the whole and leaf, respectively. The percentage error of the precipitate, for the whole plant, was greater than the percentage error of the protein recovery, 24.0 and 14.0%, respectively. This suggests that recovery of non-protein mass had a greater variation than recovery of protein mass.

The biochemical compositions of Murchison Bay, Dec-18, and West Bengal, Jan-20, whole samples demonstrated a greater lignin content for the former, and marginally lower cellulose and hemi-cellulose. This corresponded with an increase in precipitate weight, suggesting that the increase in precipitate weight was due to lignin degradation [240,271]. The relationship between structural fibres and precipitate weight must be studied further to confirm. The high protein content of WL precipitate suggests that protein release was easier than for WH, likely due to the lower cellulose content of the WL.

The raw biomass protein content of the Murchison Bay sample was marginally greater than the West Bengal sample, replicated in the protein recovery, however, when raw biomass protein was plotted against protein recovery, it produced an  $r^2$  of 0.05, demonstrating a weak relationship.



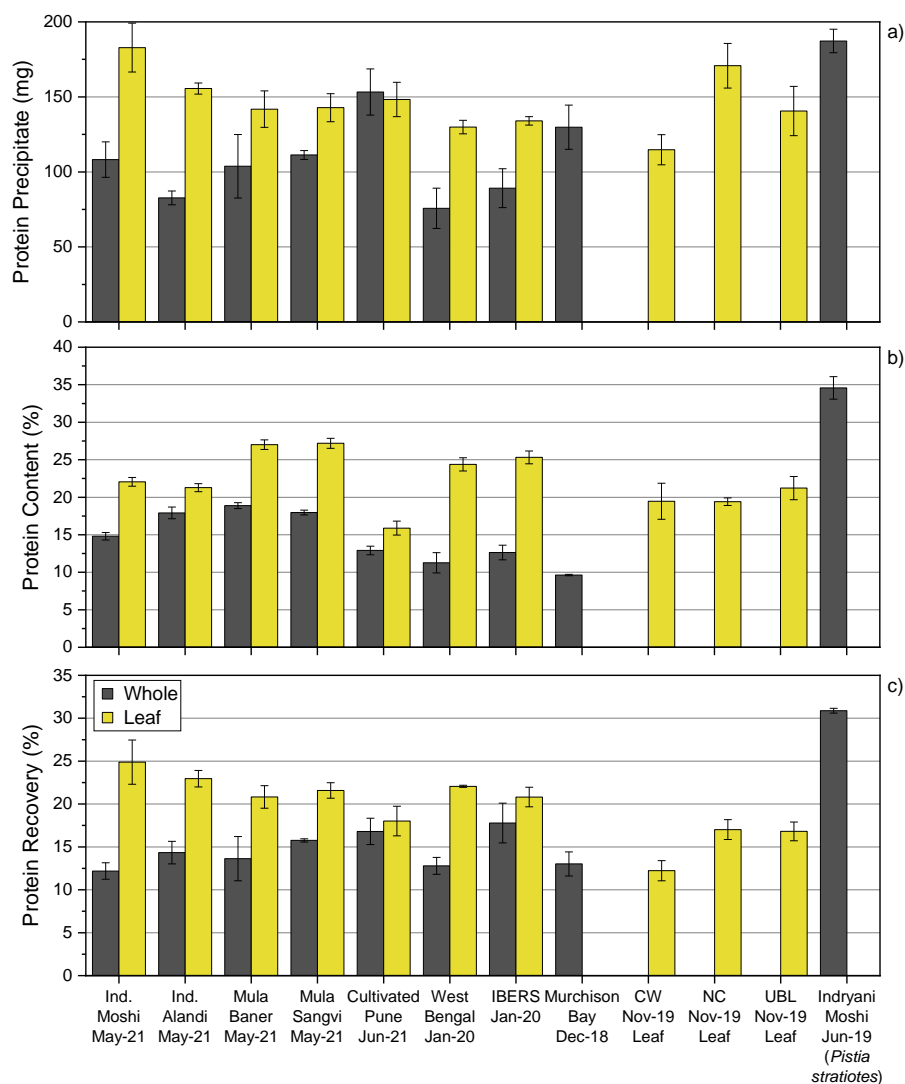


**Figure 6.2-6:** Comparison of alkali acid extraction from a variety of locations at 40°C/1.0M/150 minutes, a) precipitate weight; b) protein content; c) protein recovery. Error bars demonstrate the replicate variation.

The biochemical components were individually plotted against the AAE outputs, a linear fit was then applied and an analysis of variance test (ANOVA) carried out on each comparison. An example of the fitted line is displayed in Figure 6.2-7. This was carried out to determine if the variation in biochemical composition may have impacted the precipitation.

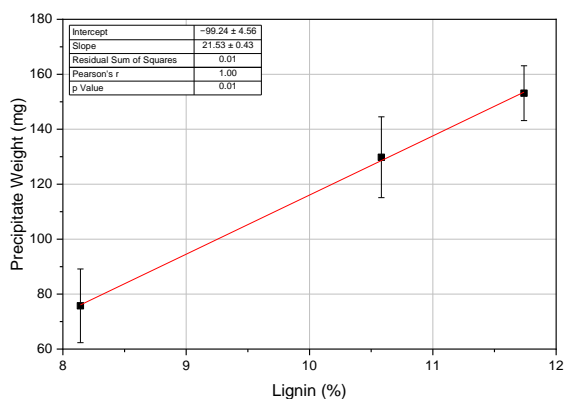


**Figure 6.2-7:** Example of a linear fit of a biochemical component plotted against an alkali acid extraction result- lignin and precipitate weight. Error bars demonstrate the replicate variation.

The PR value and p-value, obtained via the ANOVA test, from each fit, was then plotted to demonstrate the significance of each biochemical component on the alkali extraction outputs; this is displayed in Table 6.2-2. The p-value defines the significance of the slope, defined as: “above 0.05, the slope is not significantly different from 0”. This demonstrates that the relationship between lignin and precipitate weight was the only significant relationship (0.01). Whereas the impact of lignin content on protein content and protein recovery was insignificant. The PR value indicates that there was a strong fit between the raw biomass cellulose and protein content with the precipitate protein content and protein recovery. The cellulose content was suggested to have a negative impact on the protein recovery [200], this was corroborated by a negative slope for the fit of cellulose and precipitate protein content and protein recovery, -2.69 and -1.16, respectively. However, the high error presented resulted in a slope that was not significantly different from zero.

**Table 6.2-2:** Statistical analysis of the relationship between biochemical components and alkali acid extraction outputs for whole plants (Indrayani Mosh Jun-19 *Pistia stratiotes*; West Bengal Jan-20; and Murchison Bay Dec-18).

Biochemical Component	Precipitate Weight		Protein Content		Protein Recovery	
	p-value	PR value	p-value	PR value	p-value	PR value
Cellulose	0.41	-0.80	0.11	-0.99	0.06	-1.00
Hemicellulose	0.17	-0.96	0.34	-0.86	0.30	-0.89
Lignin	0.01*	1.00	0.50	0.71	0.46	0.75
Protein	0.36	0.84	0.15	0.97	0.11	0.99

\*Slope shows statistical significance

Only three samples were included in the previous analysis, due to the limited cross over between the biochemical analysis study and AAE, therefore, these results must be interpreted with caution. However, the leaf, root and petiole samples from Indrayani

Moshi June 2019, did fit this cross over. Initially, only the whole plants were included in this analysis; because of the significant variation in composition that occurs in the different parts of the plant and the known variations in extraction potential. An example of this is the high concentration of ash within the root, an element that may impact the extraction and reduce impact of other factors on extraction, thereby reducing the significance of the results. However, when they were included in the fit, a greater number of results were statistically significant, see Table 6.2-3. This included protein content on precipitate weight and protein content (of the precipitate), and cellulose content on protein content and protein recovery. The impact of lignin content on precipitate weight was no longer significant. Further work must be conducted here to understand what components impact the process.

This study was limited due to the limited number of samples, but also the linear fit: it is unknown if these relationships fulfil a linear relationship, however, the lack of data points means that linear was the only option. Therefore, further analysis of this relationship should be conducted. Sari *et al.* suggested that at 20°C, for 24 hours, cellulose and ash were negatively correlated with protein recovery, whereas at 60°C, for one hour, sugar, hemicellulose and ash were negatively correlated [200], indicating that there are further relationships to be examined.

**Table 6.2-3:** Statistical analysis of the relationship between biochemical components and alkali acid extraction outputs for water hyacinth parts and whole plants (Indrayani Moshi Jun-19 *Pistia stratiotes*; West Bengal Jan-20; Murchison Bay Dec-18; leaf, root and petiole Indrayani Moshi Jun-19).

Biochemical Component	Precipitate Weight		Protein Content		Protein Recovery	
	p-value	PR value	p-value	PR value	p-value	PR value
Cellulose	0.15	-0.66	0.02*	-0.87	0.00*	-0.96
Hemicellulose	0.35	-0.46	0.43	-0.40	0.81	-0.12
Lignin	0.29	0.52	0.39	0.43	0.54	0.32
Protein	0.03*	0.87	0.04*	0.83	0.16	0.65

\*Slope shows statistical significance

### 6.2.2.3. Comparison of alkali acid extraction from wet and dry

The process of drying biomass before utilisation is an expensive and potentially time consuming, therefore, it is important to understand if the extraction can occur on wet biomass, as opposed to dry. Figure 6.2-8 depicts the variations that occurred between dry and wet samples from a heavy metal spiked growth trial at IBERS, Aberystwyth (unpublished). The whole plants showed no difference between the wet and dry samples, whereas the dry leaf produced 44% more precipitate than the wet leaf. This suggests that the root and/or the petiole may be more susceptible to the alkali acid extraction when wet than dry, whereas the wet leaf was more susceptible when dry.

The wet whole plant precipitate had a slightly higher protein content than the dry whole plant, whereas the dry leaf was higher than the wet leaf. The final protein recovery was higher for the dry biomass than the wet. The results demonstrate that drying the biomass increases the success of the AAE, however, the expense of the drying may result in a net loss, therefore, further investigation will occur in Chapter 7.

Whilst the calculation of protein content has assumed to account for chlorophyll-based N, and other non-protein N, this is an indirect method and is therefore a lower reliability than direct analysis. The difference in protein recovery between dry and wet could be attributed to the behaviour of chlorophyll in the different circumstances. Further work should be conducted to understand this, in particular the analysis of the precipitate for amino acid content to confirm the protein content and quality of the precipitate.

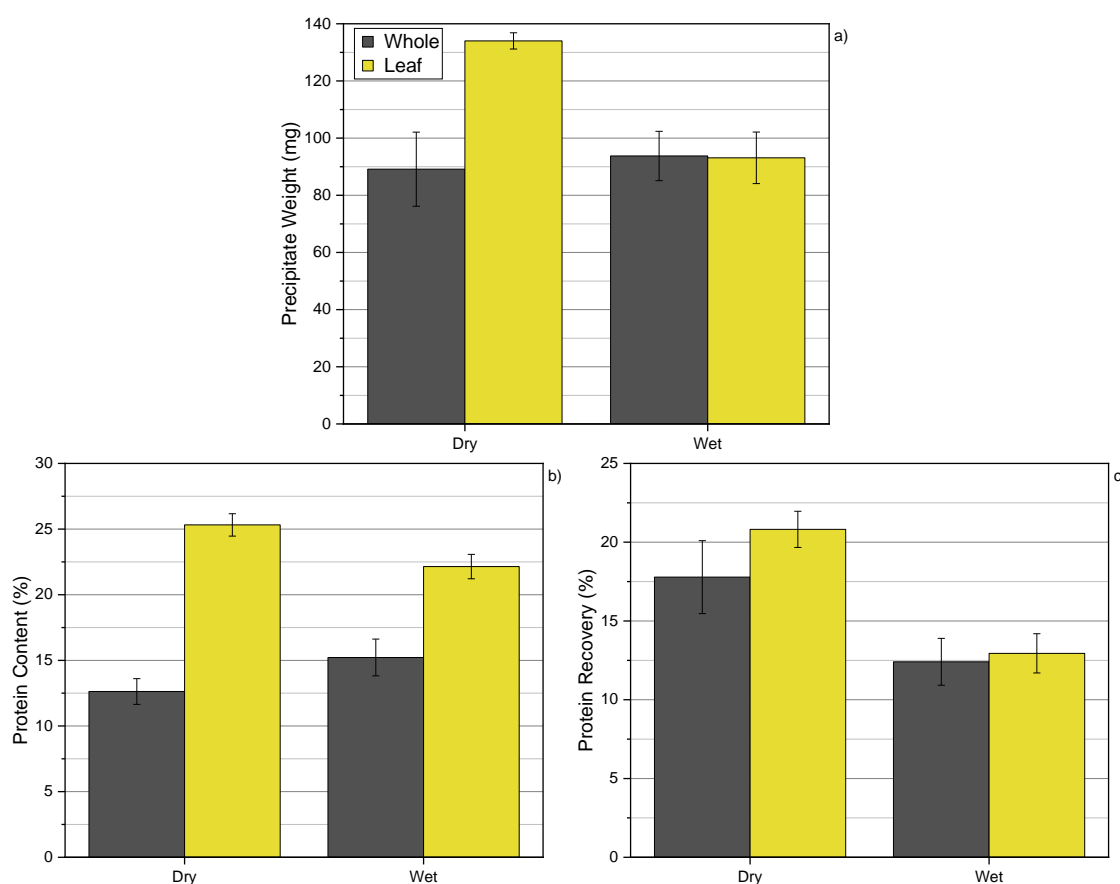


**Figure 6.2-8:** Comparison of alkali acid extraction from wet and dry samples from an IBERS heavy metal spiked small-crate trial at 40°C/1.0M/150 minutes, a) precipitate weight; b) protein content; c) protein recovery. Error bars demonstrate the replicate variation.

### 6.2.3. Fate of trace elements

WH biomass has been shown to contain toxic contaminants, particularly HMs, above the level that would be tolerated by humans [343]. Therefore, it is possible that the precipitate contains equal amounts of HMs. This is unlikely based on the solubility of HMs as a function of pH: Ca, Cd, Co, Cu, Fe, Mn, Ni, Pb and Zn have all been shown

to have a peak solubility below pH 2, the solubility then decreased as pH increased [344]. This suggests that the any bound metals would not be soluble during the alkali treatment and free metals may be soluble and therefore remain in the acidic solution after centrifugation. However, HMs associated with peptides, like phytochelatins, a HM chelating peptide [345,346], could be present in the final product. Secondly, any HMs associated with structural fibres, or other carbohydrates, could follow the same trend.

Figure 6.2-9 displays the elemental analysis of the three WH tissues, for the raw biomass and protein precipitate. The results suggest that elements such as Co, Cu, Ni, Pb and Zn were concentrated within the precipitate, whereas elements such as Al, Cr, Fe, Mo and Ti were reduced. Cu, Pb and Zn are HMs that have been shown to penetrate root tissue, whereas Al, Fe and Ti tend to be present in higher concentration on the surface of roots [149]. This suggests that the HMs present within the root tissue are associated with compounds that are soluble under alkaline conditions and are therefore present in the final precipitate. An increase in Cu was also found by Hontiveros and Serrano, who soaked WH in NaOH at pH 9, and precipitated at pH 2 utilising HCl, at 60-80°C [212]. An increase in Pb was not observed, however, the sample utilised was WH leaf which contained low levels of Pb in comparison with the root. Hontiveros and Serrano demonstrated that the essential amino acid content of the WH precipitate was similar to that of a chicken egg [212], however, methionine and lysine were limiting factors.

The HM content of the raw biomass showed that the root contained the highest HM content, followed by petiole and then leaf. Whilst the root precipitate contained the highest HM content, the leaf contained greater concentrations of Ni than the petiole, which resulted in a greater precipitate total HM content. The greatest difference between the raw and precipitate was the increase in Na for all of the tissues. This was due to the presence of sodium sulphate, resulting in the increase of both Na and S. The S was not included in Figure 6.2-9 due the high concentration; the S content was 11.8, 13.0 and 9.2% for the leaf, root and petiole precipitates, respectively.

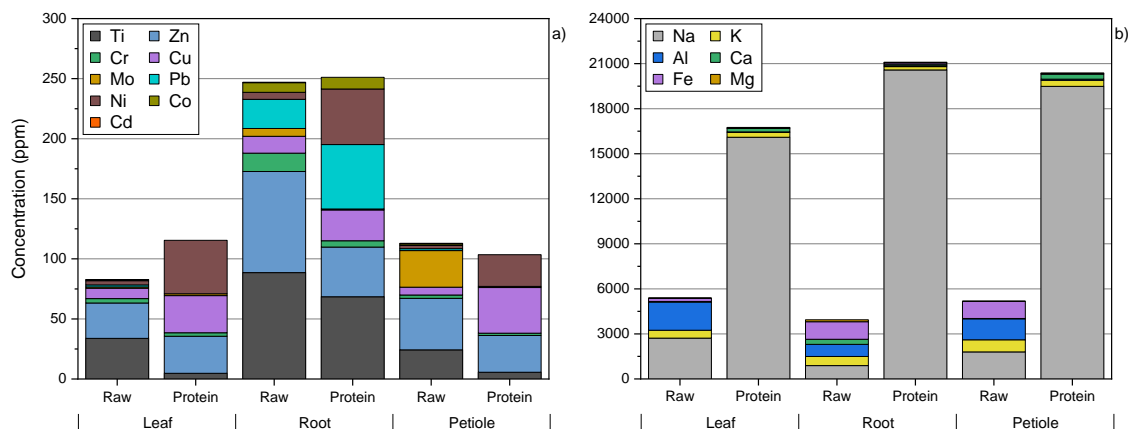


**Figure 6.2-9:** Trace elemental composition of raw water hyacinth tissues and protein extract from Indrayani Moshi Jun-19, utilising alkali acid extraction at 40°C/1.0M/150 minutes- a) low concentration elements; b) high concentration elements.

Three samples were analysed to understand the difference between the HM flow when utilising whole plants as compared with the WH leaf. Figure 6.2-10 shows the elemental composition for two whole samples and a leaf. The Na concentration showed no trend and did not appear to be correlated with the original Na content, corroborating that the addition of NaOH and H<sub>2</sub>SO<sub>4</sub> produced sodium sulphates. Therefore, it is likely that the variations in Na content were due to contamination when decanting the liquid from the protein rather than an increased sodium content within the precipitate. The same was true for the S content: the content was 7.3, 7.0 and 11.4% for the WL, cultivated whole and cultivated leaf samples, respectively. This shows no trend with the raw biomass, which was BDL for the WH and 0.3% for the WL, for the S content. Further work was conducted to reduce the Na and S content through washing the precipitate to remove the excess liquid and solubilise the sodium sulphate.

The HM concentration showed similar trends to the previous samples: Cu, Ni and Zn all were concentrated in the precipitate. However, Ni was reduced for WL and the leaf precipitate; Al, Ca, Cr, Fe and Ti were also reduced. The whole precipitate contained greater quantities of HMs than the leaf precipitate; WL showed similar total concentration to the cultivated WH sample, however, it contained less Ni and greater Cu concentrations.

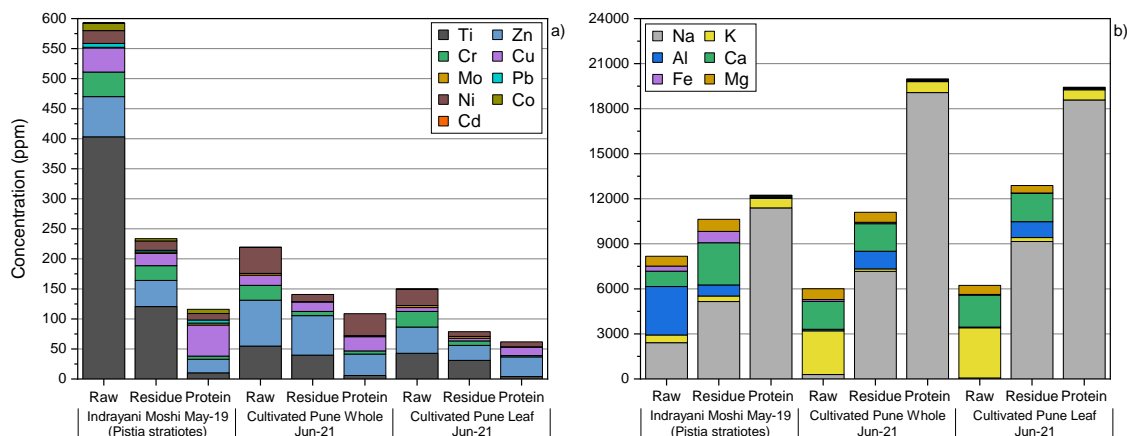


**Figure 6.2-10:** Elemental composition of raw biomass, residue from alkali extraction and protein precipitate from acid precipitation for whole water lettuce plant, cultivated water hyacinth whole plant and leaf sample- a) low concentration elements; b) high concentration elements.

When considering WH precipitate, the MPL of metals within ‘foodstuffs’ must be considered. The European Union Law does not have a category specific to protein extracts, precipitates or concentrates, therefore the value for ‘food supplements’ was utilised. The MPL for Cd, Hg and Pb were stated as 1, 0.1 and 3 ppm, respectively. Cd was BDL for all protein samples and demonstrated a peak concentration of 0.5 ppm in the whole samples. However, results from Chapter 4 showed that Cd could reach >100 ppm in WH root tissue suggesting that these samples would be unfit for extraction. Pb showed significant variation between the samples, ranging from BDL to >50 ppm. However, the majority of samples were <3 ppm with the only exception being WL and WH root. Further analysis would be required to understand the cause of this. Hg was not considered for this study after the initial analysis showed all samples BDL. These results suggest that WH would be a possible choice for a protein supplement in human diets, in particular leaf tissue. However, the reduction of Na and S must be investigated.

The recommended daily intake (RDA), for the elements listed in Figure 6.2-10, is listed in Table 6.2-4, along with the nutritional information for ‘Holland & Barrett ABC to Z Vegan Multivitamins’ and a pea protein. The weight required of the cultivated Pune leaf Jun-21 precipitate to fulfil the RDA requirements, and the same nutrient composition as the vegan multivitamin, was calculated. This demonstrates that the precipitate contains less nutrients than the multivitamin, per 100g of precipitate, however, the presence of protein suggests that it would still hold value. The precipitate would provided 19% of the protein available from the pea protein, as well as containing less Ca, Fe, Mg and Zn. This suggests that WH leaf precipitate would have a significantly lower value than pea protein. If it was assumed that WH precipitate was valued at 19% of the pea protein described in Table 6.2-4, the precipitate would be valued at £13.30 per kg

[347]. Based on the value of average market pea protein isolates, from Petersen *et al.*, valued at \$6.5-8.1 per kg [196], this appears to be an overestimation. Secondly, the trace nutrient content of WH could result in a reduction in price.

The nutrient value of the precipitate ranges from 1.4- 922.7% of the RDA, suggesting that some nutrients are in excessive amounts. Cr has been shown to have anti-inflammatory properties, although this has been shown to be contradictory [348], however, elevated Cr supplementation of 1 mg/day did not have adverse effects. Whilst copper is in elevated concentration in the precipitate, the lethal dose of copper has been suggested to be 10-20 g [349], therefore, above 6.9 kg of the precipitate could prove fatal in an adult. However, it is unlikely that this would be consumed by an adult, however, this must be investigated further if this was to be a commercially available product, due to issues with concentration.

**Table 6.2-4:** Recommended daily allowance of various trace elements and protein compared with protein precipitate, from cultivated Pune leaf Jun-21; a commercial vegan multivitamin; and a commercial pea protein.

Nutrient	RDA (mg/day)*	Vegan multivitamin‡ (mg per tablet)	Pea Protein^ (mg/100g)	Precipitate (mg/100g)	%RDA for 100g of precipitate (%)
Al	18.57	-	-	2.36	12.68
Ca	700.00	120.00	10.00	8.53	1.22
Cd	1.00†	-	-	0.00	-
Co	0.01	-	-	0.00	-
Cr	0.03	0.04	0.01	0.23	922.68
Cu	1.20	1.00	0.60	1.43	118.81
Fe	8.70	14.00	16.00	1.73	19.89
K	3500.00	-	50.00	68.18	1.95
Mg	300.00	60.00	12.00	4.27	1.42
Mo	0.05	-	0.03	0.03	67.83
Na	2400.00	-	-	1857.99	77.42
Ni	-	-	-	0.82	-
Pb	3.00†	-	-	0.00	-
Ti	0.40	-	-	0.41	102.30
Zn	9.50	10.00	6.00	3.27	34.38
Protein	56000.00	-	84000.00	15915.20	28.42

\*[350]; †Value taken from MPL [343]; ‡[351]; ^[347]

The high HM concentrations in WH precipitate suggests that animal feed would be a sensible option for a marketing strategy. However, animal feed has a significantly lower target price; for example, the global value of soybean meal was valued at £0.37 per kg, as of the 29<sup>th</sup> September 2022 [214], this was over 35 times lower than the predicted value of WH precipitate as a human food supplement and over 15 times lower than the bottom end of the range suggested by Petersen *et al.* for pea protein isolate [196]. The



average Indian soybean meal was quoted as almost twice that of the global price, at £0.65 per kg [215], this was still much cheaper than protein isolate.

The European commission set limits of 0.2 ppm and 10 ppm for Cd and Pb, respectively, for animal feeds [352], suggesting that WH precipitate would be acceptable as an animal feed. Table 6.2-5 compares the trace nutrient and protein content of the cultivated Pune leaf Jun-21 precipitate and Indian soybean meal. This shows that the precipitate was lower than soybean meal for all nutrients and contained 34% of the protein present in soybean meal.

**Table 6.2-5:** Trace nutrient and protein composition of water hyacinth precipitate, from cultivated Pune leaf Jun-21, in comparison with Indian soybean meal.

Nutrient	Water Hyacinth Precipitate (mg/100g)	Soybean Meal (mg/100g)*
Al	2.36	ND
Ca	8.53	436
Cd	0.00	ND
Co	0.00	ND
Cr	0.23	ND
Cu	1.43	1.69
Fe	1.73	84.30
K	68.18	2,020
Mg	4.27	364
Mo	0.03	ND
Na	-	18.00
Ni	0.82	ND
Pb	0.00	ND
Ti	0.41	ND
Zn	3.27	5.52
Protein	15,915	46,300

\*[353]; ND- no data

The comparison between pea protein and soybean meal suggests that WH would be poor a substitute for human or animal consumption. However, WH is an invasive species that can be cultivated at high rates, therefore, the harvesting and cultivation of WH may result in the plant becoming profitable, if the ecosystem services provided by clear water systems are included. Another option would be to blend WH precipitate with high value soy to create a lower cost product. However, the key analysis here was that a WH precipitate can be produced that was safe for animal consumption.

#### 6.2.4. Alkali acid extraction solid residue analysis

The AAE produced a precipitate that accounted for ~7.5- 20.0% of the mass, therefore, it is important to understand the composition and potential utilisation of the remaining residue. Two residues were selected for ultimate, proximate and elemental analysis, as

well as  $BMP_{ex}$ . The samples selected were residues of cultivated Pune Jun-21, leaf and whole.

Table 6.2-6 shows the composition of the raw biomass and residue for the cultivated whole plant and the leaf from Maharashtra June 2021. The residue had a decrease in VM, FC, C, H, N and O; whilst the ash content, C:N ratio and maximum  $BMP_{th}$  was increased. The reduced protein content and HHV suggests that the only option, out of the options considered, would be AD. However, if the biomass was dried then pellets or biochar could be produced, these would be more effective than the raw biomass due to the reduced N content of the residue.

**Table 6.2-6:** Comparison of the composition of raw biomass and residue from alkali acid extraction on cultivated Pune Jun-21 whole plant and leaf samples at 40°C/1.0M/150 minutes.

Sample	Cultivated Pune Whole Jun-21		Cultivated Pune Leaf Jun-21	
	Raw Biomass	Residue	Raw Biomass	Residue
VM (% db)	67.8 ± 0.7	52.9 ± 0.1	72.9 ± 0.2	47.6 ± 0.0
FC (% db)	14.6 ± 0.5	7.3 ± 0.1	11.7 ± 0.0	3.0 ± 0.0
Ash (% db)	17.6 ± 1.2	36.5 ± 0.2	15.4 ± 0.1	41.0 ± 0.0
C (% db)	34.0 ± 1.1	30.7 ± 0.1	35.5 ± 0.8	28.1 ± 0.1
H (% db)	4.3 ± 0.3	3.6 ± 0.5	4.4 ± 0.1	3.3 ± 0.3
N (% db)	2.5 ± 0.2	1.9 ± 0.1	2.8 ± 0.1	2.1 ± 0.0
S (% db)	0.0 ± 0.0	0.0 ± 0.0	0.0 ± 0.0	0.0 ± 0.0
O* (% db)	41.6 ± 0.1	27.3 ± 0.6	49.6 ± 0.7	25.5 ± 0.3
C:N	13.5 ± 1.6	16.0 ± 0.7	12.6 ± 0.9	13.7 ± 0.3
Protein <sup>+</sup> (%)	11.8 ± 1.0	8.9 ± 0.3	13.1 ± 0.7	9.5 ± 0.2
HHV (MJ/kg)	13.6 ± 0.5	11.6 ± 0.4	14.4 ± 0.3	10.6 ± 0.2
Max $BMP_{th}$ (mL CH <sub>4</sub> /g VS)	335.9 ± 18.0	440.9 ± 28.6	285.4 ± 13.7	430.1 ± 18.3
$BMP_{ex}$ (mL CH <sub>4</sub> /g VS)	112.2 ± 1.4	199.0 ± 11.8	- ± -	216.4 ± 6.4
BI (%)	33.4 ± 0.1	45.2 ± 0.4	- ± -	50.3 ± 0.3

\*Calculated by difference; <sup>+</sup>Calculated with co-efficient (4.64) multiplied by nitrogen.

The trace elemental analysis, presented in Figure 6.2-11, showed that the residue contained lower amounts of all elements, with the exception of Al and Na. This was in contrast to the protein precipitate which concentrated certain elements. This left some elements unaccounted for and therefore suggests that HMs may be concentrated in the liquid fraction discarded at the end of the experiments. At this time, the liquid fraction was assumed as an acidic waste, however, the presence of HMs could result in a greater cost in disposal, therefore, further work must be conducted before this process could be commercialised.

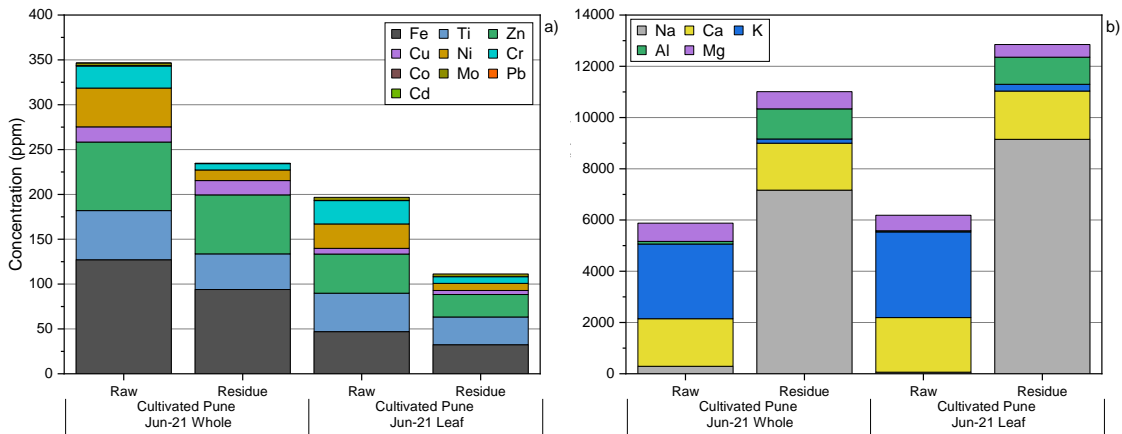


**Figure 6.2-11:** Trace elemental comparison of raw biomass and residue from alkali acid extraction on cultivated Pune Jun-21 whole plant and leaf samples at 40°C/1.0M/150 minutes.

The maximum  $BMP_{th}$  of the residue has been shown to increase and suggested that the alkali treatment of WH could result in increased biogas yield from AD. Secondly, the use of NaOH, as pre-treatment for AD, has been shown to increase methane yield from 61% to 71% [354], suggesting that alkali treatment from the AAE would improve methane yields. Figure 6.2-12 demonstrates the yields achieved by experimental  $BMP$  ( $BMP_{ex}$ ): for the cultivated whole sample, the methane yield was increased by over 77%. The methane yield of the cultivated leaf residue was greater than the whole sample. However, due to errors in experimentation, the leaf raw biomass was not recorded, however, based on the BI for similar leaf samples, see Chapter 4, it can be assumed that the methane yield would be improved. However, the raw leaf biomass had a marginally higher BI than the raw whole biomass, so the leaf residue may not improve as greatly as the whole residue. The increased methane yield from the residue would add value to utilising WH biomass for AAE.

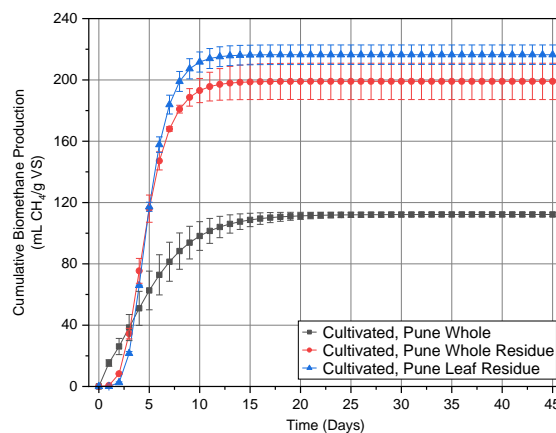


**Figure 6.2-12:** Experimental bio-methane potential of raw biomass and residue from alkali acid extraction on cultivated water hyacinth Pune Jun-21 whole plant and leaf samples at 40°C/1.0M/150 minutes. Error bars demonstrate the replicate variation.

### 6.3. Comparison of alkali acid extraction conditions on water lettuce

AAE from WH and WL demonstrated that WL outperformed WH in terms of total precipitate, protein content of the precipitate and protein yield. Secondly, the ash and HM content in the WL precipitate was not greater than the WH precipitate, despite higher levels of ash and HMs in the raw biomass. Therefore, WL was selected as a reference material to understand the impact of the process conditions on the extraction of protein. The sample utilised for this investigation was from Indrayani Moshi June 2019, described in Table 6.2-1.

The composition of the raw WL biomass, and comparative WH samples, are displayed in Table 6.3-1 and Figure 6.3-1. WL had a higher N and protein content than WH and subsequently a lower C:N ratio, suggesting that WH would be a better feedstock for AD [312]. This was compounded by a lower maximum  $BMP_{th}$  for WL. As previously discussed, WH had a greater cellulose content than WL, which could lead to reduced protein extraction. WH also had a greater hemicellulose content and a lower lignin content, however, this was dependent on the location. In the literature, the maximum reported lignin content of WH was 26.4, suggesting that the two species could have similar lignin contents, depending on the location [54]. With the exception of N, most nutrients and HMs overlap between WL and the range given by the different WH samples, however, WL appears to have a greater concentration of Al, Ti and Na. This was seen in the transfers of metals to the protein where WL had a greater concentration of Al and Ti than any of the WH samples, Na was inflated by the addition of NaOH.

**Table 6.3-1:** Composition of water lettuce reference material for alkali acid extraction and comparative water hyacinth samples.

Plant	Water Lettuce		Water Hyacinth	
Location	Indrayani Moshi	Indrayani Moshi	Mula Baner	Lake Victoria
Date of Collection	Jun-19	May-21	Jun-19	Dec-18
VM (% db)	64.2 ± 0.3	67.1 ± 0.8	76.8 ± 1.7	54.1 ± 0.1
FC (% db)	8.8 ± 0.0	12.1 ± 0.3	15.3 ± 1.1	8.4 ± 0.3
Ash (% db)	26.9 ± 0.4	20.8 ± 0.4	7.8 ± 0.6	37.5 ± 0.4
C (% db)	28.7 ± 0.0	36.6 ± 0.2	38.9 ± 0.1	28.0 ± 0.1
H (% db)	3.0 ± 0.0	4.5 ± 0.0	4.2 ± 0.3	3.1 ± 0.6
N (% db)	3.7 ± 0.1	2.8 ± 0.0	3.2 ± 0.1	2.1 ± 0.0
S (% db)	0.3 ± 0.0	0.0 ± 0.0	0.2 ± 0.0	0.2 ± 0.0
O* (% db)	37.3 ± 0.0	35.3 ± 0.2	45.7 ± 0.5	29.0 ± 0.6
C:N	7.8 ± 0.1	12.9 ± 0.2	12.3 ± 0.4	13.1 ± 0.1
Cellulose (%)	14.1 ± 0.9	-	26.4 ± 0.9	33.2 ± 0.6
Hemicellulose (%)	14.8 ± 0.3	-	16.1 ± 0.2	16.2 ± 0.4
Lignin (%)	11.7 ± 1.0	-	7.9 ± 0.5	10.6 ± 0.2
Protein (%)	17.1 ± 0.3	13.1 ± 0.1	14.7 ± 0.5	10.0 ± 0.1
HHV (MJ/kg)	10.9 ± 0.0	14.4 ± 0.1	15.2 ± 0.2	10.5 ± 0.4
Max BMP <sub>th</sub> (mL CH <sub>4</sub> /g VS)	274.7 ± 0.3	412.6 ± 3.7	326.9 ± 11.1	374.7 ± 30.6

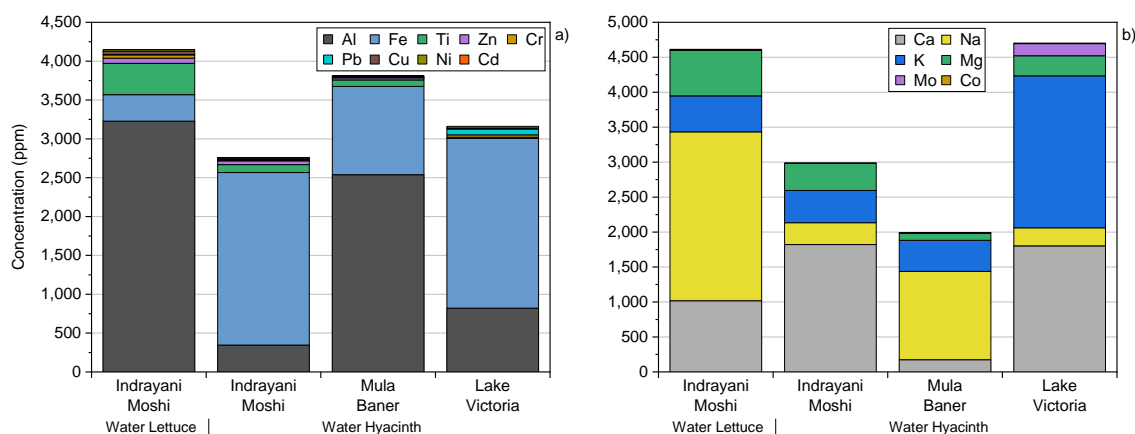


**Figure 6.3-1:** Composition of water lettuce reference material for alkali acid extraction and comparative water hyacinth samples- a) heavy metals; b) nutrients.

The extraction parameters considered were extraction time, temperature and total amount of alkali; these were suggested as the greatest influences on protein extraction by Sari *et al.* [255], and discussed in section 2.5.

### 6.3.1. Effect of extraction time on alkali acid extraction

Time is vital parameter in any process; however, the impact of time is dependent on the feedstock and conditions applied. Urribarrí *et al.* demonstrated that extraction yield peaked at 30 minutes for Dwarf Elephant grass, under the conditions of calcium hydroxide at pH 10, 60°C and a 1:10 solid to liquid ratio [355]. However, yield increase was from 33.7 to 34.9%, suggesting that the influence of extraction time was minimal. The peak extraction time was similar to that found by Khalil, who found that extraction from Guar seed powder peaked at 40 minutes. The increase in yield was dependent on the extraction solvent, with the change in protein yield ranging from a 21.7 to 41.3% increase [356]. In contrast, Shen *et al.* demonstrated that extraction from green tea leaves at 30°C, 0.06 M NaOH, and a 1:35 solid-liquid ratio, improved extraction from below 20% yield to almost 40% [357]. The increase in yield was rapid in the first two hours of extraction, before slowing until 5 hours were it appeared to plateau [357]. Whereas, Zhang *et al.* demonstrated that extraction time was insignificant after just 2 hours of extraction [256].

To understand how extraction time impacted AAE, extraction was carried out over three temperatures (40°C; 65°C; and 90°C) and two alkali concentration (0.1 and 1.0 M NaOH). The extraction times considered were 0, 1, 5, 15, 30, 45, 60, 90, 120, 150, 180, 240 and 300 minutes.

The variations in precipitate weight demonstrated that for all conditions, other than 40°C/0.1M and 65°C/0.1M, the precipitate weight peaked before 150 minutes, Figure 6.3-2. This suggests that these conditions released the protein before 150 minutes and further extraction time resulted in either no increase in yield or hydrolysis of the protein. The first condition, 40°C/0.1M, demonstrated a large increase from 180 to 240 minutes, 183.2%, suggesting that this condition had not fully released the protein. The yield decreased at 300 minutes in comparison, therefore, another extraction time period was added to determine if this decrease was due to error or if a plateau would occur. As can be seen in Figure 6.3-2, the protein yield at 360 minutes showed no increase from 300 minutes, suggesting that a maximum yield had occurred. Whilst the yield from 65°C/0.1M did not peak before 150 minutes, the increase beyond 150 minutes was <8.5%. Therefore, it was assumed that the increase was unlikely to continue beyond 300 minutes.

Table 6.3-2 displays the percentage increase from the minimum protein yield for each condition. It demonstrates that all conditions had a minimum value after 1 minute, with the exception of 40°C/0.1M, which gave a yield of ~0 mg at 1 minute, and 90°C/1.0M, which resulted in large reductions in yield after its maximum due to protein hydrolysis. However, for the purposes of demonstrating the percentage increase due to extraction

time, these values were ignored. Whilst all conditions utilising 1.0 M NaOH resulted in a greater maximum protein yield, the initial protein yields were greater than 0.1 M NaOH conditions, therefore the percentage change was lower. The same was true for temperature: as the temperature increased, the percentage increase reduced. This suggests that at conditions that have a greater hydrolysis and protein solubilisation potential, higher alkali concentration and higher temperature, extraction time was less significant. This was similar to the results found by Khalil, who demonstrated that extraction time had a greater impact on extraction utilising distilled water than NaOH [356].

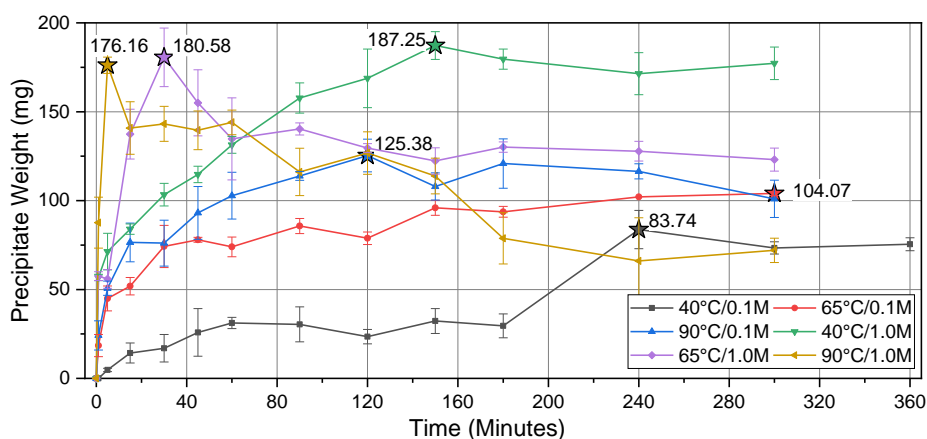


**Figure 6.3-2:** The effect of extraction time on the precipitate weight from water lettuce utilising alkali acid extraction (☆ - maximum value for condition with data label). Error bars demonstrate the replicate variation.

**Table 6.3-2:** Percentage change in precipitate weight with respect to extraction time.

	Minimum*		Maximum		Percentage increase (%)
	Yield (mg)	Time (minutes)	Yield (mg)	Time (minutes)	
40°C/0.1M	4.7	5	83.7	240	1663.0
65°C/0.1M	18.5	1	104.1	300	463.6
90°C/0.1M	24.2	1	125.4	120	418.5
40°C/1.0M	56.8	1	187.3	150	229.9
65°C/1.0M	56.0	1	180.6	30	222.8
90°C/1.0M	87.6	1	176.2	5	101.1

\*Excluding 0 mg yield and yields after maximum

The total quantity of precipitate is not the only result suggesting success from AAE; another indicator is the protein content in the precipitate, see Figure 6.3-3 and Table 6.3-3. The results suggest that protein content had little variation due to extraction time: with the exception of a small number of anomalies, like 51.0% at 5 minutes of 65°C/0.1M, and all results after 150 minutes of 90°C/1.0M, there was little variation in the protein content with respect to extraction time, see Table 6.3-3. This suggests that

protein solubilisation occurred at the same rate as the solubilisation of non-protein compounds.

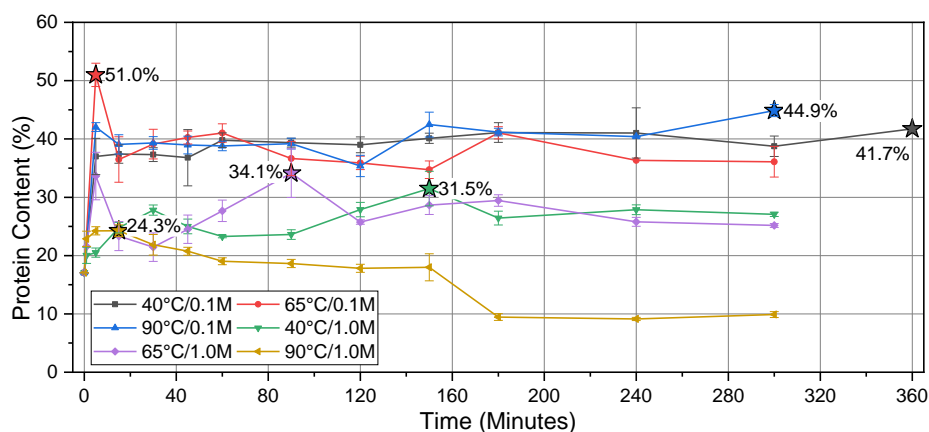


**Figure 6.3-3:** The effect of extraction time on the protein concentration from water lettuce utilising alkali acid extraction (☆ - maximum value for condition with data label). Error bars demonstrate the replicate variation.

**Table 6.3-3:** Percentage change in protein content of precipitate with respect to extraction time.

Conditions	Raw Sample protein content (%)	Maximum Protein content (%)	Time (minutes)	Percentage increase (%)	Overall protein content SD* (%)
40°C/0.1M	17.1%	41.7%	360	144.7%	1.7%
65°C/0.1M		51.0%	5	199.0%	2.4%
90°C/0.1M		44.9%	300	163.1%	2.5%
40°C/1.0M		31.5%	150	84.6%	3.3%
65°C/1.0M		34.1%	90	100.2%	4.2%
90°C/1.0M		24.3%	15	42.2%	2.6%

\*SD- Standard Deviation, calculated with anomalies removed (1 minute of 40°C/0.1M, 65°C/0.1M, 90°C/0.1M; 5 minutes of 65°C/0.1M; 180-300 minutes of 90°C/1.0M)

Utilising the total precipitate weight and protein content of the precipitate it was possible to calculate the percentage of protein recovery from the raw sample via Equation 6-1 and Equation 6-2. The protein recovery incorporates both quantity of precipitate and the protein content of the precipitate, displayed in Figure 6.2-4. The peak protein recovery occurred from 150-240 minutes for 40°C/0.1M, 65°C/0.1M, 90°C/0.1M and 40°C/1.0M; 90 minutes for 65°C/1.0M; and 5 minutes for 90°C/1.0M. Three of the conditions showed different peaks in comparison to the precipitate weight peaks.

**Equation 6-1:** Protein weight in precipitate.

$$\text{Protein in precipitate (mg)} = \text{Protein content of precipitate (\%)} \times \text{Precipitate weight (mg)}$$



**Equation 6-2:** Protein recovery percentage.

$$\text{Protein Recovery (\%)} = \frac{\text{Protein in Precipitate (mg)}}{\text{Protein in Original Sample (mg)}} \times 100$$

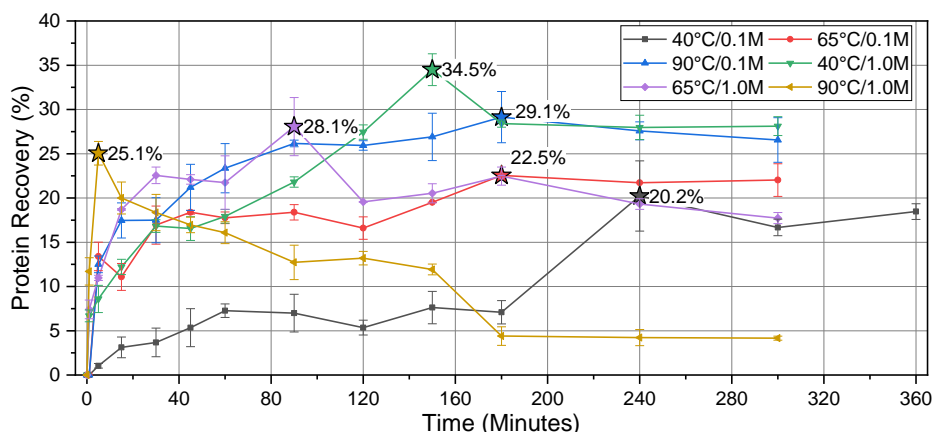


**Figure 6.3-4:** The effect of extraction time on the protein recovery from water lettuce utilising alkali acid extraction (☆ - maximum value for condition with data label). Error bars demonstrate the replicate variation.

The ash content of the precipitate, see Figure 6.3-5, showed little variation, with respect to extraction time, for all conditions except for 90°C/1.0M. The 90°C/1.0M condition appears to follow the inverse of the protein content of the precipitate; this suggests that the ratio of ash to other non-protein compounds does not change within the precipitate, with respect to extraction time, rather the protein recovery diminishes.

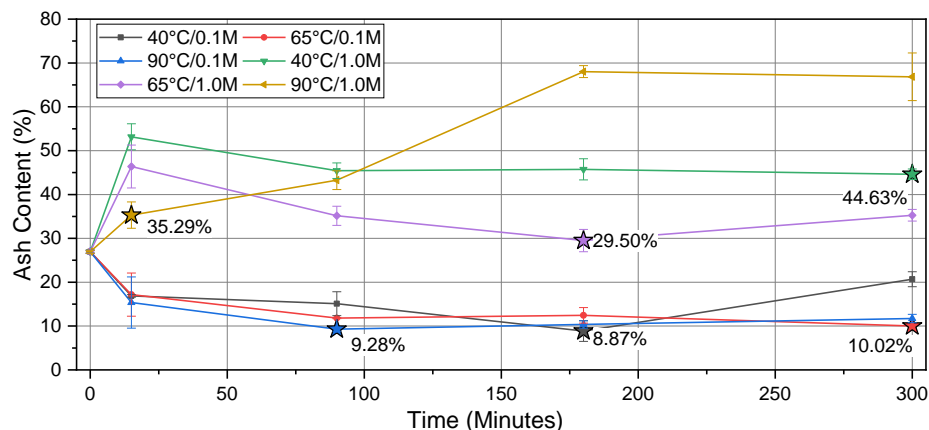


**Figure 6.3-5:** The effect of extraction time on the ash content from water lettuce utilising alkali acid extraction (☆ - minimum value for condition with data label). Error bars demonstrate the replicate variation.

**6.3.2. Effect of temperature on alkali acid extraction**

Increased temperatures have been shown to benefit protein extraction [255,357], however, prolonged periods of increased temperature are costly, can cause protein hydrolysis and cause protein coagulation [256], thereby reducing protein yield and increasing costs. To examine the impact of temperature on AAE from WL, three

temperatures were selected: 40°C; 65°C; and 90°C. The increase in temperature during AAE has been shown to significantly increase protein solubilisation when compared with room temperature [230,256], therefore, 40°C was selected as the base temperature. However, increasing the temperature above 100°C can lead to the hydrolysis of proteins, particularly above 140°C [240], and cause protein coagulation at higher alkalinities. Therefore, 90°C was selected as the maximum temperature in this study.

Figure 6.3-6 depicts the precipitate weight that was generated using 0.1 M and 1.0 M NaOH at the different temperatures. Figure 6.3-6a demonstrates that increased temperature had a direct increase in the total precipitate weight: at all time points, 40°C was lower than both 65 and 90°C conditions and at all time points (with the exception of 300 minutes), 65°C was lower than 90°C. In contrast, Figure 6.3-6b demonstrated that at the higher alkalinity, 1.0 M NaOH, temperature had a larger negative impact on precipitate weight; 40°C appeared to follow a similar trend to 65°C and 90°C for 0.1 M NaOH, demonstrating a steady increase until 150 minutes where the rate plateaus and reaches a steady state. Due to the low temperature, there did not appear to be any protein hydrolysis, loss of 8.4% weight was marginally greater than the SD. Whereas, for 65 and 90°C, the rate of recovery was greater, peaking at 30 and 5 minutes, respectively. However, the precipitate weight then decreased substantially, resulting in a loss of 32.3% for 65°C and 59.1% for 90°C.

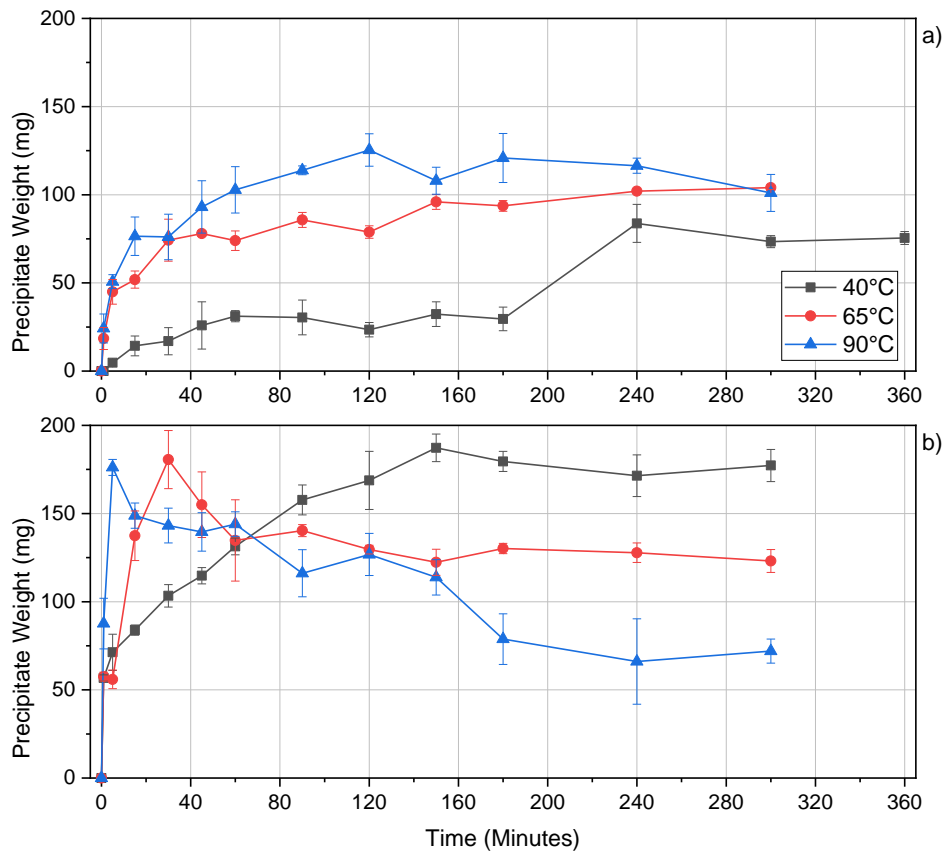


**Figure 6.3-6:** The effect of temperature on the precipitate weight from water lettuce utilising alkali acid extraction. Error bars demonstrate the replicate variation. a) 0.1M NaOH; b) 1.0M NaOH.

As suggested by the issues of high temperatures on protein coagulation and hydrolysis, under conditions of 0.1 M NaOH, the impact of temperature appeared to be extraction time dependent. Utilising Equation 6-3 and Equation 6-4, the percentage relative difference of the precipitate weights, with respect to extraction time, can be calculated to determine the impact of temperature at each extraction time. Where  $W_{t,a}$  and  $W_{t,b}$  are the precipitate weights at time  $t$  for conditions a and b;  $\Delta W_t$  is the relative change between precipitate weights at time  $t$ ; and  $\%RPD_t$  is the percentage relative difference between the precipitate weights, at time  $t$ .

**Equation 6-3:** Relative difference between precipitate weights, under conditions a and b, at time  $t$ .

$$\Delta W_t = W_{t,a} - W_{t,b}$$

**Equation 6-4:** Percentage relative difference between precipitate weight at time  $t$ .

$$\%RPD_t = \Delta W_t / \left( \frac{W_{t,a} + W_{t,b}}{2} \right)$$

Figure 6.3-7 depicts  $\%RPD_t$  and demonstrates that the impact of temperature, in 0.1 M NaOH, was greater from 40°C to 65°C, than 65°C to 90°C. However, due to the high standard deviation, there appears to be no significant difference in the  $\%RPD_t$  of

90°C/65°C. There is a clear decline of the %RPD<sub>t</sub> from 5 minutes and a plateau, or steady state, from ~30 minutes and onwards for 90°C/65°C, until 240 minutes where there is a reduction. In 1.0 M NaOH, there was no relationship that could be discerned between the temperatures, however, all reduced with time due to loss or dilution of protein.

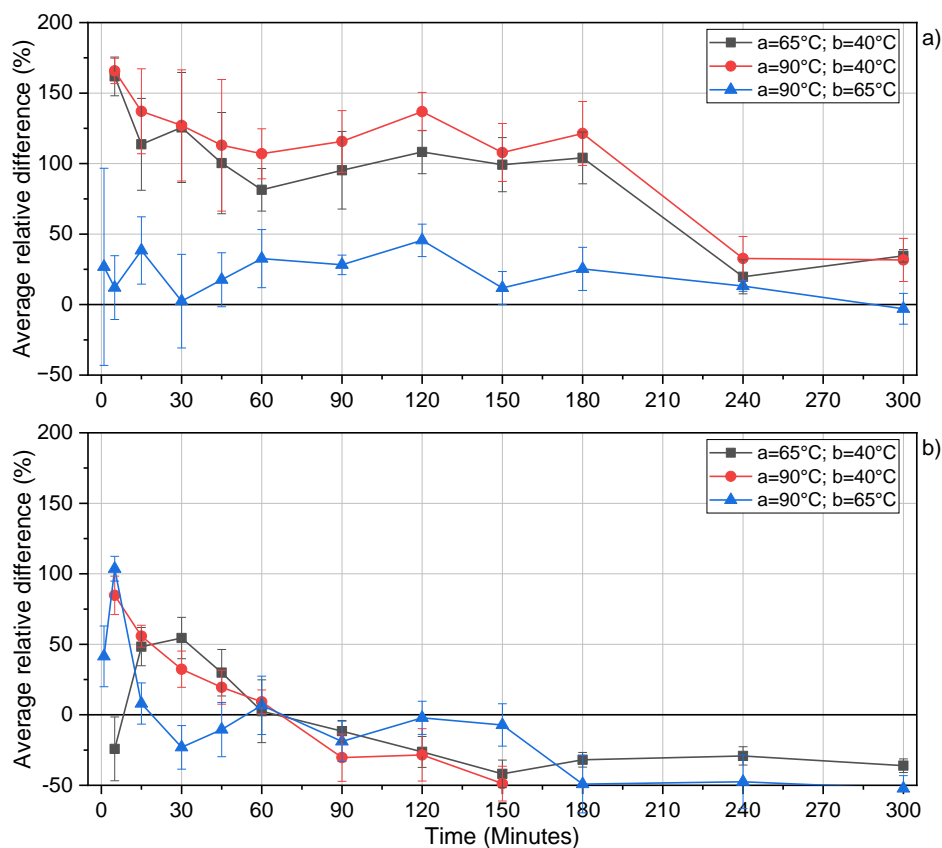


**Figure 6.3-7:** Percentage relative difference (calculated via Equation 6-4) between precipitate of each condition, with respect to extraction time, for alkali acid extraction. Error bars demonstrate the replicate variation. a) 0.1 M NaOH; b) 1.0 M NaOH.

To understand if the loss in precipitate weight, experienced in the 90°C/0.1M, 65°C/1.0M and 90°C/1.0M, was due to protein hydrolysis, or loss of non-protein compounds from the precipitate, the protein content of the precipitate was analysed. Figure 6.3-8a demonstrates that the difference between the protein content was minimal for 0.1 M NaOH, with the exception of 65°C/0.1M at 5 minutes. This suggests that the rate of recovery of protein was equal to non-protein compounds; it is possible that this was due to greater hydrolysis of complex carbohydrate occurring with longer time allowances. The lack of decrease at the higher extraction times implies that the decrease in precipitate weight of 90°C/0.1M, at 200 minutes, was due to loss of both non-protein compounds and protein hydrolysis.

In contrast, at the higher alkali conditions protein hydrolysis occurred at 90°C from 30 minutes and onwards, resulting in a up to 15.1% lower protein content (9.14 to 24.3%).

The protein content stabilised at 180 minutes, suggesting that the remaining protein structures had a greater heat resistance. The hydrolysis of protein was a result of the higher temperature and alkali concentration, whilst this was less obvious for the other temperatures at 1.0 M NaOH, they both exhibit a reduction in protein content at longer extraction times (between 8-9% from peak).

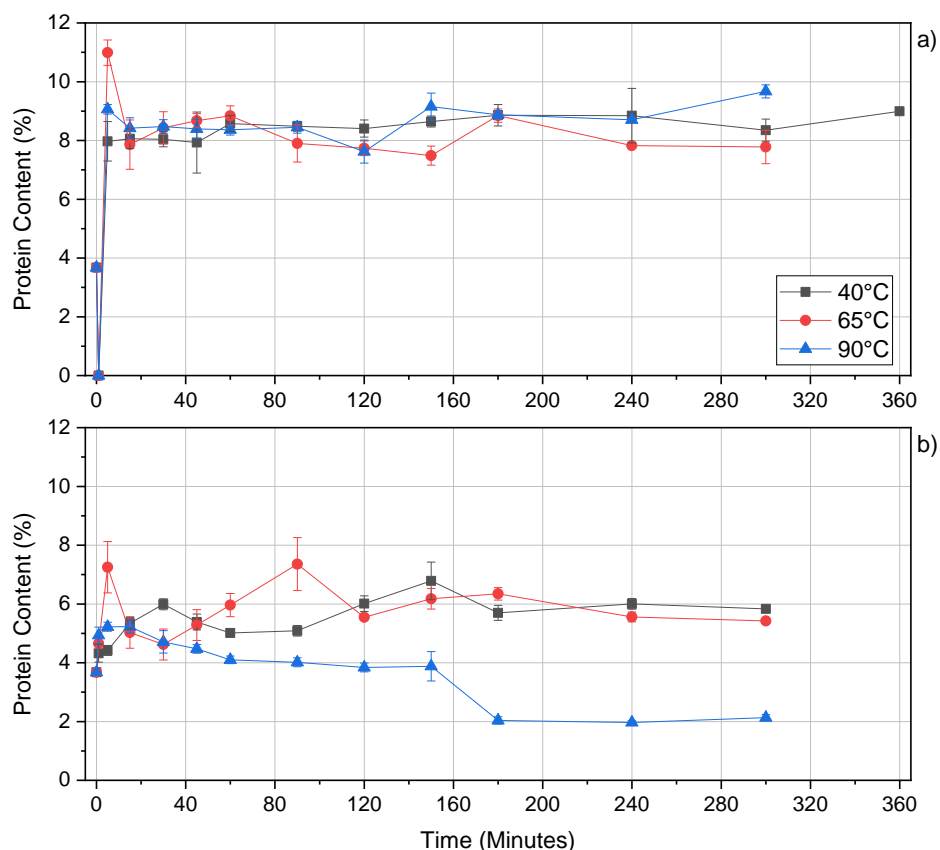


**Figure 6.3-8:** The effect of temperature on the protein content of protein precipitate from water lettuce utilising alkali acid extraction. Error bars demonstrate the replicate variation. a) 0.1M NaOH; b) 1.0M NaOH.

A selected number of precipitate samples were analysed for ash content to determine the trend across the whole set, the results are displayed in Figure 6.3-10. The ash content at 0.1M shows that, compared to the raw plant biomass, a reduction occurred as a result of the extraction, followed by a minor reduction with respect to extraction time and temperature. This suggests that AAE at 0.1 M NaOH has a significant reduction on ash content, however, it is unlikely that temperature has an impact on the ash content at this alkalinity. At 300 minutes, for 40°C/0.1M, there was a slight increase in ash content, suggesting that ash plays a role in the increased precipitate weight from 180 minutes. This is in contrast to all other analysis (C, H, N and S) which showed no percentage increase over this extraction time.

The protein recovery, depicted in Figure 6.3-9, showed similar trends to protein weight: temperature improved recovery at 0.1 M NaOH, whereas at 1.0 M, temperature reduced recovery as extraction time was increased.

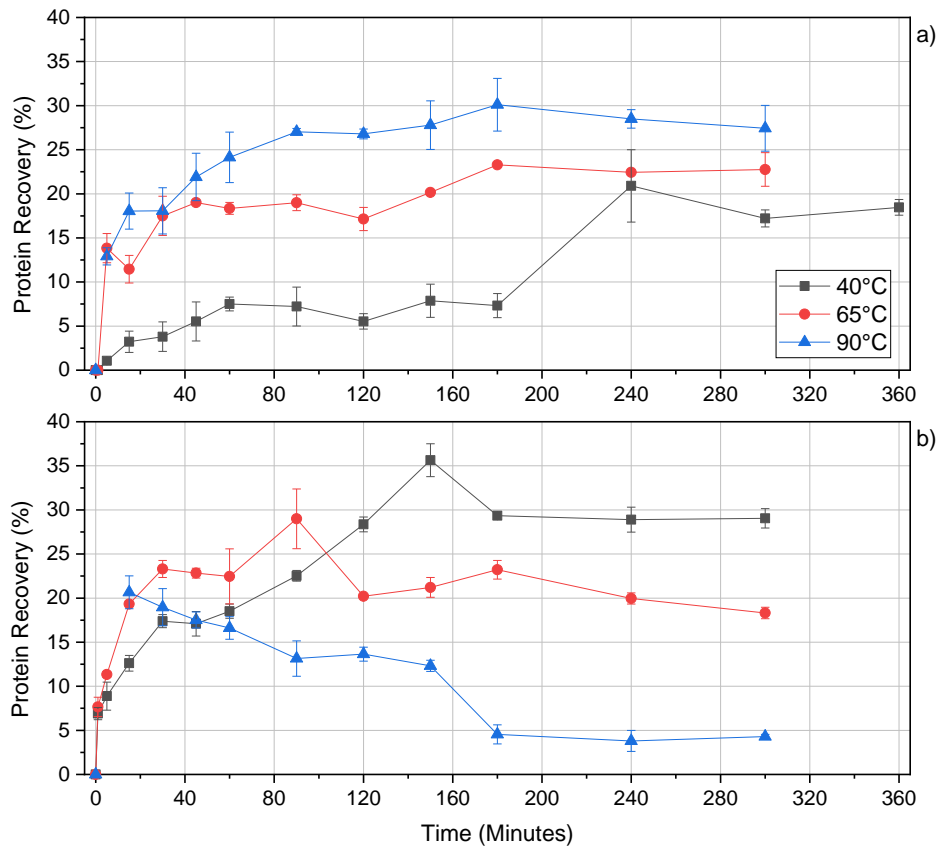


**Figure 6.3-9:** The effect of temperature on the protein recovery from water lettuce utilising alkali acid extraction. Error bars demonstrate the replicate variation. a) 0.1M NaOH; b) 1.0M NaOH.

At 1.0M NaOH, the ash content showed an increase on the raw plant sample, likely due to the higher concentration of Na and SO<sub>4</sub> salts, and showed little variation for 40 and 65°C, see Figure 6.3-10b. In contrast to 0.1 M conditions, there was a distinct difference between the ash content of each temperature condition. The ash content at 65°C was lower, at all measured points, than 40°C, whilst 90°C increased until 180 minutes, where it appeared to plateau. The increase demonstrates the inverse of protein content and precipitate weight, suggesting that the ash content did not change, rather the proportion. To examine this, the total ash weight was calculated via Equation 6-5, where  $Ash_t$  is the ash weight at time t; and  $Ash\%_t$  is the percentage ash content at time t. Figure 6.3-11 displays the results.

**Equation 6-5:** Ash weight at time t.

$$Ash_t = Ash\%_t \times W_t$$

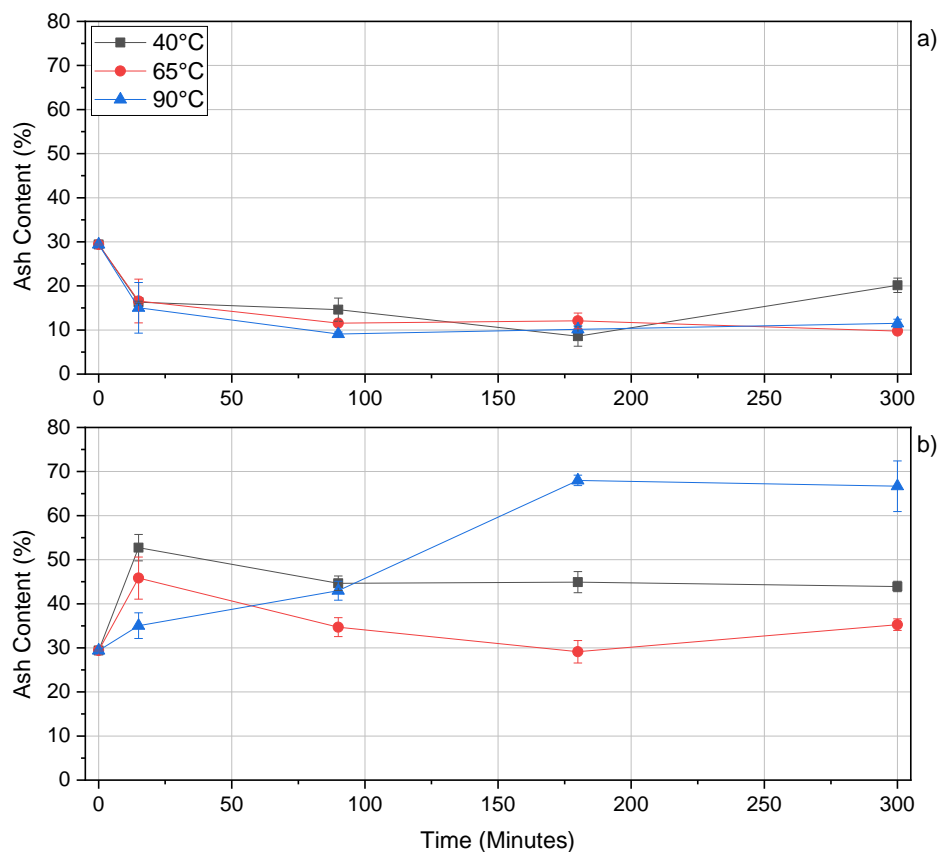


**Figure 6.3-10:** The effect of temperature on the ash content from water lettuce utilising alkali acid extraction. Error bars demonstrate the replicate variation. a) 0.1M NaOH; b) 1.0M NaOH.

Figure 6.3-11a shows that the ash increase was responsible for 27.5% of the increase in precipitate weight, at 240 minutes for 40°C/0.1M. Whilst the percentage ash content only has a percentage increase of 133%, the ash weight increase by 479%. The majority of the increased weight is likely to have come from organic compounds.

Figure 6.3-11b shows that whilst the percentage ash content increased for 90°C/0.1M, the weight did not change, demonstrating that temperature and extraction time had no impact on ash weight, but the reduction in protein content or increased organic recovery resulted in the increased ash proportion.

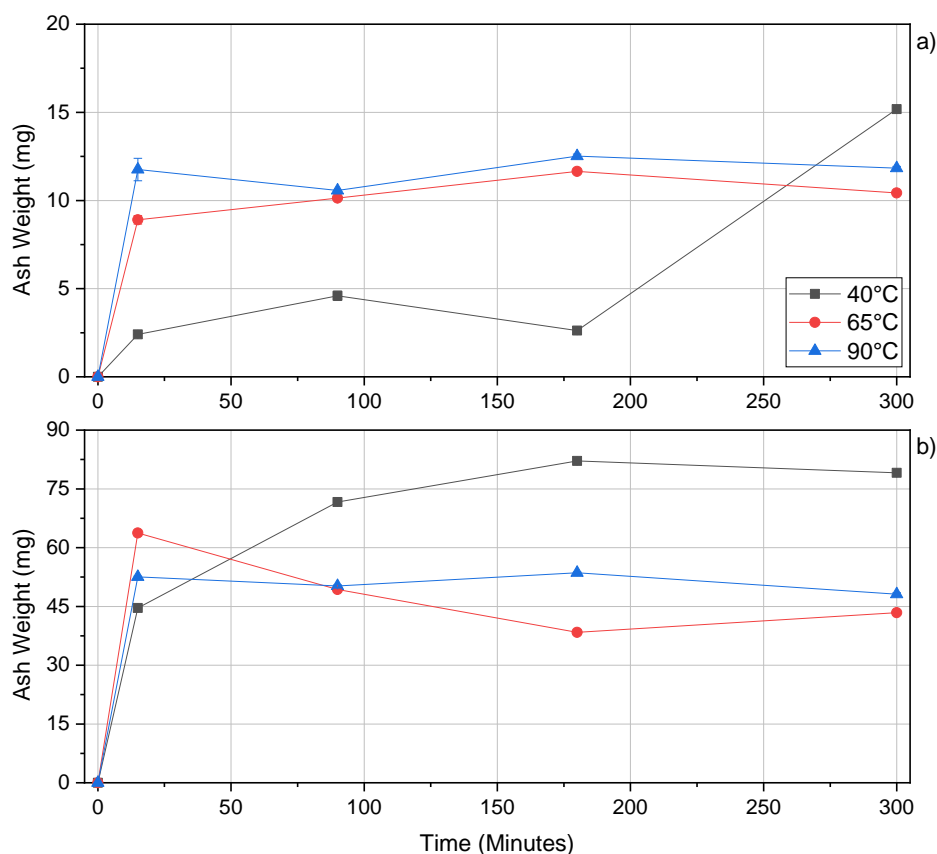


**Figure 6.3-11:** The effect of temperature on the total ash weight from water lettuce utilising alkali acid extraction. Error bars demonstrate the replicate variation. a) 0.1M NaOH; b) 1.0M NaOH.

The results of the impact of temperature on AAE suggest that at conditions of high hydrolysis potential, both high temperature and alkalinity, temperature had the greater impact on the precipitate weight and protein content, than at conditions of lower hydrolysis potential. Secondly, temperature can cause protein hydrolysis at long exposure extraction time or high alkalinity. Prolonged periods of high temperatures can be costly and cause protein hydrolysis/coagulation, resulting in lower yields for a greater price, therefore lower temperature must be considered where possible.

### 6.3.3. Influence of alkali concentration on alkali acid extraction

It has been suggested that the absolute amount of alkali has the defining role in in alkali-acid extractions [256]; this is in relation to the pH/agent concentration and solid-liquid ratio [240]. For the purposes of comparing extraction conditions, the solid-liquid ratio was maintained at 40 ml to 1 g feedstock, as suggested by Shen *et al.*, whereas the pH/agent concentration was varied.

Two concentrations were selected: 0.1 and 1.0 M of NaOH. The precipitate weight variations are depicted in Figure 6.3-12; this highlights the impact of increased alkalinity, however, this impact appears to be variable, depending on extraction time and temperature. At 40°C, the percentage increase of the precipitate weight appears to



be greater than at 65 or 90°C, across the whole of the experiment. To illustrate the increase, the %RPD<sub>t</sub> was calculated and displayed in Figure 6.3-13; this confirmed the assumption, whilst also suggesting that there was no significant difference between this impact of agent concentration at the higher temperatures. As suggested by temperature, the increase in precipitate weight was greater during shorter experiments before the increase plateaued from ~15 to 180 minutes.

Utilising 1.0 M NaOH appears to be the optimal choice based on precipitate weight, however, the optimal temperature is still unknown. At 40°C/1.0M the precipitate weight peaked at 187.25 ± 7.85 mg; 65°C/1.0M reached 180.58 ± 16.47 mg; and 90°C/1.0M peaked at 176.16 ± 4.56 mg. The error observed demonstrates that all three temperatures overlap, therefore the protein content and recovery must be analysed.

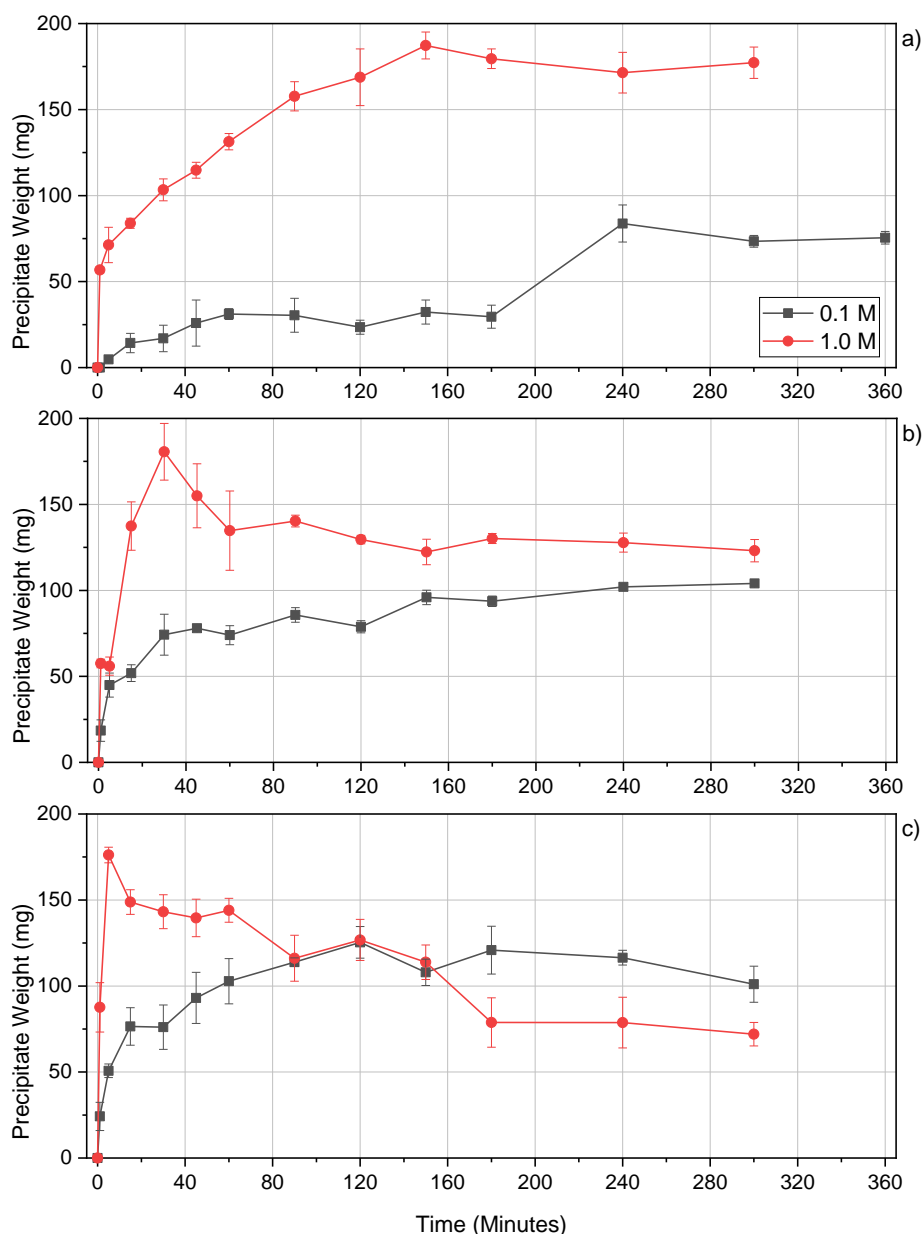


**Figure 6.3-12:** The effect of alkali concentration on the precipitate weight from water lettuce utilising alkali acid extraction. Error bars demonstrate the replicate variation. a) 40°C; b) 65°C c) 90°C.

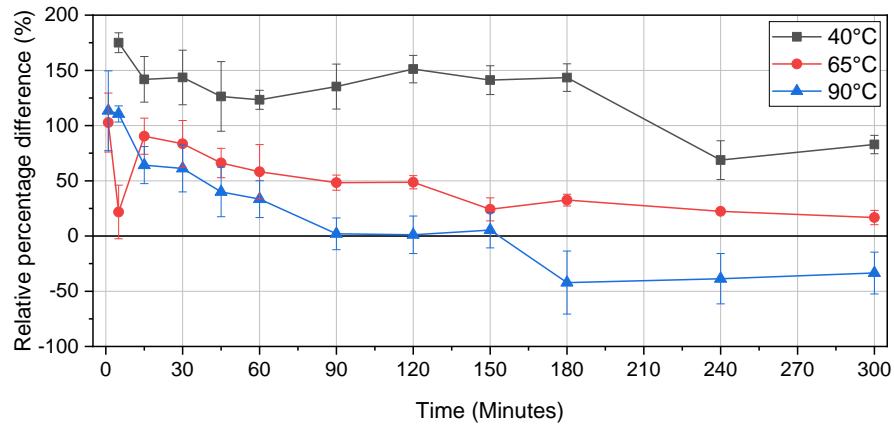


**Figure 6.3-13:** Percentage relative difference (calculated via Equation 6-4) between precipitate of 0.1 and 1.0 M of NaOH, with respect to extraction time. a= 0.1 M NaOH; b= 1.0 M NaOH. Error bars demonstrate the replicate variation.

The agent concentration appeared to have the greatest impact, of the three parameters studied, on the final precipitate protein content, see Figure 6.3-14. At all temperature conditions, the 1.0 M concentration demonstrated a lower percentage protein content within the precipitate, with 90°C demonstrating the lowest content, likely due to the hydrolysis caused by higher temperatures and alkalinity.

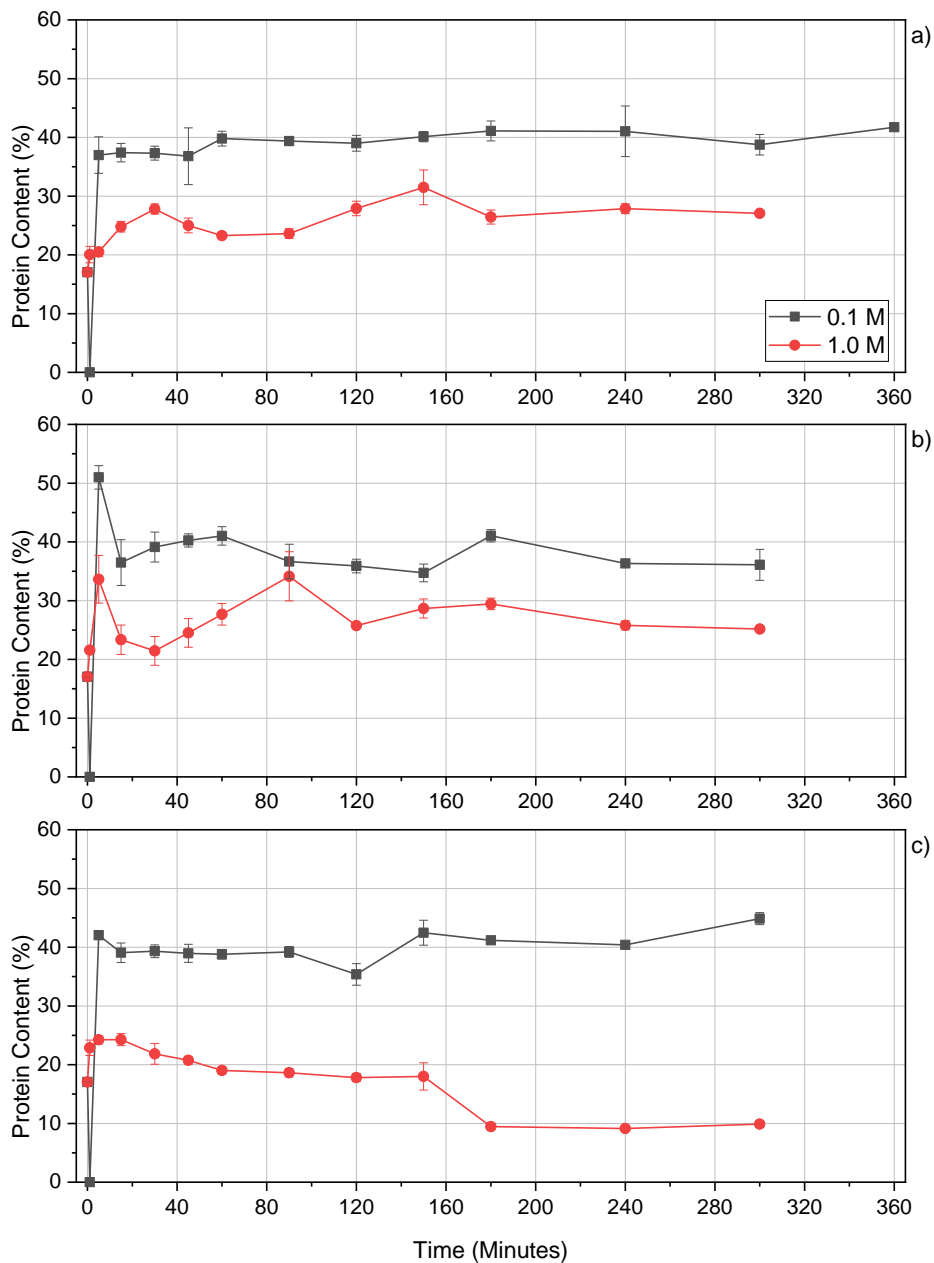


**Figure 6.3-14:** The effect of alkali concentration on the protein concentration of the protein precipitate from water lettuce utilising alkali acid extraction. Error bars demonstrate the replicate variation. a) 40°C; b) 65°C c) 90°C.

The impact of alkalinity on protein content of the precipitate, had a dramatic effect on the protein recovery. Whilst the precipitate weight was similar for the peak at each temperature for 1.0 M, the protein yield was not. Figure 6.3-15 shows that the recovery peaks at  $34.50 \pm 1.80\%$  for 40°C/1.0M;  $28.07 \pm 3.28\%$  for 65°C/1.0M; and  $25.06 \pm 1.33\%$  for 90°C/1.0M. The recovery was not higher for 1.0 M at all temperatures: the peak recovery at 40°C was 34.50% for 1.0M compared with 20.23% for 0.1M, and shows an %RPD of 12.5% recovery yield, across all time points. In comparison, 65°C had a peak recovery of 28.07% for 1.0M compared with 22.55% for 0.1M, with an ARD of 2.52%. At 90°C, the impact of higher alkalinity reversed, resulting in a greater

recovery at 0.1 M: the peak recovery for 1.0 M was 25.06% compared with 29.14% for 0.1 M, and showed an ARD of -7.35%. The increased hydrolysis potential at high temperatures and alkalinities would result in a greater and more rapid release of protein, therefore, the protein was exposed to higher temperatures and alkalinities for greater periods of extraction time, which can result in hydrolysis and coagulation.

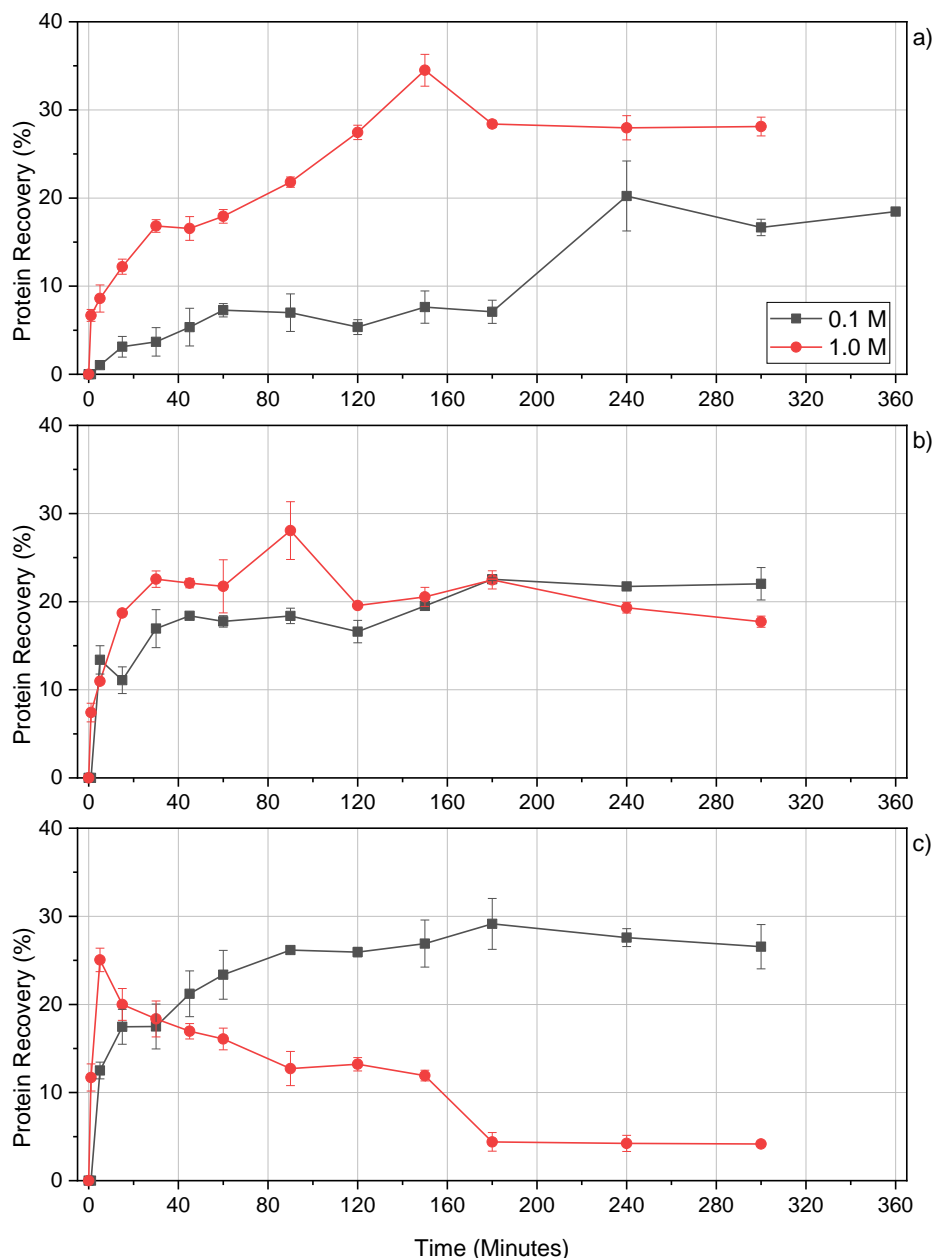


**Figure 6.3-15:** The effect of alkali concentration on the protein recovery from water lettuce utilising alkali acid extraction. Error bars demonstrate the replicate variation. a) 40°C; b) 65°C c) 90°C.

The decreased protein content at 1.0 M did not result in a lower protein recovery, at lower temperatures. This was likely due to the increased precipitate weight and increase of non-protein compounds. This was evidenced by the increase of ash content in 1.0 M, in comparison to 0.1 M, see Figure 6.3-16. During precipitation, greater

H<sub>2</sub>SO<sub>4</sub> was required to acidify the solution, due to the presence of more OH<sup>-</sup> ions, therefore, a greater amount of sodium sulphates formed. These salts are likely to cause the increased ash content at 1.0 M; evidence of this came from the proximate analysis via TGA. The selected precipitates were ashed at 550°C, rather than the standard 900°C, to ensure no evaporation of Na or K [137]. As a comparison, a select number of samples were analysed at 900°C as an estimation of Na content. However, due to the presence of Na and S, low melting point sodium sulphates [358], and possibly higher melting point sodium-aluminium silicates (due to high Ca content) [359], were likely to be present. These formed a glass like substance in the base of the crucible, see Plate 6.3-1. The result produced an increase in weight during ashing and voided the results. Therefore, further analysis was conducted on the fate of heavy metals within the extraction through elemental analysis.

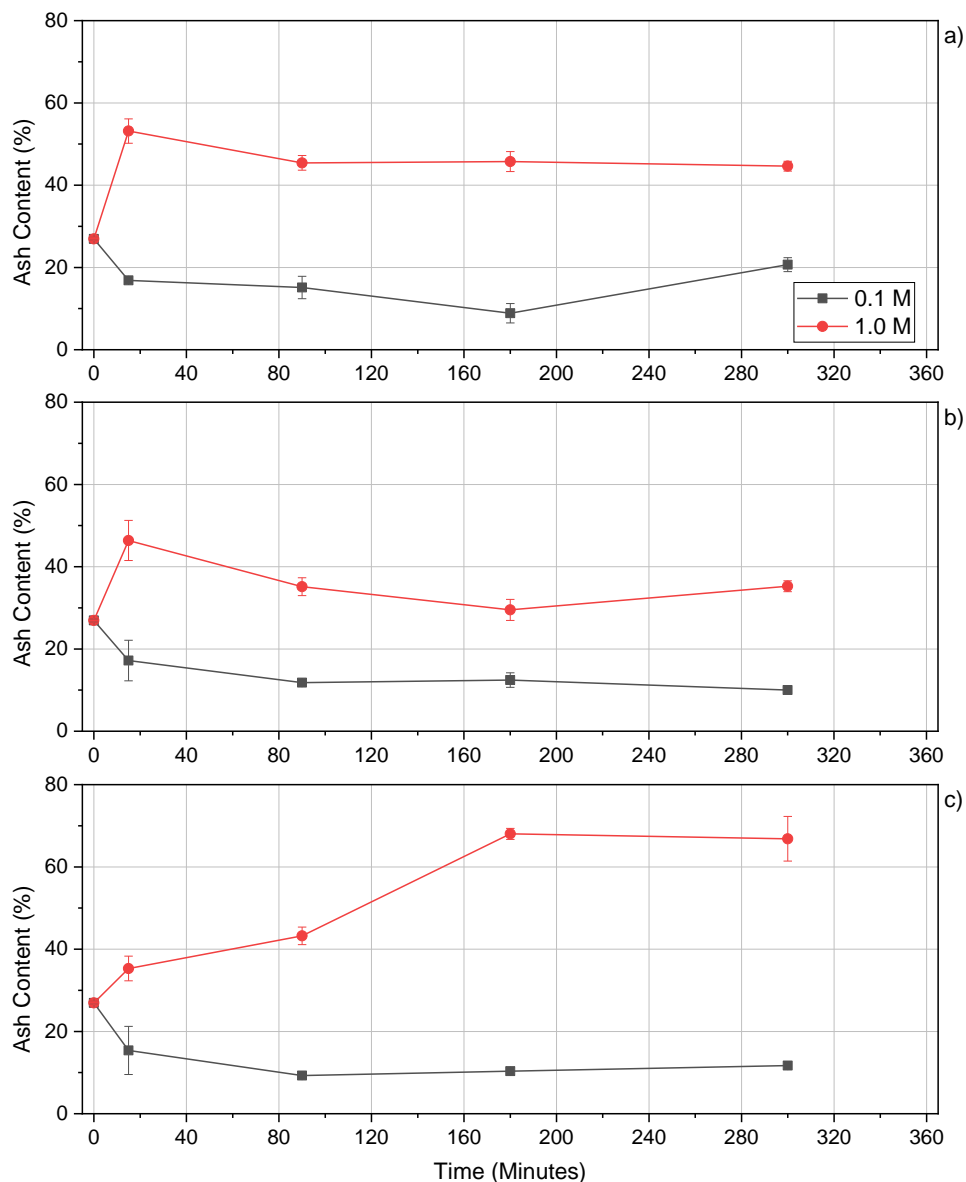


**Figure 6.3-16:** The effect of alkali concentration on the percentage ash content of protein precipitate from water lettuce utilising alkali acid extraction. Error bars demonstrate the replicate variation. a) 40°C; b) 65°C c) 90°C.

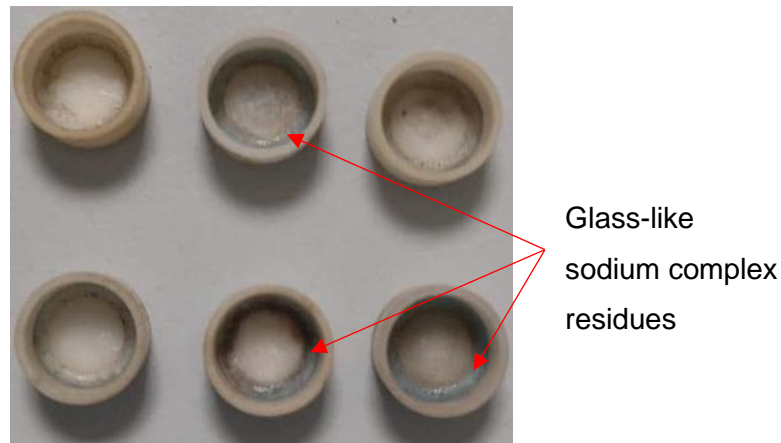


**Plate 6.3-1:** Product formed in the thermo-gravimetric analysis crucible at 900°C.

#### 6.3.4. Fate of trace nutrients and heavy metals in water lettuce

As demonstrated in section 6.2.3, the precipitate did not contain high levels of HMs, however, it did contain high levels of Na and S. However, it is possible that the different conditions may not have followed this rule. Figure 6.3-17 demonstrates the HM content of four precipitates. These were selected as the peak precipitate weight from each condition, that contained enough product to fulfil a single replicate, with the exception of 40°C/1.0M/150 which was conducted in duplicate. Therefore, these results must be interpreted with caution.

The results demonstrated that the HM content of the precipitate followed a similar trend as demonstrated by 6.2.3: the HMs were contained within the residue, with a smaller proportion located in the precipitate. However, the whole samples were above the MPL for human consumption [343] and whilst there was little legislation on animal feed, it is likely these values would be considered dangerous, due to the high levels of Cr (3.3-12.5 ppm), Cu (38.6-70.3 ppm), Pb (3.5-5.7 ppm) and Zn (22.7- 65.5 ppm). In comparison, the Na and S content was greatly increased. Whilst it was not possible to estimate the impact of each parameter, due to the variances of extraction time between each sample, it was clear that increased agent concentration resulted in a greater Na and S concentration. The results of HMs and Na and S, suggest that this was not a suitable for human or animal consumption at current levels. Secondly, the recovery yields were relatively low, though this is not unexpected for alkali acid extractions, therefore, optimisation of the extraction may be possible to improve both the inorganic content and the yield.

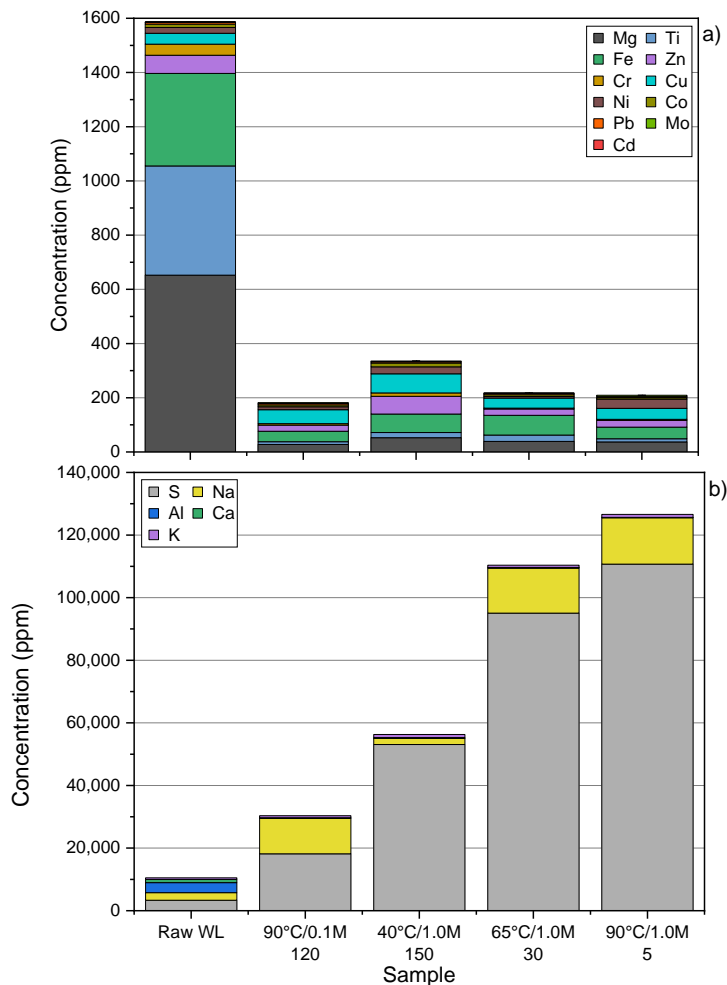


**Figure 6.3-17:** Elemental composition of precipitate from water lettuce utilising alkali acid extraction at a variety of conditions- temperature (°C) / alkali concentration (M) time (minutes). a) low concentration elements; b) high concentration elements.

### 6.3.5. Residue analysis in water lettuce

The residue analysis in section 6.2.4, demonstrated that the residue had increased  $BMP_{ex}$  and decreased HM content; the same analysis was conducted on WL. Table 6.3-4 demonstrates that WL residue followed a different trend to the WH samples: the VM, C, N, and O were all reduced, whereas the FC, ash, H, C:N and maximum  $BMP_{th}$  increased. The increase in ash content was 34% for WL compared with over 100% for both of the WH samples. The N content reduction was also significantly different: the reduction of WL N was 56% compared with an average of 26% for the WH samples. The larger N decrease resulted in a greater C:N ratio increase, in comparison to the WH samples. Whilst the maximum  $BMP_{th}$  increased, it was less than shown by the WH samples, increasing by 18% compared with 31 and 51% for the WH whole and leaf samples, respectively.

**Table 6.3-4:** Composition of raw biomass and residue from alkali acid extraction on water lettuce at 40°C/1.0m/150 minutes.

Sample	Raw Biomass	Residue
VM (% db)	64.2 ± 0.3	46.6 ± 0.9
FC (% db)	8.8 ± 0.0	13.6 ± 0.3
Ash (% db)	26.9 ± 0.4	35.5 ± 0.3
C (% db)	28.7 ± 0.0	26.4 ± 0.2
H (% db)	3.0 ± 0.0	3.2 ± 0.3
N (% db)	3.7 ± 0.1	1.6 ± 0.4
S (% db)	0.3 ± 0.0	0.0 ± 0.0
O* (% db)	37.3 ± 0.0	33.3 ± 0.9
C:N	7.8 ± 0.1	16.6 ± 3.5
Protein <sup>+</sup> (%)	17.1 ± 0.3	7.6 ± 1.6
HHV (MJ/kg)	10.9 ± 0.0	10.2 ± 0.3
Max BMP <sub>th</sub> (mL CH <sub>4</sub> /g VS)	274.7 ± 0.3	324.5 ± 19.5
BMP <sub>ex</sub> (mL CH <sub>4</sub> /g VS)	227.9 ± 0.0	181.1 ± 11.6
BI (%)	83.0 ± 0.0	55.8 ± 0.6

\*Calculated by difference; \*Calculated with co-efficient (4.64) by N

The trace elemental content also differed from the WH residues: the Ca, Fe and Mg concentrations increased, and the concentration of Al decreased. These were opposite the results found by the WH samples. Secondly, the increase in Na and decrease in K content was significantly lower than shown for WH. These results suggests that metal distribution and association was different in WL as to what was observed in WH. The decrease in Fe content in WH was likely due to the weak association between Fe and the surface of WH roots [149], it is possible that WL had a stronger uptake of Fe. This hypothesis was corroborated by the high TF of Fe by WL: Kumar *et al.* demonstrated that WL had a TF of ~1 under a range of conditions, in comparison, this study showed that WH had a TF of <0.5 for all but one sample, see Chapter 4. This suggests that Fe within WL was associated more strongly than the surface adsorption of Fe by WH, therefore it was not removed by an alkali treatment. Al showed the opposite trend, it is a HM associated with weak adsorption to WH roots, and therefore would likely be reduced by alkali treatment. Whilst this occurred with WL, it did not occur with the WH samples. In comparison, Ti was reduced by 75%; this was a greater reduction than WH, although this was likely due to the higher concentrations of Ti in the WL sample than WH, therefore, further analysis of a WH sample from the same river would be required for comparison to be made.



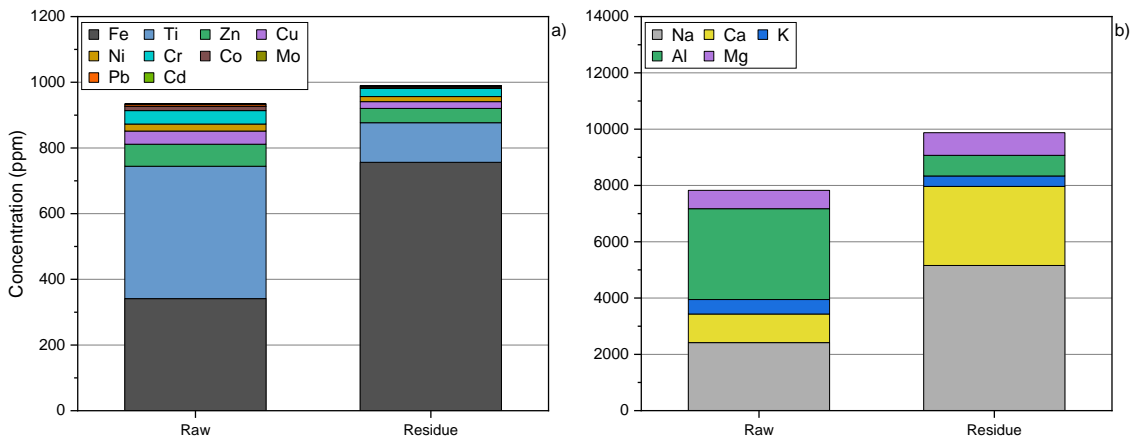


**Figure 6.3-18:** Trace elemental comparison of raw biomass and residue from alkali acid extraction on cultivated water lettuce at 40°C/1.0M/150 minutes. low concentration elements; b) high concentration elements.

The high lignin and low cellulose content of WL suggests that it would be a poor choice for AD [137,319], however, the  $BMP_{ex}$  of raw WL was over twice what was shown by raw WH, 228 and 112 mL  $CH_4/g$  VS, respectively. This did not translate to improved methane production from the WL residue, which showed a 21% decrease as compared with raw biomass, Figure 6.3-19.

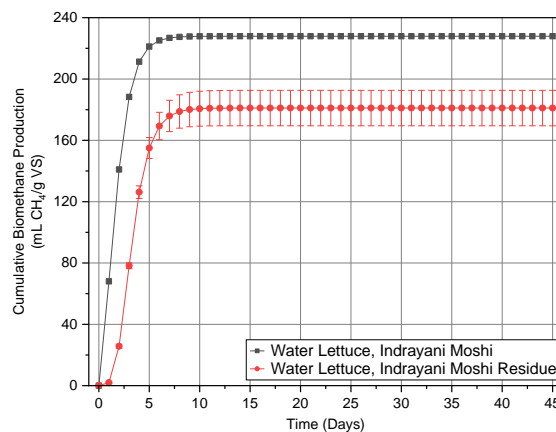


**Figure 6.3-19:** Experimental bio-methane potential of raw biomass and residue from alkali acid extraction on water lettuce at 40°C/1.0M/150 minutes. Error bars demonstrate the replicate variation.

### 6.3.6. Optimisation of extraction

To optimise the extraction, three experiments were conducted: removal of sodium sulphate contaminants; precipitation pH; and solid-to-liquid ratio. All optimisation experiments were conducted at the optimum protein recovery yield: 40°C/1.0 M/150 minutes.

#### 6.3.6.1. Removal of sodium sulphate contaminants

The elemental and proximate analysis of the protein precipitate demonstrated that the precipitate contained high concentrations of Na and S, as well as HMs above the MPL

for human consumption. Removing these HMs could be challenging, as it is possible that these HMs were not directly associate with protein, but have formed compounds, like aluminosilicate [359], that have an extremely low solubility [360]. Therefore, the target of this experiment was to remove sodium sulphate compounds, which have a high solubility in water [361]. After the solution was centrifuged and decanted, to separate the precipitate, the precipitate was washed with warm water, shaken and centrifuged. Table 6.3-5 displays the analysis of the raw biomass, precipitate and the precipitate after it had been washed.

This demonstrated that some precipitate was removed/lost during the washing process; some of this loss was protein, with a reduction in recovery by 7.6%, however, the protein content was increased by over 10%. This was due to the substantial reduction in ash content, which was reduced by over 30%. This demonstrated that the washing of precipitate could be a vital part of the process for producing protein via alkali acid extraction to ensure the protein is of sufficient quality. The precipitate was then analysed for elemental composition to understand if the HM, Na or S content had been reduced as part of the washing process.

**Table 6.3-5:** Analysis of protein precipitate after washing in comparison to reference and raw biomass.

Sample Reference	Precipitate Weight (mg)	Protein Recovery (%)	Protein Content (%)	Ash Content (%)
Raw Biomass	-	-	17.1 ± 0.3	26.9 ± 0.4
40C/1.0M/150	154.1 ± 19.9	31.4 ± 2.6	34.1 ± 2.8	36.6 ± 0.0
40C/1.0M/150 Wash	84.0 ± 13.2	23.8 ± 3.3	45.5 ± 0.7	3.8 ± 0.6

Figure 6.3-20 compares the three samples for the elemental composition. The extraction process reduced the concentration of Al, Ca, Cr, Fe, Mg, Ni, K, Ti and Zn, however, the concentrations of Cu, Na, Pb and S were increased. The washing step resulted in an increase of Al, Co, Cu, Fe, Ni, Pb, Ti and Zn; the most important of the changes were Cu (54% increase); K (87% decrease); Na (92% decrease); Ni (117% increase); Pb (49% increase); and S (81% decrease).

The washing step clearly decreases the sodium sulphates that formed during the precipitation step, resulting in a 92 and 81% decrease in Na and S, respectively. However, both of these were still higher than the raw biomass, 104 and 311%, respectively. It may be possible to reduce this by further utilising higher temperature water, multiple rinses or longer residence time; further investigation would be required.

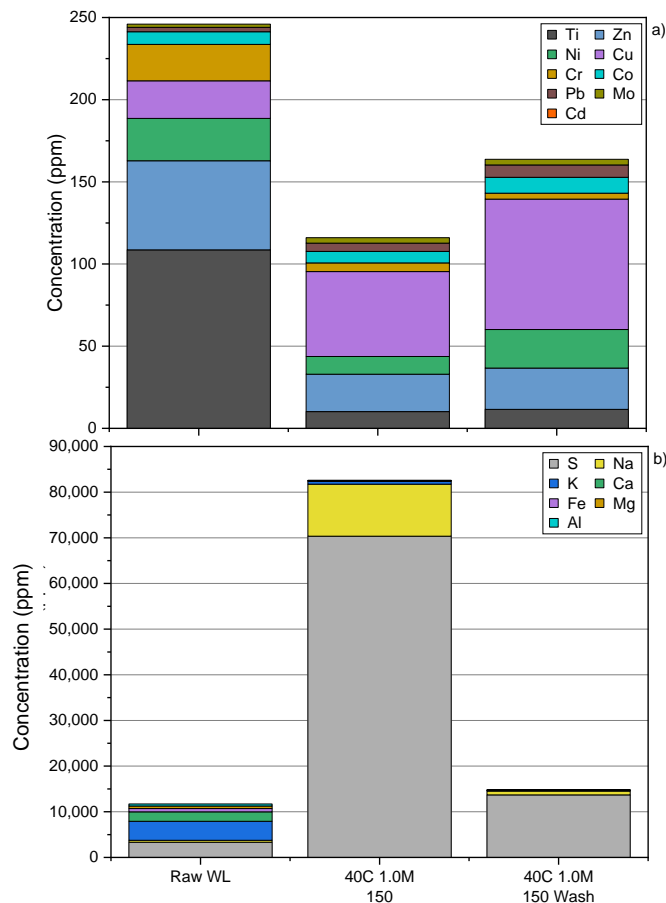


**Figure 6.3-20:** The effect of washing on elemental composition of precipitate from water lettuce utilising alkali acid extraction - a) low concentration elements; b) high concentration elements.

### 6.3.6.2. Isoelectric precipitation pH

The optimal isoelectric point varies depending on the feedstock: *Ulva sp.* was shown to have an increased protein recovery when the pH was reduced from 5 to 2 [242]. Similar to *Saccharina latissimi*, which had a peak precipitation at pH 2/3. In contrast, *Spirulina platensis* [270], alfalfa leaves [268] and green tea residue [256], all showed a peak precipitation at pH 3.5-4. Spent brewer's grain also had an optimum precipitation at pH 3-5 [269]. To analyse this impact on WL protein, two conditions (40°C/1.0 M/150 minutes and 40°C/0.1 M/150 minutes) were conducted and the precipitation pH varied from 3-5.

The precipitate weight increased from pH 5 to 4, then showed little variation between pH 4 and 3. The impact of pH was greater at 0.1 M NaOH, increasing by the weight by 135% from pH 5 to 3, whereas, at 1.0 M NaOH, the increase was only 16%.

The protein content demonstrated a similar trend, increasing as pH was increased, however, for 0.1 M NaOH, the protein content peaked at pH 4. The protein content also showed a greater increase for 0.1 M NaOH, a maximum increase of 30%, compared with 7% for 1.0 M.

The impact of precipitation pH was exaggerated for protein recovery: at 0.1 M NaOH, the increase was 240%, whereas for 1.0 M NaOH, the increase was just 24%, from pH 5 to pH 3. This demonstrated that the optimal pH for precipitation of WH protein was between pH 3-4; further investigation would be required to narrow this range.

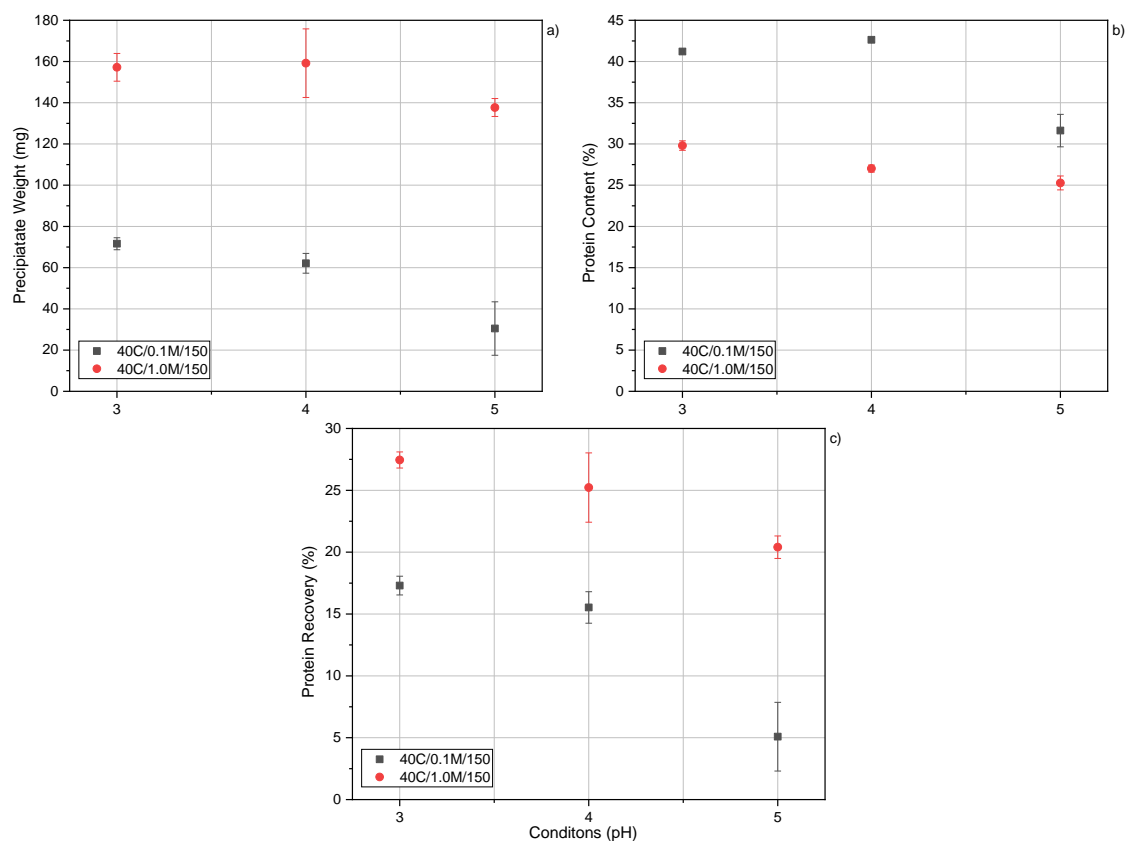


**Figure 6.3-21:** The impact of changing the precipitation pH. Error bars demonstrate the replicate variation. a) precipitate weight; b) protein content; c) protein recovery.

### 6.3.6.3. Solid-to-liquid ratio

The absolute amount of alkali has been stated as the critical parameter in AAE [256], the concentration of the alkali was selected to understand this impact, however, the solid-to-liquid ratio (S:L ratio) must also be investigated. A low S:L ratio is unlikely to be implemented on a industrial scale due to the high running costs [255], unless the recovery could be drastically increased. Shen *et al.* demonstrated that decreasing the S:L ratio from 1:20 to 1:40 (g/mL) doubled the protein recovery, however, from 1:40 to 1:50 there was only a marginal increase [357]. Three S:L ratios were selected, 1:20, 1:40 and 1:60, see Figure 6.3-22.

The precipitate weight showed a linear increase as the S:L ratio was decreased, the overall increase was 143%. In contrast, the protein content peaked at 1:40, then decreased at 1:20 and 1:60. This was reflected by the protein recovery which was lowest at 1:20, then showed little difference between 1:40 and 1:60, similar to what

Shen *et al.* demonstrated when decreasing the S:L ratio beyond 1:40. Therefore, it is likely that 1:40 would be utilised at scale to reduce costs.

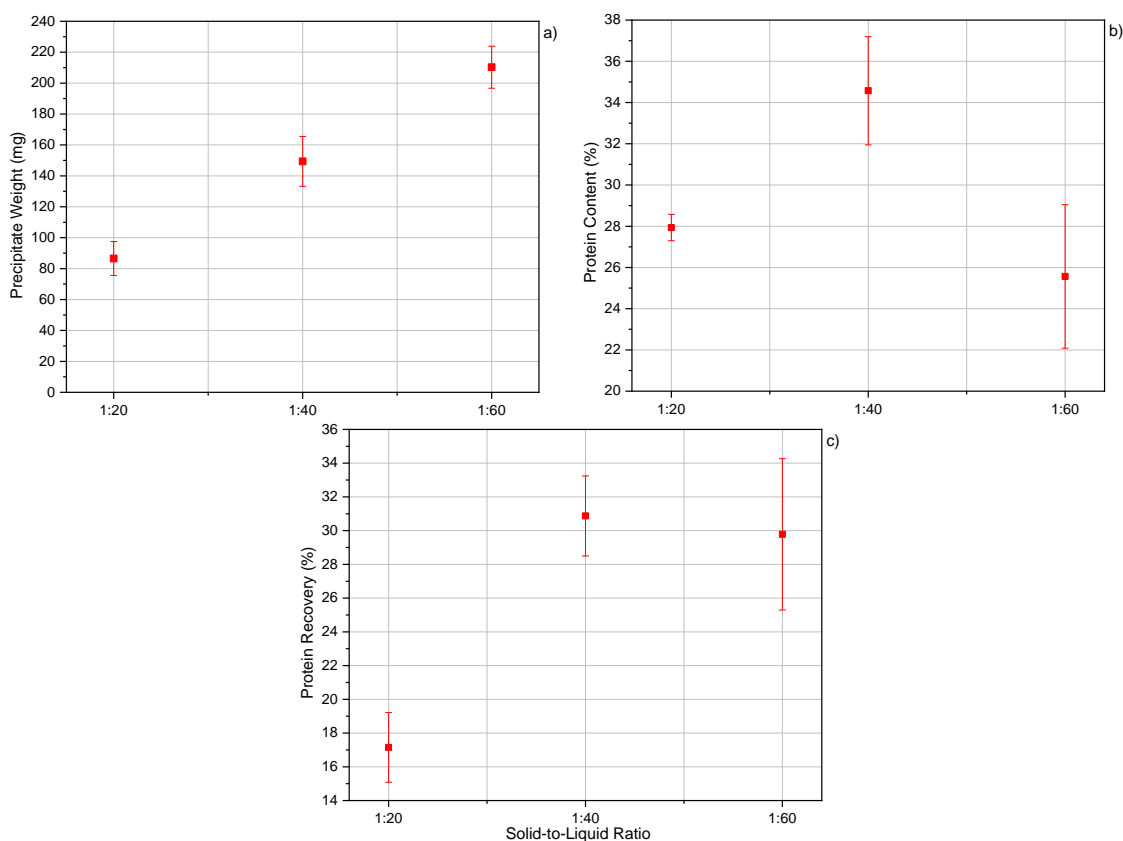


**Figure 6.3-22:** The impact of changing the precipitation pH. Error bars demonstrate the replicate variation. a) precipitate weight; b) protein content; c) protein recovery.

## 6.4. Conclusions

This chapter aimed to investigate the potential for protein extract from WH and WL, via alkali solubilisation and acidic precipitation. Including, the determination of the effect of feedstock variation on protein yield; understanding the effect of extraction conditions on protein yield; and investigating the potential for improving the extraction yield.

A selection of 24 samples were selected for AAE at 40°C and 1.0 M NaOH for 150 minutes. These samples had varied plant parts, with the majority focussing on leaf and whole plants. The samples originated from a variety of locations, including: Pune, both harvested from a river and cultivated samples; West Bengal pond samples; Murchison Bay samples harvested from different locations in the bay within Lake Victoria; IBERS cultivated samples, both wet and dry samples; and a sample of WL from Pune. The residue, from the alkali treatment, and the precipitates, from the alkali acid treatment, were analysed to understand the protein yield, ash content and the fate of heavy metals. The optimal sample was then selected for condition analysis, to understand the impact of varying conditions. This sample then underwent extraction optimisation via

the removal of sodium sulphates, varying the pH of precipitation and the solid-to-liquid ration.

Several samples were selected for a small-scale biochemical analysis comparison, this showed that the petiole would most likely be the plant tissue that yielded the poorest protein yield, based on the high cellulose and low protein content, followed by the root and finally the leaf. The experimental results showed that the leaf had the highest protein recovery, whilst the root and petiole showed no significant difference. However, the petiole did show the greatest protein increase in content from raw biomass to the precipitate.

The location study showed a high variability in both structural fibre content and protein content. This suggests that environmental conditions play a significant role in structural fibre ratios and protein content. The WL sample had a more optimal structural fibre ratio and protein content, as compared with the WH samples, demonstrating a low cellulose content and high lignin and protein content. The range in biochemical analysis was mirrored in the results of AAE; the precipitate showed a range of 77.5 and 68.1 mg over the whole and leaf samples, respectively. The protein recovery showed a lower percentage error, the range was 5.6 and 12.7%. The comparison of biochemical analysis across the locations indicated that lignin content had a statistically significant positive impact on precipitate weight. However, when the sample size was increased to include different parts of the plant, this relationship was insignificant. In contrast, the impact of raw plant protein content on the precipitate weight and the precipitate protein content, and the cellulose content on protein content and protein recovery, were significant. However, the limited sample size and assumption of a linear relationship means that further research should be conducted.

The comparison of dry and wet biomass demonstrated a greater protein recovery for the dry leaf and whole plant, however, further information on the energy balance of drying the biomass may illuminate this further.

The comparison of HMs, in the protein precipitate from different tissues, indicated that the leaf and petiole contained similar concentrations of all trace nutrients and HMs, with the exception of Na which was attributed to the methodology error. In contrast, the root precipitate contained over twice the total concentration of trace elements, excluding Na, largely due to the presence of Pb and Ti. This suggests that roots are not an appropriate feedstock for AAE. The cultivated WH leaf sample demonstrated the lowest concentrations of trace elements, however, it contained high enough levels of Cu that >500g of precipitate could be considered toxic to adult humans. WH precipitate was a poor substitute for human and animal consumption, in comparison with pea protein and soybean meal, respectively. However, as an invasive and damaging plant, WH could

be attained cheaply and easily, whilst the removal also provides ecosystem services to local areas, therefore, it could be considered an alternative, especially if the improvements to local ecosystems could be quantified.

The analysis of residues from the AAE demonstrated that the alkali treatment improves the BI of the biomass and therefore improves the  $BMP_{ex}$  by >77% for whole samples. This would increase the value of the extraction: if all energy use could be offset by biogas production from the residue. However, the N and K concentrations in the residue were lower than the raw biomass, suggesting that the digestate produced may be a poor source of nutrients. This could be offset by digesting leaf residue with raw petioles and roots, of which the former contained high levels of N.

In the comparison of extraction conditions on AAE from WL, it was shown that extraction increased with extraction time up to 150 minutes for 5 out of 6 conditions studied; the final condition had the weakest hydrolysis potential and therefore required longer time for hydrolysis to occur. At lower alkalinity, 0.1 M NaOH, temperature improved AAE over all extraction time points; however, at increased alkalinity, 1.0 M NaOH, the higher temperature caused protein hydrolysis as time progressed. The impact of alkalinity appeared to have the greatest impact at lower temperatures, with the greatest increase in yield, between 0.1 M and 1.0 M NaOH, occurring at 40°C. There appeared to be little variation between the conditions analysed for trace element concentration, the largest difference occurring between the different alkali conditions, where 1.0 M NaOH produced a precipitate with significantly more Na and S content than 0.1 M NaOH. The residue analysis was different to that shown by WH: the elemental analysis showed that Fe content increased in the residue, resulting in a greater total concentration of the selected HMs. The concentration of N and K was still low, however, the BI was reduced and a lower  $BMP_{ex}$  achieved for the residue in comparison to the raw biomass.

The optimisation of the extraction showed that sodium sulphate compounds could be easily removed with a warm water wash, however, trace elements, like Cu and Ni, were increased by the wash. The variation of precipitation pH demonstrated that pH 3 and 4 showed little variation, whereas pH 5 performed poorly. The solid to liquid ratio demonstrated that there was little variation between 1:40 and 1:60, whereas 1:20 showed an 80% reduction in protein recovery. It is likely that 1:40 would be utilised at scale to reduce production costs.

The overall research aim of examining AAE from WH and WL was achieved, and it was demonstrated that both WH and WL were suitable feedstocks for alkali acid extraction, however, WL out performed WH.

## Chapter 7.

# Development of an Aquatic biomass biorefinery

### 7.1. Introduction

The previous chapters have demonstrated the potential for WH as a resource, and showed that whilst WH had variations in composition by time period and location, the biomass was likely to contain high concentrations of HMs and protein. WH has significant potential for extraction of protein due to its ability to survive in a range of conditions and to proliferate to produce large populations at a high plant density. However, there were some drawbacks, with AAE, which need to be addressed. A proposed biorefinery would have access to large quantities of biomass, that has been deemed a nuisance, and by removing the biomass it would restore rivers, as well as removing toxic heavy metals and excess nutrients from the ecosystem.

The objective of this chapter was to demonstrate the opportunities and challenges for WH as a wild resource or cultivated resource, to produce protein and bioenergy, in the form of biogas. To answer this, the results from the three previous chapters, coupled with literature data, were utilised to demonstrate the potential opportunities for WH in a set area.

The examples described in this chapter explore scenarios that could be implemented if harvesting biomass from a natural waterbody or closed system. However, as demonstrated, there can be significant geographical and phenological variation. Therefore, all results were used as assumptions in a proposed biorefinery. The proposed biorefinery utilises WH, either harvested from a large natural waterbody or cultivated in smaller closed systems, as a feedstock to produce a protein rich product for incorporation into ruminant feed or in a protein extraction process, combined with the production of biogas via AD.

In the wild scenarios, the Goyal Para ponds were not considered due to the limited supply, this would have resulted in a costly start up and unsustainable system. In the closed cultivation system, the nutrients would come from local wastewater, like a farming family's household waste; digestate; or CM. Whilst digestate was demonstrated to have a detrimental impact on growth rate and protein content, it was assumed that this was due to the increased water N concentration, therefore if a lower



quantity of digestate was utilised, this impact could be reduced. The size of the cultivation systems would be too small to consider protein extraction, therefore, only anaerobic digestion was considered for these systems. Large scale cultivation was not considered due to the high start up costs.

## 7.2. Scenario description

There were two categories of scenarios: wild harvested WH; and cultivated under semi-controlled conditions. It was assumed that all systems within the scenarios were closed, therefore, any material that was added to the systems would be retained in the final products or wastes.

### 7.2.1. Wild harvested scenarios

Under the wild harvested scenario, two locations were considered: Kampala, Uganda; and Pune, India. Two biorefineries were suggested for each location; the first is described in Figure 7.2-1. This displays a flow chart for the process of a WH biorefinery utilising wild harvested WH biomass for AD, labelled as scenario wild anaerobic digestion (W-AD). This would require the use of a WH harvester, shredder/chopper, and an anaerobic digestion unit. The whole plant would be harvested and shredded to produce material for digestion. Due to the difficulty of obtaining fresh WH plants, only dried plants were examined, however, this would be a poor option for WH utilisation. Therefore, the dry methane potential was utilised whilst the loading rate assumed to be the FW.

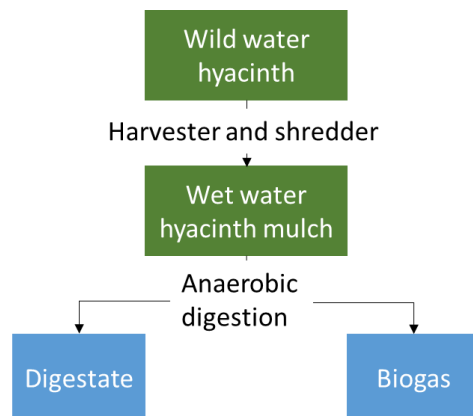


**Figure 7.2-1:** Process flow of water hyacinth biorefinery, utilising wild harvested, dried and shredded biomass to produce biogas via anaerobic digestion. Green= raw plant biomass; blue= end product.

The second process utilised AAE to produce a protein product, followed by AD of the solid residue, see Figure 7.2-2, labelled scenario wild alkali acid extraction (W-AAE). This would require the use of a WH harvester, shredder/chopper, mechanical dryer, solid-liquid separation unit, bioreactor and an anaerobic digestion unit. The process was split into four scenarios as comparison: scenario 1 utilised the whole biomass in

the alkali extraction and used the residue for biogas production; scenario 2 utilised just the leaf then added the residue to the raw petiole biomass for biogas production; scenario 3 utilised just the leaf then added the residue to the raw petiole and root biomass for biogas production; and scenario 4 just utilised the whole biomass for biogas production (the same as scenario W-AD, Figure 7.2-1). The biomass would be harvested, and separated depending on the scenario, then shredded and dried. The selected biomass would then undergo an alkali extraction, including filtering to remove the residue, followed by a solid-liquid separation to produce a liquid and solid residue. The solid residue would undergo treatment by AD, alongside the raw petioles and/or roots depending on the scenario. In Chapter 6, the residue was dried before digestion, however, this was due to logistics rather than as a process, it was assumed that the drying of the residue would have minimal impact on the methane yield due to the low moisture content of the feedstock. The liquid fraction would be acidified, to ~pH 3.75, to form a protein precipitate which would be extracted via a solid-liquid separation. This would produce a solid precipitate and a liquid waste; the liquid waste would either be recycled into the process as an acid, or neutralised and added to the digestate as a nutrient source. The first option would be dependent on the level of contamination in the acid and further investigation into the number of iterations would be required. The second option would be dependent on the acid and alkali used in the process: in Chapter 6 sodium hydroxide and sulphuric acid were used, these would be poor additions to digestate due to the high levels of sodium sulphate. However, if different agents were used, for example phosphoric acid; acetic acid; or potassium chloride, then the liquid waste would be more applicable as a fertiliser addition. Further investigation should be conducted here; for the purposes of this study, it was assumed that acid could be recycled back into the process with limited contamination. This would need to be confirmed experimentally, however, a nutrient and mass balance of the process indicated the levels of contamination.

Due to the difficulty to obtain fresh WH plants, only dried plants were examined in the BMP experiments, therefore, to compare dry against wet it was assumed that there was no impact on the digestion of residue when the alkali extraction feedstock was fresh. Further experimental work should be conducted to confirm this.

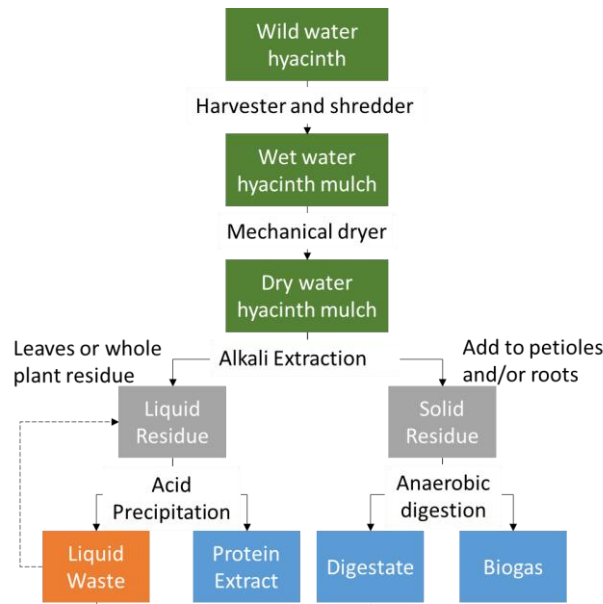


**Figure 7.2-2:** Process flow of water hyacinth biorefinery, utilising wild harvested, dried and shredded biomass to produce protein extract and biogas via alkali acid extraction and anaerobic digestion. Green= raw biomass; grey= interim product; blue= end product; orange= potential waste; broken line= potential flow.

### 7.2.2. Cultivated scenarios

The cultivated scenarios were viewed on a small-scale where a single family was cultivating and processing the biomass. The scenarios, demonstrated in Figure 7.2-3, were split into three, depending on the source of nutrients: digestate; CM; and domestic wastewater. The digestate setup demonstrated a closed system where the WH was harvested, labelled as scenario cultivated anaerobic digestion (C-AD), then chopped or shredded and then processed in an AD unit. The resulting digestate is then fed back into the WH system as a source of nutrients. The CM setup follows a similar design, labelled as scenario cultivated cow manure (C-CM), where the WH mulch is used to supplement the diet of a ruminant, assumed to be a cow; the manure is then fed back into the WH system as a source of nutrients. The next setup utilises digestate as a nutrient source, but co-digests WH alongside cow manure, likely externally purchased, labelled as scenario cultivated co-digestion (C-CoD).

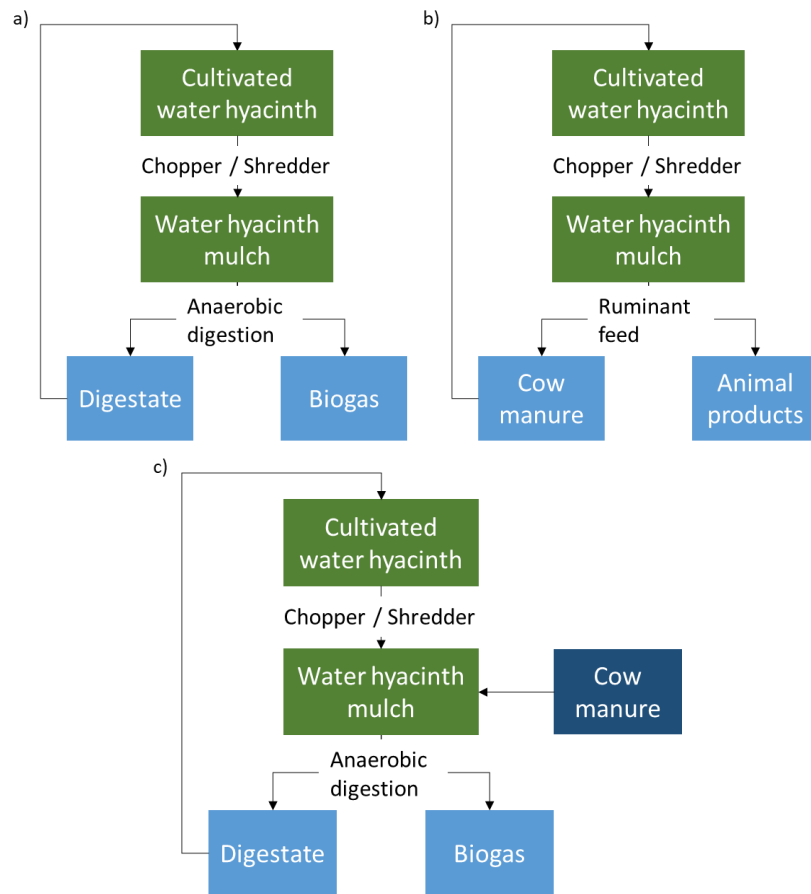


**Figure 7.2-3:** Process flow of water hyacinth biorefinery, utilising wild harvested, dried and shredded biomass to produce biogas via anaerobic digestion. Green= raw biomass; grey= interim product; blue= end product; dark blue= external product. a) scenario cultivated anaerobic digestion; b) scenario cultivated cow manure; c) scenario cultivated co-digestion.

Whilst wastewater was not directly analysed by this study, literature has demonstrated that WH can be used to reliably treat domestic or urban wastewater [33,57,96,101]. It could be assumed that WH would reduce the nutrient content of domestic wastewater to levels that would allow the water to be utilised for farm-based irrigation or discharged, whilst the suspended solids would settle during the treatment and could be removed from the base of the tank. The sludge at the base of the tank could be utilised as an AD feedstock or as a fertiliser. The domestic wastewater setup could utilise any of the previous processes, labelled as scenario cultivated domestic wastewater anaerobic digestion (C-DoAD), scenario cultivated domestic wastewater ruminant feed (C-DoRF) and scenario cultivated domestic wastewater co-digestion (C-DoCo), see Figure 7.2-4. The biomass would be fed nutrients in the form of domestic wastewater, over a period of time the biomass would reduce the pollutant concentration in the water, resulting in a nutrient rich sludge at the bottom of the cultivation pond/tank; water that could be used in non-potable scenarios; and the cultivated biomass. The biomass would then be chopped or shredded and utilised in AD or as feed supplement.

The sludge could be used as a fertiliser or as an addition to the feedstock for AD. Due to the lack of experimental data on this scenario, the growth rate and methane potential could not be estimated and would result in no costings difference to scenarios C-AD, C-CM and C-CoD, other than the cost of nutrient material in C-CoD. Therefore, only the cultivation and cleaning of this step were analysed. However, it should be noted that this scenario could reduce the costs of domestic wastewater treatment and further analysis of the cultivation of WH with domestic wastewater should be conducted, as well as the influence of the sludge on digestion capabilities.

Information on growth rate was only available from India, therefore, no other location was considered. It was assumed that the surrounding area of Pune would have similar growth rates to the experimental results in Chapter 5.

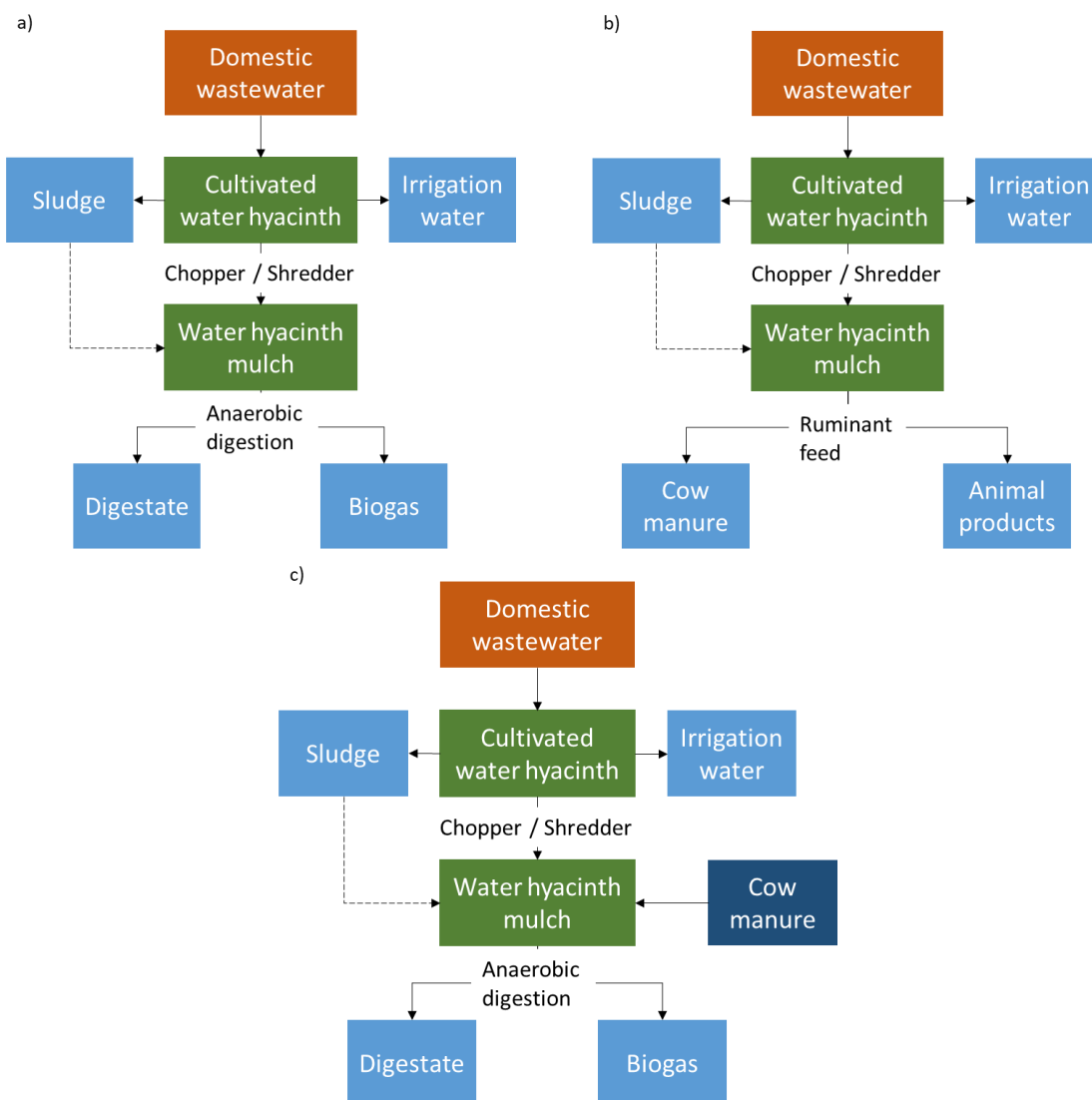


**Figure 7.2-4:** Process flow of water hyacinth biorefinery, utilising wild harvested, dried and shredded biomass to produce biogas via anaerobic digestion. Green= raw biomass; blue= end product; brown= external nutrient source; dark blue= external product; broken line= potential flow. a) scenario cultivated domestic wastewater anaerobic digestion; b) scenario cultivated domestic wastewater ruminant feed; c) scenario cultivated domestic wastewater co-digestion.

### 7.3. Cost assumptions

Assumptions for the capital and operational costs are presented here. Assumptions for the value of the products are also presented here.

#### 7.3.1. Capital cost

In the scenarios described, there were four types of equipment required: a WH harvester; industrial drying unit; AD unit; and protein extraction vessel. Quotes were obtained from suppliers in Uganda, India or China (where necessary).

There were two types of harvester considered, the modified clam-bucket device described by Wolverton and McDonald [33], and a harvester similar to the boat and cutter described by Dar [127] and Valk [55].

The cost of the modified clam-bucket device was determined by assuming that the modification of a 21 ton excavator would be nominal compared with the cost of the excavator, as suggested by Wolverton and McDonald [33]. Quotes for an excavator are displayed in Table 7.3-1 and Table 7.3-2. Assuming that the excavators were utilised for 3 months of the year, it would take 10- 14.5 years to make purchasing an excavator worth the investment. However, the excavators could be rented out during the off-season to recoup the investment, therefore, purchasing was chosen and a value of INR 6- 7.8 million was attributed to the value in India and UGX 320- 365 million in Uganda.

**Table 7.3-1:** Quotes for heavy duty excavator for use in Pune, India.

Unit Details	Hire		Purchase		Diesel Consumption (L/hr)	Reference
	Rs/ month	£*/ month	Million INR	£*		
CAT336E	-	-	6	58,200	-	[362]
Hyundai 245LR	-	-	7.8	75,660	-	[363]
Volvo EC210DL	-	-	7.5	72,750	24-27	[364]
Hitachi EX200	200,000	1,940	-	-	14-16	[365]
Hitachi EX200	180,000	1,746	-	-	14-16	[366]
JCB 245XR	195,000	1,892	-	-	-	[367]

\*Based on 1 INR: GBP £0.0097 [368]

**Table 7.3-2:** Quotes for heavy duty excavator for use in Kampala, Uganda.

Unit Details	UGX	£*	Fuel Consumption (L/hr)	Reference
Komatsu PC220	365,000,000	80,300	-	[369]
CAT320C	365,000,000	80,300	23.4	[370,371]
CAT320B	320,000,000	70,400	13.3	[372]

\*Based on UGX 1: GBP £0.00022 [373]

The cost of the boat and cutter harvester was assigned a value of £67,436; this was based on the price of a small boat and cutter harvester from Aquamarine [374]. This was £13,403 more expensive than the same model in 2018 [375]. A similar harvester, used by Valk [55], required ~6 L of diesel per hour.

A quote for a belt dryer, capable of reducing biomass moisture content to ~10% at 500 kg/hour throughput, was utilised for the biomass dryer. The quote included a heat exchange furnace, feed in conveyor, drying unit and burner, discharge conveyor and control panel. The would be supplied for ~£39,500 per unit.

The value of the industrial AD units were estimated based on quotes from a company based in Guangdong, China, see Table 7.3-3. The quotes included processing units to shred the biomass post collection.

**Table 7.3-3:** Anaerobic digester unit and associated equipment costs.

Feedstock Loading Rate (kg FW/day)	Cost of Unit (£) <sup>1,2</sup>	Cost of associated equipment (£) <sup>1,3</sup>	Total (£) <sup>1,2,3</sup>	Power (kW)
250	2,903	9,920	12,823	5
1,250	6,935	22,080	29,015	15
5,000	21,452	46,720	68,172	80

<sup>1</sup>Based on \$1 USD: GBP £0.80 [376]; <sup>2</sup>Included a biogas generator, biogas pressure boost and desulfurization system; <sup>3</sup>Included a shredder, vertical mixer, feeding pump with cutter, circulation mixing pump, portable assembly biogas digester 15 m<sup>3</sup>, biogas storage bag 20 m<sup>3</sup> and electrical control box; †

These units would be unlikely to be used in a rural environment or small-scale cultivation scenario. For the cultivation scenarios, Deenbandhu fixed dome digesters were employed. The costings were estimated based on the information provided by Samar *et al.* [377], incorporating adjusted costs for inflation [378]. The values are described in Table 7.3-4; the costings include material and labour costs.

**Table 7.3-4:** Deenbandhu fixed dome digesters costs.

Size (m <sup>3</sup> )	Feedstock Loading Rate (kg FW/day)	Cost*	
		INR	GBP <sup>+</sup>
1	50	22,256	216
2	100	31,158	302
3	150	40,061	389
4	200	50,424	489
6	300	62,734	609

\*Includes material and labour costs; <sup>+</sup>Based on 1 INR: GBP £0.0097 [368].

A temperature-controlled bioreactor was utilised as a comparable unit to use as a protein extraction vessel. The cost was estimated based on quotes from a company based in Pune, India, for a SIP Economy Model reactor, see Table 7.3-5. The quote

included a vessel, aeration system, agitation system, sterilisation system, temperature control system, chilling unit and pH control system.

**Table 7.3-5:** Bioreactor unit and associated equipment costs.

Reactor Capacity (L)	Total Cost (GBP)*	Total Cost (million INR)*	Power Requirements (kW)
500	24,662	2.54	3.3 <sup>+</sup>
1,000	35,677	3.68	3.7
2,500	62,192	6.41	5.0 <sup>+</sup>
5,000	101,069	10.42	7.0 <sup>+</sup>
10,000	176,275	18.17	11.2

\*Includes a vessel, aeration system, agitation system, sterilisation system, temperature control system, chilling unit and pH control system; <sup>+</sup>Estimated based on similar units

A two-phase solid-liquid disc centrifuge was utilised for the separation biomass from NaOH and protein precipitate from the alkali acid mixture; a quote was obtained for a unit capable of processing 2,000- 5,000 L/ hr and unit capable of processing 5,000- 10,000 L/hr. The quote included the unit and an electric control chamber and was valued at US\$29,800 per unit for the former and US\$66,800 for the latter. The smaller motor had power requirements of 15 kW whilst the latter was 18.5 kW.

### 7.3.2. Annual operating costs

The industrial-scale equipment described in 7.3.1., were assumed to have a maintenance cost of 5%, of the original cost, per year. Example maintenance costs of the largest pieces of equipment are listed in Table 7.3-6. The fixed dome digester was not included based on the small size of the digester and robust nature of the design [377].

**Table 7.3-6:** Maintenance cost of biorefinery equipment in Kampala and Pune.

Equipment	Description	Cost (£)		Maintenance costs (£/year)	
		Uganda*	India <sup>+</sup>	Uganda*	India <sup>+</sup>
Water hyacinth harvester	Modified excavator	77,000	68,870	3,850	3,444
	Boat and cutter	67,436		3,372	
Industrial dryer	400-500kg/h; output of 10- 12% moisture; belt dryer	39,516		1,976	
Anaerobic digester	5,000 kg FW/day	68,172		3,409	
Bioreactor	10,000 L SIP Economy Model	176,275		8,814	

\*Based on UGX 1: GBP £0.00022 [373]; <sup>+</sup>Based on 1 INR: GBP £0.0097 [368].



The cost of the energy carriers were estimated to be included in the annual operating costs. The cost of diesel was valued at £1.10 per litre in Uganda [379] and £0.90 per litre in India [380]. In Maharashtra, the average electricity cost over 24 hours, from January to June 2023, was INR 5,736.17 per MWh or 0.06 £/kWh [381]. In Uganda, the price varied depending on the size of the end-user, described in Table 7.3-7. It was assumed that a large industrial commercial connection would be acceptable. The specification of the digester required a maximum voltage of 400 V and rated power of 98 kVa, however, multiple digesters would be required, therefore a cost of UGX 384 was attributed to the value of electricity. The same value, in both locations, was assumed as the value of electricity deployed back to the grid from biogas electricity generation.

**Table 7.3-7:** Electricity cost in Uganda [382].

Tariff	Description	Cost (per kWh)	
		UGX	£*
Commercial	415V; 3 phase; Maximum load <100 amps	612	0.13
Medium Industrial Commercial	415V; 3 phase; Maximum load >100 amps; <500kVa	462	0.10
Large Industrial Commercial	33,000V; <15,000 kVa	384	0.08
Extra Large Industrial Commercial	No Information	325	0.07

\*Based on UGX 1: GBP £0.00022 [373].

The labour costs are described in Table 7.3-8. The values in Uganda could only be obtained for any unskilled or skilled workers across the country, whereas for India, the wages were extracted for Maharashtra workers within the engineering sector. It was assumed that each process, alkali acid extraction and AD, would require two fulltime equivalent unskilled workers to run the process and two fulltime equivalent skilled workers to oversee the whole biorefinery.

**Table 7.3-8:** Labour costs for skilled and unskilled workers in India and Uganda.

Country	Unskilled (£/month)	Skilled (£/month)	Reference
Uganda*	94.66	131.99	[383]
India*	122.14	133.78	[384]

\*Based on UGX 1: GBP £0.00022 [373]; \*Based on 1 INR: GBP £0.0097 [368].

The cost assumptions for the chemicals are described in Table 7.3-9, quotes were obtained from suppliers in India and Uganda. De-sulphurising agent was not included as this was supplied by the digestion company. This was valued at £484 for six months

of the chemical, for a 500 kg/day loading rate unit. This would be scaled to £4,839 for the 5000 kg/day loading rate unit. Due to the limited data on 60 mL NaOH to 1 g feedstock, a ratio of 40 mL, of 1.0M NaOH, to 1 g DW was utilised. For sulphuric acid (H<sub>2</sub>SO<sub>4</sub>), approximately 1.5 mL per sample of concentrated H<sub>2</sub>SO<sub>4</sub> was required, therefore, 1.5L to 1 kg feedstock was assumed.

**Table 7.3-9:** Cost of chemicals for biorefinery in India and Uganda.

Chemical	Uganda (£/ton) <sup>1,3</sup>	India (£/ton) <sup>2,4</sup>
NaOH	924	485
H <sub>2</sub> SO <sub>4</sub>	481	63

<sup>1</sup>Based on UGX 1: GBP £0.00022 [373]; <sup>2</sup>Based on 1 INR: GBP £0.0097 [368].

### 7.3.3. Product value

Biomethane was valued at 89% of the value of LPG, based on the energy content of methane compared with LPG [385]. In Pune, the value of LPG was INR 1,106 for a 14.2 kg cylinder [386]. In Kampala, the value of LPG was given as UGX 118,000 for a 12.5 kg cylinder [387–389]. The equivalent would be £0.76 per kg in Pune [368] and £2.08 in Kampala [373].

No value was associated to the digestate, due to the low value [377,390,391].

The protein precipitate was attributed a value of £1.10- 1.41 per kg for the whole plant and £1.41- 1.76 per kg for the leaf. This was based on the protein content of the precipitate as a proportion of pea protein, valued at £6.50 per kg [196].

## 7.4. Wild water hyacinth scenarios

### 7.4.1. Wild water hyacinth as a resource

#### 7.4.1.1. Biomass availability and compositional range

Wild WH has been demonstrated to be a significant problem across tropical regions, destroying ecosystems, blocking transport channels and impacting the livelihoods and health of local people. Utilising satellite imagery, an analysis of Murchison Bay, Uganda, demonstrated that the bay contained >200,000 t FW of harvestable biomass each year, or ~541 g DW/m<sup>2</sup>/yr [392], assuming a moisture content of 95%. The resolution of the phenological variations were poor in this study due to the high levels of cloud cover reducing visibility during a significant portion of the year. However, Ongore *et al.* were able to show that WH biomass varies across the year, with coverage maximising in September through to January then reducing until April [393]; this is likely due to the lower precipitation and higher temperature and irradiance from August to March [73]. Assuming that the peak harvestable biomass in Murchison Bay,

the data point was from February 2020 where temperature was highest for the year, and the minimum biomass reached ~16.6% coverage, as suggested by Ongore *et al.* [73], then phenological coverage can be assumed, see Figure 7.4-1. This figure was calculated based on the assumption that the biomass was at maximum coverage from October to February, and minimum coverage from April to July; a polynomial fit of order 4 was then performed with a p-value of <0.05. This curve suggests the resource availability for Murchison Bay, demonstrating the variations that would be likely to occur based on environmental conditions.

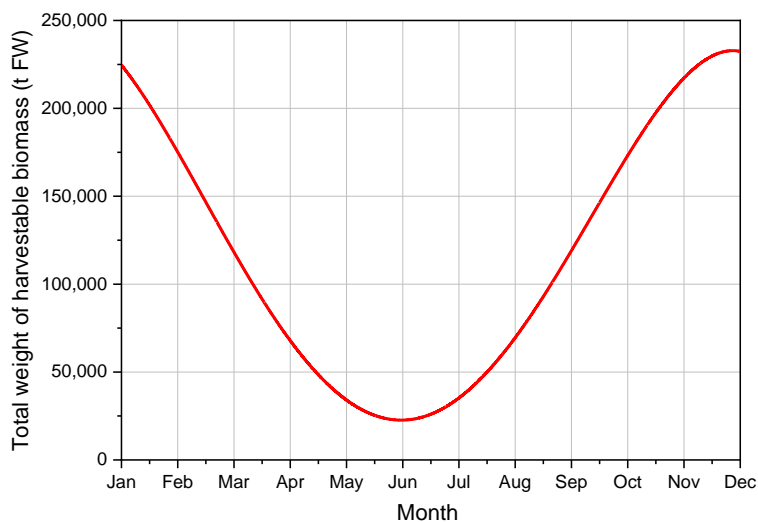


**Figure 7.4-1:** Phenological assumptions for biomass availability in Murchison Bay, Lake Victoria.

Assuming that the CW site, in Murchinson Bay, was an accurate representation for the background levels of biomass composition, then the minimum and maximum range can be calculated, see Table 7.4-1. However, the point source pollution caused by sewage or brewery wastewater resulted in increased contamination and therefore changed the composition, the maximum results analysed in Murchison Bay are also displayed in Table 7.4-1. It was assumed that the biomass could be processed wet and would demonstrate similar digestion behaviour as the BMP experiments, further work should be conducted to examine this. It has been assumed that plant part proportions did not vary significantly across the year.

**Table 7.4-1:** Biomass composition range from Murchison Bay, Lake Victoria

Parameter	Plant Part	Range at CW site		All sites maximum
		Minimum	Maximum	
Total heavy metal concentration (mg/kg)	Leaf	326.0	592.3	632.4 ± 21.1
	Root	1040.4	1732.8	3925.4 ± 201.9
	Petiole	348.7	647.8	761.9 ± 73.7
Protein Content (% DW)	Leaf	12.7	18.2	20.1 ± 0.0
	Root	8.6	14.7	16.3 ± 0.7
	Petiole	6.9	9.4	13.8 ± 0.0
BMP <sub>th</sub> (mL CH <sub>4</sub> /g VS)*	Leaf	188.8	287.8	287.8
	Root	64.8	79.6	83.7
	Petiole	216.7	316.3	375.6
Carbon (% DW)	Leaf	39.4	42.4	44.4 ± 0.2
	Root	34.8	38.3	38.5 ± 0.4
	Petiole	34.7	37.3	39.6 ± 0.2
Nitrogen (% DW)	Leaf	2.7	3.9	4.3 ± 0.0
	Root	1.9	3.2	3.5 ± 0.0
	Petiole	1.5	2.0	3.0 ± 0.0
Potassium (% DW)	Leaf	0.13	0.54	0.54 ± 0.19
	Root	0.22	0.35	0.50 ± 0.00
	Petiole	0.31	0.55	0.70 ± 0.04

\*Calculated utilising the biodegradability index from Table 4.2-3.

The important HMs when producing a protein rich extract were demonstrated to be Cu, Ni, Pb, Ti and Zn, the range and maximum for these metals are displayed in Table 7.4-2.

**Table 7.4-2:** Cu, Ni, Pb, Ti and Zn concentration range from Murchison Bay, Lake Victoria.

Element	Plant Part	Concentration range at CW site (mg/kg)	All sites maximum concentration (mg/kg)
Cu	Leaf	1 - 6	7 ± 1.5
	Root	3 - 43	20 ± 0.8
	Petiole	0 - 4	5 ± 0.4
Ni	Leaf	1 - 2	2 ± 0.3
	Root	2 - 7	7 ± 1.4
	Petiole	1 - 2	2 ± 0.3
Pb	Leaf	1 - 34	49 ± 1.0
	Root	2 - 101	200 ± 0.1
	Petiole	0 - 27	48 ± 3.7
Ti	Leaf	1 - 27	29 ± 1.8
	Root	2 - 71	71 ± 0.0
	Petiole	1 - 23	23 ± 0.5
Zn	Leaf	1 - 43	49 ± 3.3
	Root	7 - 85	179 ± 8.7
	Petiole	0 - 29	44 ± 1.9

The same calculations can be made for WH available in Pune; however, in Pune, there would be no biomass available after the monsoon. The density of the biomass was not analysed during this study; however, the density can be assumed based on the logistic growth model. The density could not be estimated until the biomass reached 100% coverage, at this point, it was assumed that the density would be equal to the carrying capacity of dwarf WH plants (640 g DW/m<sup>2</sup>) [106], at this point the plants would grow vertically, increasing their density to the carrying capacity, assumed to be the average calculated from literature (2690 g DW/m<sup>2</sup>). This is demonstrated in Figure 7.4-2; this figure was calculated assuming two steps of growth, firstly the horizontal growth from no plants in December to dwarf plants in early March, and secondly, vertical from dwarf plants to carrying capacity in June. These steps were utilised to produce a density curve of order 2, the curve then dropped to zero in July to illustrate the impact of the monsoon: regardless of biomass availability at this time, the conditions would not be appropriate for collection. The total harvestable biomass was calculated to illustrate the amount of biomass available at a set location in Pune. The area utilised was the stretch of river between Moshi and Alandi on the Indrayani River; this portion was 6.28 km long [281], and was calculated using google maps in satellite view to determine river area [394].

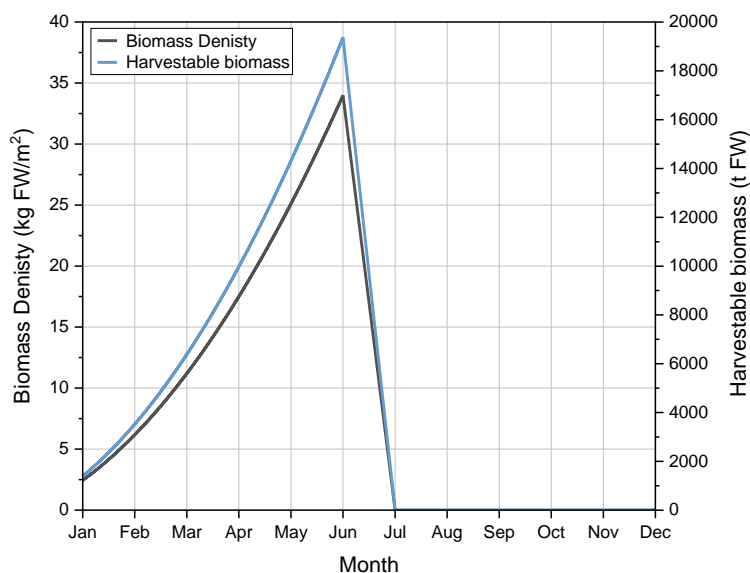


**Figure 7.4-2:** Estimated biomass density in a Pune river.

As with Uganda, there was a range of composition in the Pune rivers, therefore, the composition range is displayed in Table 7.4-3 and Table 7.4-4. It was assumed that biomass would only be harvested from May onwards, therefore only the composition of collections in May were included in this range. As with Lake Victoria, the moisture content was assumed to be 95%.

**Table 7.4-3:** Biomass composition range from Pune Rivers, May 2021.

Plant Part	Leaf	Root	Petiole
Total heavy metal concentration (mg/kg)	574 - 834	3112 - 5240	680 - 1036
Protein Content (%)	14 - 18	11 - 12	10 - 13
Maximum BMP <sub>th</sub> (mL CH <sub>4</sub> /g VS)	150 - 164	69 - 92	170 - 217
Carbon (% DW)	35.7 - 38.6	21.7 - 29.3	30.5 - 34.3
Nitrogen (% DW)	3.1 - 4.0	2.3 - 2.6	2.1 - 2.8
Potassium (% DW)	0.24 - 0.40	0.06 - 0.12	0.34 - 0.60

**Table 7.4-4:** Cu, Ni, Pb, Ti and Zn concentration range from Pune Rivers, May 2021.

Plant Part	Concentration range (mg/kg)				
	Cu	Ni	Pb	Ti	Zn
Leaf	7 - 17	3 - 8	9 - 89	1 - 41	3 - 59
Root	32 - 146	18 - 29	61 - 488	1 - 226	10 - 313
Petiole	6 - 13	3 - 5	11 - 107	1 - 40	2 - 76

#### 7.4.1.2. Harvestable biomass

In Uganda, the biomass could be harvested throughout the year, however, the amount that could be harvested must be considered. It was suggested that a weekly harvest of 9.1% of the total area would be sustainable across the population [395]; utilising the assumed biomass availability curve, it was possible to determine the amount of biomass that would be sustainable, see Table 7.4-5. This suggests that 135,414 t FW of biomass would be available for harvest without reducing the total population, however, the issues that WH creates may mean that a greater amount would be harvested, particularly in months of high availability.

**Table 7.4-5:** Harvestable biomass from Murchison Bay, Lake Victoria.

Month	Total Biomass (t FW*)	Harvestable Biomass per week (t FW*)
January	224,635	20,421
February	175,135	15,921
March	118,213	10,747
April	67,894	6,172
May	34,103	3,100
June	22,661	2,060
July	35,286	3,208
August	69,596	6,327
September	119,105	10,828
October	173,225	15,748
November	217,265	19,751
December	232,434	21,130
Total	1,489,553	135,414

The month of highest harvestable material, December, would require >4,250 t FW to be harvested per day, assuming a 5-day week. As described in Chapter 2, there was a range of harvesting potential for different mechanical harvesters, ranging from 0.6- 9.3 t/ hr. Assuming a working day of 8 hours, this would mean that 4.8- 74.4 t could be harvested per day, by one harvester. For the lower end of this range, 886 harvesters would be required to harvest the required area; the upper end of the range would require 58. Dar described a WH harvester that could achieve 1.7 t/hr [127]; these harvesters cost between US\$69,980 to 199,980 [133], therefore, to harvest 4250 t FW/day, it would cost between US\$22- 62 million in capital costs. This is a considerable sum of money and therefore unlikely to be cost effective, especially due to the suggestions of poor durability for WH harvesters and high level of clogging that can occur [33,127]. This raises the question of whether smaller scale operations are potentially more viable. However, another available option would be the use of boats to manipulate biomass close to the shore where it could be harvested with a crab bucket crane. This would increase harvest capabilities and reduce costs as common place equipment could be modified, as opposed to purchase of specialist equipment. The cost of modifying equipment for mechanical harvesting cannot be estimated, however, it can be assumed that this would be the cheapest option. For the purposes of this study, it was assumed that a single crab bucket harvester was utilised with pusher boats, resulting with an average harvesting speed of 9.2 t/hr and maximum speed of 12.3 t /hr. Therefore, an average of 73.6 t FW/day would be available, with a maximum of 98.4 t FW/day; this would translate to 26,864- 35,916 t FW/year.

In India, the biomass was assumed to only be sustainably harvestable from May and would be lost during monsoon, suggested to start in July. This would require 323 t FW to be harvested per day to ensure that the biomass was removed before the monsoon. The best harvesters for a river would be either a conveyor or crab bucket due to proximity to the banks, therefore, the harvesting rate can be assumed would be likely to be at the highest end of that range. The biomass density would be 25- 34 kg FW/m<sup>2</sup>, suggesting that one harvester, operating at 73.6 t/day, could cover 2,188- 2,976 m<sup>2</sup>/day. The number of days to harvest the Indrayani River, from Moshi to Alandi, is displayed in Figure 7.4-3; this demonstrates that to harvest the biomass within the time period, the low density (25 kg FW/m<sup>2</sup>) would require 4 harvesters, whilst the higher density would require 5. However, this assumes that the biomass does not grow back significantly during this period, which would be unlikely. Another issue in this scenario was the short timescale of the harvest: fresh biomass would require utilisation in a

short time period to ensure it was not spoilt, this would leave no biomass available for the majority of the year; therefore, drying facilities could be required.

For the purposes of this study, it was assumed that 5 harvesters were required; this would produce 368- 492 t FW/day, but due to the small harvesting window, less biomass than Kamapala would be available over the year, 22,387- 29,930 t FW/year.

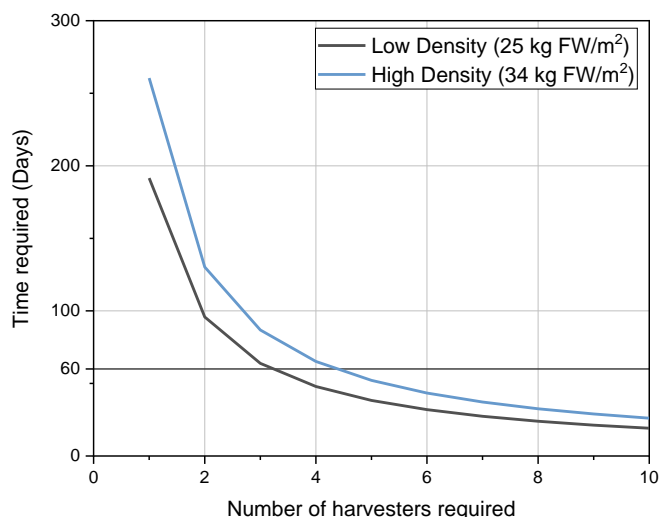


**Figure 7.4-3:** Time required for different numbers of harvesters to clear Indrayani River of water hyacinth, from Moshi to Alandi.

The processing of the biomass would require mechanical treatment to ensure that it was ready for conversion or extraction. The majority of harvesters are described with processing units installed into the harvester [33,55,127,396], however, on the harvester described by Valk was able to split the roots and the above water tissues [55]. Due to the high concentration of HMs and low protein content, this design would be ideal to separate tissues in a cost-effective manner. If a harvester without a processing unit was chosen, like the crab bucket modification method, then a shredder or chopper would be required; Valk valued a chopper at EUR €250,000, however, models capable of processing 5 tons of wet biomass per hour are available for < USD \$20,000 [397].

The challenge of harvesting and processing has been clearly demonstrated here and is a major barrier to the mass utilisation of WH biomass, both in terms of infrastructure and economics.

## 7.4.2. Scenario wild anaerobic digestion (W-AD)

### 7.4.2.1. Scenario W-AD production and flow

As described previously, it was assumed that a minimum of 73.6 t FW/day of biomass was available for digestion at any site in Murchison Bay, Lake Victoria, with a possibility of a maximum of 98.4 t FW/day. The amount of methane that could be produced per day is described Table 7.4-6. This demonstrates a biogas production range of



~305,000- 593,000 litres per day from the CW site. This biomethane would be valued at ~UGX 1.9- 3.7 million or £424- 823 per day, with a maximum possible value of UGX 4.1 million or £916. In contrast, if this was burnt to produce electricity, assuming an energy content of 15.4 MJ/kg [385], this would be valued at just £74- 143 per day with a maximum production of £159 per day.

**Table 7.4-6:** Biomethane potential of wild harvested water hyacinth biomass parts in Murchison Bay, Lake Victoria.

Parameter	Plant Part	Range at CW* site		All sites maximum
		Minimum	Maximum	
Theoretical Biomethane Potential (mL CH <sub>4</sub> /g DW)	Leaf	105.8	161.3	161.25
	Root	30.9	38.0	39.96
	Petiole	108.5	158.3	187.98
	Whole <sup>+</sup>	83.0	120.5	134.20
Biomass Available (t DW/day)	Leaf	0.88	1.18	1.18
	Root	1.18	1.57	1.57
	Petiole	1.62	2.16	2.16
	Whole	3.68	4.92	4.92
Methane Available (1000 L CH <sub>4</sub> /day)	Leaf	93.4	190.4	190.4
	Root	36.4	59.9	62.9
	Petiole	175.6	342.7	406.9
	Whole	305.5	593.0	660.3

\*CW = Clean Water; <sup>+</sup>Calculated by proportion of parts.

To estimate the composition of the digestate, a nutrient flow was conducted based on the BI of the average biomass composition from the CW site. It was assumed that the AD unit was a closed system, therefore, all nutrients that were not lost in the biogas remained in the digestate. The C flow was calculated utilising the BI and the Buswell and Neave equation for the conversion of any C<sub>x</sub>H<sub>y</sub>O<sub>z</sub> compound, corresponding to the dry fraction of an organic compound) into CH<sub>4</sub> and CO<sub>2</sub> [305]. The N flow was calculated utilising the BI to assume that all N digested was converted to ammonia. The scenario utilised 73.6 t of fresh biomass, see Table 7.4-7, and resulted in 4.2 t of the original biomass contained within the digestate, or ~169,000 L of digestate, containing a maximum of 1.35, 0.10 and 0.03 t of C, N and K. As compared with CM, this would supply 28 and 85% less N and P [138], suggesting that it would be of little value.

**Table 7.4-7:** Digestate quantity and nutrient content from anaerobic digestion of water hyacinth from biomass in Murchison Bay, Lake Victoria.

Parameter	Range at CW site		All sites maximum
	Minimum	Maximum	
Feedstock (kg DW/day)	3,680	4,920	4,920
Digestate (L/day)	169,280	226,320	226,320
Carbon (kg DW/day)	902	1,306	1,349
Nitrogen (kg DW/day)	42	85	101
Potassium (kg DW/day)	9	24	29

It has been shown that the inclusion of roots in digestion reduces the biomethane production, therefore, a scenario has been proposed where only the leaf and petiole is digested. This was calculated by adding the leaf and petiole methane production and nutrient flows, however, the actual digestion behaviour may be different, therefore, further investigation should be conducted into this. The methane production and nutrient flow to the digestate are described in Table 7.4-8. By removing the roots, the amount of the biogas would be reduced by 9.5-11.9%. The nutrient content would be reduced by an average of 41, 48 and 27% for C, N and K, respectively. As digestate has a relatively low value, from INR 0-4 per kg [377,390,391], this reduction is assumed to have little impact on value, despite almost half the C and N being lost.

**Table 7.4-8:** Mass, biomethane production and digestate quantity and nutrient content from anaerobic digestion of water hyacinth leaf and petiole from Murchison Bay, Lake Victoria.

Parameter	Range at CW site		All sites maximum
	Minimum	Maximum	
Feedstock (kg DW/day)	2502	3346	3346
Methane Available (1000 L CH <sub>4</sub> /day)	269	533	597
Digestate (L/day)	115,110	153,898	153,898
Carbon (kg DW/day)	533	759	801
Nitrogen (kg DW/day)	22	42	52
Potassium (kg DW/day)	6	18	22

A similar analysis was conducted on the biomass from India. To ensure that all biomass collected before the monsoon, 5 harvesters must be used in conjunction with pusher boats. This would result in a collection of 368-492 t FW /day. This would produce a methane yield of 1.4- 1.6 million litres per day, see Table 7.4-9; this would be valued at INR 72,500- 84,000 or £703- 815 per day. The high value in Uganda was due to the increased value of LPG within the country, with a cost of almost 3 times compared with India. In contrast, if this was burnt to produce electricity, assuming an

energy content of 15.4 MJ/kg [385], this would be valued at £12,300- 14,300 per day. However, due to the short harvesting period this would be worth less over the entire year, assuming that the biomass was either dried and stored, or a secondary source could be utilised.

**Table 7.4-9:** Biomethane potential of wild harvested water hyacinth biomass and plant parts in Pune, India.

Parameter	Whole	Leaf	Root	Petiole
Theoretical Methane Potential (mL Ch <sub>4</sub> / g DW)	76-88	106-127	29-43	126-128
Biomass Available (t DW/day)	18-25	5-6	6-9	7-10
Methane Available (1000 L Ch <sub>4</sub> / day)	1393-1614	486-579	184-274	938-954

\*Maximum biomass not used in calculations

The nutrient flow demonstrated that an average of 7.15 t FW of the original biomass ending up in the digestate, with a total volume of ~989,00 L of digestate containing 5.4, 0.44 and 0.07 t of C, N and K, see Table 7.4-10. As compared with CM, this would supply 0.8 and 86% less N and P [138], suggesting that it would be of little value.

**Table 7.4-10:** Mass and digestate quantity and nutrient content from anaerobic digestion of water hyacinth from biomass in Pune, India.

Parameter	Minimum	Maximum	Average
Feedstock (kg DW/day)	18,400	24,600	21,500
Digestate (L/day)	846,400	1,131,600	989,000
Carbon (kg DW/day)	3,579	7,142	5,360
Nitrogen (kg DW/day)	305	569	437
Potassium (kg DW/day)	61	81	71

The removal of the roots demonstrated marked difference in comparison to Uganda: the biogas yield was only reduced by 1.7% on average, suggesting that the roots had a less significant negative impact on the digestion, however, as stated before this must be confirmed experimentally. The nutrient content was reduced more significantly than the Ugandan samples, with a reduction of 46, 48 and 52% for the C, N and K respectively.

**Table 7.4-11:** Mass, biomethane production and digestate quantity and nutrient content from anaerobic digestion of water hyacinth leaf and petiole from Pune, India.

Parameter	Minimum	Maximum	Average
Feedstock (kg DW/day)	12,003	16,047	14,025
Methane Available (1000 L Ch <sub>4</sub> /day)	1,424	1,533	1,479
Digestate (L/day)	552	738	645
Carbon (kg DW/day)	2,268	3,285	2,777
Nitrogen (kg DW/day)	129	338	234
Potassium (kg DW/day)	34	78	56

Removing the roots would be more time consuming to prepare the biomass for digestion, unless the harvesters utilised were able to separate the biomass during harvesting, as described by Valk [55]. Valk did not experimentally examine this harvester, therefore it was assumed that it performed at a similar speed to other harvester of a similar design, where a boat was utilised to cut the biomass and distributed back the shore when full, and was designated a processing speed of 13.6 t FW/day, over 5 times less than the clamshell bucket method. This low harvesting rate reduces the maximum biomass that can be harvested and therefore reduces the maximum biomass that can be generated. A single harvester could harvest 0.8 t FW/day of leaves and petioles; however, the HM content of the parts suggests that the digestate would contain 71.3- 73.7% less HMs. The key constraint here would be the harvesting rate, therefore, if this could be increased, separation of roots from the rest of the plant appears to be the optimal method of treatment. However, disposal of the roots may prove to be a limiting factor due to the high HM content. Further work should be conducted here, as well as further work into the digestion of leaves and petioles.

#### 7.4.2.2. Scenario W-AD Costs and benefits

Due to the unknown challenges and costs of separating the biomass into parts, only the whole plant was considered for the costings. However, it is acknowledged that removing the roots would likely be optimal to reduce HM content of the feedstock. The capital costs, annual costs and income from W-AD are described in Table 7.4-12. The minimum and maximum within the table is demonstrates the variation due to harvesting rates, biomethane production and cost variations. The reduced methane potential shown by the Indian samples resulted in a significantly reduced methane production. Pune had a greater size of digester due to the large biomass harvesting; the greater annual costs were largely due to increased maintenance and running costs of the larger digester, as demonstrated in Figure 7.4-4. The lower value of LPG in Pune resulted in the scenario losing £189,000- 272,000 per year. The addition of income from renting out the water hyacinth harvester (modified excavator) would improve this

to a loss of £102,000- 185,000. Co-digestion with sewage sludge could improve the techno-economics of this scenario, however this was not analysed as part of this study. The same would occur in Uganda, with a loss of £52,800 to 111,600 per year. This demonstrates that the costs of a large-scale AD biorefinery, utilising WH as a sole feedstock, would be too expensive. The demonstration that this would be the case in multiple locations, one of which has an elevated BI and LPG value, suggests that this would be the case in a large range of scenarios.

**Table 7.4-12:** Capital costs, annual costs, income and payback time of the scenario wild anaerobic digestion based in Kampala and Pune.

Location	Capital Costs (million £)		Annual Costs (100,000 £/yr)		Annual Income Methane (100,000 £/yr)		Payback (years)	
	Min	Max	Min	Max	Min	Max	Min	Max
Kampala	1.14	1.51	2.66	3.87	1.55	3.34	N/A	N/A
Pune	1.19	1.58	2.32	3.38	0.43	0.66	N/A	N/A

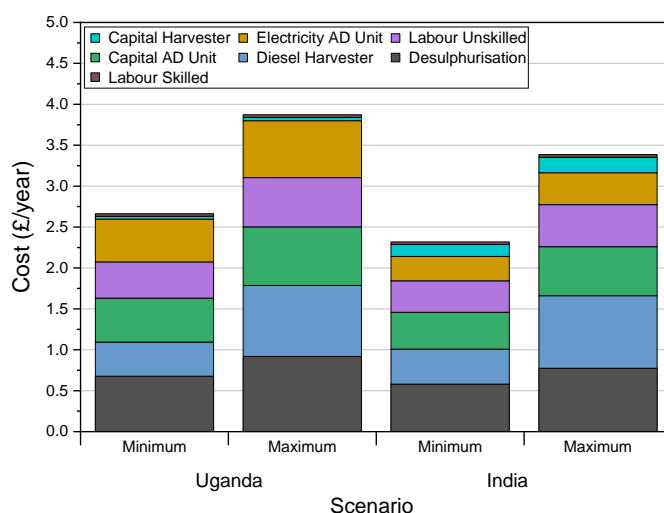


**Figure 7.4-4:** Distribution of annual costs for scenario wild anaerobic digestion.

### 7.4.3. Scenario wild alkali acid extraction (W-AAE)

#### 7.4.3.1. Scenario W-AAE production and flow

As described previously, it was assumed that 73.6-98.4 t FW/day of biomass was available for processing at any site in Murchison Bay, Lake Victoria. The protein production was calculated based on the average of all samples, from section 6.2; the amount of protein that could be produced per day is described in Table 7.4-1. This demonstrated that 279- 754 kg/day of protein could be produced from the whole plant, compared with 82- 216 kg/day for the leaf. The value of the precipitate would result in a range of £305- 1030 and 116- 379 per day for the leaf and whole plant, respectively.

**Table 7.4-13:** Protein production of wild harvested water hyacinth whole plant and leaf in Murchison Bay, Lake Victoria.

		Whole	Leaf
Precipitate (mg/g DW)	Minimum	75.7	93.11
	Maximum	153.3	182.87
Biomass Available (t DW/day)	Minimum	3.68	0.88
	Maximum	4.92	1.18
Precipitate Production (kg/day)	Minimum	278.7	82.2
	Maximum	754.1	215.9

Table 7.4-14 and Table 7.4-15 demonstrate the mass and nutrient flow of the alkali acid protein extraction. This demonstrates that whilst the leaves have greater protein content and low HM content, the whole plant produces a larger amount of the protein product due to a greater amount of biomass. It also demonstrates that up to half of the carbon and nitrogen, whilst almost all of the potassium is lost in the liquid waste, based on calculations by difference, and therefore using this waste product as a fertiliser could be the optimal choice. However, further investigation must be undertaken with other solvents to demonstrate this. The proportion of the whole raw biomass within the liquid, based on the values in Table 7.4-14, is an average of  $15.4 \pm 6.3\%$ , this will be used as an assumption of the mass lost resulting in a reduction in the solid residue weight to 2,550- 3,954 kg DW. For the leaf this would be an average of  $23.7 \pm 6.1\%$ , reducing the solid residue weight to 532- 834 kg DW.

**Table 7.4-14:** Mass and nutrient flow for protein precipitation from water hyacinth whole plant from Murchison Bay, Lake Victoria.

	Weight (kg DW)		C (kg DW)		H (kg DW)		N (kg DW)		K (kg DW)	
	Min	Max	Min	Max	Min	Max	Min	Max	Min	Max
Raw	3680	4920	1202	1989	115	287	65.6	171	7.09	27.7
Protein Extract	397	531	10.0	13.3	0.9	1.2	1.7	2.3	0.029	0.039
Solid Residue	3255	4352	882	1180	103.5	138.4	55.2	73.8	0.053	0.071
Liquid Waste*	-	-	310	795	10.1	147.9	8.7	94.7	7.00	27.6

\*Calculated by difference

**Table 7.4-15:** Mass and nutrient flow for protein precipitation from water hyacinth leaf from Murchison Bay, Lake Victoria.

	Weight (kg DW)		C (kg DW)		H (kg DW)		N (kg DW)		K (kg DW)	
	Min	Max	Min	Max	Min	Max	Min	Max	Min	Max
Raw	883	1181	328	525	27.5	69	23.0	51	0.93	5.9
Protein Extract	129	173	5.1	6.9	0.5	0.6	0.9	1.2	0.009	0.012
Solid Residue	757	1012	183	244	21.5	28.7	13.3	17.8	0.020	0.027
Liquid Waste*	-	-	140	274	5.5	39.6	8.8	32.2	0.90	5.9

\*Calculated by difference

To calculate the methane production from the residue of the alkali extraction process, the impact of the process on residue composition was calculated. This was then applied to the composition of the raw material from Lake Victoria, to predict the composition of the residue. This was utilised to determine the  $BMP_{th}$  of the residue and utilised in four scenarios: scenario 1 utilised all the biomass in the alkali extraction and used the residue for biogas production; scenario 2 utilised just the leaf then added the residue to the raw petiole biomass; scenario 3 utilised just the leaf then added the residue to the raw petiole and root biomass; and scenario 4 just utilised the raw biomass for biogas production.

The potential methane production, from the four scenarios, is described in Table 7.4-16. This demonstrates that the alkali extraction improved the biomethane yield; secondly, whilst removing the roots from the digester improved the  $BMP_{th}$ , it had a detrimental effect on the overall biomethane yield, however, this does not consider the impact of HM contamination within the digestate. The  $BMP_{th}$  for the scenarios was calculated by the proportion of the feedstock within the digester, rather than an experimental value, therefore, the digester may not behave in the way, in particular the negative impacts of the root on digestion. However, an experimental analysis of a petiole and root composite demonstrated that the  $BMP_{ex}$  was 124 mL  $CH_4/g$  VS. In comparison, by multiplying the  $BMP_{ex}$  of the individual parts by their corresponding proportions within the sample, a theoretical  $BMP_{ex}$  of 118 mL  $CH_4/g$  VS was generated, suggesting that the theoretical method may underestimate the methane production. In contrast, the whole plant demonstrated a  $BMP_{ex}$  of 104 mL  $CH_4/g$  VS, whereas the theoretical method resulted in a theoretical  $BMP_{ex}$  of 120 mL  $CH_4/g$  VS, a significant over estimation. Further work on the impact of the roots on anaerobic digestion behaviour should be conducted.

**Table 7.4-16:** Biomethane potential of four scenarios containing water hyacinth biomass parts from Murchison Bay, Lake Victoria.

Scenario	Theoretical Biomethane Potential (mL CH <sub>4</sub> /g DW)		Feedstock available (t DW/day)		Methane Production (1000 L CH <sub>4</sub> /day)	
	Min	Max	Min	Max	Min	Max
1	128.89	207.11	2.75	3.68	354.93	762.51
2	249.06	400.69	2.20	2.94	256.88	571.28
3	215.34	337.93	3.37	4.51	290.32	632.57
4	81.77	133.46	3.68	4.92	300.91	656.61

The mass and nutrient content of the raw whole biomass and the processed biomass from the four scenarios is described in Table 7.4-17. This demonstrated that the alkali treated whole biomass in scenario 2 had a significantly lower nutrient content than the non-treated whole biomass, in particular K, however as this was estimated, experimental work should be carried out to confirm this. The removal of the roots did not significantly reduce the nutrient content of the digestate.

Whilst it has been stated that a reduction in nutrient content of the digestate may not reduce its value significantly, this is a greater reduction and is more likely to reduce the value. As compared with CM, the digestate had significantly reduced nutrient content, ranging from 49- 73% for N and 92-99% for P, see Table 7.4-23.

**Table 7.4-17:** Mass and nutrient content of digestate and raw biomass from four scenarios, in Murchison Bay, Lake Victoria.

Scenario	Feedstock (kg DW)		Carbon (kg DW)		Nitrogen (kg DW)		Potassium (kg DW)	
	Min	Max	Min	Max	Min	Max	Min	Max
Raw Biomass	3680	4920	1202	1989	66	171	7	28
1	2754	3682	367	505	15	36	0.42	0.64
2	579	775	98	132	5	11	0.15	0.23
3	581	776	99	132	5	11	0.15	0.24
4	3680	4920	829	1332	38	98	7	28

For the Indian scenario, 368-492 t FW /day of biomass was available for processing; this would be able to produce 1,394- 3,771 kg of protein precipitate per day from the whole biomass, compared with 426- 1118 kg/day from the leaf biomass. This amount of protein would be valued at £1,527- 5,149 and £600- 1,964 per day, for the whole and leaf biomass, respectively.



**Table 7.4-18:** Protein production of wild harvested water hyacinth whole plant and leaf in Pune, India.

		Whole	Leaf
Precipitate (mg/g DW)	Minimum	75.7	93.1
	Maximum	153.3	182.9
Biomass Available (t DW/day)	Minimum	18.40	4.57
	Maximum	24.60	6.11
Precipitate Production (kg/day)	Minimum	1393.5	425.7
	Maximum	3770.6	1117.9

The impact of dry feedstock compared with wet was described in section, resulting in a slight increase in precipitate formation for the whole plant, averaged at 7.1%, and a decrease from the leaf, averaged at 31.0%. These values were utilised when comparing the costs and benefits of dry versus wet biomass.

The nutrient and mass flows are described in Table 7.4-19 and Table 7.4-20. The results were based on variations in all protein extraction samples; therefore, the results were similar to the Ugandan results, with only the variation in total amount flowing due to variations in raw biomass composition and total weight.

The proportion of the whole raw biomass within the liquid, based on the values in Table 7.4-19, was an average of  $10.8 \pm 5.0\%$ , this will be used as an assumption of the mass lost resulting in a reduction in the solid residue weight to 13,691- 20,500 kg DW. For the leaf the loss was  $20.3 \pm 2.2\%$ , reducing the solid residue weight to 3,036- 4,290 kg DW.

Based on the average contamination content between India and Uganda, it was assumed that the recycled liquid waste was 13.1 less effective each reuse, at 75% contamination it was deemed a waste and disposed of. The most economical use of the acid would be to replace after five cycles.

**Table 7.4-19:** Mass and nutrient flow for protein precipitation from water hyacinth whole plant from Pune, India

	Weight (kg DW)		C (kg DW)		H (kg DW)		N (kg DW)		K (kg DW)	
	Min	Max	Min	Max	Min	Max	Min	Max	Min	Max
Raw	18400	24600	5260	8997	654	1108	410	761	8.9	83
Protein Extract	1985	2654	50	67	4.37	5.84	8.4	11.3	0.14	0.19
Solid Residue	16274	21758	4412	5899	518	692	276	369	0.27	0.36
Liquid Waste	-	-	798	3031	132	410	125	380	8.5	82

**Table 7.4-20:** Mass and nutrient flow for protein precipitation from water hyacinth leaf from Pune, India.

	Weight (kg DW)		C (kg DW)		H (kg DW)		N (kg DW)		K (kg DW)	
	Min	Max	Min	Max	Min	Max	Min	Max	Min	Max
Raw	4572	6113	1634	2362	201	299	142	242	10.4	23.9
Protein Extract	668	893	26.6	35.6	2.42	3.23	4.68	6.3	0.05	0.06
Solid Residue	3919	5240	945	1263	111	149	69	92	0.10	0.14
Liquid Waste	-	-	663	1063	87	147	69	144	10.3	23.7

The total methane generation is displayed in Table 7.4-21, for the four scenarios. As with Uganda, the removal of the roots reduced the total methane yield due to the reduction in the biomass availability. If we assume that the removal of the roots would reduce the total available biomass, as suggested in section 7.4.2, then this would reduce the applicability of removing the roots. It would be more important to make the decision based on the HM content of the precipitate.

**Table 7.4-21:** Biomethane potential of four scenarios containing water hyacinth biomass parts from Pune, India.

Scenario	Theoretical Biomethane Potential (mL CH <sub>4</sub> /g DW)		Feedstock available (t DW/day)		Methane Production (1000 L CH <sub>4</sub> /day)	
	Min	Max	Min	Max	Min	Max
1	127.01	165.77	3.25	4.35	413	721
2	275.58	323.01	8.85	11.84	1,084	1,824
3	242.50	281.71	14.74	19.71	1,324	2,253
4	80.58	106.82	18.40	24.60	1,483	2,628

The nutrient and mass content of the digestate showed similar trends to the Ugandan data, see Table 7.4-22. As compared with CM, the digestate had significantly reduced nutrient content, ranging from 11- 57% for N and 92-99% for P, see Table 7.4-23.

**Table 7.4-22:** Mass and nutrient content of raw biomass compared with digestate from four scenarios, in Pune, India.

Scenario	Mass (kg DW)		Carbon (kg DW)		Nitrogen (kg DW)		Potassium (kg DW)	
	Min	Max	Min	Max	Min	Max	Min	Max
Raw Biomass	18400	24600	5260	8997	410	761	9	83
1	8641	11552	1905	1792	110	187	2.48	3.79
2	1668	2230	613	662	43	69	1.00	1.54
3	1669	2231	614	664	43	70	1.00	1.55
4	7837	10478	3632	5310	235	437	9	83

**Table 7.4-23:** Reduction in nutrient content of digestate, as compared with cow manure [138].

Scenario	Uganda		India	
	Nitrogen (%)	Potassium (%)	Nitrogen (%)	Potassium (%)
1	73	99	57	99
2	55	99	34	99
3	55	99	34	99
4	49	92	11	92

#### 7.4.3.2. Scenario W-AAE costs and benefits

Due to the unknown challenges of separating the biomass into parts, only the whole plant was considered for the costings. However, it is acknowledged that removing the roots would likely be optimal to reduce HM content of the feedstock.

The capital costs, annual costs and income from W-AAE are described Table 7.4-24. The minimum and maximum within the table is demonstrates the variation due to harvesting rates, biomethane production and cost variations. This demonstrates that no scenario examined would be economically profitable. Whilst, the annual income was greater for W-AAE then W-AD, the annual costs were over 10 times greater; this was predominantly due to the cost of the chemicals used in protein extraction, see Figure 7.4-5. For the wet feedstock, the chemicals accounted for 92 and 72% of the annual costs in Uganda and India, respectively. For the dried scenario, the gas requirements were higher than the gas produced by anaerobic digestion, and the gas purchased accounted for 44 and 86% in Uganda and India, respectively.

**Table 7.4-24:** Capital costs, annual costs, income and payback time of the scenario wild alkali acid extraction based in Kampala and Pune.

Location	Condition	Capital Costs (million £)		Annual Costs (100,000 £/yr)		Annual Income (100,000 £/yr)		Payback (years)	
		Min	Max	Min	Max	Min	Max	Min	Max
Kampala	Wet	1.4	1.7	33.5	44.7	3.7	9.0	N/A	N/A
	Dry	1.3	1.6	57.6	76.2	1.1	3.8	N/A	N/A
Pune	Wet	1.4	1.8	8.8	11.9	1.9	5.5	N/A	N/A
	Dry	1.3	1.7	55.7	74.6	0.9	3.1	N/A	N/A

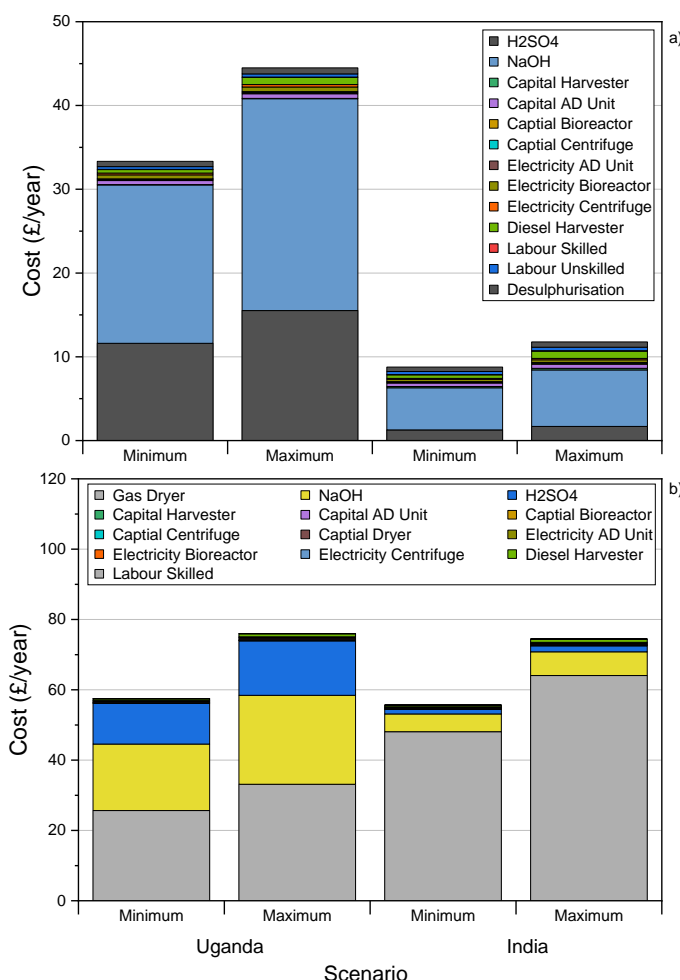


**Figure 7.4-5:** Distribution of annual costs for scenario wild alkali acid scenario. a) wet feedstock; b) dry feedstock.

A method of reducing the cost would be to vary the alkali, however, when other alkalis were investigated, all were of a similar cost. In soybean extractions, sodium bicarbonate ( $\text{NaHCO}_3$ ) has been utilised [141], however, a greater amount would be required to achieve the same alkali concentration. Secondly, quotes from suppliers demonstrated no significant cost reduction per ton of  $\text{NaHCO}_3$ . It is likely that this was more economical in soybean extractions due to the lower pH required for extraction as compared with biomass like WH [141].

#### 7.4.4. Secondary benefits of the wild scenarios

The results demonstrate that W-AD and W-AAE were largely economically unsustainable, with only Kampala W-AD resulting in a profit. This was especially evident for W-AAE where the cost of chemicals were an obvious barrier to the biorefinery. However, in all scenarios the no secondary services were accounted for, in particular ecosystem services. The removal of WH from the water bodies is a significant task and is one of the major barriers to the reducing the impact of the plant, therefore this removal has economic value to the local community, however the calculation of this value is extremely challenging. In Pune, the rivers are completely blocked by WH for two to four months of year, whilst on Lake Victoria economic losses due to WH mats are issues all year round [398]. These plants also are site for disease and many other issues, as discussed in Chapter 2, all of which cannot be valued.

Another service this provides is the removal of heavy metals from the waterbodies. In India, the rivers are used for drinking, washing, religious activities, amongst other things. Therefore, the removal of these HMs is a significant result. Currently, biomass is either left to be removed by the impact of monsoon or harvested and left to rot on the banks of the river, where the HMs will eventually leach back into the waterbody.

Therefore, by removing these metals and stopping them from entering the river again, could be considered a significant positive of the scenarios. For example, based on the range of HM content within the whole biomass, the harvesting of 368 t FW of WH could remove between 40,700- 63,550 kg of HMs per year, from the Pune waterbodies.

Whilst this was not part of the scope of this study, the potential opportunity for phytomining of HMs from WH could be a secondary process to improve viability.

### 7.5. Cultivated water hyacinth scenarios

#### 7.5.1. Cultivated biomass as a resource

##### 7.5.1.1. Biomass availability and compositional range

It has been demonstrated that cultivated WH can be reliably produce biomass at a high growth rate, utilising low grade nutrient sources. Whilst this study did not focus on wastewater in cultivated tanks, the evidence from the literature analysis and the wild biomass suggests that this would not be a barrier to cultivation. Cultivated biomass could be conducted in shallow tanks, similar to the tanks used in this study, or a variety of closed system waterbodies, including artificial ponds, canals, drainage ditches or farm ponds. These waterbodies could be fed with CM, digestate or local wastewater, however, this study aimed to demonstrate the potential for this cultivation utilising low-cost nutrients like CM and digestate. Therefore, despite the variation in nutrient feed within the scenarios, the growth rates are assumed to fit within the ranges stated.

The biorefinery considered for cultivation tanks would be considerably different to harvesting wild biomass: the wild harvest biomass is an example of large-scale biorefinery, valorising a problematic invasive species, whereas the cultivated refinery would most likely be integrated with wastewater treatment or small-scale biogas production. Therefore, this biorefinery scenario was considered on a small scale, detailing the potential from a single farm pond of 10 m<sup>2</sup>. The pond would be fed with CM, digestate or domestic wastewater, with the growth assumed to follow the equations detailed in Chapter 5, Equation 5-4 and Equation 5-5. The value for  $r_N$  can then be utilised in Equation 7-1 to produce a final growth rate ( $r_x$ ), that assumed a  $N_0$  of 60 mg N/L. The results of the seasonal growth rates and expected farm pond yield are described in Table 7.5-1. The final density represents the density achieved from 42 days of growth, as described in Chapter 5, and would therefore have two harvests per season; whilst the farm pond yield assumed a 10 m<sup>2</sup> pond that was harvested back to an original density of 4 kg FW/m<sup>2</sup>, every 42 days.

**Equation 7-1:** Final growth rate calculated utilising normalised growth rate for nitrogen content.

$$r_x = r_N \cdot N_0$$

**Table 7.5-1:** Intrinsic growth rate and final harvest yield.

Season	$r_x$ (g/g/m <sup>2</sup> /day)	Final density (g DW/m <sup>2</sup> )	Farm pond yield (kg FW)
Spring	0.1050	957	303
Summer	0.1063	959	304
Monsoon	0.0950	934	294
Winter	0.0627	777	231
Total	-	3626	1131

The biomass would require harvesting once every 42 days, due to the small-scale nature of the scenario, it is likely that this would be conducted manually. If a single person can recover 200 kg FW per hour, then it would take one person less than one day to harvest a full farm pond. The processing of this biomass could be conducted locally, simple farm-based shredders are likely to be present for the processing of grass and hay for animal fodder, whilst air drying would be the most likely method employed. The ponds would likely require dredging of material after several harvests to remove the WH debris.

The composition assumptions are described in Table 7.5-2 and Table 7.5-3, however, the HM concentration and the leaf maximum BMP were only based on the summer trial. The levels of HM in the biomass relate to the HM in the nutrient source and/or

water used to cultivate the biomass. Data presented is from real world trials although it is possible that HM content can be minimised by controlling nutrient and source.

**Table 7.5-2:** Biomass composition range for large tank cultivated biomass.

Plant Part	Total heavy metal concentration (mg/kg)*	Protein Content (%)	Maximum BMP <sub>th</sub> (mL CH <sub>4</sub> /g VS)
Whole	1149 – 1180	12 - 16	336 - 395
Leaf	830 – 862	13 - 18	276 – 295*

\*Data only available for summer trial

**Table 7.5-3:** Cu, Ni, Pb, Ti and Zn concentration range for large tank cultivated biomass.

Plant Part	Concentration range (mg/kg)*				
	Cu	Ni	Pb	Ti	Zn
Whole	16 - 18	15 - 72	0.0 - 0.1	49 - 61	70 - 83
Leaf	5 - 8	10 - 45	0.0 - 0.0	46 - 39	43 - 44

\*Data only available for summer trial

#### 7.5.1.2. Requirements for cultivation

Cultivation of WH would require water and nutrients, it is important to understand these requirements for ease of use by an end-use operator. Water is a significant requirement of any WH system due to the high transpiration rate of WH, which can be up to three times higher than local fauna [23,25,71]. In a 10 m<sup>2</sup> farm pond the depth would need to a minimum of 0.3 m to ensure that the roots had space to grow, and the debris would not suffocate them. The large tanks were filled to ~80% of maximum capacity, to ensure no overspill, plant or nutrient loss; therefore, assuming the farms ponds received the same amount of water, they would require an initial 2,400 L of water. The tanks were refilled to ~80% capacity every 7 days, in summer, this was estimated to require 10% of original volume per week, or 35 L. Whilst this value would have differed for each season, this is assumed to be the highest and will be used for all seasons. Assuming that the farm pond would require a similar level of water, 240 L of water per week, or 1,440 L or 60% the original volume over a 42-day harvest cycle, plus the original 2,400 L of starting water would be required.

For C-AD assumptions were made on digestate production from co-digestion of CD/WH in an AD reactor; based on experimental results from a 200 L semi-batch reactor, ~2.3 L of digestate were produced for every kg FW of feedstock [138]. In the large tanks, 70 L of digestate was added at the start with no further digestate added, resulting in a  $N_0$  of ~140 mg N/L and a reduced growth rate for the first 10 days. Therefore, the suggested digestate addition was reduced to 30 L, or ~85 mL of

digestate per L of water, and addition increased to every two weeks, like the CM. Assuming an average harvest of 141.5 kg FW biomass per harvest in a 10 m<sup>2</sup> farm pond, 325.5 L of digestate could be produced, whilst only 202 L would be required to fertilise the pond. The remaining digestate can be used as an organic fertiliser for crops. This disparity increases as the size of the tank increases, resulting in a greater difference between required and produced, see Figure 7.5-1.

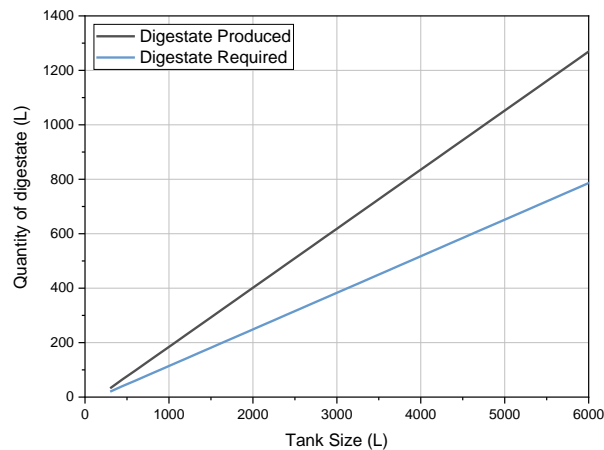


**Figure 7.5-1:** Quantity of digestate produced and required by a farm pond cultivating water hyacinth for anaerobic digestion.

In C-CM, the amount of manure produced by a single cow was assumed to be 20 kg FW/day [399]. In the large tanks, 12.75 kg of CM was added every two weeks to achieve the required N concentration, whilst in winter this value was too high and the water N concentration peaked at >200 mg N/L, it is assumed that no operator would have the capabilities to analyse for N concentration, therefore a single value for addition would be more applicable. In a 10 m<sup>2</sup> farm pond, ~87.5 kg FW of CM every two weeks, or ~262 kg FW over a 42-day harvest cycle, would be required. This amount could be produced by a single cow, accounting for just under one third of the manure produced by a cow. A single cow could produce enough nutrients for a pond of ~47.6 m<sup>2</sup>.

If the nutrients were to come from domestic wastewater, C-Do, the quantity of the wastewater and speed of treatment must be assumed. The amount of domestic wastewater produced was assumed to be 100 L of wastewater per day [400]. Aremu *et al.* demonstrated that after 28-days raw sewage was sufficiently cleaned to be used for non-drinking purposes and produced a sludge that could be used as a fertiliser [401], or a feedstock in AD for co-digestion. Assuming the original water was already present, over a 28-day period, 2,800 L of domestic wastewater would be produced. If this was used to replace the water lost, a pond surface area of ~30 m<sup>2</sup> would be required.



### 7.5.2. Scenario cultivated anaerobic digestion (C-AD)

For the cultivated scenarios, a 10 m<sup>2</sup> pond could produce 142.7 kg FW would be every 6 weeks, on average. This results in a range of 0.12- 0.17 kg DW/day. This could produce 9.9- 16.3 L CH<sub>4</sub>/day, see Table 7.5-4. Removing the roots was not considered due the small-scale nature of the process.

**Table 7.5-4:** Biomethane potential of wild harvested water hyacinth biomass cultivated in Pune, India.

Parameter	Spring	Summer	Monsoon	Winter	Average
Methane Potential (mL CH <sub>4</sub> /g DW)	91.2-97.2	59.7-60.1	82.3-89.5	90.0-94.6	80.8-85.3
Biomass Available (g DW/day)	164-167	166-166	160-174	124-129	153-159
Methane Available (L CH <sub>4</sub> /day)	15.0-16.3	9.9-10.0	13.1-15.6	11.1-12.2	12.4-13.6

The biomass from a 10 m<sup>2</sup> pond would contribute an average of just 6.1- 6.4% of the feedstock requirements for a 50 kg/day fixed dome digester. To produce enough biomass for a 50 kg/day digester a surface area of 144- 202 m<sup>2</sup> would be required, a size that is unlikely to be fulfilled on any farm. This suggests that WH could not be utilised in a digester as a single feedstock but there could be possibility for a co-digestion scenario.

The mass and nutrient flows are described in Table 7.5-5. This would result in an average of 35.3 L of digestate left over, once it was utilised in the cultivation pond.

**Table 7.5-5:** Digestate quantity and nutrient content from anaerobic digestion of water hyacinth from biomass cultivated in India.

Parameter	Minimum	Maximum	Average
Feedstock (g DW/week)	1,074	1,114	1,094
Digestate (L/week)	49.4	51.3	50.3
Carbon (g DW/week)	269	294	281
Nitrogen (g DW/week)	19.5	23.6	21.6
Potassium (g DW/week)	3.13	3.25	3.19

### 7.5.3. Scenario cultivated cow manure (C-CM)

It was demonstrated in Chapter 2 that the addition of WH into the diets of ruminants can have positive or negative effects, depending on the proportion of diet supplementation. If WH was included, up to 30% of a dairy cows diet, then the negative impacts were reduced, whilst daily weight gain were increased [202,203]. The inclusion of WH as 30% of the diet in dairy cattle required 7,840 g FW/day [204]. The available biomass from a 10 m<sup>2</sup> farm pond would be an average of 3,070- 3,184 g FW/day, suggesting that a farm pond could not provide enough biomass to contribute 30% towards 1 animal. This suggests that WH could not be utilised in this scenario, as the farm pond would have to >20 m<sup>2</sup>, see Table 7.5-6, and as WH cannot be used as a sole source of feed, other uses of the biomass may be better suited. Secondly, the manure produced by the cows would not be large enough to support the cultivation of the biomass for the majority of scenarios.

**Table 7.5-6:** Surplus water hyacinth and cow manure after cultivation and diet supplementation, based on the cultivation area and requirements of the cattle.

Cultivation Area (m <sup>2</sup> )	Maximum number of cows that could be fed on WH*	Surplus water hyacinth (g FW/ day)*	Surplus cow manure (kg FW/day)*
10	0	3127	-4.2
20	0	6254	-8.4
30	1	1541	7.4
40	1	4668	3.2
50	1	7795	-1.0

\*Based on the average growth rate across the year

### 7.5.4. Scenario cultivated co-digestion (C-CoD)

For the co-digestion trials, WH was co-digested in a 200 L semi-batch reactor, as described by Bray *et al.* [138]. The tests were performed on fresh, shredded biomass, producing 182.0 mL CH<sub>4</sub> / g VS at a concentration of 57.3% within the biogas. This would be the equivalent of 33.3 mL CH<sub>4</sub>/g FW, which is typical for co-digestion of WH with CM in a fixed dome digester [138].

In the co-digestion, the fresh weight ratio was 7.5% WH, 30% CM and rest was water. Therefore, to produce enough biomass for a 50 kg/day digester, a farm pond of 12 m<sup>2</sup> would be required, as well the purchasing of 15 kg of cow manure per day, whilst the digestate would be in surplus by 25.8 L/day, described in Table 7.5-7. This demonstrates that this a feasible alternative to the previous cultivation scenarios. The nutrient balance could not be calculated as the raw biomass was not characterised fully

so a digestion factor could not be estimated, however, the digestate was analytically determined to contain 0.04, 0.01 and 0.04% FW of N, P and K, respectively.

**Table 7.5-7:** Area and digestate required for water hyacinth cultivation to fulfil requirements of co-digestion with cow manure.

Loading rate (kg FW/day)	WH Required (kg FW)	Area required (m <sup>2</sup> )	Cow Manure Required (kg/day)	Digestate (L/day)	
				Required	Surplus
50	3.75	12	15	17.3	25.8
100	7.5	24	30	34.6	51.7
150	11.25	36	45	51.8	77.5
200	15	48	60	69.1	103.4
300	22.5	72	90	103.7	155.1

#### 7.5.5. Costings of the cultivated water hyacinth scenarios

Only C-CoD was deemed to be feasible based on the nutrient requirements and closed system would be unlikely to be feasible. The costs utilised in C-CoD would be a fixed dome digester, described in section 7.3.1; cow manure, assumed to be INR 1 per kg; and water hyacinth, INR 0.5 per kg was assigned as the costs associated with the harvesting and maintenance of a fully stocked pond. The capital costs of the biomass shredder was not considered as it was assumed that this machinery was required for animal feed on rural farms. It was assumed that no labour costs were incurred after the installation of the digester as the installation process included training in usage and maintenance for the recipient. As for the WH harvesting, it was assumed that this could be achieved by the family based on practical experience when cultivating the biomass and the assumed harvesting rates of 200 kg FW/hour. The income from the process would be from the offsetting of LPG cylinders, assumed to cost INR 1106 per 14.2 kg cylinder [386].

Six scenarios were analysed where 1- 3.5 LPG cylinders were offset per month, as described in Table 7.5-8. This was chosen due to a maximum size of Deenbandhu digesters, of 6 m<sup>3</sup>, as described by Samar *et al.* [377]. Beyond 4 LPG cylinders per month, a digester of over 6 m<sup>3</sup> would be required and therefore the costs could not be estimated. The loading rates of WH, CM and water are then displayed in Table 7.5-9.

**Table 7.5-8:** Scenarios considered for liquid petroleum gas consumption and methane requirement to meet demand.

Scenario	LPG Offset Cylinders per month	LPG Consumption (kg/day)	Bio-methane Requirement (kg/day)*
1	1	0.47	0.53
2	1.5	0.71	0.80
3	2	0.95	1.06
4	2.5	1.18	1.33
5	3	1.42	1.60
6	3.5	1.66	1.86

**Table 7.5-9:** Daily inventory of water hyacinth, cow manure and water for digester operation.

Scenario	WH Loading (kg/day)	CM Loading (kg/day)	Water Addition (kg/day)	Total Loading (kg/day)
1	5.7 ± 1.0	22.7 ± 4.1	47.2 ± 8.4	75.6 ± 13.5
2	8.5 ± 1.5	34.0 ± 6.1	70.9 ± 12.7	113.4 ± 20.3
3	11.3 ± 2.0	45.4 ± 8.1	94.5 ± 16.9	151.2 ± 27.0
4	14.2 ± 2.5	56.7 ± 10.1	118.1 ± 21.1	189.0 ± 33.8
5	17.0 ± 3.0	68.0 ± 12.2	141.7 ± 25.3	226.8 ± 40.5
6	19.8 ± 3.5	79.4 ± 14.2	165.4 ± 29.6	264.6 ± 47.3

The installation costs, presented in Table 7.3-4, were calculated as a factor of the loading in accordance with Samar et al. [377], based on the loading for each scenario. However, subsidies were available from the Ministry of New and Renewable Energy for AD systems of 1-25m<sup>3</sup>, therefore the subsidised costings are displayed Table 7.5-10, alongside the cost of the raw material, WH and CM, and the value of the product, LPG offsetting. The digestate would be utilised for cultivation of WH and any excess would either be disposed of or spread to land.

**Table 7.5-10:** Subsidised installation costs, material costs and value of liquid petroleum gas offset.

Scenario	Subsidised Installation Costs (Rs)	Material Costs (Rs/month)	LPG Offset Value (Rs/month)
1	25,524 ± 6,313	776 ± 139	1,106
2	40,910 ± 6,252	1,164 ± 208	1,659
3	56,297 ± 12,626	1,552 ± 277	2,212
4	73,959 ± 15,783	1,940 ± 347	2,765
5	91,621 ± 18,939	2,328 ± 416	3,318
6	109,283 ± 22,096	2,716 ± 485	3,871

The payback time of the installation cost was calculated based on the amount of LPG offset minus the cost of the raw materials. This demonstrates that as the digester size was increased, the returns were reduced and the payback time increased. If the cost of the digester was assumed to follow the trajectory of the digesters presented by Samar *et al.*, a digester that could offset 14 LPG cylinders would have a payback time of ~8.8 years, over one year longer than the smallest digester.

Due to the limited returns for increasing the size of the biogas plant, the lowest payback time was for the scenarios offsetting 1 and 2 cylinders per month.

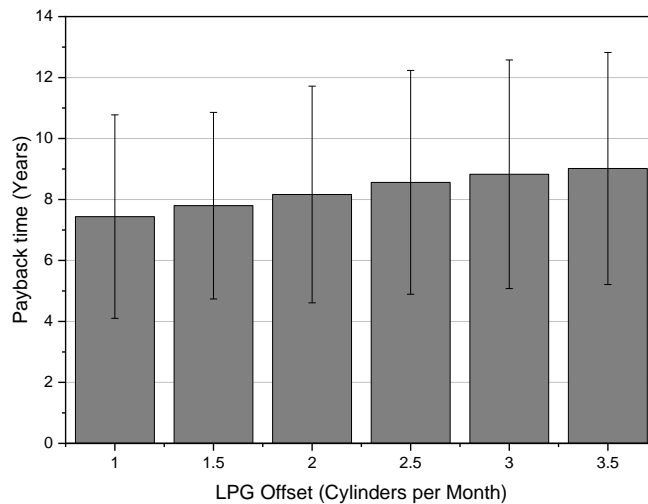


**Figure 7.5-2:** Payback period for each liquid petroleum gas replacement scenario, where digestate is utilised by the user. Error bars demonstrate the impact on economic performance based on variations in feedstock methane yield.

## 7.6. Conclusions

The aim of this chapter was to demonstrate the opportunities and challenges of WH as a wild or cultivated resource, looking at producing a protein precipitate and bioenergy, in the form of biogas.

Six scenarios were proposed, two utilising wild harvested WH and four utilising cultivated biomass. Firstly, the wild biomass available was estimated; in the wild scenarios, a single harvester was used in Kampala due to the costs of harvesting more. Whereas in India, more biomass per day must be harvested to ensure the river was harvested before the monsoon removes the biomass. Five harvesters would ensure the biomass was harvested in time. Scenario wild anaerobic digestion (W-AD) harvested wild biomass and utilised the biomass to produce biogas via anaerobic digestion.

In Kamapala, 73.6- 98.4 t FW/day could be harvested by a single harvester, this produced 111,500- 241,000 m<sup>3</sup> CH<sub>4</sub>/year and 61.8- 82.6 million L/year of digestate. In India, biomass could only be harvested for two months of the year, due to the

monsoon, therefore, 5 harvesters were required, decreasing the daily biomass availability to an average of 61- 82 t FW/day, over the entire year, or 368- 492 t FW/day during the harvesting period. This would produce 84,700- 131,250 m<sup>3</sup> CH<sub>4</sub>/year and 51.5- 68.8 million L/year of digestate. The lower BI and biomass harvest in Pune reduced the biomethane that could be produced; the biorefinery would not be sustainable even when the harvesters rented out during the off-season. Despite the higher LPG value, the scenario in Kamapala would also not be sustainable. This suggests that regardless of the location, large scale processing of WH by AD would not be sustainable when WH is the sole feedstock. Co-digestion should be examined further.

In scenario wild alkali acid extraction (W-AAE), the fresh feedstock scenario was more successful than the dry. In Kampala, the same harvest potential produced 109- 296 t/year of protein precipitate; 156,600- 288,300 m<sup>3</sup> CH<sub>4</sub>/year and 55.9- 64.0 million L/year of digestate from the residue. In Pune, the equivalent process produced 91- 247 t/year of protein; 135,350- 258,200 m<sup>3</sup> CH<sub>4</sub>/year and 48.3- 57.3 million L/year of digestate. The cost of chemicals proved to be the biggest barrier to this scenario, accounting for 92 and 72% in Uganda and India, respectively. Whilst none of these scenarios demonstrated profitability, their secondary benefits could not be accounted for. These include ecosystem restoration; economic viability of the waterbody bodies; disease prevention; and heavy metal removal from the waterbodies.

The cultivated scenarios were split based on their nutrient source. Scenario cultivated anaerobic digestion (C-AD) demonstrated that a cultivation pond would need a surface area of 144- 202 m<sup>2</sup> would be required to produce enough biomass to fulfil a 50 kg/day fixed dome digester, a size that is unlikely to be achievable on a small-scale. The same issue was found for the scenario cultivated cow manure, where a cultivation pond of >32 m<sup>2</sup> in surface area would be required to guarantee enough biomass to feed a single cow. Whilst this is more feasible than C-AD, the WH would only contribute to 30% of the animal's diet, suggesting that it is unlikely to reduce costs substantially. The final scenario that was examined in detail was the cultivated co-digestion; this demonstrated that a cultivation pond of just 12 m<sup>2</sup> could provide enough biomass for co-digestion with cow manure, producing a surplus of 25.8 L/day of digestate. This scenario was then examined in depth by examining a variety of options for offsetting LPG usage by a single family. This demonstrated that the payback time varied from 4 to 13 years depending on the biogas production and the size of the digester. The optimal sized digester was less than 150 kg/day due to the increased cost of installation and materials, whilst the subsidy reduction was less impactful as the size of digester increased.

Another cultivation scenario was postulated but not examined as it was out of scope for the experimental work. It was suggested that a 30 m<sup>2</sup> cultivation pond could be utilised to clean domestic wastewater from a single family in India. This would produce a biomass that could be co-digested with the sludge that forms at the base of the pond. Whilst this is theoretically possible, no experimental analysis was conducted on cultivation of WH with domestic wastewater, nor co-digestion of WH with the sludge. Finally, health and safety issues may occur with the cleaning of the tanks/collection of the sludge, suggesting a bespoke cultivation system could be required, adding costs.

Based on the information gathered in this chapter, small-scale decentralised WH systems would be more effective than large scale biorefineries. This was largely due to the cost of harvesting, low biomethane potential and high processing costs of the alkali acid extraction. However, the impact of removing the WH biomass from the waterbodies may have non-quantifiable benefits that make it an overall positive mechanism, therefore, further investigation into optimisation should occur to increase the value of the process. Options include improvement of protein precipitation and co-digestion of the biomass with cheap waste products, like sewage sludge.

## Chapter 8.

# Conclusions and Future Work

The overall aim of this thesis was to demonstrate the potential utilisation of water hyacinth in a biorefinery, examining the breadth of the variation in composition that could occur geographically or phenologically. The following section will outline the key conclusions of the thesis and how these achieved the overall aims and objectives of the study. In addition, future directions of this work are proposed, in order to valorise WH biomass and produce an economically viable biorefinery.

Summary of the aims and objectives

### 8.1. Conclusions

This thesis was split into three key objectives: water hyacinth as resource, in controlled conditions and utilised in a biorefinery. This section outlines the key conclusions obtained through these objectives.

*Objective 1: Water hyacinth in the wild.*

An in-depth literature review determined that WH roots contained the highest concentration of contaminants but that little was known about those variations across the growth cycle. The variations geographically were more obvious, with a significant range of composition proposed. However, analysis of the reasons behind these variations was lacking; this study would investigate the pollution sources of the local area to determine if this impacted the composition.

WH samples were collected from three locations: Lake Victoria, Uganda; West Bengal, India; and Maharashtra, India. The results demonstrated that whilst the Pune rivers would be considered the most polluted, due to the high levels of raw sewage, they contained the lowest levels of nitrogen and heavy metal contamination, suggesting that either biomass was able to remove pollutants from the water or the high flow rate reduced the concentration of contaminants that could occur in water with a high residence time. The ponds in Goyal Para had the lowest level of pollution and lower levels of TKN and TSS than all sites in Lake Victoria, these were used as the baseline for a “clean waterbody”. This was shown in the ash content where Goyal Para for the whole plant, as well as the leaf, petiole and root tissues. Whilst the Lake Victoria whole plant had a greater ash content than the Pune rivers, all parts of the plant had a lower ash content, suggesting that the whole plant may have been an anomaly. The roots contain a greater ash content and heavy metal content than the rest of plant, when



comparing the total heavy metal content of the roots, it demonstrated that the Pune rivers were the most contaminated plants; they also contained the highest concentration of protein. It is suggested that the higher flow rate in Pune rivers increased the exposure of the plants to inorganics and therefore increased the total uptake of inorganics.

The phenological analysis demonstrated that all sites had peaks across the respective collection periods. In Lake Victoria, this was most likely due to the variations in environmental conditions, resulting in changes in growth rate and exposure to pollutants. The biomass with the highest number and size of peaks was the site exposed to sewage pollution. At all sites, the protein content was lowest at times when the heavy metal content was highest, suggesting that if protein recovery was the primary concern, then heavy metal contamination would be minimised. Whereas if the focus was on heavy metal recovery or removal, then protein extraction would be a poor method of utilisation both due to the high contamination and low protein content. In Pune, the biomass was only available for a small portion of the year due to monsoon. The biomass was then characterised by two distinct growth periods; the first was a horizontal growth mechanism, characterised by high asexual reproduction and short plants with long roots and bulbous petioles. This method was utilised by WH to dominate a waterbody as quickly as possible. These plants appeared to have a reduction in heavy metal and calcium content and increased nitrogen and potassium concentration. Once the plants were restricted for space, the plants switched growth mechanism and began to grow vertically. These plants were characterised by long tubular petioles, large dark leaves and short feathery roots. At this stage the plants reduced their nitrogen and potassium content, whilst the heavy metal and calcium concentrations increased. This demonstrated similar results to Uganda, where protein and heavy metal content were inverses of each other. However, in Pune, the period of high protein was the period of lowest biomass yield and therefore would be a sub-optimal time to harvest biomass; by harvesting at the end of the growth season, total protein weight would be increased and heavy metal removal from the river would be maximised. Due to lack of sampling points, the phenological variations in Goyal Para could be not identified, however, it was shown that plants had low protein content at the end of the growth season. In contrast to the other sites, heavy metal content did not increase at this point, possible due to the impact of monsoon resulting in a dilution of heavy metal contamination.

In comparison to water lettuce, WH had a similar ash and nutrient content, theoretical higher heating value, and maximum theoretical biomethane potential. Whereas protein content and heavy metal content were lower in WH. Based on this WH could be

considered the sub-optimal choice, however, it has been demonstrated that WH has a greater growth rate and plant density.

This objective resulted in a range of WH samples and demonstrated an expected range of organic and inorganic composition, as well as utilisation potential indicators, including higher heating value, biomethane potential and protein content. The pollution sources suggested that water flow had a greater impact on biomass composition than point source pollution. In contrast, phenological variations were more obvious when a clear growth season could be identified. Once identified, it may be possible to estimate the biomass composition changes, provided no point source pollution events change the conditions significantly.

*Objective 2: Water hyacinth in controlled conditions.*

The literature identified that under semi-controlled conditions, WH growth rate could be estimated based on the N concentration of the water, however, the data was limited, the nutrient sources varied and no consistent methodology. Therefore, it was proposed that a consistent methodology could be applied to WH cultivation under semi-controlled conditions to determine the impact of water N concentration has on growth rate. Other parameters investigated were temperature and biomass density.

WH was cultivated under conditions of known nutrient addition, specifically focussed on the variations of nitrogen loading. In small crate trials, utilising cow manure as the sole source of nutrients, a strong and statistically significant linear fit was observed up to 30 mg N/L, with an equation of  $y = (1.20 \pm 0.11)x + (1.97 \pm 1.32)$ . When compared with other nutrient source, there was variation in nitrogen solubilisation within the water, which contributed to the variation in growth rates seen. Cooked food waste and an artificial fertiliser were trialled but due a low growth rate or high cost, respectively, they were discounted. Buffalo manure showed no improvement to cow manure. Digestate had a high nitrogen solubilisation that reduced growth rate, however, due to its potential in a closed system biorefinery, it was utilised in large growth trials. The filtered cow manure was also utilised in large growth trials due to the reduction in surface tension and viscosity, as compared to cow manure. When cultivated in large tanks, the growth was similar to that in small crates, however, high nitrogen concentration had less impact on the growth rate. Filtered cow manure was the best nutrient source due to its high growth rate, low surface tension and low viscosity. Digestate had a lower growth rate than filtered cow manure, however this may have been due to the high nitrogen solubilisation. The N concentration of the leaf confirmed literature analysis that increasing the N concentration in the water increased the N concentration in the leaf. Utilising the logistic growth model, the impact of plant density on growth rate was demonstrated to vary depending on the water N concentration. By normalising for

water N concentration, it was demonstrated that temperature was a significant factor in growth rate, but solar irradiance was not.

The work in this objective demonstrated that WH growth rate could be manipulated by varying the water N concentration but other factors, including density and temperature, should be considered. Secondly, the growth rate appeared to vary due to nutrient source, but within an expected margin of error. In particular, filtered cow manure demonstrated a high growth rate and suitable growth conditions, whilst digestate resulted in a higher level of nutrient solubilisation.

### *Objective 3: Water hyacinth in a biorefinery*

An investigation into the literature determined that two methods appeared to show promise for WH: protein extraction and anaerobic digestion. WH has been used as flour or hay in various diets for different animals and undergone various processing techniques for protein extraction. However, due to the poor digestion properties of WH it could only account for <30% of an animal's diet. Whilst as a feedstock for extraction, WH demonstrated poor yields and only the leaves were investigated due to the high HM content. Therefore, a simple extraction process was proposed that could utilise the whole biomass and reduce processing costs and biomass waste. AD was investigated as a secondary option due to its ability to process wet biomass, the possibilities of co-digestion and the production of digestate for use as a nutrient source in WH.

The analysis of conditions demonstrated that the optimal time varied depending on the other conditions, although beyond 150 minutes extraction time appeared to be insignificant for most conditions. For the temperature, 40 or 65°C was optimal, and the highest alkali strength, of 1.0M, gave greater yields. The higher alkali strength required greater quantity of acid to acidify and resulted in higher concentrations of sodium sulphates in the final product, however, gentle washing in water removed the majority of this. To optimise yields, certain parameters were altered: increasing the solid-to-liquid ratio increase yields; a precipitation pH of 3.75 showed little difference when lowered to 3 or raised to 4.

WH samples were then utilised at the optimal condition, 40°C; 1.0M; and 150 minutes, to demonstrate the variations that could occur between different samples. This demonstrated that the leaf had the highest protein recovery, whilst the root and petiole were similar, despite the highest protein concentration coming from the petiole. The analysis of biochemical composition of the raw biomass demonstrated that protein content and cellulose content had significant impact on the precipitate weight and protein content of the precipitate. The variability of WH composition suggests that this variability could impact the economic viability of this process, however, a greater number of samples would be required to analysis this. The impact of utilising wet

feedstock, as opposed to dry, showed a reduction in total protein recovery for both the leaf and whole plant.

The analysis of the solid residue demonstrated that the biomethane potential of the whole plant was increased by >77%, however, a mass balance indicated that digestate would have 49- 73%, 92-99% less N and P, respectively, than CM.

The analysis of the protein precipitate demonstrated that it contained low enough concentrations of HMs to be consumed in small amounts by humans, however, only the leaf and petiole would be safe. If the biomass could be blended with other cheap forms of protein, e.g., soy meal, it could be ingested safely and as a low-cost food additive for animals or humans.

The data from all the objectives was presented in the form of six scenarios: wild anaerobic digestion; wild alkali acid extraction; cultivated cow manure; cultivated anaerobic digestion; and cultivated co-digestion. Two case studies were developed for the wild scenarios, one in Kampala and one in Pune. This demonstrated the scale of the problem that is WH: huge capital costs would be required in order to harvest the biomass, on top of the costs associated with processing. In Kampala, WH could be harvested sustainably, i.e., the biomass would grow back faster than could be harvested, by a single harvester; whilst in Pune, a minimum of 5 harvesters would be required in order to harvest the section of the river selected before the monsoon removed the biomass.

The first wild scenario, W-AD, demonstrated that the high capital costs, and high running costs of producing the biogas, resulted in economically unsustainable process in both case study locations. It was concluded that the poor digestibility of WH was the predominant factor in this, therefore, co-digestion should be investigated further, examples could include food waste, sewage sludge or agricultural wastes. Other options could include pre-treatment which has been shown to increase digestion of WH. However, the second wild scenario, W-AAE, also demonstrated that despite the production of protein, the treatment of WH with NaOH was not economically sustainable, largely due to the cost of NaOH and the high solid-to-liquid ratio. If protein was not the target product, a significant reduction in the cost of chemicals would occur, for example, the use of KOH as pretreatment utilises over 50 times less per kg of feedstock than was used in the W-AAE scenario [138], however, this is unlikely to solubilise a significant portion of the protein, but could improve the economic viability of the W-AD scenario.

The first two of the cultivated scenarios, C-CM and C-AD, demonstrated a similar result to the previous two: the utilisation of WH as sole feedstock was unable to provide enough biomass to fulfil the requirements of the scenario. In the C-CM scenario a pond

of over 30 m<sup>2</sup> would be required to feed a single animal, whilst in the C-AD scenario, a pond of over 140 m<sup>2</sup> would be required. An examination of WH as a feedstock in a co-digestion scenario, with CM, demonstrated a significant improvement: the pond requirements were just 12 m<sup>2</sup> for a 50 kg/day digester. When investigating the offsetting of LPG for a single family, the payback period ranged from 4-13 years, but the optimal size was 150 kg/day digester.

Whilst options exist for increasing the viability of the wild harvest scenarios, the most important aspect are non-direct financial reasons for removing the biomass, therefore a private company is unlikely to harvest the biomass but the impacts on local economics of removing the biomass could interest local government involvement, provided the processing options exist in the area. However, these results suggest that WH has more viability as a feedstock in decentralised AD units, as compared to large scale digestion.

## **8.2. Future work**

This work has investigated the potential for HM contaminated WH to be utilised as a feedstock under a variety of scenarios, however, significant questions still exist surrounding its potential. These surround the non-direct financial reasons for WH harvesting; and the options for increasing the economic viability of the wild harvesting and cultivation scenarios.

### **8.2.1. Bioaccumulation and the role of water hyacinth in urban water bodies**

The potential for WH to perform a role in the removal of HMs has been investigated in literature, however, the variations that occur phenologically suggests that this process could be optimised to remove the HMs from the waterbodies. A limitation of the literature is the lack of information on the concentration of pollution within the waterbodies and therefore the relationship within WH. This study attempted to remedy this by examining the water quality indicators, however, due to COVID19, a full set of data could not be delivered, therefore, a detailed set of phenological variations in WQIs and biomass composition should be considered, to understand the role that WH plays in the removal of pollutants from urban water bodies.

In the particular case of Pune, two areas should be studied further: the difference between the water quality during low WH density (post-monsoon to mid-winter); and the impact of WH on point source pollution events. The first suggested study was not part of the initial scope of this study and the facilities were not available to access the rivers outside of the WH growth period. However, the levels of pollution within the rivers and the biomass suggests that biomass may have significant impacts on the water quality. This would be a vital study due to the needs of the river for the local population: the rivers in Pune are utilised for drinking water, bathing and recreation, therefore,

before the WH recovers post monsoon, the water could contain significantly higher levels of pollution.

The second study was alluded to in Chapter 4, where it was demonstrated that at one site the HM content within the plants was reduced along the river, suggesting that WH acts as a filter for the pollutants and therefore the plants are subjected to lower concentrations as the river moves through the city. In contrast, on the other river, the biomass was not significantly different between the two sites, due to the regular influxes of pollution along the river. An analysis along the rivers would demonstrate the role that WH plays within urban rivers and demonstrate the need for removing these pollutants from the river, increasing the value of the biorefinery. A greater understanding of the variations would also identify the possibility of utilising WH for phytomining.

### 8.2.2. Increasing the economic sustainability of a water hyacinth biorefinery

There were multiple options identified for the optimisation of the WH biorefinery, described here are some of the examples.

#### *8.2.2.1. Analysis of digestate and digestate value*

In the scenarios described in Chapter 7, the digestate was assigned no value, despite the significant variation in the concentration of nutrients. It has been suggested that digestate has a value [377,391], particularly in a scenario where it could be utilised locally as a fertiliser offset. Bray *et al.* demonstrated that the sale of digestate was the most significant impact on economic viability of small-scale AD [138]. In the wild harvested scenarios, the sale of digestate for 0.5 Rs/kg would result in the generation of ~£250,000- 400,000 in the W-AD scenarios, making the Uganda case study an economically viable option. However, the mass flow produced in Chapter 7, suggest that the digestate of WH as a sole feedstock would have less nutrient content than CM, therefore, the digestate should be analysed directly to understand its value as fertiliser and the potential issues that may arise from the HM content of the roots. This analysis may suggest that the extra processing costs of removing the roots may be the optimal route due to the presence of HMs in the digestate, potentially labelling the digestate as a mass-produced waste that must be disposed of, as opposed to a low value product.

#### *8.2.2.2. Alternative feedstock as a source of nutrients or co-digestion material*

The cultivation of WH has been demonstrated to have a strong relationship between starting water N concentration and growth rate, however, this was based off CM. Whilst other sources of nutrients showed to be within a 95% confidence, only a selected number were investigated. It has been suggested that domestic wastewater could be

used as a source of nutrients and that literature suggests it could clean the water within a suitable timeframe for a single family, assuming a pond size of ~30 m<sup>2</sup>. However, the practicalities of this cultivation were not within the scope of this study. Firstly, the safety of utilising this water should be investigated, particularly around the attraction of pests to a highly polluted water body. Secondly, production and recovery of sewage sludge: the solid matter would eventually settle to base of the water body, this matter must be removed periodically or the build-up of sludge and WH detritus would eventually start to cause hypoxic zones, which could have impacts that have previously not been accounted for. Secondly, sewage sludge is a useful feedstock for AD [402], therefore, it would be a wasted resource. However, the co-digestion of the sludge with WH should be investigated to determine the biomethane potential, both on a small-scale and large scale as secondary source of feedstock in large-scale AD, either to enhance the methane yield or account for lower biomass yields during the monsoon and winter in rain affected locations.

#### *8.2.2.3. Optimisation of the protein extraction methodology*

The production of protein substitutes is an important topic in the current climate, therefore, if a safe WH protein precipitate could be produced economically sustainably then WH could offer significant ecosystems services as well as a viable product. However, this study has shown that WH was a poor feedstock choice as compared with WL due to the increased cellulose content of the biomass. However, optimisation of this process could improve the recovery, or alternative methods may reduce the costs of the process. Here are some examples of cost reduction and optimisation methods that were not part of the scope in this study. However, the study was limited by the inability to determine the quality of the protein extract, therefore, any further work should include the analysis of the amino acid content of the extract.

Firstly, a limitation of this study was utilisation of one set of conditions for the different stocks, as shown in the literature, optimal conditions vary significantly depending on the feedstock, therefore it is likely that variation in biomass may result in variation in the yield. A more detailed set of conditions and on a wider sample set would demonstrate the optimal conditions for extractions. This includes the utilisation of fresh feedstock in this analysis: the current study demonstrated that dry feedstock had a greater recovery than wet feedstock, the theory behind this cannot be explained and therefore should be examined further.

Other methods for optimising AAEs, that were not part of the scope of this work, are microwave assisted and ultrasound assisted extraction. These have been shown to double protein recovery depending on the feedstock and the conditions [244,249].

Another method not considered in this study was the acidic fermentation of WH to produce a protein product, liquid product and solid residue. An example of this is the lactic acid fermentation of feedstocks to produce a protein rich product, fibre rich residue and nutrient rich liquid residue [239]. This process was able to produce 6- 13 kg of protein product per ton of fresh feedstock, as compared with 4- 8 kg/ton FW for AAE. Secondly, the process produced a nutrient rich liquid containing a highly valuable chemical product in lactic acid [235]. Other fermentation process could also be studied, for example, acetic acid fermentation [403]; acetic acid is a bioproduct of anaerobic digestion through acetogenesis, and the addition of acetic acid into a digester can improve methane yields by 70%. Therefore, the production of a fibre rich press cake and acetic acid rich liquid could improve methane yields from WH significantly. However, the fermentation of WH must be investigated to understand the potential of this method.

Finally, the selection chemicals in AAE, and their potential secondary uses should be examined experimentally. It has been shown that the use of NaOH was a major barrier to the economic viability of scenario W-AAE, as well the production of sodium sulphates a bio-product of utilising NaOH and H<sub>2</sub>SO<sub>4</sub>. Whilst it has been suggested that the liquid waste could be recycled back into the process, this was not examined experimentally. Another option to this would be to utilise alternative chemicals for the AAE. Examples include KOH or urea as the solubilising agent, and organic or phosphoric acids as the precipitation agent. The advantage of these options is the by-products of the process would be suitable as fertilisers or as an additive to AD.



# References

1. Fawzy S, Osman AI, Doran J, Rooney DW. (2020). Strategies for mitigation of climate change: a review. *Environ Chem Lett.* 18(6): 2069–94. **10.1007/s10311-020-01059-w**
2. United Nations. 2022. The Sustainable Development Goals. Accessed February 25, 2023. <https://unstats.un.org/sdgs/report/2022/The-Sustainable-Development-Goals-Report-2022.pdf>
3. Gould CF, Urpelainen J. (2018). LPG as a clean cooking fuel: Adoption, use, and impact in rural India. *Energy Policy.* 122(C): 395–408. **10.1016/j.enpol.2018.07.042**
4. Lu J, Fu Z, Yin Z. (2008). Performance of a water hyacinth (*Eichhornia crassipes*) system in the treatment of wastewater from a duck farm and the effects of using water hyacinth as duck feed. *Journal of Environmental Sciences.* 20(5): 513–9. **10.1016/S1001-0742(08)62088-4**
5. UNESCO World Water Assessment Programme. (2021). The United Nations world water development report 2021: valuing water. Paris; 187 p. Accessed February 25, 2023. <https://unesdoc.unesco.org/ark:/48223/pf0000375724>
6. Förstner U, Wittmann GTW. (1981). *Metal Pollution in the Aquatic Environment*. 2nd ed. Berlin, Heidelberg: Springer Berlin Heidelberg; 504 p. (Springer Study Edition). **10.1007/978-3-642-69385-4\_2**
7. Laws EA. (2017). *Aquatic Pollution: An Introductory Text*. John Wiley & Sons; 758 p.
8. Glibert PM. (2017). Eutrophication, harmful algae and biodiversity — Challenging paradigms in a world of complex nutrient changes. *Marine Pollution Bulletin.* 124(2): 591–606. **10.1016/j.marpolbul.2017.04.027**
9. Istvánovics V. (2009). Eutrophication of Lakes and Reservoirs. In: Likens GE, editor. *Encyclopedia of Inland Waters*. Oxford: Academic Press; p. 157–65. **10.1016/B978-012370626-3.00141-1**
10. Wurtsbaugh WA, Paerl HW, Dodds WK. (2019). Nutrients, eutrophication and harmful algal blooms along the freshwater to marine continuum. *WIREs Water.* 6(5): e1373. **<https://doi.org/10.1002/wat2.1373>**
11. Selman M, Greenhalgh S. (2009). *Eutrophication: Sources and Drivers of Nutrient Pollution*. Accessed December 28, 2020. <https://www.wri.org/publication/eutrophication-sources-and-drivers-nutrient-pollution>
12. Sharma S. (2014). *Heavy Metals In Water: Presence, Removal and Safety*. **10.1039/9781782620174**
13. Majumdar A, Barla A, Upadhyay MK, Ghosh D, Chaudhuri P, Srivastava S, Bose S. (2018). Vermiremediation of metal(loid)s via *Eichhornia crassipes* phytomass extraction: A sustainable technique for plant amelioration. *Journal of Environmental Management.* 220: 118–25. **10.1016/j.jenvman.2018.05.017**

14. Chernykh NA, Ngo TC, Chan HK, Baeva YI, Grachev VA. (2018). The regularities of heavy metals and arsenic accumulation in the vegetation of riverside depending on the level of technogenic load. *Journal of Pharmaceutical Sciences and Research*. 10(4): 800–4.
15. Förstner U, Prosi F. (1979). Heavy Metal Pollution in Freshwater Ecosystems. In: *Biological Aspects of Freshwater Pollution*. Elsevier; p. 129–61. **10.1016/B978-0-08-023442-7.50011-6**
16. Bradl H. (2005). *Heavy Metals in the Environment: Origin, Interaction and Remediation*. Elsevier; 283 p. <https://www.elsevier.com/books/heavy-metals-in-the-environment-origin-interaction-and-remediation/bradl/978-0-12-088381-3>
17. Alvarado S, Guédez M, Lué-Merú MP, Nelson G, Alvaro A, Jesús AC, Gyula Z. (2008). Arsenic removal from waters by bioremediation with the aquatic plants Water Hyacinth (*Eichhornia crassipes*) and Lesser Duckweed (*Lemna minor*). *Bioresource Technology*. 99(17): 8436–40. **10.1016/j.biortech.2008.02.051**
18. Sharma A, Aggarwal NK, Saini A, Yadav A. (2016). Beyond biocontrol: water hyacinth-opportunities and challenges. *Journal of Environmental Science and Technology*. 9(1): 26–48. **10.3923/jest.2016.26.48**
19. Azimi A, Azari A, Rezakazemi M, Ansarpour M. (2017). Removal of Heavy Metals from Industrial Wastewaters: A Review. *ChemBioEng Reviews*. 4(1): 37–59. **10.1002/cben.201600010**
20. Hakeem K, Sabir M, Ozturk M, Mermut AR. (2014). *Soil Remediation and Plants: Prospects and Challenges*. Academic Press; 771 p. <https://www.elsevier.com/books/soil-remediation-and-plants/hakeem/978-0-12-799937-1>
21. Saha P, Shinde O, Sarkar S. (2017). Phytoremediation of industrial mines wastewater using water hyacinth. *Int J Phytoremediation*. 19(1): 87–96. **10.1080/15226514.2016.1216078**
22. Susarla S, Medina VF, McCutcheon SC. (2002). Phytoremediation: An ecological solution to organic chemical contamination. *Ecological Engineering*. 18(5): 647–58. **10.1016/S0925-8574(02)00026-5**
23. Penfound WmT, Earle TT. (1948). *The Biology of the Water Hyacinth*. Ecological Monographs. 18(4): 447–72. **10.2307/1948585**
24. Jones JL, Jenkins RO, Haris PI. (2018). Extending the geographic reach of the water hyacinth plant in removal of heavy metals from a temperate Northern Hemisphere river. *Scientific Reports*. 8(1). **10.1038/s41598-018-29387-6**
25. Gopal B. (1987). *Water Hyacinth: Aquatic Plant Study*. Elsevier; 492 p.
26. Williams AE. (2006). *Water Hyacinth*. In: *Van Nostrand's Scientific Encyclopaedia*. American Cancer Society; **10.1002/0471743984.vse7463.pub2**
27. EU. Nov 4, 2014. Regulation (EU) No 1143/2014 of the European Parliament and of the Council of 22 October 2014 on the prevention and management of the introduction and spread of invasive alien species. OJ L, 32014R1143. Accessed February 27, 2019. <http://data.europa.eu/eli/reg/2014/1143/oj/eng>

28. Guna V, Ilangoan M, Anantha Prasad MG, Reddy N. (2017). Water Hyacinth: A Unique Source for Sustainable Materials and Products. *ACS Sustainable Chem Eng.* 5(6): 4478–90. **10.1021/acssuschemeng.7b00051**
29. Ellis AT. (2011). Water Hyacinth, *Eichhornia crassipes*. : 7. **[http://depts.washington.edu/oldenlab/wordpress/wp-content/uploads/2013/03/Eichhornia-crassipes\\_Ellis.pdf](http://depts.washington.edu/oldenlab/wordpress/wp-content/uploads/2013/03/Eichhornia-crassipes_Ellis.pdf)**
30. Malik A. (2007). Environmental challenge vis a vis opportunity: The case of water hyacinth. *Environment International.* 33(1): 122–38. **10.1016/j.envint.2006.08.004**
31. Prasad MNV, De Oliveira Freitas HM. (2003). Metal hyperaccumulation in plants - Biodiversity prospecting for phytoremediation technology. *Electronic Journal of Biotechnology.* 6(3): 110–46. **10.2225/vol6-issue3-fulltext-6**
32. Kateregga E, Sterner T. (2007). Indicators for an invasive species: Water hyacinths in Lake Victoria. *Ecological Indicators.* 7(2): 362–70. **10.1016/j.ecolind.2006.02.008**
33. Wolverson BC, McDonald RC. (1979). Water hyacinth (*Eichhornia Crassipes*) productivity and harvesting studies. *Econ Bot.* 33(1): 1–10. **10.1007/BF02858205**
34. Kumar K, Mishra SK, Shrivastav A, Park MS, Yang J-W. (2015). Recent trends in the mass cultivation of algae in raceway ponds. *Renewable and Sustainable Energy Reviews.* 51: 875–85. **10.1016/j.rser.2015.06.033**
35. EPPO. (2019). EPPO Global Database. <https://gd.eppo.int>
36. Bolorunduro PI. (2002). Perspectives in water weeds infestation: the Lake Chad experience. In New Bussa, Nigeria; p. 165–74. Accessed November 4, 2019. <http://aquaticcommons.org/952/>
37. Brundu G, Camarda I. (2004). The Exotic Flora of Chad: A First Contribution. *Weed Technology.* 18: 1226–31.
38. Kriticos DJ, Brunel S. (2016). Assessing and Managing the Current and Future Pest Risk from Water Hyacinth, (*Eichhornia crassipes*), an Invasive Aquatic Plant Threatening the Environment and Water Security. *PLOS ONE.* 11(8): e0120054. **10.1371/journal.pone.0120054**
39. Programme UNE, Topfer K. (1999). *Global Environment Outlook 2000.* Earthscan; 438 p.
40. Tamiru G. (2017). Invasive Alien Weed Species Distribution, Impacts on Agriculture, Challenge and Reaction in Ethiopia: A Review. In.
41. Secretariat I. (2003). Identification of risks and management of invasive alien species using the IPPC framework. In: *Proceedings of the workshop on invasive alien species and the International Plant Protection Convention, Braunschweig, Germany.* Braunschweig, Germany; p. 22–6. <http://www.fao.org/3/y5968e/y5968e10.htm#TopOfPage>
42. Poddar K, Mandal L, Banerjee GC. (1991). Studies on water hyacinth (*Eichhornia crassipes*)- chemical composition of the plant and water from different habitats. *Indian Veterinary Journal.* 68(9): 833–7.

43. Sudiarto SIA, Renggaman A, Choi HL. (2019). Floating aquatic plants for total nitrogen and phosphorus removal from treated swine wastewater and their biomass characteristics. *Journal of Environmental Management*. 231: 763–9. **10.1016/j.jenvman.2018.10.070**
44. Güngören Madenoğlu T, Jalilnejad Falizi N, Kabay N, Güneş A, Kumar R, Pek T, Yüksel M. (2019). Kinetic analysis of methane production from anaerobic digestion of water lettuce (*Pistia stratiotes* L.) with waste sludge. *Journal of Chemical Technology & Biotechnology*. 94(6): 1893–903. **10.1002/jctb.5968**
45. Yang M, Zhang X, Wang K, Zhu S, Ye Z, Sheng K, Zhang X. (2022). Investigation of cascade valorization of *Pistia stratiotes* L. by hydrothermal treatment. *Fuel*. 324: 124473. **10.1016/j.fuel.2022.124473**
46. Nisha SN, Geetha B. (2017). Effect of partial replacement of fishmeal with aquatic weed *Pistia stratiotes* meal on growth, biochemical composition, haematological parameters and digestive enzymes in Indian major carp *Labeo rohita*. *Int J Fish Aquat Stud*. 5(2): 527–32.
47. Górnicki K, Kaleta A, Winiczenko R. (2020). Estimating the higher heating value of forest and agricultural biomass. Jewiarz M, editor. *E3S Web Conf*. 154: 01002. **10.1051/e3sconf/202015401002**
48. Wolverton BC, McDonald RC. (1978). Nutritional composition of water hyacinths grown on domestic sewage. *Econ Bot*. 32(4): 363–70. **10.1007/BF02907930**
49. Patel V, Desai M, Madamwar D. (1993). Thermochemical pretreatment of water hyacinth for improved biomethanation. *Appl Biochem Biotechnol*. 42(1): 67–74. **10.1007/BF02788902**
50. Das A, Ghosh P, Paul T, Ghosh U, Pati BR, Mondal KC. (2016). Production of bioethanol as useful biofuel through the bioconversion of water hyacinth (*Eichhornia crassipes*). *3 Biotech*. 6(1). **10.1007/s13205-016-0385-y**
51. Yan J, Wei Z, Wang Q, He M, Li S, Irbis C. (2015). Bioethanol production from sodium hydroxide/hydrogen peroxide-pretreated water hyacinth via simultaneous saccharification and fermentation with a newly isolated thermotolerant *Kluyveromyces marxianus* strain. *Bioresource Technology*. 193: 103–9. **10.1016/j.biortech.2015.06.069**
52. Bolenz S, Omran H, Gierschner K. (1990). Treatments of water hyacinth tissue to obtain useful products. *Biological Wastes*. 33(4): 263–74. **10.1016/0269-7483(90)90130-K**
53. Abdelhamid DAM, Gabr DAA. (1991). Evaluation of water hyacinth as a feed for ruminants. *Archiv für Tierernaehrung*. 41(7–8): 745–56. **10.1080/17450399109428519**
54. Chanakya HN, Borgaonkar S, Meena G, Jagadish KS. (1993). Solid-phase biogas production with garbage or water hyacinth. *Bioresource Technology*. 46(3): 227–31. **10.1016/0960-8524(93)90125-U**
55. Valk VA. (2015). Valorization of water hyacinth as a renewable source of animal feed and biogas: A business case for Lake Victoria, Kenya. [Netherlands]: Wageningen University; Accessed May 16, 2019. <http://resolver.tudelft.nl/uuid:415bce32-3782-49ba-99ce-1a433d826143>

56. Center TD, Spencer NR. (1981). The phenology and growth of water hyacinth (*Eichhornia crassipes* (Mart.) Solms) in a eutrophic north-central Florida lake. *Aquatic Botany*. 10: 1–32. **10.1016/0304-3770(81)90002-4**
57. Lugo AE, Ultsch GR, Brinson MM, Kane E. (1978). Metabolism and biomass of water hyacinth-dominated ponds and canals in the vicinity of Gainesville, Florida. *Geol Ecol Trop*. (2): 415–41.
58. Center TD, Dray Jr F Allen, Jubinsky GP, Grodowitz MJ. (1999). Biological Control of Water Hyacinth Under Conditions of Maintenance Management: Can Herbicides and Insects Be Integrated? *Environmental Management*. 23(2): 241–56. **10.1007/s002679900183**
59. Barrett SCH. (1980). Sexual Reproduction in *Eichhornia crassipes* (Water Hyacinth). II. Seed Production in Natural Populations. *Journal of Applied Ecology*. 17(1): 113–24. **10.2307/2402967**
60. Barrett SCH. (1977). Tristyly in *Eichhornia crassipes* (Mart.) Solms (Water Hyacinth). *Biotropica*. 9(4): 230–8. **10.2307/2388140**
61. Wasagu RS, Lawal M, Shehu S, Alfa HH, Muhammad C. (2013). Nutritive values, Mineral and Antioxidant properties of *Pistia stratiotes* (Water lettuce). *Nigerian Journal of Basic and Applied Sciences*. 21(4): 253–7. **10.4314/njbas.v21i4.2**
62. Abdel Shafy HI, Farid MR, El-Din AM. (2016). Water-hyacinth from Nile River: chemical contents, nutrient elements and heavy metals. *Egyptian Journal of Chemistry*. 59(2): 131.
63. Lara-Serrano JS, Rutiaga-Quiñones OM, López-Miranda J, Fileto-Pérez HA, Pedraza-Bucio FE, Rico-Cerda JL, Rutiaga-Quiñones JG. (2016). Physicochemical Characterization of Water Hyacinth (*Eichhornia crassipes* (Mart.) Solms). *BioResources*. 11(3). **10.15376/biores.11.3.7214-7223**
64. Sivasankari B, David Ravindran A. (2016). A Study on Chemical Analysis of Water Hyacinth (*Eichhornia crassipes*), Water Lettuce (*Pistia stratiotes*). *International Journal of Innovative Research in Science, Engineering and Technology*. 5(10): 17566–70. **10.15680/IJRSET.2016.0510010**
65. Preussler KH, Mahler CF, Maranhão LT. (2015). Performance of a system of natural wetlands in leachate of a posttreatment landfill. *International Journal of Environmental Science and Technology*. 12(8): 2623–38. **10.1007/s13762-014-0674-0**
66. Victor KK, Ladji M, Adjiri AO, Cyrille YDA, Sanogo TA. (2016). Bioaccumulation of Heavy Metals from Wastewaters (Pb, Zn, Cd, Cu and Cr) in Water Hyacinth (*Eichhornia crassipes*) and Water Lettuce (*Pistia stratiotes*). *International Journal of ChemTech Research*. 9(2): 189–95.
67. Shirinpur-Valadi A, Hatamzadeh A, Sedaghatoor S. (2019). Study of the accumulation of contaminants by *Cyperus alternifolius*, *Lemna minor*, *Eichhornia crassipes*, and *Canna x generalis* in some contaminated aquatic environments. *Environmental Science and Pollution Research*. 26(21): 21340–50. **10.1007/s11356-019-05203-0**
68. Tabla-Hernandez J, Rodriguez-Espinosa PF, Mendoza-Pérez JA, Sánchez-Ortíz E, Martínez-Tavera E, Hernandez-Ramirez AG. (2019). Assessment of potential

- toxic metals in a Ramsar wetland, Central Mexico and its self-depuration through *Eichhornia crassipes*. *Water* (Switzerland). 11(6). **10.3390/w11061248**
69. Ayaz T, Khan S, Khan AZ, Lei M, Alam M. (2020). Remediation of industrial wastewater using four hydrophyte species: A comparison of individual (pot experiments) and mix plants (constructed wetland). *Journal of Environmental Management*. 255. **10.1016/j.jenvman.2019.109833**
  70. Eid EM, Shaltout KH, Almuqrin AH, Aloraini DA, Khedher KM, Taher MA, Alfarhan AH, Picó Y, Barcelo D. (2021). Uptake prediction of nine heavy metals by *Eichhornia crassipes* grown in irrigation canals: A biomonitoring approach. *Science of the Total Environment*. 782. **10.1016/j.scitotenv.2021.146887**
  71. McKeown AE, Bugyi G. (2015). *Impact of Water Pollution on Human Health and Environmental Sustainability*. IGI Global; Accessed April 24, 2019. <https://www.igi-global.com/book/impact-water-pollution-human-health/134812>
  72. Nesslage GM, Wainger LA, Harms NE, Cofrancesco AF. (2016). Quantifying the population response of invasive water hyacinth, *Eichhornia crassipes*, to biological control and winter weather in Louisiana, USA. *Biol Invasions*. 18(7): 2107–15. **10.1007/s10530-016-1155-9**
  73. NASA. (2022). Prediction of Worldwide Energy Resources (POWER). Langley Research Center (LaRC) <https://power.larc.nasa.gov/data-accessviewer/>. Published 2022. Accessed April 20, 2022. <https://power.larc.nasa.gov/data-accessviewer/>
  74. Rai PK. (2019). Heavy metals/metalloids remediation from wastewater using free floating macrophytes of a natural wetland. *Environmental Technology and Innovation*. 15. **10.1016/j.eti.2019.100393**
  75. Gutiérrez EL, Ruiz EF, Uribe EG, Martínez JM. (2000). Biomass and Productivity of Water Hyacinth and Their Application in Control Programs. 102.
  76. Giraldo E, Garzón A. (2002). The potential for water hyacinth to improve the quality of Bogota River water in the Muña Reservoir: Comparison with the performance of waste stabilization ponds. 103 p. (*Water Science and Technology*; vol. 45). <https://www.scopus.com/inward/record.uri?eid=2-s2.0-0036166580&partnerID=40&md5=f07d7a211e28ec7fc888baf7c68e8b44>
  77. Hermoso-López Araiza JP, Quecholac-Piña X, Beltrán-Villavicencio M, Espinosa-Valdemar RM, Vázquez-Morillas A. (2016). Integral Valorization of the Water Hyacinth from the Canals of Xochimilco: Production of Edible Mushrooms and Forage. *Waste and Biomass Valorization*. 7(5): 1203–10. **10.1007/s12649-016-9526-0**
  78. Knipling EB, West SH, Haller WT. (1970). Growth characteristics, yield potential, and nutritive content of water hyacinths. In: *Soil and Crop Science Society of Florida*. p. 51–63. Accessed April 27, 2019. <http://agris.fao.org/agris-search/search.do?recordID=US201302332072>
  79. Van Driesche R, Blossey B, Hoddle M, Lyon S, Reardon R. 2002. Biological control of invasive plants in the Eastern United States. Accessed April 27, 2019. <https://www.cabdirect.org/cabdirect/abstract/20043196936>

80. Imaoka T, Teranishi S. (1988). Rates of nutrient uptake and growth of the water hyacinth (*Eichhornia crassipes* (Mart.) Solms). *Water Research*. 22(8): 943–51. **10.1016/0043-1354(88)90140-6**
81. Wilson JR, Holst N, Rees M. (2005). Determinants and patterns of population growth in water hyacinth. *Aquatic Botany*. 81(1): 51–67. **10.1016/j.aquabot.2004.11.002**
82. Evans AC. (1963). The grip of the Water Hyacinth. *New Scientist*. 19(358). [https://books.google.co.in/books?id=WQVsn4hDiAUC&pg=PA666&lpq=PA666&dq=The+grip+of+water+hyacinth+new+scientist+1963&source=bl&ots=ARsF9eu hkh&sig=ACfU3U33CgTZIpLXhGttXjJvuHDqJFjaug&hl=en&sa=X&ved=2ahUKE wjPylSX5e\\_hAhVI73MBHTulBvAQ6AEwAnoECAkQAQ#v=onepage&q&f=false](https://books.google.co.in/books?id=WQVsn4hDiAUC&pg=PA666&lpq=PA666&dq=The+grip+of+water+hyacinth+new+scientist+1963&source=bl&ots=ARsF9eu hkh&sig=ACfU3U33CgTZIpLXhGttXjJvuHDqJFjaug&hl=en&sa=X&ved=2ahUKE wjPylSX5e_hAhVI73MBHTulBvAQ6AEwAnoECAkQAQ#v=onepage&q&f=false)
83. de Casabianca M-L, Laugier T. (1995). *Eichhornia crassipes* production on petroliferous wastewaters: Effects of salinity. *Bioresource Technology*. 54(1): 39–43. **10.1016/0960-8524(95)00112-3**
84. Muramoto S, Oki Y. (1988). Effects of surface-active agents on the salinity tolerance of water hyacinth (*Eichhornia crassipes*). *Journal of Environmental Science and Health Part A: Environmental Science and Engineering*. 23(6): 603–11. **10.1080/10934528809375437**
85. Toy A. (2005). Water Hyacinth Adaptation to Higher Saline Levels.
86. Sooknah RD, Wilkie AC. (2004). Nutrient removal by floating aquatic macrophytes cultured in anaerobically digested flushed dairy manure wastewater. *Ecological Engineering*. 22(1): 27–42. **10.1016/j.ecoleng.2004.01.004**
87. Reddy KR, Agami M, Tucker JC. (1990). Influence of phosphorus on growth and nutrient storage by water hyacinth (*Eichhornia crassipes* (Mart.) Solms) plants. *Aquatic Botany*. 37(4): 355–65. **10.1016/0304-3770(90)90021-C**
88. Reddy KR, Sutton DL. (1984). Water hyacinths for water quality improvement and biomass production. *J Environ Qual*; (United States). 13:1. <https://www.osti.gov/biblio/7192772-water-hyacinths-water-quality-improvement-biomass-production>
89. Fox LJ, Struik PC, Appleton BL, Rule JH. (2008). Nitrogen Phytoremediation by Water Hyacinth (*Eichhornia crassipes* (Mart.) Solms). *Water Air Soil Pollut*. 194(1): 199–207. **10.1007/s11270-008-9708-x**
90. Boyd CE. (1976). Accumulation of Dry Matter, Nitrogen and Phosphorus by Cultivated Water Hyacinths. *Economic Botany*. 30(1): 51–6.
91. Boyd CE, Scarsbrook E. (1975). Influence of nutrient additions and initial density of plants on production of Water Hyacinth (*Eichhornia crassipes*). *Aquatic Botany*. 1: 253–61. **10.1016/0304-3770(75)90026-1**
92. Debusk TA, Ryther JH, Hanisak MD, Williams LD. (1981). Effects of seasonality and plant density on the productivity of some freshwater macrophytes. *Aquatic Botany*. 10: 133–42. **10.1016/0304-3770(81)90016-4**
93. Reddy KR, Debusk WF. (1984). Growth characteristics of aquatic macrophytes cultured in nutrient-enriched water: I. Water hyacinth, water lettuce, and pennywort. *Economic Botany*. 38(2): 229–39. **10.1007/BF02858838**

94. Reddy KR, Tucker JC. (1983). Productivity and nutrient uptake of water hyacinth, *Eichhornia crassipes* L. Effect of nitrogen source. *Econ Bot.* 37(2): 237–47. **10.1007/BF02858790**
95. Tucker CS, Debusk TA. (1981). Seasonal growth of *Eichhornia crassipes* (Mart.) solms: Relationship to protein, fiber, and available carbohydrate content. *Aquatic Botany.* 11: 137–41. **10.1016/0304-3770(81)90055-3**
96. Wooten JW, Dodd JD. (1976). Growth of water hyacinths in treated sewage effluent. *Econ Bot.* 30(1): 29–37. **10.1007/BF02866781**
97. Reddy KR, Agami M, Tucker JC. (1989). Influence of nitrogen supply rates on growth and nutrient storage by water hyacinth (*Eichhornia crassipes*) plants. *Aquatic Botany.* 36(1): 33–43. **10.1016/0304-3770(89)90089-2**
98. Delgado M, Guardiola E, Bigeriego M. (1995). Organic and inorganic nutrients removal from pig slurry by water hyacinth. *Journal of Environmental Science and Health Part A: Environmental Science and Engineering and Toxicology.* 30(7): 1423–34. **10.1080/10934529509376275**
99. Fernando PUD. (2003). Modelling of growth cycle of water hyacinth: an application to Bolgoda Lake [Master of Science in Environmental Water Resources Engineering and Management]. University of Moratuwa; Accessed May 3, 2019. <http://dl.lib.mrt.ac.lk/handle/123/1317>
100. Gossett DR, Norris WE. (1971). Relationship between nutrient availability and content of nitrogen and phosphorus in tissues of the aquatic macrophyte, *Eichornia Crassipes* (Mart.) Solms. *Hydrobiologia.* 38(1): 15–28. **10.1007/BF00036789**
101. Ho YB, Wong W. (1994). Growth and macronutrient removal of water hyacinth in a small secondary sewage treatment plant. *Resources, Conservation and Recycling.* 11(1): 161–78. **10.1016/0921-3449(94)90087-6**
102. Reddy KR, D'Angelo EM. (1990). Biomass yield and nutrient removal by water hyacinth (*Eichhornia crassipes*) as influenced by harvesting frequency. *Biomass.* 21(1): 27–42. **10.1016/0144-4565(90)90045-L**
103. Sahai R, Sinha AB. (1970). Contribution to the ecology of Indian aquatics. *Hydrobiologia.* 35(3): 376–82. **10.1007/BF00184564**
104. Eid EM, Shaltout KH. (2017). Population dynamics of *Eichhornia crassipes* (C. Mart.) Solms in the Nile Delta, Egypt. *Plant Species Biology.* 32(4): 279–91. **10.1111/1442-1984.12154**
105. Greco MKB, de Freitas JR. (2002). On two methods to estimate production of *Eichhornia crassipes* in the eutrophic Pampulha reservoir (MG, Brazil). *Braz J Biol.* 62(3): 463–71. **10.1590/s1519-69842002000300010**
106. Mitsch JW. (1974). Systems analysis of nutrient disposal in cypress wetlands and lake ecosystems in Florida [PhD]. University of Florida, Gainesville;
107. Tipping PW, Martin MR, Pokorny EN, Nimmo KR, Fitzgerald DL, Dray FA, Center TD. (2014). Current levels of suppression of waterhyacinth in Florida USA by classical biological control agents. *Biological Control.* 71: 65–9. **10.1016/j.biocontrol.2014.01.008**



108. Kumar V, Singh J, Chopra AK. (2018). Assessment of phytokinetic removal of pollutants of paper mill effluent using water hyacinth (*Eichhornia crassipes* [Mart.] Solms). Environmental Technology (United Kingdom). 39(21): 2781–91. **10.1080/09593330.2017.1365944**
109. Putra RS, Hastika FY. (2018). Removal of heavy metals from leachate using electro-assisted phytoremediation (EAPR) and up-take by water hyacinth (*eichornia crassipes*). Indonesian Journal of Chemistry. 18(2): 306–12. **10.22146/ijc.29713**
110. Sidek NM, Abdullah SRS, Ahmad NU, Draman SFS, Rosli MMM, Sanusi MF. (2018). Phytoremediation of abandoned mining lake by water hyacinth and water lettuces in constructed wetlands. Jurnal Teknologi. 80(5): 87–93. **10.11113/jt.v80.10992**
111. Gulzar F, Mahmood Q, Bhatti ZA, Zeb BS, Shaheen S, Hayat T, Shahid N, Zeb T. (2018). Industrial wastewater treatment in internal circulation bioreactor followed by wetlands containing emergent plants and algae. World Journal of Microbiology and Biotechnology. 34(8). **10.1007/s11274-018-2496-6**
112. Palihakkara CR, Dassanayake S, Jayawardena C, Senanayake IP. (2018). Floating wetland treatment of acid mine drainage using *Eichhornia crassipes* (water hyacinth). Journal of Health and Pollution. 8(17): 14–9. **10.5696/2156-9614-8.17.14**
113. Sumual H, Warouw F, Kamagi M. (2018). Design of water hyacinth utilization as renewable electricity energy source in Tondano Lake. In. **10.1051/mateconf/201819713004**
114. Li F, He X, Srishti A, Song S, Tan HTW, Sweeney DJ, Ghosh S, Wang C-H. (2021). Water hyacinth for energy and environmental applications: A review. Bioresource Technology. 327: 124809. **10.1016/j.biortech.2021.124809**
115. Elbasiouny H, Darwesh M, Elbeltagy H, Abo-alhamd FG, Amer AA, Elsegaiy MA, et al. (2021). Ecofriendly remediation technologies for wastewater contaminated with heavy metals with special focus on using water hyacinth and black tea wastes: a review. Environ Monit Assess. 193(7): 449. **10.1007/s10661-021-09236-2**
116. Sindhu R, Binod P, Pandey A, Madhavan A, Alphonsa JA, Vivek N, Gnansounou E, Castro E, Faraco V. (2017). Water hyacinth a potential source for value addition: An overview. Bioresource Technology. 230: 152–62. **10.1016/j.biortech.2017.01.035**
117. Ali S, Abbas Z, Rizwan M, Zaheer IE, Yavaş İ, Ünay A, et al. (2020). Application of Floating Aquatic Plants in Phytoremediation of Heavy Metals Polluted Water: A Review. Sustainability. 12(5): 1927. **10.3390/su12051927**
118. Thamaga KH, Dube T. (2018). Remote sensing of invasive water hyacinth (*Eichhornia crassipes*): A review on applications and challenges. Remote Sensing Applications: Society and Environment. 10: 36–46. **10.1016/j.rsase.2018.02.005**
119. Sun L, Zhu ZS. (2014). A Decision Model for Harvesting *Eichhornia crassipes* Once a Week. AMR. 889–890: 1660–3. **10.4028/www.scientific.net/AMR.889-890.1660**

120. Chassany de Casabianca M-L. (1985). *Eichhornia crassipes*: Production in repeated harvest systems on waste water in the Languedoc Region (France). *Biomass*. 7(2): 135–60. **10.1016/0144-4565(85)90039-3**
121. Lorber MN, Mishoe JW, Reddy PR. (1984). Modeling and analysis of waterhyacinth biomass. *Ecological Modelling*. 24(1): 61–77. **10.1016/0304-3800(84)90055-3**
122. Greenfield BK, Siemering GS, Andrews JC, Rajan M, Andrews SP, Spencer DF. (2007). Mechanical shredding of water hyacinth (*Eichhornia crassipes*): Effects on water quality in the Sacramento-San Joaquin River Delta, California. *Estuaries and Coasts: J ERF*. 30(4): 627–40. **10.1007/BF02841960**
123. Moorthy MVS, Dhamodharan.S, Chandru.G. (2018). Fabrication of Water Hyacinth Harvester. *International Journal of Engineering Research & Technology*. 5(7). **10.17577/IJERTCONV5IS07043**
124. Su W, Sun Q, Xia M, Wen Z, Yao Z. (2018). The Resource Utilization of Water Hyacinth (*Eichhornia crassipes* [Mart.] Solms) and Its Challenges. *Resources*. 7(3): 46. **10.3390/resources7030046**
125. Gunnarsson CC, Petersen CM. (2007). Water hyacinths as a resource in agriculture and energy production: A literature review. *Waste Management*. 27(1): 117–29. **10.1016/j.wasman.2005.12.011**
126. Ramaprabhu J, Ramchandran V. (1984). Developments in aquatic weed control research in India relating to fisheries. *Journal of Aquatic Plant Management*. 22: 97–100.
127. Dar B. 2018 Jun. Evaluation of Water Hyacinth Harvester and WH Management of Lake Tana, Ethiopia. *Global Coalition For Lake Tana Restoration*; Accessed December 9, 2022. <http://tanacoalition.org/wp-content/uploads/2018/10/Water-Hyacinth-Harvesting-Machine-Performance-Report-06072018-COITBD-1.pdf>
128. Heyduk A. (2016). Bulk density estimation using a 3-dimensional image acquisition and analysis system. Kowalczyk PB, Drzymala J, editors. *E3S Web Conf*. 8: 01060. **10.1051/e3sconf/20160801060**
129. Mathur SM, Singh P. (2004). Development and Performance Evaluation of a Water Hyacinth Chopper cum Crusher. *Biosystems Engineering*. 88(4): 411–8. **10.1016/j.biosystemseng.2004.04.007**
130. Greenfield BK, David N, Hunt J, Wittmann M, Siemering G. 2004 Apr. Review of Alternative Aquatic Pest Control Methods For California Waters. San Francisco Estuary Institute; (Aquatic Pesticide Monitoring Program).
131. Van Dyke JM. (1972). Mechanical Harvesting of water hyacinth *Eichhornia crassipes* in Shell Creek Reservoir, Charlotte County, Florida. In Department of the Army, Office of the Chief of Engineers; <https://apps.dtic.mil/sti/citations/AD0745895>
132. Musil CF, Breen CM. (1977). The application of growth kinetics to the control of *Eichhornia crassipes* (Mart) solms. Through nutrient removal by mechanical harvesting. *Hydrobiologia*. 53(2): 165–71. **10.1007/BF00029295**

133. Durgin PR, Bormann EJ, Gladu AC. (2021). Evaluating the Feasibility and Effectiveness of Duckweed Phytoremediation in Lake Sevan. Worcester Polytechnic Institute;
134. Greenfield BK, Blankinship M, Mcnabb TJ. (2006). Control Costs, Operation, and Permitting Issues for Non-chemical Plant Control: Case Studies in the San Francisco Bay-Delta Region, California. *J Aquat Plant Manage.* 44: 40–9.
135. Monlau F, Barakat A, Trably E, Dumas C, Steyer J-P, Carrère H. (2013). Lignocellulosic Materials Into Biohydrogen and Biomethane: Impact of Structural Features and Pretreatment. *Critical Reviews in Environmental Science and Technology.* 43(3): 260–322. **10.1080/10643389.2011.604258**
136. Montingelli ME, Tedesco S, Olabi AG. (2015). Biogas production from algal biomass: A review. *Renewable and Sustainable Energy Reviews.* 43: 961–72. **10.1016/j.rser.2014.11.052**
137. Brown AE. (2021). Integration of Hydrothermal Conversion and Anaerobic Fermentation for the Valorisation of High Ash Feedstocks. University of Leeds; <https://etheses.whiterose.ac.uk/30260/>
138. Bray DG, Nahar G, Grasham O, Dalvi V, Rajput S, Dupont V, Camargo-Valero MA, Ross AB. (2022). The Cultivation of Water Hyacinth in India as a Feedstock for Anaerobic Digestion: Development of a Predictive Model for Scaling Integrated Systems. *Energies.* 15(24): 9599. **10.3390/en15249599**
139. Brown AE, Adams JMM, Grasham OR, Camargo-Valero MA, Ross AB. (2020). An Assessment of Different Integration Strategies of Hydrothermal Carbonisation and Anaerobic Digestion of Water Hyacinth. *Energies.* 13(22): 27. **10.3390/en13225983**
140. Bencko V, Symon K. (1977). Health aspects of burning coal with a high arsenic content: I. Arsenic in hair, urine, and blood in children residing in a polluted area. *Environmental Research.* 13(3): 378–85. **10.1016/0013-9351(77)90018-4**
141. Preece KE, Hooshyar N, Zuidam NJ. (2017). Whole soybean protein extraction processes: A review. *Innovative Food Science & Emerging Technologies.* 43: 163–72. **10.1016/j.ifset.2017.07.024**
142. Rahman MA, Hasegawa H. (2011). Aquatic arsenic: Phytoremediation using floating macrophytes. *Chemosphere.* 83(5): 633–46. **10.1016/j.chemosphere.2011.02.045**
143. Rai PK. (2018). Heavy metal phyto-technologies from Ramsar wetland plants: green approach. *Chemistry and Ecology.* 34(8): 786–96. **10.1080/02757540.2018.1501476**
144. Gameda S, Gabbiye N, Alemu A. (2019). Phytoremediation potential of free floating plant species for chromium wastewater: The case of duckweed, water hyacinth, and water lilies. 519 p. (Lecture Notes of the Institute for Computer Sciences, Social-Informatics and Telecommunications Engineering, LNICST; vol. 274). **10.1007/978-3-030-15357-1\_42**
145. Sampanpanish P, Pinpa K. (2018). Cadmium Removal from Contaminated Sediment Using EDTA and DTPA with Water Hyacinth. *International Journal of Environmental Research.* 12(4): 543–51. **10.1007/s41742-018-0114-y**

146. Fawzy MA, Badr NE, El-Khatib A, Abo-El-Kassem A. (2012). Heavy metal biomonitoring and phytoremediation potentialities of aquatic macrophytes in River Nile. *Environ Monit Assess.* 184(3): 1753–71. **10.1007/s10661-011-2076-9**
147. Sutton DL, Blackburn RD. (1971). Uptake of copper by water hyacinth. *Hyacinth control J.* 9: 18–20.
148. Gunathilakae N, Yapa N, Hettiarachchi R. (2018). Effect of arbuscular mycorrhizal fungi on the cadmium phytoremediation potential of *Eichhornia crassipes* (Mart.) Solms. *Groundwater for Sustainable Development.* 7: 477–82. **10.1016/j.gsd.2018.03.008**
149. Vesk PA, Nockolds CE, Allaway WG. (1999). Metal localization in water hyacinth roots from an urban wetland. *Plant, Cell & Environment.* 22(2): 149–58. **10.1046/j.1365-3040.1999.00388.x**
150. Aggarwal A, Sharma I, Tripathi B, Munjal A, Baunthiyal M, Sharma V. (2011). Metal Toxicity and Photosynthesis. In: *Photosynthesis: Overviews on Recent Progress and Future Perspectives.* p. 16: 229-236.
151. Küpper H, Küpper F, Spiller M. (1996). Environmental relevance of heavy metal-substituted chlorophylls using the example of water plants. *Journal of Experimental Botany.* 47(2): 259–66. **10.1093/jxb/47.2.259**
152. Küpper H, Šetlík I, Šetliková E, Ferimazova N, Spiller M, Küpper FC. (2003). Copper-induced inhibition of photosynthesis: limiting steps of in vivo copper chlorophyll formation in *Scenedesmus quadricauda*. *Funct Plant Biol.* 30(12): 1187–96. **10.1071/FP03129**
153. Fazal S, Zhang B, Mehmood Q. (2015). Biological treatment of combined industrial wastewater. *Ecological Engineering.* 84: 551–8. **10.1016/j.ecoleng.2015.09.014**
154. Shuvaeva OV, Belchenko LA, Romanova TE. (2013). Studies on Cadmium Accumulation by Some Selected Floating Macrophytes. *International Journal of Phytoremediation.* 15(10): 979–90. **10.1080/15226514.2012.751353**
155. Aurangzeb N, Nisa S, Bibi Y, Javed F, Hussain F. (2014). Phytoremediation potential of aquatic herbs from steel foundry effluent. *Brazilian Journal of Chemical Engineering.* 31(4): 881–6. **10.1590/0104-6632.20140314s00002734**
156. Swarnalatha K, Radhakrishnan B. (2015). Studies on removal of Zinc and Chromium from aqueous solutions using water Hyacinth. *Pollution.* 1(2): 193–202. **10.7508/pj.2015.02.007**
157. Prasad B, Maiti D. (2016). Comparative study of metal uptake by *Eichhornia crassipes* growing in ponds from mining and nonmining areas—a field study. *Bioremediation Journal.* 20(2): 144–52. **10.1080/10889868.2015.1113924**
158. Abbas Z, Arooj F, Ali S, Zaheer IE, Rizwan M, Riaz MA. (2019). Phytoremediation of landfill leachate waste contaminants through floating bed technique using water hyacinth and water lettuce. *International Journal of Phytoremediation.* 21(13): 1356–67. **10.1080/15226514.2019.1633259**
159. Alifa D, Moersidik SS, Priadi CR. (2019). *Eichhornia crassipes* Potency as Hyperaccumulator Macrophyte in Phytoremediation of Acid Mine Drainage Containing Zn. In. **10.1088/1755-1315/355/1/012064**

160. Eid EM, Shaltout KH, Moghanm FS, Youssef MSG, El-Mohsnawy E, Haroun SA. (2019). Bioaccumulation and translocation of nine heavy metals by *Eichhornia crassipes* in Nile delta, Egypt: Perspectives for phytoremediation. *International Journal of Phytoremediation*. 21(8): 821–30. **10.1080/15226514.2019.1566885**
161. Adelodun AA, Afolabi NO, Chaúque EFC, Akinwumiju AS. (2020). The potentials of *Eichhornia crassipes* for Pb, Cu, and Fe removal from polluted waters. *SN Applied Sciences*. 2(10). **10.1007/s42452-020-03392-9**
162. Du L, Arauzo PJ, Meza Zavala MF, Cao Z, Olszewski MP, Kruse A. (2020). Towards the Properties of Different Biomass-Derived Proteins via Various Extraction Methods. *Molecules*. 25(3): 488. **10.3390/molecules25030488**
163. Elizabeth J, Yuniati R, Wardhana W. (2020). The capacity of water hyacinth as biofilter and bioaccumulator based on its size. In. **10.1088/1757-899X/902/1/012067**
164. Peng H, Wang Y, Tan TL, Chen Z. (2020). Exploring the phytoremediation potential of water hyacinth by FTIR Spectroscopy and ICP-OES for treatment of heavy metal contaminated water. *International Journal of Phytoremediation*. 22(9): 939–51. **10.1080/15226514.2020.1774499**
165. Gaballah MS, Ismail K, Aboagye D, Ismail MM, Sobhi M, Stefanakis AI. (2021). Effect of design and operational parameters on nutrients and heavy metal removal in pilot floating treatment wetlands with *Eichhornia crassipes* treating polluted lake water. *Environmental Science and Pollution Research*. **10.1007/s11356-021-12442-7**
166. Zhang Y, Liu H, Yan S, Wen X, Qin H, Wang Z, Zhang Z. (2019). Phosphorus removal from the hyper-eutrophic Lake Caohai (China) with large-scale water hyacinth cultivation. *Environ Sci Pollut Res*. 26(13): 12975–84. **10.1007/s11356-019-04469-8**
167. Iamchaturapatr J, Yi SW, Rhee JS. (2007). Nutrient removals by 21 aquatic plants for vertical free surface-flow (VFS) constructed wetland. *Ecological Engineering*. 29(3): 287–93. **10.1016/j.ecoleng.2006.09.010**
168. Yi N, Gao Y, Long X, Zhang Z, Guo J, Shao H, Zhang Z, Yan S. (2014). *Eichhornia crassipes* Cleans Wetlands by Enhancing the Nitrogen Removal and Modulating Denitrifying Bacteria Community. *CLEAN – Soil, Air, Water*. 42(5): 664–73. **10.1002/clen.201300211**
169. Polomski RF, Taylor MD, Bielenberg DG, Bridges WC, Klaine SJ, Whitwell T. (2008). Nitrogen and Phosphorus Remediation by Three Floating Aquatic Macrophytes in Greenhouse-Based Laboratory-Scale Subsurface Constructed Wetlands. *Water Air Soil Pollut*. 197(1): 223–32. **10.1007/s11270-008-9805-x**
170. Caldelas C, Iglesia-Turiño S, Arous JL, Bort J, Febrero A. (2009). Physiological responses of *Eichhornia crassipes* [Mart.] Solms to the combined exposure to excess nutrients and Hg. *Brazilian Journal of Plant Physiology*. 21(1): 1–12. **10.1590/S1677-04202009000100002**
171. Lu X, Gao Y, Luo J, Yan S, Wang T, Liu L, Zhang Z. (2016). Interactive Effects of Tetracyclines and Copper on Plant Growth and Nutrient Uptake by *Eichhornia crassipes*. *Clean - Soil, Air, Water*. 44(1): 96–104. **10.1002/clen.201400662**

172. Rezania S, Md Din MF, Mohanadoss P, Md Sairan F, Kamaruddin S. (2013). Nutrient uptake and wastewater purification with Water Hyacinth and its effect on plant growth in a batch system. *Journal of environmental treatment techniques*. 1: 81–5.
173. Feng W, Xiao K, Zhou W, Zhu D, Zhou Y, Yuan Y, et al. (2017). Analysis of utilization technologies for *Eichhornia crassipes* biomass harvested after restoration of wastewater. *Bioresource Technology*. 223: 287–95.  
**10.1016/j.biortech.2016.10.047**
174. Friedl A, Padouvas E, Rotter H, Varmuza K. (2005). Prediction of heating values of biomass fuel from elemental composition. *Analytica Chimica Acta*. 544(1): 191–8. **10.1016/j.aca.2005.01.041**
175. Biswas B, Singh R, Krishna BB, Kumar J, Bhaskar T. (2017). Pyrolysis of azolla, sargassum tenerrimum and water hyacinth for production of bio-oil. *Bioresource Technology*. 242: 139–45. **10.1016/j.biortech.2017.03.044**
176. Rezania S, Ponraj M, Din MFM, Songip AR, Sairan FM, Chelliapan S. (2015). The diverse applications of water hyacinth with main focus on sustainable energy and production for new era: An overview. *Renewable and Sustainable Energy Reviews*. 41: 943–54. **10.1016/j.rser.2014.09.006**
177. Munjeri K, Ziuku S, Maganga H, Siachingoma B, Ndlovu S. (2016). On the potential of water hyacinth as a biomass briquette for heating applications. *International Journal of Energy and Environmental Engineering*. 7(1): 37–43.  
**10.1007/s40095-015-0195-8**
178. Rezania S, Md Din MF, Kamaruddin SF, Taib SM, Singh L, Yong EL, Dahalan FA. (2016). Evaluation of water hyacinth (*Eichhornia crassipes*) as a potential raw material source for briquette production. *Energy*. 111: 768–73.  
**10.1016/j.energy.2016.06.026**
179. Carnaje NP, Talagon RB, Peralta JP, Shah K, Paz-Ferreiro J. (2018). Development and characterisation of charcoal briquettes from water hyacinth (*Eichhornia crassipes*)-molasses blend. Nath AJ, editor. *PLOS ONE*. 13(11): e0207135. **10.1371/journal.pone.0207135**
180. Davies RM, Davies OA. (2013). Physical and Combustion Characteristics of Briquettes Made from Water Hyacinth and Phytoplankton Scum as Binder. *Journal of Combustion*. 2013: 1–7. **10.1155/2013/549894**
181. Davies RM, Davies OA, Mohammed US. (2013). Combustion Characteristics of Traditional Energy Sources and Water Hyacinth Briquettes. *International Journal of Scientific Research in Environmental Sciences*. 1(7): 144–51.  
**10.12983/ijsres-2013-p144-151**
182. Ighodalo OA, Zoukumor K, Egbon C, Okoh S, Odu K. (2011). Processing water hyacinth into biomass Briquettes for cooking purposes. *J Emerg Trends Eng Appl Sci (JETEAS)*. 2(2): 305–7.
183. Rodrigues AJ, Odero MO, Hayombe PO, Akuno W, Kerich D, Maobe I. (2014). Converting water hyacinth to briquettes: a beach community based approach. *Int J Sci Basic Appl Res*. 15(1): 358e78.
184. Elliott DC, Sealock LJ, Butner RS. (1988). Product Analysis from Direct Liquefaction of Several High-Moisture Biomass Feedstocks. In: Soltes EJ, Milne

TA, editors. Pyrolysis Oils from Biomass. Washington, DC: American Chemical Society; p. 179–88. **10.1021/bk-1988-0376.ch017**

185. Singh R, Balagurumurthy B, Prakash A, Bhaskar T. (2015). Catalytic hydrothermal liquefaction of water hyacinth. *Bioresource Technology*. 178: 157–65. **10.1016/j.biortech.2014.08.119**
186. Singhal V, Rai JPN. (2003). Biogas production from water hyacinth and channel grass used for phytoremediation of industrial effluents. *Bioresource Technology*. 86(3): 221–5. **10.1016/S0960-8524(02)00178-5**
187. Verma VK, Singh YP, Rai JPN. (2007). Biogas production from plant biomass used for phytoremediation of industrial wastes. *Bioresource Technology*. 98(8): 1664–9. **10.1016/j.biortech.2006.05.038**
188. Patil JH, AntonyRaj Mal, Gavimath CC, Hooli VR. (2011). A Comperative Study On Anaerobic Co-Digestion Of Water Hyacinth With Poultry Litter And Cow Dung. : 9.
189. Mathew AK, Bhui I, Banerjee SN, Goswami R, Chakraborty AK, Shome A, Balachandran S, Chaudhury S. (2015). Biogas production from locally available aquatic weeds of Santiniketan through anaerobic digestion. *Clean Technologies and Environmental Policy*. 17(6): 1681–8. **10.1007/s10098-014-0877-6**
190. Takaya CA. (2016). Nutrient sorption potential of treated and untreated hydrochars and biochars derived from various waste feedstocks [Doctor of Philosophy]. The University of Leeds;
191. Singh J, Kalamdhad AS, Lee B-K. (2015). Reduction of eco-toxicity risk of heavy metals in the rotary drum composting of water hyacinth: Waste lime application and mechanisms. *Environmental Engineering Research*. 20(3): 212–22. **10.4491/eer.2015.024**
192. Singh J, Kalamdhad AS. (2016). Effect of lime on speciation of heavy metals during composting of water hyacinth. *Frontiers of Environmental Science and Engineering*. 10(1): 93–102. **10.1007/s11783-014-0704-7**
193. Tereshchenko NN, Akimova EE, Pisarchuk AD, Yunusova TV, Minaeva OM. (2015). Utilizing heavy metal-laden water hyacinth biomass in vermicomposting. *Environmental Science and Pollution Research*. 22(9): 7147–54. **10.1007/s11356-014-3943-z**
194. Jordão CP, Fialho LL, Neves JCL, Cecon PR, Mendonça ES, Fontes RLF. (2007). Reduction of heavy metal contents in liquid effluents by vermicomposts and the use of the metal-enriched vermicomposts in lettuce cultivation. *Bioresource Technology*. 98(15): 2800–13. **10.1016/j.biortech.2006.06.023**
195. Calzadilla A, Rehdanz K, Betts R, Falloon P, Wiltshire A, Tol RSJ. (2013). Climate change impacts on global agriculture. *Climatic Change*. 120(1): 357–74. **10.1007/s10584-013-0822-4**
196. Petersen AM, Annoh-Quarshie J, van Rensburg E, Görgens JF. (2020). Optimizing the processes of extracting proteins from yellow peas and ethanol production from spent pea residues. *Biomass Conv Bioref*. **10.1007/s13399-020-00851-6**

197. Wu W, Sun Y. (2011). Dietary safety evaluation of water hyacinth leaf protein concentrate. *Hum Exp Toxicol*. 30(10): 1514–20. **10.1177/09603271110392085**
198. de Vasconcelos GA, Vêras RML, de Lima Silva J, Cardoso DB, de Castro Soares P, de Morais NNG, Souza AC. (2016). Effect of water hyacinth (*Eichhornia crassipes*) hay inclusion in the diets of sheep. *Trop Anim Health Prod*. 48(3): 539–44. **10.1007/s11250-015-0988-z**
199. Taylor KG, Bates RP, Robbins RC. (1971). Extraction of protein from water hyacinth. *Hyacinth Control J*. 9(1): 20–2.
200. Sari YW, Syafitri U, Sanders JPM, Bruins ME. (2015). How biomass composition determines protein extractability. *Industrial Crops and Products*. 70: 125–33. **10.1016/j.indcrop.2015.03.020**
201. Mekuriaw S, Tegegne F, Tsunekawa A, Ichinohe T. (2018). Effects of substituting concentrate mix with water hyacinth (*Eichhornia crassipes*) leaves on feed intake, digestibility and growth performance of Washera sheep fed rice straw-based diet. *Tropical Animal Health and Production*. 50(5): 965–72. **10.1007/s11250-018-1519-5**
202. Islam S, Khan MJ, Islam MN. (2009). Effect of feeding wilted water hyacinth (*Eichhornia crassipes*) on the performance of growing bull cattle. *Indian Journal of Animal Sciences*. 79(5): 494–7.
203. Hò TT, Udén P. (2015). Effect of fresh water Hyacinth (*Eichhornia crassipes*) on intake and digestibility in cattle fed rice straw and molasses-urea cake.
204. Ho Thanh T. (2012). Water Hyacinth (*Eichhornia crassipes*) – Biomass Production, Ensilability and Feeding Value to Growing Cattle [Doctor of Philosophy]. Swedish University of Agricultural Sciences;
205. Aregheore EM, Cawa K. (2000). Voluntary intake by crossbred Anglo-Nubian goats of water hyacinth (*Eichhornia crassipes*) fed in two states plus guinea grass (*Panicum maximum*) in confinement. *Scientia Agriculturae Bohemica*. 31(4): 261–71.
206. Mako AA. (2013). Performance of West African Dwarf goats fed graded levels of sun-cured water hyacinth (*Eichhornia crassipes* Mart. Solms-Laubach) replacing Guinea grass. *Livestock Research for Rural Development*. 25(7): 2013.
207. Mani AMM. (2019). Utilization leaf meal of water hyacinth (*Eichhornia crassipes*) as a replacement protein source for growing Awassi lambs. *International Journal of Veterinary Science*. 8(1): 54–60.
208. Fouzi MNM, Deepani ML a. NR. (2018). Water hyacinth (*Eichhornia crassipes*) leaves as an alternative protein source for feeding early phase of Tilapia (*Oreochromis niloticus*). *Sri Lanka Veterinary Journal*. 65(1): 5–12. **10.4038/slvj.v65i1.30**
209. Moses T, Vya B, C K, FNA O. (2020). Composition of Water Hyacinth (*Eichhornia crassipes*) Plant Harvested from the Volta Lake in Ghana and its Potential Value as a Feed Ingredient in Rabbit Rations. *Advances in Animal and Veterinary Sciences*. 9(2): 230–7. **10.17582/JOURNAL.AAVS/2021/9.2.230.237**
210. Wu W, Guo X, Huang M. (2014). Evaluation of acute toxicity potential of water hyacinth leaves. *Toxicol Ind Health*. 30(5): 426–31. **10.1177/0748233712458138**



211. LabChem. Ascorbic Acid- Safety Data Sheet. Accessed February 3, 2023. <https://www.labchem.com/tools/msds/msds/LC11530.pdf>
212. Hontiveros GJS, Serrano Jr AE. (2015). Nutritional value of water hyacinth (*Eichhornia crassipes*) leaf protein concentrate for aquafeeds. *Aquaculture, Aquarium, Conservation & Legislation*. 8(1): 26–33.
213. Adeyemi O, Osubor CC. (2016). Assessment of nutritional quality of water hyacinth leaf protein concentrate. *The Egyptian Journal of Aquatic Research*. 42(3): 269–72. **10.1016/j.ejar.2016.08.002**
214. International Monetary Fund. (2022). Global price of Soybean Meal. FRED, Federal Reserve Bank of St. Louis. FRED, Federal Reserve Bank of St. Louis; Published 2022. Accessed October 31, 2022. <https://fred.stlouisfed.org/series/PSMEAUSDM>
215. Byrne J. (2022). Indian soymeal continues to be outpriced globally. *feednavigator.com*. Published 2022. Accessed October 31, 2022. <https://www.feednavigator.com/Article/2022/03/08/Indian-soymeal-continues-to-be-outpriced-globally>
216. Kimura Athletic. (2022). Pea Protein Amino Acid Profile. Kimura Athletic. Published 2022. Accessed February 3, 2023. <https://kimuraathletic.com/performance-centre/pea-protein-amino-acid-profile/>
217. Gorissen SHM, Crombag JJR, Senden JMG, Waterval WAH, Bierau J, Verdijk LB, van Loon LJC. (2018). Protein content and amino acid composition of commercially available plant-based protein isolates. *Amino Acids*. 50(12): 1685–95. **10.1007/s00726-018-2640-5**
218. Snow AM, Ghaly AE. (2008). A Comparative Study of the Purification of Aquaculture Wastewater Using Water Hyacinth, Water Lettuce And Parrot's Feather. *American Journal of Applied Sciences*. 5(4): 440–53. **10.3844/ajassp.2008.440.453**
219. Gupta P, Roy S, B. Mahindrakar A. (2012). Treatment of Water Using Water Hyacinth, Water Lettuce and Vetiver Grass - A Review. *RE*. 2(5): 202–15. **10.5923/j.re.20120205.04**
220. Purnamawati R, Taufikurahman T, Rahmawati A, Putra C, Din D, Rahmatilah, Ashgi F. (2020). The Physiological Responses of Water Hyacinth (*Eichhornia crassipes* (Mart.) Solms) and Water Lettuce (*Pistia stratiotes* L.) as Trivalent Chromium Bioaccumulator. *3BIO: Journal of Biological Science, Technology and Management*. 2: 2655–8777. **10.5614/3bio.2020.2.1.2**
221. Adebayo A, Briski E, Kalaci O, Hernandez M, Ghabooli S, Beric B, et al. (2011). Water hyacinth (*Eichhornia crassipes*) and water lettuce (*Pistia stratiotes*) in the Great Lakes: playing with fire? *Aquatic Invasions*. 6(1): 91–6. **10.3391/ai.2011.6.1.11**
222. Ali EF, Galal TM, Hassan LM, Al-Yasi HM, Dakhil MA, Eid EM. (2021). Seasonal potential of *Pistia stratiotes* in nutrient removal to eliminate eutrophication in Al-Sero Drain (South Nile Delta, Egypt). *Journal of Freshwater Ecology*. 36(1): 173–87. **10.1080/02705060.2021.1915397**

223. Arber A. (1920). The vegetative morphology of *Pistia* and the Lemnaceae. *Proceedings of the Royal Society of London Series B, Containing Papers of a Biological Character*. 91(636): 96–103.
224. Global Invasive Species Database. (2023). Species profile: *Pistia stratiotes*. Published 2023. Accessed December 10, 2023. <https://iucngisd.org/gisd/species.php?sc=285>
225. Galal TM, Dakhil MA, Hassan LM, Eid EM. (2019). Population dynamics of *Pistia stratiotes* L. *Rend Fis Acc Lincei*. 30(2): 367–78. **10.1007/s12210-019-00800-0**
226. Milićević DB. (2023). Modeling the growth dynamics of water lettuce, *Pistia stratiotes* L. in wastewater. *Archives of Biological Sciences*. (00): 31–31.
227. Larsen SU, Jørgensen H, Bukh C, Schjoerring JK. (2019). Green biorefining: Effect of nitrogen fertilization on protein yield, protein extractability and amino acid composition of tall fescue biomass. *Industrial Crops and Products*. 130: 642–52. **10.1016/j.indcrop.2019.01.016**
228. Bals B, Dale BE. (2011). Economic comparison of multiple techniques for recovering leaf protein in biomass processing. *Biotechnology and Bioengineering*. 108(3): 530–7. **10.1002/bit.22973**
229. Zhang C, Slegers PM, Wisse J, Sanders JPM, Bruins ME. (2018). Sustainable scenarios for alkaline protein extraction from leafy biomass using green tea residue as a model material. *Biofuels, Bioproducts and Biorefining*. 12(4): 586–99. **10.1002/bbb.1870**
230. Brouwer P, Nierop KGJ, Huijgen WJJ, Schluempmann H. (2019). Aquatic weeds as novel protein sources: Alkaline extraction of tannin-rich *Azolla*. *Biotechnology Reports*. 24: e00368. **10.1016/j.btre.2019.e00368**
231. Lorenzo-Hernando A, Ruiz-Vegas J, Vega-Alegre M, Bolado-Rodríguez S. (2019). Recovery of proteins from biomass grown in pig manure microalgae-based treatment plants by alkaline hydrolysis and acidic precipitation. *Bioresource Technology*. 273: 599–607. **10.1016/j.biortech.2018.11.068**
232. Yang Y, Ge Y, Zeng H, Zhou X, Peng L, Zeng Q. (2017). Phytoextraction of cadmium-contaminated soil and potential of regenerated tobacco biomass for recovery of cadmium. *Scientific Reports*. 7(1): 1–10. **10.1038/s41598-017-05834-8**
233. Khan LH, Varshney VK. (2018). Chemical Utilization of *Albizia lebbek* Leaves for Developing Protein Concentrates as a Dietary Supplement. *Journal of Dietary Supplements*. 15(4): 386–97. **10.1080/19390211.2017.1349232**
234. Chiesa S, Gnansounou E. (2011). Protein extraction from biomass in a bioethanol refinery – Possible dietary applications: Use as animal feed and potential extension to human consumption. *Bioresource Technology*. 102(2): 427–36. **10.1016/j.biortech.2010.07.125**
235. Santamaría-Fernández M, Ambye-Jensen M, Damborg VK, Lübeck M. (2019). Demonstration-scale protein recovery by lactic acid fermentation from grass clover – a single case of the production of protein concentrate and press cake silage for animal feeding trials. *Biofuels, Bioproducts and Biorefining*. 13(3): 502–13. **10.1002/bbb.1957**

236. Russin TA, Arcand Y, Boye JI. (2007). Particle Size Effect on Soy Protein Isolate Extraction. *Journal of Food Processing and Preservation*. 31(3): 308–19. <https://doi.org/10.1111/j.1745-4549.2007.00127.x>
237. Vishwanathan KH, Singh V, Subramanian R. (2011). Influence of particle size on protein extractability from soybean and okara. *Journal of Food Engineering*. 102(3): 240–6. **10.1016/j.jfoodeng.2010.08.026**
238. Hildebrand B, Boguhn J, Rodehutschord M. (2011). Investigations on the effect of forage source, grinding, and urea supplementation on ruminal fermentation and microbial protein flow in a semi-continuous rumen simulation system. *Archives of Animal Nutrition*. 65(5): 402–14. **10.1080/1745039X.2011.609751**
239. Santamaría-Fernández M, Molinuevo-Salces B, Kiel P, Steinfeldt S, Uellendahl H, Lübeck M. (2017). Lactic acid fermentation for refining proteins from green crops and obtaining a high quality feed product for monogastric animals. *Journal of Cleaner Production*. 162: 875–81. **10.1016/j.jclepro.2017.06.115**
240. Contreras M del M, Lama-Muñoz A, Manuel Gutiérrez-Pérez J, Espínola F, Moya M, Castro E. (2019). Protein extraction from agri-food residues for integration in biorefinery: Potential techniques and current status. *Bioresource Technology*. 280: 459–77. **10.1016/j.biortech.2019.02.040**
241. Santamaría-Fernández M, Molinuevo-Salces B, Lübeck M, Uellendahl H. (2018). Biogas potential of green biomass after protein extraction in an organic biorefinery concept for feed, fuel and fertilizer production. *Renewable Energy*. 129: 769–75. **10.1016/j.renene.2017.03.012**
242. Juul L, Møller AH, Bruhn A, Jensen SK, Dalsgaard TK. (2021). Protein solubility is increased by antioxidant addition during protein extraction from the green macroalga, *Ulva* sp. *J Appl Phycol*. 33(1): 545–55. **10.1007/s10811-020-02285-z**
243. Chemat F, Rombaut N, Sicaire A-G, Meullemiestre A, Fabiano-Tixier A-S, Abert-Vian M. (2017). Ultrasound assisted extraction of food and natural products. Mechanisms, techniques, combinations, protocols and applications. A review. *Ultrasonics Sonochemistry*. 34: 540–60. **10.1016/j.ultsonch.2016.06.035**
244. Li K, Ma H, Li S, Zhang C, Dai C. (2017). Effect of Ultrasound on Alkali Extraction Protein from Rice Dreg Flour. *Journal of Food Process Engineering*. 40(2): e12377. <https://doi.org/10.1111/jfpe.12377>
245. Sánchez-Zurano A, Morillas-España A, González-López CV, Lafarga T. (2020). Optimisation of Protein Recovery from *Arthrospira platensis* by Ultrasound-Assisted Isoelectric Solubilisation/Precipitation. *Processes*. 8(12): 1586. **10.3390/pr8121586**
246. Xu Y, Li Y, Bao T, Zheng X, Chen W, Wang J. (2017). A recyclable protein resource derived from cauliflower by-products: Potential biological activities of protein hydrolysates. *Food Chemistry*. 221: 114–22. **10.1016/j.foodchem.2016.10.053**
247. Gil-Chávez GJ, Villa JA, Ayala-Zavala JF, Heredia JB, Sepulveda D, Yahia EM, González-Aguilar GA. (2013). Technologies for Extraction and Production of Bioactive Compounds to be Used as Nutraceuticals and Food Ingredients: An Overview. *Comprehensive Reviews in Food Science and Food Safety*. 12(1): 5–23. <https://doi.org/10.1111/1541-4337.12005>

248. Ye X, Li L. (2012). Microwave-Assisted Protein Solubilization for Mass Spectrometry-Based Shotgun Proteome Analysis. *Anal Chem.* 84(14): 6181–91. **10.1021/ac301169q**
249. Varghese T, Pare A. (2019). Effect of microwave assisted extraction on yield and protein characteristics of soymilk. *Journal of Food Engineering.* 262: 92–9. **10.1016/j.jfoodeng.2019.05.020**
250. Ho KKHY, Ferruzzi MG, Liceaga AM, San Martín-González MF. (2015). Microwave-assisted extraction of lycopene in tomato peels: Effect of extraction conditions on all-trans and cis-isomer yields. *LWT - Food Science and Technology.* 62(1, Part 1): 160–8. **10.1016/j.lwt.2014.12.061**
251. Wang W, de Dios Alché J, Rodríguez-García MI. (2007). Characterization of olive seed storage proteins. *Acta Physiol Plant.* 29(5): 439–44. **10.1007/s11738-007-0053-2**
252. Sawada MM, Venâncio LL, Toda TA, Rodrigues CEC. (2014). Effects of different alcoholic extraction conditions on soybean oil yield, fatty acid composition and protein solubility of defatted meal. *Food Research International.* 62: 662–70. **10.1016/j.foodres.2014.04.039**
253. Capellini MC, Giacomini V, Cuevas MS, Rodrigues CEC. (2017). Rice bran oil extraction using alcoholic solvents: Physicochemical characterization of oil and protein fraction functionality. *Industrial Crops and Products.* 104: 133–43. **10.1016/j.indcrop.2017.04.017**
254. Roselló-Soto E, Barba FJ, Parniakov O, Galanakis CM, Lebovka N, Grimi N, Vorobiev E. (2015). High Voltage Electrical Discharges, Pulsed Electric Field, and Ultrasound Assisted Extraction of Protein and Phenolic Compounds from Olive Kernel. *Food Bioprocess Technol.* 8(4): 885–94. **10.1007/s11947-014-1456-x**
255. Sari YW, Mulder WJ, Sanders JPM, Bruins ME. (2015). Towards plant protein refinery: Review on protein extraction using alkali and potential enzymatic assistance. *Biotechnology Journal.* 10(8): 1138–57. **10.1002/biot.201400569**
256. Zhang C, Sanders JPM, Bruins ME. (2014). Critical parameters in cost-effective alkaline extraction for high protein yield from leaves. *Biomass and Bioenergy.* 67: 466–72. **10.1016/j.biombioe.2014.05.020**
257. Ashori A, Ornelas M, Sheshmani S, Cordeiro N. (2012). Influence of mild alkaline treatment on the cellulosic surfaces active sites. *Carbohydrate Polymers.* 88(4): 1293–8. **10.1016/j.carbpol.2012.02.008**
258. Cookman DJ, Glatz CE. (2009). Extraction of protein from distiller's grain. *Bioresource Technology.* 100(6): 2012–7. **10.1016/j.biortech.2008.09.059**
259. Naseri A, Jacobsen C, Sejberg JJP, Pedersen TE, Larsen J, Hansen KM, Holdt SL. (2020). Multi-Extraction and Quality of Protein and Carrageenan from Commercial *Spinosum* (*Eucheuma denticulatum*). *Foods.* 9(8): 1072. **10.3390/foods9081072**
260. Naseri A, Marinho GS, Holdt SL, Bartela JM, Jacobsen C. (2020). Enzyme-assisted extraction and characterization of protein from red seaweed *Palmaria palmata*. *Algal Research.* 47: 101849. **10.1016/j.algal.2020.101849**

261. Bandyopadhyay K, Chakraborty C, Barman AK. (2012). Effect of Microwave and Enzymatic Treatment on the Recovery of Protein from Indian Defatted Rice Bran Meal. *J Oleo Sci.* 61(10): 525–9. **10.5650/jos.61.525**
262. Sari YW, Bruins ME, Sanders JPM. (2013). Enzyme assisted protein extraction from rapeseed, soybean, and microalgae meals. *Industrial Crops and Products.* 43: 78–83. **10.1016/j.indcrop.2012.07.014**
263. Solati Z, Manevski K, Jørgensen U, Labouriau R, Shahbazi S, Lærke PE. (2018). Crude protein yield and theoretical extractable true protein of potential biorefinery feedstocks. *Industrial Crops and Products.* 115: 214–26. **10.1016/j.indcrop.2018.02.010**
264. Solati Z, Jørgensen U, Eriksen J, Søgaard K. (2017). Dry matter yield, chemical composition and estimated extractable protein of legume and grass species during the spring growth. *Journal of the Science of Food and Agriculture.* 97(12): 3958–66. **<https://doi.org/10.1002/jsfa.8258>**
265. Licitra G, Hernandez TM, Van Soest PJ. (1996). Standardization of procedures for nitrogen fractionation of ruminant feeds. *Animal Feed Science and Technology.* 57(4): 347–58. **10.1016/0377-8401(95)00837-3**
266. Salcedo-Chávez B, Osuna-Castro JA, Guevara-Lara F, Domínguez-Domínguez J, Paredes-López O. (2002). Optimization of the Isoelectric Precipitation Method To Obtain Protein Isolates from Amaranth (*Amaranthus cruentus*) Seeds. *J Agric Food Chem.* 50(22): 6515–20. **10.1021/jf020522t**
267. Jiang J, Xiong YL, Chen J. (2010). pH Shifting Alters Solubility Characteristics and Thermal Stability of Soy Protein Isolate and Its Globulin Fractions in Different pH, Salt Concentration, and Temperature Conditions. *J Agric Food Chem.* 58(13): 8035–42. **10.1021/jf101045b**
268. Hojilla-Evangelista MP, Selling GW, Hatfield R, Digman M. (2017). Extraction, composition, and functional properties of dried alfalfa (*Medicago sativa* L.) leaf protein. *Journal of the Science of Food and Agriculture.* 97(3): 882–8. **<https://doi.org/10.1002/jsfa.7810>**
269. Connolly A, Piggott CO, FitzGerald RJ. (2013). Characterisation of protein-rich isolates and antioxidative phenolic extracts from pale and black brewers' spent grain. *International Journal of Food Science & Technology.* 48(8): 1670–81. **10.1111/ijfs.12137**
270. Parimi NS, Singh M, Kastner JR, Das KC, Forsberg LS, Azadi P. (2015). Optimization of Protein Extraction from *Spirulina platensis* to Generate a Potential Co-Product and a Biofuel Feedstock with Reduced Nitrogen Content. *Front Energy Res.* 3. **10.3389/fenrg.2015.00030**
271. Rommi K, Niemi P, Kemppainen K, Kruus K. (2018). Impact of thermochemical pre-treatment and carbohydrate and protein hydrolyzing enzyme treatment on fractionation of protein and lignin from brewer's spent grain. *Journal of Cereal Science.* 79: 168–73. **10.1016/j.jcs.2017.10.005**
272. Koschuh W, Povoden G, Thang VH, Kromus S, Kulbe KD, Novalin S, Krotscheck C. (2004). Production of leaf protein concentrate from ryegrass (*Lolium perenne* x *multiflorum*) and alfalfa (*Medicago sativa* subsp. *sativa*). Comparison between heat coagulation/centrifugation and ultrafiltration. *Desalination.* 163(1): 253–9. **10.1016/S0011-9164(04)90197-X**

273. Magomya AM, Kubmarawa D, Ndahi JA, Yebpella GG. (2014). Determination Of Plant Proteins Via The Kjeldahl Method And Amino Acid Analysis: A Comparative Study. *International Journal Of Scientific & Technology Research*. 3(4): 5.
274. Bjarnadóttir M, Aðalbjörnsson BV, Nilsson A, Slizyte R, Roleda MY, Hreggviðsson GÓ, Friðjónsson ÓH, Jónsdóttir R. (2018). *Palmaria palmata* as an alternative protein source: enzymatic protein extraction, amino acid composition, and nitrogen-to-protein conversion factor. *J Appl Phycol*. 30(3): 2061–70. **10.1007/s10811-017-1351-8**
275. Biorefine. The production of green protein. *BioRefine*. Accessed February 10, 2023. <https://biorefine.dk/p/produktion>
276. Montealegre C, Esteve C, García MC, García-Ruiz C, Marina ML. (2014). Proteins in Olive Fruit and Oil. *Critical Reviews in Food Science and Nutrition*. 54(5): 611–24. **10.1080/10408398.2011.598639**
277. Jiang L, He L, Fountoulakis M. (2004). Comparison of protein precipitation methods for sample preparation prior to proteomic analysis. *Journal of Chromatography A*. 1023(2): 317–20. **10.1016/j.chroma.2003.10.029**
278. Crowell AMJ, Wall MJ, Doucette AA. (2013). Maximizing recovery of water-soluble proteins through acetone precipitation. *Analytica Chimica Acta*. 796: 48–54. **10.1016/j.aca.2013.08.005**
279. Kadam SU, Álvarez C, Tiwari BK, O'Donnell CP. (2017). Extraction and characterization of protein from Irish brown seaweed *Ascophyllum nodosum*. *Food Research International*. 99: 1021–7. **10.1016/j.foodres.2016.07.018**
280. Vesik PA, Allaway WG. (1997). Spatial variation of copper and lead concentrations of water hyacinth plants in a wetland receiving urban run-off. *Aquatic Botany*. 59(1): 33–44. **10.1016/S0304-3770(97)00032-6**
281. Maharashtra Pollution Control Board. 2019. Report On Action Plan For Clean-Up Of Polluted Stretch Of Indrayani River. Accessed June 20, 2022. [https://www.mpcb.gov.in/sites/default/files/river-polluted/action-plan-priority/priority\\_II\\_INDRAYANI\\_28052019.pdf](https://www.mpcb.gov.in/sites/default/files/river-polluted/action-plan-priority/priority_II_INDRAYANI_28052019.pdf)
282. The Energy and Resources Institute. 2022. Water Quality- State of Maharashtra 2020-21. Accessed June 20, 2022. [https://mpcb.gov.in/sites/default/files/wqr\\_report\\_04052022.pdf](https://mpcb.gov.in/sites/default/files/wqr_report_04052022.pdf)
283. Klean Environmental Consultants PVT.LTD. 2018. Comprehensive study of polluted river stretches of Bhīma River. Maharashtra Pollution Control Board; Accessed June 20, 2022. [https://mpcb.gov.in/sites/default/files/focus-area-reports-documents/BhimaRiverReport%20\\_CPCBguidelines%2018thNovember15.pdf](https://mpcb.gov.in/sites/default/files/focus-area-reports-documents/BhimaRiverReport%20_CPCBguidelines%2018thNovember15.pdf)
284. Maharashtra Industrial Development Corporation. Accessed May 19, 2023. <https://www.midcindia.org/>
285. Maharashtra Pollution Control Board. 2020. 10. NWMP Station Details: Surface Water. [https://mpcb.gov.in/sites/default/files/water-quality/monitoring\\_network/NWMPresultgroundsurface26102020.pdf](https://mpcb.gov.in/sites/default/files/water-quality/monitoring_network/NWMPresultgroundsurface26102020.pdf)

286. Maharashtra Pollution Control Board. 2019. Report On Action Plan For Clean-Up Of Polluted Stretch Of Mula River. Accessed June 20, 2022. [https://www.mpcb.gov.in/sites/default/files/river-polluted/action-plan-priority/priority\\_I\\_MULA\\_28052019.pdf](https://www.mpcb.gov.in/sites/default/files/river-polluted/action-plan-priority/priority_I_MULA_28052019.pdf)
287. BSI. 2015. Solid biofuels. Determination of moisture content. Oven dry method. Total moisture. Reference method. Report No.: BS EN ISO 18134-1:2015. <https://bsol.bsigroup.com/Bibliographic/BibliographicInfoData/000000000030275466>
288. BSI. 2016. Water quality. Sampling. Guidance on quality assurance and quality control of environmental water sampling and handling. Report No.: BS EN ISO 5667-14:2016. <https://bsol.bsigroup.com/Bibliographic/BibliographicInfoData/000000000030332572>
289. Grasham O, Dupont V, Camargo-Valero MA, García-Gutiérrez P, Cockerill T. (2019). Combined ammonia recovery and solid oxide fuel cell use at wastewater treatment plants for energy and greenhouse gas emission improvements. *Applied Energy*. 240: 698–708. **10.1016/j.apenergy.2019.02.029**
290. APHA. (2017). Standard methods for the examination of water and wastewater. 23rd edition. Baird RB, Eaton AD, Rice EW, editors. Vol. 10. Washington, DC: American Public Health Association; 1 p.
291. Kjeldahl J. (1883). New method for the determination of nitrogen in organic substances. *Fresenius, Zeitschrift f anal Chemie*. 22(1): 366–82. **10.1007/BF01338151**
292. Baethgen WE, Alley MM. (1989). A manual colorimetric procedure for measuring ammonium nitrogen in soil and plant Kjeldahl digests. *Communications in Soil Science and Plant Analysis*. 20(9–10): 961–9. **10.1080/00103628909368129**
293. BSI. 2006. Animal feeding stuffs. Determination of amylase-treated neutral detergent fibre content (aNDF). Report No.: BS EN ISO 16472:2006. Accessed February 12, 2023. <https://bsol.bsigroup.com/Bibliographic/BibliographicInfoData/000000000030127855>
294. BSI. 2008. Animal feeding stuffs. Determination of acid detergent fibre (ADF) and acid detergent lignin (ADL) content. Report No.: BS EN ISO 13906:2008. Accessed February 12, 2023. <https://bsol.bsigroup.com/Bibliographic/BibliographicInfoData/000000000030200218>
295. EPA. 1978. Nitrogen, Kjeldahl, Total (Colorimetric, Automated Phenate). p. 8. Report No.: Method 351.1: Nitrogen, Kjeldahl, Total (Colorimetric, Automated Phenate) by Autoanalyzer. [https://www.epa.gov/sites/default/files/2015-08/documents/method\\_351-1\\_1978.pdf](https://www.epa.gov/sites/default/files/2015-08/documents/method_351-1_1978.pdf)
296. Allee WC, Oesting R. (1934). A Critical Examination of Winkler's Method for Determining Dissolved Oxygen in Respiration Studies with Aquatic Animals. *Physiological Zoology*. 7(4): 509–41.
297. Hach. 2015 Sep. Nitrogen, Ammonia-Salicylate Method 8155. Report No.: DOC316.53.01077. <https://www.hach.com/asset-get.download-en.jsa?id=7639983745>

298. American Public Health Association. (1992). APHA Method 2320: Standard Methods for the Examination of Water and Wastewater. Washington DC: American Water Works Association (AWWA) and Water Pollution Control Federation (WPCF); <http://archive.org/details/gov.law.apha.method.2320.1992>
299. ASTM. (2018). Standard Test Method for Elements in Water by Inductively-Coupled Plasma Atomic Emission Spectroscopy. Vol. 11.01. ASTM International; 15 p. <https://www.astm.org/d1976-18.html>
300. Buswell AM, Mueller HF. (1952). Mechanism of Methane Fermentation. *Ind Eng Chem.* 44(3): 550–2. **10.1021/ie50507a033**
301. Boyle WC. (1976). Energy Recovery From Sanitary Landfills - A Review. In: *Microbial Energy Conversion*. Pergamon; p. 119–38. **10.1016/B978-0-08-021791-8.50019-6**
302. Deng C, Lin R, Kang X, Wu B, O'Shea R, Murphy JD. (2020). Improving gaseous biofuel yield from seaweed through a cascading circular bioenergy system integrating anaerobic digestion and pyrolysis. *Renewable and Sustainable Energy Reviews.* 128: 109895. **10.1016/j.rser.2020.109895**
303. Kanwar SS, Gupta RK, Guleri RL, Singh SP. (1994). Performance evaluation of a 1 m<sup>3</sup> modified, fixed-dome Deenbandhu biogas plant under hilly conditions. *Bioresource Technology.* 50(3): 239–41. **10.1016/0960-8524(94)90096-5**
304. Quintana-Najera J, Blacker AJ, Fletcher LA, Bray DG, Ross AB. (2022). The Influence of Biochar Augmentation and Digestion Conditions on the Anaerobic Digestion of Water Hyacinth. *Energies.* 15(7): 2524. **10.3390/en15072524**
305. Buswell AM, Neave SL. 1930. Laboratory studies of sludge digestion. *Illinois State Water Survey; Report No.:* 30. <https://www.isws.illinois.edu/pubdoc/b/iswsb-30.pdf>
306. Demirbaş A. (1997). Calculation of higher heating values of biomass fuels. *Fuel.* 76(5): 431–4. **10.1016/S0016-2361(97)85520-2**
307. Sheng C, Azevedo JLT. (2005). Estimating the higher heating value of biomass fuels from basic analysis data. *Biomass and Bioenergy.* 28(5): 499–507. **10.1016/j.biombioe.2004.11.008**
308. Demirbaş A, Demirbaş AH. (2004). Estimating the Calorific Values of Lignocellulosic Fuels. *Energy Exploration & Exploitation.* 22(2): 135–43. **10.1260/0144598041475198**
309. da Silva Oliveira A, Bocio A, Beltramini Trevilato TM, Magosso Takayanagui AM, Domingo JL, Segura-Muñoz SI. (2007). Heavy metals in untreated/treated urban effluent and sludge from a biological wastewater treatment plant. *Env Sci Poll Res Int.* 14(7): 483. **10.1065/espr2006.10.355**
310. Bakare BF, Adeyinka GC. (2022). Evaluating the Potential Health Risks of Selected Heavy Metals across Four Wastewater Treatment Water Works in Durban, South Africa. *Toxics.* 10(6): 340. **10.3390/toxics10060340**
311. Allen E, Wall DM, Herrmann C, Murphy JD. (2016). A detailed assessment of resource of biomethane from first, second and third generation substrates. *Renewable Energy.* 87: 656–65. **10.1016/j.renene.2015.10.060**



312. Nugraha WD, Syafrudin, Senduk AT, Matin HHA, Budiyo. (2018). Optimization of Biogas Production by Solid State Anaerobic Digestion (SS-AD) Method from Water Hyacinth with Response Surface Methodology (RSM). E3S Web Conf. 73: 01016. **10.1051/e3sconf/20187301016**
313. Mæhre HK, Dalheim L, Edvinsen GK, Elvevoll EO, Jensen I-J. (2018). Protein Determination—Method Matters. *Foods*. 7(1): 5. **10.3390/foods7010005**
314. Chang SKC, Zhang Y. (2017). Protein Analysis. In: Nielsen SS, editor. *Food Analysis*. Cham: Springer International Publishing; p. 315–31. (Food Science Text Series). **10.1007/978-3-319-45776-5\_18**
315. Jenkins BM, Baxter LL, Miles TR, Miles TR. (1998). Combustion properties of biomass. *Fuel Processing Technology*. 54(1): 17–46. **10.1016/S0378-3820(97)00059-3**
316. Shailaja G, Gautam G. (2017). Risk assessment of trace elements distribution in soils of basaltic aquifers, southern Maharashtra, India. 5: 11.
317. Team Urban Update. (2020). Toxic foam engulfs Indrayani River in Pune. Urban Update. Published 2020. Accessed June 20, 2022. <https://urbanupdate.in/toxic-foam-engulfs-indrayani-river-in-pune/>
318. Google Maps. (2022). Pimpri Chinchwad. Accessed June 20, 2022. <https://tinyurl.com/indrayaniscrap>
319. Khan MU, Ahring BK. (2019). Lignin degradation under anaerobic digestion: Influence of lignin modifications -A review. *Biomass and Bioenergy*. 128: 105325. **10.1016/j.biombioe.2019.105325**
320. Mohammed M, Merga B, Ahmed A. (2019). Effects of Brewery waste sludge on potato (*Solanum tuberosum* L.) productivity and soil fertility. Yildiz F, editor. *Cogent Food & Agriculture*. 5(1): 1707053. **10.1080/23311932.2019.1707053**
321. Khanal B, Shah SC, Sah SK, Shriwastav CP, Acharya B. (2014). Heavy Metals Accumulation in Cauliflower (*Brassica Oleracea* L. var. *Botrytis*) Grown in Brewery Sludge Amended Sandy Loam Soil. **10.14355/IJAST.2014.0203.01**
322. Obasi A, Agwu O. (2017). Bioremoval of Heavy Metals from a Nigerian Brewery Wastewater by Bacterial Application. *Food and Applied Bioscience*. 5(3): 165–75. **10.14456/fabj.2017.14**
323. Tesfahun W, Zerfu A, Shumuye M, Abera G, Kidane A, Astatkie T. (2021). Effects of brewery sludge on soil chemical properties, trace metal availability in soil and uptake by wheat crop, and bioaccumulation factor. *Heliyon*. 7(1): e05989. **10.1016/j.heliyon.2021.e05989**
324. Kumar R, Rani M, Gupta H, Gupta B, Park D, Jeon B-H. (2017). Distribution of trace elements in flowing surface waters: Effect of seasons and anthropogenic practices in India. *International Journal of Environmental Analytical Chemistry*. 97(7): 637–56. **10.1080/03067319.2017.1339035**
325. Outa JO, Kowenje CO, Plessl C, Jirsa F. (2020). Distribution of arsenic, silver, cadmium, lead and other trace elements in water, sediment and macrophytes in the Kenyan part of Lake Victoria: spatial, temporal and bioindicative aspects. *Environ Sci Pollut Res*. 27(2): 1485–98. **10.1007/s11356-019-06525-9**

326. Bray DG. (2023). Dataset for 'The potential utilisation of contaminated biomass following phytoremediation'. University of Leeds; <https://doi.org/10.5518/1367>
327. Abdel-sabour MF, Abdel-Haleem AS, Zohny E. (1996). Chemical composition of water hyacinth (*Eichhronia Crassipes*) a comparison indication of heavy metal pollution in egyptian water bodies Vol 4. In p. 1760. [http://inis.iaea.org/search/search.aspx?orig\\_q=RN:28029291](http://inis.iaea.org/search/search.aspx?orig_q=RN:28029291)
328. Smith AM, Singh S, Ross AB. (2016). Fate of inorganic material during hydrothermal carbonisation of biomass: Influence of feedstock on combustion behaviour of hydrochar. *Fuel*. 169: 135–45. **10.1016/j.fuel.2015.12.006**
329. Eid EM, Shaltout KH. (2017). Growth dynamics of water hyacinth (*Eichhornia crassipes*): a modeling approach. *Rend Fis Acc Lincei*. 28(1): 169–81. **10.1007/s12210-016-0589-4**
330. Joint Expert Committee on Food Additives, editor. (2004). Evaluation of certain food additives and contaminants: sixty-first report of the Joint FAO/WHO Expert Committee on Food Additives ; [meeting of the Joint FAO/WHO Expert Committee on Food Additives, Rome 2003]. Geneva: WHO; 176 p. (WHO technical report series).
331. The European Commission. Dec 19, 2006. Commission Regulation (EC) No 1881/2006 of 19 December 2006 setting maximum levels for certain contaminants in foodstuffs. OJ L 364/5. Accessed June 2, 2022. <http://data.europa.eu/eli/reg/2006/1881/oj/eng>
332. Sangomla A. (2021). Climate change is real: 600-900% excess rain in many Maharashtra districts. Published 2021. Accessed December 20, 2022. <https://www.downtoearth.org.in/news/climate-change/climate-change-is-real-600-900-excess-rain-in-many-maharashtra-districts-78095>
333. Shahfahad, Talukdar S, Ali R, Nguyen K-A, Naikoo MW, Liou Y-A, Islam ARMdT, Mallick J, Rahman A. (2022). Monitoring drought pattern for pre- and post-monsoon seasons in a semi-arid region of western part of India. *Environ Monit Assess*. 194(6): 396. **10.1007/s10661-022-10028-5**
334. Center TD, Wright AD. (1991). Age and Phytochemical Composition of Waterhyacinth (*Pontederiaceae*) Leaves Determine their Acceptability to *Neochetina eichhorniae* (Coleoptera: Curculionidae). *Environmental Entomology*. 20(1): 323–34. **10.1093/ee/20.1.323**
335. Bui D-C, Nguyen Q-M, Chu X-Q, JiHoon K, KiTae P, Doan V-H, Do Q-T. (2019). Effects of copper and zinc on the anaerobic co-digestion process of waste activated sludge and septic tank sludge. *Desalination and Water Treatment*. 173: 34–40.
336. Huurman S, van der Weide R, van Dijk W. 2017. Cultivation of aquatic plants on cow manure digestate. *ACRRES*; Accessed May 16, 2019. <http://www.acrres.nl/en/publications/cultivation-of-aquatic-plants-on-cow-manure-digestate/>
337. Ofulla AVO, Karanja D, Omondi R, Okurut T, Matano A, Jembe T, Abila R, Boera P, Gichuki J. (2010). Relative abundance of mosquitoes and snails associated with water hyacinth and hippo grass in the Nyanza gulf of Lake Victoria. *Lakes & Reservoirs: Science, Policy and Management for Sustainable Use*. 15(3): 255–71. **10.1111/j.1440-1770.2010.00434.x**

338. Isalkar U. (2018). Spread of water hyacinth triggers mosquito menace. The Times of India.
339. Food and Agriculture Organization of the United Nations. (2022). FAOSTAT. Food and Agriculture Organization of the United Nations. Published 2022. Accessed April 24, 2022. <https://www.fao.org/faostat/en/#home>
340. Santamaría-Fernández M. (2018). A Novel Green Biorefinery Concept: Protein refining by lactic acid fermentation and biogas production from green biomass [phd]. Aalborg University; p. 1–185. Accessed February 24, 2021. <https://orgprints.org/33337/>
341. Ting WHT, Tan IAW, Salleh SF, Wahab NA. (2018). Application of water hyacinth (*Eichhornia crassipes*) for phytoremediation of ammoniacal nitrogen: A review. *Journal of Water Process Engineering*. 22: 239–49. **10.1016/j.jwpe.2018.02.011**
342. Bals B, Teachworth L, Dale B, Balan V. (2007). Extraction of Proteins from Switchgrass Using Aqueous Ammonia within an Integrated Biorefinery. *Appl Biochem Biotechnol*. 143(2): 187–98. **10.1007/s12010-007-0045-0**
343. The European Commission. Apr 29, 2011. Consolidated text: Commission Regulation (EC) No 1881/2006 of 19 December 2006 setting maximum levels for certain contaminants in foodstuffs. 420/2011 Queen’s Printer of Acts of Parliament; p. 9. Accessed April 27, 2022. <https://webarchive.nationalarchives.gov.uk/eu-exit/20201231120835/https://eur-lex.europa.eu/legal-content/EN/TXT/?uri=CELEX:02006R1881-20201014>
344. Tack FM, Callewaert OWJJ, Verloo MG. (1996). Metal solubility as a function of pH in a contaminated, dredged sediment affected by oxidation. *Environmental Pollution*. 91(2): 199–208. **10.1016/0269-7491(95)00049-6**
345. Grill E, Winnacker E-L, Zenk MH. (1987). Phytochelatins, a class of heavy-metal-binding peptides from plants, are functionally analogous to metallothioneins. *Proc Natl Acad Sci U S A*. 84(2): 439–43.
346. Narender Reddy G, Prasad MNV. (1990). Heavy metal-binding proteins/peptides: Occurrence, structure, synthesis and functions. A review. *Environmental and Experimental Botany*. 30(3): 251–64. **10.1016/0098-8472(90)90037-5**
347. Nuzest. All About Pea Protein Nutrition – Nuzest SG. Accessed October 28, 2022. <https://nuzest.sg/blogs/news/all-about-pea-protein-nutrition>
348. Moradi F, Maleki V, Saleh-Ghadimi S, Kooshki F, Pourghassem Gargari B. (2019). Potential roles of chromium on inflammatory biomarkers in diabetes: A Systematic. *Clinical and Experimental Pharmacology and Physiology*. 46(11): 975–83. **10.1111/1440-1681.13144**
349. Gray JP, Suhali-Amacher N, Ray SD. (2017). Metals and Metal Antagonists. In: Ray SD, editor. *Side Effects of Drugs Annual*. Elsevier; p. 197–208. (A Worldwide Yearly Survey of New Data in Adverse Drug Reactions; vol. 39). **10.1016/bs.seda.2017.07.001**
350. NHS. (2017). Vitamins and minerals. nhs.uk. Published 2017. Accessed October 28, 2022. <https://www.nhs.uk/conditions/vitamins-and-minerals/>

351. Holland & Barrett. H&B Vegan Multivitamin & Mineral Tablets. Accessed October 28, 2022. <https://www.hollandandbarrett.com/shop/product/holland-barrett-vegan-multivitamin-mineral-tablets-60012166>
352. May 12, 2014. Commission Regulation (EU) No 488/2014 of 12 May 2014 amending Regulation (EC) No 1881/2006 as regards maximum levels of cadmium in foodstuffs (Text with EEA relevance). 488/2014 Queen's Printer of Acts of Parliament; Accessed October 31, 2022. <https://www.legislation.gov.uk/eur/2014/488>
353. Ibáñez MA, de Blas C, Cámara L, Mateos GG. (2020). Chemical composition, protein quality and nutritive value of commercial soybean meals produced from beans from different countries: A meta-analytical study. *Animal Feed Science and Technology*. 267: 114531. **10.1016/j.anifeedsci.2020.114531**
354. Patil J, AntonyRaj Mal, Gavimath C. (2011). Study on effect of pre-treatment methods on biomethanation of water hyacinth. *International Journal of Advanced Biotechnology and Research*. 2: 143–7.
355. Urribarrí L, Ferrer A, Colina A. (2005). Leaf Protein from Ammonia-Treated Dwarf Elephant Grass (*Pennisetum purpureum* Schum cv. Mott). In: Davison BH, Evans BR, Finkelstein M, McMillan JD, editors. *Twenty-Sixth Symposium on Biotechnology for Fuels and Chemicals*. Totowa, NJ: Humana Press; p. 721–30. (ABAB Symposium). **10.1007/978-1-59259-991-2\_60**
356. Khalil MM. (2001). Biochemical and technological studies on the production of isolated guar protein. *Mol Nutr Food Res*. 45(1): 21–4. **10.1002/1521-3803(20010101)45:1<21::AID-FOOD21>3.0.CO;2-J**
357. Shen L, Wang X, Wang Z, Wu Y, Chen J. (2008). Studies on tea protein extraction using alkaline and enzyme methods. *Food Chemistry*. 107(2): 929–38. **10.1016/j.foodchem.2007.08.047**
358. Sevonius C, Yrjas P, Lindberg D, Hupa L. (2019). Impact of sodium salts on agglomeration in a laboratory fluidized bed. *Fuel*. 245: 305–15. **10.1016/j.fuel.2019.02.034**
359. Li G, Wang C, Yan Y, Jin X, Liu Y, Che D. (2016). Release and transformation of sodium during combustion of Zhundong coals. *Journal of the Energy Institute*. 89(1): 48–56. **10.1016/j.joei.2015.01.011**
360. Fernández-Jiménez A, Palomo A. (2009). Nanostructure/microstructure of fly ash geopolymers. In: Provis JL, van Deventer JSJ, editors. *Geopolymers*. Woodhead Publishing; p. 89–117. (Woodhead Publishing Series in Civil and Structural Engineering). **10.1533/9781845696382.1.89**
361. PubChem. Sodium Sulphate. Accessed October 7, 2022. <https://pubchem.ncbi.nlm.nih.gov/compound/24436>
362. IndiaMART. (2023). Catepillar CAT336E. IndiaMART. Published 2023. Accessed May 21, 2023. <https://www.indiamart.com/proddetail/cat-336e-hybrid-hydraulic-excavator-24753689973.html>
363. IndiaMART. (2023). Hyundai 245LR. IndiaMART. Published 2023. Accessed May 21, 2023. <https://www.indiamart.com/proddetail/hyundai-245lr-smart-plus-construction-excavator-22177090597.html>

364. Indiamart. (2023). Volvo EC210DL. indiamart.com. Published 2023. Accessed May 21, 2023. <https://www.indiamart.com/proddetail/volvo-hydraulic-excavator-14344764473.html>
365. IndiaMART. (2023). Hitachi EX200- 2 Lakh. IndiaMART. Published 2023. Accessed May 21, 2023. <https://www.indiamart.com/proddetail/excavators-hiring-services-20162125533.html>
366. IndiaMART. (2023). Hitachi EX200- 1.8 Lakh. IndiaMART. Published 2023. Accessed May 21, 2023. <https://www.indiamart.com/proddetail/ex-200-hitachi-excavator-hiring-service-22252022412.html>
367. IndiaMART. (2023). JCB 245XR. indiamart.com. Published 2023. Accessed May 21, 2023. <https://www.indiamart.com/proddetail/excavator-rental-service-22950262355.html>
368. Bing. (2023). INR to GBP- 21/05/2023. Published 2023. Accessed May 21, 2023. <https://www.bing.com/search?q=INR+to+GBP&qs=n&form=QBRE&sp=-1&ghc=1&lq=0&pq=inr+to+gbp&sc=11-10&sk=&cvid=3FD1BE81F1E24FCA89071B5A6C44A9BF&ghsh=0&ghacc=0&ghpl=>
369. Jiji. (2023). Komatsu PC220 (2013). Published 2023. Accessed May 21, 2023. <https://jiji.ug/nakawa/heavy-equipments-machinery/excavator-2013-model-BTKJgPTSIO0m7SWuVjR1nssL.html>
370. Jiji. (2023). Caterpillar CAT320C (2009). Published 2023. Accessed May 21, 2023. <https://jiji.ug/nakawa/heavy-equipments-machinery/excavator-2009-model-6qCnRFaIsABaBbGIFJEKlooW.html>
371. Matar M, Osman H, Georgy M, Abou-Zeid A, Moheebelsaid, Professor A. (2016). Systems engineering approach to measuring the environmental impacts of open trenching construction operations. In.
372. Jiji. (2023). Caterpillar CAT320B (2012). Published 2023. Accessed May 21, 2023. <https://jiji.ug/central-division/heavy-equipments-machinery/cat-excavator-tractor-long-hand-fork-rUeHD6OO7PNrPjjopToigQgm.html>
373. Bing. (2023). UGX to GBP- 21/05/2023. Published 2023. Accessed May 21, 2023. <https://www.bing.com/search?pglt=43&q=UGX+to+gbp&cvid=1a5c651432a54531ad8f75b971fbfed1&aqs=edge..69i57j69i64.2805j0j1&FORM=ANNTA1&PC=U531>
374. Aquamarine Inc. (2023). Aquamarine- aquatic plant and weed harvesting technology. Published 2023. Accessed May 21, 2023. <https://www.aquamarine.ca/>
375. Tana Coalition. (2018). First Purchase of Modern Water Hyacinth Harvester. GLOBAL COALITION FOR LAKE TANA RESTORATION. Published 2018. Accessed May 21, 2023. <http://tanacoalition.org/first-modern-water-hyacinth-harvester/>
376. Bing. (2023). USD to GBP- 04/06/2023. Bing. Published 2023. Accessed June 4, 2023. <https://www.bing.com/search?pglt=43&q=USD+to+£&cvid=6f84e46f40a5430795cd0a6565433a76&aqs=edge..69i57j0i8.3311j0j1&FORM=ANNTA1&PC=U531>

377. Samar KK, Sharma D, Meena GL. (2016). The Solid State Biogas Plant: A Boon for Water Scarce Areas. <https://mnre.gov.in/img/documents/uploads/f93373e7bb8143fd9665e46ea4e5cbda.pdf>. 9(4): 16–21.
378. The World Bank. (2023). Inflation, consumer prices (annual %) - India. World Development Indicators. Published 2023. Accessed June 4, 2022. <https://data.worldbank.org/indicator/FP.CPI.TOTL.ZG?locations=IN>
379. GlobalPetrolPrices.com. (2023). Uganda diesel prices. GlobalPetrolPrices.com. Published 2023. Accessed June 4, 2023. [https://www.globalpetrolprices.com/Uganda/diesel\\_prices/](https://www.globalpetrolprices.com/Uganda/diesel_prices/)
380. My Petrol Price. (2023). Cost of Diesel in Pune. My Petrol Price. Published 2023. Accessed June 4, 2023. <https://www.mypetrolprice.com/7/Diesel-price-in-Pune>
381. India Energy Exchange. (2023). Area Prices. India Energy Exchange. Published 2023. Accessed June 4, 2023. <https://www.iexindia.com/marketdata/areaprice.aspx>
382. UEDCL. (2023). Electricity End User Tariffs and Charges. Uganda Electricity Distribution Company Limited. Published 2023. Accessed June 4, 2023. <https://www.uedcl.co.ug/approved-tariffs/>
383. Wage Indicator Foundation. (2023). Wages in Context- Uganda. Wage Indicator Foundation. Published 2023. Accessed June 5, 2023. <https://mywage.org/uganda/salary/wages-in-context>
384. Wage Indicator Foundation. (2023). Minimum Wage Maharashtra – Engineering Industry. Wage Indicator Foundation. Published 2023. Accessed June 5, 2023. <https://paycheck.in/salary/minimumwages/18640-maharashtra/18790-engineering-industry>
385. (2001). Engineering ToolBox. Published 2001. Accessed April 25, 2022. <https://www.engineeringtoolbox.com/>
386. Goodreturn. (2023). LPG Price in Pune. Goodreturn. Published 2023. Accessed May 13, 2023. <https://www.goodreturns.in/lpg-price-in-pune.html#1683916200>
387. Dorothy Nakaweesi. (2022). Cooking gas prices rise by 30 percent. Daily Monitor.
388. Pricegator. (2023). Compare Cooking Gas Prices in Uganda. Prigator. Published 2023. Accessed June 7, 2023. <https://dignited.com/pricegator/cooking-gas/>
389. TotalEnergies MS Uganda. (2019). About Total Gas. TotalEnergies MS Uganda. Published 2019. Accessed June 7, 2023. <https://services.totalenergies.ug/about-total-gas>
390. Raha D, Mahanta P, Clarke ML. (2014). The implementation of decentralised biogas plants in Assam, NE India: The impact and effectiveness of the National Biogas and Manure Management Programme. *Energy Policy*. 68: 80–91. **10.1016/j.enpol.2013.12.048**
391. Dey B, Roy B, Kumar N. (2019). The Status And Impact of National Biogas And Manure Management Programme At Aizawl In North-East India. ICTEA:

International Conference on Thermal Engineering. 2019. Accessed April 27, 2022. <https://journals.library.ryerson.ca/index.php/ictea/article/view/1271>

392. Jorry B. (2021). Phytoremediation of contaminated water using *Eichhornia crassipes* (Water Hyacinth) and application of the biomass for energy and biomaterials [Masters in Energy and Environment]. University of Leeds;
393. Ongore CO, Aura CM, Ogari Z, Njiru JM, Nyamweya CS. (2018). Spatial-temporal dynamics of water hyacinth, *Eichhornia crassipes* (Mart.) and other macrophytes and their impact on fisheries in Lake Victoria, Kenya. *Journal of Great Lakes Research*. 44(6): 1273–80. **10.1016/j.jglr.2018.10.001**
394. Google Maps. (2022). Google Maps. Accessed June 20, 2022. <https://www.google.co.uk/maps/@18.6852895,73.8615569,2357m/data=!3m1!1e3>
395. Sun L, Zhu ZS. (2014). A Maximum Sustainable Area Model for Harvesting *Eichhornia crassipes* in Environmental Phytoremediation. *AMM*. 513–517: 2975–8. **10.4028/www.scientific.net/AMM.513-517.2975**
396. Zoolfakar MR, Chacha II. (2021). A Water Hyacinth Harvester. In: Ismail A, Dahalan WM, Öchsner A, editors. *Advanced Engineering for Processes and Technologies II*. Cham: Springer International Publishing; p. 193–207. (Advanced Structured Materials). **10.1007/978-3-030-67307-9\_18**
397. Alibaba. (2023). Alibaba Biomass Choppers. Biomass Chopper-Biomass Chopper Manufacturers, Suppliers and Exporters on Alibaba.com Feed Processing Machines. Published 2023. Accessed April 9, 2023. [https://www.alibaba.com/trade/search?fsb=y&IndexArea=product\\_en&clusterId=6500042427&keywords=biomass+chopper&tab=all&viewtype=L&](https://www.alibaba.com/trade/search?fsb=y&IndexArea=product_en&clusterId=6500042427&keywords=biomass+chopper&tab=all&viewtype=L&)
398. Nakweya G. (2019). Kenya warms to the water hyacinth as wonder source of biofuel. *The Guardian*.
399. Widodo TW, Hendriadi A. (2005). Development of Biogas Processing for Small Scale Cattle Farm.
400. Vasudevan P, Thapliyal A, Srivastava RK, Pandey A, Dastidar MG, Davies P. (2010). Fertigation potential of domestic wastewater for tree plantations. 69.
401. Aremu A, Ojoawo S, Alade G. (2012). Water Hyacinth (*Eichhornia crassipes*) culture in sewage: nutrient removal and potential applications of by-products. *Transnational Journal of Science and Technology*. 2.
402. Khanh Nguyen V, Kumar Chaudhary D, Hari Dahal R, Hoang Trinh N, Kim J, Chang SW, et al. (2021). Review on pretreatment techniques to improve anaerobic digestion of sewage sludge. *Fuel*. 285: 119105. **10.1016/j.fuel.2020.119105**
403. Patel R, Pandya HN. (2015). Production of acetic acid from molasses by fermentation process. *International Journal of Advance Research and Innovative Ideas in Education*. 1(2): 58–60.

## Appendix A. Global distribution of water hyacinth

**Table A-1:** List of Countries for the Global Distribution of Water Hyacinth

Africa		Asia	Europe	South America	North America	Oceania
Benin	Malawi	Bangladesh	France	Bermuda	Bahamas	American Samoa
Burkina Faso	Mauritius	Brunei Darussalam	Italy	Brazil	Costa Rica	Australia
Burundi	Morocco	Cambodia	Portugal	Chile	Cuba	Cook Islands
Cameroon	Mozambique	China	Russia	Colombia	Dominican Republic	Fiji
Congo	Nigeria	India	Spain	Ecuador	Guatemala	French Polynesia
DR Congo	Reunion	Indonesia	Turkey	Peru	Haiti	Guam
Cote d'Ivoire	Rwanda	Israel		Puerto Rico	Honduras	Marshall Islands
Egypt	Senegal	Japan		Venezuela	Jamaica	Micronesia
Equatorial Guinea	Sierra Leone	Jordan			Mexico	Nauru
Ethiopia	South Africa	Jordan			Nicaragua	New Caledonia
Gabon	Sudan	Lao			Panama	New Zealand
Ghana	Swaziland	Lebanon			USA	Northern Mariana Islands
Guinea	Tanzania	Malaysia				Palau
Guinea-Bissau	Togo	Maldives				Papua New Guinea
Kenya	Uganda	Myanmar				Samoa
Liberia	Zambia	Philippines				Solomon Islands
Madagascar	Zimbabwe	Singapore				US minor outlying islands
		Sri Lanka				Vanuatu
		Syria				
		Taiwan				
		Thailand				
		Viet Nam				



## Appendix B. Analysis of individual sites

### B.1. Phenological analysis of water quality indicators

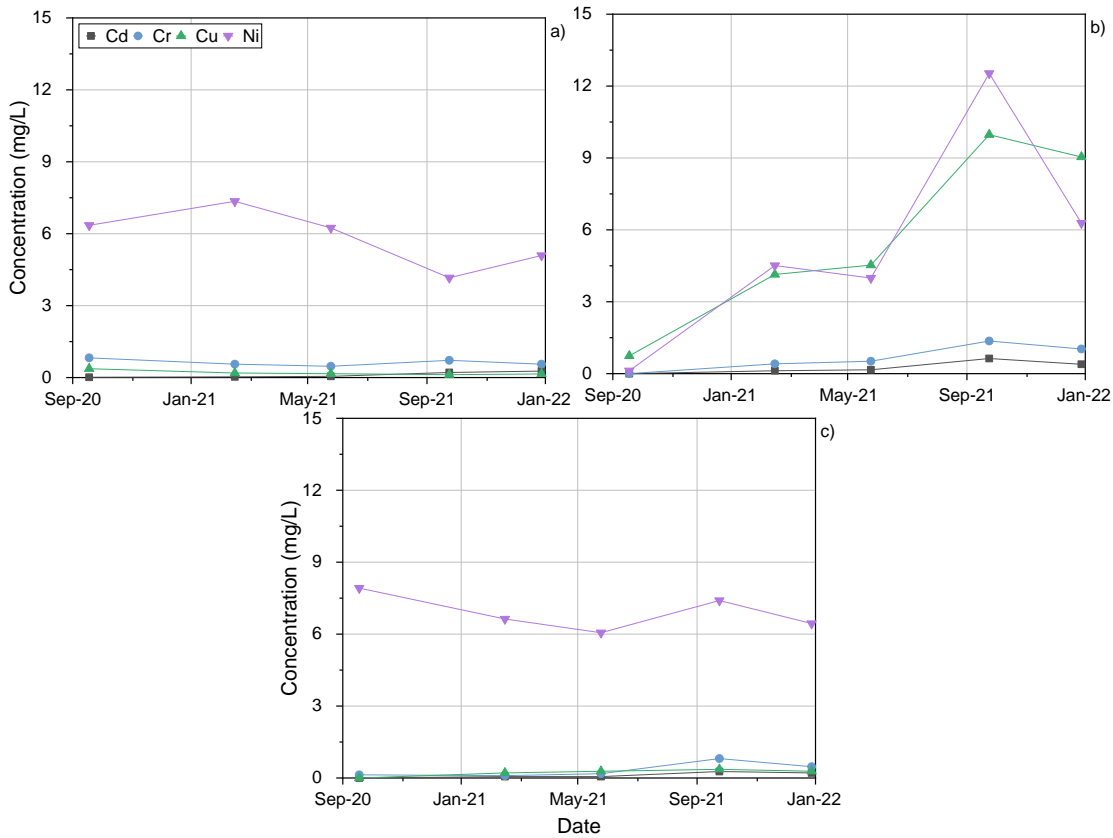


**Figure B.1-1:** Phenological variations of heavy metal water concentration of Murchison Bay, Lake Victoria, Uganda. a) clean water; b) Nakivubo channel; c) Ugandan Brewery Ltd.

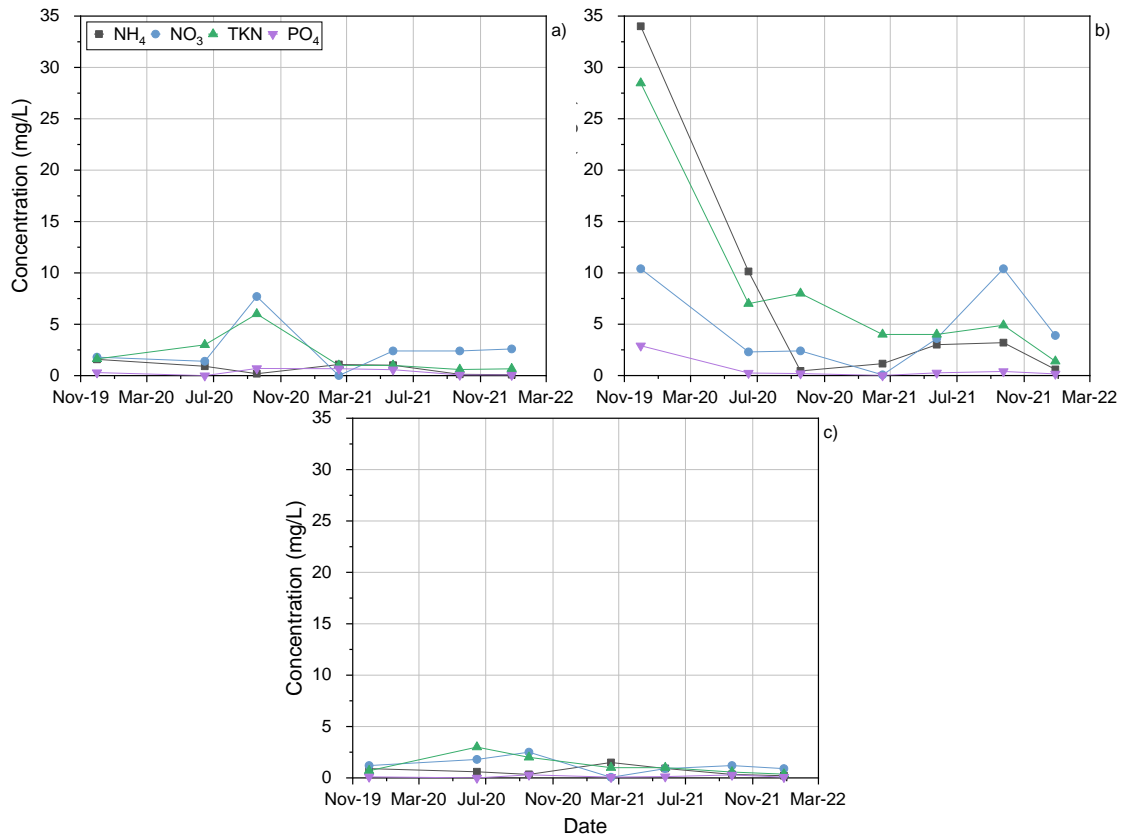


**Figure B.1-2:** Phenological variations of nitrogen and phosphorus concentration of Murchison Bay, Lake Victoria, Uganda. a) clean water; b) Nakivubo channel; c) Ugandan Brewery Ltd.

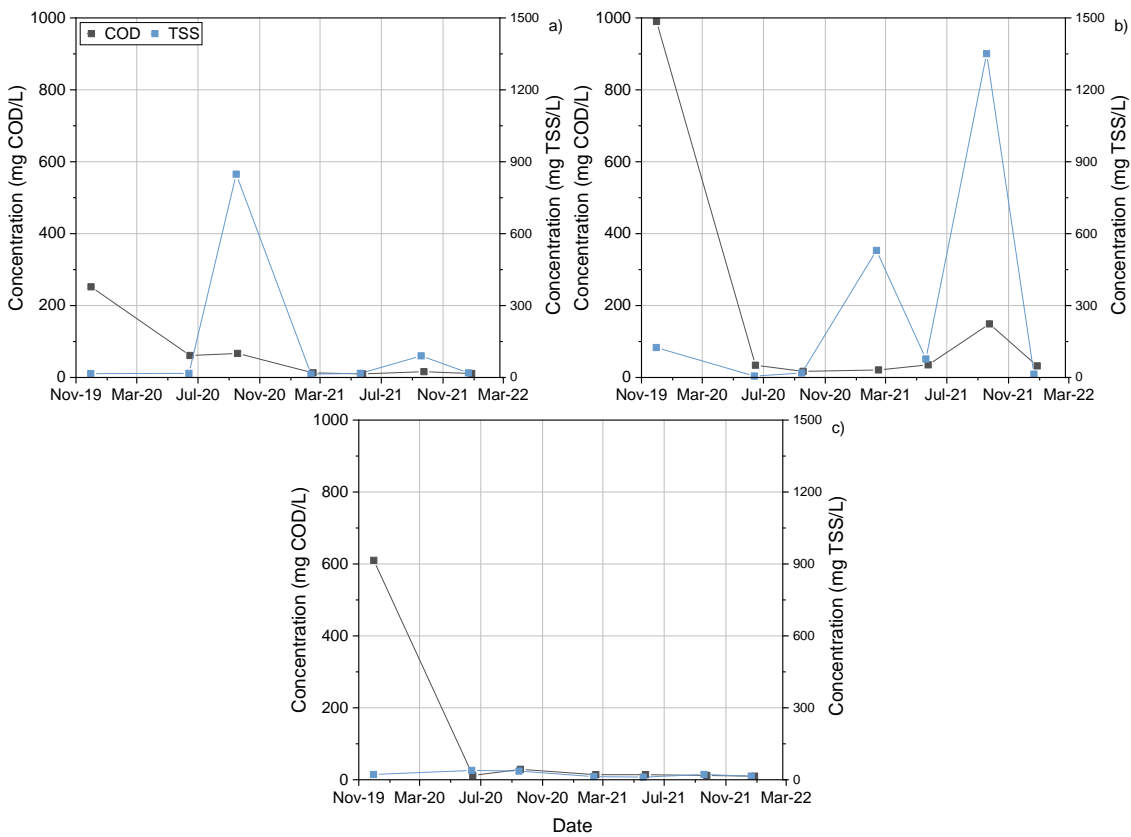


**Figure B.1-3:** Phenological variations of chemical oxygen demand and total suspended solids concentration of Murchison Bay, Lake Victoria, Uganda. a) clean water; b) Nakivubo channel; c) Ugandan Brewery Ltd.

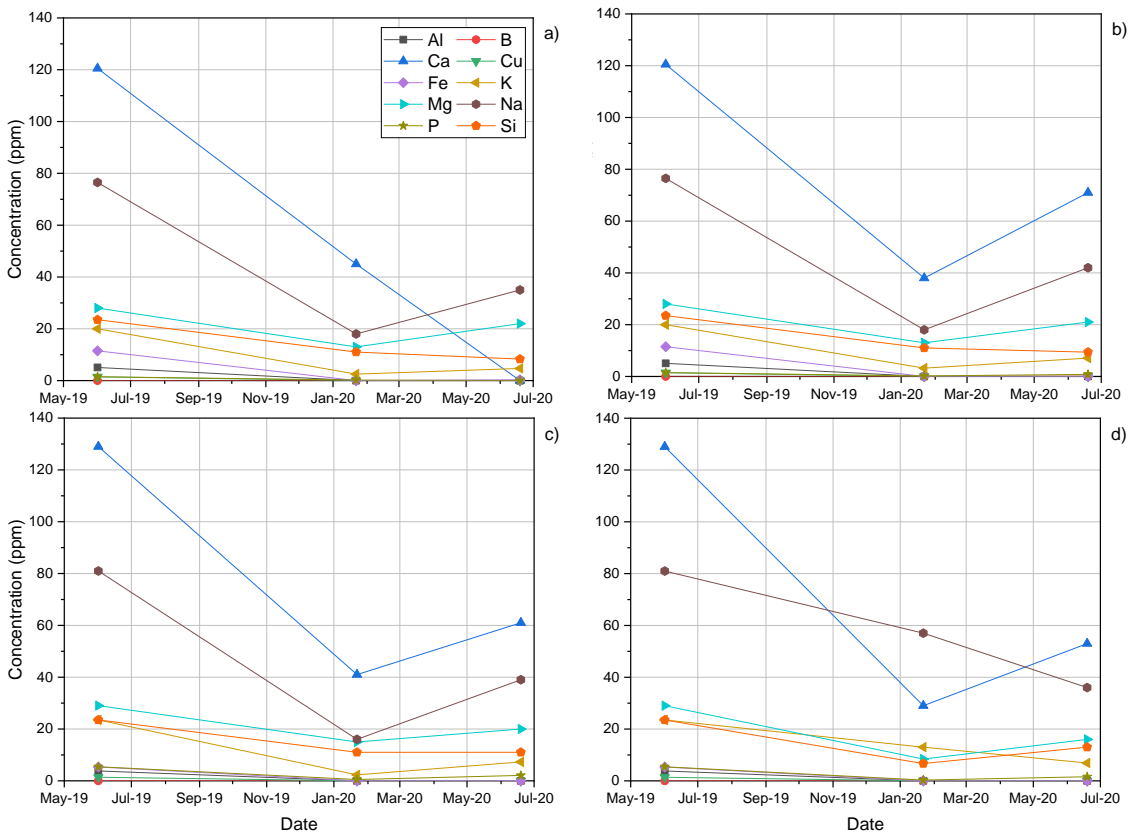


**Figure B.1-4:** Phenological variations of water quality indicators of Pune, Maharashtra, India. a) Indrayani Moshi; b) Indrayani Alandi; c) Mula Baner; d) Mula Sangvi).

## B.2. Biomass composition of water hyacinth samples for geographical and pollution analysis

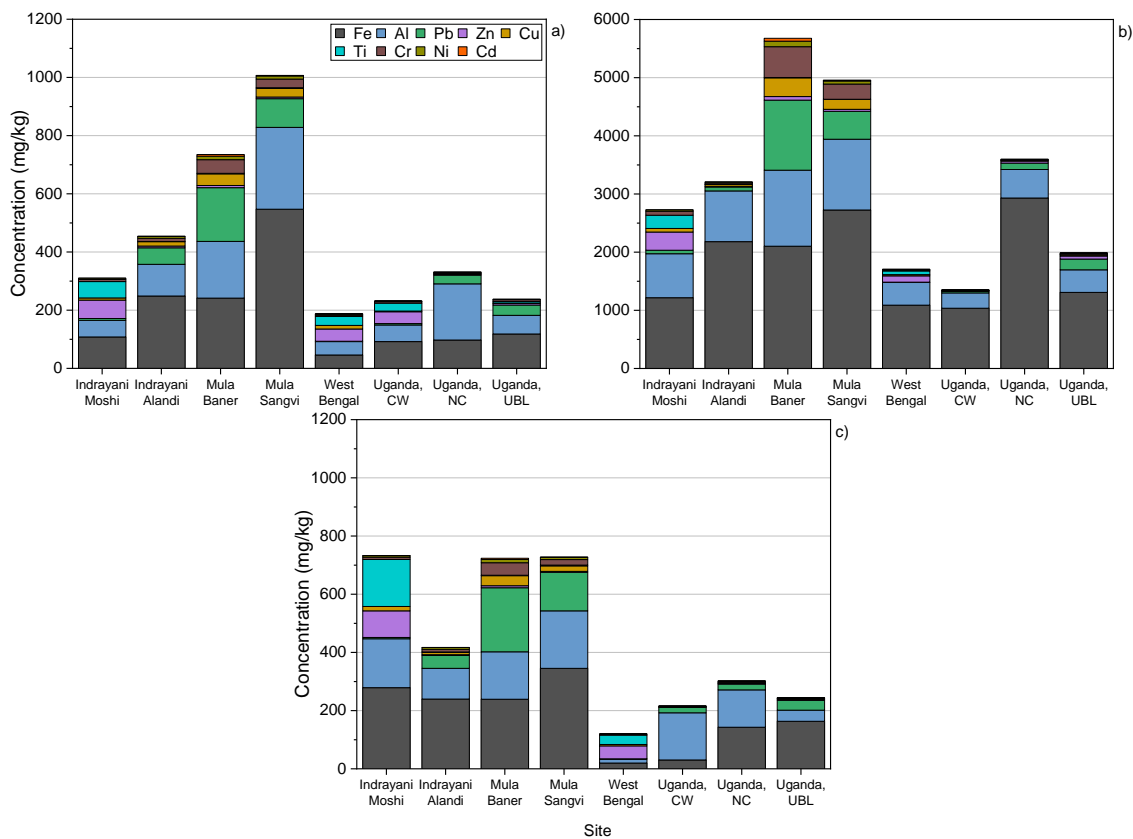


**Figure B.2-1:** Minimum and maximum inorganic composition (heavy metals) of water hyacinth samples for geographical and pollution analysis. a) leaf; b) root; c) petiole.

## Appendix C. Nutrient composition in growth trials

**Table C-1:** Composition of cow manure, from small crate nutrient Trial 1 via ICP-OES, vs. Hoagland's solution.

Element	Cow Manure (ppm)	Hoagland's Solution (ppm)
Aluminium	292	-
Barium	14	-
Boron	23	0.5
Cadmium	< 1	-
Calcium	5253	200
Chromium	1.3	-
Copper	20	0.02
Iron	524	2.9
Lead	1.7	-
Magnesium	5978	48.6
Manganese	110	0.5
Molybdenum	< 0.1	0.05
Nickel	< 1	-
Nitrogen	2178	210
Phosphorous	2438	31
Potassium	6129	235
Silicon	2272	64
Silver	< 1	-
Sodium	3067	1.2
Tin	3.1	-
Titanium	47	-
Vanadium	1.7	-
Zinc	42	0.05